UNIVERSITAT DE BARCELONA

New Catalytic Methods for Pauson-Khand Reactions, Isomerization and Asymmetric Hydrogenations

Application to the Synthesis of Bioactive Compounds

Albert Cabré Montesinos

New Catalytic Methods for Pauson-Khand Reactions, Isomerization and Asymmetric Hydrogenations.

Application to the Synthesis of Bioactive Compounds.

Albert Cabré Montesinos

Doctoral programme: Química Orgànica

Thesis director: **Antoni Riera Escalé**

Facultat de Química

Departament de Química Inorgànica i Orgànica

Secció de Química Orgànica

Universitat de Barcelona

UNIVERSITAT DE BARCELONA

Memòria presentada per l'Albert Cabré Montesinos per a optar al grau de DOCTOR en Química Orgànica per la Universitat de Barcelona

Albert Cabré Montesinos

El **Prof. Antoni Riera Escalé**, catedràtic del department de Química Inorgànica i Orgànica, Secció de Química Orgànica, de la Facultat de Química de la Universitat de Barcelona,

CERTIFICA: que la present tesi doctoral titulada "New catalytic methods for Pauson-Khand reactions, isomerizations and asymmetric hydrogenations. Application to the synthesis of bioactive compounds" presentada per **Albert Cabré Montesinos** per optar al títol de doctor per la Universitat de Barcelona, ha estat realitzada sota la seva direcció.

Prof. Dr. Antoni Riera Escalé

Barcelona, desembre de 2019

Aquest treball s'ha realitzat des del setembre de 2015 al desembre de 2019 amb el suport econòmic del Ministerio de Educación, Cultura y Deporte (beca predoctoral FPU – Formación de profesorado universitario; FPU16/07199) i de l'IRB Barcelona amb una beca predoctoral durant el curs 2015-2016. La tasca s'ha finançat pels projectes de recerca del Ministeri d'Economia i Competitivitat (CTQ2014-56361-P i CTQ2017-87840-P).

El treball experimental s'ha dut a terme al laboratori "Unitat de Recerca en Síntesi Asimètrica" (URSA) de l'Institut de Recerca Biomèdica (IRB Barcelona), ubicat al Parc Científic de Barcelona (PCB).

Acknowledgments

Tot inici té un final. I el final està a punt d'arribar. Bé, no és un final. És un punt i apart. El camí continua, però s'acaba una de les etapes que més m'han marcat. Un abans i un després en el meu creixement i desenvolupament professional. També a nivell personal.

I és que la vida són etapes. Etapes durant les quals et trobes camins planers, pujades, baixades, corbes. Camins sense sortides. Camins paral·lels, que creies eterns, però que després es tornen perpendiculars. Generant cruïlles. I n'hi ha moltes, de cruïlles. Algunes són insignificants. D'altres, transcendentals. A nivell acadèmic, puc dir que n'he viscut dues de gran importància. La primera, quan vaig escollir ser químic. Tenia dubtes, no ho negaré, però quan vaig decidir-me vaig estar-ne convençut, plenament. Resumia tot allò que m'agradava: aprendre, investigar, dissenyar. Crear. I, justament per això, vaig posar la mirada en la química orgànica. Particularment, en la síntesi i la catàlisi –també, val a dir-ho, gràcies a professors que em van motivar, apostant per mi, des d'un primer moment. Tenir al davant un trencaclosques, on només dues peces encaixen. Trobar la forma d'unir-les, generant-ne una de nova, que pugui ser de gran utilitat. En definitiva, vaig percebre que aquesta disciplina m'oferia la oportunitat de generar idees, on notava que m'hi sentia a gust. I, quan em va passar això, vaig ser feliç. Havia escollit bé. Però d'il·lusions no es viu: cal passar a l'acció.

Tenia clar que volia fer el doctorat. No en vaig tenir cap dubte. Però valia la pena estudiar-ho bé: en definitiva, són 4 anys de la meva vida. De química en veuria, sí, molta. Però, en una època de maduresa, tots els factors compten (directa o indirectament, ja que l'èxit –també en la química- va lligat a això). Sense saber-ho, estava immers a la segona cruïlla. Recordo que era un tarda, al mes de gener. Em vaig dirigir al Parc Científic, per primera cop. Havia contactat amb el professor Antoni Riera per una entrevista i, molt amablement, em va obrir les portes del seu laboratori. Quan vam acabar de xerrar, ho tenia clar: volia que aquell espai fos la meva segona casa durant els 4 anys següents.

Durant aquests anys, ha estat un pare a nivell professional, però també a nivell personal. I sóc conscient que no tothom pot dir-ho: em sento molt afortunat. Un gran mentor, sempre disposat a parlar i a ajudar-te quan faci falta. Que sempre té una resposta a oferir-te, a donar-te tot el que estigui al seu abast perquè aconsegueixis allò que et proposes. Atent per tal de no baixar la guàrdia, però relaxant-te en moments d'estrès. En definitiva, el millor mentor que em podia imaginar. Algú que et marca a la teva vida, i que mai li estaràs prou agraït per tot el que t'ha donat. Em sento realment feliç d'haver-te tingut com a director de tesis, Toni. Gràcies.

De la mateixa manera, vull agrair al Prof. Xavier Verdaguer tota la seva ajuda durant aquests anys. La seva disposició a parlar, compartir i discutir sobre química. Gràcies, Xevi, per totes les xerrades i consells que m'has donat. La teva experiència m'ha servit (i em servirà) de molt.

URSA és un gran equip. Gràcies a tots els membres que han contribuït a que la meva estada allà hagi estat tant i tant bona. Des dels primers que vaig conèixer i que ja no hi són, com

fins els membres actuals. | Marta, vam començar aquest camí junts, quan –el dia de les entrevistes, i sense saber-ho- vaig decidir a obrir conversa amb tu. No sé perquè em vaig decidir per tu i no pels altres, suposo que era el destí. Els dos volíem anar a URSA, i ho vam aconseguir –tot i que semblava ben i ben difícil. Era l'inici d'una veritable amistat. Gràcies per convertir-te en una de les meves millors amigues, i el millor suport per aquest viatge que és el PhD. Per tots els moments viscut dins i fora del lab, val la pena haver fet el doctorat només per conèixer-te. Vals moltíssim! | Amparo, mi postdoc preferida. También empecé contigo este trayecto. Fuiste mi "role model", aunque... a veces no hiciera caso de tus consejos. Reponsable, cuidadosa, trabjadora... aunque no te lo creas, fuiste un soporte vital. Girarme y ver que estabas ahí. Hablarnos con la mirada y empezar a reír. Eso era química! Gracias por todo! Y por tus abrazos. Bueno, justamente por eso no... Antetodo, respeto a la presidenta del pasillo guay. | Anna, la teva capacitat d'organització, distensió i detallista és indiscutible. Em vas rebre amb els braços oberts (me'n recordo en la primera Welcome Party), i et vas convertir en un pilar indispensable al grup. Valoro –moltíssim- que sempre hagis apostat per mi, tant fa un temps enrere com ara. Intentaré que tota aposta es faci realitat. | Craig, you've been exactly what I consider to be an excellent labmate: helpful, hard worker and kind. Your "Scottish" jokes –that sometimes I do not understand- makes you unique. NYC will remind me of you as well. Thanks for being like you are! | Ernest, durant tot aquests anys crec que hem après molt l'un de l'altre, i estic molt content d'haver-te conegut. La flor al cul la tens, sí, però no apareix per art de màgia. Gràcies per ensenyar-me a hidrogenar i a ajudar-me a prendre la vida amb més filosofia. | Alessandro, the crazy postdoc. Your crazy but effective ideas, what an inspirational source. Thanks for all the advices you gave to me: in the lab and outside the lab. You'll rock it. | Joan Matarín (lololo) em vas caure bé des del minut 0. Ets d'aquelles persones que no fa falta ni parlar-hi: només observant-te ja es pot comprovar que ets una grandíssim persona. Bon amic, bon químic, responsable, cocinillas, el yerno perfecto. Et repeteixo el que et vaig dir fa poc: d'aquí uns anys, seguirem igual. | Enric, el secretari del pasillo (tot i que es cregui el president). Ets un gran col·lega, un currante, fas que la vida al lab sigui molt amena. Tot i que a vegades et passis amb tant de jugueteo, saps que t'aprecio molt. Totes les converses de futbol, política, química i de la vida en general amb tu, s'agraeixen. Ens tornarem a trobar, segur! | Pep, ets un crack. Vas començar com a màster (quina sort que poguessis entrar), i mica en mica vas fer-te el lloc. I mira't ara, el veterano del grup!! La teva paciència i constància et farà arribar lluny. Fas que les coses siguin fàcils, amb tu és difícil tenir problemes. Ànims amb tot, que vals molt! | Carolina, la mejor research assistant que ha tenido y tendrá URSA. Chica, cuántos años llevamos juntos ya? Por tu sonrisa eterna, tus enfados y chillos espontáneos, tus miradas de complicidad, y el soporte. Eres complidora, trabajadora y te haces querer. ¿Acaso se puede pedir más? No llores cuando me eches de menos, anda. | I, al tornar de l'estada internacional, vaig conèixer dues persones més. Guillem, en pocs mesos ens hem agafat molta confiança, i de fet ja ets el personal trainer oficial! Amb les teves cares i gestos és impossible no agafar-te complicitat, fins i tot ens expliques marujeos! Quién te ha visto y quién te ve. Tinc ben clar que els protacs estan en bones mans! | I finalment la meva compi de pasillo, proyecto y casi de vitrina. Marina, ens vam conèixer via mail. Con el parrafote ese. Però en vivo y en directo fue todo mucho mejor! Riures, confesiones, discussions –de química també-, y miradas de complicidad que lo dicen todo! Recorda: vísteme despacio que tengo prisa. Ets una tia plena de personalitat, carisma i energia. Sé que trobaràs a faltar els meus massatges, però tot té

solució. Espero que triomfis amb les PK i els teus complexes d'iridi. Ho tens tot per tirar-ho endavant! Gràcies per tant, en relativament tant poc temps. | També vull donar les gràcies a antics membres del grup com l'Héléa i en Dan.

Finalment hi ha altres persones que també hi han contribuït molt. He tingut la sort de compartir projectes amb molts estudiants (TFG i TFM). I de tots ells m'emporto coses bones, apart de l'experiència com a mentor. | Martí G. el meu primer màster. Un noi brillant, començar el PhD amb tu va ser tot molt més fàcil, a base de resoldre misteris. | Elia, tu buen hacer fue un lujo. Constante, responsable y trabajador. Y mejor persona. | Sergi, ets un crack, l'amo del salseo. Vas ser un gran descobriment: gràcies eternes pel teu amor incondicional als oxetans, fins al final. Diu molt de tu. | Juanjo, per tota la feina que vas fer. Molts d'encerts. | Laura, mi primera TFG! Gracias por tu simpatía durante esos meses. | Lorenzo, el ejemplo de humildad, responsable y trabajador. Ese finde en Bolonia que no olvidaré. Eres un grande. | Pol M., només vam coincidir un més, però m'hagués agradat guiar-te més temps. El teu esforç és innegable, aconseguiràs allò que et proposis. | I d'altres estudiants que també han passat pel lab: Marta D., Helena F., Javi, Ruben, Pol H., Marc, Oriol, Jacqueline, Dominique, Medea. Gràcies a tots.

Durant els dos últims anys de tesis, també he tingut la sort de realitzar pràctiques docents al grau de Química de la UB. Particularment, agrair a la Sonia, al Cesc, a l'Andrea i a la Gemma. Van ser només tres setmanes, però en vam tenir prou: sou simplement genials!

També vull agrair als companys de l'UB. A l'Albert i a l'Arnald, els nostres companys inorgànics, tots els meetings, xerrades i bons moments que hem passat junts. També al servei d'Espectrometria de masses: a la Irene i a la Laura, per rebre'm sempre amb un somriure tot i portar-li's 20 mostres de cop. Al Josep, d'IR, per tot el suport i excel·lent tracte. I al servei de RMN, Vicky i M. Antònia, per l'ajut quan us he necessitat. De l'IRB, a la Clara i a l'Anna, per l'ajuda amb les beques. Al Parc Científic he tingut la sort de col·laborar amb l'empresa ENANTIA. Vull donar infinites gràcies a l'Esther i a l'Adela. És un luxe comptar amb professionals com vosaltres. També a la Mònica i al Toni, per la seva gran amabilitat. I també a altres membres del Parc: Montse, por el cariño y cuidarme tan bien.

D'altra banda, fer la tesis doctoral té molts avantatges. He tingut la gran sort de poder anar de congrés en diverses ocasions. Dels quals m'emporto molts records (Tolouse, Sitges, Heidelberg, Oxford, Donosti, Santiago) i molts amics. Companys de l'ICIQ, Laura de la UAM,... i especial menció als meus amics de Farmàcia: Mar, em vas acollir amb els teus companys, ets una noia genial!!! Sergi, Aina, Míriam, Rosa,.... I al Pau, que com jo, érem els infiltrats del grup. Congressos que m'han fet créixer, i han estat font d'inspiració per tenir noves idees, i fer networking.

I, òbviament, Princeton. 6 mesos de la meva vida que mai oblidaré: New York, Philly, Boston, Washington, Chicago. L'estada internacional que sempre havia somiat. I will always be grateful to Prof. David MacMillan for giving me the opportunity to be part of his prestigious research group. During 6 months I appreciated how much brilliant they are,

making new chemistry from the scratch. Discussing and (even arguing!) to find the best approach. Always in a cooperative manner, because science is based on this. Patrick and Ian, my fumehood labmates. Sebastian and Junyong, for being my friends in and outside the lab, for all those afternoons at the gym. Many thanks to Dani, Gabby, Xiahang, Tomer, Tim, Tiffany,...and all the rest of the MacMillan's group. You guys made my stay there simply amazing. I remember the Frickmas' Party, where I knew I did not want to leave Princeton. També al Martí i al Gerard, i al Carles; els meus amics matemàtics, que ens vam trobar de casualitat, i quina sort! Per tots els viatges i dinars plegats: gràcies, em vau fer sentir com si fos a Catalunya. Y, por supuesto, a vosotras: Maria y Laura. Por las tardes juntos, en el lab, comiendo Ramen, en Cape May, en Boston. Por las noches de cine. Fueron 6 meses inoblidables. María, gracias por tu soporte incondicional, aunque fueras rancia (a propósito) conmigo. Por nuestras charlas en la cocina, todas las noches en el bus y por ese fin de año 2018 juntos en NYC. Te echo de menos, te mereces lo mejor.

Fer la tesis al IRB Barcelona m'ha servit per conèixer d'altres àmbits científics, com la biomedicina. Però, sobretot, per estar en contacte amb altres persones fora del meu camp. La meva promoció: Mireia, Alícia, Jorge, Núria, Diana, Rafa i Manu. De tots ells m'emporto records valuosíssims: Barcelona, Grècia i Eivissa. Com m'agradaria tornar enrere. Recordo aquells moments i és inevitable somriure. | Mireia, t'has convertit en algú vital, gràcies per tot.

També vull esmentar als meus amics. Els que, desde fora del laboratori, em donen suport incondicional. Ja sigui des de l'època de La Salle, o de la URV. Sempre he pensat que conservar als amics és de mutu acord. Clara, Aleix, Carlota F., Carlos, Anna M., Glòria, Anna R., Emma, Eva, Laura F. i Isaque, Carlota B.,... amb vosaltres ho he aconseguit. No vull que mai canvii. I, d'altres que, aquí a Barcelona, o en etapes anteriors, he tingut la sort de creuar-m'hi i convertir-se en amics: Manel, Dani, Nadia, Hugo, Quim, Glòria S., Ivan, Cristofe, Alex, Alícia, Veronica i Joan G.

Finalment, a la meva família: tiet Ton, Glòria, Gerard, Karin, Adam, Mari. I a la meva padrina i a la meva tieta, que des del cel estic segur que estan orgulloses d'on he arribat. Des de petit us he tingut aprop, i no puc estar-ne més agraït. A vosaltres, i als meus pares. Papis, gràcies de tot cor per convertir l'Albertito en qui sóc actualment. Us ho dec tot a vosaltres.

Gràcies de tot cor, a tots els que formeu part d'aquests agraïments.

I a qui hagi d'arribar: ens trobarem a la propera cruïlla.

"Que tot està per fer, I tot és possible"

- Miquel Martí i Pol

"No hay mal que por bien no venga"

- Refrán popular

"Action expresses priorities"

- Mahatma Gandhi

"L'essential est invisible pour les yeux"

- Antoine de Saint-Euxupéry

"Imagination is more important than knowledge. Knowledge is limited whereas imagination embraces the entire world".

Albert Einstein

"I learned (what I suppose I really knew already) that one can never go back, that one should not ever try to go back -that the essence of life is going forward. Life is really a one-way street, ins't it?"

Agatha Christie

This thesis is dedicated to my parents. For being beside me all the time: for all the love, for all the advices, for all their support. I am what I am simply because of them. Gràcies.

Abbreviations

AMPA	α-amino-3-hydroxy-5-methyl-4-isoxazolepropionic acid receptor
aq	aqueous
ATR	Attenuated total reflection
BA_r^F	tetrakis[3,5-bis(trifluoromethyl)phenyl]borate
Boc	tert-Butyloxycarbonyl
Bz	benzoyl
c	concentration
calc.	calculated
COD	cyclooctadiene
conv.	conversion
DCE	dichloroethane
DCM	dichloromethane
DFT	Density functional theory
DIBAL-H	Diisobutylaluminium hydride
DMAP	4-Dimethylaminopyridine
DMF	dimethylformamide
DMSO	dimethyl sulfoxide
EDG	electron-donating group
ee	enantiomeric excess
equiv.	equivalent
ESI	electrospray ionization
EWG	electron-withdrawing group
GC	gas chromatography
HOMO	Highest occupied molecular orbital
HPLC	High-performance liquid chromatography
HRMS	High resolution mass spectrometry
IPA	2-propanol
IR	infrared
J	coupling constant
LMO	localized molecular orbital
LUMO	Lowest unoccupied molecular orbital
m.p.	melting point
m/z	mass-to-charge ratio
mCPBA	meta-Chloroperoxybenzoic acid
MEG	monoethylene glycol
MS	mass spectrometry
NBD	norbornadiene
NBO	natural bond orbital
NBS	N-Bromosuccinimide
NMDA	N-methyl-D-aspartate receptor
NMO	N-Methylmorpholine N-oxide
NMR	Nuclear Magnetic Resonance
NOESY	Nuclear Overhauser Effect Spectroscopy
on	overnight
PES	Potential energy Surface
PK	Pauson-Khand
PKR	Pauson-Khand Reaction
PTFE	Polytetrafluoroethylene
pyr	pyridine
rac	racemic
RT	room temperature
TBAF	Tetra-n-butylammonium fluoride
TBS	t-butyldimethylsilyl
TFA	Trifluoroacetic acid
THF	Tetrahydrofuran
TLC	Thin Layer Chromatography
TMSCl	Trimethylsilyl
TMSCl	trimethylsilyl chloride
TON	turnover number
t_R	retention time
Ts	tosyl; p-toluenesulfonyl
TS	transition state
δ	chemical shift

List of publications

The experimental results of this thesis are presented through eight chapters (from Chapter 2 to Chapter 9). Each of them corresponds to scientific publications that have been accepted (or submitted under revision) during the doctoral period.

I. Ethylene Glycol Assisted Intermolecular Pauson-Khand Reaction
Cabré, A.; Verdaguer, X.; Riera, A.

Synthesis **2017**, *49*, 3945-3951. Highlighted in *Synfacts* ***2017****, 13(11), 1143*

Formulated the research question and shared the task of solving the research problem, performed the experimental work and co-write the article with A. Riera and X. Verdaguer as research supervisors.

II. Catalytic Pauson-Khand Reaction in Ethylene Glycol-Toluene. Activity, Selectivity and Catalyst Recyclability
Cabré, A.; Verdaguer, X.; Riera, A.

Synthesis **2018**, *50* (19), 3891-3896.

Shared the task for formulating and solving the research problem, performed the experimental work and co-write the article with A. Riera and X. Verdaguer as research supervisors.

III. Total synthesis of (*R*)-Sarkomycin Methyl Ester Via Regioselective Intermolecular Pauson-Khand Reaction and Iridium-Catalyzed Asymmetric Isomerization
Cabré, A.; Khaizourane, H.; Garçon, M.; Verdaguer, X.; Riera, A.

Org. Lett. ***2018****, 20* (13), 3953-3957.

Shared the task for formulating and solving the research problem, performed most of the experimental work and co-write the article with A. Riera and X. Verdaguer as research supervisors. H. Khaizourane synthesized (*rac*)-Sarkomycin. The DFT calculations were performed by M. Garçon.

IV. **Mild Iridium-Catalysed Isomerization of Epoxides. Computational Insights and Application to the Synthesis of β-Alkyl Amines**
Cabré, A.; Cabezas-Giménez, J.; Sciortino, G.; Ujaque, G.; Verdaguer, X.; Lledós, A.; Riera, A.

Adv. Synth. Catal. **2019**, *361*, 3624-3631.

Shared the task for formulating and solving the research problem, performed the initial key experimental work and synthesis of the substrates, supervised and guided Juanjo Cabezas-Giménez (Master student) who did part of the experimental work, and co-write the article with A. Riera, A. Llédos and X. Verdaguer as research supervisors. G. Sciortino, in collaboration with G. Ujaque, performed the DFT calculations.

V. **Iridium-Catalyzed Isomerization of *N*-Sulfonyl Aziridines to Allyl Amines**
Cabré, A.; Sciortino, G.; Ujaque, G.; Verdaguer, X.; Lledós, A.; Riera, A.

Org. Lett. **2018**, *20* (18), 5747-5751.

Formulated the research question and shared the task of solving the research problem. Performed the experimental work and co-write the article with A. Riera, A. Lledós and X. Verdaguer as research supervisors. G. Sciortino, in collaboration with G. Ujaque, performed the DFT calculations.

VI. **Catalytic Regioselective Isomerization of 2,2-Disubstituted Oxetanes to Homoallylic Alcohols**
Cabré, A.; Rafael, S.; Sciortino, G.; Ujaque, G.; Verdaguer, X.; Lledós, A.; Riera, A.

Submitted manuscript.

Formulated the research question and shared the task of solving the research problem. Performed the initial key experimental work and the last experiments (asymmetric hydrogenation), supervised and guided Sergi Rafael (Bachelor student) who did part of the experimental work, and co-write the article with A. Riera, A. Lledós and X. Verdaguer as research supervisors. G. Sciortino, in collaboration with G. Ujaque, performed the DFT calculations.

VII. Enantioselective Synthesis of β-Methyl Amines via Iridium-Catalyzed Asymmetric Hydrogenation of *N*-Sulfonyl Allyl Amines

Cabré, A.; Verdaguer, X.; Riera, A.

Adv. Synth. Catal. **2019**, *361,* 4196-4200 (VIP: Very Important Publication).

Shared the task for formulating and solving the research problem, performed the experimental work and co-write the article with A. Riera and X. Verdaguer as research supervisors.

VIII. Highly Enantioselective Iridium-Catalyzed Hydrogenation of *N*-Allyl Phthalimides

Cabré, A.; Romagnoli, E.; Martínez-Balart, P.; Verdaguer, X.; Riera, A.

Org. Lett. **2019**, DOI 10.1021/acs.orglett.9b03865.

Formulated the research question and shared the task of solving the research problem. Performed the initial key experimental work and the last experiments (synthetic applications), supervised and guided Elia Romagnoli (Master student) and Pol Martínez-Balart (Bachelor student) who did part of the experimental work; and co-write the article with A. Riera and X. Verdaguer as research supervisors.

Table of contents

Chapter 1

General introduction and Objectives

Most of the pharmaceuticals, materials, and other chemicals important to modern society are procured by synthetic organic chemistry. The heart of this discipline is the construction of carbon-carbon bonds, yet reactions that achieve this goal often require undesirable starting materials or inefficient strategies. There is a need, thus, to find new synthetic transformations to expand the chemical space. In this sense, the development of new chemical reactions with a low environmental impact is a major concern for the chemists. Efficiency of a process can be defined in terms of complexity, selectivity and atom economy. Catalysis meets all these criteria and is a key technology for green chemistry.[1]

In parallel to this, the prevalence of chiral stereocenters in many natural products, drugs and pharmaceuticals has attracted a growing interest in the development of enantioselective methods. The need of optically pure substances is mainly driven because of the different behavior and biological responses of the two enantiomers: when interacting with one enantiomer, a chiral drug may have a desired beneficial effect while the other may be inactive or cause serious and undesirable side effects.[2] Among all the approaches for gaining access to enantiomerically pure compounds, asymmetric catalysis is considered as one of the ultimate solutions as it provides an efficient, clean and atom economical approach, usually using transition metals in combination with chiral ligands. Due to the increasing number of available methodologies, the scope of asymmetric catalysis[3] has greatly expanded to include a broad range of chemical transformations. Ideally, an asymmetric catalytic reaction should provide high yields and selectivity (chemo-, diastereo- and enantioselectivity) for a wide range of substrates, whilst being sustainable and with a high catalytic efficiency (low catalyst loading for a high TON). Therefore, the design of novel chiral catalysts and the development of new asymmetric methodologies for the synthesis of biologically active compounds are urged.

At the Unitat de Recerca en Síntesi Asimètrica (URSA) research group, the design, synthesis and catalytic evaluation of novel *P*-stereogenic ligands have been carried out during the last decades.[4] These ligands were typically coordinated to transition metals such as cobalt, rhodium or iridium. Particularly, the resulting metal complexes were tested in catalytic reactions such as the Pauson-Khand reaction and asymmetric hydrogenation. Due to the expertise of the group in this field, this doctoral thesis is focused on:

- The development of new synthetic protocols for the catalytic and stoichiometric **Pauson-Khand reaction (PKR)** to afford PK adducts with enhanced yields and selectivity.

- The design of new synthetic strategies based on (asymmetric) **isomerization reactions** of allylic and heterocyclic compounds.
- The application of iridium-P,N complexes on the **asymmetric hydrogenation** of minimally functionalized olefins.

Moreover, and in all the chapters, the atom economy is taken into account, following the green chemistry principles, in order to minimize reagents or solvents that may have hazardous effects on human health and the environment. Regarding to this, isomerization and hydrogenation reactions perfectly accomplishes this requirement. Overall, this doctoral thesis describes innovative catalytic platforms to improve the means by which a variety of important chemicals are accessed, which would impact public health as well as into a number of other sectors that rely on fine chemicals.

1.1. The Pauson-Khand Reaction

The Pauson-Khand Reaction, first discovered by P. L. Pauson and I. U. Khand, is formally a [2+2+1] cycloaddition between an alkyne, an alkene and a carbon monoxide molecule, usually promoted by a cobalt (0) complex, in stoichiometric or catalytic manner.[5] The reaction leads to the formation of a cyclopentenone, with three new carbon-carbon bonds and, if the alkene is disubstituted, two new stereocenters are formed, thus enhancing its synthetic potential. This reaction can proceed in stoichiometric (by quantitative formation of alkynyl-hexacarbonyl dicobalt complexes) or catalytic manner (using CO pressure and catalytic amount of metal complex).

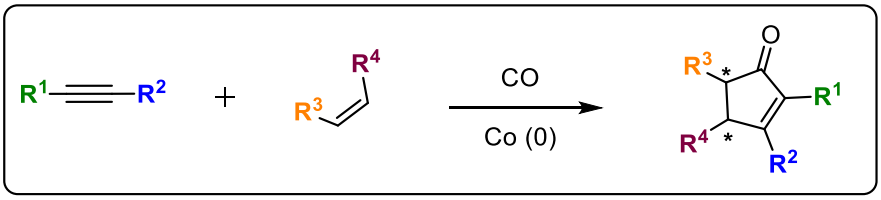

Scheme 1.1. General scheme for the Pauson-Khand reaction (PKR).

In fact, the Pauson-Khand reaction is a textbook method for the construction of cyclopentanic rings[6] and has been typically employed for the synthesis of a wide variety of natural products or bioactive compounds[7] containing a cyclopentenone as structural core motif, mostly in the intramolecular fashion. However, our research group has exploited the

intermolecular PKR for the synthesis of other bioactive compounds, such as (+)-brefeldine-A,[8] 13-epi-12-oxo-PDA,[9] (-)-carbovir[10] and deoxy-J1-phytoprostanes,[11] dPPJ$_1$-I and dPPJ$_1$-II (Figure 1.1).

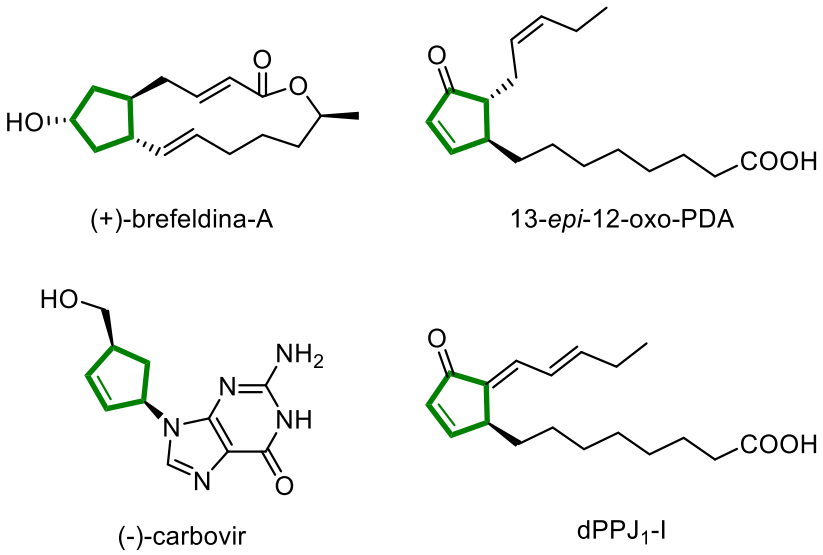

Figure 1.1. Some products of biological interest synthesized by the PKR.

The asymmetric version of the Pauson-Khand has been investigated in our research group during the last decades.[12] The introduction of chirality in the PKR began with the use of chiral auxiliaries attached either to the alkene or the alkyne. Our group has a long-standing experience in the development of asymmetric approaches for the intermolecular PKR using either chiral auxiliaries or ligands. Particularly, hemilabile chiral bidentate *N*-phosphino sulfonamides (PNSO) were tested with high efficiency in the enantioselective, intermolecular PKR of terminal alkynes[12a,b] and disubstituted internal alkynes[12c] (Scheme 1.2). In the intramolecular fashion, our group also described the asymmetric, catalytic, intramolecular Pauson-Khand reaction of several 1,6-enynes, catalyzed by [Rh(COD)(MaxPHOX)]BF$_4$.[13] PK-adducts were afforded in moderate yields and selectivities of up to 86% ee (Scheme 1.3).

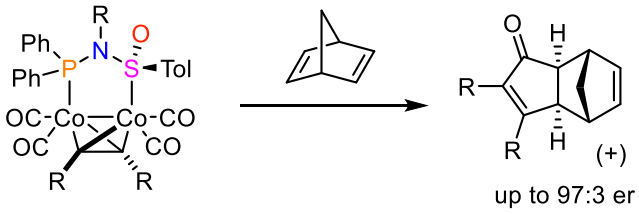

Scheme 1.2. Asymmetric Intermolecular PKR of symmetrically substituted alkynes.

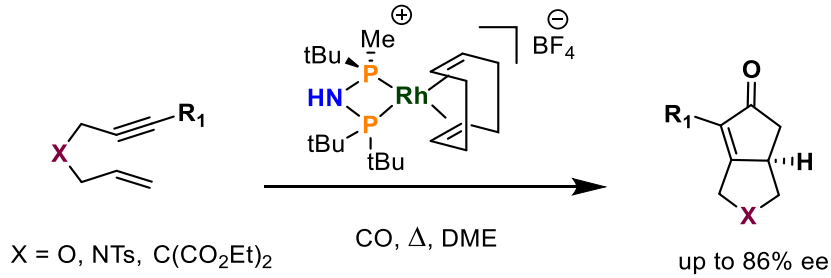

Scheme 1.3. Rh-catalyzed asymmetric and intramolecular catalytic PKR.

However, and despite all the efforts, the intermolecular Pauson-Khand reaction with a wide substrate scope in high enantioselectivities remains as one of the current challenges in this field, and our group reported, in 2015, the precedent with best results reported so far (Scheme 1.4) using the ThaxPHOS catalyst.

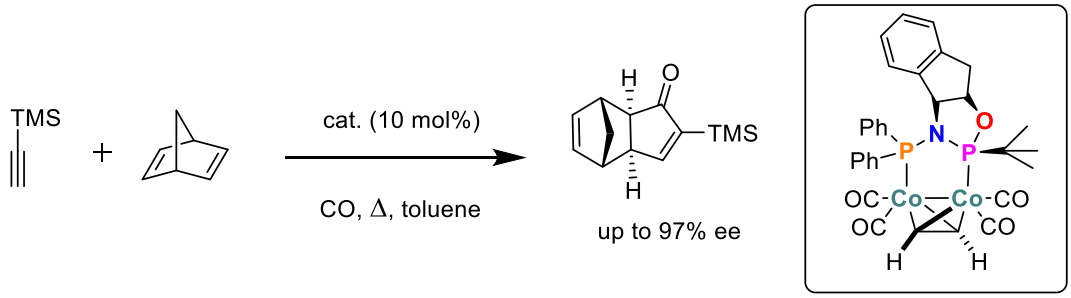

Scheme 1.4. Co-catalyzed asymmetric and intermolecular catalytic PKR.

On the other hand, the regiochemical outcome of the intermolecular Pauson-Khand reaction is an issue to take into account. Whereas terminal alkynes afford cyclopentenones with the substituent in α to the carbonyl group, asymmetrical internal alkynes can lead to a mixture of regioisomers.[14] It must be also highlighted that the PKR is sensitive to steric and electronic effects of both the alkene and the alkyne. Sterically hindered substrates tend to be low yielding, and terminal alkynes are known to react easier that internal alkynes. In terms of electronic effects, non-symmetrical internal alkynes tend to afford cyclopentenones with the EDG groups in α to the carbonyl group and EWG groups in β position (Scheme 1.4).

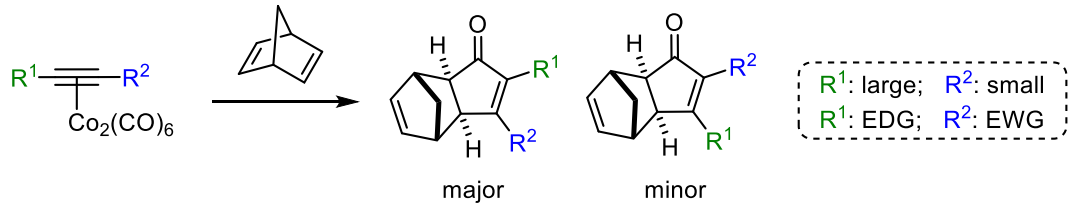

Scheme 1.4. General regiochemical outcome of the PKR.

When executed in intramolecular fashion, the Pauson-Khand reaction has been the most used version of this reaction as it leads to complex polycyclic structures in very few synthetic steps and it shows minor reactivity requirements. However, and despite its great synthetic potential, the intermolecular PKR has been less investigated. One of the main reasons for this is that the intermolecular PKR shows a small range of applicability regarding the alkene. Only small alkenes, such as ethylene, or strained alkenes, such as norbornene, norbornadiene or cyclopropane, react with synthetically useful yields.

Regarding to this, there are few examples of intermolecular PKR using poor-coordinating or non-strained alkenes, with the exception of ethylene. Baran and co-workers reported, in 2011, the total synthesis of (±)-Axinellamines A and B (Scheme 1.5).[15] During the course of this work, they proposed that one of the key steps was an ethylene glycol assisted Pauson-Khand cycloaddition. To promote the reaction, they employed *N*-methyl morpholine *N*-oxide (NMO) as activator. The Pauson-Khand reaction has been typically activated by heating, displacing the CO molecules from the cobalt complex and thus allowing alkene coordination. However, and in some cases, this methodology suffered from low yields or poor selectivity. For that reason, *N*-oxides emerged as promising alternative to perform the reaction at room temperature while enhancing the reaction activity.[16] Moreover, at that work, the use of ethylene glycol as an additive was highlighted to be essential. Otherwise, the reaction did not proceed due to the poor reactive alkene employed. However, and since that report, the effect of ethylene glycol had not been further investigated when we started our work (present thesis).

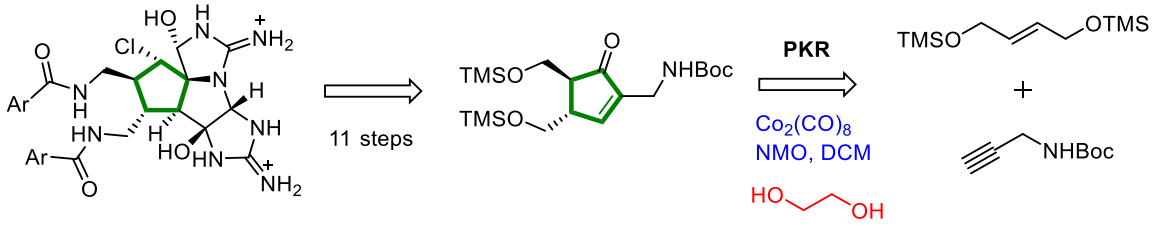

Scheme 1.5. Total synthesis of (±)-Axinellamines A and B (*Baran et al., 2011*).

At that point, our group considered that a study about the role that ethylene glycol can have as additive in the Pauson-Khand reaction, both in intramolecular and intermolecular fashion, would be beneficial for the field. Moreover, the impact of ethylene glycol in the catalytic version would be in high demand to explore uncovered reactivity.

Therefore, the first objective of this thesis was to investigate the effects that ethylene glycol produce to the outcome of the PKR in stoichiometric manner, as explained in **Chapter 2**. Afterwards, the role of ethylene glycol in the catalytic PKR was studied, in terms of yield, activity and selectivity, as detailed in **Chapter 3**.

Afterwards, we sought for a target compound that could be synthesized by means of this methodology. Among the wide variety of cyclopentanic compounds that are biologically activity, (*R*)-Sarkomycin is a nice example to illustrate the utility of our methodology (Fig. 1.2).[17] Although its structure is relatively simple, with only one stereogenic center, a large number of synthestic approaches toward sarkomycin (or sarkomycin derivatives) have been reported.[18] However, some of these syntheses addressed the racemic mixture and involved a relatively large number of steps. In other cases, the desired enantiopurity was obtained via (a) kinetic resolution, (b) the chiral auxiliary approach, or (c) classical racemic resolution. To the best of our knowledge, the only precedent that employed asymmetric catalysis was the work reported by Von Zezschwitz and co-workers (Scheme 1.6).[19] They described a five-step sequence based on the Rh-catalyzed asymmetric conjugate addition of hexenyl chain to cyclopentenone.

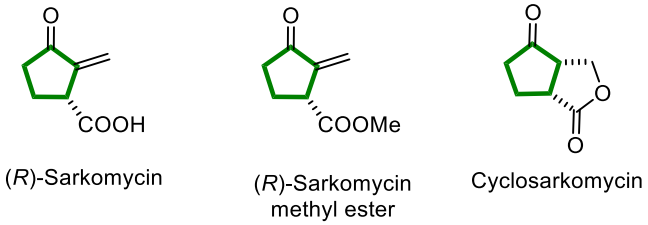

Figure. 1.2. (*R*)-Sarkomycin and some of its derivatives.

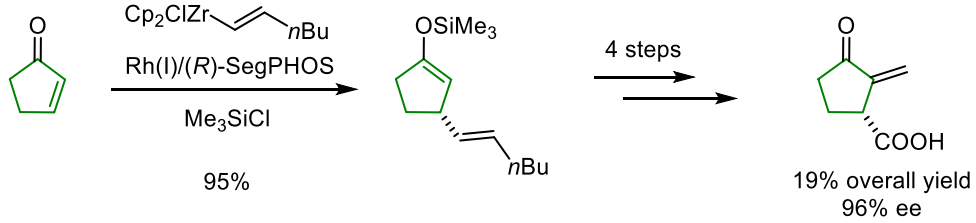

Scheme 1.6. Rh-Catalyzed Asymmetric Conjugate Addition (*von Zezschwitz et al., 2013*)

Therefore, and following the work performed in the doctoral thesis of Dr. Héléa Khaizourane, we envisioned that the cyclopentane ring of (*R*)-Sarkomycin could be rapidly

assembled by an intermolecular Pauson-Khand reaction, followed by an asymmetric hydrogenation using chiral iridium complexes.

Our research group has a long-standing expertise in the synthesis of *P*-stereogenic ligands, which are coordinated to transition metals (Rh, Co or Ir), and their application to asymmetric catalysis, with special emphasis in asymmetric hydrogenation. We recently developed a novel route to bulky *P*-stereogenic phosphine ligands through S_N2@P reactions.[20] This synthetic strategy provided access to a library of phosphine-oxazoline ligands that were coordinated to iridium, thus generating the Ir-MaxPHOX family (Fig 1.3).[21] The general structure of Ir-MaxPHOX catalyst is depicted in Scheme 1.7. A feature of this ligand system (MaxPHOX) is that it contains three stereogenic centers that can be introduced from three simple building blocks: an amino alcohol, an amino acid, and a *P*-stereogenic phosphinous acid. One of the key advantages of the MaxPHOX ligands is the structural diversity arising from its possible configurations and substitution patterns, which can be adapted to a specific reaction, and modulating the steric hinderance by modifying the oxazoline substituent.

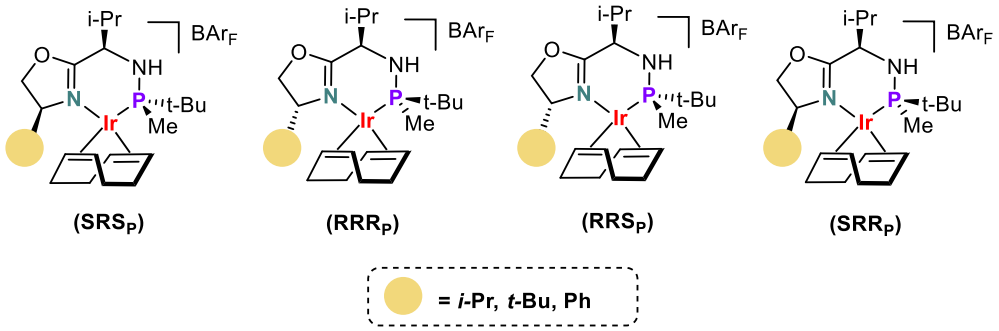

Figure. 1.3. The four diastereoisomers of the Ir-MaxPHOX family of catalysts.

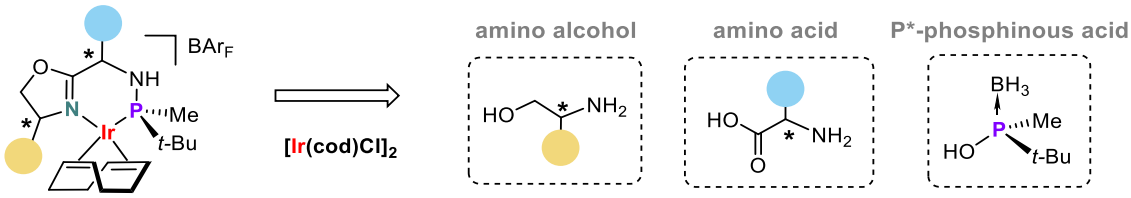

Scheme 1.7. General structure of the Ir-MaxPHOX catalysts.

These Ir-MaxPHOX complexes have been successfully applied to the asymmetric hydrogenation of cyclic enamides[21], and aryl[22] and alkyl imines,[23] showing excellent activities and enantioselectivities for all cases. However, we were prompted to find other enantioselective catalytic applications for these catalysts.

Consequently, the third aim of this thesis was the total synthesis of (*R*)-Sarkomycin (or derivatives) by means of regioselective intermolecular PKR using ethylene glycol as additive and asymmetric catalysis using iridium MaxPHOX complexes. This total synthesis is detailed in **Chapter 4**.

1.2. Isomerization processes

Isomerization reactions constitute an important field in homogeneous catalysts, as they offer excellent atom economy while providing useful synthetic transformations. Proof of this, the rhodium-catalyzed asymmetric isomerization of allylic amines into the corresponding enamines stands out as one of the major achievements in asymmetric catalysis.[24] This transformation, first developed by Noyori, became a breakthrough towards the enantiopure synthesis of menthol in the industry.

Apart from allylic amines, during the last decades, some efforts have been put towards the asymmetric isomerization of other substrates, such as allylic alcohols (Scheme 1.8).[25]

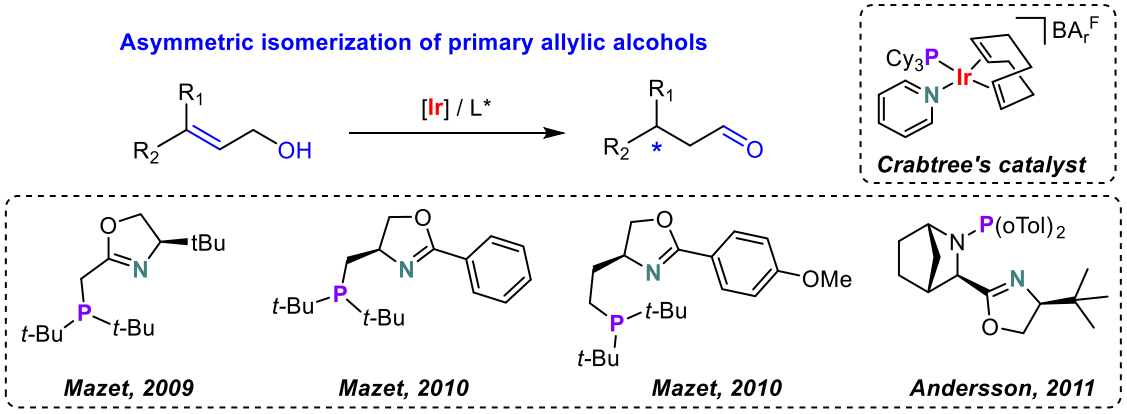

Scheme 1.8. Chiral P,N-ligands used in asymmetric isomerization of allylic alcohols.

In contrast, the isomerization of **heterocyclic compounds** has been less explored if compared to allylic compounds. Heterocyclic compounds are present in numerous pharmaceuticals, materials and natural products. They present at least one heteroatom in their chemical structure. Particularly, in this thesis, we envisaged the isomerization of strained heterocycles (epoxides, oxetanes and aziridines).

Epoxides are oxygenated 3-membered rings which are versatile and highly useful synthetic intermediates in organic synthesis.[26] Epoxides are inherently reactive due to the strained ring, which makes them feasible to be interconverted into other functional groups. Regarding to rearrangement processes, the selective isomerization to the carbonyl group, avoiding the formation of other byproducts or side reactivity is highly desired. This reaction, that bears substantial synthetic potential, is also called Meinwald rearrangement,[27] and it is usually catalyzed by Lewis acids, such as $BF_3 \cdot Et_2O$, lithium salts and $MgBr_2$. Other catalysts were also described to perform the reaction selectively: $InCl_3$,[28] $IrCl_3$[29] and copper salts.[30] However, a number of limitations due to the toxicity or high catalyst loadings remain to be addressed when employing catalytic conditions. In this sense, several organometallic complexes have been designed and applied to the selective isomerization of epoxides. Particularly, Mazet and co-workers reported the most relevant breakthrough using novel palladium[31] and iridium[32] complexes. However, high temperatures were needed in both cases (Scheme 1.9).

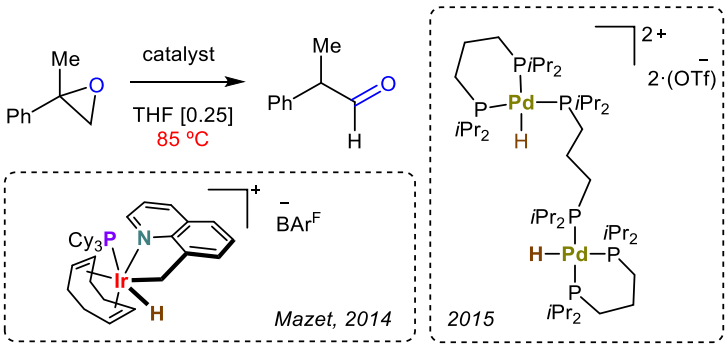

Scheme 1.9. Pd- and Ir-catalyzed selective isomerization of epoxides (*Mazet, 2014-2015*).

Moreover, the Meinwald rearrangement can lead to cascade or tandem reactions, taking advantage of the carbonyl group formed to generate other synthetically useful compounds. For example, Otte and co-workers reported, in 2016, a $B(C_6F_5)_3$-catalyzed tandem Meinwald rearrangement – reductive amination.[33] As result, several β-alkyl amines were synthesized starting for readily available epoxide substrates. However, the scope was limited to the use of anilines.

Therefore, the fourth aim of this doctoral thesis was to find a suitable metal catalyst for the regioselective isomerization of epoxides using mild conditions and to perform a tandem process. The results and discussion are found in **Chapter 5**.

Nitrogenated heterocyclic compounds have also found widespread use, as they are present in multiple drug candidates and key synthetic intermediates. For this reason, studying their both synthesis and reactivity is crucial. There are several synthetic protocols in the literature to afford aziridines in good yields. The reactivity of aziridines is mainly focused in ring opening reactions, ring expansion or 1,3-dipolar cycloadditions. Surprisingly, a general synthetic protocol for the selective isomerization of aziridines, or the aza-version of the Meinwald rearrangement, has received little attention.[34] There were only few works related to this, but lacked of synthetic potential. For example, in 2002, Nakayama and co-workers described the BF_3-promoted aza-pinacol rearrangement of various *N*-tosyl aziridines to give the corresponding *N*-tosyl imines.[35] Later on, in 2003, Ney and co-workers reported a palladium-catalyzed isomerization of monosubstituted *N*-tosyl aziridines to sulfonyl ketimines (Scheme 1.10).[36]

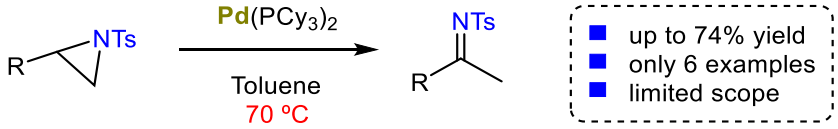

Scheme 1.10. Palladium-catalyzed isomerization of monosubstituted *N*-tosyl aziridines to sulfonyl ketimines (Ney, 2003).

The ring strain, the facility of preparation and the further utility of the potential products make aziridines the ideal substrates to study new catalytic isomerization reactions.

Therefore, and disclosed in the **Chapter 6**, the sixth aim of this doctoral thesis was the discovery of an unprecedented selective isomerization of N-sulfonyl aziridines, to afford synthetically useful organic intermediates that can be further interconverted into valuable compounds.

Finally, another important class of oxygenated heterocyclic compounds are oxetanes,[37] which are four-membered strained rings.

The reactivity of oxetanes is mainly focused on ring-opening and ring-expansion reactions.[38] C-H functionalization of oxetanes has been also reported.[39] However, the selective isomerization of oxetanes still remains a challenge and, to the best of our knowledge, there was no precedent in the literature. Probably, the easy polymerization of oxetanes,[40] has

prevented the scientific community to disclose their isomerization to monomeric compounds.

The following aim of this doctoral thesis, therefore, was the catalyst screening and further reaction optimization for the selective isomerization of 2,2-disubstituted oxetanes, followed by the scope evaluation to find the strengths and weakness of the methodology. This will be detailed in **Chapter 7**.

1.3. Asymmetric Hydrogenation

Metal-catalyzed asymmetric hydrogenation has attracted considerable interest because it is one of the best methods for the preparation of optically active compounds.[41] From an industrial perspective, the direct hydrogenation of unsaturated compounds is a much more desirable process compared to hydrosilylations,[42] transfer-hydrogenation reactions[43] or acid-catalyzed reductions.[44] Moreover, catalytic hydrogenation is an excellent process in terms of atom economy, low catalyst loadings, mild reaction conditions and sustainability.

In the literature, numerous efficient catalytic systems based on Ru, Rh and Ir provide excellent selectivity in the hydrogenation of various prochiral alkenes. However, for some substrates, attaining high (enantio)selectivity remains a challenge. One of these types of substrate are unfunctionalized, or minimally functionalized, olefins.[45] In the absence of a coordinating group, rhodium and ruthenium generally show low reactivity and unsatisfactory enantioselectivity. Thus, their application is restricted to certain class of properly functionalized substrates. However, iridium can overcome these limitations and, in fact, it emerged as an alternative to those metals. In the late ninetees, Pfaltz and co-workers used phosphinooxazoline ligands to design a chiral analogue of Crabtree's catalyst, that showed high enantioselectivities when using prochiral imines. Since then, many iridium-based catalysts bearing chelating P,N donors as stereodirecting ligands were designed,[46] that were able to hydrogenate with high enantioselectivities even in compounds lacking of coordinating groups.

Focusing in minimally functionalized olefins, 1,1-disubstituted olefins containing a neighboring polar group have been successfully hydrogenated in enantioselective manner using iridium-P,N chiral complexes. As shown in Scheme 1.11, Pfaltz, Diéguez and

Andersson pioneered this enantioselective transformation for different substrates, such allylic alcohols, allylic acetates and allylic silanes with excellent results.[47] However, the asymmetric hydrogenation of 1,1-disubstituted allylic amines using iridium catalysis was still undisclosed.

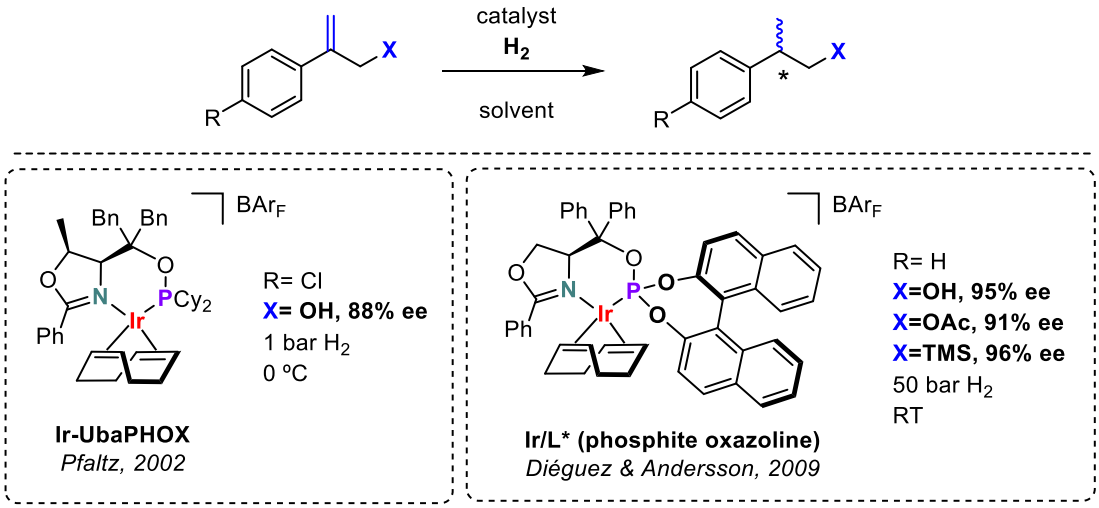

Scheme 1.11. Asymmetric hydrogenation of 1,1-disubstituted terminal olefins containing a neighboring polar group using iridium-P,N chiral complexes.

Many active natural products, pharmaceuticals and agrochemicals contain chiral amines. In this regard, there is considerable interest in developing catalytic methods that provide single enantiomers, thus avoiding the use of inefficient racemate resolutions. Particularly, chiral amines bearing a β-methyl group on the chiral center and their derivatives are key structural elements in a wide variety of bioactive compounds.[48] Some examples are depicted in Figure 1.4.

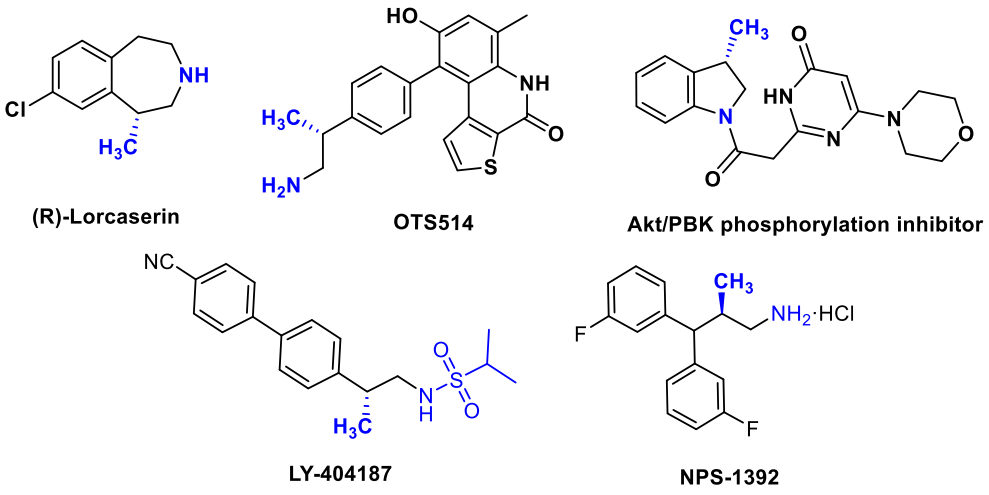

Figure 1.4. Examples of biologically active compounds containing β-methyl chiral amines.

The asymmetric hydrogenation of imines, enamides and allyl amines is a direct strategy to afford enantioenriched compounds containing chiral amines. Whereas the enantioselective hydrogenation of the former ones has been well-established, also employing iridium catalysis, allyl amines remain unexplored. Particularly, and as best of our knowledge, there are scarcely few methods for the asymmetric hydrogenation of terminal 1,1-disubstituted allyl amines. In 2005, Zhang and co-workers reported an efficient method for the asymmetric synthesis of β-methyl chiral amines using a Ru-C_3-TunePhos catalyst with excellent enantioselectivities (67-98% ee),[49] as shown in Scheme 1.12. However, this transformation suffered from some limitations, such: i) harsh conditions: extremely high H_2 pressure for a terminal alkene and heating, ii) long reaction times, iii) the R substituent was limited to alkyl groups. When the substituent was an aryl group, the enantiomeric excess dropped dramatically.

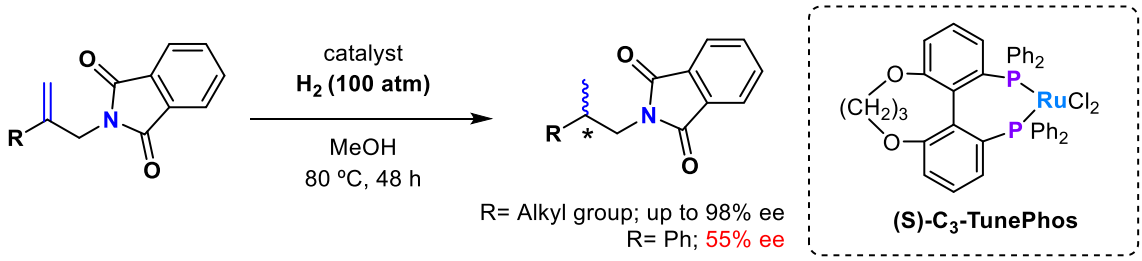

Scheme 1.12. Ru-catalyzed asymmetric hydrogenation of allyl phthalimides (*Zhang, 2005*).

Consequently, the development of new asymmetric methodologies for the catalytic hydrogenation of 2-aryl allyl *N*-protected amines is in high demand. In this sense, our research group envisioned that the highly modular Ir-P,N MaxPHOX family would be suitable catalysts for this transformation to afford enantioenriched products containing chiral amines.

Therefore, in **Chapters 8 and 9**, the last two objectives of this thesis will be presented. The asymmetric hydrogenation of 1,1-disubstituted allyl amines using chiral Ir-P,N complexes, with a particular emphasis to MaxPHOX ligands, has been studied. To showcase the utility of the developed methodology, several bioactive compounds have been synthesized.

References

(1) Anastas, P. T.; Warner, J. C. *Green Chemistry: Theory and Practice*; Oxford University Press: Oxford, **1998**.

(2) Blaser, H.-U.; Federsel, H.-J.; Ed. Asymmetric Catalysis on Industrial Scale: Challenges, Approaches and Solutions; 2 ed.; Wiley-VCH: Weinheim, **2010**.

(3) (a) *Catalytic Asymmetric Synthesis*. (Ed.I. Ojima), Wiley-VCH: Weinheim, **2000**; (b) *Applied Homogeneous Catalysis with Organometallic Compounds*, (Eds.: B. Cornils, W. A. Herrmann), Wiley-VCH: Weinheim, **2002**; (c) S. Akutagawa in Comprehesive Asymmetric Catalysis, Vol. 2 (Eds.: E. N. Jacobsen, A. Pfaltz, H. Yamamoto), Springer, Berlin, 1999, Chapter 23; (d) S. Akutagawa, K. Tani in Catalytic Asymmetric Synthesis, 2nd ed. (Ed.: I. Ojima), Wiley, New York, 2000, pp. 145–161; (e) Noyori, R. Asymmetric Catalysis in Organic Synthesis; Wiley and Sons, Inc.; New York, 1994.

(4) (a) Cristóbal-Lecina, E.; Etayo, P.; Doran, S.; Revés, M.; Martín-Gago, P.; Grabulosa, A.; Costantino, A. R.; Vidal-Ferran, A.; Riera, A.; Verdaguer, X. *Adv. Synth. Catal.* **2014**, *356* (4), 795–804. (b) Salomó, E.; Orgué, S.; Riera, A.; Verdaguer, X. *Synthesis* **2016**, *48* (16), 2659–2663. (c) Prades, A.; Núñez-Pertíñez, S.; Riera, A.; Verdaguer, X. *Chem. Commun.* **2017**, *53* (33), 4605–4608. (d) Salomó, E.; Prades, A.; Riera, A.; Verdaguer, X. *J. Org. Chem.* **2017**, *82* (13), 7065–7069. (e) Téllez, J.; Gallen, A.; Ferrer, J.; Lahoz, F. J.; García-Orduña, P.; Riera, A.; Verdaguer, X.; Carmona, D.; Grabulosa, A. *Dalt. Trans.* **2017**, *46* (45), 15865–15874. (f) Gallen, A.; Orgué, S.; Muller, G.; Escudero-Adán, E. C.; Riera, A.; Verdaguer, X.; Grabulosa, A. *Dalt. Trans.* **2018**, *47* (15), 5366–5379.

(5) (a) Omae, I. *Appl. Organomet. Chem.* **2007**, *21*, 318. (b) Strübing, D.; Beller, M. In *Catalytic Carbonylation Reactions*; Beller, M., Ed.; Springer Berlin Heidelberg: Berlin, Heidelberg, **2006**, 165. (c) Pérez-Castells, J. In *Metal Catalyzed Cascade Reactions*; Müller, T. J. J., Ed.; Springer Berlin Heidelberg: Berlin, Heidelberg, **2006**, 207. (d) Laschat, S.; Becheanu, A.; Bell, T.; Baro, A. *Synlett* **2005**, 2547. (e) Boñaga, L. V. R.; Krafft, M. E. *Tetrahedron* **2004**, *60*, 9795. (f) Rodríguez Rivero, M.; Adrio, J.; Carretero, J. C. *Eur. J. Org. Chem.* **2002**, 2881. (g) Brummond, K. M.; Kent, J. L. *Tetrahedron* **2000**, *56*, 3263. (h) Fletcher, A. J.; Christie, S. D. R. *J. Chem. Soc., Perkin Trans. 1* **2000**, 1657. (h) *The Pauson-Khand Reaction: Scope, Variations and Applications*; Ríos Torres, R. Ed.; Wiley: Chichester, UK., **2012**. (i) Lee, H.-W.; Kwong, F.-Y. *Eur. J. Org. Chem.* **2010**, 789. (j) Blanco-Urgoiti, J.; Anorbe, L.; Perez-Serrano, L.; Dominguez, G.; Perez-Castells, J. *Chem. Soc. Rev.* **2004**, *33*, 32.

(6) (a) Ricker, J. D.; Geary, L. M. *Top. Catal.* **2017**, *60*, 609–619. (b) Jeong, N. In *Comprehensive Organic Synthesis II*; Elsevier: New York, 2014; pp. 1106–1178. (c) Lee, H.-W.; Kwong, F.-Y. *Eur. J. Org. Chem.* **2010**, 789–811. (d) Park, J. H.; Chang, K. M.; Chung, Y. K. *Coord. Chem. Rev.* **2009**, *253*, 2461–2480. (e) Blanco-Urgoiti, J.; Anorbe, L.; Perez-Serrano, L.; Dominguez, G.; Perez-Castells, J. *Chem. Soc. Rev.* **2004**, *33*, 32–42.

(7) Examples of the use of PKR in total synthesis of bioactive compounds, see: (a) Castro, J.; Sorensen, H.; Riera, A.; Morin, C.; Moyano, A.; Pericàs, M. A.; Greene, A. E. *J. Am. Chem. Soc.* **1990**, *112*, 9388-9389. (b) Su, S.; Rodriguez, R. A.; Baran, P. S. *J. Am. Chem. Soc.* **2011**, *133*, 13922–13925. (c) Rodríguez Rivero, M.; De La Rosa, J. C.; Carretero, J. C. *J. Am. Chem. Soc.* **2003**, *125*, 14992–14993.

(8) Bernardes, V.; Kann, N.; Riera, A.; Moyano, A.; Pericàs, M. A.; Greene, A. E. *J. Org. Chem.* **1995**, *60*, 6670-6671.

(9) Aiguabella, N.; Pesquer, A.; Verdaguer, X.; Riera, A. *Org. Lett.* **2013**, *15*, 2696–2699.

(10) Vázquez-Romero, A.; Rodriguez, J.; Lledó, A.; Verdaguer, X.; Riera, A. *Org. Lett.* **2008**, *10*, 4509-4512.

(11) Iqbal, M; Evans, P.; Lledó, A.; Verdaguer, X.; Pericàs, M. A.; Riera, A.; Loeffler, C.; Sinha, A. K.; Mueller, M. J. *ChemBioChem* **2005**, *6*, 276-280.

(12) (a) Solà, J.; Revés, M.; Riera, A.; Verdaguer, X. *Angew. Chem. Int. Ed.* **2007**, *46*, 5020-5023; (b) Revés, M.; Achard, T.; Solà, J.; Riera, A.; Verdaguer, X. *J. Org. Chem.* **2008**, *73*, 7080-7087; (c) Ji, Y.; Riera, A.; Verdaguer, X. *Org. Lett.* **2009**, *11*, 4346-4349.

(13) Cristóbal-Lecina, E.; Constantino, A. R.; Grabulosa, A.; Riera, A.; Verdaguer, X. *Organometallics* **2015**, *34*, 4989-4993.

(14) Fager-Jokela, E.; Muuronen, M.; Khaizourane, H.; Vázquez-Romero, A.; Verdaguer, X.; Riera, A.; Helaja, J. *J. Org. Chem.* **2014**, *79*, 10999–11010.

(15) Su, S.; Rodriguez, R. A.; Baran, P. S. *J. Am. Chem. Soc.* **2011**, *133*, 13922–13925.

(16) Shambayati, S.; Crowe, W. E.; Schreiber, S. L. *Tetrahedron Lett.* **1990**, *31*, 5289-5292; b)

(17) (a) Sung, S.-C. *Antibiotics* **1967**, *1*, 156–165,751. (b) Umezawa, H.; Takeuchi, T.; Nitta, K.; Okami, Y.; Yamamoto, T.; Yamaoka, S. *J. Antibiot.* **1953**, *6*, 147–152; (c) Bickis, I. J.; Creaser, E. H.; Quastel, J. H.; Scholefield, P. G. *Nature* **1957**, *180*, 1109–1111. (d) Amri, H.; Rambaud, M.; Villieras, J. *Tetrahedron Lett.* **1989**, *30*, 7381–7382. (e) Kozikowski, A. P.; Stein, P. D. *J. Am. Chem. Soc.* **1982**, *104*, 4023–4024.

(18) (a) Kar, A.; Argade, N. P. *Synthesis* **2005**, 1234–1236. (b) Cohen, T.; Kosarych, Z.; Suzuki, K.; Yu, L. C. *J. Org. Chem.* **1985**, *50*, 2965–2968. (c) Govindan, S. V; Hudlicky, T.; Koszyk, F. J. *J. Org. Chem.* **1983**, *48*, 3581–3583.

(19) Westmeier, J.; Kress, S.; Pfaff, C.; von Zezschwitz, P. *J. Org. Chem.* **2013**, *78*, 10718–10723.

(20) Orgué, S.; Flores-Gaspar, A.; Biosca, M.; Pàmies, O.; Diéguez, M.; Riera, A.; Verdaguer, X. *Chem. Commun.* **2015**, *51* (99), 17548–17551.

(21) Salomó, E.; Orgue, S.; Riera, A.; Verdaguer, X. *Angew. Chem., Int. Ed.* **2016**, *55*, 7988-7992.

(22) Salomó, E.; Rojo, P.; Hernández-Lladó, P.; Riera, A.; Verdaguer, X. *J. Org. Chem.* **2018**, *83* (8), 4618-4627.

(23) Salomó, E.; Gallen, A.; Sciortino, G.; Ujaque, G.; Grabulosa, A.; Lledós, A.; Riera, A.; Verdaguer, X. *J. Am. Chem. Soc.* **2018**, *140*, 16967-16970.

(24) (a) Inoue, S.; Takaya, H.; Tani, K.; Otsuka, S.; Sato, T.; Noyori, R. *J. Am. Chem. Soc.* **1990**, *112* (12), 4897-4905; (b) Noyori, R.; Takaya, H. *Acc. Chem. Res.* **1990**, *23* (10), 345-350.

(25) (a) Tanaka, K.; Qiao, S.; Tobisu, M.; Lo, M. M.-C.; Fu, G. C. *J. Am. Chem. Soc.* **2000**, *122*, 9870–9871; (b) Tanaka, K.; Fu, G. C. *J. Org.Chem.* **2001**, *66*, 8177–8186. (c) Li, J.-Q.; Peters, B.; Andersson, P. G. *Chem. Eur. J.* **2011**, *17*, 11143–11145. (d) Mantilli, L.; Mazet, C. *Chimia* **2009**, *63*, 35–38; (e) Mantilli, L.; Mazet, C. *Tetrahedron* Lett. **2009**, *50*, 4141–4144. (f) Li, H.; Mazet, C. *Acc. Chem. Res.* **2016**, *49* (6), 1232-1241. (g) Mantilli, L.; Gorard, D.; Torche, S.; Besnard, C.; Mazet, C. *Angew.Chem. Int. Ed.* **2009**, *121*, 5245–5249; *Angew. Chem. Int. Ed.* **2009**, 48, 5143–5147; (h) Mantilli, M.; Mazet, C. *Chem. Commun.* **2010**, *46*, 445–447; (i) Mantilli, L.; Gorard, D.; Torche, S.; Besnard, C.; Mazet, C. *Chem. Eur. J.* **2010**, *16*, 12736–12745.

(26) (a) Paddock, R. L.; Nguyen, S. T. *J. Am. Chem. Soc.*, **2001**, *123*, 11498–11499. (b) Liao, S.; Leutzsch, M.; Monaco, M. R.; List, B. *J. Am. Chem. Soc.*, **2016**, *138*, 5230–5233. (c) Rowley

J. M.; Lobkovsky, E. B.; Coates, G. W. *J. Am. Chem. Soc.*, **2007**, *129*, 4948–4960. (d) Mulzer, M.; Tiegs, B. J.; Wang, Y.; Coates, G. W.; O'Doherty, G. A. *J. Am. Chem. Soc.*, **2014**, *136*, 10814–10820. (e) Gansäuer, A.; Otte, M.; Shi, L. *J. Am. Chem. Soc.*, **2011**, *133*, 416-417. (f) Justicia, J.; Oller-López, J. L.; Campaña, A. G.; Oltra, J. E.; Cuerva, J. M.; Buñuel, E.; Cárdenas, D. J. *J. Am. Chem. Soc.*, **2005**, *127*, 14911–14921. (g) Gansäuer, A.; Otte, M.; Piestert, F.; Fan, C. A. *Tetrahedron*, **2009**, *65*, 4984–4991. (h) Gansäuer, A.; Bluhm, H.; Pierobon, M. *J. Am. Chem. Soc.,* **1998**, *120*, 12849–12859.

(27) Meinwald, J.; Labana, S. S.; Chadha, M. S. *J. Am. Chem. Soc.* **1963**, *85*, 582–585.

(28) Ranu, B. C.; Jana, U. *J. Org. Chem.*, **1998**, *63*, 8212–8216.

(29) Karamé, I.; Tommasino, M. L.; Lemaire, M. *Tetrahedron Lett.* **2003**, *44*, 7687–7689

(30) (a) Robinson, M. W. C.; Pillinger, K. S.; Graham, A. E. *Tetrahedron Lett.,* **2006**, *47*, 5919–5921. (b) Robinson, M. W. C.; Pillinger, K. S.; Mabbett, I.; Timms, D. A.; Graham, A. E. *Tetrahedron*, **2010**, *66*, 8377–8382.

(31) Vyas, D. J.; Larionov, E.; Besnard, C.; Guénée, L.; Mazet, C. *J. Am. Chem. Soc.* **2013**, *135*, 6177–6183.

(32) Humbert, N.; Vyas, D. J.; Besnard, C.; Mazet, C. *Chem. Commun.* **2014**, *50*, 1–4.

(33) Tiddens, M. R.; Klein, J. M.; Otte, M. *Org. Lett.,* **2016**, *18*, 3714–3717.

(34) Zhang, Z. Da; Scheffold, R. *Helv. Chim. Acta* **1993**, *76*, 2602–2615.

(35) Sugihara, Y.; Iimura, S.; Nakayama, J. *Chem. Commun.* **2002**, 134–135.

(36) Wolfe, J. P.; Ney, J. E. *Org. Lett.* **2003**, *5*, 4607–4610.

(37) Bull, J. A.; Croft, R. A.; Davis, O. A.; Doran, R.; Morgan, K. F. *Chem. Rev.* **2016**, *116*, 12150-12233.

(38) (a) Gansäuer, A.; Ndene, N.; Lauterbach, T.; Justicia, J.; Winkler, I.; Mück-Lichtenfeld, C.; Grimme, S. *Tetrahedron* **2008**, *64*, 11839-11845. (b) Thakur, A.; Facer, M. E.; Louie, J. *Angew. Chem. Int. Ed.* **2013**, *52*, 12161-12165. (c) Lo, M. M.-C.; Fu, G. C. *Tetrahedron* **2001**, *57*, 2621-2634.

(39) Ravelli, D.; Zoccolillo, M.; Mella, M.; Fagnoni, M. *Adv. Synth. Catal.* **2014**, *356*, 2781-2786.

(40) Soga, T.; Kudo, H.; Nishikubo, T.; Sato, S. *Polym. J.* **2008**, *40* (9), 832-836.

(41) (a) J. M. Brown. in *Comprehensive Asymmetric Catalysis Vol. I*; (Eds: Jacobsen, E. N., Pfaltz, A., Yamamoto, Y.); Springer: Berlin, 1999. (b) Blaser, H.-U.; Pugin, B.; Spindler, F. *Top. Organomet. Chem.* **2012**, *42*, 65-102. (c) Etayo, P.; Vidal-Ferran, A. *Chem. Soc. Rev.* **2013**, *42*, 728-754. (d) Zhang, Z.; Butt, N. A.; Zhang, W. *Chem. Rev.* **2016**, *116*, 14769-14827. (e) Margarita, C.; Andersson, P. G. *J. Am. Chem. Soc.* **2017**, *139*, 1346-1356.

(42) (a) Nakajima, Y.; Shimada, S. *RSC Adv.* **2015**, *5*, 20603-20616. (b) Chen, J.; Cao, M.; Cheng, B.; Lu, Z. *Synlett* **2015**, *26* (17), 2332-2335.

(43) For selected reviews, see: (a) Wang, C.; Wu, X.; Xiao, J. *Chem. Asian. J.* **2008**, *3*, 1750-1770. (b) Wang, D.; Astruc, D. *Chem. Rev.* **2015**, *115*, 6621-6686. (c) Gladiali, S.; Alberico, E. *Chem. Soc. Rev.* **2006**, *35*, 226-236.

(44) (a) Wakchaure, V. N.; Kaib, P. S. J.; Leutzsch, M.; List, B. *Angew. Chem. Int. Ed.* **2015**, *54*, 11852-11856. (b) Li, G.; Liang, Y.; Antilla, J. C. *J. Am. Chem. Soc.* **2007**, *129* (18), 5830-5831.

(45) (a) Roseblade, S. J.; Pfaltz, A. *Acc. Chem. Res.* **2007**, *40*, 1402–1411. (b) Pàmies, O.; Andersson, P. G.; Diéguez, M. *Chem. Eur. J.* **2010**, *16*, 14232–14240. (c) Woodmansee, D. H.; Pfaltz, A. *Chem. Commun.* **2011**, *47*, 7912–7916. (d) Mazuela, J.; Pàmies, O.; Diéguez, M. *ChemCatChem* **2013**, *5*, 2410–2417. (e) Biosca, M.; Salomo, E.; de la Cruz-Sanchez, P.; Riera, A.; Verdaguer, X.; Pàmies, O.; Diéguez, M. *Org. Lett.* **2019**, *21*, 807-811.

(46) (a) Pfaltz, A.; Blankenstein, J.; Hilgraf, R.; Hörmann, E.; Mcintyre, S.; Menges, F.; Schönleber, M.; Smidt, S. P.; Bettina, W.; Zim-mermann, N. *Adv. Synth. Catal.* **2003**, *345*, 33–43. (b) Verendel, J. J.; Pàmies, O.; Diéguez, M.; Andersson, P. G. *Chem. Rev.* **2014**, *114*, 2130–2169. (c) Müller, M. A.; Gruber, S.; Pfaltz, A. *Adv. Synth. Catal.* **2018**, *360* (7), 1340–1345. (d) Lu, W. J.; Chen, Y. W.; Hou, X. L. *Adv. Synth. Catal.* **2010**, *352* (1), 103–107. (e) Trifonova, A.; Diesen, J. S.; Chapman, C. J.; Andersson, P. G. *Org. Lett.* **2004**, *6* (21), 3825–3827. (f) Li, J.-Q.; Liu, J.; Krajangsri, S.; Chumnanvej, N.; Singh, T.; Andersson, P. G. *ACS Catal.* **2016**, *6* (12), 8342–8349.

(47) (a) Blankenstein, J.; Pfaltz, A. *Angew. Chem. Int. Ed.* **2001**, *40*, 4445–4447. (b) McIntyre, S.; Hörmann, E.; Menges, F.; Smidt, S. P.; Pfaltz, A. *Adv. Synth. Catal.* **2005**, *347* (2–3), 282–288; (c) Mazuela, J.; Verendel, J. J.; Coll, M.; Bo, A.; Marcel, C. *J. Am. Chem. Soc.* **2009**, *131*, 12344–12353.

(48) Chiral amines with β-stereogenic centres: (a) Davies, H. M. L.; Ni, A. *Chem. Commun.* **2006**, 3110–3112. (b) Iii, R. N. H.; Stabler, R. S.; Repke, D. B.; Kress, J. M.; Walker, K. A.; Martin, R. S.; Brothers, J. M.; Ilnicka, M.; Lee, S. W.; Mirzadegan, T. *Bioorg. Med. Chem. Lett.* **2010**, *20* (11), 3436–3440. (c) Ramesh, P.; Suman, D. *Synlett* **2018**, *50*, 211–226. (d) Omura, S. Macrolide Antibiotics, Academic Press, Orlando, FL, 1984. (e) Lazarevski, G.; Kobrehel, G.; Metelko, B.; Duddeck, H. *J. Antibiot.* **1996**, *49*, 1066-1069.

(49) Wang, C. J.; Sun, X.; Zhang, X. *Angew. Chem., Int. Ed.* **2005**, *44*, 4933–4935.

Chapter 2

Ethylene Glycol Assisted Intermolecular Pauson-Khand Reaction

The Pauson-Khand reaction (PKR)[1] is one of the few direct methods to synthesize five-membered ring carbocycles from acyclic precursors. When executed in an intramolecular fashion, this cobalt-mediated [2+2+1] cyclization is an extremely efficient way to build up complex cyclopentane polycycles.[1,2] The intermolecular PKR has found more limited use due to the narrow scope of the alkene. In fact, only strained olefins, such as norbornadiene or cyclopropene[3] or highly unhindered alkenes such as ethylene[4] gave high yields. However, the intermolecular version has a great potential since it allows cyclopentenones to be built up from very simple starting materials, namely an alkene, an alkyne and carbon monoxide.[5]

During recent decades, much efforts has been devoted enhancing the yields of this reaction using a variety of promoters or additives.[6] In 1990, Schreiber and co-workers discovered that the PKR, which was typically performed at high temperatures (60-110 ℃), could also be promoted using *N*-oxides[7] such as *N*-methylmorpholine-*N*-oxide (NMO) in methylene chloride.[8] These conditions allowed the reaction to take place at room temperature and often gave better yields.[9]

In 2011, Baran and co-workers reported the total syntheses of (±)-Axinellamines A and B.[10] The starting material of these synthesis was a cyclopentenone prepared by an intermolecular PKR using 1,4-bis((trimethylsilyl)oxy)-2-butene (Scheme 2.1). The success of the PKR with this unstrained olefin was possible only when using NMO as promoter and adding monoethylene glycol (MEG)[11] and 4Å MS to the reaction. Under these conditions, a remarkable 46–58% yield was obtained (without MEG, yields dropped to 15–25%). Although Baran and co-workers stated that ethylene glycol was an essential additive, to the best of our knowledge, these conditions have not been used in any other PKR reported to date. We envisioned that, using this novel methodology, other olefins might give better yields and therefore a wider range of alkenes could be used.

Here we studied the role that ethylene glycol displays in the stoichiometric *N*-oxide promoted intermolecular PKR. We have tested the effect of Baran's conditions when performing the reaction with strained alkenes such as norbornadiene, poorly reactive cyclopentenes[12] and several ethylene synthetic equivalents.[13]

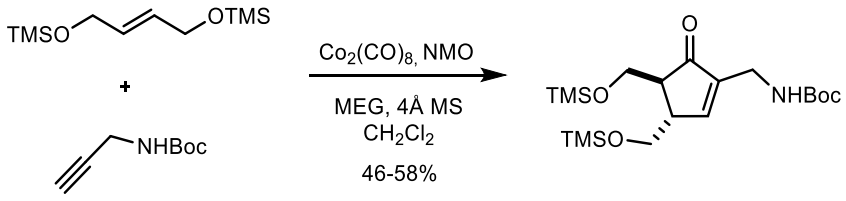

Scheme 2.1. Ethylene glycol-assisted intermolecular PKR used in Baran's synthesis of Axinellamines.

We first tested the new protocol with norbornadiene (NBD) which is the most relevant alkene substrate in intermolecular PKR. We observed that in all cases, the yields using ethylene glycol and molecular sieves (MS) as additives were substantially higher (entries 2, 4, 6 and 8; table 2.1). The reaction is usually steroselective affording the *exo* adduct as the major stereoisomer. In the case of the reactions with ethylene glycol, the stereoselectivity towards the *exo* further increased slightly. The presence of ethylene glycol lowered the reaction rate and sometimes more than 6 equivalents of NMO were needed to complete the reaction. The reaction crudes using Baran's conditions were easier to work-up because the ethylene glycol trapped the cobalt by-products, thus affording a cleaner crude.

Table 2.1. Intermolecular Pauson-Khand reactions of terminal and internal alkynehexacarbonyldicobalt complexes with norbornadiene. The reactions were performed in CH_2Cl_2. 6-10 equiv. of NMO was added in one portion.

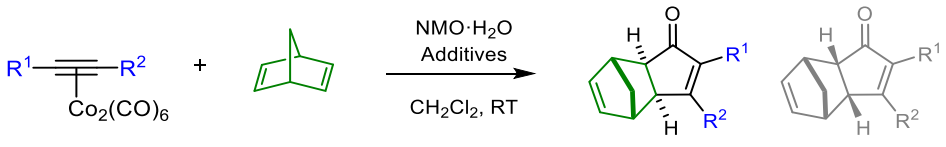

2-1a-d **2-*exo*-2a-d** **2-*endo*-2a-d**

entry	R^1	R^2	Alkyne	Additives	Time (h)	Product	Yield (%)	*exo*: *endo*
1	CH_2SPh	H	**2-1a**	-	4	**2-2a**	8	>99
2	CH_2SPh	H	**2-1a**	MEG, 4Å MS	17	**2-2a**	51	>99
3	CH_2NHBoc	H	**2-1b**	-	17	**2-2b**	65	91:9
4	CH_2NHBoc	H	**2-1b**	MEG, 4Å MS	24	**2-2b**	85	93:7
5	TMS	H	**2-1c**	-	2	**2-2c**	72	96:4
6	TMS	H	**2-1c**	MEG, 4Å MS	48-72	**2-2c**	89	98:2
7	*n*-$(CH_2)_2CH_3$	CH_2OTBS	**2-1d**	-	24	**2-2d**	79	99:1
8	*n*-$(CH_2)_2CH_3$	CH_2OTBS	**2-1d**	MEG, 4Å MS	48-72	**2-2d**	95	99:1

Another type of strained alkenes that showed satisfactory reactivity in the intermolecular PKR were medium-sized *trans*-cycloalkenes.[14] The PKR of these alkenes offered a modular, regioselective and straightforward entry to *trans* fused [n.3.0] bicylic scaffolds.[15] In general, good to excellent yields were achieved using few equivalents of alkene and NMO as promoter. However, when using protected propargylic alcohols such as **2-1e** the yield of the corresponding cyclopentenone dropped. We have found that under Baran's protocol the yield of **2-3e** increased from 38 to 60% as shown in Table 2.2.

Table 2.2. Comparative study of the intermolecular Pauson-Khand reaction using terminal alkyne **2-1e** with *trans*-cyclooctene.

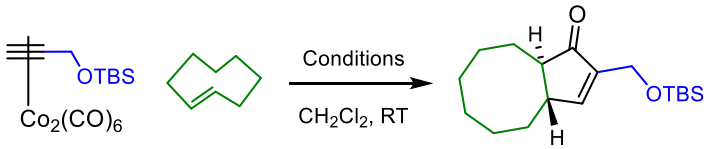

2-1e **2-3e**

Entry	Alkyne	Conditions	Product	Yield (%)
1	**2-1e**	0 °C to RT, 2h, 6 equiv. NMO	**2-3e**	38[14]
2	**2-1e**	48 h, 10 equiv. NMO, MEG-4Å MS	**2-3e**	60

Ethylene (**2-4**) is a useful alkene in intermolecular PKR. It has been used in the synthesis of Taylorione[13] and Phytoprostanes B1,[16] among others.[17] Its main drawbacks are the need of the equipment to manipulate a gas and its relatively low solubility. The later issue can be improved by adding molecular sieves[18] and/or by slowly adding NMO. Thermal activation or other promoters usually worsened the reaction yields. Several alternatives to the use of ethylene gas have been described. For example, the use of supercritical ethylene was applied in the twofold PKR of cyclic diynes[19] or in a catalytic version of the intermolecular PKR.[20] In 1999, W. J. Kerr and P. L. Pauson[13] reported the use of vinyl esters such as vinyl benzoate (**2-5**) as ethylene surrogates in the PKR (Table 2.3). Therefore, we tested Baran's protocol on several ethylene equivalents as alkenes.

Terminal alkynes **2-1b-c** were reacted with ethylene under the standard *N*-oxide promoted PKR conditions (Table 2.3). For the sake of comparison, we used the standard protocol with vinyl benzoate adding NMO in a single portion. Under these conditions the corresponding cyclopentenones **2-7b,c** were obtained in significantly lower yields than with ethylene. However, when using vinyl benzoate in the presence of ethylene glycol and 4Å MS as additives, also adding NMO in a single portion, the yields recovered or were higher than those achieved with ethylene. We also attempted, for the first time, the use of vinyl

trimethylsilane (**2-6**) as ethylene surrogate (entries 4 and 12). Olefin **2-6** showed good reactivity under these conditions, and the yields were comparable to those obtained with vinyl benzoate. However, a treatment with fluoride to cleave the silylated cyclopentenones was required.

Again, using Baran's conditions the work-up was much cleaner and all cobalt residues were easily removed by a simple decantation. In terms of reactivity, vinyl benzoate proved to be the most useful ethylene equivalent. The yields were comparable to those achieved with ethylene, and in some cases even improved (entries 3, 9 and 11). The presence of additives did not affect the C-O cleavage to take place, which still occurred spontaneously.

Table 2.3. Intermolecular Pauson-Khand reactions of internal alkynehexacarbonyldicobalt complexes with ethylene and ethylene equivalents. The reactions were performed in CH_2Cl_2. 6 equiv. of NMO was added in one portion.

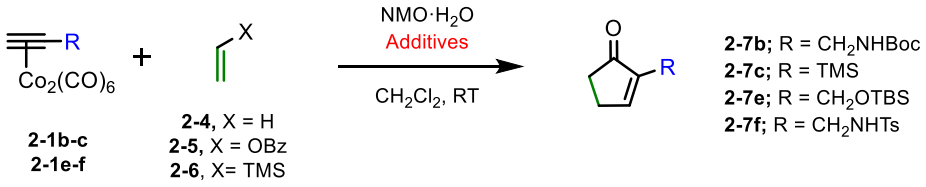

Entry	R	Alkyne	X	Alkene	Additives	Time (h)	Product	Yield (%)
1	-CH_2NHBoc	**2-1b**	H	**2-4**	-	4	**2-7b**	63
2	-CH_2NHBoc	**2-1b**	OBz	**2-5**	-	5	**2-7b**	36
3	-CH_2NHBoc	**2-1b**	OBz	**2-5**	MEG, 4Å MS	17	**2-7b**	67
4[a]	-CH_2NHBoc	**2-1b**	TMS	**2-6**	MEG, 4Å MS	17	**2-7b**	57
5	TMS	**2-1c**	H	**2-4**	-	4	**2-7c**	67
6	TMS	**2-1c**	OBz	**2-5**	-	5	**2-7c**	15
7	TMS	**2-1c**	OBz	**2-5**	MEG, 4Å MS	24	**2-7c**	43
8	-CH_2OTBS	**2-1e**	H	**2-4**	-	3	**2-7e**	20
9	-CH_2OTBS	**2-1e**	OBz	**2-5**	MEG, 4Å MS	17	**2-7e**	40
10	-CH_2NHTs	**2-1f**	OBz	**2-4**	-	5	**2-7f**	54
11	-CH_2NHTs	**2-1f**	OBz	**2-5**	MEG, 4Å MS	17	**2-7f**	72
12[a]	-CH_2NHTs	**2-1f**	TMS	**2-6**	MEG, 4Å MS	17	**2-7f**	64

[a] Once finished, the reaction was quenched with catalytic amount of HF·pyr.

Ethylene glycol can help to extend the scope of alkynes available for this transformation. In this regard, when internal alkynes are used in the intermolecular PKR reactivity decreases. To the best of our knowledge, there is no precedent in which internal alkynes have been used to synthesize α,β-substituted cyclopentenones *via* regioselective[21] PKR with ethylene

surrogates. We observed (Table 2.4) that when using ethylene equivalents with Baran's protocol, reaction yields were comparable to those obtained with ethylene in most cases (entries 5, 9 and 11). Only for the one bearing an alkyl chain, the reactivity decreased considerably (entry 2).

Table 2.4. Intermolecular Pauson-Khand reactions of internal alkynehexacarbonyldicobalt complexes with ethylene and ethylene equivalents. The reactions were performed in CH_2Cl_2. 6-10 equiv. of NMO was added.

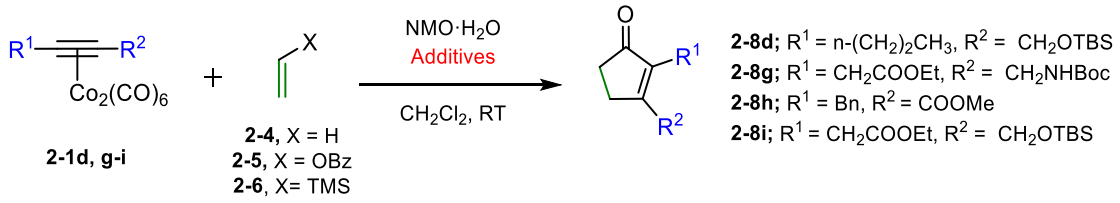

Entry	R^1	R^2	Alkyne	X	Alkene	Additives	Time (h)	8	Yield (%)
1	-$(CH_2)_2CH_3$	-CH_2OTBS	**2-1d**	H	**2-4**	-	5	**2-8d**	65
2	-$(CH_2)_2CH_3$	-CH_2OTBS	**2-1d**	OBz	**2-5**	MEG, 4Å MS	36	**2-8d**	12
3	-CH_2COOEt	-CH_2NHBoc	**2-1g**	H	**2-4**		4	**2-8g**	75
4	-CH_2COOEt	-CH_2NHBoc	**2-1g**	OBz	**2-5**		5	**2-8g**	20
5	-CH_2COOEt	-CH_2NHBoc	**2-1g**	OBz	**2-5**	MEG, 4Å MS	17	**2-8g**	64
6[a]	-CH_2COOEt	-CH_2NHBoc	**2-1g**	TMS	**2-6**	MEG, 4Å MS	17	**2-8g**	56
7	-CH_2Ph	-COOMe	**2-1h**	H	**2-4**	-	4	**2-8h**	57
8	-CH_2Ph	-COOMe	**2-1h**	OBz	**2-5**	-	5	**2-8h**	11
9	-CH_2Ph	-COOMe	**2-1h**	OBz	**2-5**	MEG, 4Å MS	24	**2-8h**	46
10	-CH_2COOEt	-CH_2OTBS	**2-1i**	H	**2-4**	-	4	**2-8i**	53
11	-CH_2COOEt	-CH_2OTBS	**2-1i**	OBz	**2-5**	MEG, 4Å MS	17	**2-8i**	49
12[a]	-CH_2COOEt	-CH_2OTBS	**2-1i**	TMS	**2-6**	MEG, 4Å MS	17	**2-8i**	43

[a] Once finished, the reaction was quenched with catalytic amount of HF·pyr

Finally, we sought to explore the effect of Baran's conditions when using other alkenes such as cyclopentene (**2-9**) or 2,3-dihydrofuran (**2-10**), which are poorly reactive and less common in PKR. *N*-Boc propargylamine and trimethylsilyl acetylene complexes (**2-1b** and **2-1c**) were selected due to their synthetic importance.[22] Using ethylene glycol as additive, the yields of N-oxide-promoted cyclizations of cyclopentene, doubled those achieved when using the standard protocol or when 4Å MS was the only additive (Table 2.5). The reaction

using of 2,3-dihydrofuran afforded the products with the biggest yield increase and with completely regioselectivity (Table 2.6).

Table 2.5. Comparative study of the intermolecular Pauson-Khand reaction using terminal alkynes and cyclopentene.

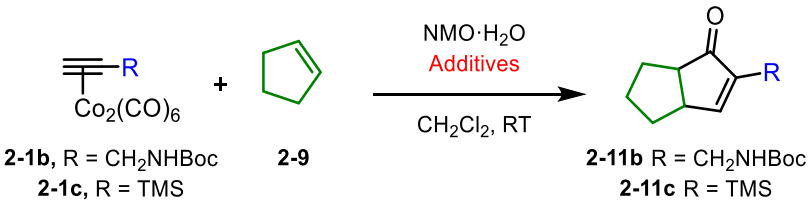

2-1b, R = CH_2NHBoc **2-1c**, R = TMS — **2-9** — **2-11b** R = CH_2NHBoc **2-11c** R = TMS

Entry	Alkyne	Additives	Time (h)	Prod.	Yield (%)
1	**2-1b**	-	3	**2-11b**	35
2	**2-1b**	4Å MS	3	**2-11b**	37
3	**2-1b**	MEG, 4Å MS	5	**2-11b**	60
4	**2-1c**	-	4	**2-11c**	16
5	**2-1c**	4Å MS	4	**2-11c**	14
6	**2-1c**	MEG, 4Å MS	48-72	**2-11c**	31

[a] The reactions were performed in CH_2Cl_2. NMO (6 equiv.) was added in one portion.

Table 2.6. Comparative study of the intermolecular Pauson-Khand reaction using terminal alkynes and 2,3-dihydrofuran.

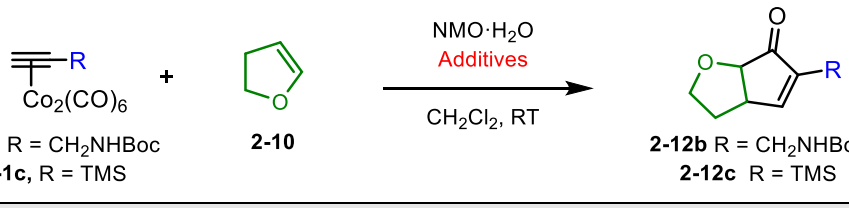

2-1b, R = CH_2NHBoc **2-1c**, R = TMS — **2-10** — **2-12b** R = CH_2NHBoc **2-12c** R = TMS

Entry	Alkyne	Additives	Time (h)	Prod.	Yield (%)
1	**2-1b**	-	17	**2-12b**	40
2	**2-1b**	MEG, 4Å MS	36	**2-12b**	57
3	**2-1c**	-	4	**2-12c**	21
4	**2-1c**	MEG, 4Å MS	24	**2-12c**	82

[a] The reactions were performed in CH_2Cl_2. NMO (6 equiv.) was added in one portion.

In conclusion, we have shown that the use of ethylene glycol as additive consistently improves the *N*-oxide-promoted intermolecular PKR in terms of yield, stereoselectivity and practicality. When using norbornadiene as alkene, which is the most reactive alkene in the intermolecular PKR, a slight increase in both yield and stereoselectivity was observed. Using ethylene surrogates such as vinyl benzoate and vinyltrimethylsilane, we obtained the corresponding cyclopentenones with similar yields that those achieved with ethylene gas. The greatest advantage was found when using less activated alkenes such as cyclopentene or 2,3-dihydrofuran. This methodology greatly facilitates the work-up of the reactions because the ethylene glycol absorbs the cobalt by-products. Moreover, since the reaction rate decreases, the addition of the *N*-oxide promoter can be done in a single portion. We believe that the

main effect of ethylene glycol is to stabilize the unsaturated cobalt complexes that are the key intermediates of the PKR. This new protocol may help to address one of the most important drawbacks of the intermolecular PKR, namely the limited range of reactive alkenes.

References

(1) (a) Omae, I. *Appl. Organomet. Chem.* **2007**, *21*, 318. (b) Strübing, D.; Beller, M. In *Catalytic Carbonylation Reactions*; Beller, M., Ed.; Springer Berlin Heidelberg: Berlin, Heidelberg, **2006**, 165. (c) Pérez-Castells, J. In *Metal Catalyzed Cascade Reactions*; Müller, T. J. J., Ed.; Springer Berlin Heidelberg: Berlin, Heidelberg, **2006**, 207. (d) Laschat, S.; Becheanu, A.; Bell, T.; Baro, A. *Synlett* **2005**, 2547. (e) Boñaga, L. V. R.; Krafft, M. E. *Tetrahedron* **2004**, *60*, 9795. (f) Rodríguez Rivero, M.; Adrio, J.; Carretero, J. C. *Eur. J. Org. Chem.* **2002**, 2881. (g) Brummond, K. M.; Kent, J. L. *Tetrahedron* **2000**, *56*, 3263. (h) Fletcher, A. J.; Christie, S. D. R. *J. Chem. Soc., Perkin Trans. 1* **2000**, 1657.

(2) (a) Chuang, K. V; Xu, C.; Reisman, S. E. *Science,* **2016**, *353*, 912–915. (b) Verdaguer, X. *Science* **2016**, *353*, 866. (c) Gibson, S. E.; Mainolfi, N. *Angew. Chem. Int. Ed.* **2005**, *44*, 3022.

(3) Marchueta, I.; Verdaguer, X.; Moyano, A.; Pericàs, M. A.; Riera, A. *Org. Lett.* **2001**, *3*, 3193.

(4) Other Pauson–Khand reactions with ethylene: a) Donker-Voort, J. G.; Gordon, A. R.; Johnstone, W. C.; Kerr, J.; Lange, U. *Tetrahedron* **1996**, *52*, 7391; b) Gordon, A. R.; Johnstone, C. W.; Kerr, J. *Synlett* **1995**, 1083; c) Rautenstrauch, V.; Megard, P.; Conesa, J.; Kuester, W. *Angew. Chem. Int. Ed. Engl.* **1990**, *29*, 1413.

(5) (a) *The Pauson-Khand Reaction: Scope, Variations and Applications*; Ríos Torres, R. Ed.; Wiley: Chichester, UK., **2012**. (b) Lee, H.-W.; Kwong, F.-Y. *Eur. J. Org. Chem.* **2010**, 789. (c) Blanco-Urgoiti, J.; Anorbe, L.; Perez-Serrano, L.; Dominguez, G.; Perez-Castells, J. *Chem. Soc. Rev.* **2004**, *33*, 32.

(6) To see other additives tried in the intermolecular PKR see: (a) Wang, Y.; Xu, L.; Yu, R.; Chen, J.; Yang, Z. *Chem. Commun.* **2012**, *48*, 8183. (b) Gibson, S. E.; Johnstone, C.; Stevenazzi, A. *Tetrahedron* **2002**, *58*, 4937. (c) Hayashi, M.; Hashimoto, Y.; Yamamoto, Y.; Usuki, J.; Saigo, K. *Angew. Chem. Int. Ed.* **2000**, *39*, 631. (d) Sugihara, T.; Yamaguchi, M. *Synlett* **1998**, 1384. (e) Jeong, N.; Hwang, S. H.; Lee, Y.; Chung, Y. K. *J. Am. Chem. Soc.* **1994**, *116*, 3159

(7) (a) Kerr, W. J.; McLaughlin, M. J.; Pauson, P. L.; Robertson, S. M. *J. Organomet. Chem.* **2001**, *630*, 104. (b) Jeong, N.; Chung, Y. K.; Lee, B. Y.; Lee, S. H.; Yoo, S.-E. *Synlett* **1991**, *1991*, 204.

(8) Shambayani, S.; Crowe, W. E.; Schreiber, S. L. *Tetrahedron Lett.* **1990**, *31*, 5289.

(9) Hay, A. M.; Kerr, W. J.; Kirk, G. G.; Middlemiss, D. *Organometallics* **1995**, *14*, 4986.

(10) Su, S.; Rodriguez, R. A.; Baran, P. S. *J. Am. Chem. Soc.* **2011**, *133*, 13922.

(11) To see other examples of MEG as cobalt NPs stabilizer, see: Muller, J.-L.; Klankermayer, J.; Leitner, W. *Chem. Commun.* **2007**, 1939.

(12) (a) Ford, J. G.; Kerr, W. J.; Kirk, G. G.; Lindsay, D. M.; Middlemiss, D. *Synlett* **2000**, *10*, 1415. (b) Kerr, W. J.; Lindsay, D. M.; Watson, S. P. *Chem. Commun.* **1999**, 2551.

(13) (a) Kerr, W. J.; McLaughlin, M.; Pauson, P. L.; Robertson, S. M. *J. Organomet. Chem.* **2001**, *630*, 104. (b) Kerr, W. J.; McLaughlin, M.; L. Pauson, P.; M. Robertson, S. *Chem. Commun.* **1999**, 2171.

(14) Lledo, A.; Fuster, A.; Reves, M.; Verdaguer, X.; Riera, A. *Chem. Commun.* **2013**, *49*, 3055.

(15) This system is typically accessed by indirect routes involving ring expansion reactions: (a) Fan, X.; Zhuo, L.-G.; Tu, Y. Q.; Yu, Z.-X. *Tetrahedron* **2009**, *65*, 4709. (b) Shinohara, I.; Nagaoka, H. *Tetrahedron Lett.* **2004**, *45*, 1495. (c) Roxburgh, C. J. *Tetrahedron* **1993**, *49*, 10749.

(16) (a) Vázquez-Romero, A.; Verdaguer, X.; Riera, A. *Eur. J. Org. Chem.* **2013**, 1716. (b) Vázquez-Romero, A.; Cárdenas, L.; Blasi, E.; Verdaguer, X.; Riera, A. *Org. Lett.* **2009**, *11*, 3104.

(17) (a) Jahn, U.; Galano, J.-M.; Durand, T. *Angew. Chem. Int. Ed.* **2008**, *47*, 5894. (b) Das, U. N. *Biotechnol. J.* **2006**, *1*, 420. (c) Marks, F.; Fürstenberger, G. *Prostaglandins, Leukotrienes and other Eicosanoids*; Wiley-VCHG.; Weinheim, **1999**. (d) Rokach, J.; Khanapure, S. P.; Hwang, S.-W.; Adiyaman, M.; Lawson, J. A.; FitzGerald, G. A. *Prostaglandins* **1997**, *54*, 823.

(18) (a) Blanco-Urgoiti, J.; Casarrubios, L.; Domínguez, G.; Pérez-Castells, J. *Tetrahedron Lett.* **2002**, *43*, 5763. (b) Pérez-Serrano, L.; Casarrubios, L.; Domínguez, G.; Pérez-Castells, J. *Org. Lett.* **1999**, *1*, 1187.
(19) Rausch, B. J.; Becker, H.; Gleiter, R.; Rominger, F. *Synlett* **2002**, 723.
(20) Jeong, N.; Hwang, S. H. *Angew. Chem. Int. Ed.* **2000**, *39*, 636.
(21) Fager-Jokela, E.; Muuronen, M.; Khaizourane, H.; Vázquez-Romero, A.; Verdaguer, X.; Riera, A.; Helaja, J. *J. Org. Chem.* **2014**, *79*, 10999.
(22) (a) Aiguabella, N.; Pesquer, A.; Verdaguer, X.; Riera, A. *Org. Lett.* **2013**, *15*, 2696. (b) Vázquez-Romero, A.; Rodríguez, J.; Lledó, A.; Verdaguer, X.; Riera, A. *Org. Lett.* **2008**, *10*, 4509. (c) Shih, C.; Fritzen, E. L.; Swenton, J. S. *J. Org. Chem.* **1980**, *45*, 4462.
(23) Iqbal, M.; Li, Y.; Evans, P. *Tetrahedron* **2004**, *60*, 2531.
(24) Bonazzi, S.; Binaghi, M.; Fellay, C.; Wach, J.-Y.; Gademann, K. *Synthesis* **2010**, 631.

Experimental Section

Reactions were carried out under N_2 in vials or round-bottomed flasks previously oven-dried. CH_2Cl_2 was degassed and dried with a solvent purification system (SPS PS-MD-3). Reactions were monitored by TLC analysis using Merck silica gel 60 F-254 thin layer plates. Solvents were removed under reduced pressure with a rotary evaporator. Silica gel chromatography was performed using an automated chromatography system (PuriFlash® 430, Interchim). NMR spectra were run at 400 MHz for ^1H and at 101 MHz for ^{13}C. Chemical shifts (δ) are given in ppm and referenced to internal solvent resonances and reported relative to TMS (tetramethylsilane). The coupling constants (*J*) are reported in Hertz (Hz). High-resolution mass spectra (ESI) were recorded on a LC/MSD-TOF G1969A (Agilent Technologies).

General procedure for the intermolecular Pauson-Khand Reaction using the standard protocol.

Method A. The corresponding hexacarbonyl dicobalt complex (1.0 equiv.) was dissolved in anhydrous CH_2Cl_2 (11 mL/mmol complex) and charged to a vial which was previously purged with nitrogen. Alkene (5.0 equiv.; otherwise indicated) was then added. The reaction was stirred 10 minutes. A solution of NMO (6 equiv.; otherwise indicated) in anhydrous CH_2Cl_2 was added in a single portion. The reaction was monitored by TLC until no cobalt complex was observed. Then, the crude was filtered through a plug of SiO_2 and washed with CH_2Cl_2 (x3). The solvent was concentrated under vacuum and the crude was purified by column chromatography on SiO_2 using mixtures of hexanes/AcOEt of increasing polarities.

General procedures for the ethylene glycol-assisted intermolecular Pauson-Khand Reaction

Method B. The corresponding hexacarbonyl dicobalt complex (1.0 equiv.) was dissolved in anhydrous CH_2Cl_2 (11 mL/mmol complex) and charged to a vial containing 4Å MS (317 mg/mmol complex), which was previously purged with nitrogen. Alkene (5.0 equiv.; otherwise indicated) and ethylene glycol (1.7 mL/mmol complex) were then added. The reaction was stirred 10 minutes. A solution of NMO (6 equiv.; otherwise indicated) in anhydrous CH_2Cl_2 was added in a single portion. The reaction was monitored by TLC until no cobalt complex was observed. Then, the crude was filtered through a plug of neutral Al_2O_3 and washed with CH_2Cl_2 (x3). The solvent was concentrated under vacuum and the crude was purified by column chromatography on SiO_2 using mixtures of hexanes/AcOEt of increasing polarities.

Method C. The corresponding hexacarbonyl dicobalt complex (1.0 equiv.) was dissolved in anhydrous CH_2Cl_2 (11 mL/mmol complex) and charged to a vial containing 4Å MS (317 mg/mmol complex), which was previously purged with nitrogen. Vinyltrimethylsilane (5.0 equiv.) and ethylene glycol (1.7 mL/mmol complex) were then added. The reaction was stirred 10 minutes. A solution of NMO (6 equiv.; otherwise indicated) in anhydrous CH_2Cl_2 was added in a single portion. The reaction was monitored by TLC until no cobalt complex was observed. Once finished, the reaction was quenched with catalytic amount of HF·pyridine and it was stirred 10 minutes. Afterwards, the mixture was quickly filtered by a short plug of neutral Al_2O_3. The solvent was concentrated under vacuum and the crude was purified by column chromatography on SiO_2 using mixtures of hexanes/AcOEt of increasing polarities.

(3aR,4S,7R,7aR)-2-((Phenylthio)methyl)-3a,4,7,7a-tetrahydro-1H-4,7-methanoinden-1-one, 2-2a.

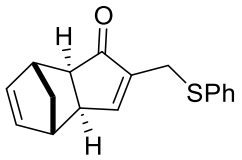

Starting from 0.33 mmol of Co complex **2-1a**. Isolated yield. Method A: 7 mg, 8%; Method B: 46 mg, 51% (off white solid). **^{1}H NMR** (400 MHz, $CDCl_3$) δ 7.33 – 7.21 (m, 5H), 7.20 – 7.14 (m, 1H), 6.24 (dd, *J* = 5.6, 3.1 Hz, 1H), 6.18 (dd, *J* = 5.6, 3.0 Hz, 1H), 3.74 – 3.58 (m, 2H), 2.91 (p, *J* = 1.4 Hz, 1H), 2.68 (dhept, *J* = 5.4, 1.3 Hz, 1H), 2.57 (dt, *J* = 2.9, 1.5 Hz, 1H), 2.31 (dt, *J* = 5.0, 1.4 Hz, 1H), 1.30 (dp, *J* = 9.4, 1.6 Hz, 1H), 1.07 (dd, *J* = 9.4, 1.6 Hz, 1H). The analytical data for this compound were in excellent agreement with the reported.[22a]

***Tert*-butyl (((3aR,4S,7R,7aR)-1-oxo-3a,4,7,7a-tetrahydro-1H-4,7-methanoinden-2-yl)methyl)carbamate, 2-2b.**

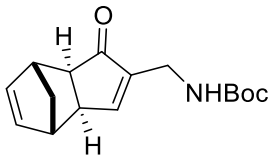

Starting from 0.30 mmol of Co complex **2-1b**. Isolated yield. Method A: 54 mg, 65%; Method B: 70 mg, 85% (off white solid). **^{1}H NMR** (400 MHz, $CDCl_3$) δ 7.33 (d, *J* = 2.6 Hz, 1H), 6.27 (dd, *J* = 5.6, 3.1 Hz, 1H), 6.18 (dd, *J* = 5.6, 3.0 Hz, 1H), 5.04 (br s, 1H), 3.85 (t, *J* = 6.5 Hz, 2H), 2.89 (t, *J* = 1.8 Hz, 1H), 2.74 (ddp, *J* = 5.3, 2.6, 1.3 Hz, 1H), 2.70 – 2.65 (m, 1H), 2.29 (dt, *J* = 5.1, 1.4 Hz, 1H), 1.41 (s, 9H), 1.38 – 1.33 (m, 1H), 1.21 – 1.16 (m, 1H). The analytical data for this compound were in excellent agreement with the reported data.[22a]

(3aS,4S,7R,7aR)-2-(Trimethylsilyl)-3a,4,7,7a-tetrahydro-1H-4,7-methanoinden-1-one, 2-2c.

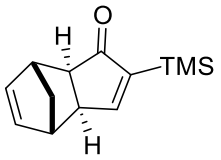

Starting from 0.36 mmol of Co complex **2-1c**. Isolated yield. Method A: 69 mg, 72%; Method B: 53 mg, 89% (white solid). **^{1}H NMR** (400 MHz, $CDCl_3$) δ 7.59 (d, *J* = 2.5 Hz, 1H), 6.27 (dd, *J* = 5.7, 3.1 Hz, 1H), 6.20 (dd, *J* = 5.6, 3.0 Hz, 1H), 2.91 (d, *J* = 2.8 Hz, 1H), 2.83 (s, 1H), 2.69 (s, 1H), 2.28 (d, *J* = 5.2 Hz, 1H), 1.37 (d, *J* = 9.3 Hz, 1H), 1.19 (d, *J* = 9.3 Hz, 1H), 0.17 (s, 9H). The analytical data for this compound were in excellent agreement with the reported data.[23]

(3aS,4S,7R,7aR)-3-(((*Tert*-butyldimethylsilyl)oxy)methyl)-2-propyl-3a,4,7,7a-tetrahydro-1H-4,7-methanoinden-1-one, 2-2d.

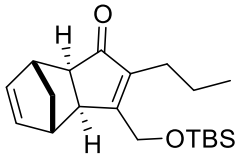

Starting from 0.27 mmol of Co complex **2-1d**. Isolated yield. Method A: 69 mg, 79%; Method B: 84 mg, 95% (off white solid). 10 equiv. of NMO were used in both cases. **^{1}H NMR** (400 MHz, $CDCl_3$) δ 6.19 (dd, *J* = 5.6, 3.1 Hz, 1H), 6.12 (dd, *J* = 5.6, 2.9 Hz, 1H), 4.51 (d, *J* = 15.1 Hz, 1H), 4.41 (dd, *J* = 15.1, 1.0 Hz, 1H), 2.83 (dd, *J* = 3.0, 1.6 Hz, 1H), 2.81 – 2.75 (m, 2H), 2.19 (dd, *J* = 5.2, 1.5 Hz, 1H), 2.13 – 2.08 (m, 1H), 2.02 (dt, *J* = 7.5, 6.2 Hz, 1^{i}H), 1.37 – 1.26 (m, 3H), 1.10 (dtd, *J* = 9.2, 1.4,

0.7 Hz, 1H), 0.87 (s, 9H), 0.80 (d, *J* = 7.3 Hz, 3H), 0.04 (s, 6H). The analytical data for this compound were in excellent agreement with the reported.[21]

(3aS,9aR)-2-(((tert-butyldimethylsilyl)oxy)methyl)-3a,4,5,6,7,8,9,9a-octahydro-1H-cyclopenta[8]annulen-1-one, 2-3e.

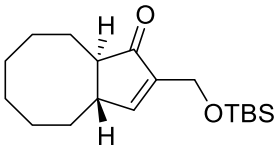

Starting from 0.22 mmol of Co complex **2-1e**. Isolated yield. Method A: 38%[14]; Method B (using 10 equiv. of NMO): 31 mg, 60% (colourless oil). In both cases, 3 equiv. of alkene were used. **^{1}H NMR** (400 MHz, $CDCl_3$) δ 7.28 (q, *J* = 2.0 Hz, 1H), 4.34 (dd, *J* = 2.9, 1.9 Hz, 2H), 2.68 (dq, *J* = 12.3, 3.0 Hz, 1H), 2.20 – 1.20 (m, 13H), 0.91 (s, 9H), 0.07 (s, 6H). The analytical data for this compound were in excellent agreement with the reported data.[14]

Tert-butyl ((5-oxocyclopent-1-en-1-yl)methyl)carbamate, 2-7b.

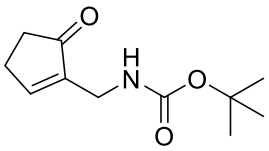

Starting from 0.23 mmol of Co complex **2-1b**. Isolated yield. Method A: 17 mg, 36%; Method B: 32 mg, 67%; Method C: 28 mg, 57% (pale orange oil). **^{1}H NMR** (400 MHz, $CDCl_3$) δ 7.49 (s, 1H), 5.02 (br s, 1H), 3.91 (d, *J* = 6.7 Hz, 2H), 2.69 – 2.55 (m, 2H), 2.47 – 2.38 (m, 2H), 1.44 (s, 9H). **^{13}C NMR** (101 MHz, $CDCl_3$) δ 209.22, 159.29, 155.81, 143.05, 79.43, 36.09, 34.81, 28.33, 26.61. **HRMS** (ESI) calculated for $C_{11}H_{17}NNaO_3$ 234.1101, found 234.1099 $[M+Na]^+$. **IR** (ATR-FTIR) ν_{max} = 3368, 2981, 2928, 1735, 1698 cm^{-1}.

2-(trimethylsilyl)cyclopent-2-en-1-one, 2-7c.

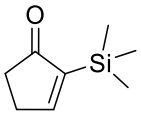

Starting from 0.22 mmol of Co complex **2-1c**. Isolated yield. Method A: 6 mg, 15%; Method B: 16 mg, 43% (colourless oil). **^{1}H NMR** (400 MHz, $CDCl_3$) δ 7.79 (t, *J* = 2.6 Hz, 1H), 2.66 (dt, *J* = 7.5, 2.5 Hz, 2H), 2.37 – 2.30 (m, 2H), 0.18 (s, 9H). The analytical data for this compound were in excellent agreement with the reported data.[22c]

2-(((*Tert*-butyldimethylsilyl)oxy)methyl)cyclopent-2-en-1-one, 2-7e.

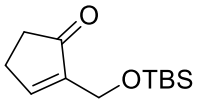

Starting from 0.41 mmol of Co complex **2-1e**. Isolated yield. Method B: 36 mg, 40% (colourless oil). **^{1}H NMR** (400 MHz, $CDCl_3$) δ 7.53 (ddd, *J* = 4.6, 2.7, 1.9 Hz, 1H), 4.37 (td, *J* = 2.8, 1.8 Hz, 2H), 2.66 – 2.57 (m, 2H), 2.54 – 2.42 (m, 2H), 0.92 (s, 9H), 0.08 (s, 6H). The analytical data for this compound were in excellent agreement with the reported data.[24]

4-Methyl-N-((5-oxocyclopent-1-en-1-yl)methyl)benzenesulfonamide, 2-7f.

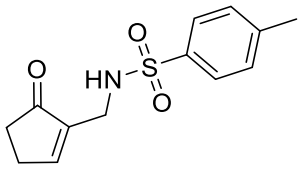

Starting from 0.22 mmol of Co complex **2-1f**. Isolated yield. Method B: 43 mg, 72%; Method C: 38 mg, 64% (colourless oil). **^{1}H NMR** (400 MHz, $CDCl_3$) δ 7.73 – 7.68 (m, 2H), 7.41 (tt, *J* = 2.7, 1.3 Hz, 1H), 7.32 – 7.27 (m, 2H), 5.14 (t, *J* = 6.4 Hz, 1H), 3.80 (dtd, *J* = 6.6, 1.8, 1.2 Hz, 2H), 2.51 – 2.45 (m, 2H), 2.42 (s, 3H), 2.28 – 2.24 (m, 2H). **^{13}C NMR** (101 MHz, $CDCl_3$) δ 208.98, 160.31, 143.48, 140.71, 136.93, 129.60, 127.24, 39.18, 34.53, 26.87, 21.49. **HRMS** (ESI) calculated for $C_{13}H_{16}NO_3S$ 266.0845, found 266.0844 $[M+H]^+$. **IR** (ATR-FTIR) ν_{max} = 3270, 3017, 1689 cm^{-1}.

3-(((*Tert*-butyldimethylsilyl)oxy)methyl)-2-propylcyclopent-2-en-1-one, 2-8d.

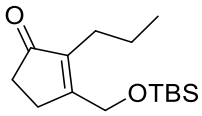

Starting from 0.18 mmol of Co complex **2-1d.** Isolated yield. Method B (using 10 equiv. of NMO): 6 mg, 12% (colourless oil). **^{1}H NMR** (400 MHz, $CDCl_3$) δ 4.54 (s, 2H), 2.59 (dtd, *J* = 7.1, 2.3, 1.2 Hz, 2H), 2.41 – 2.33 (m, 2H), 2.21 – 2.10 (m, 2H), 1.39 (dq, *J* = 14.8, 7.4 Hz, 2H), 0.92 (s, 9H), 0.87 (t, *J* = 7.4 Hz, 3H), 0.10 (s, 6H). **^{13}C NMR** (101 MHz, $CDCl_3$) δ 210.07, 171.72, 139.49, 61.36, 34.19, 27.09, 25.96, 25.20, 21.91, 18.47, 14.20, -5.29. **HRMS** (ESI) calculated for $C_{15}H_{29}O_2Si$ 269.1931, found 269.193 $[M+H]^+$. **IR** (ATR-FTIR) ν_{max} = 2950, 1770, 1464, 840 cm^{-1}.

Ethyl 2-(2-(((tert-butoxycarbonyl)amino)methyl)-5-oxocyclopent-1-en-1-yl)acetate, 2-8g.

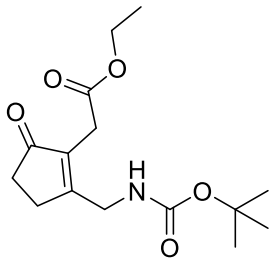

Starting from 0.23 mmol of Co complex **2-1g**. Isolated yield. Method A: 14 mg, 20%; Method B: 43 mg, 64%; Method C: 37 mg, 56% (colourless oil). **^{1}H NMR** (400 MHz, $CDCl_3$) δ 5.05 (br s, 1H), 4.17 – 4.10 (m, 2H), 4.12 (s, 2H), 3.30 (s, 2H), 2.69 – 2.58 (m, 2H), 2.48 – 2.40 (m, 2H), 1.46 (s, 9H), 1.25 – 1.28 (m, 3H). **^{13}C NMR** (101 MHz, $CDCl_3$) δ 208.04, 172.77, 171.21, 170.73, 156.13, 134.01, 80.01, 61.29, 60.46, 40.85, 33.90, 28.42, 21.11, 14.27. **HRMS** (ESI) calculated for $C_{15}H_{24}NO_5$ 298.1649, found 298.1650 $[M+H]^+$. **IR** (ATR-FTIR) ν_{max} = 3359, 2972, 1701, 1693, 1650 cm^{-1}.

Methyl 2-benzyl-3-oxocyclopent-1-ene-1-carboxylate, 2-8h.

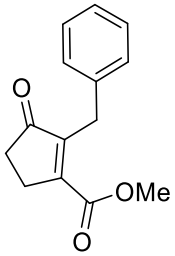

Starting from 0.36 mmol of Co complex **2-1h**. Isolated yield. Method A: 9 mg, 11%; Method B: 36 mg, 46% (colourless oil). **^{1}H NMR** (400 MHz, $CDCl_3$) δ 7.30 (ddt, *J* = 7.6, 1.5, 0.7 Hz, 2H), 7.27 –

7.21 (m, 2H), 7.20 – 7.14 (m, 1H), 3.91 (s, 2H), 3.87 (s, 3H), 2.81 – 2.75 (m, 2H), 2.50 – 2.44 (m, 2H). **^{13}C NMR** (101 MHz, $CDCl_3$) δ 209.03, 165.57, 154.54, 149.60, 138.28, 129.00, 128.36, 126.32, 52.14, 33.97, 29.65, 26.65. **HRMS** (ESI) calculated for $C_{14}H_{15}O_3$ 231.1016, found 231.1022 $[M+H]^+$. **IR** (ATR-FTIR) ν_{max} = 2976, 2954, 1715, 1709 cm^{-1}.

Ethyl 2-(2-(((tert-butyldimethylsilyl)oxy)methyl)-5-oxocyclopent-1-en-1-yl)acetate, 2-8i.

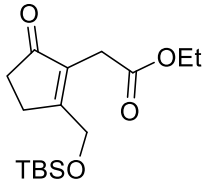

Starting from 0.22 mmol scale of Co complex **2-1i**. Isolated yield. Method B: 34 mg, 49%; Method C: 29 mg, 43% (colourless oil). **^{1}H NMR** (400 MHz, $CDCl_3$) δ 4.58 (s, 2H), 4.12 (q, *J* = 7.1 Hz, 2H), 3.32 (s, 2H), 2.64 (dtd, *J* = 7.1, 2.3, 1.2 Hz, 2H), 2.44 – 2.39 (m, 2H), 1.25 (t, *J* = 7.1 Hz, 3H), 0.92 (s, 9H), 0.10 (s, 6H). **^{13}C NMR** (101 MHz, $CDCl_3$) δ 208.41, 174.71, 170.44, 132.66, 62.44, 61.04, 33.80, 28.67, 27.55, 25.95, 18.46, 14.30, -5.40. **HRMS** (ESI) calculated for $C_{16}H_{29}O_4Si$ 313.1830, found 313.1834 $[M+H]^+$. **IR** (ATR-FTIR) ν_{max} = 2958, 2923, 2856, 1734, 1702 cm^{-1}.

***Tert*-butyl ((1-oxo-1,3a,4,5,6,6a-hexahydropentalen-2-yl)methyl) carbamate, 2-11b.**

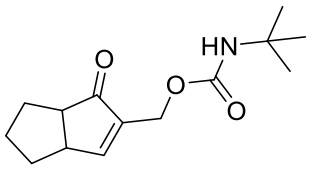

Starting from 0.23 mmol of Co complex **2-1b**. Isolated yield. Method A: 20 mg, 35%; Method B: 35 mg, 60% (colourless oil). **^{1}H NMR** (400 MHz, $CDCl_3$) δ 7.32 – 7.26 (m, 1H), 5.02 (br s, 1H), 3.86 (d, *J* = 6.2 Hz, 2H), 3.33 – 3.18 (m, 1H), 2.74 (ddd, *J* = 10.1, 5.6, 1.8 Hz, 1H), 1.91 – 1.83 (m, 1H), 1.75 – 1.65 (m, 2H), 1.63 – 1.54 (m, 2H), 1.42 (s, 9H), 1.19 (qt, *J* = 12.4, 6.5 Hz, 1H). **^{13}C NMR** (101 MHz, $CDCl_3$) δ 212.36, 162.22, 155.79, 143.11, 79.44, 50.51, 44.25, 36.04, 30.07, 29.35, 28.33, 23.55. **HRMS** (ESI) calculated for $C_{14}H_{22}NO_3$ 252.1594, found 252.1591 $[M+H]^+$. **IR** (ATR-FTIR) ν_{max} = 2937, 2869, 1724, 1525, 758 cm^{-1}.

2-(Trimethylsilyl)-4,5,6,6a-tetrahydropentalen-1(3aH)-one, 2-11c.

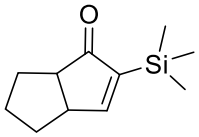

Starting from 0.23 mmol of Co complex **2-1c**. Isolated yield. Method A: 7 mg, 16%; Method B: 14 mg, 31% (colourless oil). **^{1}H NMR** (400 MHz, $CDCl_3$) δ 7.57 (d, *J* = 2.6 Hz, 1H), 3.30 (ddt, *J* = 8.5, 5.4, 2.5 Hz, 1H), 2.71 – 2.62 (m, 1H), 1.89 (dd, *J* = 12.7, 6.3 Hz, 1H), 1.75 – 1.61 (m, 2H), 1.56 (dt, *J* = 12.5, 6.0 Hz, 2H), 1.13 (ddq, *J* = 18.8, 12.5, 6.4 Hz, 1H), 0.16 (s, 9H). **^{13}C NMR** (101 MHz, $CDCl_3$) δ 216.84, 174.91, 147.66, 50.81, 47.85, 30.60, 29.75, 23.50, -1.64. **HRMS** (ESI) calculated for $C_{11}H_{19}OSi$ 195.1200, found 195.1197 $[M+H]^+$. **IR** (ATR-FTIR) ν_{max} = 2918, 2850, 1734, 1215, 758 cm^{-1}.

Tert-butyl ((6-oxo-3,3a,6,6a-tetrahydro-2H-cyclopenta[b]furan-5-yl)methyl)carbamate, 2-12b.

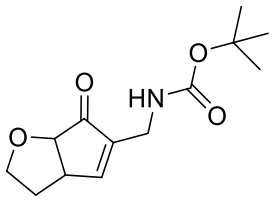

Starting from 0.23 mmol scale of Co complex **2-1b**. Isolated yield. Method A: 23 mg, 40%; Method B: 33 mg, 57% (colourless oil). **^{1}H NMR** (400 MHz, $CDCl_3$) δ 7.35 (d, *J* = 2.7 Hz, 1H), 5.02 (br s, 1H), 4.33 (d, *J* = 5.6 Hz, 1H), 3.96 (ddd, *J* = 9.3, 7.4, 2.0 Hz, 1H), 3.88 (d, *J* = 6.9 Hz, 2H), 3.56 – 3.48 (m, 1H), 3.46 – 3.38 (m, 1H), 2.07 (dddd, *J* = 10.9, 7.5, 3.4, 2.2 Hz, 1H), 1.79 (ddt, *J* = 12.6, 5.4, 2.1 Hz, 1H), 1.41 (s, 9H). **^{13}C NMR** (101 MHz, $CDCl_3$) δ 206.00, 159.05, 155.76, 143.56, 80.48, 67.48, 42.88, 35.96, 30.06, 28.31. **HRMS** (ESI) calculated for $C_{13}H_{20}NO_4$ 254.1387, found 254.1382 $[M+H]^+$. **IR** (ATR-FTIR) ν_{max} = 2955, 2917, 2850, 1715, 1168, 758 cm^{-1}.

5-(trimethylsilyl)-2,3,3a,6a-tetrahydro-6H-cyclopenta[b]furan-6-one, 2-12c.

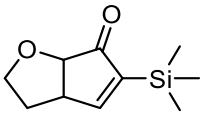

Starting from 0.23 mmol scale of Co complex **2-1c**. Isolated yield. Method A: 9mg, 21%; Method B: 35 mg, 82% (colourless oil). **^{1}H NMR** (400 MHz, $CDCl_3$) δ 7.62 (d, *J* = 2.7 Hz, 1H), 4.28 (d, *J* = 5.7 Hz, 1H), 3.95 (ddd, *J* = 9.3, 7.4, 2.0 Hz, 1H), 3.52 – 3.41 (m, 2H), 2.08 (dddd, *J* = 12.5, 10.9, 9.8, 7.4 Hz, 1H), 1.79 (ddt, *J* = 12.5, 5.5, 2.0 Hz, 1H), 0.18 (s, 9H). **^{13}C NMR** (101 MHz, $CDCl_3$) δ 210.18, 171.32, 148.39, 80.92, 67.25, 46.04, 30.41, -1.80. **HRMS** (ESI) calculated for $C_{10}H_{17}O_2Si$ 197.0992, found 197.0996 $[M+H]^+$. **IR** (ATR-FTIR) ν_{max} = 2955, 2859, 1706, 1248, 841 cm^{-1}.

^{1}H NMR and ^{13}C NMR spectra

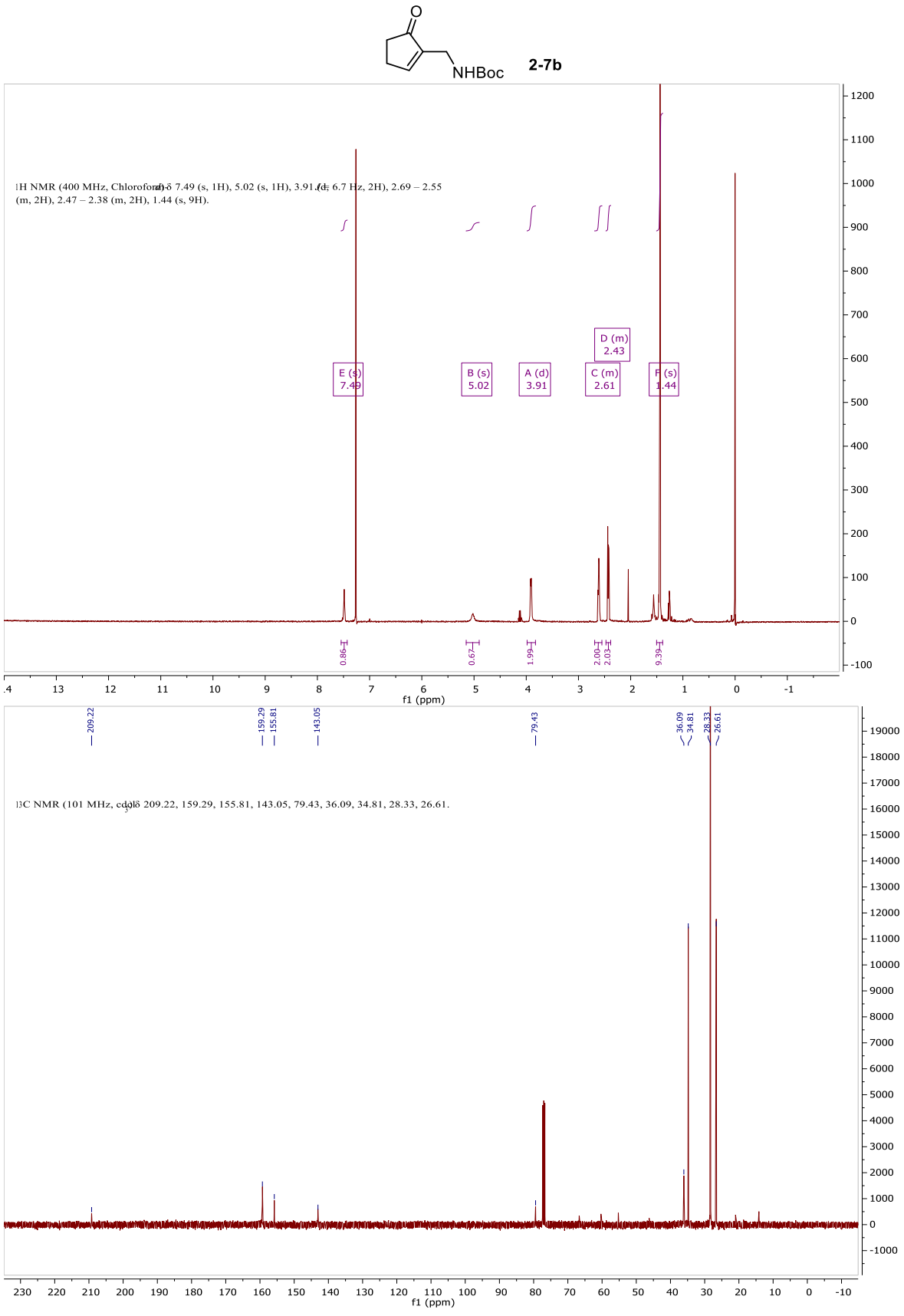

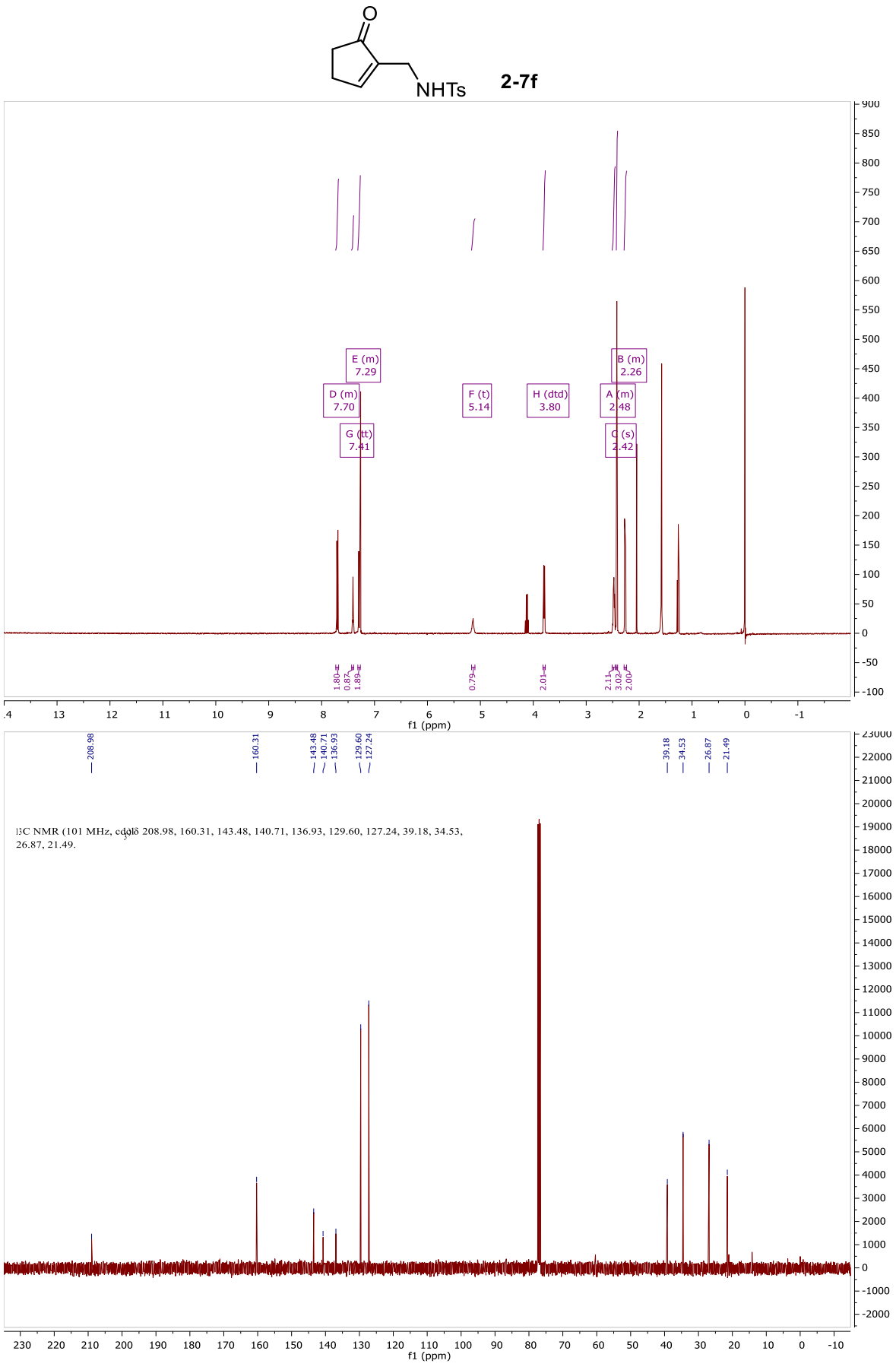
O
NHTs
2-7f
E (m) 7.29
D (m) 7.70
G (tt) 7.41
F (t) 5.14
H (dtd) 3.80
B (m) 2.26
A (m) 2.48
C (s) 2.42
1.80
0.87
1.89
0.79
2.01
2.11
3.02
2.00
f1 (ppm)
208.98
160.31
143.48
140.71
136.93
129.60
127.24
39.18
34.53
26.87
21.49
13C NMR (101 MHz, cdcl3) δ 208.98, 160.31, 143.48, 140.71, 136.93, 129.60, 127.24, 39.18, 34.53, 26.87, 21.49.
f1 (ppm)

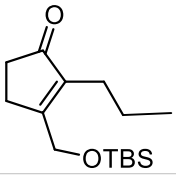

2-8d

^{1}H NMR (400 MHz, Chloroform-*d*) δ 4.54 (s, 2H), 2.59 (dtd, *J* = 7.1, 2.3, 1.2 Hz, 2H), 2.41 – 2.33 (m, 2H), 2.21 – 2.10 (m, 2H), 1.39 (dq, *J* = 14.8, 7.4 Hz, 2H), 0.92 (s, 9H), 0.87 (t, *J* = 7.4 Hz, 4H), 0.10 (s, 6H).

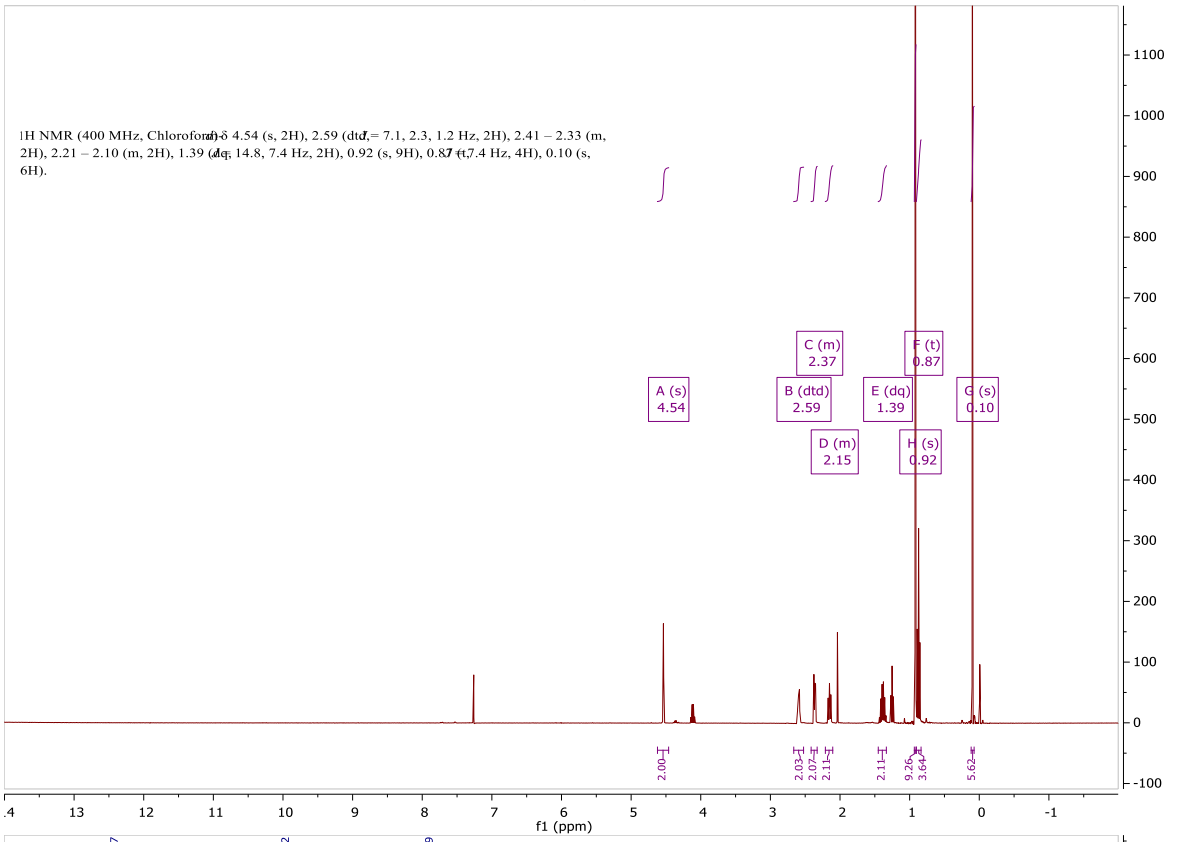

^{13}C NMR (101 MHz, cdcl$_3$) δ 210.07, 171.72, 139.49, 61.36, 34.19, 27.09, 25.96, 25.20, 21.91, 18.47, 14.20, -5.29.

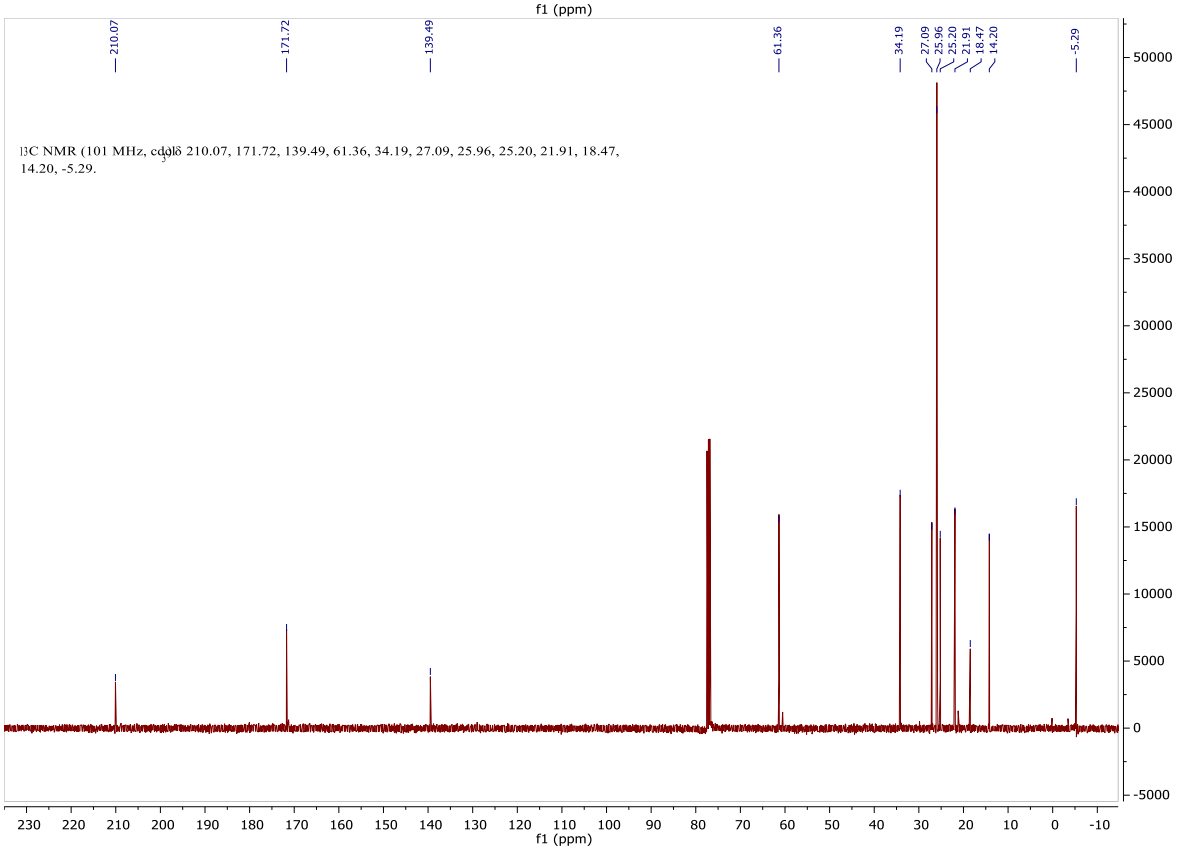

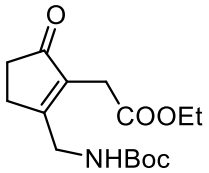

2-8g

^{1}H NMR (400 MHz, Chloroform-d) δ 5.05 (s, 1H), 4.12 (d, J = 7.1 Hz, 4H), 3.30 (s, 2H), 2.69 – 2.58 (m, 2H), 2.48 – 2.40 (m, 2H), 1.46 (s, 9H), 1.27 (s, 3H).

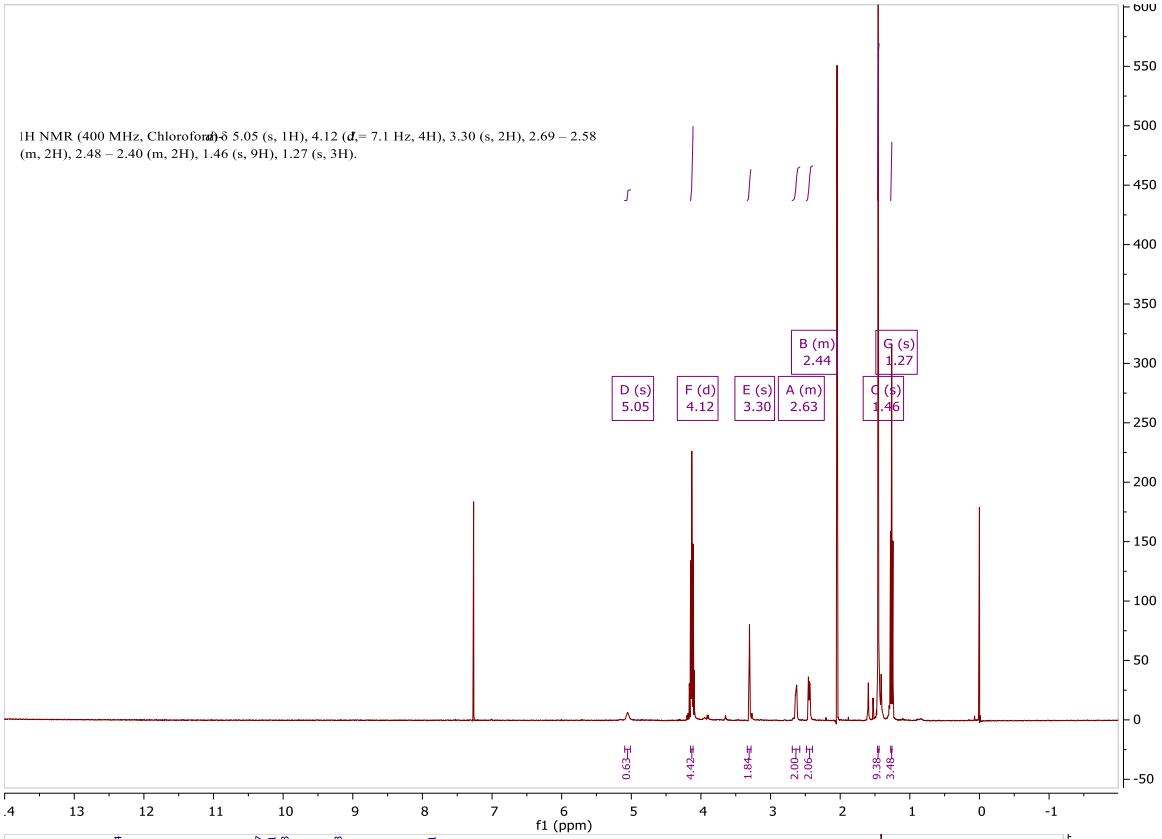

^{13}C NMR (101 MHz, cdcl3) δ 208.04, 172.77, 171.21, 170.73, 156.13, 134.01, 80.01, 61.29, 60.46, 40.85, 33.90, 28.42, 21.11, 14.27.

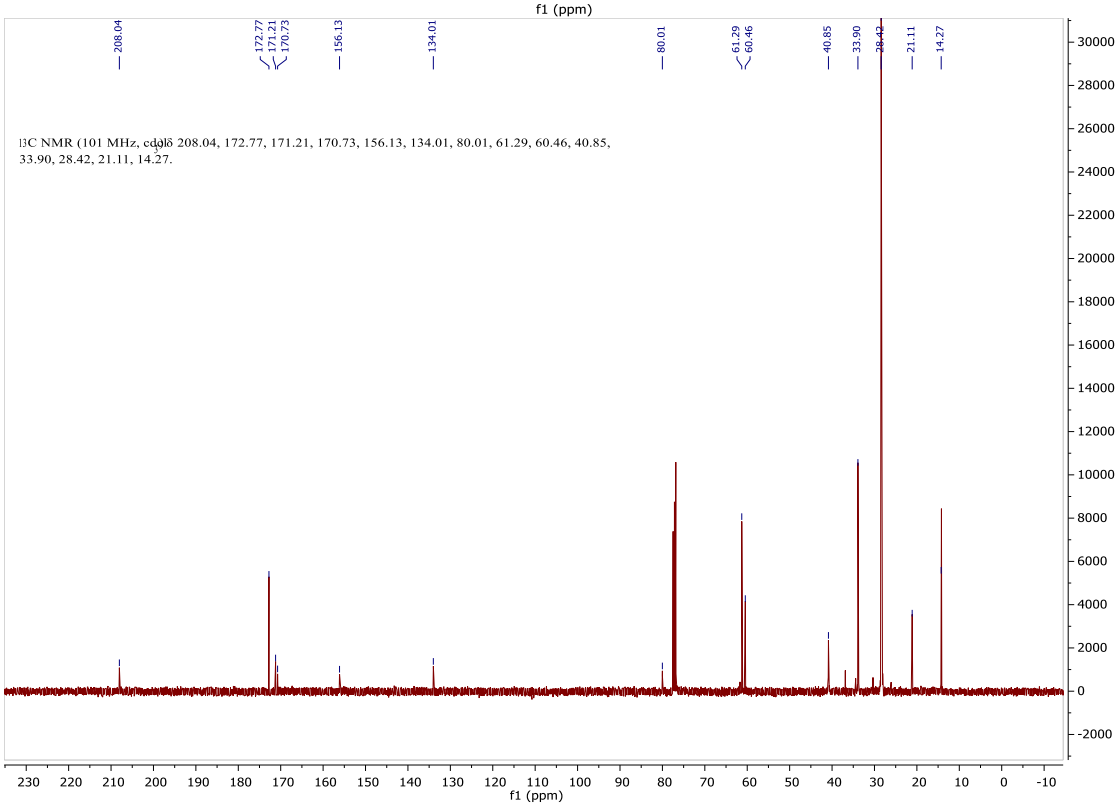

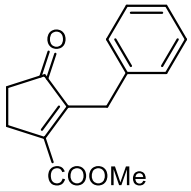

2-8h

^{1}H NMR (400 MHz, Chloroform-*d*) δ 7.30 (ddt, *J* = 7.6, 1.5, 0.7 Hz, 2H), 7.27 – 7.21 (m, 2H), 7.20 – 7.14 (m, 1H), 3.91 (s, 2H), 3.87 (s, 3H), 2.81 – 2.75 (m, 2H), 2.50 – 2.44 (m, 2H).

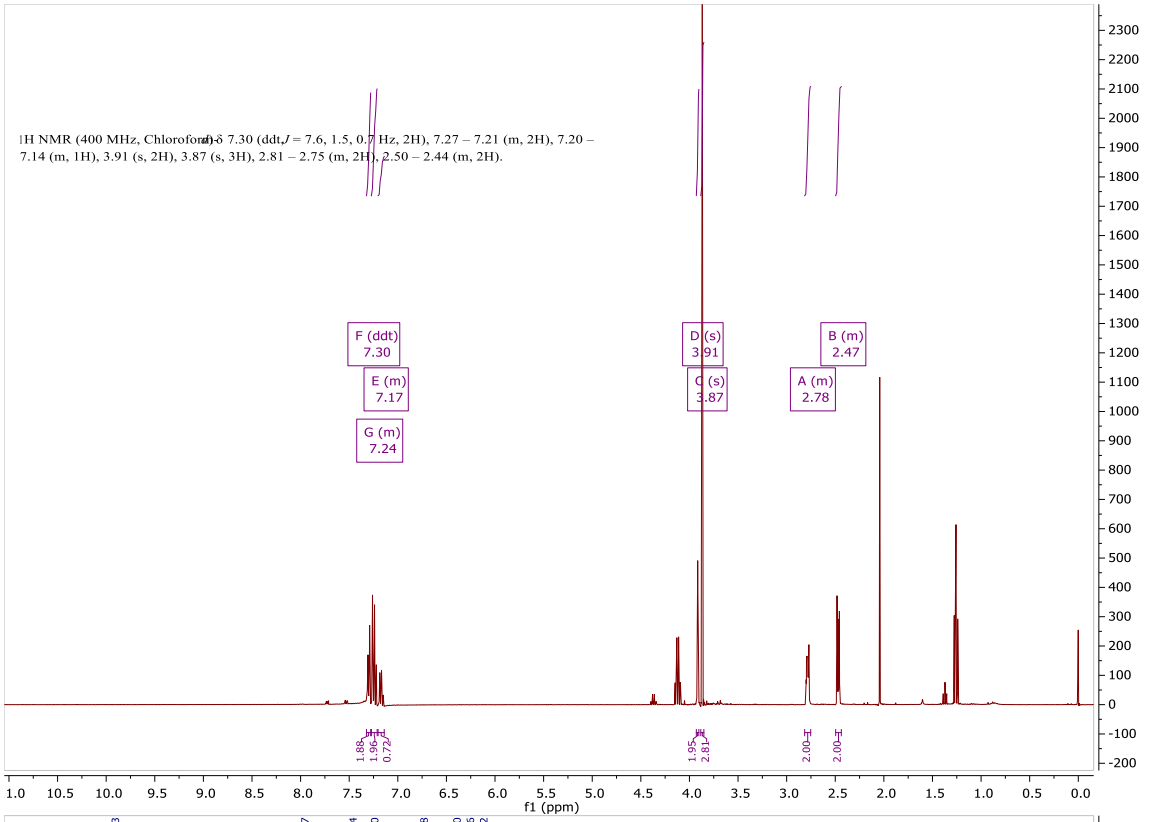

^{13}C NMR (101 MHz, $CDCl_3$) δ 209.03, 165.57, 154.54, 149.60, 138.28, 129.00, 128.36, 126.32, 52.14, 33.97, 29.65, 26.65.

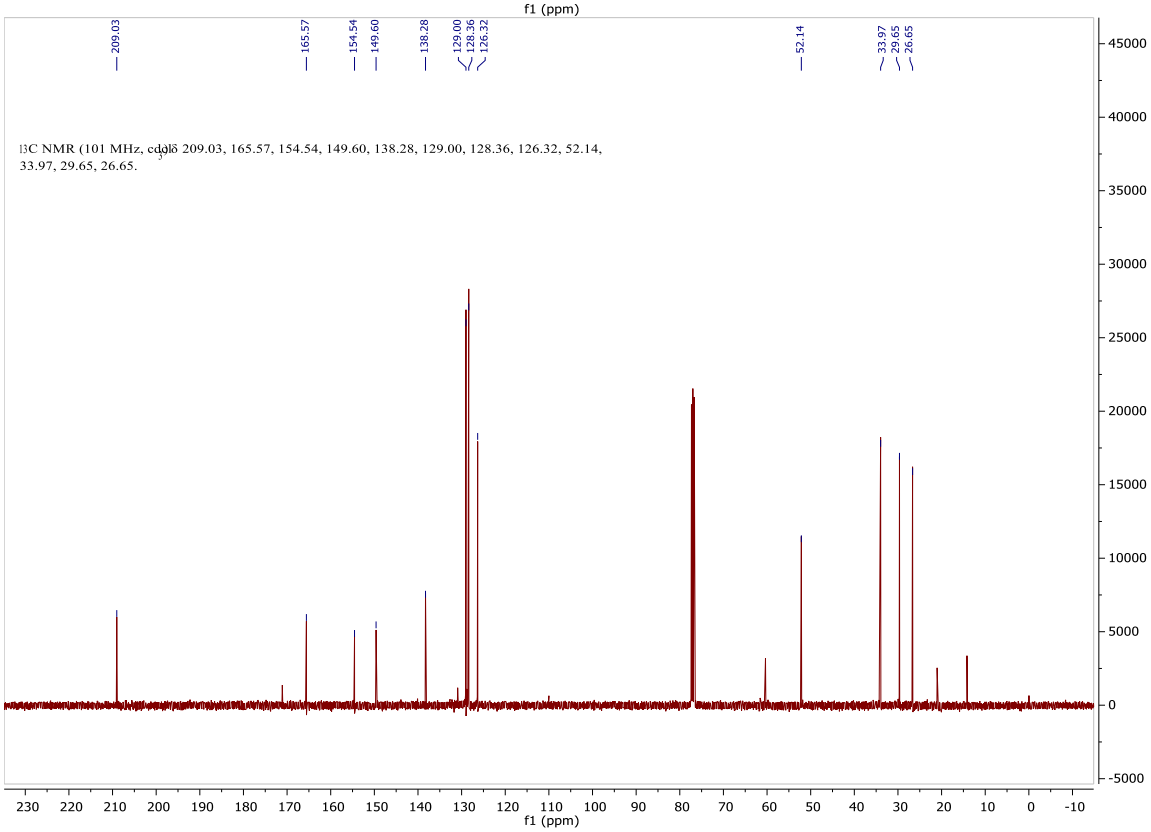

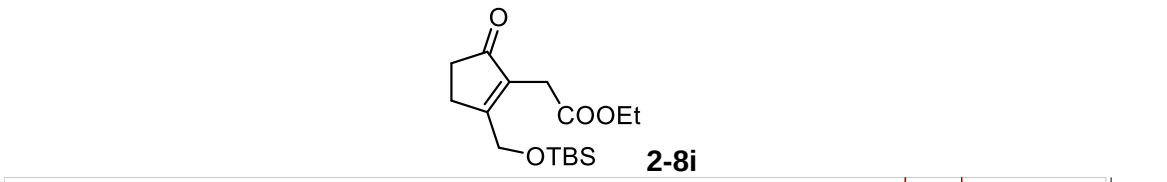

2-8i

^{1}H NMR (400 MHz, Chloroform-d) δ 4.58 (s, 2H), 4.12 (q, J = 7.1 Hz, 2H), 3.32 (s, 2H), 2.64 (dtd, J = 7.1, 2.3, 1.2 Hz, 2H), 2.44 – 2.39 (m, 2H), 1.25 (t, J = 7.1 Hz, 3H), 0.92 (s, 9H), 0.10 (s, 6H).

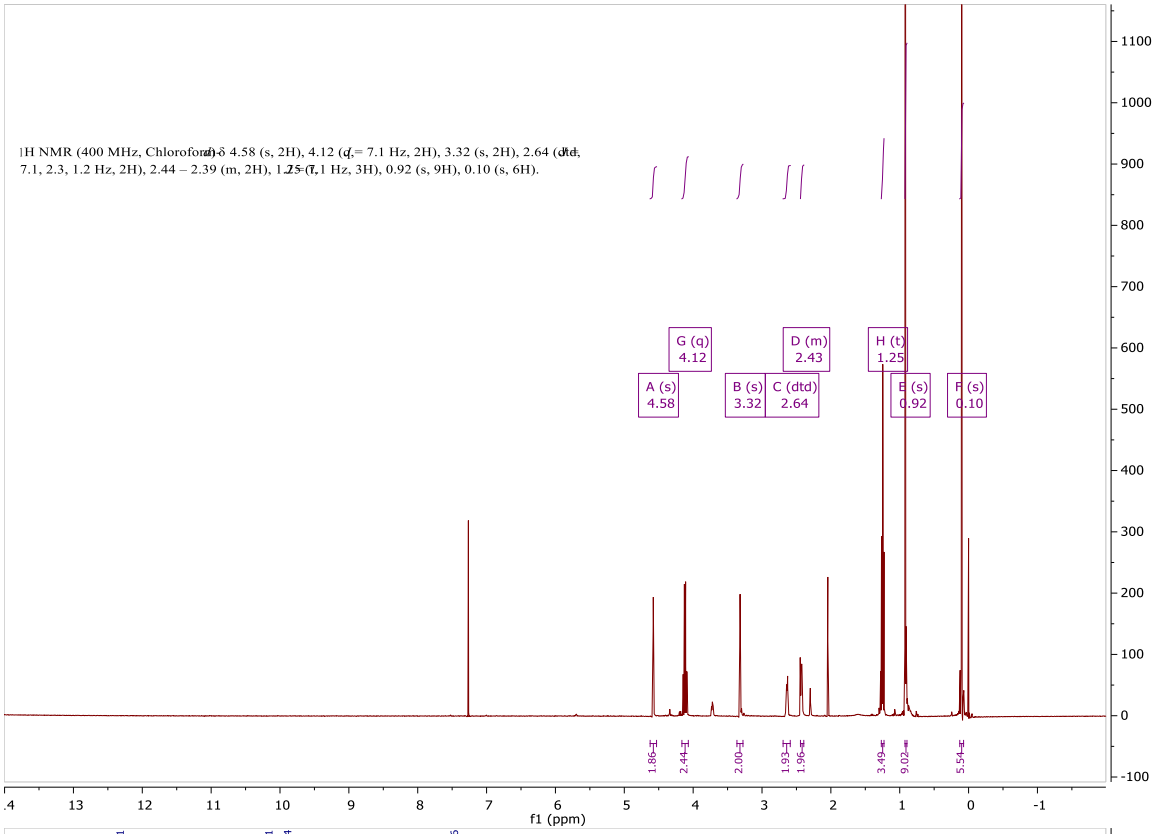

^{13}C NMR (101 MHz, cdcl$_3$) δ 208.41, 174.71, 170.44, 132.66, 62.44, 61.04, 33.80, 28.67, 27.55, 25.95, 18.46, 14.30, -5.40.

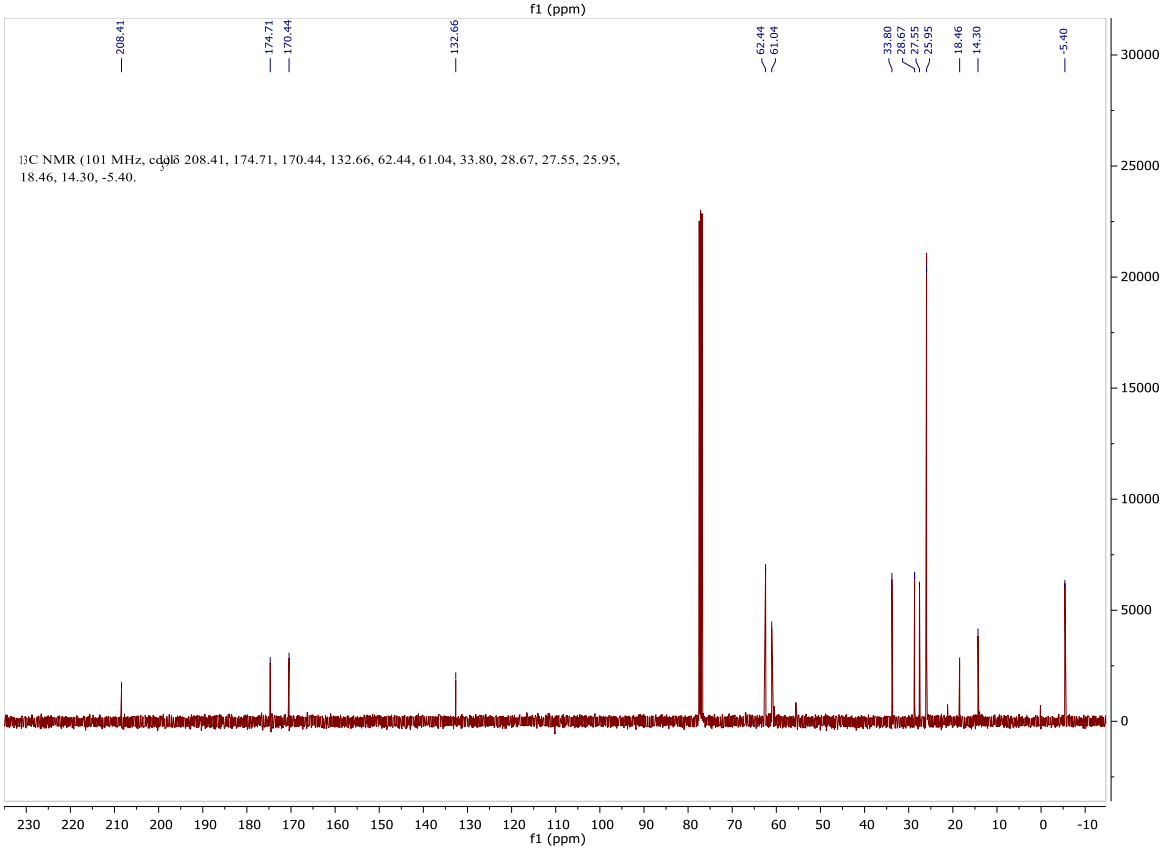

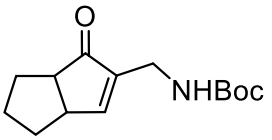

2-11b

^{1}H NMR (400 MHz, Chloroform-*d*) δ 7.32 – 7.26 (m, 1H), 5.02 (s, 1H), 3.86 (d, *J* = 6.2 Hz, 2H), 3.33 – 3.18 (m, 1H), 2.74 (ddd, *J* = 10.1, 5.6, 1.8 Hz, 1H), 1.91 – 1.83 (m, 1H), 1.75 – 1.65 (m, 2H), 1.63 – 1.54 (m, 2H), 1.42 (s, 9H), 1.19 (qt, *J* = 12.4, 6.5 Hz, 1H).

^{13}C NMR (101 MHz, $CDCl_3$) δ 212.36, 162.22, 155.79, 143.11, 79.44, 50.51, 44.25, 36.04, 30.07, 29.35, 28.33, 23.55.

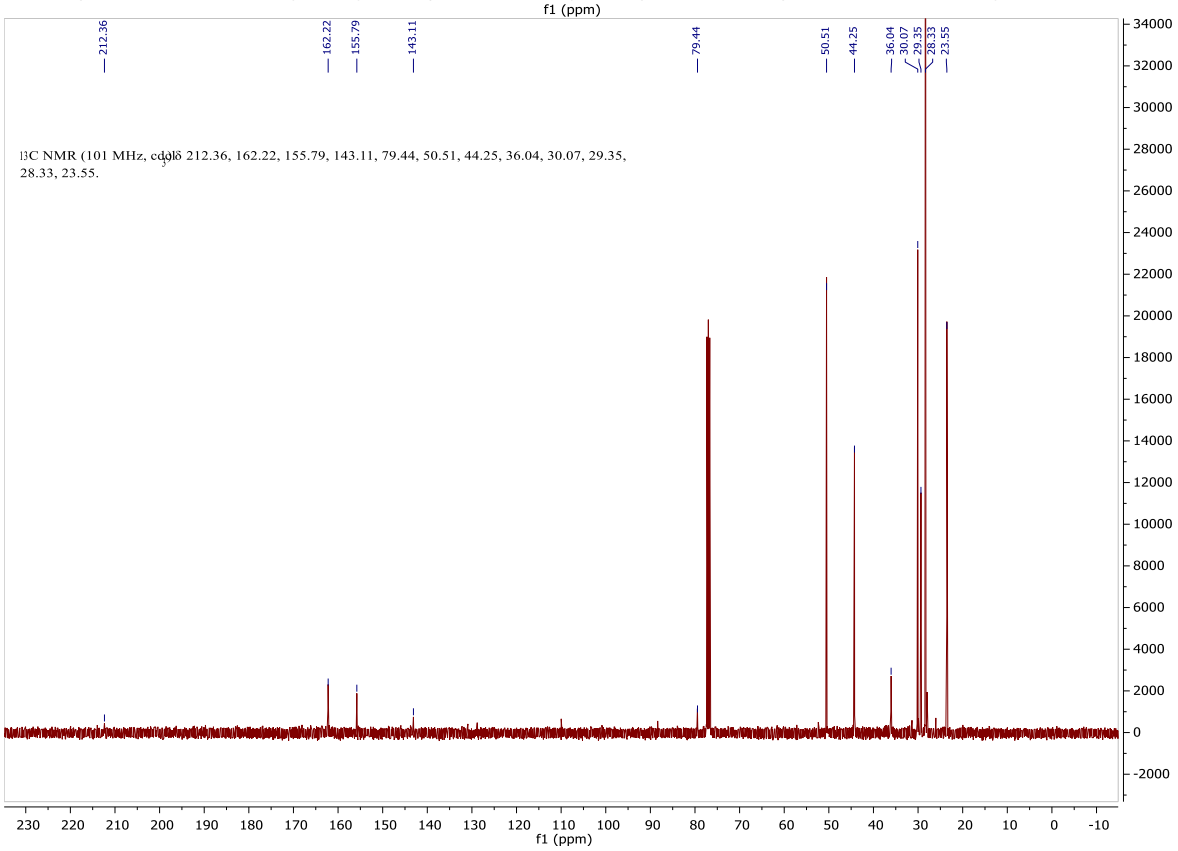

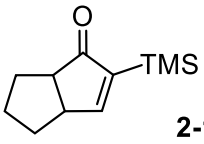
O
TMS

2-11c

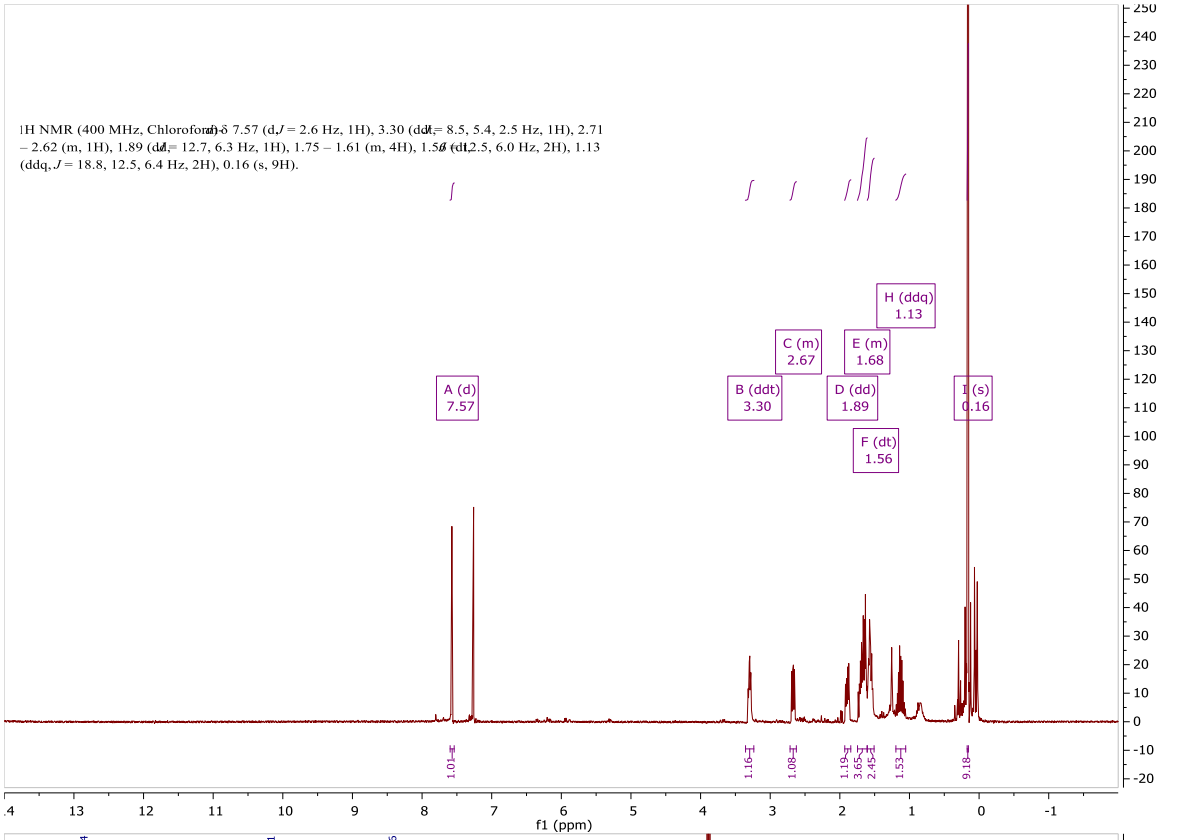
A (d)
7.57
B (ddt)
3.30
C (m)
2.67
D (dd)
1.89
E (m)
1.68
F (dt)
1.56
H (ddq)
1.13
I (s)
0.16
1.01
1.16
1.08
1.19
3.65
2.45
1.53
9.18
f1 (ppm)

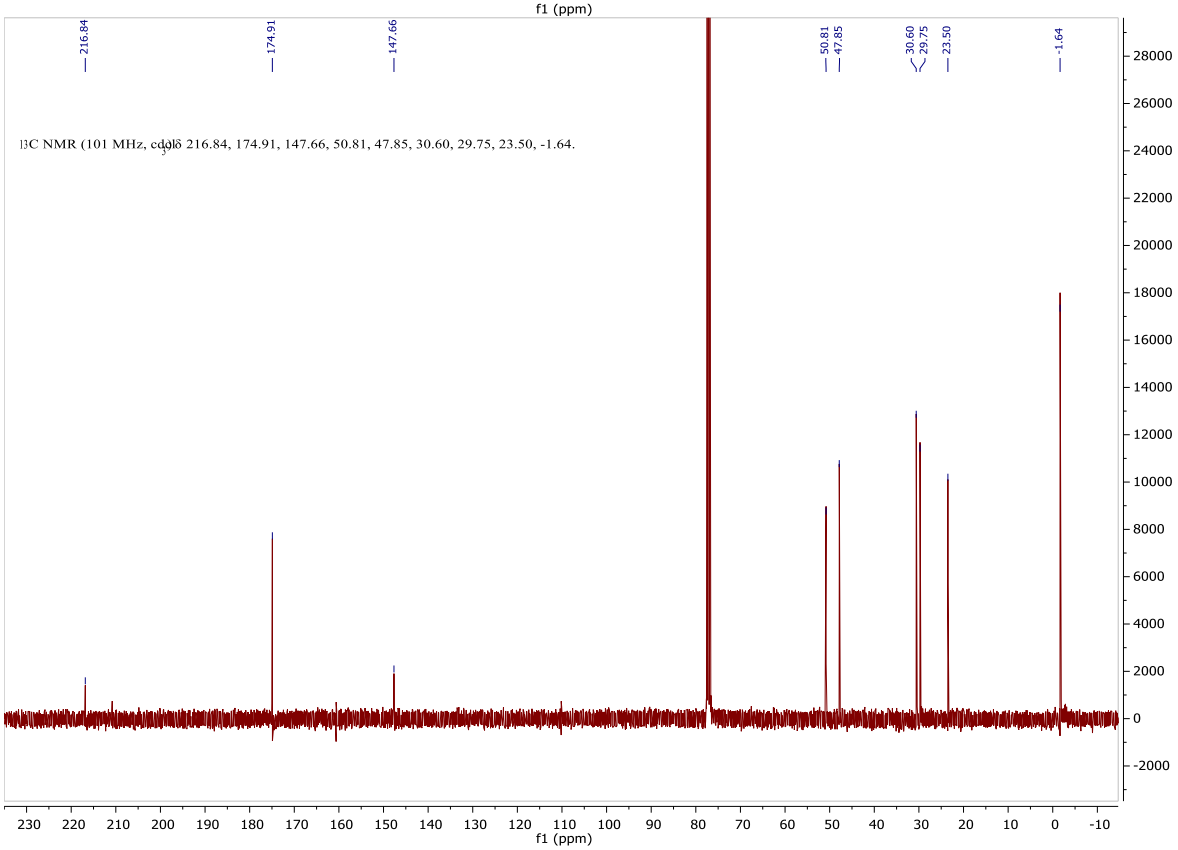
216.84
174.91
147.66
50.81
47.85
30.60
29.75
23.50
-1.64
f1 (ppm)

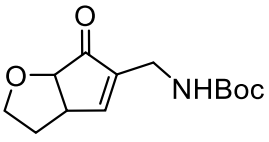
O
O
NHBoc

2-12b

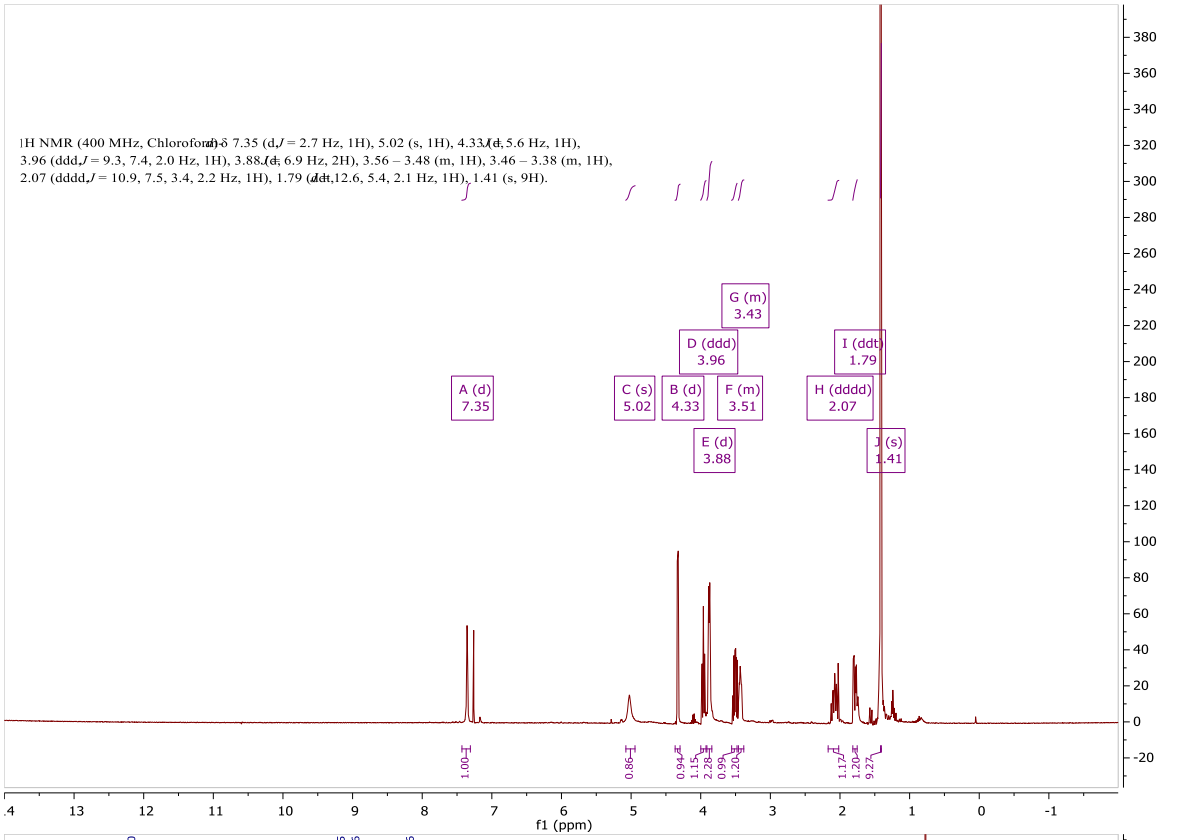
A (d) 7.35
C (s) 5.02
B (d) 4.33
F (m) 3.51
E (d) 3.88
D (ddd) 3.96
G (m) 3.43
H (dddd) 2.07
I (ddt) 1.79
J (s) 1.41
1.00
0.86
0.94
1.15
2.28
0.99
1.20
1.17
1.20
9.27
f1 (ppm)

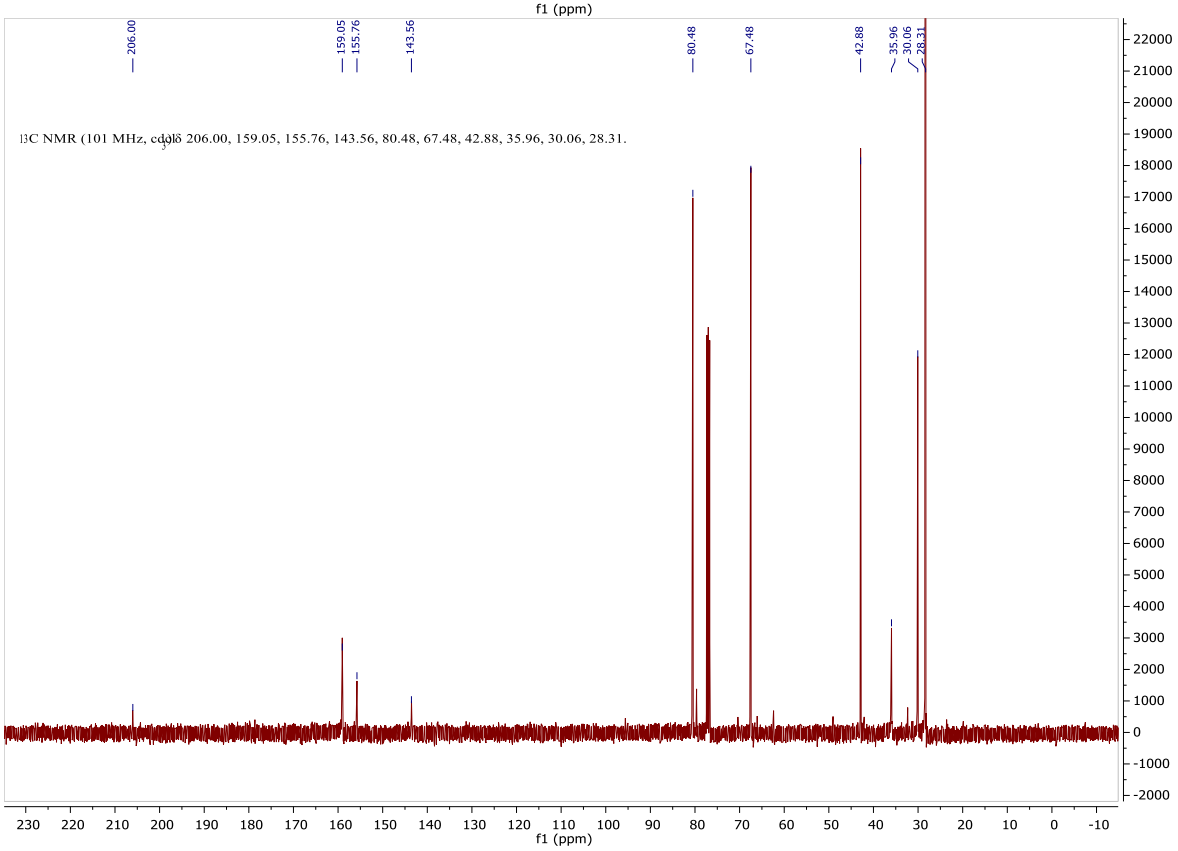
206.00
159.05
155.76
143.56
80.48
67.48
42.88
35.96
30.06
28.31
f1 (ppm)

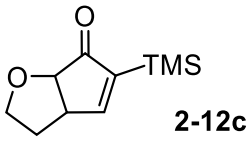

2-12c

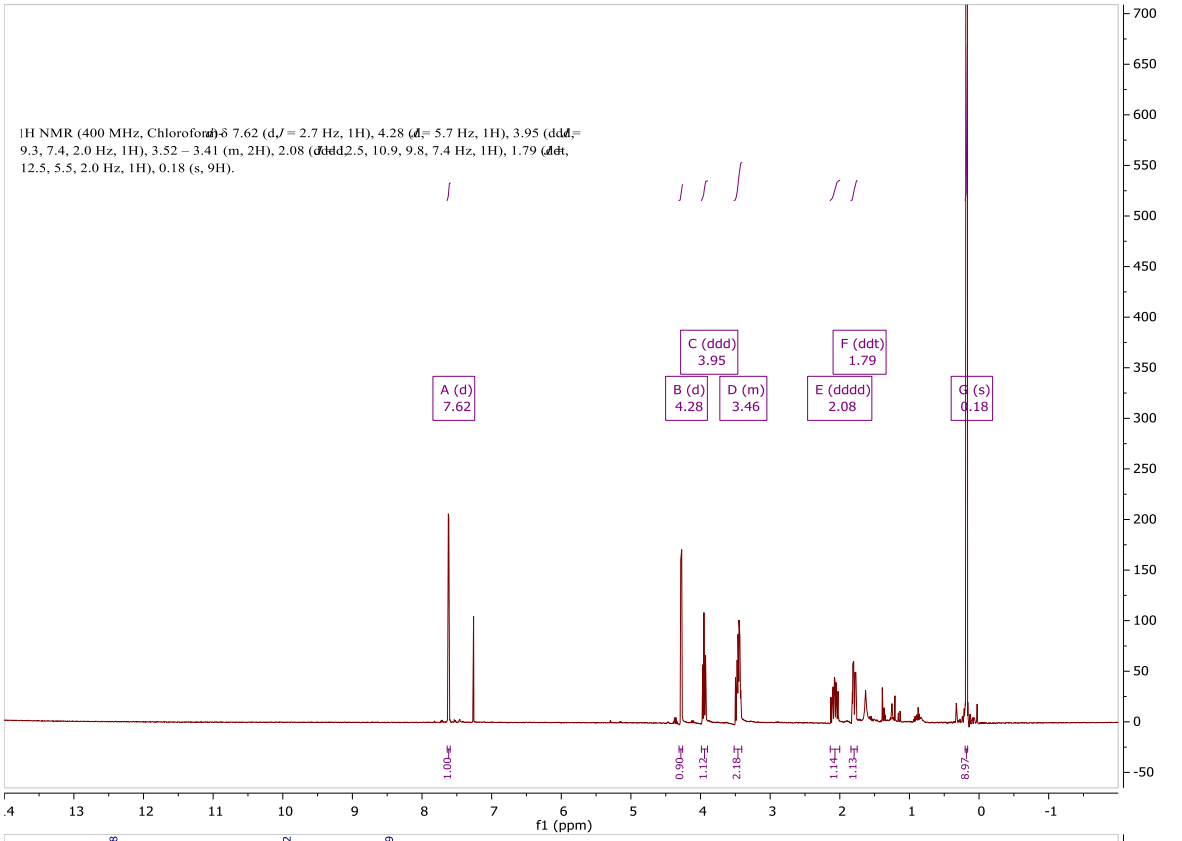

^{1}H NMR (400 MHz, Chloroform-d) δ 7.62 (d, J = 2.7 Hz, 1H), 4.28 (d, J = 5.7 Hz, 1H), 3.95 (ddd, J = 9.3, 7.4, 2.0 Hz, 1H), 3.52 – 3.41 (m, 2H), 2.08 (dddd, J = 12.5, 10.9, 9.8, 7.4 Hz, 1H), 1.79 (ddt, J = 12.5, 5.5, 2.0 Hz, 1H), 0.18 (s, 9H).

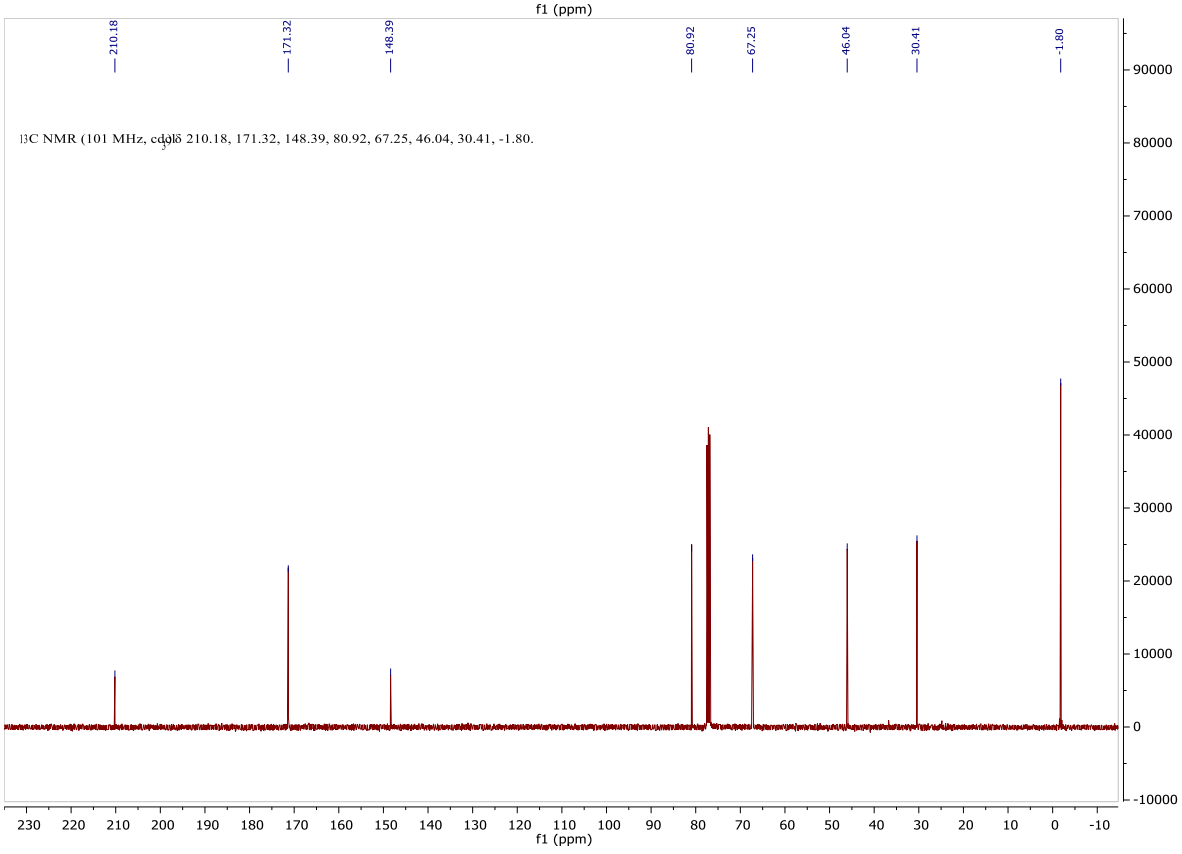

^{13}C NMR (101 MHz, $CDCl_3$) δ 210.18, 171.32, 148.39, 80.92, 67.25, 46.04, 30.41, -1.80.

Chapter 3

Catalytic Pauson-Khand Reaction in Ethylene Glycol-Toluene. Activity, Selectivity and Catalyst Recyclability

The Pauson-Khand reaction (PKR),[1,2] a metal-catalysed [2+2+1] cycloaddition coupling an alkyne, an alkene and CO is one of the most powerful synthetic tools with which to prepare cyclopentenones.[3,4] The stoichiometric version of the reaction uses large amounts of dicobalt octacarbonyl with the subsequent drawbacks of price, residue disposal and difficult purification of the final product. In this regard, the development of catalytic methodologies to reduce the amount of metal are required for large scale preparations. Several catalytic versions of the PKR involving the use of other metals such as Ti,[5] Ru,[6] Rh,[7] Ni[8] and Ir[9] or bimetallic species, have been described.[10] However, the use of cobalt complexes is probably the most practical and economical approach. Although the catalytic system can be prepared *in situ* by reducing $CoBr_2$ with Zn under CO pressure,[11] dicobalt octacarbonyl continues to be the most common catalyst.[12]

Many additives have been described to improve the yields in the cobalt-catalysed PKR. Ureas such as tetramethyl thiourea (TMTU),[13] phosphites,[14] triphenylphosphines,[15] hard Lewis bases[16] and sulphides[17] are the most relevant. However, the use of large amounts of additives usually hinders the purification of the product.

Catalyst recycling is clearly desirable. Several heterogeneous catalytic systems such as colloidal cobalt nanoparticles (NPs),[19] cobalt on charcoal[20] or cobalt Raney[21]have been described for the PKR.[18]. However, to the best of our knowledge, there are no precedents of catalyst recycling in homogenous systems.

Based on a previous methodology developed by Baran and co-workers,[4a] our group recently reported that, ethylene glycol (MEG) can enhance the alkene range in the stoichiometric N-Oxide promoted intermolecular PKR (Scheme 3.1).[22] In the present study we report that this additive also has a positive effect on cobalt-catalysed PKR, allowing the reaction to be performed with very low catalyst loadings, reducing undesired by-products, facilitating the purification of the final product and permitting the catalyst recycling by simple liquid-liquid separation.

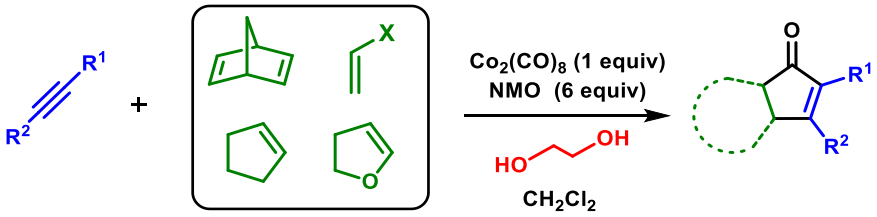

Scheme 3.1. Previous work of MEG-assisted intermolecular PKR.

We chose three standard enynes **3-1a-c** to test the intramolecular catalytic PKR. As expected, the reaction proceeded smoothly in toluene using 5 mol % of $Co_2(CO)_6$ to afford the corresponding bicyclic cyclopentenones in moderate to good yields. The yields of the oxygen-containing enyne **3-1c** were slightly lower than those of **3-1a** and **3-1b**. Under the same conditions but using MEG/toluene (15% v/v) instead of pure toluene (entries 1-3, Table 3.1) the yields consistently increased by approximately 10 points. Although the increase in yield was moderate, the reaction crudes were much cleaner in MEG-toluene, thus allowing easier work-up and purification.

We then, turned our attention to the intermolecular version. Terminal alkynes **3-1d-j** were reacted with norbornadiene (NBD) or norbornene (entries 1-7 and 8, respectively, Table 3.2) under CO pressure using dicobalt octacarbonyl as catalyst affording cyclopentenones **3-2d-j** in good to excellent yield. Except in one case (entry 7) the yields clearly improved when using the MEG/toluene mixture. Moreover, a significant improvement in terms *exo:endo* selectivity was also achieved in all cases. In entry 4, for instance, only traces of trimerization of phenylacetylene –a common byproduct in catalytic PKR that is usually avoided by adding triphenylphosphine- was detected. In addition, no *endo* adduct was observed. It is worth noting that **3-2d** and **3-2e** are the most interesting substrates from the synthetic point of view since they have been used in the synthesis of several biologically active compounds.[4b-d]

Table 3.1. Catalytic Intramolecular Pauson-Khand Reaction.[a]

Entry	Enyne	Cyclopentenone	Yield (%)[b]
1	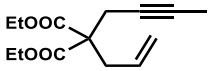 3-1a	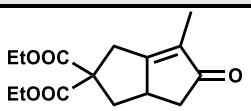 3-2a	A: 81 B: 90
2	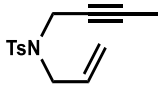 3-1b	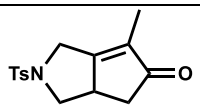 3-2b	A: 83 B: 91
3	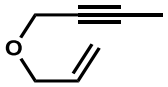 3-1c	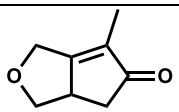 3-2c	A: 47 B: 60

[a] Reaction conditions A: enyne (100 mg, 1.0 equiv.), $Co_2(CO)_8$ (0.05 equiv.) in toluene at 80 °C under CO (1 atm), overnight. Reaction conditions B: Same but using MEG–toluene (15% v/v) as additive. [b] Isolated yields.

Table 3.2. Catalytic Intermolecular Pauson-Khand Reaction.[a]

Entry	Alkyne	Cyclopentenone	*exo:endo*	Yield (%) [b]
1	 3-1d	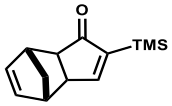 3-2d	A: 93:7 B: 93:7	A: 75 B: 99
2	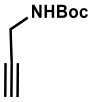 3-1e	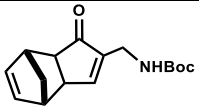 3-2e	A: 83:17 B: 93:7	A: 60 B: 93
3	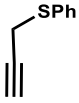 3-1f	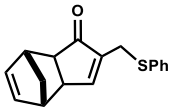 3-2f	A: 93:7 B: 96:4	A: 79 B: 93
4	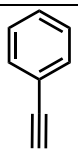 3-1g	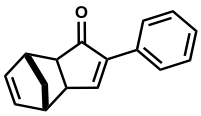 3-2g	A: 98:2 B: >99	A: 89 B: 91
5	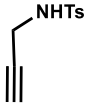 3-1h	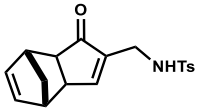 3-2h	A: 93:7 B: 95:5	A: 80 B: 85
6	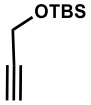 3-1i	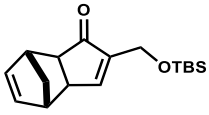 3-2i	A: 93:7 B: 95:5	A: 56 B: 70

7	 3-1j	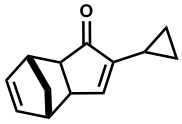 3-2j	A: 93:7 B: >99	A: 75 B: 72
8[c]	 3-1d	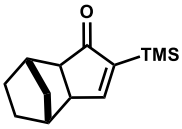 3-3	A:86:14 B: >99	A: 94 B: 98

[a] Reaction conditions. A: norbornadiene (5.0 equiv.), alkyne (100 mg, 1.0 equiv.), $Co_2(CO)_8$ (0.05 equiv.) in toluene at 80 °C under CO (1 atm), overnight. B: Ethylene glycol (15% v/v) was added as additive. [c] Norbornene was used as alkene.

Apart from the effect of MEG on the yield and *exo*/*endo* selectivity, the addition of this compound to the reaction mixture also gave a much cleaner crude product. In fact, after completion of the reaction, two phases were clearly observed: a slightly coloured upper toluene layer and a dark red lower MEG layer (Figure 3.1). Therefore, when the reaction finished, toluene and MEG formed two immiscible liquid layers. We assumed that most of the product remained in the organic phase whereas most of the cobalt species were trapped in the MEG layer.

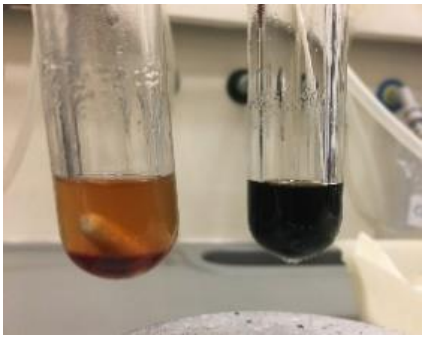

Figure 3.1. Reaction crude of **3-3** after 17 hours of heating (entry 8, Table 3.2). With MEG as additive (left) and without MEG (right).

To test this assumption, the upper layer was separated and a solution of alkyne and alkene in toluene was added to the MEG phase. Heating at 80ºC under CO (1 atm) the PKR proceeded again thereby proving that the cobalt species that remain into the MEG phase were catalytically active. This observation prompted us to use the novel methodology to test the recycling of $Co_2(CO)_8$. For this purpose, **3-1d** and N-protected propargyl amine acetylenes **3-1e** and **3-1h** were selected as alkynes and norbornadiene as alkene. The reaction was performed using an initial loading of 10 mol% of $Co_2(CO)_8$ in MEG/toluene (15% v/v).

The reaction mixture was stirred at 80 °C overnight under CO (1 atm). Then, the reactor was depressurized and the supernatant organic layer was separated. A fresh toluene solution of alkyne and NBD was added to the MEG layer containing the cobalt complexes. The second catalytic cycle finished after 36 h (monitored by TLC) and the operation was repeated. Finally, the third catalytic cycle lasted 72 h. Each of the toluene layers was collected, evaporated and chromatographed affording the corresponding PK-adducts (Table 3.3). The overall yields were excellent and less than 10% of the product was found in the final MEG layer. Therefore, it was possible to perform up to three catalytic cycles (Table 3.3). In this case, the *exo:endo* selectivities were similar to those obtained with the previous methodology.

Table 3.3. Catalytic Recyclability.[a]

Entry	Alkyne	Cyclopentenone	Yield (cycle)[b]	Overall yield (*exo:endo*)[c]
1	 3-1d	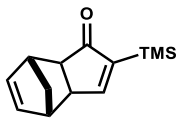 3-2d	95 (first) 90 (second) 71 (third)	85 % (90:10)
2	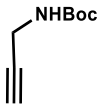 3-1e	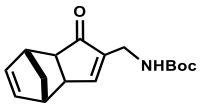 3-2e	99 (first) 93 (second) 85 (third)	92% (92:8)
3	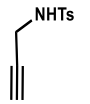 3-1h	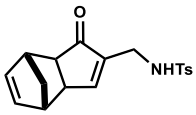 3-2h	99 (first) 92 (second) 85 (third)	92% (95:5)

[a]Reaction conditions C. Three cycles of alkyne (200 mg, 1.0 equiv.) and norbornadiene (5.0 equiv.), were run with $Co_2(CO)_8$ (10 mol%) MEG-toluene (15% v/v) at 80 °C under CO (1 atm); [b]Yield after each catalytic cycle. [c]Isolated overall yield. In parentheses, overall *exo:endo* ratio.

The MEG-phase containing the cobalt residues degraded during each catalytic cycle, until it became inactive (Figure 3.2). As far as we know, this is the first example of catalyst recycling done homogeneously by simple liquid-liquid separation. In this regard, the amount of cobalt catalyst was reduced to 3 mol%.

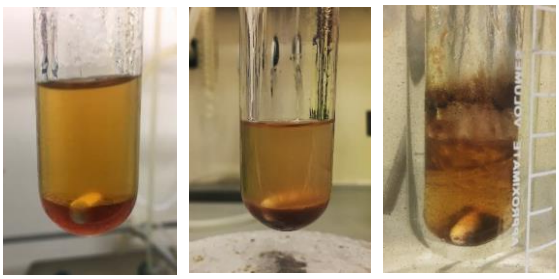

Figure 3.2. Catalytic intermolecular PKR of **3-1e** with NBD recycling the catalyst that remain in the MEG phase. After the first cycle (left), after the second cycle (center) and after the third cycle (right).

The process was scaled up to gram scale, and catalyst loading was reduced to 1 mol% without the need of catalyst recycling (Scheme 3.2). To the best of our knowledge, this is the lowest catalyst loading successfully used in the intermolecular PKR.

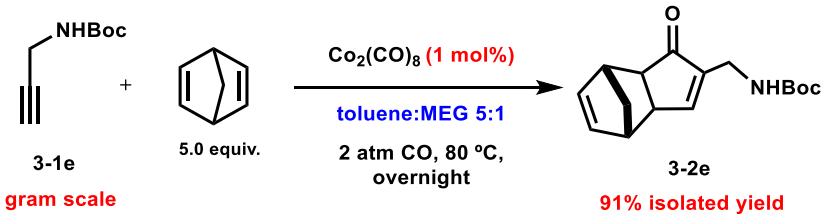

Scheme 3.2. Gram-scale intermolecular PKR using MEG/toluene as solvent. Alkyne **3-1e** (1g), norbornadiene (5.0 equiv.) and 1 mol% of $Co_2(CO)_8$ were used.

In summary, we have demonstrated that the mixture of MEG-toluene (15% v/v) enhances the PKR allowing the use 1mol% of $Co_2(CO)_8$ as catalyst under low CO pressure (1 atm). When the reactions were finished, the toluene and MEG formed immiscible layers thus facilitating the work-up because the toluene layer contained most of the product. Since the MEG layer contains most of the cobalt species it can be reused by adding a fresh solution of alkyne and alkyne. This new synthetic protocol for catalytic PKR is efficient, practical and has the lowest catalyst loading reported to date in cobalt-catalysed PKR.

References

(1) *The Pauson-Khand Reaction: Scope, Variations and Applications*; Rios, R., Ed.; Wiley: Chichester, U.K., 2012.

(2) Selected reviews: (a) J. D. Ricker, L. M. Geary, *Top. Catal.* **2017**, *60*, 609–619. (b) P. Evans, *Appl. Organomet. Chem.* **2013**, *27*, 261–262. (c) Strübing, D.; Beller, M. In *Catalytic Carbonylation Reactions*; Beller, M., Ed.; Springer Berlin Heidelberg: Berlin, Heidelberg, **2006**, 165. (d) Omae, I. *Appl. Organomet. Chem.* **2007**, *21*, 318 (e) Pérez-Castells, J. In *Metal Catalyzed Cascade Reactions*; Müller, T. J. J., Ed.; Springer Berlin Heidelberg: Berlin, Heidelberg, **2006**, 207. (f) Laschat, S.; Becheanu, A.; Bell, T.; Baro, A. *Synlett* **2005**, 2547. (g) Blanco-Urgoiti, J.; Añorbe, L.; Pérez-Serrano, L.; Domínguez, G.; Pérez-Castells, *J. Chem. Soc. Rev.* **2004**, *33*, 32–42. (h) Rodríguez Rivero, M.; Adrio, J.; Carretero, J. C. *Eur. J. Org. Chem.* **2002**, 2881. (i) Brummond, K. M.; Kent, J. L. *Tetrahedron* **2000**, *56*, 3263.

(3) Selected synthetic applications of the intramolecular PKR: (a) N. Zhao, S. Yin, S. Xie, H. Yan, P. Ren, G. Chen, F. Chen, J. Xu, *Angew. Chemie, Int. Ed.* **2018**, *57*, 3386–3390. (b) Chuang, K. V; Xu, C.; Reisman, S. E. *Science,* **2016**, *353*, 912–915. (c) Verdaguer, X. *Science* **2016**, *353*, 866. (d) K. Fujioka, H. Yokoe, A. Inoue, K. Soga, M. Tsubuki, K. Shishido, *J. Org. Chem.* **2014**, *79*, 7512–7519. (e) J. J. Crawford, W. J. Kerr, M. McLaughlin, A. J. Morrison, P. L. Pauson, G. J. Thurston, *Tetrahedron* **2006**, *62*, 11360–11370. (f) J. Castro, A. Moyano, M. A. Pericàs, A. Riera, A. E. Greene, A. Alvarez-Larena, J. F. Piniella, *J. Org. Chem.* **1996**, *61*, 9016–9020.

(4) Selected applications of the intermolecular PKR: (a) Su, S.; Rodriguez, R.A.; Baran, P.S. *J. Am. Chem. Soc.* **2011**, *133*, 13922–13925. (b) N. Aiguabella, A. Pesquer, X. Verdaguer, A. Riera, *Org. Lett.* **2013**, *15*, 2696–2699. (c) A. Vázquez-Romero, L. Cárdenas, E. Blasi, X. Verdaguer, A. Riera, *Org. Lett.* **2009**, *11*, 3104–7. (d) A. Vazquez-Romero, J. Rodriguez, A. Lledo, X. Verdaguer, A. Riera, *Org.Lett.; Org. Lett.* **2008**, *10*, 4509–4512. (e)Gibson, S. E.; Mainolfi, N. *Angew. Chem. Int. Ed.* **2005**, *44*, 3022. (f) V. Bernardes, N. Kann, A. Riera, A. Moyano, M. A. Pericàs, A. E. Greene, *J. Org. Chem.* **1995**, *60*, 6670–6671.

(5) (a) Hicks, F.A.; Buchwald, S.L. *J. Am. Chem. Soc.* **1996**, *118*, 11688–11689. (b) Sturla, S. J.; Buchwald, S. L. *J. Org. Chem.* **1999**, *64*, 5547-5550.

(6) (a) Kondo, T.; Suzuki, N.; Okada, T.; Mitsudo, T.-A. *J. Am. Chem Soc.* **1997**, *119*, 6187-6188. (b) Morimoto, T.; Chatani, N.; Fukumoto, Y.; Murai, S. *J. Org. Chem.* **1997**, *62*, 3762-3765.

(7) (a) Kwong, F.Y.; Lee, H.W.; Qiu, L.; Lam, W.H.; Li, Y.-M.; Kwong, H.L.; Chan, A.S.C. *Adv. Synth. Catal.* **2005**, *347*, 1750–1754. (b) Jeong, N.; Sung, B. K.; Choi, Y. K. *J. Am. Chem. Soc.* **2000**, *122*, 6771-6772. (c) Cristóbal-Lecina, E.; Constantino, A.R.; Grabulosa, A.; Riera, A.; Verdaguer, X. *Organometallics* **2015**; *34*: 4989–4993.

(8) Zhang, M.; Buchwald, S. L. *J. Org. Chem.* **1996**, *61*, 4498-4499.

(9) Shibata, T.; Takagi, K. *J. Am. Chem. Soc.* **2000**, *122*, 9852-9853.

(10) For heterogeneous bimetallic catalysts Co/M (M=Rh, Ru) see: K. H. Park, K.H.; Chung, Y.K.; *Adv. Synth. Catal.* **2005**, *347*, 854 – 866; Park, K.H.; Son, S.U.; Chung, Y.K. *Chem. Commun.* **2003**, 1898 – 1899.

(11) Wang, Y.; Xu, L.; Yu, R.; Chen, J.; Yang, Z. *Chem. Commun.* **2012**, *48*, 8183–8185.

(12) (a) Cabot, R.; Lledo, A.; Reves, M.; Riera, A.; Verdaguer, X. *Organometallics* **2007**, *26*, 1134. (b) Gibson, S.E.; Stevenazzi, A. *Angew. Chem. Int. Ed.* **2003**, *42*, 1800–1810.

(13) (a) Tang, Y.; Deng, L.; Zhang, Y.; Dong, G.; Chen, J.; Yang, Z. *Org. Lett.* **2005**, *7*, 593–595. (b) Tang, Y.; Deng, L.; Zhang, Y.; Dong, G.; Chen, J.; Yang, Z. *Org. Lett.* **2005**, *7*, 1657–1659.

(14) Jeong, N.; Hwang, S.H.; Lee, Y.; Chung, Y.K. *J. Am. Chem. Soc.* **1994**, *116*, 3159-3160.

(15) Gibson, S. E.; Johnstone, C.; Stevenazzi, A. *Tetrahedron* **2002**, *58*, 4937-4942.

(16) Sugihara, T.; Yamaguchi, M.; Nishizawa, M. *Chem. Eur. J.* **2001**, *7*, 1589–1595.

(17) Hayashi, M.; Hashimoto, Y.; Yamamoto, Y.; Usuki, J.; Saigo, K. *Angew. Chem. Int. Ed.* **2000**, *39* (3), 631-633.

(18) (a) Chung, Y.K. Heterogeneous Catalytic Pauson-Khand Reaction. In ref 1. Chapter 9, pp 239-273. (b) Kim, S.-W.; Son, S.U.; Lee, S.I.; Hyeon, T.; Chung, Y.K. *J. Am. Chem. Soc.* **2000**, *122* (7), 1550-1551.

(19) (a) For poly(ethylene glycol) stabilized Co nanoparticles, see: Muller, J.-L.; Klankermayer, J.; Leitner, W. *Chem. Commun.* **2007**, 1939-1941. (b) Kim, S.-W.; Son, S.U.; Lee, S.S.; Hyeon, T.; Chung, Y.K. *Chem. Commun.* **2001**, 2212–2213. (c) Son, S.U.; Lee, S.I.; Chung, Y.K.; Kim, S.-W.; Hyeon, T. *Org. Lett.* **2002**, *4*, 277–279.

(20) Son, S.U.; Park, K.H.; Chung, Y.K. *Org. Lett.* **2002**, *4*, 3983–3986.

(21) Muller, J.-L.; Rickers, A.; Leitner, W. *Adv. Synth. Catal.* **2007**, *349*, 287–291.

(22) Cabré, A.; Verdaguer, X., Riera, A. *Synthesis* **2017**, *49*, 3945–3951.

(23) Kwong, F.Y.; Li, Y.M.; Lam, W.H.; Qiu, L.; Chan, K.S.; Chan, A.S.C. *Chem. Eur. J.* **2005**, *11*, 3872-3880.

(24) Lee, H.W.; Chan, A.S.C; Kwong, F.K. *Chem. Commun.* **2007**, 2633-2635.

(25) Garçon, M.; Cabré, A.; Verdaguer, X.; Riera, A. *Organometallics* **2017**, *36*, 1056-1065.

(26) Fager-Jokela, E.; Kaasalainen, E.; Leppänen, K.; Helaja, J. *Tetrahedron* **2008**, *65*, 10381-10387.

Experimental Section

Reactions were carried out under CO in an oven-dried pressure tube. Anhydrous toluene was obtained from commercial suppliers. Reactions were monitored by TLC analysis using Merck silica gel 60 F-254 thin layer plates. Solvents were removed under reduced pressure with a rotary evaporator. Silica gel chromatography was performed using an automated chromatography system (PuriFlash® 430, Interchim). NMR at 400 MHz for ^{1}H and at 101 MHz for ^{13}C. Chemical shifts (δ) are given in ppm and referenced to internal solvent resonances and reported relative to tetramethylsilane (TMS). Coupling constants (*J*) are reported in Hertz (Hz). High-resolution mass spectra (ESI) were recorded on a LC/MSD-TOF G1969A (Agilent Technologies). Enynes **3-1a**,[7c] **3-1b**[7c] and **3-1c**[23] were prepared following the literature. Terminal alkynes **3-1h** and **3-1e** were prepared by following our previously reported procedure.[20]

General procedure for the catalytic Pauson-Khand Reaction.

Method A. In a flame-dried pressure tube containing a magnetic stirrer, the corresponding 1,6-enyne (100 mg, 1.0 equiv.) or alkyne (100 mg, 1 equiv) was dissolved in anhydrous toluene (0.3 M). $Co_2(CO)_8$ (5 mol% or 1 mol% as indicated) was added. In intermolecular reactions norbornadiene or norbornene (5.0 equiv) were also added. The pressure vessel was first purged with N_2 and then with CO (x3). Finally, it was charged with 1-2 bar of CO and heated to 80 ºC. The reaction was stirred overnight. The CO was removed using the vacuum line and the biphasic solution was concentrated under reduced pressure. The crude was purified by column chromatography using hexanes:EtOAc mixtures of increasing polarity.

Method B. Same procedure but MEG (15% v/v) was added to the mixture

General procedure for catalyst recycling in catalytic ethylene glycol-assisted Pauson-Khand Reaction (Method C).

In a flame-dried pressure tube containing a magnetic stirrer, the corresponding alkyne (200 mg, 1.0 equiv.) and alkene (5.0 equiv.) were dissolved in anhydrous toluene (0.3 M). Then, MEG (15% v/v) and $Co_2(CO)_8$ (10 mol%) were added. The pressure vessel was first purged with N_2 and then with CO (x3). Finally, it was charged with 1-2 bar of CO and heated it up to 80 ºC. The reaction was left stirring overnight. Afterwards, the CO was removed in the vacuum line. The biphasic solution was separated and the supernatant phase was collected. The MEG-containing phase was kept in the pressure tube and alkyne (200 mg, 1.0 equiv.), alkene (5.0 equiv.) and freshly anhydrous toluene were added. The same procedure as above was carried out and the reaction was left during 36 h (second cycle). For the third cycle, the methodology was repeated again and the reaction was stirred for 48-72 h. Finally, each organic phase was concentrated under reduced pressure and purified by column chromatography using hexane:EtOAc mixtures of increasing polarity.

Diethyl 6-methyl-5-oxo-3,3a,4,5-tetrahydropentalene-2,2(1H)-dicarboxylate, 3-2a.

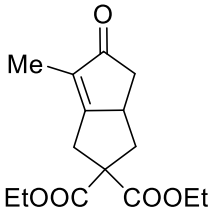

Starting from 0.40 mmol of alkyne **3-1a**; isolated yield; Method A: 91 mg (81%); Method B: 101 mg (90%); colourless oil. **^{1}H NMR** (400 MHz, $CDCl_3$) δ 4.23 (dq, *J* = 15.8, 7.1 Hz, 4H), 3.28 – 3.13 (m, 2H), 2.97 (s, 1H), 2.78 (dd, *J* = 12.7, 7.4 Hz, 1H), 2.65 (ddd, *J* = 17.9, 6.3, 0.8 Hz, 1H), 2.08 (dd, *J* = 17.9, 3.1 Hz, 1H), 1.72 (ddd, *J* = 2.5, 1.7, 1.0 Hz, 3H), 1.65 (t, *J* = 12.6 Hz, 1H), 1.27 (dt, *J* = 9.8, 7.1 Hz, 6H). The analytical data for this compound were in excellent agreement with the reported data.[7c]

6-Methyl-2-tosyl-2,3,3a,4-tetrahydrocyclopenta[c]pyrrol-5(1H)-one, 3-2b.

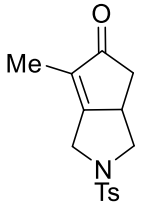

Starting from 0.38 mmol of alkyne **3-1b**; isolated yield; Method A: 92 mg (83%); Method B: 101 mg (91%); off white solid. **^{1}H NMR** (400 MHz, $CDCl_3$) δ 7.78 – 7.69 (m, 2H), 7.40 – 7.33 (m, 2H), 4.24 (d, *J* = 16.1 Hz, 1H), 4.00 (dd, *J* = 6.8, 2.5 Hz, 1H), 3.97 (d, *J* = 2.7 Hz, 1H), 3.01 (s, 1H), 2.65 – 2.54 (m, 2H), 2.44 (s, 3H), 2.07 – 1.98 (m, 1H), 1.68 (ddd, *J* = 2.5, 1.7, 0.9 Hz, 3H). The analytical data for this compound were in excellent agreement with the reported data.[7c]

6-Methyl-3a,4-dihydro-1H-cyclopenta[c]furan-5(3H)-one, 3-2c.

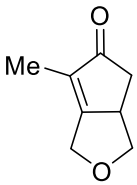

Starting from 0.91 mmol of alkyne **3-1c**; isolated yield; Method A: 59 mg (47%); Method B: 75 mg (60%); pale orange oil. **^{1}H NMR** (400 MHz, $CDCl_3$) δ 4.63 – 4.44 (m, 2H), 4.31 (d, *J* = 5.0 Hz, 1H), 3.18 (d, *J* = 3.8 Hz, 2H), 2.71 – 2.62 (m, 1H), 2.12 (dd, *J* = 18.0, 2.6 Hz, 1H), 1.76 (s, 3H). The analytical data for this compound were in excellent agreement with the reported data.[24]

(4S,7R)-2-(Trimethylsilyl)-3a,4,7,7a-tetrahydro-1H-4,7-methanoinden-1-one, 3-2d.

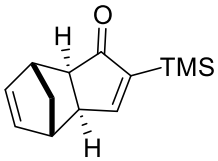

Starting from 1.02 mmol of alkyne **3-1d**; isolated yield; Method A: 167 mg (75%); Method B: 220 mg (99%); off-white solid. Method C: 1st cycle: 421 mg (95%); 2nd cycle: 400 mg (90%); 3rd cycle 315 mg (71%). **^{1}H NMR** (400 MHz, $CDCl_3$) δ 7.59 (dd, *J* = 2.5, 0.5 Hz, 1H), 6.28 – 6.23 (m, 1H), 6.22 – 6.16 (m, 1H), 2.91 (d, *J* = 2.1 Hz, 1H), 2.84 (ddt, *J* = 5.2, 2.3, 1.1 Hz, 1H), 2.69 (dtt, *J* = 3.1, 1.6, 0.8 Hz, 1H), 2.28 (ddd, *J* = 5.2, 1.6, 1.1 Hz, 1H), 1.39 – 1.36 (m, 1H), 1.20 – 1.16 (m, 1H), 0.17 (s, 9H). The analytical data for this compound were in excellent agreement with the reported data.[22]

***tert*-Butyl (((4S,7R)-1-oxo-3a,4,7,7a-tetrahydro-1H-4,7-methanoinden-2-yl)methyl)carbamate, 3-2e.**

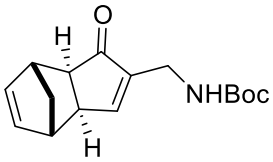

Starting from 0.64 mmol of alkyne **3-1e**; isolated yield; Method A: 106 mg (60%); Method B: 164 mg (93%); pale orange oil. Method C: 1st cycle: 349 mg (99%); 2nd cycle: 318 mg (93%); 3rd cycle 300 mg (85%). **^{1}H NMR** (400 MHz, $CDCl_3$) δ 7.34 (s, 1H), 6.29 (dd, *J* = 5.6, 3.1 Hz, 1H), 6.20 (dd, *J* = 5.7, 3.0 Hz, 1H), 5.01 (s, 1H), 3.87 (d, *J* = 6.0 Hz, 2H), 2.91 (s, 1H), 2.78 – 2.72 (m, 1H), 2.72 – 2.66 (m, 1H), 2.31 (dt, *J* = 5.0, 1.4 Hz, 1H), 1.43 (s, 9H), 1.30 – 1.18 (m, 2H). The analytical data for this compound were in excellent agreement with the reported data.[22]

(4S,7R)-2-((Phenylthio)methyl)-3a,4,7,7a-tetrahydro-1H-4,7-methanoinden-1-one, 3-2f.

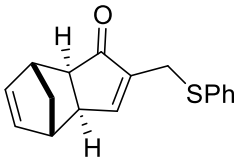

Starting from 0.67 mmol of alkyne **3-1f**; isolated yield; Method A: 142 mg (79%); Method B: 167 mg (93%); pale orange oil. **^{1}H NMR** (400 MHz, $CDCl_3$) δ 7.37 – 7.21 (m, 5H), 7.20 – 7.16 (m, 1H), 6.25 (dd, *J* = 5.6, 3.1 Hz, 1H), 6.18 (dd, *J* = 5.6, 3.0 Hz, 1H), 3.73 – 3.56 (m, 2H), 2.91 (d, *J* = 2.9 Hz, 1H), 2.70 – 2.65 (m, 1H), 2.58 (d, *J* = 2.9 Hz, 1H), 2.31 (dq, *J* = 5.0, 1.2 Hz, 1H), 1.31 (dd, *J* = 9.5, 2.1 Hz, 1H), 1.08 (d, *J* = 9.4 Hz, 1H). The analytical data for this compound were in excellent agreement with the reported data.[22]

(4S,7R)-2-Phenyl-3a,4,7,7a-tetrahydro-1H-4,7-methanoinden-1-one, 3-2g.

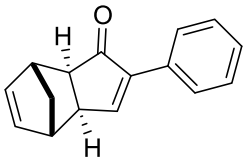

Starting from 0.98 mmol of alkyne **3-1g**; isolated yield; Method A: 194 mg (89%); Method B: 198 mg (91%); off-white solid. **^{1}H NMR** (400 MHz, $CDCl_3$) δ 7.73 – 7.67 (m, 3H), 7.41 – 7.32 (m, 3H), 6.34 (dd, *J* = 5.6, 3.1 Hz, 1H), 6.26 (dd, *J* = 5.6, 2.9 Hz, 1H), 3.03 (s, 1H), 2.87 – 2.82 (m, 1H), 2.79 (s, 1H), 2.48 (dt, *J* = 5.1, 1.4 Hz, 1H), 1.43 (dt, *J* = 9.4, 1.6 Hz, 1H), 1.35 (d, *J* = 9.7 Hz, 1H). The analytical data for this compound were in excellent agreement with the reported data.[25]

4-Methyl-N-(((4S,7R)-1-oxo-3a,4,7,7a-tetrahydro-1H-4,7-methanoinden-2-yl)methyl) benzenesulfonamide, 3-2h.

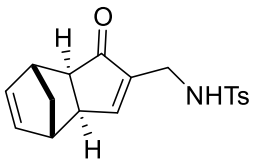

Starting from 0.48 mmol of alkyne **3-1h**; isolated yield; Method A: 126 mg (80%); Method B: 134 mg (85%); pale orange oil. Method C: 1st cycle: 312 mg (99%); 2nd cycle: 291 mg (92%); 3rd cycle 268 mg (85%). **^{1}H NMR** (400 MHz, $CDCl_3$) δ 7.71 (dd, *J* = 8.3, 2.0 Hz, 2H), 7.31 (d, *J* = 8.8 Hz, 1H), 7.29 – 7.27 (m, 2H), 6.26 (dd, *J* = 5.6, 3.0 Hz, 1H), 6.17 (dd, *J* = 5.6, 3.0 Hz, 1H), 5.10 – 5.02 (m, 1H), 3.76 (d, *J* = 5.9 Hz, 2H), 2.85 – 2.80 (m, 1H), 2.65 – 2.62 (m, 2H), 2.41 (s, 3H), 2.18 (dt, *J* = 4.9, 1.4 Hz, 1H), 1.32 (dt, *J* = 9.6, 1.5 Hz, 1H), 1.06 – 0.99 (m, 1H). **^{13}C NMR** (101 MHz, $CDCl_3$) δ 209.07, 161.35, 144.81, 143.55, 138.43, 136.99, 136.78, 129.70, 127.19, 52.83, 48.16, 43.55, 42.76, 41.13, 39.16,

21.49. **HRMS** (ESI): *m/z* $[M+H]^+$ calcd for $C_{18}H_{20}NO_3S$: 330.1158; found: 330.1165. **IR** (ATR-FTIR): 3270, 2977, 2371, 2256, 1692, 1325, 1160 cm^{-1}.

(4S,7R)-2-(((*tert*-Butyldimethylsilyl)oxy)methyl)-3a,4,7,7a-tetrahydro-1H-4,7-methanoinden-1-one, 3-2i.

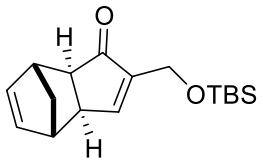

Starting from 0.59 mmol of alkyne **3-1i**; isolated yield; Method A: 96 mg (56%); Method B: 120 mg (70%); colourless oil. **^{1}H NMR** (400 MHz, $CDCl_3$) δ 7.38 (q, *J* = 2.2 Hz, 1H), 6.29 (dd, *J* = 5.6, 3.1 Hz, 1H), 6.20 (dd, *J* = 5.6, 3.0 Hz, 1H), 4.35 (td, *J* = 2.1, 0.9 Hz, 2H), 2.91 (s, 1H), 2.77 (s, 1H), 2.71 (s, 1H), 2.35 – 2.30 (m, 1H), 1.40 (d, *J* = 9.3 Hz, 1H), 1.27 – 1.24 (m, 1H), 0.92 (s, 9H), 0.08 (s, 6H). The analytical data for this compound were in excellent agreement with the reported data.[23]

(4S,7R)-2-Cyclopropyl-3a,4,7,7a-tetrahydro-1H-4,7-methanoinden-1-one, 3-2j.

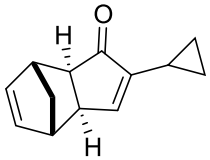

Starting from 1.51 mmol of alkyne **3-1j**; isolated yield; Method A: 211 mg (75%); Method B: 203 mg (72%); colourless oil. **^{1}H NMR** (400 MHz, $CDCl_3$) δ 6.85 (d, *J* = 2.8 Hz, 1H), 6.26 (dd, *J* = 5.6, 3.0 Hz, 1H), 6.19 (dd, *J* = 5.6, 3.0 Hz, 1H), 2.90 (p, *J* = 1.5 Hz, 1H), 2.69 – 2.57 (m, 2H), 2.29 (dt, *J* = 5.0, 1.4 Hz, 1H), 1.56 (dddt, *J* = 9.4, 8.5, 5.2, 1.0 Hz, 1H), 1.35 (dp, *J* = 9.2, 1.6 Hz, 1H), 1.19 (dt, *J* = 9.3, 1.6 Hz, 1H), 0.86 – 0.77 (m, 2H), 0.60 (ddt, *J* = 6.6, 3.8, 1.3 Hz, 2H). The analytical data for this compound were in excellent agreement with the reported data.[24]

(4R,7S)-2-(Trimethylsilyl)-3a,4,5,6,7,7a-hexahydro-1H-4,7-methanoinden-1-one, 3-3.

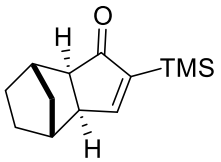

Starting from 1.02 mmol of alkyne **3-1d**; isolated yield; Method A: 211 mg (94%); Method B: 220 mg (98%); colourless oil. **^{1}H NMR** (400 MHz, $CDCl_3$) δ 7.56 (d, *J* = 2.6 Hz, 1H), 2.65 (dd, *J* = 5.4, 2.5 Hz, 1H), 2.38 (s, 1H), 2.17 (d, *J* = 4.2 Hz, 1H), 2.12 (d, *J* = 5.3 Hz, 1H), 1.66 (ddd, *J* = 16.5, 8.5, 4.1 Hz, 1H), 1.60 – 1.57 (m, 1H), 1.54 (s, 9H), 1.27 (d, *J* = 10.0 Hz, 3H), 0.17 (s, 9H). The analytical data for this compound were in excellent agreement with the reported data.[26]

Chapter 4

Total synthesis of (*R*)-Sarkomycin Methyl Ester *Via* Regioselective Intermolecular Pauson-Khand Reaction and Iridium-Catalyzed Asymmetric Isomerization

(R)-Sarkomycin **4-1**, first isolated in 1953 from the soil microorganism *Streptomyces erythrochromogenes*,[1] is a cyclopentenone that rapidly gained relevance not only for its antibiotic activity, but also for its strong inhibitory effect on several human tumors and carcinoma cell lines.[2,3] Due to its chemical instability,[4] several stable derivatives such as its methyl ester[5] **4-2** or the cyclic lactone **4-3**, so called cyclosarkomycin,[6] have been developed.

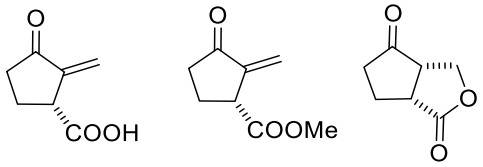

4-1 **4-2** **4-3**

Figure 4.1. Natural sarkomycin **4-1** and stable derivatives.

Although its structure is relatively simple, with only one stereogenic center,[7] a large number of synthetic approaches toward sarkomycin (or sarkomycin derivatives) have been reported, being often used as a benchmark for new synthetic methodologies. Some of the syntheses addressed the racemic mixture and involves a relatively large number of steps.[8] In other cases, the desired enantiopurity was obtained via: (a) kinetic resolution,[9] (b) the chiral auxiliary approach,[10] or (c) classical racemic resolution.[11] However, most of these processes gave low overall yields. A recent report by Von Zezschwitz and co-workers[12] was the first to use asymmetric catalysis. They described a five-step sequence based on the Rh-catalyzed asymmetric conjugate addition of a hexenyl chain to cyclopentenone. However, none of the numerous syntheses of sarkomycin published so far have exploited the Pauson-Khand reaction (PKR),[13] a text-book method for the construction of cyclopentanic compounds.[14] In most cases, they used cyclopentanic starting material. We envisioned that the cyclopentane ring of *(R)*-sarkomycin could be rapidly assembled by an intermolecular PKR[15] using an appropriate internal alkyne and ethylene. The regioselectivity of internal alkynes in the PKR has been widely studied[16] and has proven useful in the synthesis of natural compounds such as prostaglandins and phytoprostanes B1.[17]

We hypothesized that the PKR of alkyne **4-4** with ethylene would afford adduct **4-5**. The underlying challenge was the regioselective control of the reaction. In the PKR of internal alkynes with similar steric hindrance for each substituent, regioselectivity is influenced mostly by electronic factors.[16] According to previous studies, the most electron-withdrawing group (the methoxycarbonyl, in this case) should go to the β position. Therefore, we assumed that, using **4-4** as alkyne, the major isomer would be enone **4-5**. We hypothesized that the

asymmetric hydrogenation would lead to cyclopentanone **4-6**, which after hydrolysis and elimination, would afford (*R*)-sarkomycin methyl ester **4-2** (Scheme 4.1).

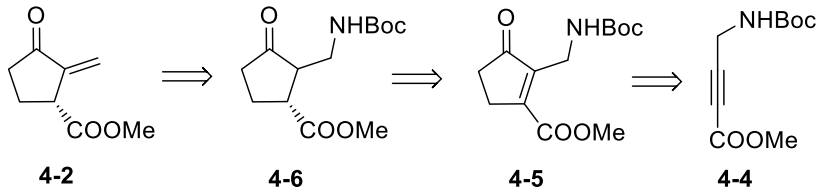

Scheme 4.1. Retrosynthetic analysis of (*R*)-Sarkomycin methyl ester **4-2**.

Here, we report a total five-step synthesis of *(R)*-sarkomycin methyl ester from acyclic precursors, using a regioselective intermolecular PKR. During our search for appropriate asymmetric hydrogenation conditions, we uncovered an unprecedented iridium-catalyzed asymmetric isomerization of allylcarbamate **4-5** that allowed us to obtain *(R)*-sarkomycin methyl ester in excellent enantiomeric excess. The iridium-catalyzed isomerization of allyl amides[18] has received very little attention in comparison to other substrates such as allyl alcohols and allyl amines.[19-22] Moreover, to the best of our knowledge, this is the first example of an asymmetric isomerization of allyl carbamates to date.

The starting material **4-4,** according to our retrosynthetic analysis, was prepared in a straightforward manner in multigram scale by carboxylation of *N*-Boc-propargyl amine with CO_2, followed by esterification in 74% overall yield (Scheme 4.2).

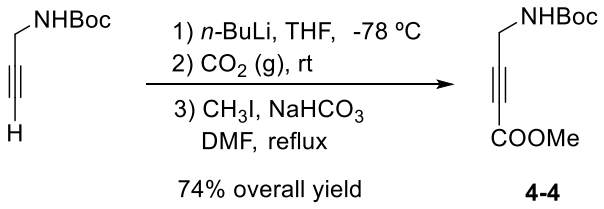

Scheme 4.2. Synthesis of internal alkyne **4-4** from *N*-Boc-propargyl amine.

With alkyne **4-4** in hand, its cobalt hexacarbonyl complex was quantitatively prepared by treatment with $Co_2(CO)_8$ in toluene. After concentration *in vacuo*, the complex was submitted to several PKR conditions (Table 4.1). Although the standard thermal conditions under 6 barG pressure of ethylene gave only trace amounts of the product, we were pleased to see that by using *N*-methylmorpholine *N*-oxide (NMO) as promoter it was obtained in 60-75%

yields with complete regioselectivity (Table 4.1, entry 1). Inspired by Baran's work,[15b] we recently reported a new synthetic protocol for intermolecular PKR using ethylene glycol (MEG) as an additive.[23] Adding 15% v/v of ethylene glycol to the reaction mixture, the yield increased up to 85% (Table 4.1, entry 2). Moreover, the crude material was cleaner and the work-up much easier. We believe that the ethylene glycol behaves as a chelating agent reducing the activating effect of NMO and allowing coordination of the alkene before decomposition of the complex.

Table 4.1. Synthesis of cyclopentenone **4-5** using Pauson-Khand reaction with ethylene.

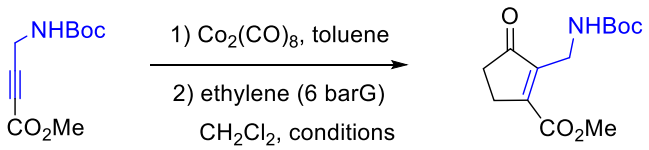

4-4 **4-5**

entry	conditions	additives	yeld (%)[a]
1	NMO (10 equiv), rt, 4 h	-	60-75
2	NMO (6 equiv), rt, 4 h	4 Å MS, MEG	85

[a] Isolated yield.

With the Pauson-Khand adduct **4-5** in hand, we then studied its hydrogenation into the corresponding cyclopentanone **6**. Catalytic hydrogenation using Pd/C afforded the racemic methyl ester **4-6** (Table 4.2, entry 1). Somewhat surprisingly for a tetrasubstituted olefin, the hydrogenation took place in quantitative yield at 3 barG or even with a hydrogen balloon. The stereochemistry of the hydrogenated product was determined to be *trans* by 2D-NMR spectroscopy. In some occasions we have observed the presence of a mixture of *cis* and *trans* stereoisomers. However, the former equilibrates to the more stable *trans* under acid catalysis and even on standing in chloroform solution.

Table 4.2. Hydrogenation/isomerization of **4-6.**

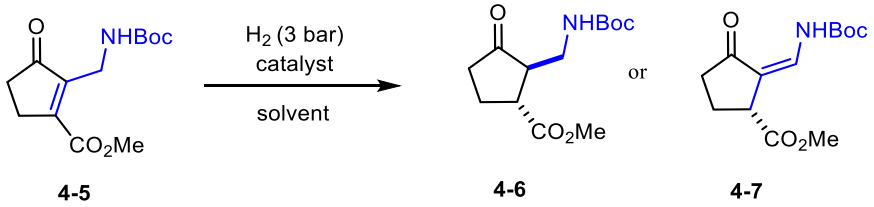

4-5 **4-6** **4-7**

entry	catalyst	mol %	solvent	conv (%)	yield[c]	ee (%)[b]
1	**Pd/C**	20	CH_2Cl_2	100	**4-6**, 100	-
2[a]	**4-8**	5	CH_2Cl_2	53	**4-6**, nd	(*R*)-49
3[a]	**4-9**	5	CH_2Cl_2	100	**4-6,** nd	(*R*)-51
4	**4-10a**	7	THF	15	nd	nd
5	**4-11a**	7	THF	21	nd	nd
6	**4-12a**	7	THF	70	**4-7,** 56	(*R*)-93
7	**4-13a**	7	THF	55	**4-7,** 45	(*R*)-71
8[a]	**4-12a**	7	THF	68	**4-7**, 50	(*R*)-93
9	**4-12b**	7	THF	75	**4-7**, 64	(*R*)-95
10	**4-12c**	7	THF	-	-	-
11	**4-12b**	12	THF	88	**4-7**, 70	(*R*)-95
12	**4-12b**	12	CH_2Cl_2	93	**4-7,** 73	(*R*)-99

[a] 50 barG of H_2 were used. [b]Measured by HPLC Chiralpak IA on compound **4-6.** [c]Isolated yield.

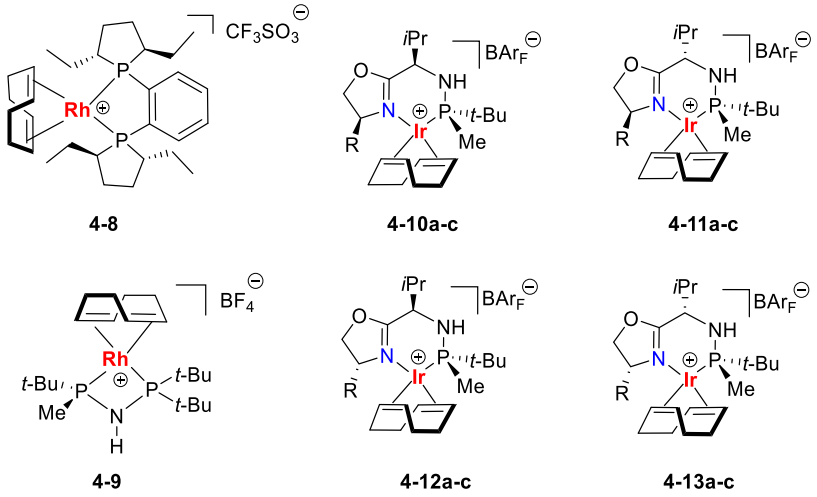

4-8 **4-10a-c** **4-11a-c**

4-9 **4-12a-c** **4-13a-c**

Scheme 4.3. Catalysts used in the hydrogenation screening. a: R = *i*Pr; b: R = Ph; c: R = *t*-Bu.

With pure **4-5** in hand, we performed a catalyst screening for the corresponding asymmetric hydrogenation. We chose as standard conditions: 50 barG of hydrogen, 5 mol % catalyst loading and stirring overnight at room temperature. Rh[(R,R)Et-DuPhos (COD)]CF_3SO_3 **4-8,** the standard Rh catalyst for asymmetric hydrogenation, afforded poor conversion (53%) with moderate enantiomeric excess (49%) (Table 4.2, entry 2). Using [Rh(COD)(*R*-MaxPHOS)]BF_4 **4-9**,[24] full conversion was achieved, but with moderate

enantiomeric excess (51%) (Table 4.2, entry 3). We then selected the iridium complexes of the *P,N*- ligands MaxPHOX developed by our group (Scheme 4.3), which are highly active for the asymmetric hydrogenation of cyclic enamides and imines, giving excellent yields and enantioselectivities.[25] These modular P,N ligands have three stereogenic centers, thus allowing the optimization of the stereoselectivity by playing with the four possible diastereoisomers. We started our hydrogenation study with the four diastereomers **4-10-13a** with isopropyl substituents as catalysts. Two of them (**4-10a** and **4-11a**) showed very low (15-20%) conversion. However, unexpectedly, the hydrogenation of **4-5** using **4-12a** and **4-13a** afforded substantial conversion (45-56%) into exocyclic enamine **4-7** with no traces of the hydrogenation product **4-6**. This observation indicates that an unprecedented isomerization process had taken place.[18] Enamine **4-7** was hydrogenated using Pd/C to the desired cyclopentanone **6**, which showed remarkable enantiomeric excess. Comparing the two best catalysts, **4-12a** (Table 4.2, entry 6) outperformed **4-13a** both in terms of conversion and enantioselectivity (Table 4.2, entry 7). An increase of hydrogen pressure to 50 bar, produced only traces of hydrogenated product; enamine **4-7** was still the major product without erosion of the enantioselectivity (Table 4.2, entry 8). We concluded that the *cis* configuration of the two bulky groups (in the oxazoline and the phosphorous atom) was necessary for the isomerization to occur. Of the two catalysts with such a requirement, **4-12a** gave the best enantioselectivity; therefore, its configuration was considered optimum. We then modified the substituent in the oxazoline ring. An increase in steric hindrance by placing a *tert*-butyl group at the oxazoline fragment (catalyst **4-12c**), did not lead to conversion (entry 10). However, when a phenyl group was placed at the oxazoline (catalyst **4-12b**), the conversion increased and, after conversion into **4-6**, the enantiomeric excess rose to 95% ee (Table 4.2, entry 9). Since the reaction was not complete, we increased the catalyst loading to 12 mol % (Table 4.2, entry 11). Finally, when performing the reaction in dichloromethane (Table 4.2, entry 12), **4-6** was obtained in an enantiopure form after hydrogenation of **4-7** with Pd/C (ee > 99).

At first sight, there was no evident driving force for the reaction to occur since the isomerisation led to a seemingly less conjugated product. In order to gain insight into the isomerisation process, DFT calculations were performed (more details in the Experimental Section – Computational details).[26] We found that the isomerization is, in fact, an exergonic process, ΔG = -5.4 kcal·mol^{-1}. The counterintuitive formation of product **7** can be

rationalized by considering two key factors, namely: *i*) conjugation, and *ii*) formation of a strong intramolecular hydrogen bond (Figure 4.2).

In contrast with product **4-5**, in which the nitrogen atom had a slightly pyramidalized geometry, the nitrogen atom in product **4-7** was completely planar. This implies that the nitrogen p-orbital can overlap with the π-orbitals of the double bond. Therefore, there is no actual loss of conjugation upon isomerization, since the fragment that goes from the carbonyl of the cyclopentanone ring to the carbonyl of the Boc group is a completely planar, conjugated π-system. Inspection of the frontier molecular orbitals clearly illustrates this point, with the HOMO and LUMO being a combination of all the aforementioned p-orbitals forming an extended, conjugated π-system.

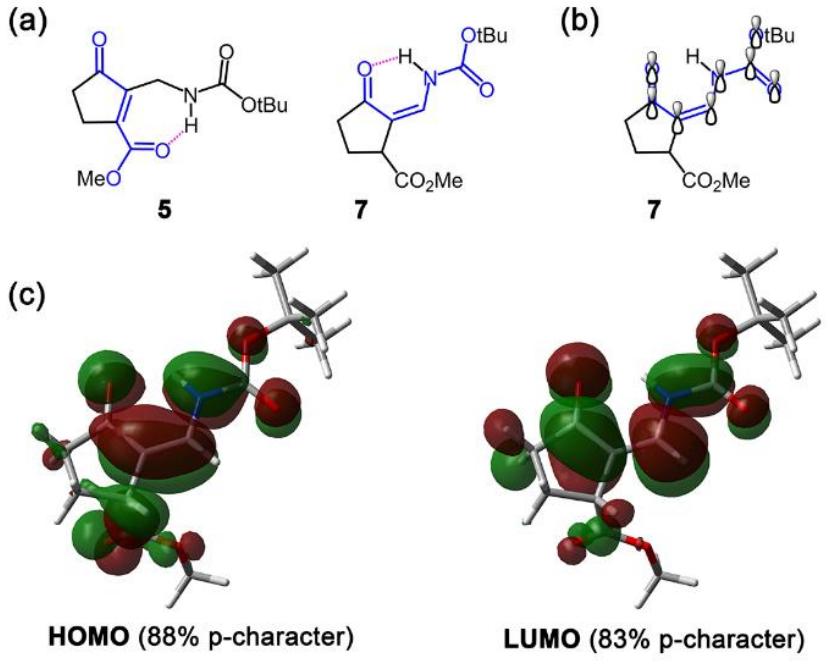

Figure 4.2. (a) Structures of the products before and after isomerisation. The planar conjugated systems are depicted in blue. Hydrogen bonds are shown in magenta. (b) Schematic representation of the conjugated π-system of product **4-7**. (c) HOMO and LUMO of product **4-7** and major atomic contributions to the molecular orbitals.

Intramolecular hydrogen bonds are also responsible for the stabilisation of product **4-7**. The strong hydrogen bond explains the experimental observation of the Z-isomer of the enamide as the only product. Although product **4-5** also has an intramolecular hydrogen bond, NBO calculations and NCI (non-covalent interactions) analysis showed that it is

significantly weaker than the hydrogen bond in product **4-7.** This could also be observed by IR (Scheme 4.4): the NH frequency of **4-7** (3301 cm-1) appears at a shorter wavelength than **4-5** (3401 cm-1) and **4-6** (3439 cm-1).

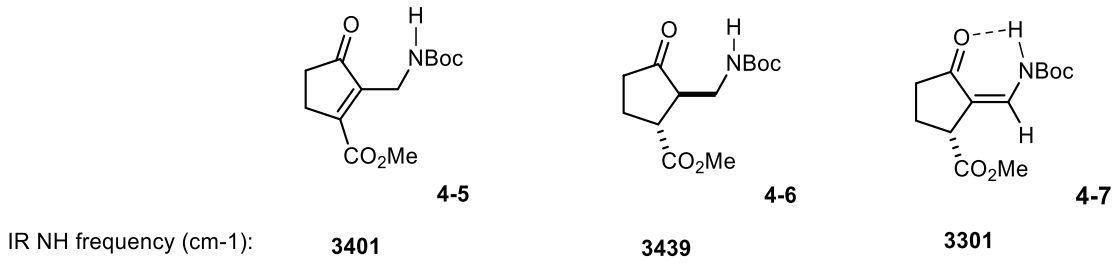

Scheme 4.4. IR frequencies of the NH. The shortest wavelength corresponds to the strongest hydrogen bond.

With the enantiopure compound **4-6** in hand, we then proceeded to perform the last steps (Scheme 4.5). Boc-deprotection was first attempted using TFA or HCl in MeOH. However, a considerable amount of base was then required to neutralize the solution. We realized that the chiral position was easily racemized in basic media and that neutral conditions were required. After much experimentation we found that TMSCl in MeOH were the best reaction conditions for the cleavage of the Boc protecting group. After evaporation of the solvent, the crude product was dissolved in DMF, and $NaHCO_3$ (4.0 equiv) and MeI (4.0 equiv) were added to form the quaternary ammonium salt which eliminated spontaneously. When the reaction was completed by TLC, it was treated with water and extracted with diethyl ether. Due to the volatility of **4-2**, great care had to be taken to evaporate the solvent. The desired (*R*)-sarkomycin methyl ester (**4-2**) was obtained in 45% yield. An enantiomeric excess of 98% was determined by HPLC analysis.

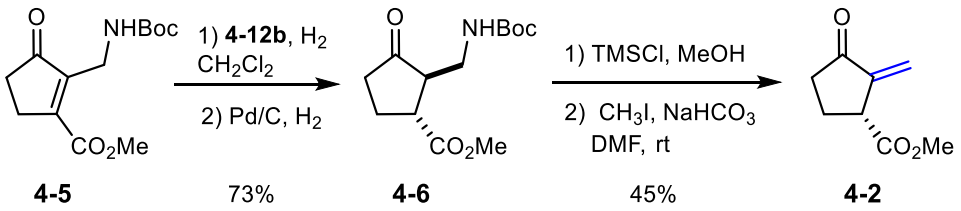

Scheme 4.5. Final steps to afford (*R*)-sarkomycin methyl ester **4-2.**

In summary, we have described an innovative, short and enantioselective synthetic route to the antibiotic (*R*)-sarkomycin methyl ester **4-2**. We were able to concisely build a significant degree of molecular complexity using a novel approach based on high-yielding and remarkably selective steps. Starting from acyclic precursors, the regioselective intermolecular PK afforded the tetrasubsituted enone in excellent yields. The use of ethylene glycol as additive improved the yield significantly. The PK adduct was then subjected to an unprecedented asymmetric isomerization catalyzed by an Ir-MaxPHOX complex. The resulting exocyclic enamine was subsequently hydrogenated and deprotected. Spontaneous elimination of the quaternary ammonium salt afforded the desired natural product as a methyl ester. The unexpected isomerization process catalyzed by a P,N-iridium complex is unprecedented and paves the way to new catalytic isomerization methodologies. The scope of this new transformation is currently being addressed by our group.

References

(1) Umezawa, H.; Takeuchi, T.; Nitta, K.; Okami, Y.; Yamamoto, T.; Yamaoka, S. *J. Antibiot.* **1953**, *6*, 147–152.

(2) (a) Sung, S.-C. *Antibiotics* **1967**, *1*, 156–165,751. (b) S.-C. Sung, J. H. Quastel, *Cancer Res.* **1963**, *23*, 1549–1550; (c) Bickis, I. J.; Creaser, E. H.; Quastel, J. H.; Scholefield, P. G. *Nature* **1957**, *180*, 1109–1111.

(3) Burchenal, J. H.; Crandall, C. E.; Gellhorn, A.; Golbey, R. B.; Karnofsky, D. A.; Magill, G. B.; Rhoads, C. P.; Stock, C. C.; Yorukoglu, S. N. *Cancer Res.* **1956**, *16*, 960–964.

(4) (a) Kondo, S. *J. Antibiot. Ser. A* **1963**, *16*, 210–219. (b) Kondo, S.; Nakamura, H.; Ikeda, Y.; Naganawa, H.; Maeda, K.; Takeuchi, T. *J. Antibiot.* **1997**, *50*, 363–365.

(5) (a) Amri, H.; Rambaud, M.; Villieras, J. *Tetrahedron Lett.* **1989**, *30*, 7381–7382. (b) Kozikowski, A. P.; Stein, P. D. *J. Am. Chem. Soc.* **1982**, *104*, 4023–4024.

(6) (a) Baker, R.; Keen, R. B.; Morris, M. D.; Turner, R. W. *J. Chem. Soc. Chem. Commun.* **1984**, 987–988.; (b) Baraldi, P. G.; Barco, A.; Benetti, S.; Pollini, G. P.; Polo, E.; Simoni, D. *J. Chem. Soc. Chem. Commun.* **1984**, 1049–1050.

(7) Hill, R. K.; Foley, P. J. J.; Gardella, L. A. *J. Org. Chem.* **1967**, *32*, 2330–2335.

(8) (a) Kar, A.; Argade, N. P. *Synthesis* **2005**, 1234–1236. (b) Cohen, T.; Kosarych, Z.; Suzuki, K.; Yu, L. C. *J. Org. Chem.* **1985**, *50*, 2965–2968. (c) Govindan, S. V; Hudlicky, T.; Koszyk, F. J. *J. Org. Chem.* **1983**, *48*, 3581–3583.

(9) Andrau, L.; Lebreton, J.; Viazzo, P.; Alphand, V.; Furstoss, R. *Tetrahedron Lett.* **1997**, *38*, 825–826.

(10) (a) García Martínez, A.; Teso Vilar, E.; García Fraile, A.; de la Moya Cerero, S.; de Oro Osuna, S.; Lora Maroto, B. *Tetrahedron Lett.* **2001**, *42*, 7795–7799. (b) Ikeda, I.; Kanematsu, K. *J. Chem. Soc. Chem. Commun.* **1995**, 453–454. (c) Linz, G.; Weetman, J.; Abdel Hady, A. F.; Helmchen, G. *Tetrahedron Lett.* **1989**, *30*, 5599–5602.

(11) Mikolajczyk, M.; Zurawinski, R.; Kielbasniski, P.; Wieczorek, M. W.; Blaszczyk, J.; Majzner, W. R. *Synthesis* **1997**, 356–365.

(12) Westmeier, J.; Kress, S.; Pfaff, C.; von Zezschwitz, P. *J. Org. Chem.* **2013**, *78*, 10718–10723.

(13) *The Pauson-Khand Reaction: Scope, Variations and Applications;* Rios, R. Ed. Wiley: Chichester, 2012.

(14) (a) Ricker, J. D.; Geary, L. M. *Top. Catal.* **2017**, *60*, 609–619. (b) Jeong, N. In *Comprehensive Organic Synthesis II*; Elsevier: New York, 2014; pp. 1106–1178. (c) Lee, H.-W.; Kwong, F.-Y. *Eur. J. Org. Chem.* **2010**, 789–811. (d) Park, J. H.; Chang, K. M.; Chung, Y. K. *Coord. Chem. Rev.* **2009**, *253*, 2461–2480. (e) Blanco-Urgoiti, J.; Anorbe, L.; Perez-Serrano, L.; Dominguez, G.; Perez-Castells, J. *Chem. Soc. Rev.* **2004**, *33*, 32–42.

(15) Examples of the use of intermolecular PKR in total synthesis of bioactive compounds, see: (a) Aiguabella, N.; Pesquer, A.; Verdaguer, X.; Riera, A. *Org. Lett.* **2013**, *15*, 2696–2699. (b) Su, S.; Rodriguez, R. A.; Baran, P. S. *J. Am. Chem. Soc.* **2011**, *133*, 13922–13925. (c) Iqbal, M.; Evans, P.; Lledo, A.; Verdaguer, X.; Pericas, M. A.; Riera, A.; Loeffler, C.; Sinha, A. K.; Mueller, M. J. *ChemBioChem* **2005**, *6*, 276–280. (d) Rodríguez Rivero, M.; De La Rosa, J. C.; Carretero, J. C. *J. Am. Chem. Soc.* **2003**, *125*, 14992–14993. (e) Bernardes, V.; Kann, N.; Riera, A.; Moyano, A.; Pericàs, M. A.; Greene, A. E. *J. Org. Chem.* **1995**, *60*, 6670–6671.

(16) (a) Fager-Jokela, E.; Muuronen, M.; Khaizourane, H.; Vázquez-Romero, A.; Verdaguer, X.; Riera, A.; Helaja, J. *J. Org. Chem.* **2014**, *79*, 10999–11010. (b) Robert, F.; Milet, A.; Gimbert, Y.; Konya, D.; Greene, A. E. *J. Am. Chem. Soc.* **2001**, *123*, 5396–5400.

(17) (a) Vázquez-Romero, A.; Verdaguer, X.; Riera, A. *Eur. J. Org. Chem.* **2013**, *2013*, 1716–1725. (b) Vázquez-Romero, A.; Cárdenas, L.; Blasi, E.; Verdaguer, X.; Riera, A. *Org. Lett.* **2009**, *11*, 3104–3107. (c) Vázquez-Romero, A.; Rodríguez, J.; Lledó, A.; Verdaguer, X.; Riera, A. *Org. Lett.* **2008**, *10*, 4509–4512.

(18) (a) Trost, B. M.; Cregg, J. J.; Quach, N. *J. Am. Chem. Soc.* **2017**, *139*, 5133–5139. (b) Kavanagh, Y.; Chaney, C. M.; Muldoon, J.; Evans, P. *J. Org. Chem.* **2008**, *73*, 8601–8604. (c) Neugnot, B.; Cintrat, J.-C.; Rousseau, B. *Tetrahedron* **2004**, *60*, 3575–3579. (d) Krompiec, S.; Pigulla, M.; Krompiec, M.; Baj, S.; Mrowiec-Białoń, J.; Kasperczyk, J. *Tetrahedron Lett.* **2004**, *45*, 5257–5261.

(19) For related allyl amine isomerization see: Akutagawa, S. In *Comprehensive Asymmetric Catalysis*, *Vol. 2*. Jacobsen, E.; Pfaltz, A.; Yamamoto, H. Eds. Springer: Berlin, 1999.

(20) Selected reviews about isomerization of allylic alcohols: (a) Li, H.; Mazet, C. *Acc. Chem. Res.* **2016**, *49*, 1232–1241. (b) Mazet, C. *Chimia* **2011**, *65*, 802–805. (c) Mantilli, L.; Mazet, C. *Chem. Lett.* **2011**, *40*, 341–344. (d) Cadierno, V.; Crochet, P.; Gimeno, J. *Synlett* **2008**, *2008*, 1105–1124. (e) Fu, G. C. in *Modern Rhodium-Catalyzed Organic Reactions*; Evans, P. A. Ed., Wiley-VCH: Weinheim, 2005. (f) Uma, R.; Crévisy, C.; Grée, R. *Chem. Rev.* **2003**, *103*, 27–52. (g) van der Drift, R. C.; Bouwman, E.; Drent, E. *J. Organomet. Chem.* **2002**, *650*, 1–24.

(21) Selected examples of enantioselective isomerization of primary allylic alcohols, see: (a) Li, H.; Mazet, C. *J. Am. Chem. Soc.* **2015**, *137*, 10720–10727. (b) Li, H.; Mazet, C. *Org. Lett.* **2013**, *15*, 6170–6173. (c) Jia-Qi, L.; Byron, P.; G., A. P. *Chem. – A Eur. J.* **2011**, *17*, 11143–11145.

(22) For other iridium-catalyzed isomerization of allylic alcohols, see: (a) Erbing, E.; Vázquez-Romero, A.; Bermejo-Gómez, A.; Platero-Prats, A. E.; Carson, F.; Zou, X.; Tolstoy, P.; Martín-Matute, B. *Chem. - A Eur. J.* **2016**, *22*, 15659–15663. (b) Gómez, A. B.; Erbing, E.; Batuecas, M.; Vázquez-Romero, A.; Martín-Matute, B. *Chem. - A Eur. J.* **2014**, *20*, 10703–10709..

(23) Cabré, A.; Verdaguer, X.; Riera, A. *Synth.* **2017**, *49*, 3945–3951.

(24) (a) Revés, M.; Ferrer, C.; León, T.; Doran, S.; Etayo, P.; Vidal-Ferran, A.; Riera, A.; Verdaguer, X. *Angew. Chem. Int. Ed. Engl.* **2010**, *49*, 9452–9455. (b) Cristóbal-Lecina, E.; Etayo, P.; Doran, S.; Revés, M.; Martín-Gago, P.; Grabulosa, A.; Costantino, A. R.; Vidal-Ferran, A.; Riera, A.; Verdaguer, X. *Adv. Synth. Catal.* **2014**, *356*, 795–804.

(25) (a) Salomó, E.; Orgué, S.; Riera, A.; Verdaguer, X. *Angew. Chem, Int. Ed.* **2016**, *55*, 7988–7992. (b) Salomó, E.; Prades, A.; Riera, A.; Verdaguer, X. *J. Org. Chem.* **2017**, *82*, 7065–7069.

(26) Frisch, M. J.; Trucks, G. W.; Schlegel, H. B.; Scuseria, G. E.; Robb, M. A.; Cheeseman, J. R.; Scalmani, G.; Barone, V.; Mennucci, B.; Petersson, G. A.; Nakatsuji, H.; Caricato, M.; Li, X.; Hratchian, H. P.; Izmaylov, A. F.; Bloino, J.; Zheng, G.; Sonnenberg, J. L.; Hada, M.; Ehara, M.; Toyota, K.; Fukuda, R.; Hasegawa, J.; Ishida, M.; Nakajima, T.; Honda, Y.; Kitao, O.; Nakai, H.; Vreven, T.; Montgomery, J. A., Jr.; Peralta, J. E.; Ogliaro, F.; Bearpark, M.; Heyd, J. J.; Brothers, E.; Kudin, K. N.; Staroverov, V. N.; Kobayashi, R.; Normand, J.; Raghavachari, K.; Rendell, A.; Burant, J. C.; Iyengar, S. S.; Tomasi, J.; Cossi, M.; Rega, N.; Millam, J. M.; Klene, M.; Knox, J. E.; Cross, J. B.; Bakken, V.; Adamo, C.; Jaramillo, J.; Gomperts, R.; Stratmann, R. E.; Yazyev, O.; Austin, A. J.; Cammi, R.; Pomelli, C.; Ochterski, J. W.; Martin, R. L.; Morokuma, K.; Zakrzewski, V. G.; Voth, G. A.; Salvador, P.; Dannenberg, J. J.; Dapprich, S.; Daniels, A. D.; Farkas, Ö.; Foresman, J. B.; Ortiz, J. V.; Cioslowski, J.; Fox, D. J. *Gaussian 09, Revision D.01*; Gaussian, Inc., Wallingford, CT, 2009.

Experimental Section

Materials

Unless otherwise indicated, materials were obtained from commercial suppliers and used without further purification. All reactions that required anhydrous conditions were performed in dried glassware under a dry nitrogen atmosphere. Anhydrous and deoxygenated dichloromethane used in the Pauson-Khand reaction was taken from a solvent purification system (SPS PS-MD-3). Solvents were removed under reduced pressure with a rotary evaporator. Silica gel chromatography was performed using an automated chromatography system (PuriFlash® 430, Interchim). MBraun UNILAB glove box system was used for the iridium-catalyzed asymmetric isomerization. Synthesis of phosphinous acid borane was carried out as previously described by us.[1]

Instrumentation

NMR spectroscopy: ^{1}H, ^{13}C, ^{31}P and 2D-NMR spectra were recorded on the NMR spectrometers of the *Centres Científics i Tecnològics de la Universitat de Barcelona*. The employed spectrometers were a Varian Mercury 400 MHz. Chemical shifts (δ) were referenced to internal solvent resonances and reported relative to TMS (tetramethylsilane). The coupling constants (*J*) are reported in Hertz (Hz). The following abbreviations are used to define multiplicities: s (singlet), d (doublet), t (triplet), q (quadruplet), dd (doublet of doublets), ddd (doublet of doublets of doublets), dt (doublet of triplets), td (triplet of doublets), tdt (triplet of doublets of triplets), dq (doublet of quadruplets), m (multiplet), br s (broad signal). The peaks marked with a * correspond to residual solvents.

High Resolution Mass Spectrometry: High resolution ESI-MS spectra were recorded in an LC/MSD-TOF G1969A (Agilent Technologies) of the *Centres Científics i Tecnològics de la Universitat de Barcelona.*

IR spectroscopy: IR spectra were measured in a Thermo Nicolet 6700 FT-IR spectrometer using an ATR system, of the Department of Inorganic and Organic Chemistry of the Universitat de Barcelona.

Optical rotations were measured at room temperature (25°C) using a Jasco P-2000 iRM- 800 polarimeter. Concentration is expressed in g/100 mL. The cell sized 10 cm long and had 1 mL of capacity, measuring λ was 589 nm, which corresponds to a sodium lamp.

Melting points were determined using a Büchi melting point apparatus and were not corrected.

[1] (a) León, T.; Riera, A.; Verdaguer, X. *J. Am. Chem. Soc.* **2011**, *133*, 5740-5743 (b) Verdaguer, X.; Orgué, S.; Flores, A.; Biosca, M.; Pàmies, O.; Diéguez, M.; Riera, A. *Chem. Commun.* **2015**, *51*, 17548-17551 (c) Salomó, E.; Orgué, S.; Riera, A.; Verdaguer, X. *Angew. Chem. Int. Ed.* **2016**, *55* (28), 7988-7992.

Experimental procedures of Sarkomycin synthesis

Methyl 4-((tert-butoxycarbonyl)amino]but-2-ynoate, 4-4

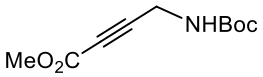

A solution of *N*-Boc-propargylamine[2] (1 g, 6.84 mmol, 1 equiv) in dry THF (23 mL) was placed in a Schlenk flask. *n*-Butyl lithium, 2.5M (3 mL, 7.52 mmol, 1.1 equiv) was added dropwise at -78 ºC. The resulting mixture was stirred for 30 min and allowed to warm up to 0 ºC. Then, a flow of CO_2 was bubbled into the mixture through a needle. The gas -generated by evaporation of dry ice pellets- was dried bubbling through conc. H_2SO_4. The reaction was allowed to warm to 0 ºC under stirring. After 1 hour stirring at 0ºC, the reaction mixture was allowed to warm to room temperature and stirred 2-3 additional hours. When the reaction was complete by TLC, it was quenched with NH_4Cl, diluted with H_2O and washed with EtOAc (x3), to ensure the removal of starting material. Then, the aqueous phase was acidified with HCl 1M to pH = 2, and extracted with EtOAc (x3). The organic layers were dried ($MgSO_4$) and concentrated. The crude, without further purification, was dissolved in anhydrous DMF (30 mL). $NaHCO_3$ (6.86g, 82 mmol, 2.55 equiv) and MeI (6.50 mL, 106 mmol, 3.3 equiv) were added. The mixture was stirred at reflux overnight. Once the reaction was complete, it was quenched with water and extracted with Et_2O (x3). The organic layer was washed with brine, dried over $MgSO_4$ and concentrated under reduced pressure. Purification over SiO_2 using hexane/EtOAc mixtures of increasing polarity afforded 74% yield of a colorless oil (1.1g, 5.06 mmol).

^{1}H NMR (400 MHz, $CDCl_3$) δ 1.45 (s, 9H), 3.78 (s, 3H), 4.07 (br s, 2H), 4.74 (br s, 1H) ppm. The analytical data for this compound were in excellent agreement with the reported data.[3]

Methyl 2-(((*tert*-butoxycarbonyl)amino)methyl)-3-oxocyclopent-1-ene-1-carboxylate, 4-5

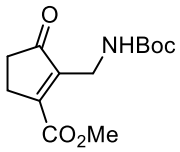

A solution of **4-4** (360 mg, 1.68 mmol, 1.0 equiv) in toluene (2 mL) was added dropwise to a round-bottom flask containing $Co_2(CO)_8$ (1.05 equiv) under stirring. The mixture was stirred at room temperature under nitrogen until the starting alkyne was completely consumed, monitoring by TLC (30-45 minutes, approximately). The crude product was evaporated to dryness and purified by silica gel chromatography with hexanes as eluent. Pure alkyne hexacarbonyl dicobalt complex was obtained in quantitative yield (840 mg, 1.68 mmol).

The corresponding dicobalt complex was dissolved in anhydrous CH_2Cl_2 (11 mL/mmol) and charged to a pressure reactor. Ethylene glycol,[4] (1.71 mL/mmol) and 4Å molecular sieves (317 mg/mmol) were also added. The reactor was purged with nitrogen and charged with ethylene at 5 barG. The reaction was stirred during 30 minutes. A solution of NMO (1.18 g, 10.08 mmol, 6 equiv) in 3 mL of anhydrous CH_2Cl_2 was added in a single portion to the reaction mixture. The reaction was monitored by TLC until completion, when no cobalt complex was observed. Afterwards, the crude was quickly filtered by a short plug of neutral Al_2O_3 and washed three times with EtOAc to eliminate cobalt residues. The solvent was concentrated at low temperature and the crude was purified by column

[2] Chachignon, H.; Scalacci, N.; Petricci, E.; Castagnolo, D. *J. Org. Chem.* **2015**, *80* (10), 5287–5295.
[3] Trost, B. M.; Taft, B. R.; Masters, J. T.; Lumb, J.-P. *J. Am. Chem. Soc.* **2011**, *133* (22), 8502–850
[4] Cabré, A.; Verdaguer, X.; Riera, A. *Synthesis* **2017**, *49*, 3945-3951.

chromatography on SiO_2 using mixtures of hexanes/EtOAc of increasing polarity to afford **4-5** as a colorless oil (389 mg, 85%).

^{1}H NMR (400 MHz, $CDCl_3$) δ: 5.46 (s, 1H), 4.27 (s, 2H), 3.90 (s, 3H), 2.90 – 2.72 (m, 2H), 2.59 – 2.39 (m, 2H), 1.42 (s, 9H) ppm. **^{13}C NMR** (101 MHz, $CDCl_3$) δ: 208.84, 165.21, 156.39, 155.45, 146.19, 79.40, 52.52, 34.76, 34.15, 28.33, 26.68 ppm. **HRMS** (ESI) Calculated for $C_{13}H_{19}NO_5$ $[M+H]^+$: 270.1338; Found: 270.1336. **IR** (ATR) ν_{max} = 3436, 3401 (NH), 2977, 1706 cm^{-1}.

Methyl 2-(((*tert*-butoxycarbonyl)amino)methyl)-3-oxocyclopentane-1-carboxylate, 4-*rac*-6.

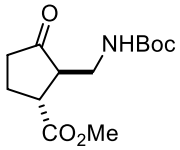

Pd/C 20% (12.7 mg, 20 mol %) was added to a solution of compound **4-7** (160 mg, 0.594 mmol, 1.0 equiv) in CH_2Cl_2 (2 mL). The suspension was introduced into a pressure reactor which was purged and charged with 3 barG of H_2. After stirring overnight at room temperature, the crude was filtered through a 0.2 μm HPLC Nylon filter and evaporated yielding **4-*rac*-6** as a colorless oil (161 mg, quantitative yield).

^{1}H NMR (400 MHz, $CDCl_3$) δ: 4.95 (br s, 1H), 3.76 (s, 3H), 3.54 – 3.31 (m, 2H), 2.91 (td, *J* = 10.9, 6.9 Hz, 1H), 2.73 – 2.58 (m, 1H), 2.48 (ddt, *J* = 18.8, 9.0, 1.8 Hz, 1H), 2.40 – 2.29 (m, 1H), 2.20 (ddd, *J* = 19.2, 10.8, 8.9 Hz, 1H), 1.97 (dtd, *J* = 12.4, 10.8, 8.8 Hz, 1H), 1.43 (s, 9H) ppm. **^{13}C NMR** (101 MHz, $CDCl_3$) δ: 216.73, 174.22, 155.94, 79.35, 53.40, 52.24, 44.59, 39.05, 37.48, 28.33, 24.59 ppm. **HRMS** (ESI) calculated for $C_{13}H_{21}NO_5$ 272.1498, found 272.1503 $[M+H]^+$. **IR** (ATR-FTIR) ν_{max} = 3439 (NH), 2967, 1733, 1704 cm^{-1}

Methyl (*1R,2R*)-2-(((*tert*-butoxycarbonyl)amino)methyl)-3-oxocyclopentane-1-carboxylate, 4-(*R*)-6 (via asymmetric hydrogenation).

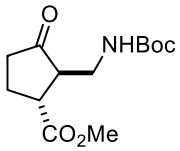

Rh[(*R*)-MaxPHOS) (COD)]BF_4 **4-9** (3 mg, 5 mol %) compound **4-7** (29 mg, 0.107 mmol, 1.0 eq.) in CH_2Cl_2 (1 mL). The suspension was introduced into a pressure reactor which was purged and charged with 50 barG of H_2. After stirring overnight at room temperature, the crude was filtered through a small plug of silica and evaporated yielding **4-6** as only product (100% conversion). The enantiomeric excess was measured by HPLC (52% ee).

Methyl (*1R,2R*)-2-(((*tert*-butoxycarbonyl)amino)methyl)-3-oxocyclopentane-1-carboxylate, 4-(*R*)-6 (via asymmetric isomerization and hydrogenation).

a) Methyl (*R,Z*)-2-(((tert-butoxycarbonyl)amino)methylene)-3-oxocyclopentane-1-carboxylate, **4-7**.

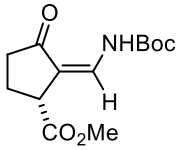

Compound **5** (1.0 equiv) and catalyst **4-14b** (12 mol %) were placed in a glass tube inside a dry box and dissolved in anhydrous CH_2Cl_2 (0.1 M). The mixture was introduced into a pressure reactor which was purged and charged with H_2 (3 barG). The reaction was stirred 48 hours at room temperature. The crude product was concentrated under vacuum and chromatographed on SiO_2 using mixtures of hexanes/AcOEt of increasing polarity affording **4-7** as an oil in 73% yield..

^{1}H NMR (400 MHz, $CDCl_3$) δ: 10.23 (d, *J* = 11.5 Hz, 1H), 7.31 (d, *J* = 11.6 Hz, 1H), 3.73 (d, *J* = 0.5 Hz, 3H), 3.69 (ddd, *J* = 8.0, 4.9, 1.5 Hz, 1H), 2.64 – 2.49 (m, 1H), 2.40 – 2.24 (m, 2H), 2.22 – 2.10 (m, 1H), 1.50 (s, 9H) ppm. **^{13}C NMR** (101 MHz, $CDCl_3$) δ: 207.34, 174.15, 135.89, 82.48, 52.46, 44.23, 37.84, 28.21, 24.43 ppm. **HRMS** (ESI) calculated for $C_{13}H_{19}NO_5$ 270.1336, found 270.1341 $[M+H]^+$. **IR** (ATR-FTIR) ν_{max} = 3301 (NH), 3025, 1731, 1689, 1606 cm^{-1}.

b) Hydrogenation of optically enriched **4-7**.

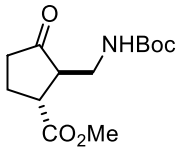

Pd/C 20% (12.7 mg, 20 mol %) was added to a solution of compound **4-7** (160 mg, 0.594 mmol, 1.0 eq.) in MeOH (2 mL). The suspension was introduced into a pressure reactor which was purged and charged with 50 barG of H_2. After 48 h stirring at room temperature, the crude was filtered through a 0.2 µm HPLC Nylon filter and evaporated yielding **4-6** as a colorless oil (161 mg, quantitative yield). The enantiomeric excess was measured by HPLC. (99% ee).

[α]$_D$: -19.0 (c 0.25, $CHCl_3$).
HPLC: CHIRALPAK IA. Heptane/EtOH 90:10, 1 mL/min, λ = 210 nm. $t_{(R)}$ = 17.2 min, $t_{(S)}$ = 20,3 min.

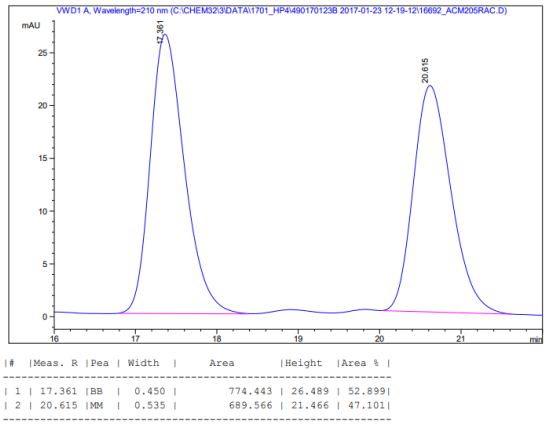

#	Meas. R	Pea	Width	Area	Height	Area %
1	17.361	BB	0.450	774.443	26.489	52.899
2	20.615	MM	0.535	689.566	21.466	47.101

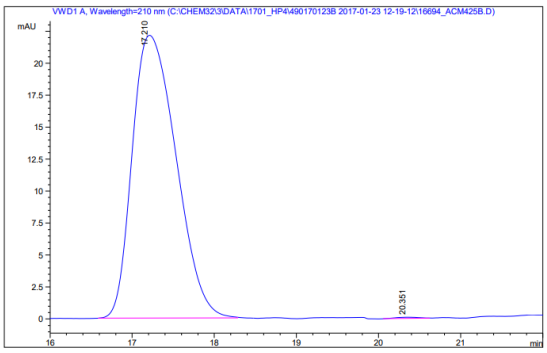

#	Meas. R	Pea	Width	Area	Height	Area %
1	17.210	BB	0.594	822.478	22.128	99.740
2	20.351	MM	0.254	2.147	0.102	0.260

Methyl (*R*)-2-methylene-3-oxocyclopentane-1-carboxylate, 4-2.

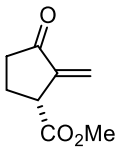

In a glass vial closed with a septum, compound **4-(*R*)-6** (174 mg, 0.64 mmol, 1 equiv) was dissolved in MeOH (5 mL). Trimethylsilyl chloride (5.0 equiv) was added via syringe and the mixture stirred overnight at room temperature. Then, the solvent was evaporated. The crude was dissolved in DMF and $NaHCO_3$ (4.0 equiv) and MeI (4.0 equiv) were added. The suspension was stirred at room temperature. After 17 hours, the reaction mixture was diluted with H_2O was extracted (x2) with diethyl ether. The organic phase was evaporated with N_2 due to the volatility of the product. Compound **2** was obtained in 45% yield (determined by NMR using 1,4-dimethoxybenzene as internal standard). Starting from 99% ee **4-(*R*)-6**, the enantiomeric excess of **4-(*R*)-2** was 98% ee. The product can be purified by chromatography on SiO_2 using pentane/ether (3:1) as eluent.

[α]$_D$: -36.0 (c 0.1, $CHCl_3$). **^{1}H NMR** (400 MHz, $CDCl_3$) δ: 6.19 – 6.14 (m, 1H), 5.59 (dd, *J* = 2.4, 0.7 Hz, 1H), 3.78 – 3.70 (m, 4H), 2.62 – 2.51 (m, 1H), 2.41 – 2.34 (m, 1H), 2.33 – 2.26 (m, 1H), 2.24 – 2.12 (m, 1H) ppm. **^{13}C NMR** (101 MHz, $CDCl_3$) δ: 204.51, 172.80, 142.29, 120.39, 52.33, 45.79, 36.66, 22.99 ppm. **HRMS** (ESI) calculated for [$C_8H_{10}O_3Na$] 177.0522, found: 177.0529. **HPLC**: CHIRALPAK IA. Heptane/EtOH 90:10, 1 mL/min, λ = 210 nm. $t_{(R)}$ = 7.99 min, $t_{(S)}$ = 9.02 min. The analytical data for this compound were in excellent agreement with the reported data.[5]

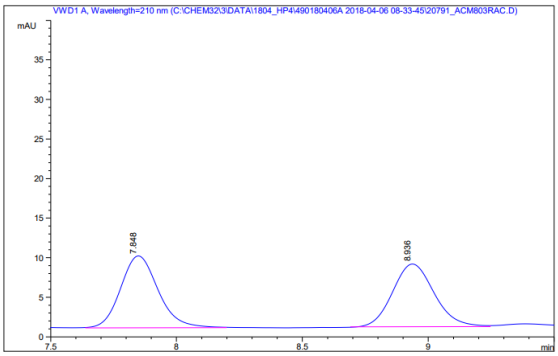

#	Meas. R	Pea	Width	Area	Height	Area %
1	7.848	BB	0.161	94.716	9.099	50.789
2	8.936	MF	0.192	91.775	7.952	49.211

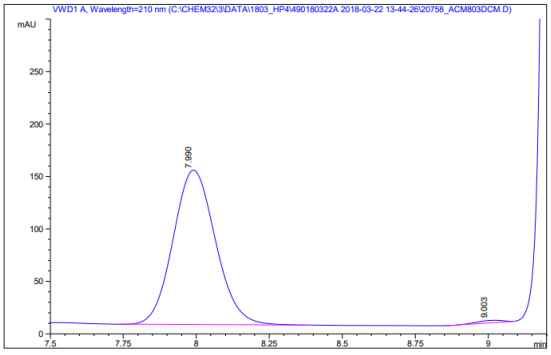

#	Meas. R	Pea	Width	Area	Height	Area %
1	7.990	MM	0.169	1493.137	147.321	98.927
2	9.003	MM	0.133	16.198	2.488	1.073

Experimental procedure for the synthesis of catalyst 4-12b

Following the experimental procedure described in the literature[1c], **4-14b** was afforded after 4 synthetic steps.

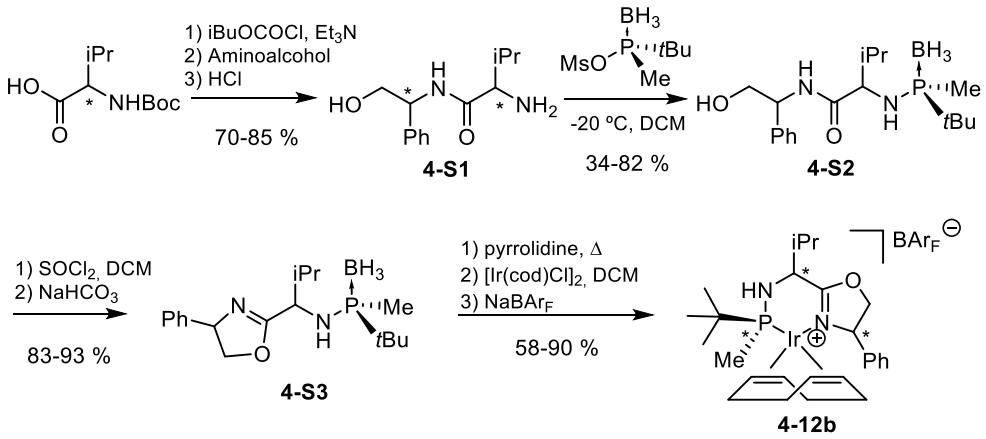

(*R*)-2-amino-N-((*R*)-2-hydroxy-1-phenylethyl)-3-methylbutanamide, 4-S1

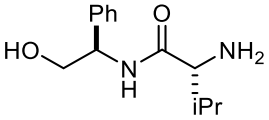

Et_3N (2 eq) and isobutylchloroformate (1.1 equiv) were slowly added to a solution of the N-Boc-protected aminoacid (1 eq, 28 mmol) in THF (0.13 M) at –30 ºC (white solid was observed when adding *i*BuOCOCl). The reaction mixture was stirred for 45 min at –30 ºC, and then the corresponding aminoalcohol (1.1 equiv) was added. The resulting mixture was left stirring at room

[5] Westmeier, J.; Kress, S.; Pfaff, C.; von Zezschwitz, P. *J. Org. Chem.* **2013**, *78* (21), 10718–10723.

temperature overnight. Then the THF was removed under reduced pressure and the oily solid was dissolved in H_2O and EtOAc. The phases were separated and the aqueous layer was extracted twice with EtOAc. The organic layers were combined, dried over $MgSO_4$ and the solvent evaporated under reduced pressure. The crude obtained was dissolved in a 1:1 mixture of MeOH and HCl (3 M, aq) (0.1 M) and stirred overnight at room temperature. The MeOH was removed under vacuum and the resulting aqueous phase was extracted with EtOAc twice to remove impurities. Then EtOAc was added over the aqueous phase and it was basified using NaOH (40%, aq) at 0 ºC. The layers were separated and the aqueous phase was extracted thrice with EtOAc. The organic phases were combined, dried over $MgSO_4$ and the solvent was removed under reduced pressure to yield the deprotected aminoalcohol **4-S1** as white solids (6.16 g, 92% yield). This was used on the next step without further purification.

m.p. 128-130 ºC. **[α]$_D$**: -32 (c 0.8, $CHCl_3$). **^{1}H NMR** (CDCl3, 400 MHz) δ: 8.05 (s, 1H), 7.39 – 7.34 (m, 2H), 7.33 – 7.27 (m, 3H), 5.06 (q, *J* = 5.9 Hz, 1H), 3.90 – 3.86 (m, 2H), 3.34 (s, 1H), 2.40 – 2.28 (m, 1H), 0.98 (d, *J* = 7.0 Hz, 3H), 0.78 (d, *J* = 6.9 Hz, 3H) ppm. **^{13}C NMR** (101 MHz, CDCl3) δ: 139.17, 129.03, 128.01, 126.85, 67.48, 56.32, 19.98, 16.15 ppm. **HRMS** (ESI) Calculated for $C_{13}H_{21}N_2O_2$ $[M+H]^+$: 237.1598; Found 237.1599. **IR** (ATR-FTIR) ν_{max} = 3324, 2892, 2834, 1645. 1543, 1055 cm^{-1}.

(*R*)-2-(((*R*)-*tert*-butyl(methyl)phosphanyl)amino)-N-((*R*)-1-hydroxy-2-phenyl)-3-methylbutanamide borane, 4-S2

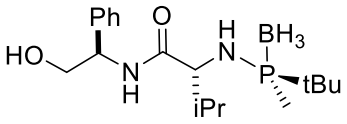

A solution of optically pure *tert*-butyl(methyl)phosphinous acid borane (1 equiv, 7.90 mmol) and methansulfonic anhydride (1.2 equiv) in CH_2Cl_2 (0.2M) was cooled to –20 ºC. To this solution, anhydrous NEt_3 (2.5 eq) was slowly added, and the mixture was stirred 1 h at –20 ºC. The corresponding amine (1.5 equiv) was then added and the solution was stirred overnight at –20 ºC. Water was added and the mixture was allowed to warm to room temperature. The organic layer was separated and the aqueous phase was extracted twice with CH_2Cl_2. The combined extracts were washed with brine and concentrated under reduced pressure. Purification by column chromatography (SiO_2, hexanes:EtOAc) yielded the corresponding compounds as white solids. **4-S2** was obtained as a white solid (1.42 g, 51% yield).

m.p. 126 - 128 ºC. **[α]$_D$**: -40 (c 0.5, $CHCl_3$). **^{1}H NMR** (CDCl3, 400 MHz) δ: 7.38 – 7.34 (m, 4H), 7.31 – 7.27 (m, 1H), 6.66 (d, *J* = 7.5 Hz, 1H), 5.06 (dt, *J* = 7.5, 5.1 Hz, 1H), 3.87 (d, *J* = 5.1 Hz, 2H), 3.52 (ddd, *J* = 10.8, 8.5, 7.0 Hz, 1H), 2.47 – 2.28 (m, 1H), 2.14 (dd, *J* = 10.8, 5.1 Hz, 1H), 1.93 (h, *J* = 6.8 Hz, 1H), 1.12 (d, *J* = 14.3 Hz, 9H), 1.06 (d, *J* = 8.9 Hz, 3H), 0.99 (d, *J* = 2.5 Hz, 3H), 0.98 (d, *J* = 2.6 Hz, 3H) ppm. **^{13}C NMR** (101 MHz, CDCl3) δ: 174.19, 138.66, 128.80, 127.87, 126.84, 66.22, 62.72, 55.85, 32.99 (d, *J* = 7.6 Hz), 30.64, 30.18, 24.38 (d, *J* = 2.5 Hz), 19.52, 18.53, 10.32 (d, *J* = 31.8 Hz) ppm. **^{31}P NMR** (202 MHz, $CDCl_3$) δ 68.9 - 68.5 (m, P-BH_3) ppm. **HRMS** (ESI) calculated for $C_{18}H_{35}BN_2O_2P$ 353.2523, found 353.2528 $[M+H]^+$. **IR** (ATR-FTIR) ν_{max} = 3310, 3266, 2968, 2383, 2361, 1652, 1556 cm^{-1}.

(*R*)-1-*tert*-butyl-1-methyl-*N*-((*R*)-2-methyl-1-((*R*)-4-phenyl-4,5-dihydrooxazol-2-yl)propyl) phosphanamine borane, 4-S3

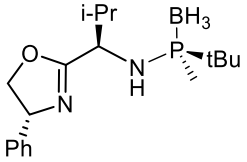

The corresponding aminophosphane (1 eq, 2.90 mmol) was dissolved in CH_2Cl_2 (0.08 M) and $SOCl_2$ (2.4 equiv) was added drop wise at 0 ºC. The solution was stirred 4 h at room temperature. The solution was then cooled down to 0 ºC and $NaHCO_3$ saturated aqueous solution was added slowly until pH 8-9. The mixture was left stirring for 15 min at room temperature. The two phases were separated and the aqueous phase was extracted twice with CH_2Cl_2. The combined organic layers were washed with brine. The organic layer was dried over $MgSO_4$ and concentrated on a rotary evaporator under reduced pressure. Purification by column chromatography (SiO_2, hexanes:EtOAc) yielded the desired product **4-S3** as an oil (0.95 g, 98% yield).

[α]$_D$: +20 (c 0.5, $CHCl_3$). **^{1}H NMR** (CDCl3, 400 MHz) δ: 7.39 – 7.33 (m, 2H), 7.29 (tdd, *J* = 5.5, 1.7, 0.9 Hz, 3H), 5.14 (dd, *J* = 10.1, 8.4 Hz, 1H), 4.66 (dd, *J* = 10.1, 8.5 Hz, 1H), 4.20 (t, *J* = 8.5 Hz, 1H), 4.08 – 3.98 (m, 1H), 2.13 – 2.03 (m, 2H), 1.30 (d, *J* = 9.0 Hz, 3H), 1.14 (d, *J* = 14.2 Hz, 9H), 1.04 (d, *J* = 6.9 Hz, 3H), 0.94 (d, *J* = 6.9 Hz, 3H) ppm. **^{13}C NMR** (101 MHz, CDCl3) δ: 170.35, 141.81, 128.72, 127.70, 126.80, 75.36, 69.48, 56.51, 32.71 (d, *J* = 6.3 Hz), 30.88, 30.43, 24.50 (d, *J* = 2.7 Hz), 19.44, 17.26, 10.32 (d, *J* = 33.1 Hz) ppm. **^{31}P NMR** (202 MHz, $CDCl_3$) δ 70.3 – 69.3 (m, P-BH_3) ppm. **HRMS** (ESI) calculated for $C_{18}H_{33}BN_2OP$ 335.2418, found 335.2420 $[M+H]^+$. **IR** (ATR-FTIR) ν_{max} = 2959, 2366, 1650, 747 cm^{-1}.

[Ir((*R,R,S*)-PheMAXPHOX)(COD)]BAr$_F$, 4-12b

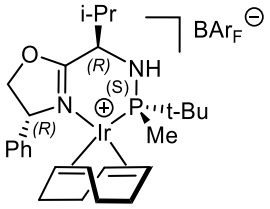

A Schlenk tube containing the corresponding borane protected ligand (1 equiv., 0.16 mmol) was evacuated and purged with N_2, dissolved in freshly distilled pyrrolidine [0.06 M] and stirred for 16 h at 90 ºC. Afterwards, and keeping the vessel under inert atmosphere, pyrrolidine was removed *in vacuo*. When no pyrrolidine remained, the crude was further dried under vacuum for 30 min at 50 ºC (the crude was under N_2 during all the procedure). Then, a solution of $[Ir(COD)(Cl)]_2$ (0.5 equiv.) in CH_2Cl_2 [0.06 M] was added to the free ligand *via* cannula. The resulting mixture was stirred for 40 min at room temperature. $NaBAr_F$ (1 equiv.) was then added and the solution was stirred 1 h more at room temperature. The resulting crude was filtered through a small plug of silica gel, (first washed with Et_2O) under N_2, eluting with hexanes:CH_2Cl_2 (50-100%). The intense orange fraction was collected and concentrated to yield the corresponding Ir complex **4-12b** as an orange solid (140 mg, 59% yield).

m. p. 226 - 230 ºC (descomposition). **[α]$_D$**: -25 (c 0.6, $CHCl_3$). **^{1}H NMR** (CDCl3, 400 MHz) δ: 7.71 (s, 10H), 7.53 (s, 5H), 7.36 (dd, *J* = 5.1, 2.0 Hz, 3H), 7.24 – 7.17 (m, 2H), 5.24 – 5.11 (m, 1H), 5.06 (dd, *J* = 9.0, 6.0 Hz, 1H), 4.76 (td, *J* = 9.8, 9.4, 5.6 Hz, 3H), 3.57 – 3.42 (m, 5H), 2.46 (h, *J* = 6.7, 6.2 Hz, 1H), 2.23 (dq, *J* = 14.1, 8.4 Hz, 6H), 2.12 (dd, *J* = 13.9, 7.0 Hz, 1H), 2.00 (h, *J* = 8.2 Hz, 1H), 1.75 – 1.62 (m, 2H), 1.28 (d, *J* = 7.7 Hz, 3H), 1.21 (t, *J* = 7.0 Hz, 2H), 1.07 (d, *J* = 6.4 Hz, 3H), 0.97 (d, *J* = 6.7 Hz, 3H), 0.84 (d, *J* = 15.5 Hz, 9H) ppm. **^{13}C NMR** (101 MHz, CDCl3) δ: 175.54, 162.40, 161.90, 161.41, 160.91, 137.29, 134.77, 129.99, 129.49, 129.32, 129.01, 128.67, 128.39, 127.13, 125.88, 123.17, 120.46, 117.49, 117.42, 117.39, 117.35, 109.99, 92.51, 92.40, 91.98, 91.85, 67.72, 65.83, 63.50, 60.48, 58.57, 40.04, 39.97, 36.47, 36.06, 34.28, 34.25, 30.60, 30.58, 30.55, 27.39, 26.32, 26.27, 19.81,

18.45, 15.25, 10.25, 9.95 ppm. **^{31}P NMR** (202 MHz, $CDCl_3$) δ 55.2 ppm. **HRMS** (ESI) calculated for $C_{26}H_{41}N_2OPIr$ 621.2580, found 621.2581 $[M+H]^+$. **IR** (ATR-FTIR) ν_{max} = 1353, 1273, 1120 cm^{-1}.

Computational details

Methods

The geometries of products were optimized using the Gaussian09 program package.[6] NBO analysis was performed using the NBO 6.0 version program.[7] QTAIM analysis was conducted with the AIMAll package.[8] Non-covalent interactions were analyzed with the NCIPLOT 3.0 program.[9]

Stationary points were characterized as minima of the Potential Energy Surface (PES) due to the absence of imaginary frequencies. The B3LYP hybrid functional was used for all calculations due to its proven accuracy for simple organic molecules. The double-ξ aug-cc-pVDZ basis set was used. A comparison with the split-valence 6-311++G(d,p) basis set was also performed and the differences in geometry and energy were negligible. For this reason, the slightly larger aug-cc-pVDZ basis set was selected.

Tight convergence criteria (opt=tight) was used for all optimizations. The default numerical integration grid was also improved using a pruned grid with 99 radial shells and 590 angular points per shell (int=ultrafine). Dispersion effects were included and modelled using Grimme's D3 correction with Becke-Johnson damping (EmpiricalDispersion=GD3BJ).[10] Solvent effects were not included since the reactions are carried out in rather nonpolar solvents.

Analysis of the intramolecular hydrogen bonds

Geometrical analysis

The strength of hydrogen bonds depends decisively on their geometry. There are many geometrical parameters that play a relevant role,[11] but the most important ones are the O···H distance, which has an average value of approximately 2 Å, the N-H···O angle, which tends to linearity (180º), and the C=O···H angle, which has to be bigger than 90º.[12] Some relevant parameters obtained from the optimized structures of products **4-5** and **4-7** are summarized in Table 4.S1.

The short distance of the hydrogen bond for product **4-7** is indicative of a significantly stronger interaction. The strength of these interactions is slightly limited due to a certain lack of directionality, as indicated by the N-H···O angle. Nevertheless, the geometrical parameters suggest that these interactions, especially for product **4-7** might be significant. Further computational analysis supports this hypothesis.

---

[6] Frisch, M. J.; Trucks, G. W.; Schlegel, H. B.; Scuseria, G. E.; Robb, M. A.; Cheeseman, J. R.; Scalmani, G.; Barone, V.; Mennucci, B.; Petersson, G. A.; Nakatsuji, H.; Caricato, M.; Li, X.; Hratchian, H. P.; Izmaylov, A. F.; Bloino, J.; Zheng, G.; Sonnenberg, J. L.; Hada, M.; Ehara, M.; Toyota, K.; Fukuda, R.; Hasegawa, J.; Ishida, M.; Nakajima, T.; Honda, Y.; Kitao, O.; Nakai, H.; Vreven, T.; Montgomery, J. A., Jr.; Peralta, J. E.; Ogliaro, F.; Bearpark, M.; Heyd, J. J.; Brothers, E.; Kudin, K. N.; Staroverov, V. N.; Kobayashi, R.; Normand, J.; Raghavachari, K.; Rendell, A.; Burant, J. C.; Iyengar, S. S.; Tomasi, J.; Cossi, M.; Rega, N.; Millam, J. M.; Klene, M.; Knox, J. E.; Cross, J. B.; Bakken, V.; Adamo, C.; Jaramillo, J.; Gomperts, R.; Stratmann, R. E.; Yazyev, O.; Austin, A. J.; Cammi, R.; Pomelli, C.; Ochterski, J. W.; Martin, R. L.; Morokuma, K.; Zakrzewski, V. G.; Voth, G. A.; Salvador, P.; Dannenberg, J. J.; Dapprich, S.; Daniels, A. D.; Farkas, Ö.; Foresman, J. B.; Ortiz, J. V.; Cioslowski, J.; Fox, D. J. *Gaussian 09, Revision D.01*; Gaussian, Inc., Wallingford, CT, 2009.

[7] *NBO 6.0*. Glendening, E. D.; Badenhoop, J. K.; Reed, A. E.; Carpenter, J. E.; Bohmann, J. A.; Morales, C. M.; Landis, C. R.; Weinhold, F. Theoretical Chemistry Institute, University of Wisconsin, Madison (2013).

[8] AIMAll (Version 13.10.19), Todd A. Keith, TK Gristmill Software, Overland Park KS, USA, 2013 (aim.tkgristmill.com).

[9] Johnson, E. R.; Keinan, S.; Mori-Sánchez, P.; Contreras-García, J.; Cohen, A. J.; Yang, W. *J. Am. Chem. Soc.* **2010**, *132*, 6498–6506.

[10] Grimme, S.; Ehrlich, S.; Goerigk, L. *J Comp. Chem.* **2011**, *32*, 1456–1465.

[11] Torshin, I. Y.; Weber, I. T.; Harrison, R. W. *Protein Eng. Des. Sel.* **2002**, *15*, 359–363.

[12] Steiner, T. *Angew. Chem. Int. Ed.* **2002**, *41*, 49–76.

Table 4.S1. Selected geometrical parameters of the hydrogen bonds in products 4-5 and 4-7. Distances in Å and angles in degrees.

	4-5 (allylamine)	**4-7 (enamide)**
O····H distance	2.25	1.96
N-H····O angle	118.36	131.06
C=O····H angle	113.22	100.75
C=O····H-N dihedral	30.92	-0.06

NCI analysis

The non-covalent interactions (NCI) were analyzed with the NCIPLOT 3.0 program. This program allows facile qualitative analysis of the non-covalent interactions of molecules, depicted as colored surfaces. Red indicates strongly repulsive interactions, yellow indicates slightly repulsive interactions, green indicates slightly attractive interactions and blue indicates strongly attractive interactions.

For both products, the aforementioned hydrogen bonds (and two irrelevant weak hydrogen bonds between the carbonyl of the Boc group and the *tert*-butyl substituents) were the only remarkable interactions.

Figure 4.S1. Plots for products 4-5 and 4-7 with a representation of the non-covalent interactions (colored surfaces).

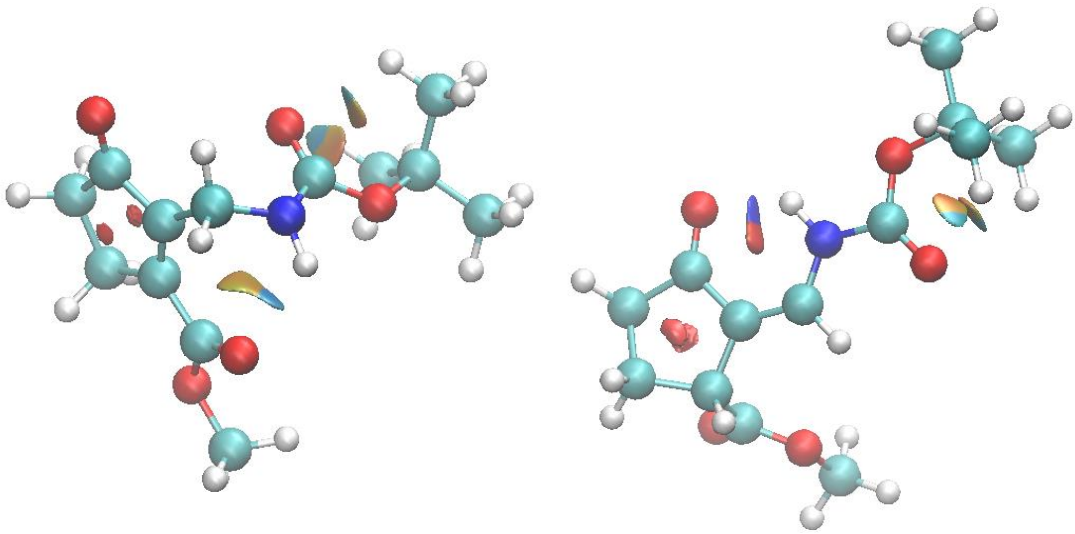

Consistent with the geometrical analysis, the interaction in product **4-5** is only slightly attractive (green) whereas the interaction in product **4-7** is strongly attractive (deep blue).

QTAIM analysis

The same interactions can be identified by Bader's Quantum Theory of Atoms In Molecules (QTAIM). As expected, there is significant electron density (ϱ) in the O···H bond. Positive values of the laplacian of the electron density ($\nabla^2\varrho$) indicate regions of charge density depletion, which is indicative of a significant ionic character of the bonding. This is consistent with the established fact that hydrogen bonds have an important electrostatic contribution.

Table 4.S2. Selected values at the bcp of the hydrogen bond.

	ϱ	$\nabla^2\varrho$	V	G
4-5 *(allylamine)*	0.0151	0.055	-0.0132	0.0135
4-7 *(enamide)*	0.0236	0.1054	-0.0247	0.0255

The values for the electron density (ϱ), the laplacian of the electron density ($\nabla^2\varrho$) and the energy density (H)[13] at the bond critical points (bcp) are consistent with standard values reported in the literature for hydrogen bonds.[14] Further analysis is beyond the scope of this work.

Figure 4.S2. Molecular graph of product 4-5. Bond critical points (bcp) are represented as green dots and ring critical points as red dots.

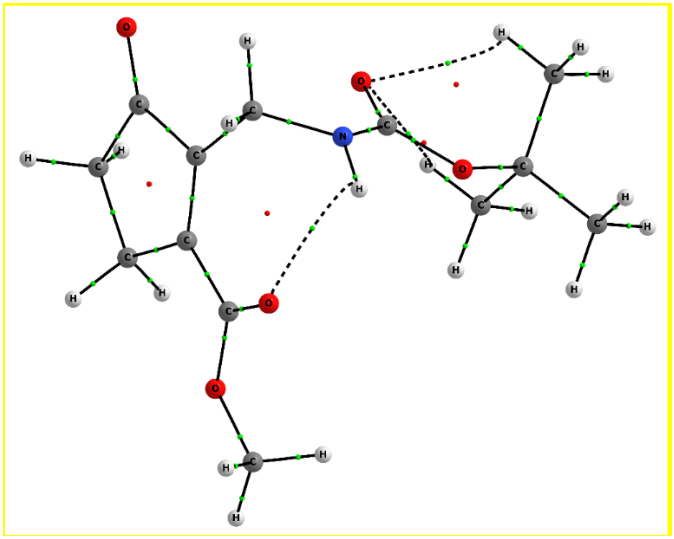

Figure 4.S3. Molecular graph of product 7. Bond critical points (bcp) are represented as green dots and ring critical points as red dots.

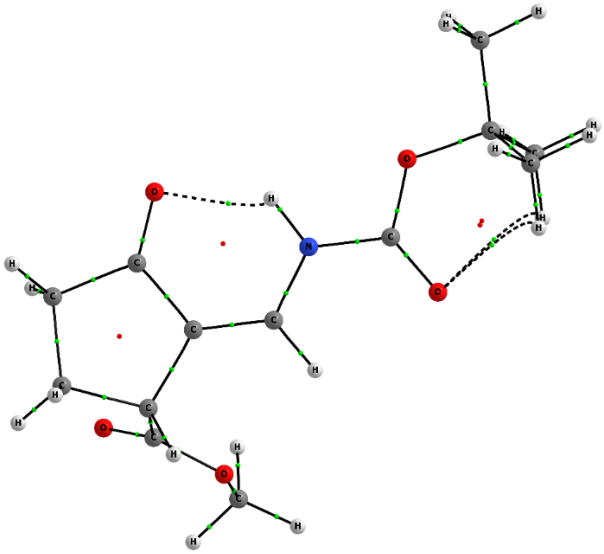

[13] The energy density H is defined as the sum of the potential energy density V and kinetic energy density G.
[14] a) Ju, Z.; Xiao, W.; Lu, X.; Liu, X.; Yao, X.; Zhang, X.; Zhang, S. *RSC Adv.* **2018**, *8*, 8209–8219. b) Hilal, R.; Aziz, S. G.; Alyoubi, A. O.; Elroby, S. *Procedia Comput. Sci.* **2015**, *51*, 1872–1877.

NBO analysis

Despite the important electrostatic character of hydrogen bonds, NBO calculations can complement the bonding description of these interactions.

For instance, the Wiberg Bond Indices (WBI) reveal a bonding interaction between the oxygen and the hydrogen atoms. Particularly, the WBI for compound **4-7** (0.0364) is around five times higher than the WBI for compound **4-5** (0.0076), suggesting a significantly stronger interaction. This difference can be further appreciated with the Second Order Pertubation Theory analysis, which quantifies the donor-acceptor interactions. The interactions corresponding to the hydrogen bonds are mainly donations from the oxygen lone pairs into the N-H σ* antibonding orbital. The stabilization energy associated with these donations is also roughly 5 times higher for compound **4-7** (2 interactions of 2.6 and 8.3 kcal·mol^{-1}, respectively) compared to compound **4-5** (2 interactions of 1.1 and 0.8 kcal·mol^{-1}, respectively).

Hence, we have provided a detailed picture of the bonding configuration of the two hydrogen bonds in product **4-5** and **4-7**, and shown both qualitatively and quantitatively that the hydrogen bond in product **4-7** is significantly stronger. Therefore, this seems to be an important contribution to the exergonic nature of the isomerization process.

Coordinates

- allylamine_2.log

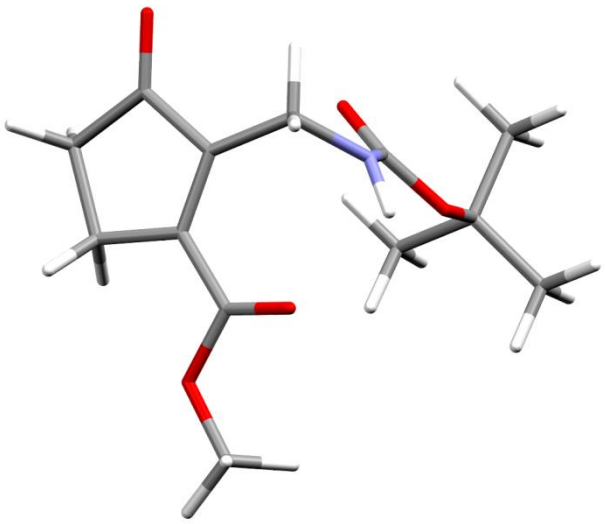

SCF (B3LYP-D3) = -937.922785167
H(0 K)= -937.610698
H(298 K)= -937.590062
G(298 K)= -937.663137
Lowest Frequency = 8.0977 cm^{-1}

C	-2.063433	2.745206	-0.328512
C	-0.089607	2.920221	-1.744843
C	-0.983217	3.722879	-0.782760
O	-3.037415	3.004612	0.349205
C	-0.115999	0.419120	-2.536839
O	-0.618214	-0.681502	-2.683347
O	1.034047	0.787831	-3.140675
C	1.645040	-0.216770	-3.973745

H	1.892698	-1.102612	-3.377442
H	2.548608	0.249593	-4.373830
H	0.962183	-0.504146	-4.781661
C	-0.934880	-0.749699	1.032397
O	-1.000887	0.211979	1.783213
O	-0.071469	-1.788212	1.137121
C	0.901743	-1.842994	2.241448
C	1.857852	-0.652231	2.155749
H	2.316445	-0.605478	1.159248
H	2.659400	-0.780024	2.895160
H	1.337827	0.287849	2.357115
C	0.171370	-1.906873	3.582935
H	0.902286	-2.085954	4.382717
H	-0.547588	-2.736101	3.583340
H	-0.358801	-0.973622	3.790096
C	1.640843	-3.150391	1.964115
H	2.127492	-3.117630	0.981218
H	0.944057	-3.997476	1.980410
H	2.409164	-3.313406	2.730453
N	-1.749588	-0.932037	-0.051899
H	-1.404130	-1.562180	-0.763287
H	-0.098859	3.322347	-2.766959
H	0.962959	2.899593	-1.433935
H	-0.440630	4.074854	0.104490
H	-1.451059	4.600075	-1.245711
C	-0.671777	1.521455	-1.717844
C	-1.741415	1.401150	-0.898465
C	-2.550513	0.191086	-0.515806
H	-3.142257	-0.158308	-1.369887
H	-3.242275	0.496800	0.277016

- enamideZ_2.log

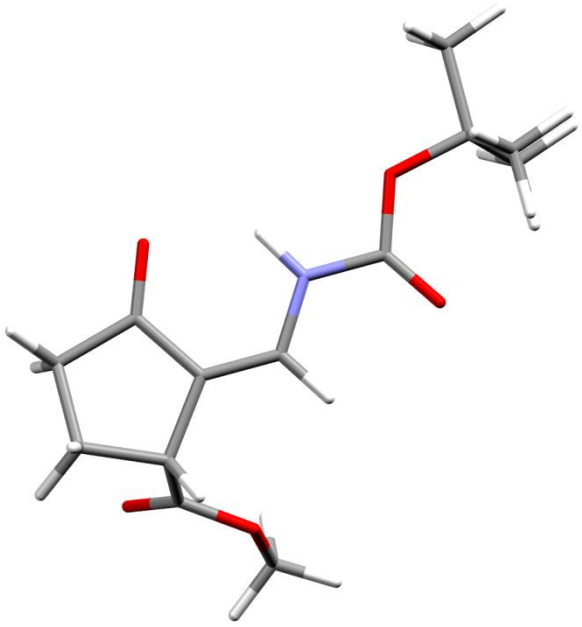

SCF (B3LYP-D3) = -937.933102859
H(0 K)= -937.620612
H(298 K)= -937.600339
G(298 K)= -937.671670

Lowest Frequency = 16.3862 cm^{-1}

C	-1.062227	2.558991	0.722612
C	-1.564131	1.446518	-0.086013
C	-2.779703	1.893302	-0.882084
C	-3.220491	3.199142	-0.171614
C	-1.947208	3.772012	0.477201
O	-0.081507	2.521082	1.469447
C	-2.365869	2.136759	-2.324830
O	-2.088602	3.212777	-2.810397
O	-2.300805	0.971404	-3.006406
C	-1.814431	1.068075	-4.359886
H	-2.472878	1.710700	-4.955565
H	-1.818354	0.044590	-4.743598
H	-0.799882	1.483529	-4.367928
C	0.716439	-1.336655	0.601778
O	0.308276	-2.262385	-0.073467
O	1.774577	-1.330218	1.425998
C	2.605740	-2.544044	1.600698
C	1.756500	-3.670632	2.187061
H	1.258935	-3.333810	3.105422
H	2.410892	-4.514365	2.442380
H	1.001806	-4.013962	1.474423
C	3.247814	-2.925491	0.267838
H	3.967635	-3.736721	0.438284
H	3.790807	-2.069170	-0.152036
H	2.499314	-3.265307	-0.452989
C	3.658587	-2.074647	2.600953
H	3.186253	-1.755305	3.538039
H	4.230842	-1.232378	2.193150
H	4.351866	-2.896319	2.819959
C	-0.980378	0.219441	-0.117092
H	-1.352467	-0.595276	-0.736591
N	0.124151	-0.081319	0.627299
H	-3.569400	1.132144	-0.883342
H	0.504287	0.667641	1.209968
H	-3.952881	2.940468	0.603949
H	-3.688787	3.897403	-0.871952
H	-1.414073	4.437631	-0.217997
H	-2.118646	4.325393	1.407326

^{1}H NMR and ^{13}C NMR spectra

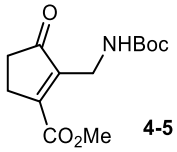

4-5

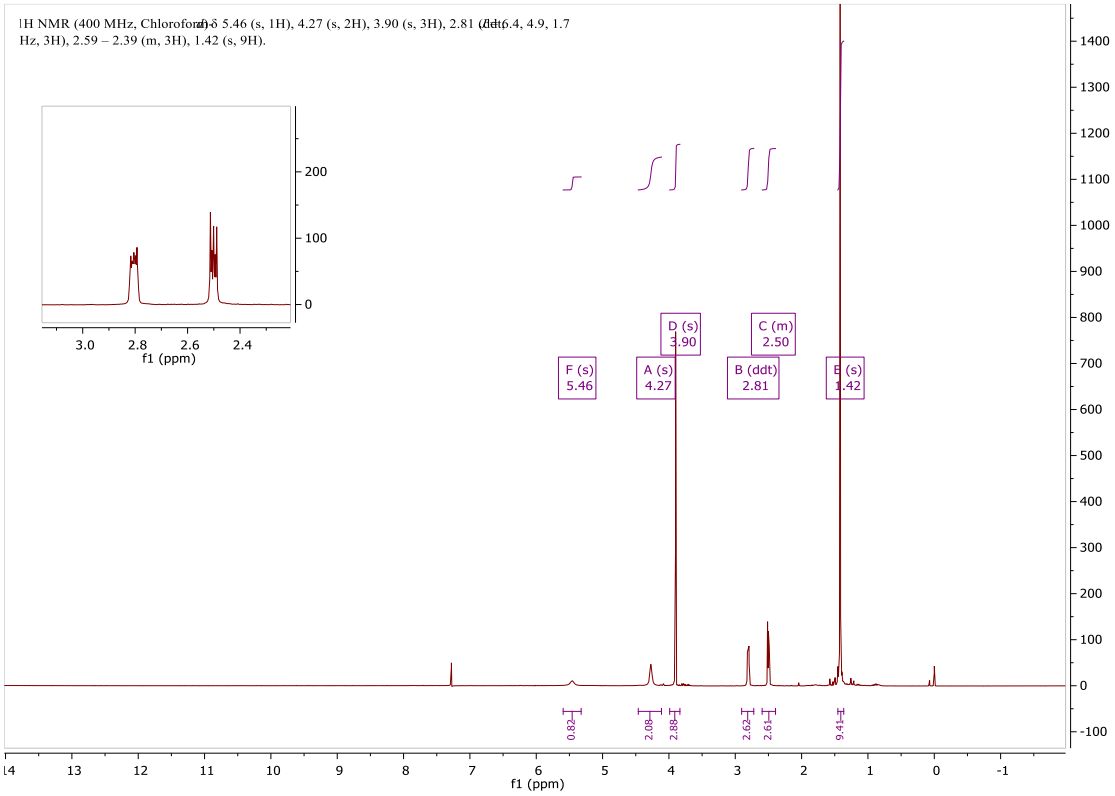

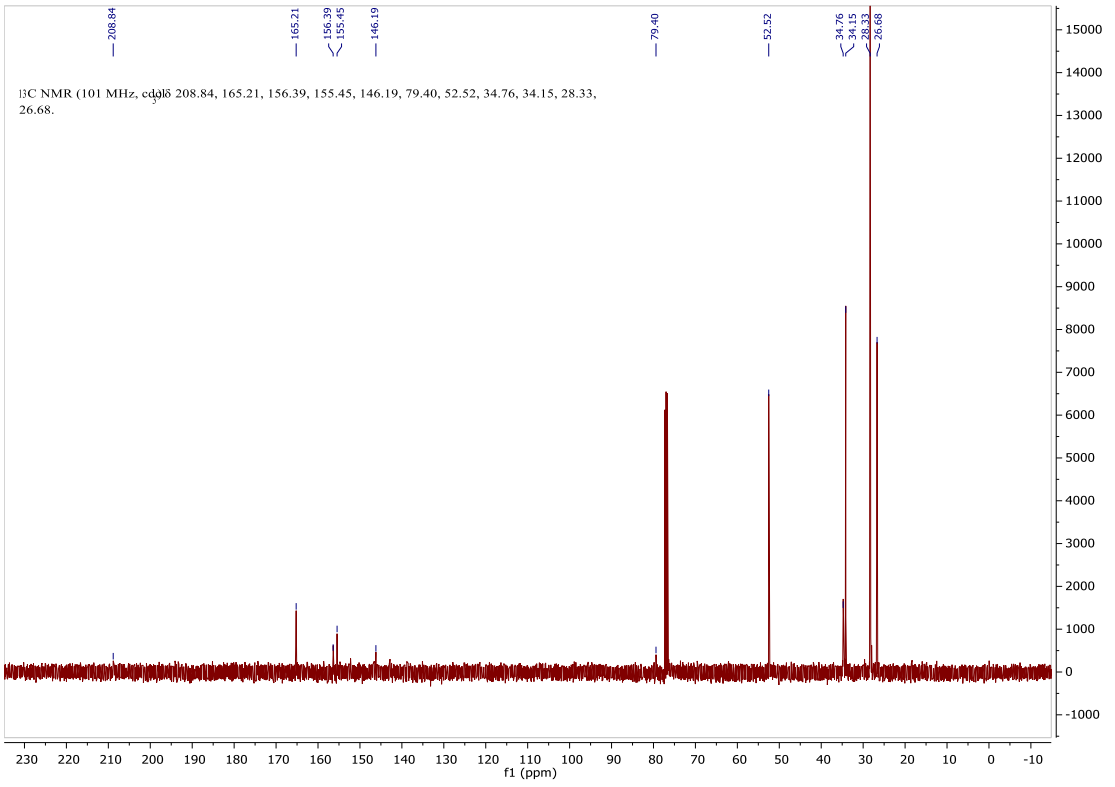

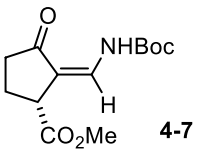
O
NHBoc
H
CO2Me

4-7

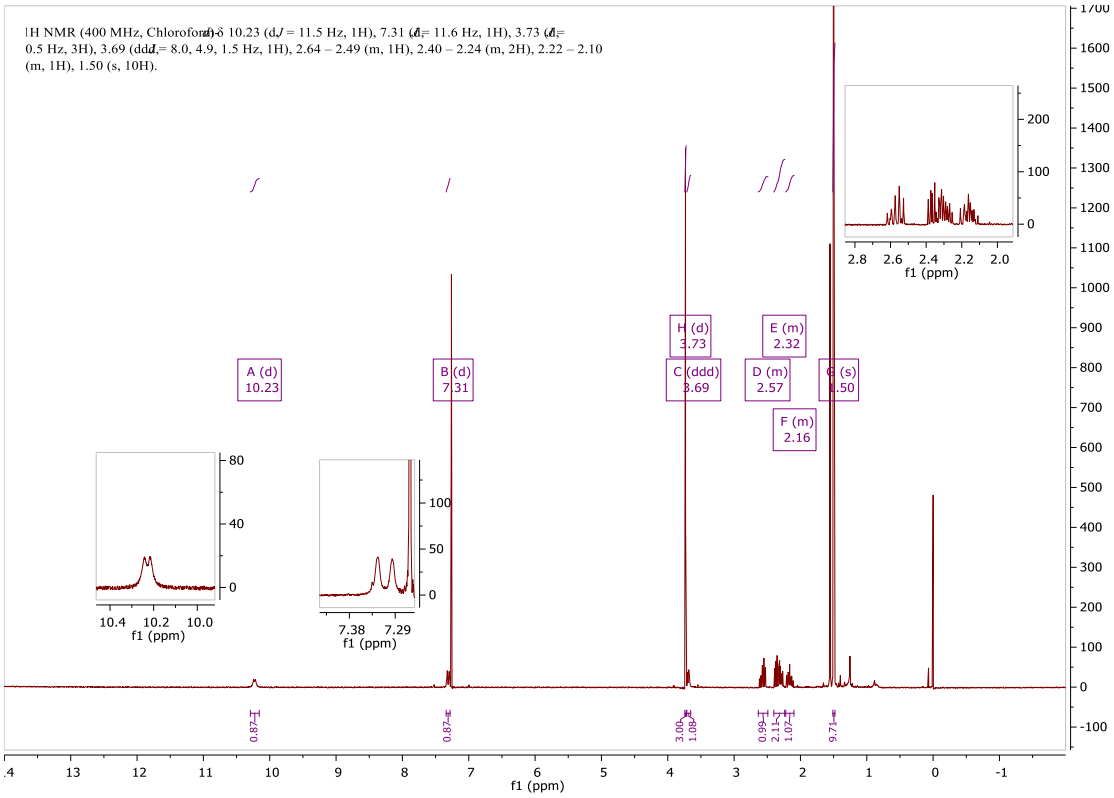
1H NMR (400 MHz, Chloroform-d) δ 10.23 (d, J = 11.5 Hz, 1H), 7.31 (d, J = 11.6 Hz, 1H), 3.73 (d, J = 0.5 Hz, 3H), 3.69 (ddd, J = 8.0, 4.9, 1.5 Hz, 1H), 2.64 – 2.49 (m, 1H), 2.40 – 2.24 (m, 2H), 2.22 – 2.10 (m, 1H), 1.50 (s, 10H).
A (d) 10.23
B (d) 7.31
C (ddd) 3.69
H (d) 3.73
D (m) 2.57
E (m) 2.32
F (m) 2.16
G (s) 1.50
f1 (ppm)

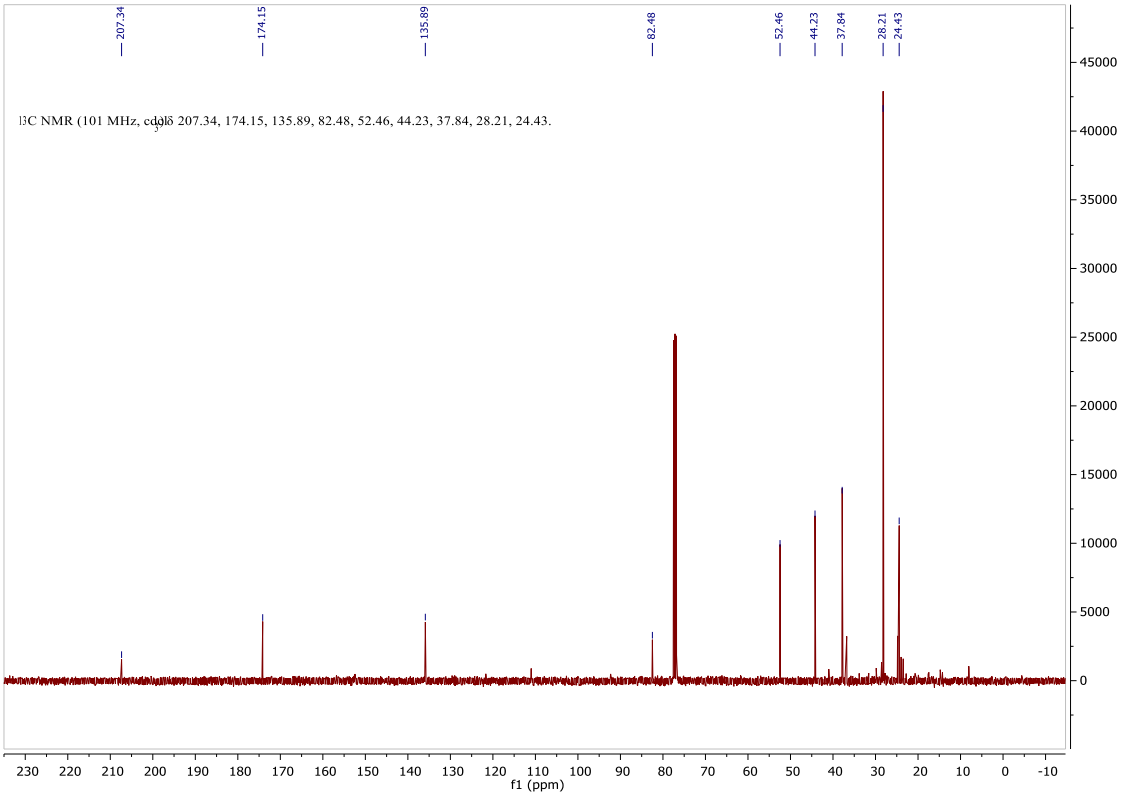
13C NMR (101 MHz, cdcl3) δ 207.34, 174.15, 135.89, 82.48, 52.46, 44.23, 37.84, 28.21, 24.43.
207.34
174.15
135.89
82.48
52.46
44.23
37.84
28.21
24.43
f1 (ppm)

NOESY Experiment.

To confirm the Z-configuration of **4-7**, a 2D-NMR experiment (NOESY) was acquired. As indicated below, there is an interaction between the alkenyl proton and the proton in α-position to ester group.

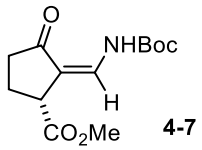

4-7

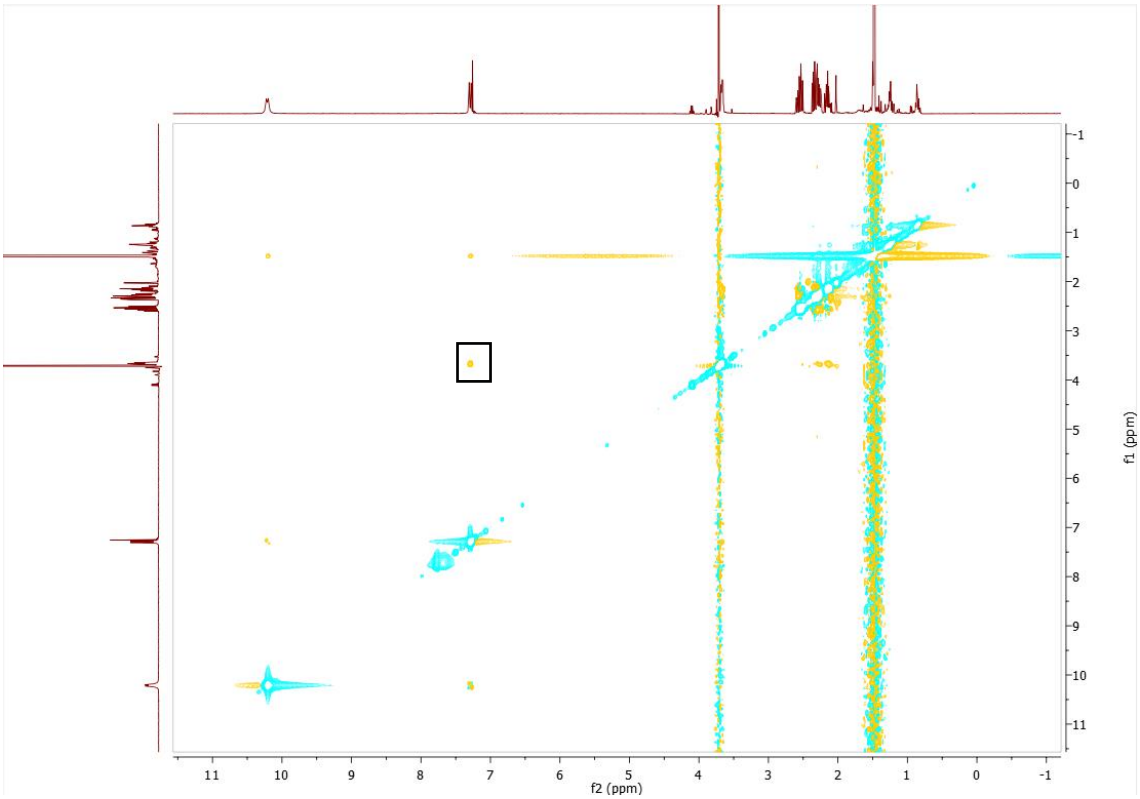

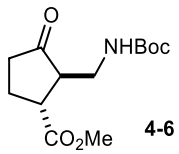
O
NHBoc
CO2Me

4-6

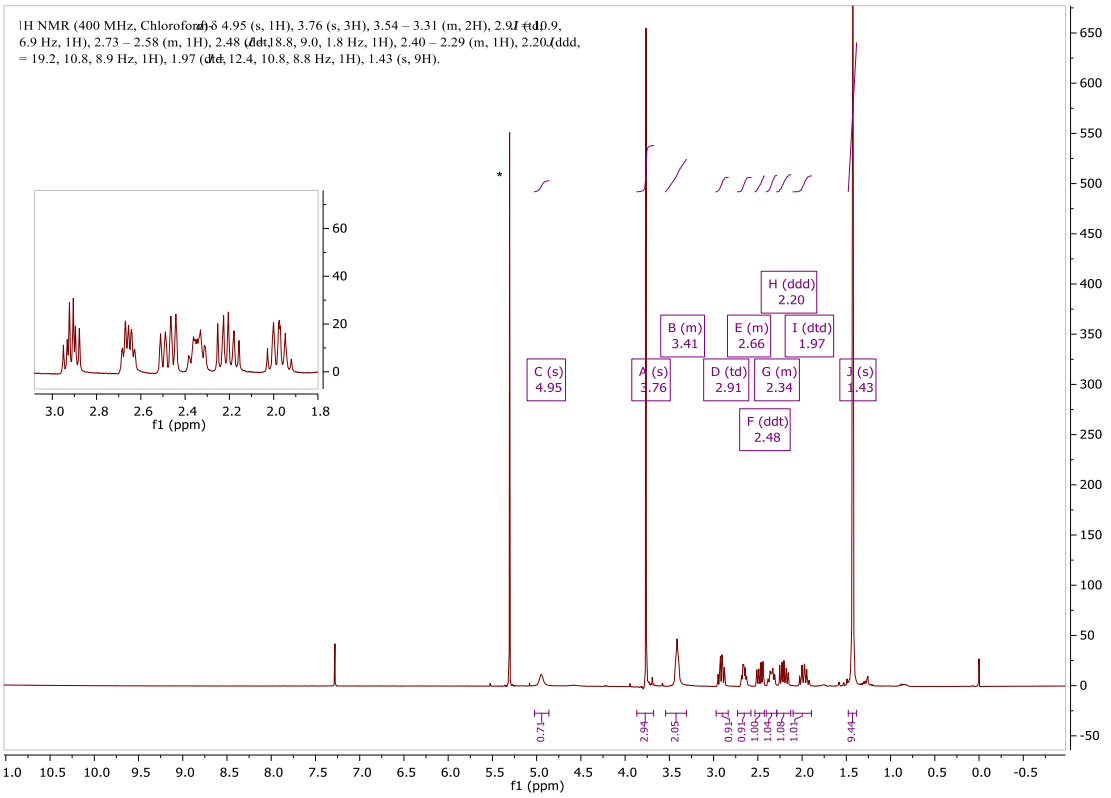
1H NMR (400 MHz, Chloroform-d) δ 4.95 (s, 1H), 3.76 (s, 3H), 3.54 – 3.31 (m, 2H), 2.91 (td, J = 10.9, 6.9 Hz, 1H), 2.73 – 2.58 (m, 1H), 2.48 (ddt, J = 18.8, 9.0, 1.8 Hz, 1H), 2.40 – 2.29 (m, 1H), 2.20 (ddd, J = 19.2, 10.8, 8.9 Hz, 1H), 1.97 (dtd, J = 12.4, 10.8, 8.8 Hz, 1H), 1.43 (s, 9H).
C (s) 4.95
A (s) 3.76
B (m) 3.41
D (td) 2.91
E (m) 2.66
F (ddt) 2.48
G (m) 2.34
H (ddd) 2.20
I (dtd) 1.97
J (s) 1.43
f1 (ppm)

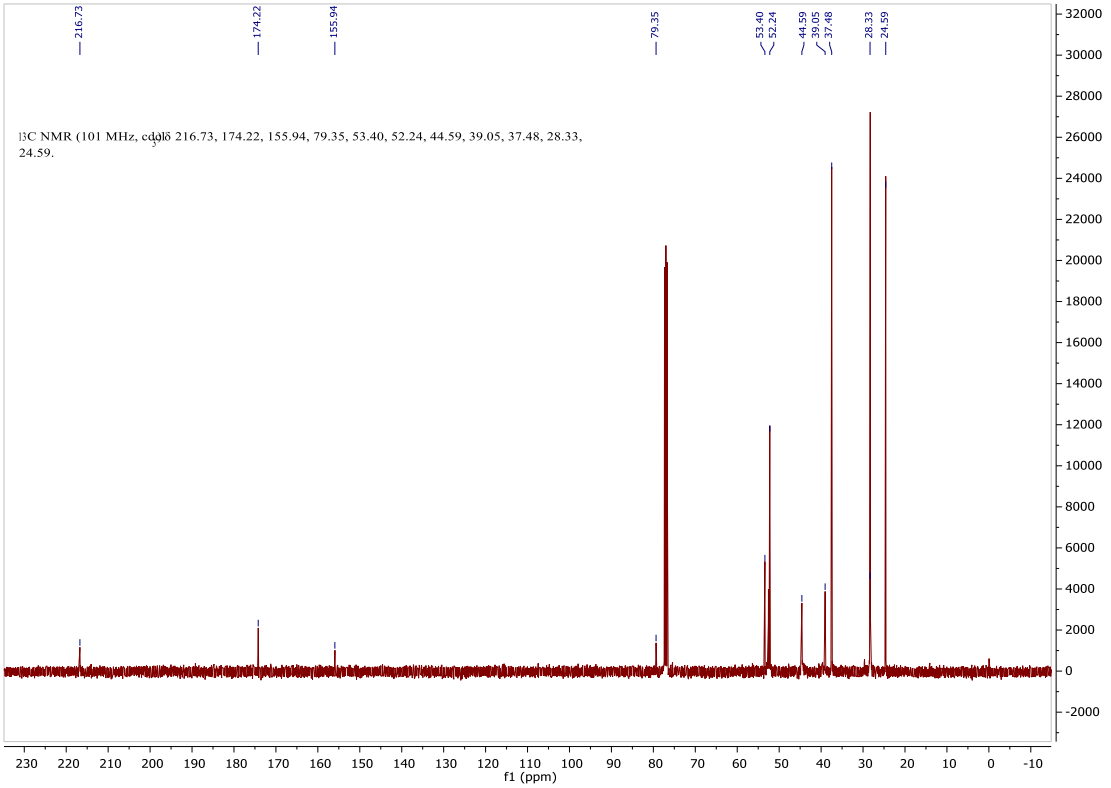
13C NMR (101 MHz, cdcl3) δ 216.73, 174.22, 155.94, 79.35, 53.40, 52.24, 44.59, 39.05, 37.48, 28.33, 24.59.
216.73
174.22
155.94
79.35
53.40
52.24
44.59
39.05
37.48
28.33
24.59
f1 (ppm)

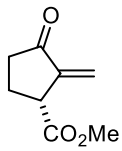
O
CO2Me

4-2

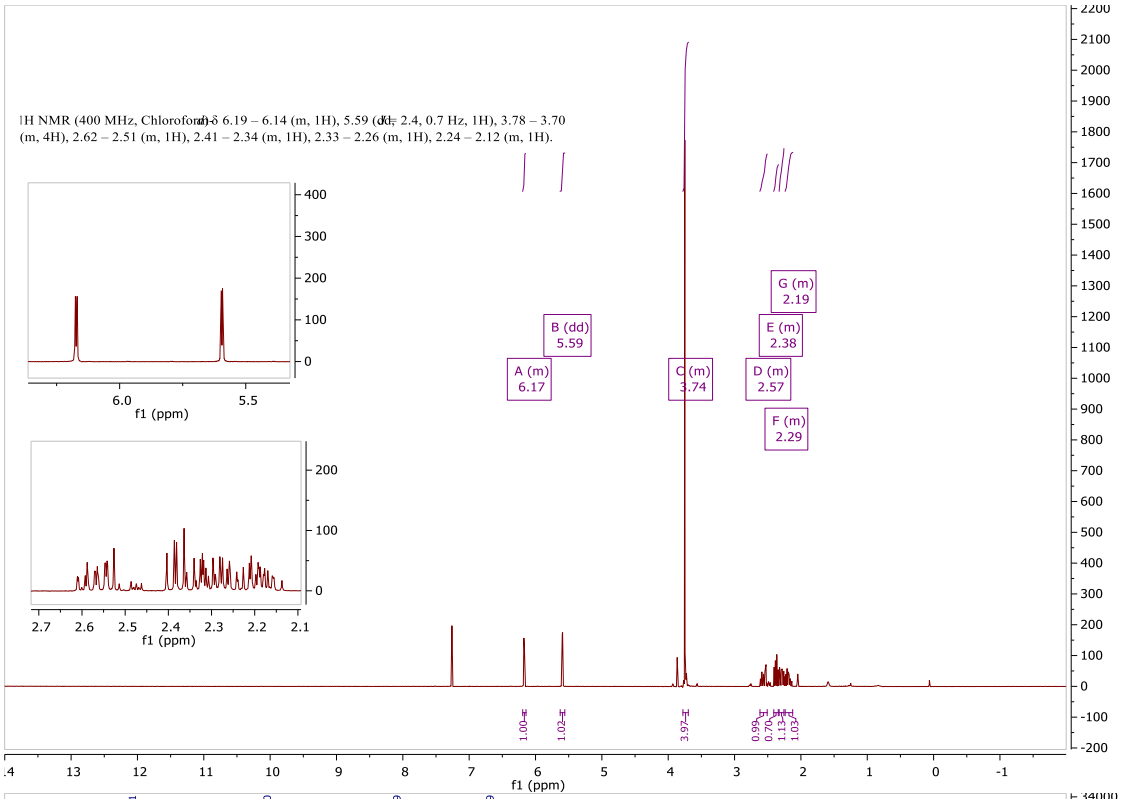
1H NMR (400 MHz, Chloroform-d) δ 6.19 – 6.14 (m, 1H), 5.59 (dd, J = 2.4, 0.7 Hz, 1H), 3.78 – 3.70 (m, 4H), 2.62 – 2.51 (m, 1H), 2.41 – 2.34 (m, 1H), 2.33 – 2.26 (m, 1H), 2.24 – 2.12 (m, 1H).
A (m) 6.17
B (dd) 5.59
C (m) 3.74
D (m) 2.57
E (m) 2.38
F (m) 2.29
G (m) 2.19
f1 (ppm)

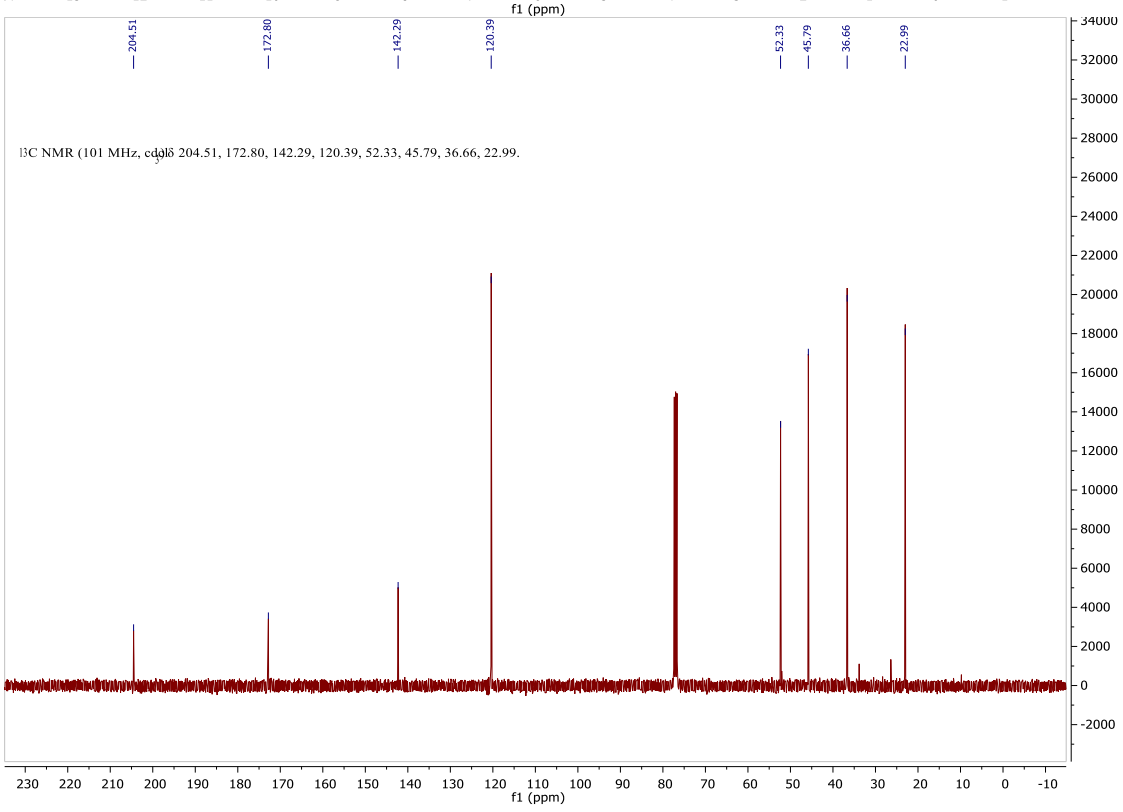
13C NMR (101 MHz, cdcl3) δ 204.51, 172.80, 142.29, 120.39, 52.33, 45.79, 36.66, 22.99.
204.51
172.80
142.29
120.39
52.33
45.79
36.66
22.99
f1 (ppm)

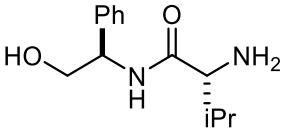
Ph
O
HO
NH2
N
H
iPr

4-S1

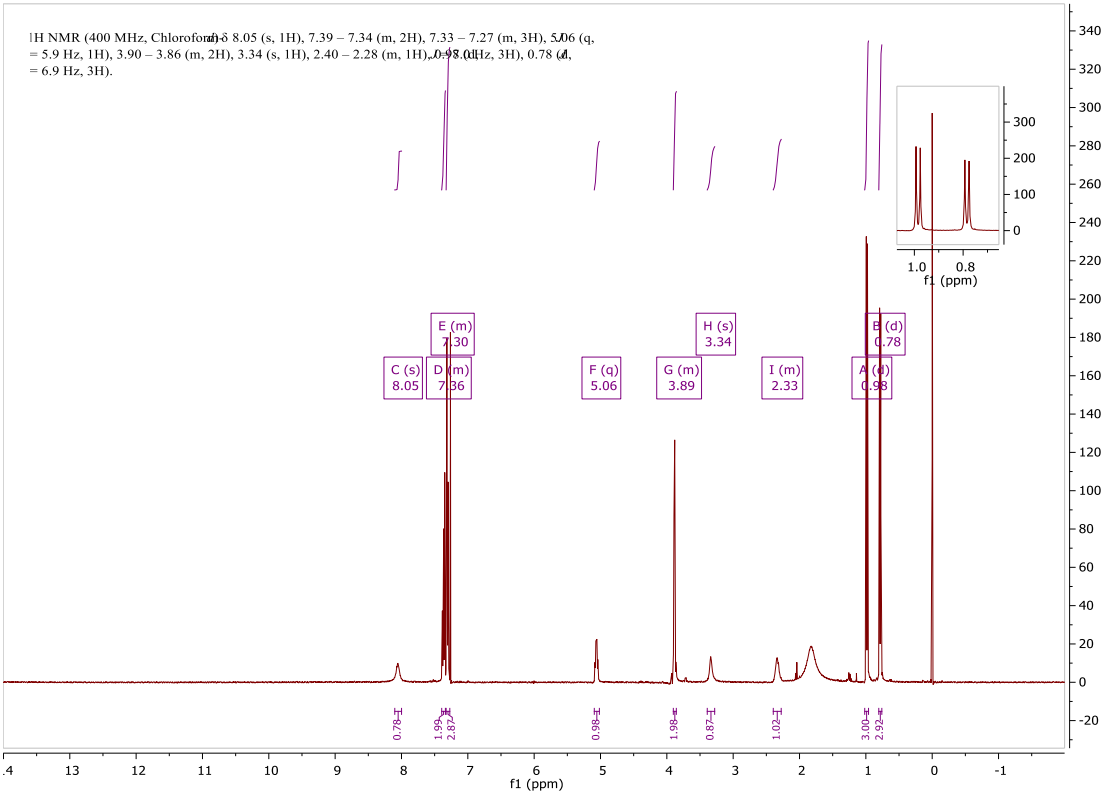
1H NMR (400 MHz, Chloroform-d) δ 8.05 (s, 1H), 7.39 – 7.34 (m, 2H), 7.33 – 7.27 (m, 3H), 5.06 (q, = 5.9 Hz, 1H), 3.90 – 3.86 (m, 2H), 3.34 (s, 1H), 2.40 – 2.28 (m, 1H), 0.98 (d, = 6.9 Hz, 3H), 0.78 (d, = 6.9 Hz, 3H).
C (s) 8.05
D (m) 7.36
E (m) 7.30
F (q) 5.06
G (m) 3.89
H (s) 3.34
I (m) 2.33
A (d) 0.98
B (d) 0.78
f1 (ppm)

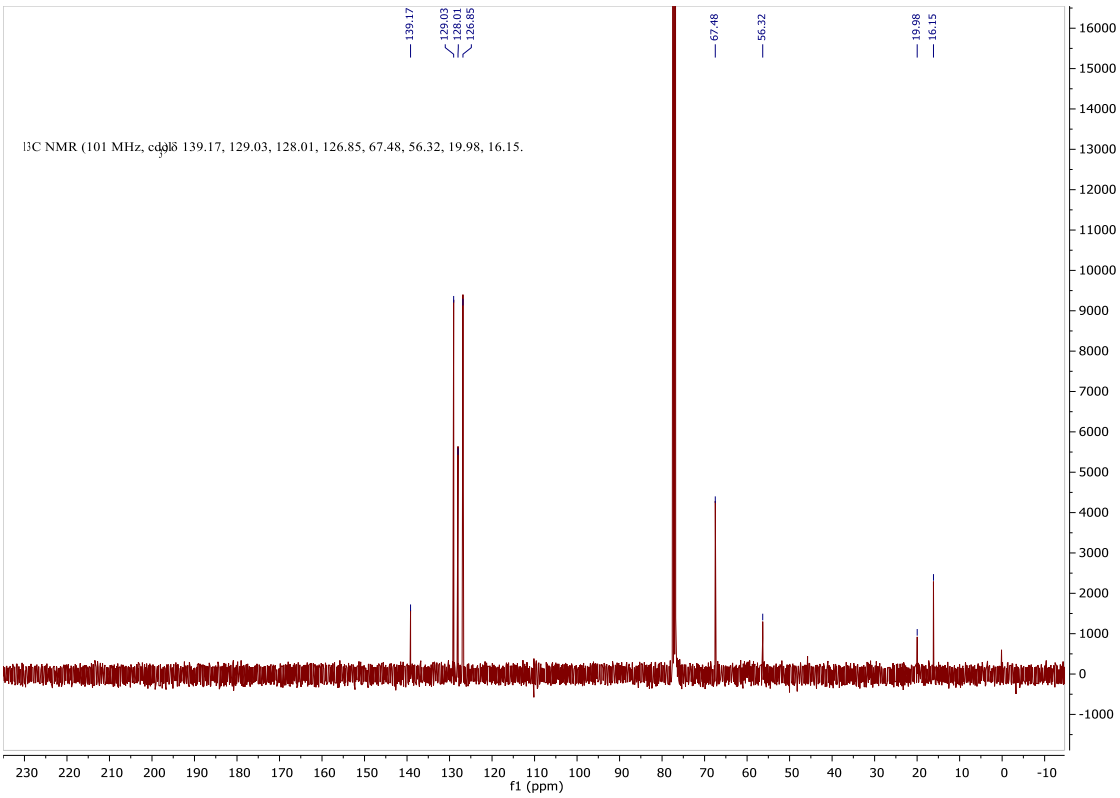
13C NMR (101 MHz, cdcl3) δ 139.17, 129.03, 128.01, 126.85, 67.48, 56.32, 19.98, 16.15.
139.17
129.03
128.01
126.85
67.48
56.32
19.98
16.15
f1 (ppm)

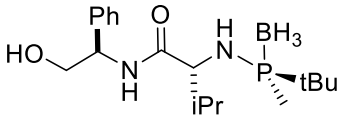

4-S2

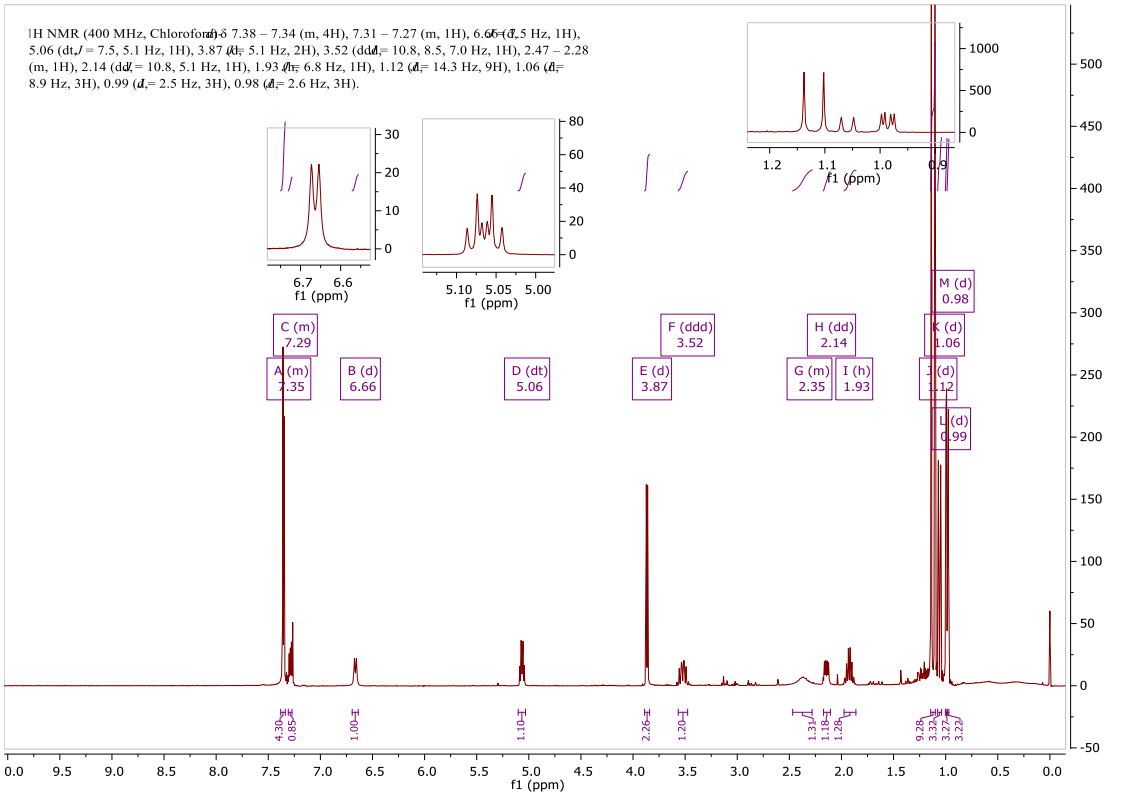

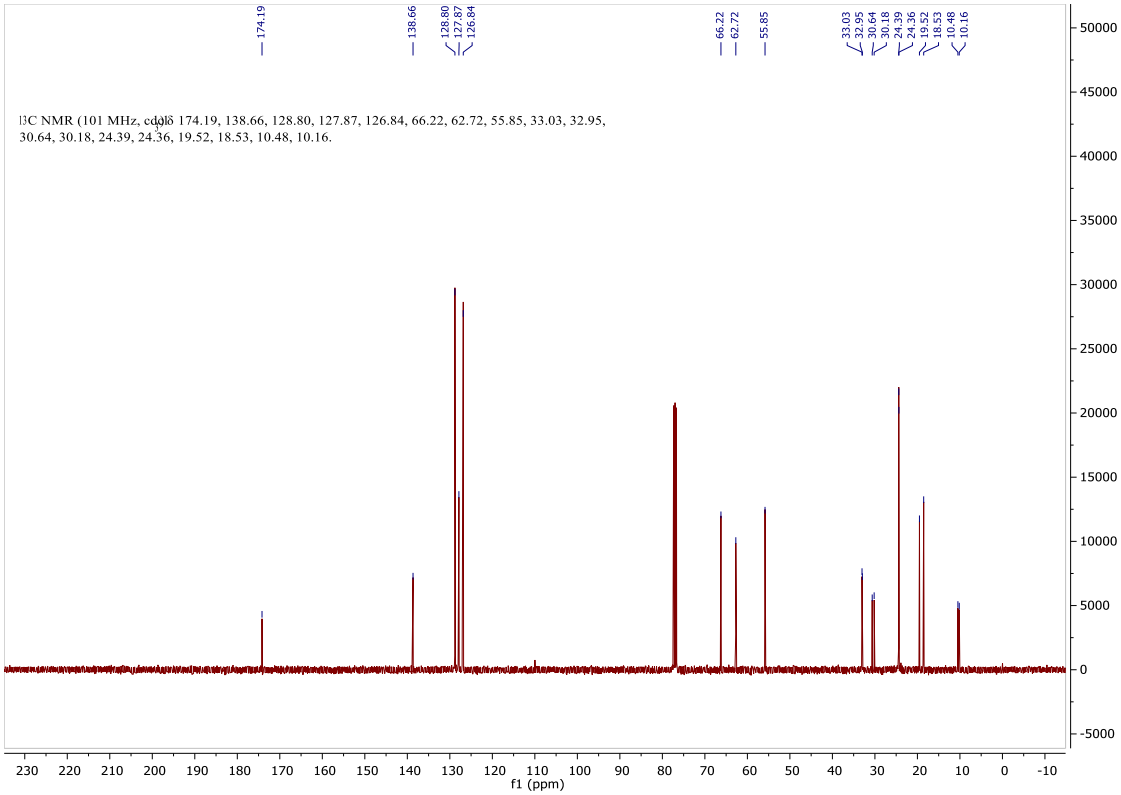

^{13}C NMR (101 MHz, cdcl$_3$) δ 174.19, 138.66, 128.80, 127.87, 126.84, 66.22, 62.72, 55.85, 33.03, 32.95, 30.64, 30.18, 24.39, 24.36, 19.52, 18.53, 10.48, 10.16.

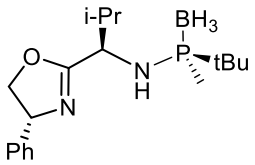
i-Pr
BH3
O
N
P
tBu
N
H
Ph

4-S3

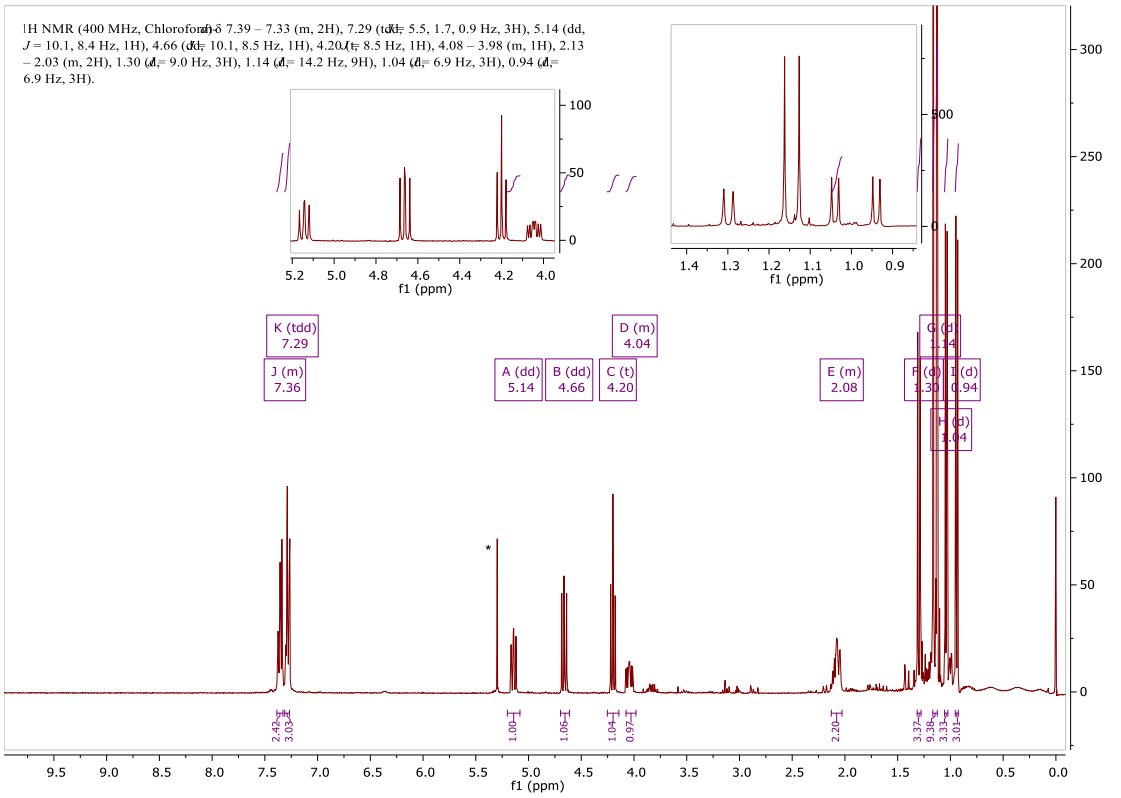
1H NMR (400 MHz, Chloroform-d) δ 7.39 – 7.33 (m, 2H), 7.29 (tdd, J = 5.5, 1.7, 0.9 Hz, 3H), 5.14 (dd, J = 10.1, 8.4 Hz, 1H), 4.66 (dd, J = 10.1, 8.5 Hz, 1H), 4.20 (t, J = 8.5 Hz, 1H), 4.08 – 3.98 (m, 1H), 2.13 – 2.03 (m, 2H), 1.30 (d, J = 9.0 Hz, 3H), 1.14 (d, J = 14.2 Hz, 9H), 1.04 (d, J = 6.9 Hz, 3H), 0.94 (d, J = 6.9 Hz, 3H).
K (tdd) 7.29
J (m) 7.36
A (dd) 5.14
B (dd) 4.66
C (t) 4.20
D (m) 4.04
E (m) 2.08
f1 (ppm)

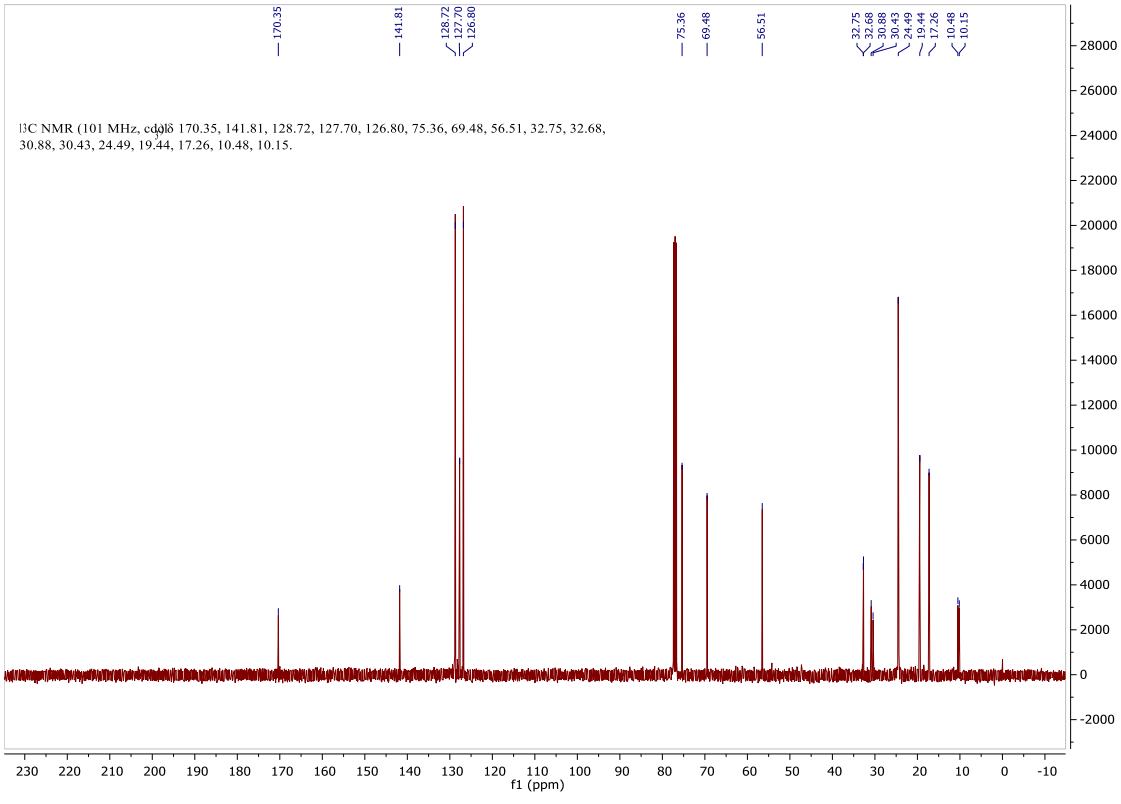
13C NMR (101 MHz, cdcl3) δ 170.35, 141.81, 128.72, 127.70, 126.80, 75.36, 69.48, 56.51, 32.75, 32.68, 30.88, 30.43, 24.49, 19.44, 17.26, 10.48, 10.15.
f1 (ppm)

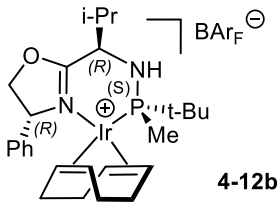

4-12b

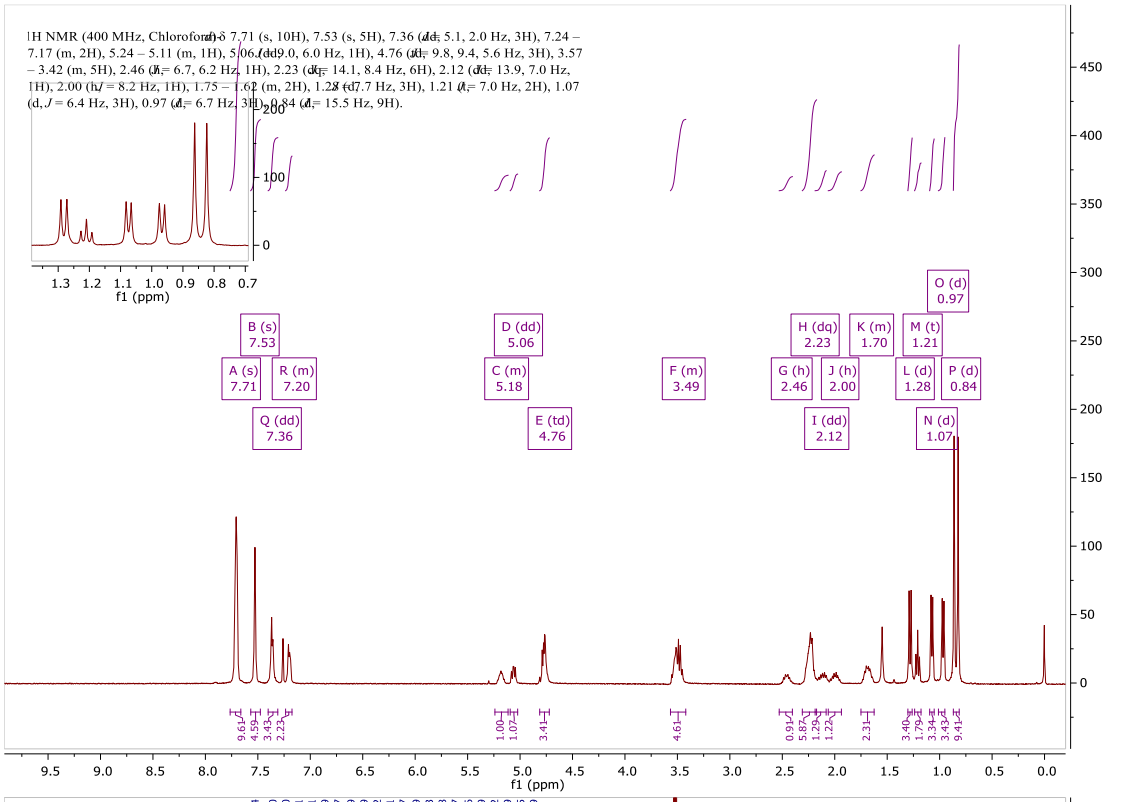

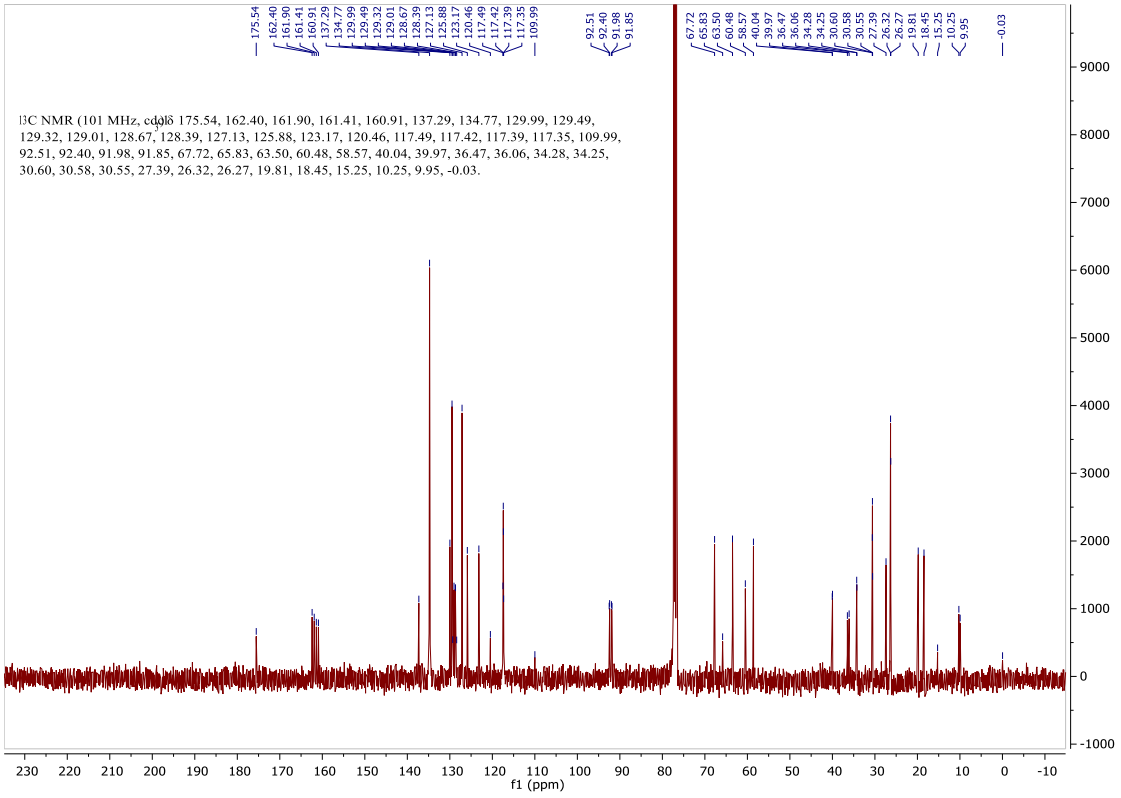

Chapter 5

Mild Iridium-Catalyzed Isomerization of Epoxides. Computational Insights and Application to the Synthesis of β-Alkyl Amines

Epoxides can be interconverted into a variety of functional groups and are thus valuable synthetic intermediates.[1] The high reactivity of the strained 3-membered ring of epoxides commonly enables a wide range of stereospecific nucleophilic ring opening reactions.[2] The isomerization into the corresponding carbonyl analogs is usually referred to as the Meinwald rearrangement.[3] Due to its excellent efficiency and atom economy, this reaction has gained relevance for the synthesis of carbonyl compounds,[4a] ring expansion reactions,[4b,c] and tandem processes.[4d,e] The Lewis acid-promoted Meinwald rearrangement has found application in fine chemistry and industrial processes.[4] However, the regiochemical outcome is a common issue since it depends on the promoter and the migratory capacity of the substituents.[5] The use of stoichiometric amounts of Lewis acids such as $BF_3 \cdot Et_2O$,[6] lithium salts[7] and magnesium bromide[8] are the most widely used conditions. The catalytic version using copper salts,[9] indium chloride[10] or iridium chloride[11] has also been described. However, a number of limitations, namely moderate product selectivity, high temperature and catalyst loading, and toxicity of the catalysts, remain to be addressed when employing catalytic conditions.

In recent years, other alternative procedures have been reported such as the use of metal-free self-assembled organic supramolecular capsules[12] or heterogeneous mesoporous aluminosilicate materials.[13] In the organometallic field, Mazet and co-workers reported the most relevant breakthrough using novel palladium[14] and iridium[15] catalysts. However, high temperatures (85-140°C and 100°C respectively) were needed in both cases.

Encouraged by this result we envisioned that other more accessible iridium catalysts (such as Crabtree's catalyst,[16,17] which is user-friendly and commercially available) could also promote the isomerization of epoxides using milder conditions. We found that, after activation,[18] Crabtree's catalyst isomerized terminal epoxides into aldehydes. One of the drawbacks of this transformation was the handling of the resulting aldehydes. Therefore, we set up a one-pot reductive amination procedure using primary amines to isolate stable, easy to handle amines.

Here, we describe the isomerization of terminal epoxides into aldehydes using Crabtree's catalyst, followed by the reductive amination of the *in situ* formed aldimines to afford synthetically useful amines (Scheme 5.1). Our one-pot procedure gave excellent selectivity. The resulting amines, containing an alkyl group in the β position, are important motifs in numerous drugs and biologically active compounds.[19]

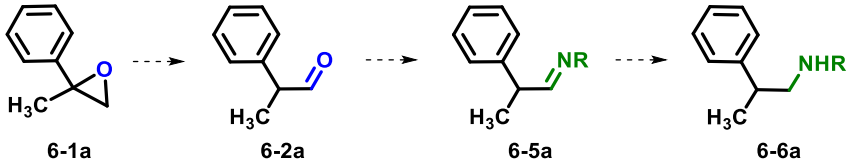

Scheme 5.1. One-pot procedure of the Meinwald rearrangement and reductive amination.

2-Methyl-2-phenyloxirane **5-1a**, easily synthesized by the Corey-Chaykosvky reaction,[20] was selected as model substrate. Isomerization of **5-1a** can, *a priori,* afford aldehyde **5-2a** or allylic alcohol **5-3a** (Table 5.1). We first tested Crabtree's catalyst (**5-4A**) in 1 mol %, without activation in dichloromethane. After 17 h, only 35% of conversion was detected by ^{1}H NMR (Table 5.1, entry 1). Aldehyde was selectively formed as the major product. We then activated the catalyst with H_2, to form a putative dihydride species.[21] Overnight stirring at room temperature increased the conversion up to 68% (Table 5.1, entry 2). Gratifyingly, the aldehyde was not affected by the presence of H_2. Therefore, we increased the catalyst loading up to 3 mol %. The reaction went to completion after 17 h, and an aldehyde/alcohol ratio of 80:20 was achieved (Table 5.1, entry 3). We then performed a solvent screening. Diethyl ether or toluene did not improve the results (Table 5.1, entries 4 and 5). This result could be explained by the low solubility of Crabtree's catalyst in these organic solvents. Therefore, we replaced PF_6 by BAr^F as counter ion. Using the Pfaltz's version of Crabtree's catalyst (**5-4B**)[22] in toluene we were pleased to see that full conversion was achieved after 17 h and with a slight improvement in selectivity (Table 5.1, entry 6). Finally, using either activated catalyst **5-4A** or **5-4B** in THF the reaction was complete after overnight stirring at room temperature reaching a selectivity of 93:7. Of note the selectivity in THF was similar in both cases (Table 5.1, entries 7 and 8). Since the hydrogen is only necessary to activate the catalyst the pressure is not important. We used 3 bars as standard procedure but the reaction can be done using hydrogen at atmospheric pressure (balloon). Purging the vessel to degas H_2 once the catalytic active species was formed did not affect neither the reactivity nor the selectivity (Table 5.1, entry 9).

Table 5.1. Optimization of the isomerization reaction.

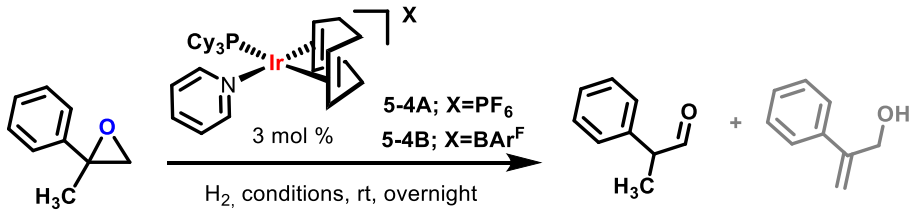

5-1a **5-2a** **5-3a**

entry	Cat.	Solvent	Conv.	Yield 5-2a (%)[a] (ratio 5-2a: 5-3a)
1 [b] [c]	**A**	CH_2Cl_2	35%	-
2 [b]	**A**	CH_2Cl_2	68%	-
3	**A**	CH_2Cl_2	>99	75 (80:20)
4	**A**	Et_2O	30%	-
5	**A**	Toluene	33%	-
6	**B**	Toluene	>99	79 (86:14)
7	**A**	THF	>99	85 (94:6)
8	**B**	THF	>99	84 (93:7)
9 [d]	**A**	THF	>99	84 (94:6)

Reactions were performed in a pressure tube, at room temperature and stirring overnight. The catalyst (3 mol %) and substrate were weighted, brought to a dry box, dissolved in anhydrous solvent and charged with hydrogen. [a] NMR yield using 1,4-dimethoxybenzene as internal standard. A small percentage of diol was observed in case of air moisture. [b] 1 mol % of catalyst was used. [c] Without external activation. [d] H_2 for 1 minute; then degas.

Once the optimal conditions for the isomerization reaction had been determined, we proceeded to study the reductive amination. Otte and co-workers pioneered a tandem Meinwald rearrangement-reductive amination using $B(C_6F_5)_3$[23] However, the scope of the amine was limited to anilines.

We reasoned that benzhydrylamine would be a convenient amine since it can be considered a synthetic equivalent of ammonia due to its easy hydrogenolysis. Therefore, we devised a two-step procedure that could be done *in situ*. To avoid the use of reagents such as $TiCl_4$ or $Ti(iPrO)_4$, which are usually required for imine formation and could interfere with our catalyst of choice we selected the aminocatalytic procedure developed by Cid and co-workers.[24] The addition of 10 mol % of pyrrolidine led to the formation of the aldimine of benzhydrylamine **5-5a** with total conversion after 2 h. With the optimal conditions for the imine formation in hand, we sought a reducing agent. Since the reduction could not be performed by hydrogen due to deactivation of iridium catalyst by the amine, we tested sodium cyanoborohydride (Table 5.2, entry 1). Conversion after 2 h was low, so we then tested a stronger reductant, $NaBH_4$, and added MeOH to the mixture. Under these

conditions the reaction went to completion and amine **5-6a** was afforded in an isolated yield of 67 % (Table 5.2, entry 2). The optimized protocol was scaled up to 1g of epoxide using only 1 mol % of iridium catalyst **5-4B**, yielding a remarkable 51% overall yield for the three steps.

Table 5.2. Optimization of the reductive amination.

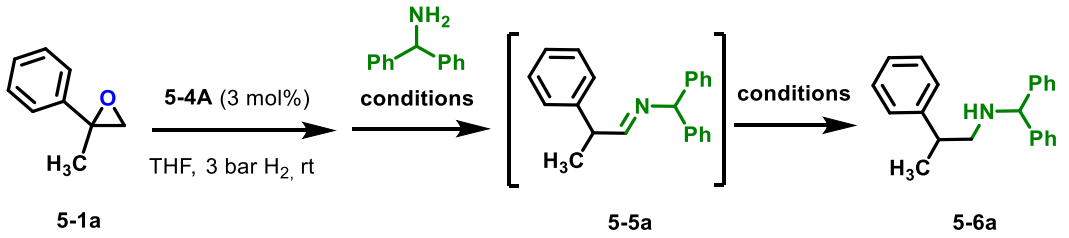

5-1a 5-5a 5-6a

entry	Conditions	Conversion[a] (3-step yield)[b]
1	1) pyrrolidine (10 mol%) 2) $NaBH_3CN$ in THF, 2h	**5-6a**: 70% (54%)
2	1) pyrrolidine (10 mol%) 2) $NaBH_4$ in MeOH, 2h	**5-6a**: 100% (67%;51%[c])

[a] Detected by ^1H NMR. [b] Isolated yield. [c] Isolated yield in gram scale, using 1 mol% of catalyst **5-4B**.

We then proceeded to study the scope of the reaction. To this end, a set of 13 2,2-disubstituted epoxides (**5-1(b-n)**) were tested (Table 5.3). The substituent pattern slightly altered the optimal conditions found for the isomerization reaction. We observed that the use of electron-withdrawing substituents was well tolerated.

Amine **5-6b** derived from 2-(4-fluorophenyl)-2-methyloxirane **5-1b** was obtained with an overall yield of 57 % (Table 5.3, entry 1). The isomerization reaction starting from the *p*-chlorophenyl oxirane **5-1b** (Table 5.3, entry 2), took place in only 2 h and the corresponding amine **5-6c** was obtained in 67 % isolated yield. In the case of *p*-Br and *p*-I derivatives **5-1(d-e)** the reaction lasted longer (48 h). However, this drawback could be solved by modifying the counter ion from PF_6 to BAr^F. In these cases, the reaction times were reduced to 12 h and the alcoholic species were minimized. After the reductive amination procedure, the resulting amines **5-6(d-e)** were obtained in synthetically useful yields (63-74 %, Table 5.3, entries 3-4).

We then studied the effect of electron-donating groups (methyl and methoxy) in *ortho* or *para*-position of the aromatic ring. Using the optimized conditions, all reactions were completed after 12 h (Table 5.3, entries 6-8) with the exception of the *ortho*-methyl compound

5-1f which due to steric hindrance, lasted 48 h (Table 5.3, entry 5). The ratio of alcoholic species formed were minimal in all cases, thus demonstrating the high selectivity of this transformation. The 2-naphthy substituent **5-1j** afforded the corresponding amine **5-6j** in 62 % yield (Table 5.3, entry 9) using standard conditions. To prove the versatility of this reaction, the methyl group was also modified. When using an ethyl substituent, the amine **5-6k** was afforded in 70 % yield and no alcoholic species were detected after the isomerization reaction (Table 5.3, entry 10).

For the branched alkyl substituent, catalyst **5-4B** was necessary for completion of the reaction. The isomerization reaction showed excellent selectivity towards the aldehyde and **5-6l** and **5-6m** were afforded in 57 % and 75 % yield, respectively (Table 5.3, entries 11-12). Finally, as an example of dialkyl epoxide, the phenethyl oxirane **5-1n** was also studied. In this regard, when using 5 mol % of **5-4B**, the reaction went to completion after 12 h with only few traces of alcohol species and afforded the corresponding amine **5-6n** in 79% yield (Table 5.3, entry 13).

The benzhydrylamine moiety can be easily removed by hydrogenolysis to afford free amines that can be further derivatized (Scheme 5.2).

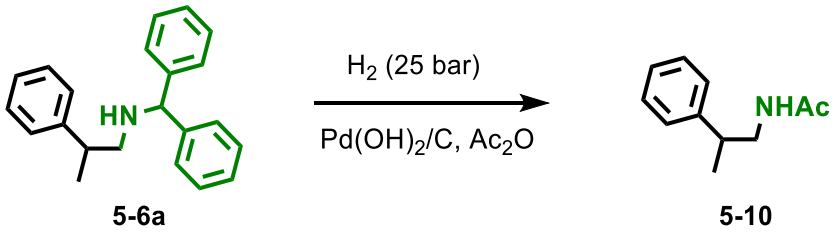

Scheme 5.2. Reaction scheme for the benzhydrylamine deprotection.

Table 5.3. Epoxide scope of the reaction. All reactions were performed in a pressure tube. Ratio **5-2: 5-3** is the selectivity towards the aldehyde when the isomerization reaction is finished, measured by ^{1}H NMR..

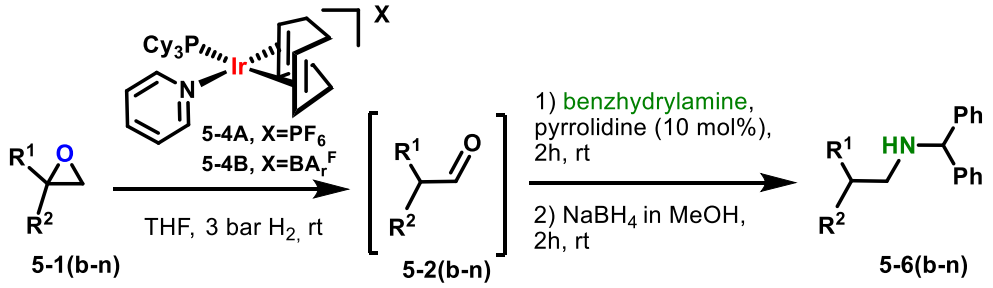

entry	5-1	R^1	R^2	cat.; time[b]	ratio 5-2: 5-3	yield (%)[c]
1	**5-1b**	*p*-F-Ph	Me	**5-4A;** 17 h	94:6	57
2	**5-1c**	*p*-Cl-Ph	Me	**5-4A;** 2h	95:5	67
3	**5-1d**	*p*-Br-Ph	Me	**5-4B;** 12h	>99	74
4	**5-1e**	*p*-I-Ph	Me	**5-4B;** 12h	92:8	63
5	**5-1f**	*o*-Me-Ph	Me	**5-4A:** 48h	97:3	80
6	**5-1g**	*p*-Me-Ph	Me	**5-4A;** 12h	94:6	45
7	**5-1h**	*o*-MeO-Ph	Me	**5-4A;** 12h	98:2	71
8	**5-1i**	*p*-MeO-Ph	Me	**5-4A;** 12h	>99	45
9	**5-1j**	2-Naphth	Me	**5-4A;** 12h	91:9	62
10	**5-1k**	Ph	Et	**5-4A;** 12h	>99	70
11	**5-1l**	Ph	iPr	**5-4B;** 3h	>99	57
12	**5-1m**	Ph	Cy	**5-4B;** 12h	>99	75
13[a]	**5-1n**	$PhCH_2CH_2$	Me	**5-4B;** 12h	98:2	79

[a] 5 mol % of catalyst **5-4B** was used. [b]Isomerization time. [c] Overall isolated yields.

The isomerization reaction also took place in epoxides with different substitution patterns. Using 1 mol % of **5-4B** in dichloromethane, 2-methyl-3-phenyloxirane **5-1o** isomerized to methyl ketone **5-2o** in excellent yield (Scheme 5.3A). In the case of trisubstituted epoxide **5-1p**, instead of hydride migration we observed phenyl migration yielding aldehyde **5-2p** as a single product (89% isolated yield), as shown in Scheme 5.3B. Again, the hydrogen pressure did not affect the reaction. 2,2-Diaryloxiranes are extremely reactive. 2-(4-Chlorophenyl)-2-phenyloxirane (**5-1q**) gave 30% yield of the corresponding aldehyde (**5-2q**), along with 65% of demethylenation product in only 2 h of reaction and using 1 mol % of **5-4A** (Scheme 5.3C).

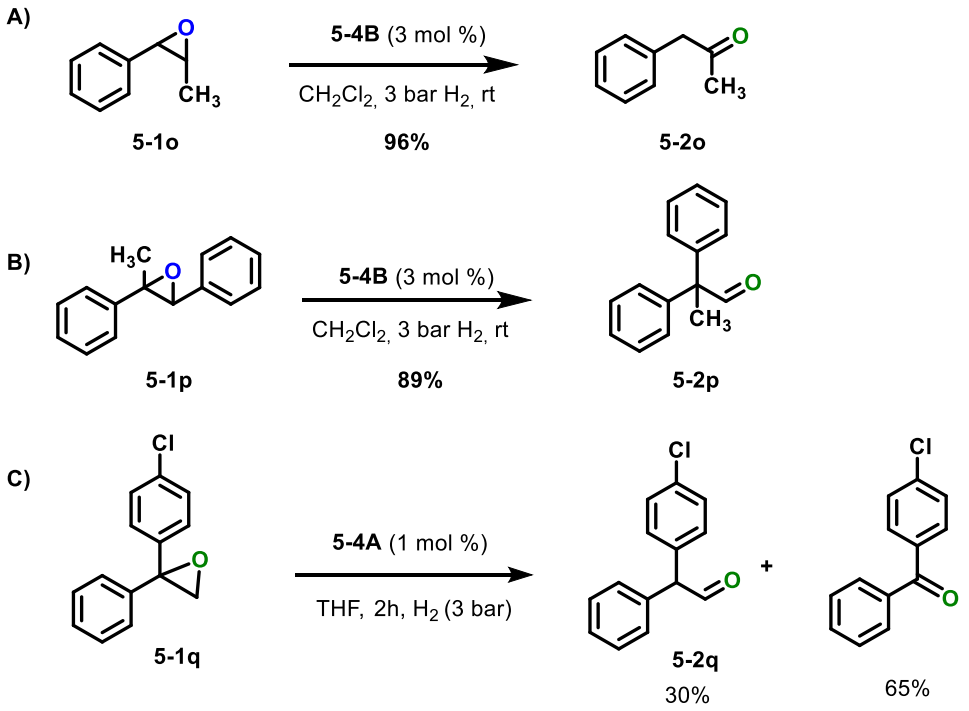

Scheme 5.3. Iridium-catalyzed isomerization of 1,2-di- and trisubstituted epoxides.

On the other hand, the amine scope could also be expanded. *p*-Methoxyaniline (Table 5.4, entry 1), benzylamine (Table 5.4, entry 2) and enantiomerically pure *(R)*-(+)-1-phenylethan-1-amine (Table 5.4, entry 3) were successfully tested with synthetically useful yields. In the latter example, the separation of the two diastereoisomers enabled the formation of enantioenriched amines after hydrogenolysis.

Table 5.4. Amine scope of the reaction. Reactions were performed in a pressure tube, using **5-4B** (5 mol %) as catalyst and 1.1 equiv. of amine.

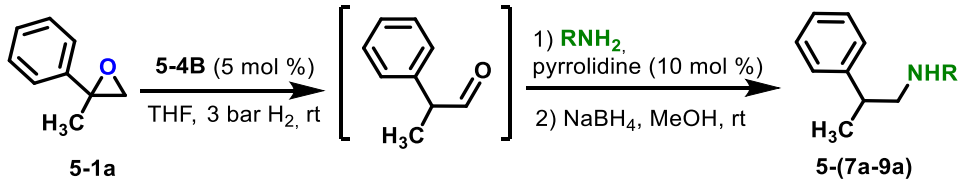

entry	amine	Yield (%)[a]
1	*p*-OMe-aniline	**5-7a,** 64%
2	Benzylamine	**5-8a,** 55%
3	*(R)*-(+)-1-Phenylethylamine	**5-9a,** 56% (3:2 dr)

[a] Isolated yields.

To gain a thorough understanding of the isomerization step, we performed a DFT study of its reaction mechanism using the B3LYP-D3[25] functional and a continuum model of the THF solvent[26] (see Experimental Part - Computational details).

We initially studied the activation of the Crabtree's catalyst, entailing hydrogenation of the COD ligand and cyclooctane release and formation of the unsaturated dihydride complex. This step is very exergonic (ΔG= -30.6 kcal·mol^{-1}) and generates the catalytic active specie $[Ir^{III}(H)_2(py)(PCy_3)]^+$ in a octahedral arrangement with two vacancies. Several possible isomers were evaluated for this species, concluding that the most stable configurations are those with the H and PCy_3 ligands mutually *cis* and the second hydride in the axial position. An isomer with the hydride *trans* to the phosphine ligand was found *ca.* 17.0 kcal·mol^{-1} above. The equatorial hydride can be coordinated *trans* a vacancy or *trans* pyridine with very similar energies (ΔG of 1.1 kcal·mol^{-1}) and easy interconversion (Gibbs energy barrier 9.0 kcal·mol^{-1}) highlighting a fast equilibrium between these two relative orientations (Scheme 5.SI1 of the Experimental Part). Between them, the species with H *trans* pyridine can better accommodate the incoming substrate and has been taken as the catalytic configuration.

The O-coordination of **5-1a** at the empty equatorial position generates intermediate **I** at 1.9 kcal·mol^{-1} and gives rise to the catalytic cycle depicted in Scheme 5.4.

The associated Gibbs energy profile can be found at the Experimental Part – Computational details (Figure 5.SI1). Subsequent concerted ring-opening and C-coordination leads to the formation of a five-member ring metallacycle, **II**, with a relative energy of 11.2 kcal·mol^{-1}, overcoming an energy barrier of 19.9 kcal·mol^{-1}, **TS$_{I\text{-}II}$** (Figure 5.2a). This transition state is the highest point in the Gibbs energy profile, making the ring-opening step the rate-determining step. Intermediate **II** is a highly distorted octahedron with the oxygen in the axial position and the equatorial hydride close to the β-carbon of **1a** (C_β ···HIr 2.219 Å). From this intermediate an easy hydride insertion to the γ-carbon-Ir bond opens the metallacycle leading to Intermediate **III**, falling at 2.4 kcal·mol^{-1}. This is practically a barrierless process with its transition sate (**TS$_{II\text{-}III}$**, Figure 5.2b) at the same energy (11.1 kcal·mol^{-1}) than intermediate **II.** According to this mechanism the reaction should proceed with retention of configuration. This was confirmed experimentally. Starting from enantiomerically pure **5-(*R*)-1a**, enantiomerically enriched **5-(*S*)-2a** was obtained, albeit with low ee (26% ee) due to substantial racemization of the aldehyde in the reaction conditions (Scheme 5.5).[27]

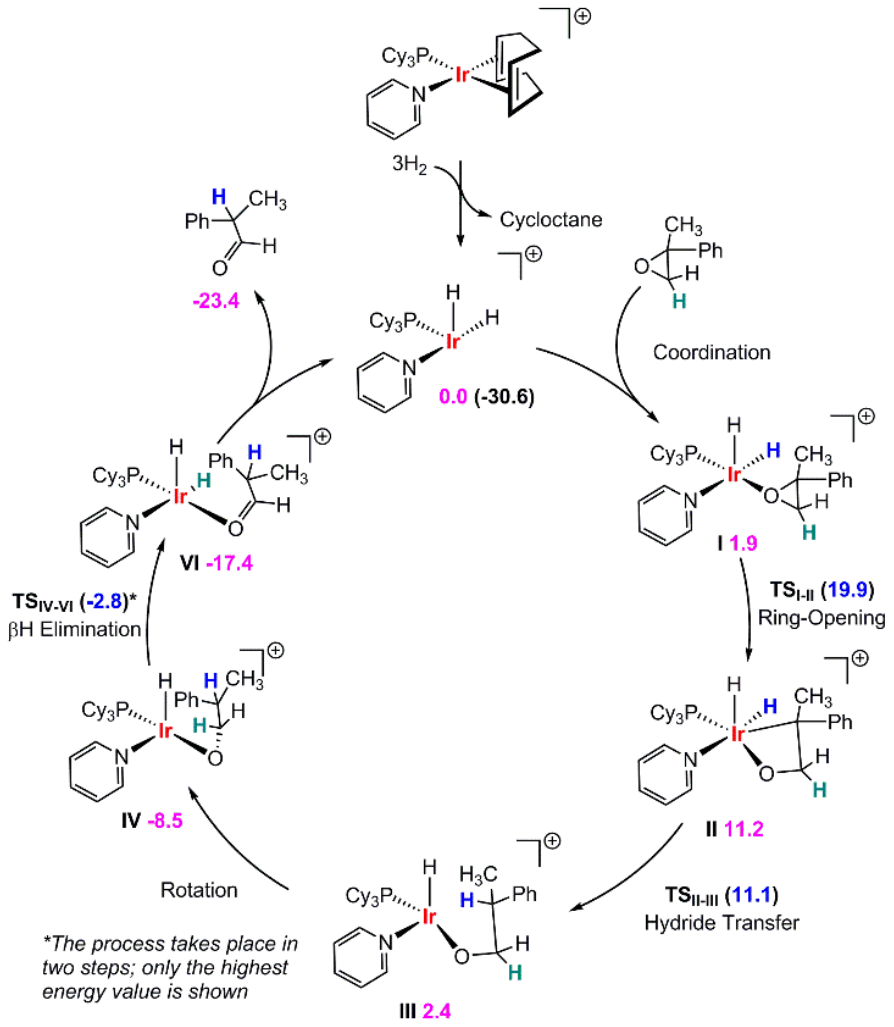

Scheme 5.4. DFT computed mechanism (B3LYP-D3 in THF) for the Ir-catalysed isomerization of epoxide **5-1a** to aldehyde **5-2a**. Relative Gibbs energies (in purple) in kcal·mol^{-1} are referred to the separated catalytically active species $[Ir^{III}(H)_2(py)(PCy_3)]^+$ and substrate **5-1a**; transition state energies are shown in parenthesis and blue.

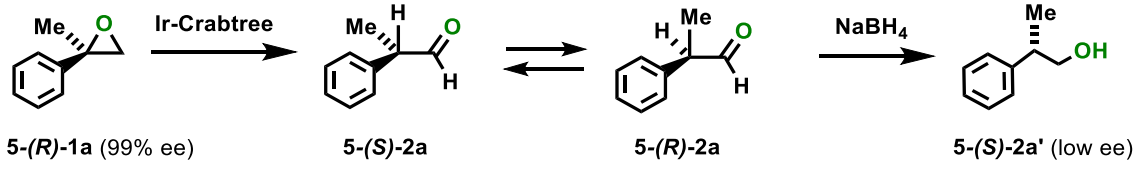

Scheme 5.5. Isomerization of enantiomerically enriched epoxides.

To complete the isomerization, a hydrogen from the substrate must end up at the metal. Consequently, β-hydride elimination is the last step of the isomerization process. Previously, substrate reorientation in intermediate **III** is required to place the β H near to the vacant equatorial position at iridium. The rotation process occurs barrierless and leads to the more stable conformation of intermediate **IV** at -8.5 kcal·mol^{-1} (βH···Ir 2.927 Å). β-hydride

elimination from intermediate **IV** is a two-step process in which, first a strong βH-Ir agostic interaction takes place (βH···Ir 1.736 Å, **V,** -7.0 kcal·mol^{-1}), followed by the β-H-C elimination, with relative Gibbs energies of -2.8 and -6.3 kcal·mol^{-1} for $\mathbf{TS_{IV\text{-}V}}$ and $\mathbf{TS_{V\text{-}VI}}$, respectively (Figures 5.2c and 5.2d). Finally, from intermediate **VI** (-17.4 kcal·mol^{-1}) the replacement of the aldehyde by a reactant molecule closes the catalytic cycle.

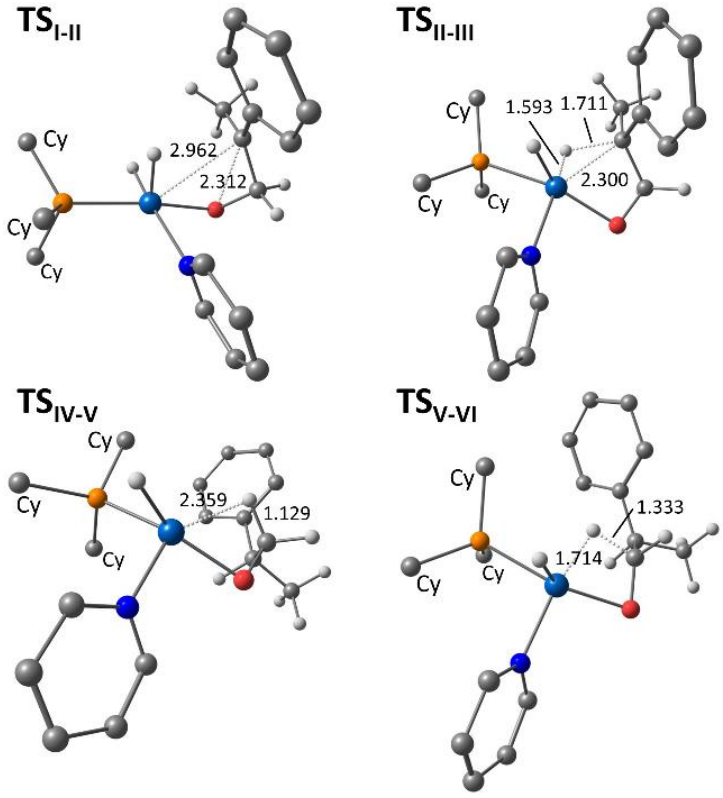

Figure 5.2. Transition state optimised geometries for: ring opening, $\mathbf{TS_{I\text{-}II}}$; hydride transfer, $\mathbf{TS_{II\text{-}III}}$; ($C_\beta$-H)-Ir agostic formation, $\mathbf{TS_{IV\text{-}V}}$; β-H elimination, $\mathbf{TS_{V\text{-}VI}}$. The most important distances are also reported in Å. Hydrogen atoms and cyclohexyl (Cy) groups have been omitted for clarity.

The general reaction sequence we have computed is equivalent to the mechanism proposed by Mazet and co-workers for the Pd-hydride catalyzed isomerization of epoxides to aldehydes.[14] Initially the metal breaks the epoxide ring and then successive hydride migration to the γ-carbon and β hydride elimination yields the aldehyde. Despite this general mechanistic similarity, some differences arise between the palladium and iridium hydride-catalysed epoxide isomerization. First, ring-opening of the epoxide is notably easier in presence of the iridium catalyst (Gibbs energy barriers in THF of 24.0 and 19.9 kcal mol^{-1} for the Pd and Ir complexes, [14,15] respectively). This behaviour can be related to the highly unsaturated nature of the Ir-catalyst, which has two vacant sites. This feature also allows the

stabilization of a metallocycle intermediate (**II**) absent in the palladium system. Correspondingly, the overall barrier for the isomerization is lower for the Ir-catalyst than for Pd (19.9 *vs.* 26.4 kcal mol^{-1}) in agreement with the milder conditions at which the reaction takes place (room temperature, see Tables 5.1 and 5.3).

In conclusion, the selective isomerization of terminal epoxides to aldehydes has been accomplished using low catalyst loadings (up to 1 mol%) of the readily available Crabtree's reagent. The pre-catalyst requires activation with hydrogen but there is no need to degas the vessel afterwards. The reaction occurs under milder conditions than in previous reports were high temperatures were required. DFT calculations reveal that the isomerization takes place via a hydride mechanism similar to that described for a palladium hydride complex,[14] but with a considerably lower barrier, in agreement with the milder reaction conditions (room temperature). The reductive amination of the resulting aldehydes can be performed *in situ*. We have optimised a one-pot protocol based on the imine formation catalysed by pyrrolidine followed by reduction with $NaBH_4$. Using benzhydrylamine, up to 14 amines have been synthesized in good to excellent yields. The reaction can be easily scaled up. Other aryl or alkyl amines –including chiral ones- have been successfully used.

References

(1) a) R. L. Paddock, S. T. Nguyen, *J. Am. Chem. Soc.*, **2001**, *123*, 11498–11499. b) S. Liao, M. Leutzsch, M. R. Monaco, B. List, *J. Am. Chem. Soc.*, **2016**, *138*, 5230–5233. c) J. M. Rowley, E. B. Lobkovsky, G. W. Coates, *J. Am. Chem. Soc.*, **2007**, *129*, 4948–4960. d) M. Mulzer, B. J. Tiegs, Y. Wang, G. W. Coates, G. A. O'Doherty, *J. Am. Chem. Soc.*, **2014**, *136*, 10814–10820. e) A. Gansäuer, M. Otte, L. Shi, *J. Am. Chem. Soc.*, **2011**, *133*, 416-417. f) J. Justicia, J. L. Oller-López, A. G. Campaña, J. E. Oltra, J. M. Cuerva, E. Buñuel, D. J. Cárdenas, *J. Am. Chem. Soc.*, **2005**, *127*, 14911–14921. g) A. Gansäuer, M. Otte, F. Piestert, C. A. Fan, *Tetrahedron*, **2009**, *65*, 4984–4991. h) A. Gansäuer, H. Bluhm, M. Pierobon, *J. Am. Chem. Soc.*, **1998**, *120*, 12849–12859.

(2) a) Q. H. Xia, H. Q. Ge, C. P. Ye, Z. M. Liu, K. X. Su, *Chem. Rev.*, **2005**, *105*, 1603–1662. b) J. G. Smith, *Synthesis*, **1984**, 629–656. c) B. M. Smith, E. J. Skellam, S. J. Oxley, A. E. Graham, *Org. Biomol. Chem.*, **2007**, *5*, 1979–1982. d) M. W. C. Robinson, R. Buckle, I. Mabbett, G. M. Grant, A. E. Graham, *Tetrahedron Lett.*, **2007**, *48*, 4723–4725.

(3) a) J. Meinwald, S. S. Labana, M. S. Chadha, *J. Am. Chem. Soc.*, **1963**, *85*, 582–585. b) B. M. Trost, *Science,* **1991**, *254*, 1471. For recent stereoselective rearrangements, see: c) K. Suda, T. Kikkawa, S. I. Nakajima, T. Takanami, *J. Am. Chem. Soc.*, **2004**, *126*, 9554–9555. d) R. Hrdina, C. E. Müller, R. C. Wende, K. M. Lippert, M. Benassi, B. Spengler, P. R. Schreiner, *J. Am. Chem. Soc.*, **2011**, *133*, 7624–7627. e) K. Suda, S. I. Nakajima, Y. Satoh, T. Takanami, *Chem. Commun.*, **2009**, 1255–1257. f) T. Kimura, N. Yamamoto, Y. Suzuki, K. Kawano, Y. Norimine, K. Ito, S. Nagato, Y. Iimura, M. Yonaga, *J. Org. Chem.*, **2002**, *67*, 6228–6231.

(4) a) J. R. Lamb, M. Mulzer, A. M. LaPointe, G. W. Coates, *J. Am. Chem. Soc.*, **2015**, *137*, 15049-15054. b) Z. Chen, Y. Xiao, J. Zhang, *Eur. J. Org. Chem.* **2013**, 4748–4751. c) A. K. Pandey, P. Banerjee, *Asian J. Org. Chem.* **2016**, *5*, 360–366. d) L. F. Wang, Z. F. Shi, X. P. Cao, B. S. Li, P. An, *Chem. Commun.* **2014**, *50*, 8061–8064. e) A. K. Pandey, A. Ghosh, P. Banerjee, *Eur. J. Org. Chem.* **2015**, 2517–2523. f) J. R. Donald, R. J. K. Taylor, *Synlett*, **2009**, 59–62. g) Y. Kita, J. Futamura, Y. Ohba, Y. Sawama, J. K. Ganesh, H. Fujioka, *J. Org. Chem.*, **2003**, *68*, 5917–5924. h) J. B. Lewis, G. W. Hedrick, *J. Org. Chem.*, **1965**, *30*, 4271–4275. i) M. Szostak, J. Aube, *J. Am. Chem. Soc.*, **2009**, *131*, 13246–13247.

(5) B. Rickborn, in *Comprehensive Organic Synthesis*, B. M. Trost, Ed., Pergamon: Oxford, **1991**, vol. 3, chapter 3.3., pp 733–775.

(6) a) Y. Kita, S. Kitagaki, Y. Yoshida, S. Mihara, D. F. Fang, M. Kondo, S. Okamoto, R. Imai, S. Akai, H. Fujioka, *J. Org. Chem.*, **1997**, *62*, 4991–4997. b) J. M. Fraile, J. A. Mayoral, L. Salvatella, *J. Org. Chem.*, **2014**, *79*, 5993–5999.

(7) R. Sudha, K. Malola Narasimhan, V. Geetha Saraswathy, S. Sankararaman, *J. Org. Chem.*, **1996**, *61*, 1877–1879.

(8) H. O. House, *J. Am. Chem. Soc.*, **1955**, *77*, 3070–3075.

(9) a) M. W. C. Robinson, K. S. Pillinger, A. E. Graham, *Tetrahedron Lett.*, **2006**, *47*, 5919–5921. b) M. W. C. Robinson, K. S. Pillinger, I. Mabbett, D. A. Timms, A. E. Graham, *Tetrahedron*, **2010**, *66*, 8377–8382.

(10) B. C. Ranu, U. Jana, *J. Org. Chem.*, **1998**, *63*, 8212–8216.

(11) I. Karamé, M. L. Tommasino, M. Lemaire, *Tetrahedron Lett.*, **2003**, *44*, 7687–7689.

(12) T. Caneva, L. Sperni, G. Strukul, A. Scarso, *RSC Adv.*, **2016**, *6*, 83505–83509.

(13) M. W. C. Robinson, A. M. Davies, R. Buckle, I. Mabbett, S. H. Taylor, A. E. Graham, *Org. Biomol. Chem.*, **2009**, *7*, 2559–2564.

(14) D. J. Vyas, E. Larionov, C. Besnard, L. Guénée, C. Mazet, *J. Am. Chem. Soc.*, **2013**, *135*, 6177–6183.

(15) N. Humbert, D. J. Vyas, C. Besnard, C. Mazet, *Chem. Commun.*, **2014**, *50*, 10592–10595.

(16) R. H. Crabtree, *Platin. Met. Rev.*, **1978**, *22*, 126–129.
(17) A. Cabré, G. Sciortino, G. Ujaque, X. Verdaguer, A. Lledós, A. Riera, *Org. Lett.*, **2018**, *20*, 5747–5751.
(18) For selected examples about H_2 activation of iridium-P,N complexes, see: a) H. Li, C. Mazet, *Acc. Chem. Res.*, **2016**, *49*, 1232–1241. b) L. Mantilli, C. Mazet, *Tetrahedron Lett.*, **2009**, *50*, 4141–4144. c) H. Li, D. Fiorito, C. Mazet, *ACS Catal.*, **2017**, *7*, 1554–1562.
(19) a) R. N. H. Iii, R. S. Stabler, D. B. Repke, J. M. Kress, K. A. Walker, R. S. Martin, J. M. Brothers, M. Ilnicka, S. W. Lee, T. Mirzadegan, *Bioorg. Med. Chem. Lett.*, **2010**, *20*, 3436–3440. b) I. Ether, G. Lazarevski, G. Kobrehel, *J. Antibiot.* **1996**, *49*, 1066–1069. c) H. M. L. Davies, A. Ni, *Chem. Commun.*, **2006**, 3110–3112. d) P. Ramesh, D. Suman, K. S. N. Reddy, *Synthesis*, **2018**, *50*, 211–226. e) G. M. Nicholas, T. F. Molinski, *Tetrahedron*, **2000**, *56*, 2921–2927.
(20) E. J. Corey, M. Chaykovsky, *J. Am. Chem. Soc.* **1965**, *87* (6), 1353-1364.
(21) E. Larionov, H. Li, C. Mazet, *Chem. Commun.,* **2014**, *50*, 9816–9826.
(22) B. Wüstenberg, A. Pfaltz, *Adv. Synth. Catal.*, **2008**, *350*, 174–178.
(23) M. R. Tiddens, R. J. M. Klein Gebbink, M. Otte, *Org. Lett.*, **2016**, *18*, 3714–3717.
(24) S. Morales, F. G. Guijarro, J. L. García Ruano, M. B. Cid, *J. Am. Chem. Soc.*, **2014**, *136*, 1082–1089.
(25) A. V. Marenich, C. J. Cramer, D. G. Truhlar, *J. Phys. Chem. B* **2009**, *113*, 6378-6396.
(26) S. Grimme, J. Antony, S.Ehrlich, H. Krieg, *J. Chem. Phys*. **2010**, *132*, 154104.
(27) After 24 h of reaction the product was racemic. However, at shorter reaction times (4 h) the reaction product had 26% ee of the right isomer (*S*) thus confirming the mechanism and indicating that the aldehyde isomerized in the reaction medium. Probably, the Lewis acid character of the iridium complexes promote the isomerization of the aldehyde which is known to be easy due to its benzylic character.[28]
(28) S. Chercheja, S. K. Nadakudity, P. Eilbracht, *Adv. Synth. Catal.* **2010**, *352*, 637–643.

Experimental Part

General procedures and materials

Unless otherwise indicated, materials were obtained from commercial suppliers and used without further purification. All reactions that required anhydrous conditions were performed in dried glassware under a dry nitrogen atmosphere. Dichloromethane and THF were degassed and anhydrised with a solvent purification system (SPS PS-MD-3). Anhydrous dichloroethane and DMF were used from Sigma Aldrich. Solvents were removed under reduced pressure with a rotary evaporator. Silica gel chromatography was performed using an automated chromatography system (PuriFlash® 430, Interchim).

Instrumentation

NMR spectroscopy: ^{1}H and ^{13}C were recorded on the NMR spectrometers of the *Centres Científics i Tecnològics de la Universitat de Barcelona*. The employed spectrometers were a Varian Mercury 400 MHz. Chemical shifts (δ) were referenced to internal solvent resonances and reported relative to TMS (tetramethylsilane). The coupling constants (*J*) are reported in Hertz (Hz). The following abbreviations are used to define multiplicities: s (singlet), d (doublet), t (triplet), q (quartet), dd (doublet of doublets), ddd (doublet of doublet of doublets), ddd (doublet of doublet of triplets), dddd (doublet of doublet of doublet of doublets), dt (doublet of triplets), td (triplet of doublets), ddq (doublet of doublet of quartets), dtd (doublet of triplet of doublets), dq (doublet of quartets), tt (triplet of triplets), qt (quartet of triplets), m (multiplet), br s (broad signal).

High Resolution Mass Spectrometry: High resolution ESI-MS spectra were recorded in an LC/MSD-TOF G1969A (Agilent Technologies) of the *Centres Científics i Tecnològics de la Universitat de Barcelona.*

IR spectroscopy: IR spectra were measured in a Thermo Nicolet 6700 FT-IR spectrometer using an ATR system, of the Department of Organic Chemistry in the Universitat de Barcelona.

Optical rotations were measured at room temperature (25°C) using a Jasco P-2000 iRM- 800 polarimeter. Concentration is expressed in g/100 mL. The cell sized 10 cm long and had 1 mL of capacity, measuring λ was 589 nm, which corresponds to a sodium lamp.

Melting points were determined using a Büchi melting point apparatus and were not corrected.

Experimental procedures and characterization

Preparation of substrates

General procedure (GP1)

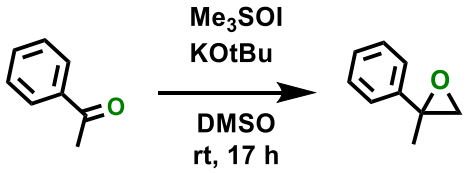

In an oven dried flask, DMSO (1.6 mL/mmol) was added to trimethylsulfoxonium iodide (1.5 equiv.). The suspension was cooled to 0 ºC, KOtBu (1.2 equiv.) was added and the resulting yellow suspension was stirred at 0 ºC for 10 min. To this suspension, a solution of ketone (1.0 equiv.) in DMSO (0.7 mL/mmol) was added dropwise and the resulting mixture was warmed gradually to r.t. and stirred at r.t. for 16 hours. Afterwards, the reaction mixture was diluted with water and extracted (x3) in hexanes. The organic extracts were collected, dried over $MgSO_4$ and concentrated to afford the desired product which was used for the next step without further purification.

General procedure (GP2)

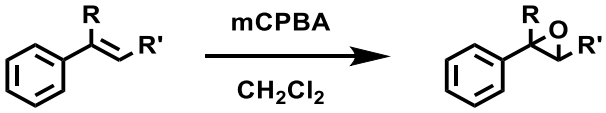

In an oven dried flask, the desired alkene (1 eq.) in dissolved in anhydrous CH_2Cl_2 (0.4 M) was placed. The vessel was purged with N_2 and cooled to 0 ºC. To this solution, *m*-CPBA (1.1 eq.) was added in a single portion. After completion of the reaction (TLC monitoring) the reaction mixture was quenched with a saturated solution of $NaHCO_3$. The aqueous phase was extracted (3x) with CH_2Cl_2. The organic phases were collected and dried over $MgSO_4$. The solvent was concentrated *in vacuo* to yield the epoxide which was directly used without any further purification.

2-methyl-2-phenyloxirane, 5-1a

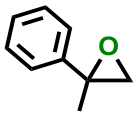

Following GP1, the product was obtained as a colorless oil (1.05 g, 94% yield). **^{1}H NMR** (400 MHz, $CDCl_3$) δ 7.39 – 7.30 (m, 4H), 7.30 – 7.26 (m, 1H), 2.98 (d, J = 5.4 Hz, 1H), 2.80 (dq, J = 5.4, 0.8 Hz, 1H), 1.72 (d, J = 0.8 Hz, 3H). The analytical data for this compound were in excellent agreement with the reported data.[1]

2-(4-fluorophenyl)-2-methyloxirane, 5-1b

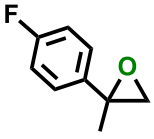

[1] Vyas, D. J.; Larionov, E.; Besnard, C.; Guénée, L.; Mazet, C. *J. Am. Chem. Soc.* **2013**, *135* (16), 6177–6183.

Following GP1, the product was obtained as a light brown oil (1.05 g, 95% yield). **^{1}H NMR** (400 MHz, $CDCl_3$) δ 7.36 – 7.30 (m, 2H), 7.05 – 6.98 (m, 2H), 2.96 (d, J = 5.3 Hz, 1H), 2.77 (dq, J = 5.3, 0.7 Hz, 1H), 1.70 (d, J = 0.6 Hz, 3H). The analytical data for this compound were in excellent agreement with the reported data.[1]

2-(4-chlorophenyl)-2-methyloxirane, 5-1c

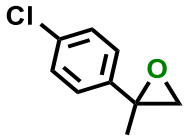

Following GP, the product was obtained as a light yellow oil (990 mg, **91%** yield). **^{1}H NMR** (400 MHz, $CDCl_3$) δ 7.30 (d, J = 0.4 Hz, 4H), 2.97 (d, J = 5.4 Hz, 1H), 2.76 (dt, J = 5.3, 0.7 Hz, 1H), 1.70 (d, J = 0.8 Hz, 3H). The analytical data for this compound were in excellent agreement with the reported data.[1]

2-(4-bromophenyl)-2-methyloxirane, 5-1d

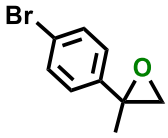

Following GP1, the product was obtained as a light yellow oil (930 mg, 87% yield). **^{1}H NMR** (400 MHz, $CDCl_3$) δ 7.48 – 7.43 (m, 2H), 7.25 – 7.21 (m, 2H), 2.97 (d, J = 5.4 Hz, 1H), 2.75 (dq, J = 5.4, 0.8 Hz, 1H), 1.69 (d, J = 0.7 Hz, 3H). The analytical data for this compound were in excellent agreement with the reported data.[1]

2-(4-iodophenyl)-2-methyloxirane, 5-1e

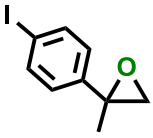

Following GP1, the product was obtained as a yellow solid (920 mg, 87% yield). **^{1}H NMR** (400 MHz, $CDCl_3$) δ 7.69 – 7.61 (m, 2H), 7.13 – 7.07 (m, 2H), 2.97 (d, J = 5.4 Hz, 1H), 2.74 (dq, J = 5.4, 0.8 Hz, 1H), 1.68 (s, 3H). The analytical data for this compound were in excellent agreement with the reported data.[1]

2-methyl-2-(*o*-tolyl)oxirane, 5-1f

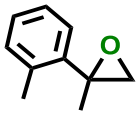

Following GP1, the product was obtained as a light yellow oil (950 mg, 86% yield). **^{1}H NMR** (400 MHz, $CDCl_3$) δ 7.39 – 7.36 (m, 1H), 7.30 – 7.23 (m, 1H), 7.20 – 7.17 (m, 1H), 7.17 – 7.12 (m, 1H), 2.97 (d, J = 5.4 Hz, 1H), 2.82 (dt, J = 5.4, 0.8 Hz, 1H), 2.42 (d, J = 0.7 Hz, 3H), 1.60 (d, J = 0.7 Hz, 3H). The analytical data for this compound were in excellent agreement with the reported data.[1]

2-methyl-2-(*p*-tolyl)oxirane, 5-1g

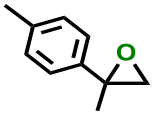

Following GP1, the product was obtained as a light yellow oil (1.08 g, 98% yield). **^{1}H NMR** (400 MHz, $CDCl_3$) δ 7.28 – 7.21 (m, 2H), 7.17 – 7.11 (m, 2H), 2.96 (d, J = 5.4 Hz, 1H), 2.79 (dq, J = 5.5,

0.8 Hz, 1H), 2.34 (s, 3H), 1.70 (d, J = 0.7 Hz, 3H). The analytical data for this compound were in excellent agreement with the reported data.[2]

2-(2-methoxyphenyl)-2-methyloxirane, 5-1h

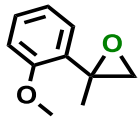

Following GP1, the product was obtained as a yellow oil (1.02 g, 93% yield). **^{1}H NMR** (400 MHz, $CDCl_3$) δ 7.35 (ddt, J = 7.4, 1.8, 0.5 Hz, 1H), 7.27 – 7.22 (m, 1H), 7.01 – 6.95 (m, 1H), 6.92 (tdd, J = 7.5, 1.1, 0.6 Hz, 1H), 3.86 (s, 3H), 2.91 (d, J = 5.3 Hz, 1H), 2.75 (dq, J = 5.3, 0.7 Hz, 1H), 1.61 (t, J = 0.7 Hz, 3H). The analytical data for this compound were in excellent agreement with the reported data.[3]

2-(4-methoxyphenyl)-2-methyloxirane, 5-1i

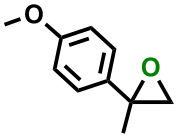

Following GP1, the product was obtained as a colorless oil (723 mg, 66% yield). **^{1}H NMR** (400 MHz, $CDCl_3$) δ 7.31 – 7.26 (m, 2H), 6.89 – 6.83 (m, 2H), 3.79 (s, 3H), 2.95 (d, *J* = 5.4 Hz, 1H), 2.79 (dq, *J* = 5.4, 0.7 Hz, 1H), 1.69 (s, 3H). The analytical data for this compound were in excellent agreement with the reported data.[1]

2-methyl-2-(naphthalene-2-yl)oxirane, 5-1j

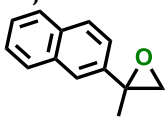

Following GP1, the product was obtained as a yellow solid (520 mg, 96% yield). **^{1}H NMR** (400 MHz, $CDCl_3$) δ 7.87 – 7.80 (m, 4H), 7.51 – 7.43 (m, 3H), 3.06 (d, J = 5.4 Hz, 1H), 2.90 (dq, J = 5.4, 0.8 Hz, 1H), 1.83 (d, J = 0.8 Hz, 3H).The analytical data for this compound were in excellent agreement with the reported data.[1]

2-ethyl-2-phenyloxirane, 5-1k

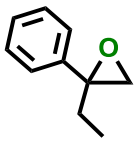

Following GP1, the product was obtained as a colorless oil (1.00 g, 91% yield). **^{1}H NMR** (400 MHz, $CDCl_3$) δ 7.38 – 7.30 (m, 3H), 7.29 – 7.24 (m, 2H), 2.97 (d, J = 5.4 Hz, 1H), 2.74 (d, J = 5.4 Hz, 1H), 2.19 (dq, J = 15.0, 7.5 Hz, 1H), 1.82 (dt, J = 14.5, 7.4 Hz, 1H), 0.94 (t, J = 7.5 Hz, 3H). The analytical data for this compound were in excellent agreement with the reported data.[1]

2-isopropyl-2-phenyloxirane, 5-1l

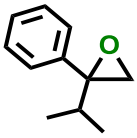

[2] Zhuang, M.; Du, H. *Org. Biomol. Chem.* **2013**, *11*, 1460-1462.
[3] Burell, R. H.; Jean, M.; Poirier, D.; Savard, S. *Can. J. Chem.* **1984**, *62*, 2822-2829.

Following GP1, the product was obtained as a colorless oil (968 mg, 88% yield). **^{1}H NMR** (400 MHz, $CDCl_3$) δ 7.38 – 7.27 (m, 4H), 2.99 (d, *J* = 5.2 Hz, 1H), 2.71 (d, *J* = 5.2 Hz, 1H), 2.08 (dq, *J* = 13.7, 6.9 Hz, 1H), 0.95 (dd, *J* = 6.9, 5.3 Hz, 6H). The analytical data for this compound were in excellent agreement with the reported data.[1]

2-cyclohexyl-2-phenyloxirane, 5-1m

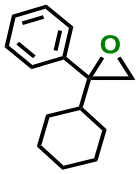

Following GP1, the product was obtained as a colorless oil (798 mg, 74% yield). **^{1}H NMR** (400 MHz, $CDCl_3$) δ 7.38 – 7.30 (m, 4H), 7.30 – 7.24 (m, 1H), 3.01 (d, J = 5.3 Hz, 1H), 2.69 (d, J = 5.3 Hz, 1H), 1.93 – 1.82 (m, 1H), 1.78 – 1.72 (m, 3H), 1.62 (dddt, J = 12.9, 4.9, 3.4, 1.6 Hz, 1H), 1.54 – 1.33 (m, 1H), 1.31 – 1.17 (m, 2H), 1.12 – 0.98 (m, 3H). The analytical data for this compound were in excellent agreement with the reported data.[1]

2-methyl-2-phenethyloxirane, 5-1n

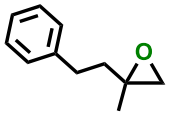

Following GP1, the product was obtained as a colorless oil (1.01 g, 92% yield).**^{1}H NMR** (400 MHz, $CDCl_3$) δ 7.28 (t, J = 7.3 Hz, 2H), 7.19 (t, J = 6.1 Hz, 3H), 2.74 (dt, J = 16.8, 7.8 Hz, 2H), 2.59 (dd, J = 10.9, 4.9 Hz, 2H), 1.96 – 1.90 (m, 1H), 1.88 – 1.80 (m, 1H), 1.38 (d, J = 3.4 Hz, 3H).The analytical data for this compound were in excellent agreement with the reported data.[1]

2-methyl-3-phenyloxirane, 5-1o

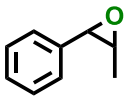

Following GP2, the product was obtained as a colorless oil (576 mg, 89% yield). **^{1}H NMR** (400 MHz, $CDCl_3$) δ 7.38 – 7.27 (m, 5H), 4.07 (d, *J* = 4.2 Hz, 1H), 3.35 (qd, *J* = 5.4, 4.2 Hz, 1H), 1.09 (d, *J* = 5.4 Hz, 3H). The analytical data for this compound were in excellent agreement with the reported data.[1]

2-methyl-2,3-diphenyloxirane, 5-1p

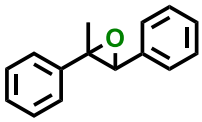

Following GP2, the product was obtained as a colorless oil (210 mg, 85% yield). **^{1}H NMR** (400 MHz, $CDCl_3$) δ 7.49 – 7.30 (m, 10H), 3.98 (s, 1H), 1.47 (s, 3H). The analytical data for this compound were in excellent agreement with the reported data.[4]

2-(4-chlorophenyl)-2-phenyloxirane, 5-1q

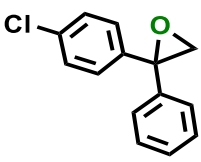

[4] Geng, X.-L.; Wang, Z.; Li, X.-Q.; Zhang, C. *J. Org. Chem.* **2005**, *70* (23), 9610-9613.

Following GP1, the product was obtained as a colorless oil (680 mg, 73% yield). **^{1}H NMR** (400 MHz, $CDCl_3$) δ 7.41 – 7.22 (m, 9H), 3.28 (d, *J* = 5.5 Hz, 1H), 3.21 (d, *J* = 5.5 Hz, 1H). **^{13}C NMR** (101 MHz, $CDCl_3$) δ 139.09, 138.36, 133.99, 128.93, 128.51, 128.49, 128.44, 128.30, 127.59, 127.31, 126.57, 124.95, 88.42, 56.92. **HRMS** (ESI) Calculated for $C_{14}H_{12}ClO$ $[M+H]^+$: 231.0571; Found: 231.0564. **IR** (ATR) ν_{max} = 3057, 3022, 1489. 1090 cm^{-1}.

One-pot iridium-catalyzed isomerization of epoxides and reductive amination.

General procedure (GP3)

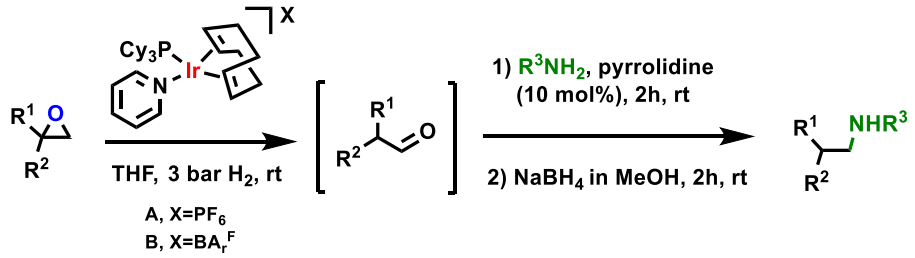

Into a glove box, the epoxide (1.0 eq.) and Crabtree's catalyst (**5-4**) **A** or **B** as indicated (3 mol%, unless otherwise indicated) were placed in a pressure tube and dissolved in anhydrous THF (0.25 M). Then, the pressure tube was purged and charged with H_2 (3 bar). The reaction was stirred for 2-48 hours at room temperature. After completion by ^{1}H-NMR monitoring, the ratio of selectivity aldehyde:alcohols was determined. Pyrrolidine (10 mol%) and the corresponding amine (1.1 eq.) were then added by pressure syringe. After 2 hours stirring vigorously, the hydrogen pressure was released and $NaBH_4$ (2.5 eq.) and MeOH (3 mL) were added. After 2 hours, the solvent was evaporated and the mixture was dissolved in EtOAc and washed with $NaHCO_3$ (aq). The aqueous layer was further extracted with EtOAc (x2), the combined organic layers were washed with brine, dried over Na_2SO_4, filtered and concentrated *in vacuo*. The crude was purified by flash column chromatography (hexanes:EtOAc = 95:5) affording the desired compound.

***N*-benzhydryl-2-phenylpropan-1-amine, 5-6a**

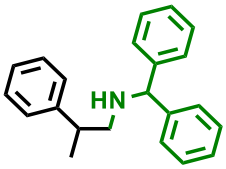

Following GP3, catalyst **A** and benzhydrylamine were used and the isomerization reaction was left for 12 hours. Aldehyde was obtained in 94% of selectivity. The desired amine was obtained as an oil (167 mg, 67% yield). When performing the reaction in gram scale and using 1 mol% of catalyst **B**, the desired amine was obtained in 51% of yield after purification. **^{1}H NMR** (400 MHz, $CDCl_3$) δ 7.37 – 7.15 (m, 15H), 4.77 (d, J = 2.2 Hz, 1H), 2.98 (hd, J = 7.1, 2.0 Hz, 1H), 2.78 – 2.72 (m, 2H), 1.48 (s, 1H), 1.27 (dd, J = 7.0, 2.0 Hz, 3H). **^{13}C NMR** (101 MHz, $CDCl_3$) δ: 145.60, 144.35, 144.33, 128.61, 128.55, 128.53, 127.41, 127.39, 127.36, 127.03, 127.02, 126.43, 67.44, 55.31, 40.35, 20.21. **HRMS** (ESI) Calculated for $C_{22}H_{23}N$ $[M+H]^+$: 302.1903; Found: 302.1904. **IR** (ATR) ν_{max} = 3399, 2977, 1750 cm^{-1}.

***N*-benzhydryl-2-(4-fluorophenyl)propan-1-amine, 5-6b**

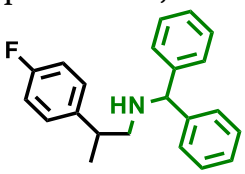

Following GP3, catalyst **A** and benzhydrylamine were used and the isomerization reaction was left for 17 hours. Aldehyde was obtained in 94% of selectivity. The desired amine was obtained as an oil

(106 mg, 57% yield). **^{1}H NMR** (400 MHz, $CDCl_3$) δ 7.34 (d, *J* = 7.1 Hz, 2H), 7.30 – 7.22 (m, 6H), 7.22 – 7.12 (m, 4H), 6.98 (t, *J* = 8.7 Hz, 2H), 4.75 (s, 1H), 2.97 (s, 1H), 2.78 – 2.67 (m, 2H), 1.23 (d, *J* = 7.0 Hz, 3H). **^{13}C NMR** (101 MHz, $CDCl_3$) δ: δ 162.65, 160.22, 144.14, 144.10, 141.10, 141.07, 128.62, 128.54, 128.44, 128.43, 127.24, 127.20, 126.96, 126.94, 115.28, 115.07, 67.34, 55.23, 39.59, 20.16. **HRMS** (ESI) Calculated for $C_{22}H_{23}N$ $[M+H]^+$: 320.1809; Found: 320.1810. **IR** (ATR) ν_{max} = 3109, 3082, 3026, 2960, 2913, 1601, 1508, 1492, 1452, 1222 cm^{-1}.

_N_-benzhydryl-2-(4-chlorophenyl)propan-1-amine, 5-6c

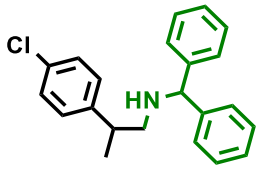

Following GP3, catalyst **A** and benzhydrylamine were used and the isomerization reaction was left for 2 hours. Aldehyde was obtained in 95% of selectivity. The desired amine was obtained as an oil (178 mg, 67% yield). **^{1}H NMR** (400 MHz, $CDCl_3$) δ 7.35 – 7.31 (m, 2H), 7.30 – 7.23 (m, 8H), 7.22 – 7.15 (m, 2H), 7.15 – 7.10 (m, 2H), 4.75 (s, 1H), 2.93 (h, J = 7.0 Hz, 1H), 2.73 – 2.70 (m, 2H), 1.23 (d, J = 7.0 Hz, 3H). **^{13}C NMR** (101 MHz, $CDCl_3$) δ 144.07, 144.04, 143.95, 131.86, 128.60, 128.53, 128.43, 128.42, 127.20, 127.17, 126.96, 126.93, 67.32, 54.99, 39.75, 19.97. **HRMS** (ESI) Calculated for $C_{22}H_{22}ClN$ $[M+H]^+$: 336.1514; Found: 336.1506. **IR** (ATR) ν_{max} = 3084, 3060, 3024, 2958, 1600, 1491, 1452 cm^{-1}.

_N_-benzhydryl-2-(4-bromophenyl)propan-1-amine, 5-6d

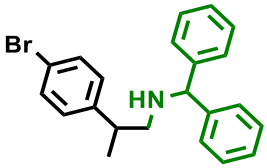

Following GP3, catalyst **B** and benzhydrylamine were used and the isomerization reaction was left for 12 hours. Aldehyde was obtained in 99% of selectivity. The desired amine was obtained as an oil (123 mg, 74% yield). **^{1}H NMR** (400 MHz, $CDCl_3$) δ 7.34 – 7.28 (m, 2H), 7.27 – 7.22 (m, 2H), 7.21 – 7.12 (m, 6H), 7.12 – 7.06 (m, 2H), 7.00 – 6.95 (m, 2H), 4.66 (s, 1H), 2.87 – 2.77 (m, 1H), 2.67 – 2.57 (m, 2H), 1.13 (d, *J* = 7.0 Hz, 3H). **^{13}C NMR** (101 MHz, $CDCl_3$) δ: δ 144.61, 144.19, 144.17, 131.60, 129.16, 128.56, 128.55, 127.33, 127.30, 127.09, 127.07, 120.04, 67.47, 55.08, 39.96, 20.05. **HRMS** (ESI) Calculated for $C_{22}H_{22}BrN$ $[M+H]^+$: 380.1008; Found: 380.1003. **IR** (ATR) ν_{max} = 3069, 3024, 2961, 2910, 2819, 1561, 1483, 1453 cm^{-1}.

_N_-benzhydryl-2-(4-iodophenyl)propan-1-amine, 5-6e

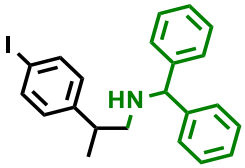

Following GP3, catalyst **B** and benzhydrylamine were used and the isomerization reaction was left for 12 hours. Aldehyde was obtained in 92% of selectivity. The desired amine was obtained as an oil (118 mg, 63% yield). **^{1}H NMR** (400 MHz, $CDCl_3$) δ 7.65 – 7.56 (m, 2H), 7.36 – 7.29 (m, 2H), 7.28 – 7.21 (m, 6H), 7.21 – 7.12 (m, 2H), 6.98 – 6.90 (m, 2H), 4.74 (s, 1H), 2.89 (h, *J* = 6.9 Hz, 1H), 2.74 – 2.66 (m, 2H), 1.45 (s, 1H), 1.21 (d, *J* = 6.9 Hz, 3H). **^{13}C NMR** (101 MHz, $CDCl_3$) δ: 145.34, 144.21, 144.19, 137.60, 129.54, 128.58, 128.57, 127.35, 127.32, 127.11, 127.09, 91.45, 67.48, 55.05, 40.06, 20.02. **HRMS** (ESI) Calculated for $C_{22}H_{22}IN$ $[M+H]^+$: 428.0870; Found: 428.0873. **IR** (ATR) ν_{max} = 3065, 3021, 2955, 2920, 2819, 1590, 1486, 1451 cm^{-1}.

_N_-benzhydryl-2-(_o_-tolyl)propan-1-amine, 5-6f

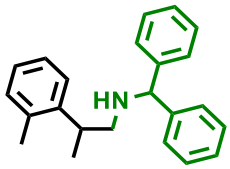

Following GP3, catalyst **A** and benzhydrylamine were used and the isomerization reaction was left for 48 hours. Aldehyde was obtained in 97% of selectivity. The desired amine was obtained as an oil (89 mg, 80% yield). **^{1}H NMR** (400 MHz, $CDCl_3$) δ 7.30 – 7.26 (m, 2H), 7.23 (dt, *J* = 3.1, 1.9 Hz, 2H), 7.21 – 7.15 (m, 4H), 7.13 – 6.96 (m, 6H), 4.69 (s, 1H), 3.18 (h, *J* = 7.0 Hz, 1H), 2.67 (ddd, *J* = 29.8, 11.7, 7.1 Hz, 2H), 2.25 (s, 3H), 1.49 (s, 1H), 1.15 (d, *J* = 6.9 Hz, 3H). **^{13}C NMR** (101 MHz, $CDCl_3$) δ 144.40, 144.29, 143.66, 136.09, 130.49, 128.56, 128.54, 127.38, 127.36, 127.07, 127.03, 126.37, 125.99, 125.39, 67.52, 54.68, 35.10, 19.73, 19.68. **HRMS** (ESI) Calculated for $C_{23}H_{25}N$ $[M+H]^+$: 316.2060; Found: 316.2066. **IR** (ATR) ν_{max} = 3059, 3021, 2955, 1597, 1490, 1452 cm^{-1}.

_N_-benzhydryl-2-(_p_-tolyl)propan-1-amine, 5-6g

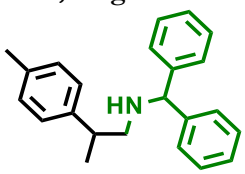

Following GP3, catalyst **A** and benzhydrylamine were used and the isomerization reaction was left for 12 hours. Aldehyde was obtained in 94% of selectivity. The desired amine was obtained as an oil (117 mg, 45% yield). **^{1}H NMR** (400 MHz, $CDCl_3$) δ 7.34 (qd, *J* = 2.3, 1.2 Hz, 2H), 7.30 – 7.23 (m, 7H), 7.20 – 7.15 (m, 2H), 7.08 (d, *J* = 8.8 Hz, 4H), 4.76 (s, 1H), 2.94 (h, *J* = 7.0 Hz, 1H), 2.71 (t, *J* = 6.0 Hz, 2H), 2.31 (d, *J* = 6.1 Hz, 3H), 1.23 (d, *J* = 7.0 Hz, 3H). **^{13}C NMR** (101 MHz, $CDCl_3$) δ 144.36, 142.50, 135.88, 129.31, 128.53, 128.52, 127.42, 127.38, 127.23, 127.02, 127.00, 67.46, 55.35, 39.86, 21.15, 20.34. **HRMS** (ESI) Calculated for $C_{23}H_{25}N$ $[M+H]^+$: 316.2060; Found: 316.2061. **IR** (ATR) ν_{max} = 3021, 2960, 2920, 2863, 1595, 1483, 1452 cm^{-1}.

_N_-benzhydryl-2-(2-methoxyphenyl)propan-1-amine, 5-6h

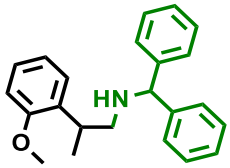

Following GP3, catalyst **A** and benzhydrylamine were used and the isomerization reaction was left for 12 hours. Aldehyde was obtained in 98% of selectivity. The desired amine was obtained as an oil (175 mg, 71% yield). **^{1}H NMR** (400 MHz, $CDCl_3$) δ 7.37 – 7.32 (m, 2H), 7.30 – 7.15 (m, 9H), 6.76 (tdd, *J* = 5.8, 5.2, 1.3 Hz, 3H), 4.76 (s, 1H), 3.79 (d, *J* = 4.3 Hz, 3H), 3.00 – 2.89 (m, 1H), 2.78 – 2.68 (m, 2H), 1.24 (d, *J* = 6.9 Hz, 3H). **^{13}C NMR** (101 MHz, $CDCl_3$) δ 159.68, 147.15, 144.17, 144.13, 129.39, 128.37, 128.36, 127.24, 127.19, 126.87, 126.85, 119.64, 113.04, 111.44, 67.27, 55.11, 55.05, 40.24, 20.05. **HRMS** (ESI) Calculated for $C_{23}H_{25}NO$ $[M+H]^+$: 332.2009; Found: 332.2008. **IR** (ATR) ν_{max} = 3059, 3024, 2951, 2828, 1598, 1583, 1487, 1452, 1257 cm^{-1}.

_N_-benzhydryl-2-(4-methoxyphenyl)propan-1-amine, 5-6i

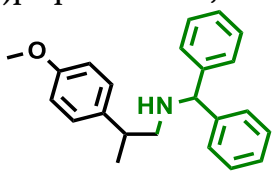

Following GP3, catalyst **A** and benzhydrylamine were used and the isomerization reaction was left for 12 hours. Aldehyde was obtained in 99% of selectivity. The desired amine was obtained as an oil (50 mg, 45% yield). **^{1}H NMR** (400 MHz, $CDCl_3$) δ δ 7.37 – 7.33 (m, 2H), 7.30 – 7.23 (m, 6H), 7.19 (ttd, *J* = 5.9, 3.3, 2.8, 1.3 Hz, 2H), 7.15 – 7.10 (m, 2H), 6.87 – 6.82 (m, 2H), 4.76 (s, 1H), 3.79 (s, 3H), 3.05 – 2.87 (m, 1H), 2.79 – 2.66 (m, 2H), 1.22 (d, *J* = 7.0 Hz, 3H). **^{13}C NMR** (101 MHz, $CDCl_3$) δ

158.10, 128.43, 128.13, 127.32, 127.29, 127.00, 113.91, 67.23, 55.25, 39.06, 29.69, 20.23. **HRMS** (ESI) Calculated for $C_{23}H_{25}NO$ $[M+H]^+$: 332.2009; Found: 332.2005. **IR** (ATR) ν_{max} = 3021, 2951, 2932, 2825, 1601, 1512, 1453, 1246 cm^{-1}.

_N_-benzhydryl-2-(naphthalen-2-yl)propan-1-amine, 5-6j

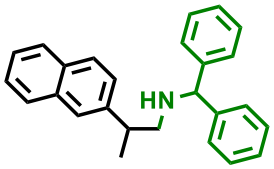

Following GP3, catalyst **B** and benzhydrylamine were used and the isomerization reaction was left for 12 hours. Aldehyde was obtained in 91% of selectivity. The desired amine was obtained as an oil (97 mg, 62% yield). **^{1}H NMR** (400 MHz, $CDCl_3$) δ 7.84 – 7.74 (m, 3H), 7.64 (dd, *J* = 1.8, 0.8 Hz, 1H), 7.49 – 7.40 (m, 2H), 7.37 – 7.31 (m, 3H), 7.29 – 7.14 (m, 8H), 4.79 (s, 1H), 3.15 (h, *J* = 7.0 Hz, 1H), 2.93 – 2.80 (m, 2H), 1.34 (d, *J* = 7.0 Hz, 3H). **^{13}C NMR** (101 MHz, $CDCl_3$) δ 144.23, 143.01, 133.74, 132.51, 128.55, 128.54, 128.25, 127.74, 127.73, 127.41, 127.39, 127.07, 127.04, 126.05, 125.94, 125.78, 125.42, 67.51, 55.11, 40.49, 20.36. **HRMS** (ESI) Calculated for $C_{26}H_{25}N$ $[M+H]^+$: 352.2060; Found: 352.2060. **IR** (ATR) ν_{max} = 3062, 3021, 2961, 2917, 2809, 1593, 1491, 1452 cm^{-1}.

_N_-benzhydryl-2-phenylbutan-1-amine, 5-6k

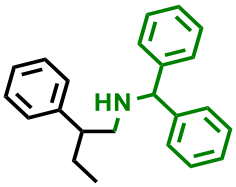

Following GP3, catalyst **A** and benzhydrylamine were used and the isomerization reaction was left for 12 hours. Aldehyde was obtained in 99% of selectivity. The desired amine was obtained as an oil (122 mg, 70% yield). **^{1}H NMR** (400 MHz, $CDCl_3$) δ 7.26 – 7.06 (m, 15H), 4.66 (s, 1H), 2.78 – 2.58 (m, 3H), 1.64 (dddd, *J* = 12.1, 9.6, 7.4, 4.9 Hz, 1H), 1.52 – 1.43 (m, 1H), 0.69 (td, *J* = 7.4, 0.7 Hz, 3H). **^{13}C NMR** (101 MHz, $CDCl_3$) δ 144.32, 144.30, 143.98, 128.55, 128.53, 128.50, 128.07, 127.39, 127.37, 127.01, 126.98, 126.46, 67.45, 53.78, 48.27, 27.42, 12.19. **HRMS** (ESI) Calculated for $C_{23}H_{25}N$ $[M+H]^+$: 316.2060; Found: 316.20 63. **IR** (ATR) ν_{max} = 3078, 3059, 3015, 2955, 2920, 2869, 1604, 1492, 1452 cm^{-1}.

_N_-benzhydryl-3-methyl-2-phenylbutan-1-amine, 5-6l

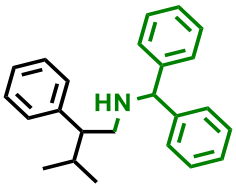

Following GP3, catalyst **B** and benzhydrylamine were used and the isomerization reaction was left for 3 hours. Aldehyde was obtained in 99% of selectivity. The desired amine was obtained as an oil (90 mg, 57% yield). **^{1}H NMR** (400 MHz, $CDCl_3$) δ 7.31 – 7.13 (m, 15H), 4.73 (s, 1H), 2.95 (dd, *J* = 11.5, 4.5 Hz, 1H), 2.78 (dd, *J* = 11.5, 9.9 Hz, 1H), 2.57 (ddd, *J* = 9.8, 8.0, 4.5 Hz, 1H), 1.91 – 1.78 (m, 1H), 0.89 (d, *J* = 6.7 Hz, 3H), 0.69 (d, *J* = 6.7 Hz, 3H). **^{13}C NMR** (101 MHz, $CDCl_3$) δ 144.30, 144.24, 142.94, 128.78, 128.50, 128.46, 128.35, 127.43, 127.34, 127.00, 126.91, 126.43, 67.47, 53.39, 51.03, 31.70, 21.24, 20.84. **HRMS** (ESI) Calculated for $C_{24}H_{27}N$ $[M+H]^+$: 330.2221; Found: 330.2216. **IR** (ATR) ν_{max} = 3059, 3025, 2957, 2917, 2866, 1593, 1492, 1451 cm^{-1}.

_N_-benzhydryl-2-cyclohexyl-2-phenylethan-1-amine, 5-6m

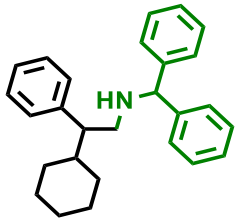

Following GP3, catalyst **B** and benzhydrylamine were used and the isomerization reaction was left for 12 hours. Aldehyde was obtained in 99% of selectivity. The desired amine was obtained as a white solid (103 mg, 75% yield). **m. p.** 85 ºC. **^{1}H NMR** (400 MHz, $CDCl_3$) δ 7.22 – 7.03 (m, 15H), 4.64 (s, 1H), 2.89 (dd, *J* = 11.5, 4.4 Hz, 1H), 2.70 (dd, *J* = 11.4, 10.0 Hz, 1H), 2.54 (ddd, *J* = 9.9, 7.9, 4.4 Hz, 1H), 1.72 – 1.54 (m, 2H), 1.49 (ddt, *J* = 10.4, 7.7, 3.8 Hz, 2H), 1.40 (ddt, *J* = 11.3, 7.8, 3.3 Hz, 1H), 1.35 – 1.24 (m, 2H), 1.15 – 0.92 (m, 3H), 0.87 – 0.75 (m, 1H), 0.67 (qd, *J* = 12.2, 3.2 Hz, 1H). **^{13}C NMR** (101 MHz, $CDCl_3$) δ 144.27, 144.23, 142.97, 128.80, 128.48, 128.44, 128.33, 128.32, 127.41, 127.32, 126.98, 126.89, 126.37, 67.45, 52.43, 50.59, 41.50, 31.56, 31.14, 26.62, 26.59, 26.56. **HRMS** (ESI) Calculated for $C_{27}H_{31}N$ $[M+H]^+$: 370.2528; Found: 370.2529. **IR** (ATR) ν_{max} = 3056, 3024, 2923, 2851, 1599, 1492, 1450 cm^{-1}.

_N_-benzhydryl-2-methyl-4-phenylbutan-1-amine, 5-6n

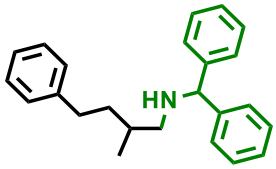

Following GP3, catalyst **B** (5 mol%) and benzhydrylamine were used and the isomerization reaction was left for 12 hours. Aldehyde was obtained in 98% of selectivity. The desired amine was obtained as an oil (112 mg, 79% yield). **^{1}H NMR** (400 MHz, $CDCl_3$) δ 7.40 (ddd, *J* = 8.1, 2.9, 1.3 Hz, 4H), 7.33 – 7.24 (m, 6H), 7.24 – 7.13 (m, 5H), 4.77 (s, 1H), 2.64 (ddd, *J* = 13.7, 9.9, 5.6 Hz, 1H), 2.59 – 2.50 (m, 2H), 2.43 (dd, *J* = 11.6, 6.8 Hz, 1H), 1.81 – 1.63 (m, 2H), 1.48 – 1.40 (m, 1H), 0.99 (d, *J* = 6.6 Hz, 3H). **^{13}C NMR** (101 MHz, $CDCl_3$) δ 144.36, 142.84, 128.42, 128.36, 128.28, 127.30, 127.28, 126.92, 125.60, 67.66, 54.37, 36.66, 33.32, 33.11, 30.92, 18.20. **HRMS** (ESI) Calculated for $C_{24}H_{27}N$ $[M+H]^+$: 330.2213; Found: 330.2216. **IR** (ATR) ν_{max} = 3082, 3062, 3018, 2961, 2930, 2863, 1596, 1492, 1452 cm^{-1}.

4-methoxy-N-(2-phenylpropyl)aniline, 5-7a

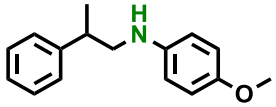

Following GP3, epoxide **5-1a** (0.2 mmol), catalyst **B** and *p*-anisidine were used and the isomerization reaction was left for 12 hours. The product was obtained as a dark oil (115 mg, 64% yield). **^{1}H NMR** (400 MHz, $CDCl_3$) δ 7.37 – 7.29 (m, 2H), 7.26 – 7.20 (m, 3H), 6.80 – 6.73 (m, 2H), 6.59 – 6.52 (m, 2H), 3.74 (s, 3H), 3.30 (dd, *J* = 12.2, 6.1 Hz, 1H), 3.20 (dd, *J* = 12.2, 8.3 Hz, 1H), 3.05 (dt, *J* = 8.2, 6.6 Hz, 1H), 1.33 (d, *J* = 6.9 Hz, 3H). **^{13}C NMR** (101 MHz, $CDCl_3$) δ 145.05, 139.25, 128.68, 128.50, 128.35, 127.28, 127.20, 126.56, 55.94, 53.54, 39.76, 20.20. **HRMS** (ESI) Calculated for $C_{16}H_{20}NO$ $[M+H]^+$: 242.1539; Found: 242.1535. The analytical data for this compound were in excellent agreement with the reported data.[5]

_N_-benzyl-2-phenylpropan-1-amine, 5-8a

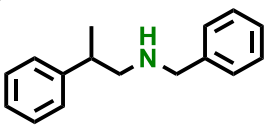

[5] Fleischer, S.; Zhou, S.; Junge, K.; Beller, M. *Chem. Asian. J.* **2011**, *6*, 2240 – 2245.

Following GP3, epoxide **5-1a** (0.2 mmol), catalyst **B** and benzylamine were used and the isomerization reaction was left for 17 hours. The product was obtained as a colorless oil (103 mg, 55% yield). **^{1}H NMR** (400 MHz, $CDCl_3$) δ 7.39 – 7.14 (m, 10H), 3.84 – 3.68 (m, 2H), 2.98 (h, *J* = 7.0 Hz, 1H), 2.85 – 2.73 (m, 2H), 1.50-1.41 (br s, 1H), 1.26 (d, *J* = 7.0 Hz, 3H). **^{13}C NMR** (101 MHz, $CDCl_3$) δ 145.05, 139.25, 128.68, 128.50, 128.35, 127.28, 127.20, 126.56, 55.94, 53.54, 39.76, 20.20. **HRMS** (ESI) Calculated for $C_{16}H_{20}N$ $[M+H]^+$: 226.1590; Found: 226.1592. The analytical data for this compound were in excellent agreement with the reported data.[6]

2-phenyl-N-((*R*)-1-phenylethyl)propan-1-amine, 5-(9a-9a')

Following GP3, epoxide **5-1a** (0.2 mmol), catalyst **B** and *(R)*-(+)-1-Phenylethylamine were used and the isomerization reaction was left for 17 hours. The desired amine was obtained as a colorless oil (106 mg in 3:2 dr, 56% yield). **(R/S)(R) isomer:** **^{1}H NMR** (400 MHz, $CDCl_3$) δ 7.34 – 7.28 (m, 6H), 7.26 – 7.19 (m, 4H), 3.71 (q, *J* = 6.6 Hz, 1H), 2.90 (h, *J* = 6.9 Hz, 1H), 2.68 (dd, *J* = 11.5, 7.8 Hz, 1H), 2.60 (dd, *J* = 11.5, 6.6 Hz, 1H), 1.28 (d, *J* = 6.6 Hz, 3H), 1.23 (d, *J* = 7.0 Hz, 3H). **^{13}C NMR** (101 MHz, $CDCl_3$) δ 145.78, 145.64, 128.62, 128.49, 127.31, 126.94, 126.78, 126.42, 58.47, 55.14, 40.26, 24.53, 20.21. **HRMS** (ESI) Calculated for $C_{17}H_{22}N$ $[M+H]^+$: 240.1747; Found: 240.1752. **IR** (ATR) ν_{max} = 2963, 2249, 1493, 1451, 1373, 1126 cm^{-1}. **(R/S)(R) isomer:** **^{1}H NMR** (400 MHz, $CDCl_3$) δ 7.39 – 7.33 (m, 1H), 7.32 – 7.27 (m, 4H), 7.25 – 7.21 (m, 2H), 7.15 (dt, *J* = 8.0, 1.2 Hz, 3H), 3.78 – 3.71 (m, 1H), 2.98 – 2.88 (m, 1H), 2.69 (dd, *J* = 11.6, 5.5 Hz, 1H), 2.65 – 2.55 (m, 1H), 1.28 (d, *J* = 6.6 Hz, 3H), 1.21 (d, *J* = 7.0 Hz, 3H). **^{13}C NMR** (101 MHz, $CDCl_3$) δ 145.67, 145.32, 128.63, 128.49, 127.36, 126.93, 126.57, 126.48, 58.15, 54.53, 40.12, 24.46, 20.51. **HRMS** (ESI) Calculated for $C_{17}H_{22}N$ $[M+H]^+$: 240.1747; Found: 240.1751. **IR** (ATR) ν_{max} = 3026, 2968, 2923, 2251, 1493, 1451, 1373, 1123 cm^{-1}.

Iridium-catalyzed isomerization of di- and tri-substituted epoxides

General procedure (GP4)

Into a dry box, the epoxide (1.0 equiv.) and Crabtree's catalyst **5-4A** or **5-4B** (1 mol%) were placed in a pressure tube and dissolved in the indicated anhydrous solvent (0.1 M). The pressure tube was purged and charged with H_2 (3 barG). The reaction was stirred 16 hours –otherwise indicated- at room temperature. After completion by ^{1}H NMR, the solvent was evaporated and the crude mixture was filtered over celite to yield the corresponding carbonyl compound.

1-phenylpropan-2-one, 5-2o

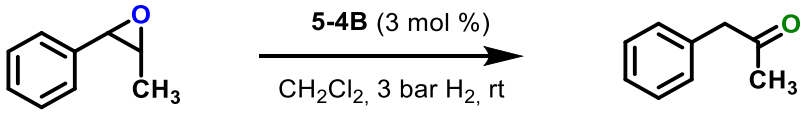

96%

Following GP4, using 2-methyl-3-phenyloxirane and catalyst **B** in CH_2Cl_2, the product was obtained as a colorless oil (112 mg, 96% yield). **^{1}H NMR** (400 MHz, $CDCl_3$) δ 7.29 – 7.22 (m, 5H), 3.72 (s, 2H), 2.18 (s, 3H). The analytical data for this compound were in excellent agreement with the reported data.[7]

[6] Horrillo-Martinez, P.; Hultzsch, K. C.; Gil, A.; Branchadell, V. *Eur. J. Org. Chem.* **2007**, 3311 - 3325.
[7] Zimbron, J. M.; Seeger-Weibel, M.; Hirt, H.; Gallou, F. *Synthesis* **2008**, *8*, 1221 – 1226.

2,2-diphenylpropanal, 5-2p

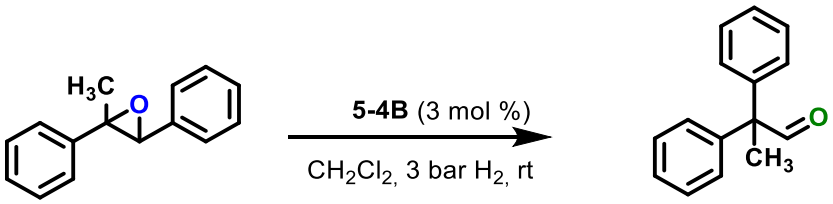

89%

Following GP4, using 2-methyl-2,3-diphenyloxirane and catalyst **B** in CH_2Cl_2, the product was obtained as a colorless oil (134 mg, 89% yield). **^{1}H NMR** (400 MHz, $CDCl_3$) δ 9.92 (s, 1H), 7.40 – 7.34 (m, 4H), 7.33 – 7.28 (m, 3H), 7.20 – 7.17 (m, 3H), 1.78 (s, 3H). The analytical data for this compound were in excellent agreement with the reported data.[8]

2-(4-chlorophenyl)-2-phenylacetaldehyde, 5-2q

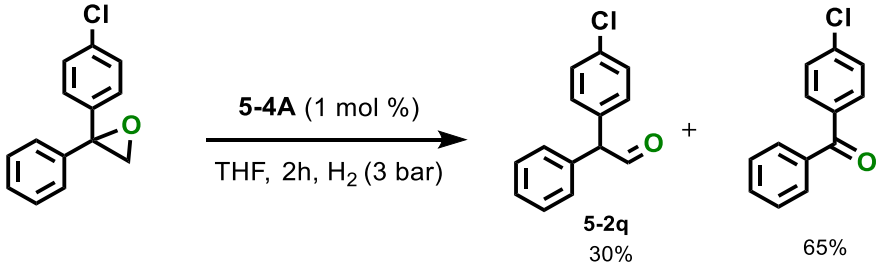

Following GP4, using 2-(4-chlorophenyl)-2-phenyloxirane and catalyst **A** (1 mol %) in THF, the reaction showed full conversion after only 2 hours. The product **5-2q** was obtained as a colorless oil (31 mg, 30% yield), along with 65% of demethylenation product. **^{1}H NMR** (400 MHz, $CDCl_3$) δ 9.92 (d, J = 2.2 Hz, 1H), 7.45 – 7.18 (m, 9H), 4.97 (d, J = 13.2 Hz, 1H). The analytical data for this compound were in excellent agreement with the reported data.[9]

Iridium-catalyzed isomerization of enantiomerically enriched epoxides.

Synthesis of the epoxide 5-(*R*)-1a.

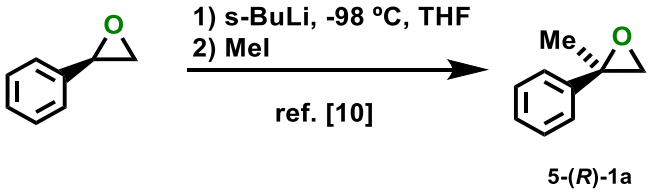

Following a literature procedure,[10] **5-(*R*)-1a** was synthesized from *(R)*-phenyloxirane via stereospecific α-lithiation and trapping the reaction with MeI as electrophile (68 mg, 79% yield, 99% ee). The enantiomeric excess was determined by chiral **HPLC**: CHIRALPAK IC. Heptane/IPA 99:1, 0.5 mL/min, λ = 210 nm. $t_{(R)}$ = 20.0 min, $t_{(S)}$ = 22.0 min. The analytic data for this were in excellent agreement with the reported data.[1]

[8] Nagai, W.; Hirata, Y. *J. Org. Chem.* **1989**, *54*, 635-640.
[9] Cul, W.; Mao, M.; He, Z.; Zhu, G. *J. Org. Chem.* **2013**, *78* (19), 9815-9821.
[10] Capriati, V.; Florio, S.; Luisi, R.; Salomone, A. *Org. Lett.* **2002**, *4* (14), 2445-2448.

Isomerization of epoxide 5-(*R*)-1a

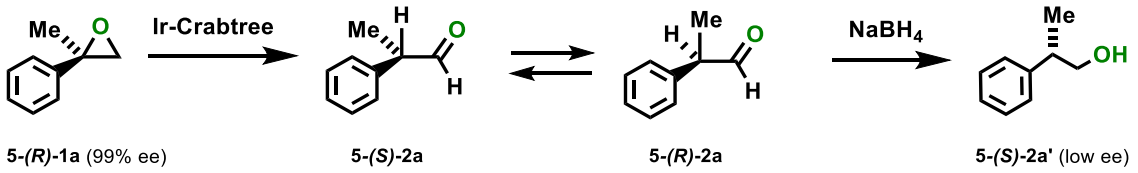

5-(*R*)-1a (99% ee) **5-(*S*)-2a** **5-(*R*)-2a** **5-(*S*)-2a'** (low ee)

Into a glove box, the epoxide **5-(*R*)-1a** (1.0 eq.) and Crabtree's catalyst **5-4A** as indicated (5 mol%) were placed in a pressure tube and dissolved in anhydrous THF (0.25 M). Then, the pressure tube was purged and charged with H_2 (3 bar). The reaction was stirred for **4 hours** at room temperature and reduced in situ with $NaBH_4$ (1.5 eq.) in 1 mL of MeOH. After stirring for 2 hours, the solvent was evaporated, redissolved with EtOAc and washed with H_2O. The aqueous phase was extracted (x2) with EtOAc. The combined organic phases were dried over $MgSO_4$ and concentrated under vacuum to afford the corresponding chiral alcohol **5-(*S*)-2a'** (50 mg, 70% yield, 26% ee). After 24 h of reaction, the product was racemic.

HPLC: CHIRALPAK IA. Heptane/EtOH 95:5, 0.5 mL/min, λ = 254 nm. $t_{(S)}$ = 14.1 min, $t_{(R)}$ = 16.6 min. The analytic data for this were in excellent agreement with the reported data.[1]

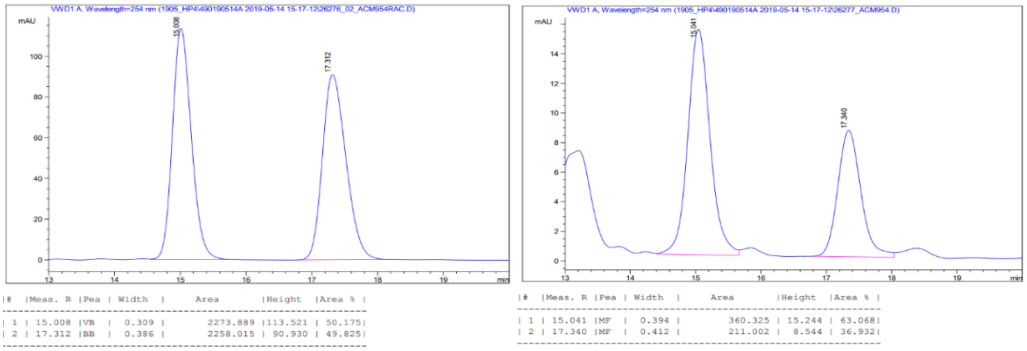

Deprotection-derivatization of amine 5-6a

Into a high pressure reactor, amine **5-6a** (121 mg, 0.4 mmol, 1.0 equiv.) was dissolved in CH_2Cl_2 (0.1 M). $Pd(OH)_2/C$ (20 mol%, 20% w/t) and Ac_2O (1.5 equiv.) were then added to the solution. The pressure reactor was purged and charged with H_2 (25 barG) and the reaction mixture was stirred overnight at 40 °C. Afterwards, the solution was filtered through a plug of celite and concentrated under reduced pressure. The crude was purified by flash column chromatography (Hexanes:EtOAc increasing polarity) to afford **5-10** as colorless oil (52 mg, 74% yield).

***N*-(2-phenylpropyl)acetamide, 5-10**

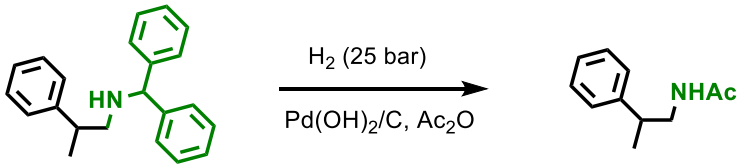

5-6a **5-10**

^{1}H NMR (400 MHz, $CDCl_3$) δ 7.29 – 7.21 (m, 2H), 7.21 – 7.16 (m, 1H), 7.14 – 7.10 (m, 2H), 5.30 (s, 1H), 3.56 (ddd, *J* = 13.2, 7.1, 5.9 Hz, 1H), 3.14 (ddd, *J* = 13.5, 8.8, 4.8 Hz, 1H), 2.91 – 2.80 (m, 1H), 1.81 (s, 3H), 1.20 (d, *J* = 7.0 Hz, 3H). **^{13}C NMR** (101 MHz, $CDCl_3$) δ 170.13, 144.20, 129.04, 128.85, 128.56, 127.30, 126.85, 126.16, 46.25, 39.83, 23.41, 19.58. The analytical data for this compound were in excellent agreement with the reported data.[11]

[11] Zhang, J.; Liu, C.; Zhang, Z.; Zhang, W. *Chem. Commun.* **2018**, *54*, 6024-6027.

Computational Details

Theoretical calculations were performed at DFT theory level through Gaussian09 software,[1] using the same methodology than that employed for the isomerization of aziridines with the Crabtree's reagent.[2] All intermediates and transition states were optimized in tetrahydrofuran solvent (THF, ε= 7.4257) with the SMD continuum model[3] using the B3LYP functional[4] combined with the Grimme's D3 correction for dispersion.[5] In the optimizations, the 6-31G(d,p) basis set was used for the main group elements,[6] and the scalar relativistic Stuttgart-Dresden SDD pseudopotential and its associated double-ζ basis set,[7] complemented with a set of *f* polarization functions,[8] for the iridium atom (BS1). Frequency calculations were carried out for all the optimized geometries in order to characterize the stationary points as either minima or transition states. It was confirmed that transition states connect with the corresponding intermediates by usual intrinsic reaction coordinate (IRC) calculations and subsequent optimization to minima.
Gibbs energies in THF were computed at 298.15 K adding the thermal and entropic correction obtained in the optimization stage to the potential energy computed as single point extending the basis set (BS2) at 6-311++G(2d,p) basis set for the main group elements[8] and quadruple-ζ def2-QZVP basis set for Ir.[9] A correction of 1.89 kcal mol^{-1} was applied to all Gibbs values to change the standard state from the gas phase (1 atm) to solution (1 M) at 298.15 K.[10]

Catalyst Hydrogenation

Since the catalyst hydrogenation can leads to different isomers of the Ir-dihydride complex, a preliminary analysis of this species was carried out. Excluding the species with *trans* hydrides, among the possible isomers, those with the equatorial hydride and cyclohexyl phosphine (PCy_3) in *cis* to each other result energetically favoured (about 17.0 kcal·mol^{-1}) over *trans* phosphine-hydride (Scheme 5.SI1). Concerning the relative position of hydrides, the equatorial H can be coordinated *trans* py or *trans* a vacancy with a Gibbs energy difference of only 1.1 kcal·mol^{-1}. For sake of completeness the transition state between the two most stables isomers has been computed, obtaining a low barrier of 9.0 kcal·mol^{-1}, which denotes a fast equilibrium between the two isomers. Between them, the species with H *trans* py can better accommodate the incoming substrate and has been taken as the active catalyst of the cycle described in Scheme 5.3.

Scheme 5.SI1. Possible isomers of the active catalyst $[Ir(H)_2(py)(PCy_3)(COD)]^+$. Relative Gibbs energy in THF reported in kcal mol^{-1} and referred to the most stable isomer taken as zero.

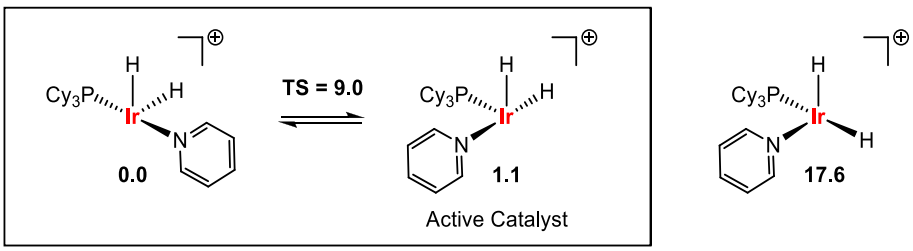

We have also evaluated the thermodynamics of the hydrogenation reaction that yields the dihydride and releases cycloctane (Table 5.SI1).

Table 5.SI1. Gibbs energy values for the hydrogenation of the catalyst $[Ir(py)(PCy_3)(COD)]^+$ in THF solvent. ΔG reported in kcal·mol^{-1}.

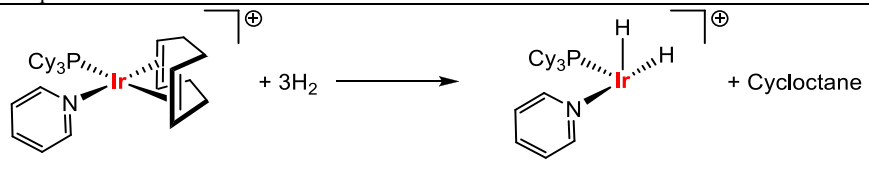

Active Catalyst

Specie	G_{THF}, BS1 (a.u)	G_{THF}, BS2 (a.u)
$[Ir^{I}(py)(Pcy_3)(COD)]^+$	-1711.356425	-1400.870925
H_2	-1.179342	-1.180441
$[Ir^{III}(H)_2(py)(Pcy_3)]^+$ [a]	-1400.601423	-1711.696601
Cycloctane	-314.333883	-314.409768

Reaction	ΔG_{THF}, BS1 [b]	ΔG_{THF}, BS2 [b]
$[Ir^{I}(py)(Pcy_3)(COD)]^+ + 3H_2 \rightarrow [Ir^{III}(H)_2(py)(Pcy_3)]^+ +$Cycloctane	-29.4	-30.6

[a] Active catalyst reported in scheme 5.S1. [b] Values in kcal·mol^{-1}.

Gibbs Energy Profile for the Isomerization Reaction

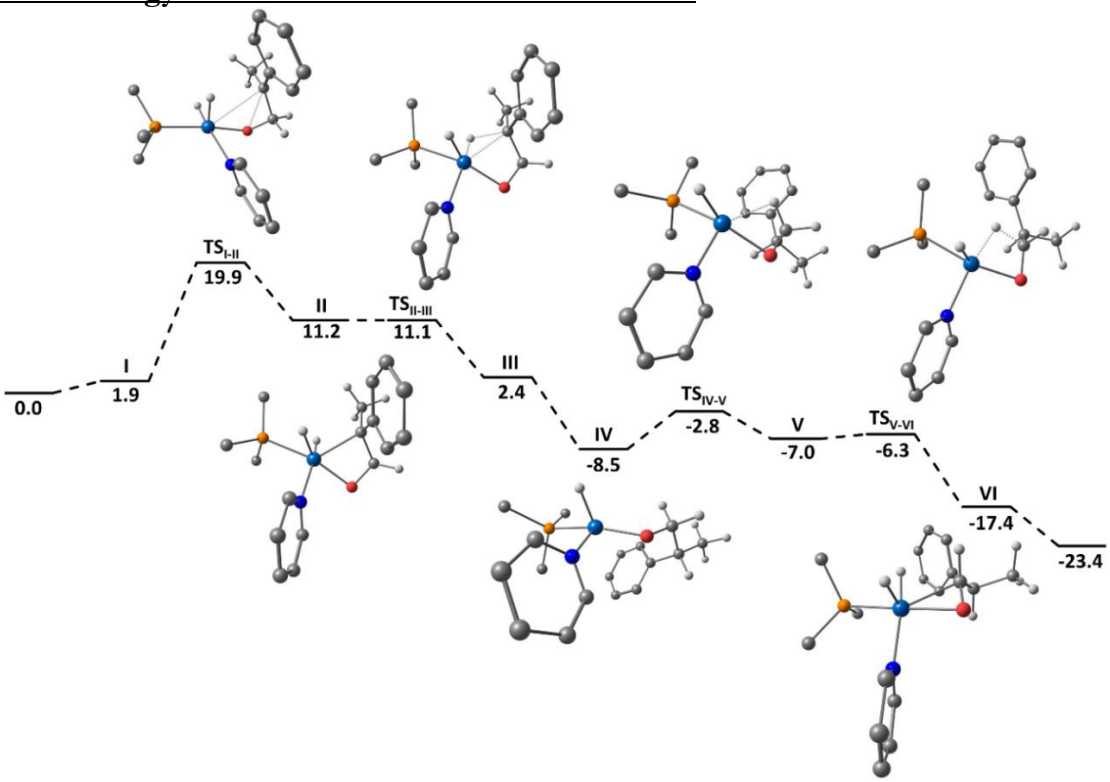

Figure 5.SI1. Gibbs energy profiles in THF for the isomerization process of epoxide **5-1a** to aldehyde **5-2a**. Energy values reported in kcal·mol^{-1}. The separated catalytically active species $[Ir(H)_2(py)(PCy_3)]^+$ and substrate **5-1a** are taken as zero-energy. The Transition states and the most representative intermediates are depicted. Cyclohexyl groups and hydrogen atoms have been omitted for clarity.

Cartesian Coordinates and Absolute E and G energies in THF of the Optimized Structures[11]

The cartesian coordinates are published online on Advanced Synthesis and Catalysis. They can be found in the Supporting Information file, which is available free of charge on the Wiley website at DOI: 10.1002/adsc.201900372

^{1}H and ^{13}C NMR spectra

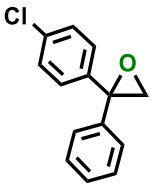

5-1q

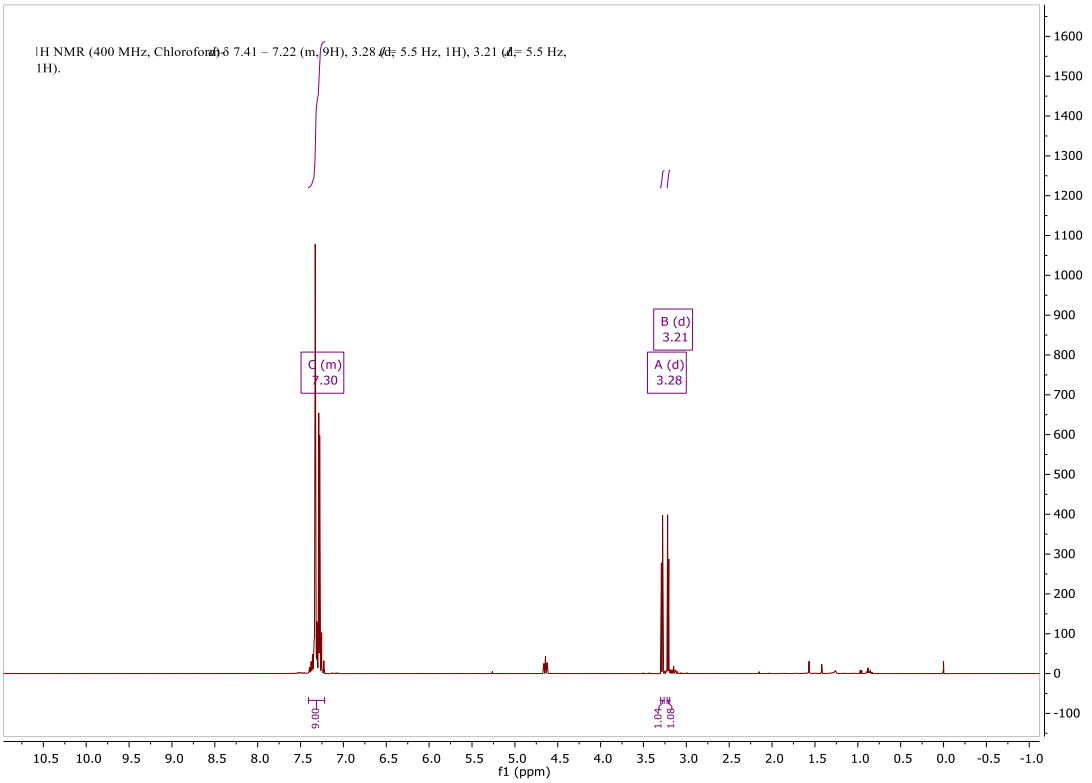

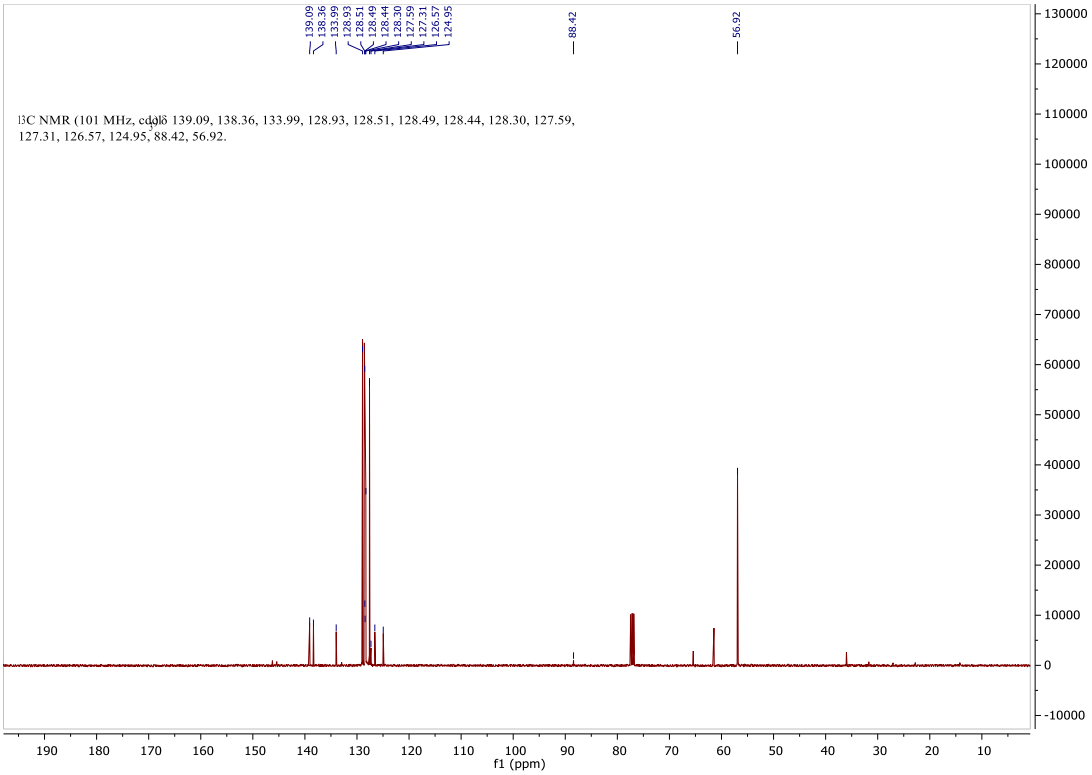

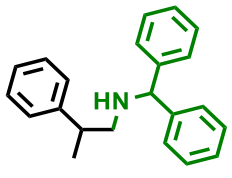

5-6a

^{1}H NMR (400 MHz, Chloroform-d) δ 7.38 – 7.15 (m, 15H), 4.77 (d, J = 2.2 Hz, 1H), 2.98 (hd, J = 7.1, 2.0 Hz, 1H), 2.75 (dd, J = 7.5, 1.5 Hz, 1H), 1.48 (s, 1H), 1.27 (dd, J = 7.0, 2.0 Hz, 3H).

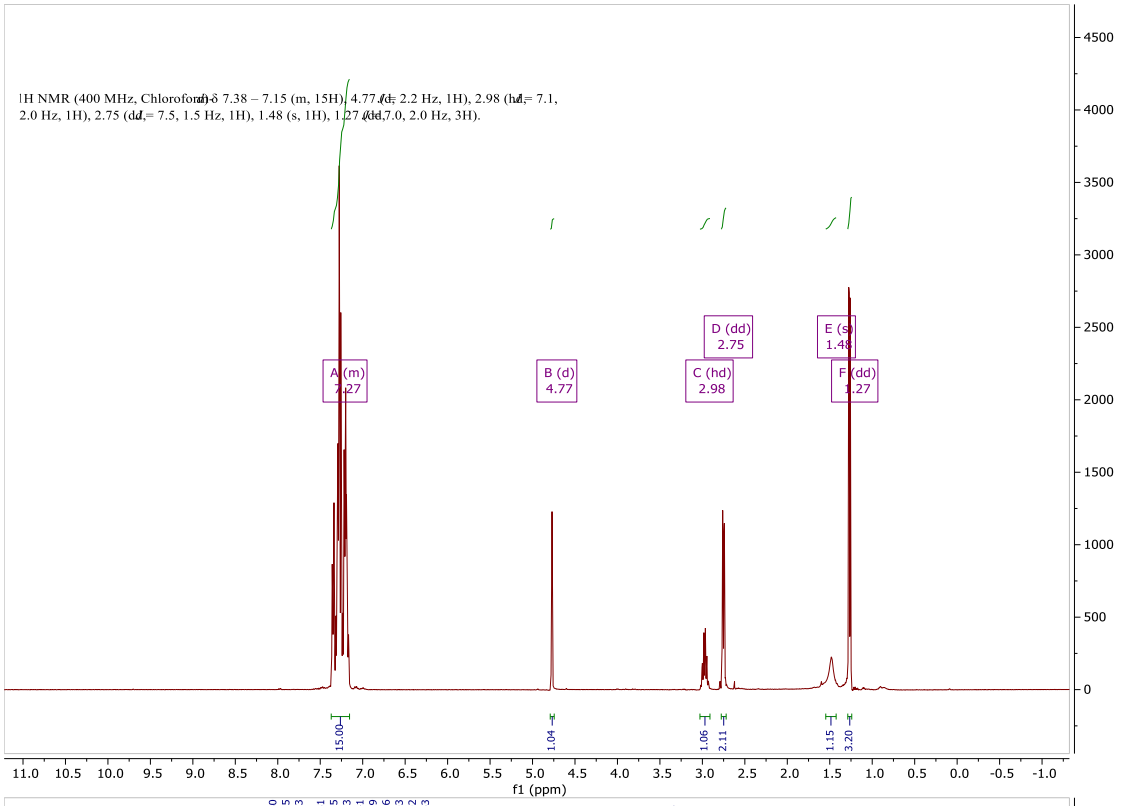

^{13}C NMR (101 MHz, cdcl$_3$) δ 145.60, 144.35, 144.33, 128.61, 128.55, 128.53, 127.41, 127.39, 127.36, 127.03, 127.02, 126.43, 67.44, 55.31, 40.35, 20.21.

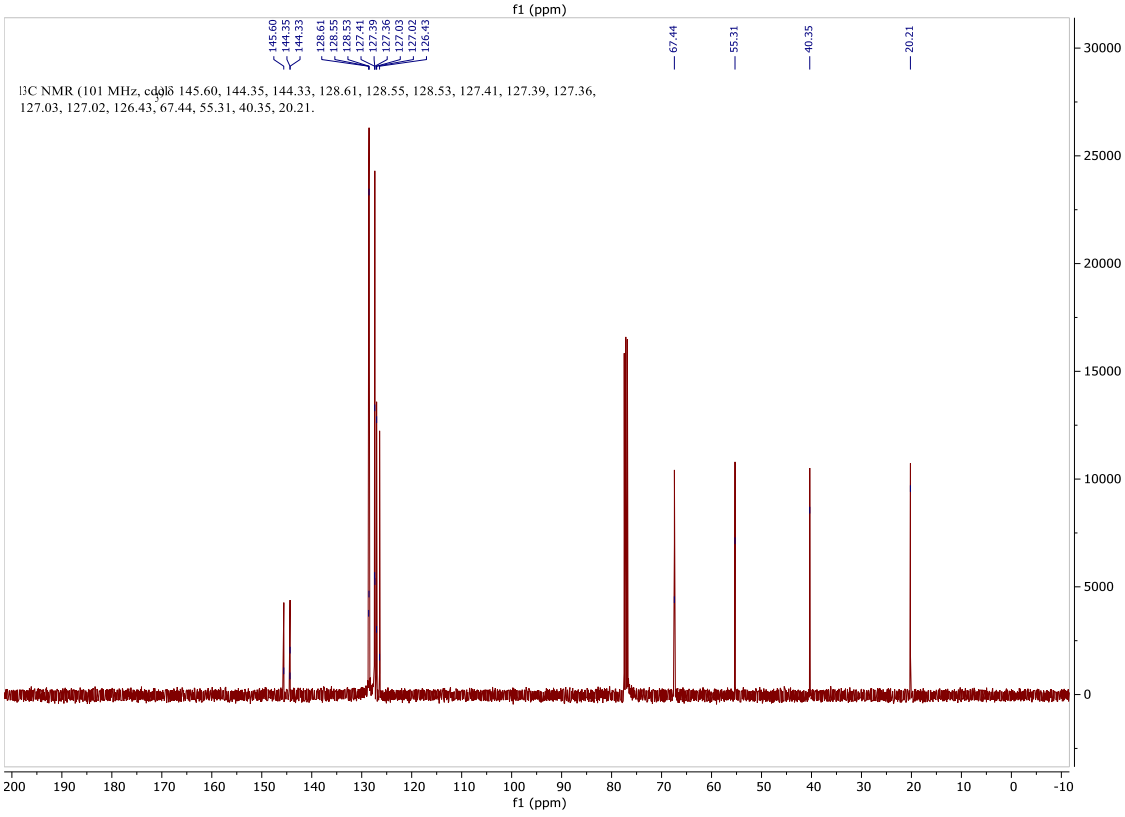

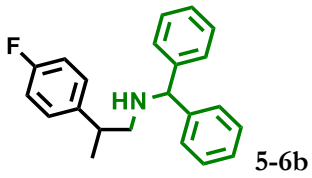

5-6b

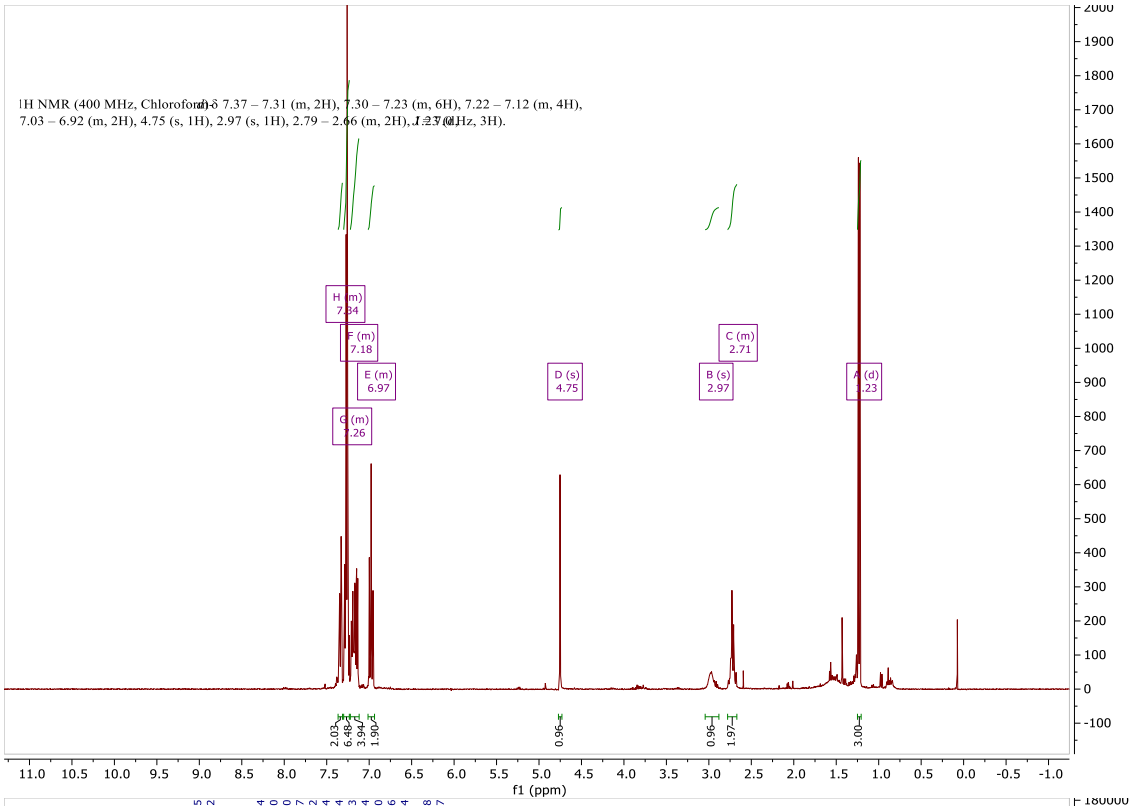

^{1}H NMR (400 MHz, Chloroform-d) δ 7.37 – 7.31 (m, 2H), 7.30 – 7.23 (m, 6H), 7.22 – 7.12 (m, 4H), 7.03 – 6.92 (m, 2H), 4.75 (s, 1H), 2.97 (s, 1H), 2.79 – 2.66 (m, 2H), 1.23 (d, J = 6.4 Hz, 3H).

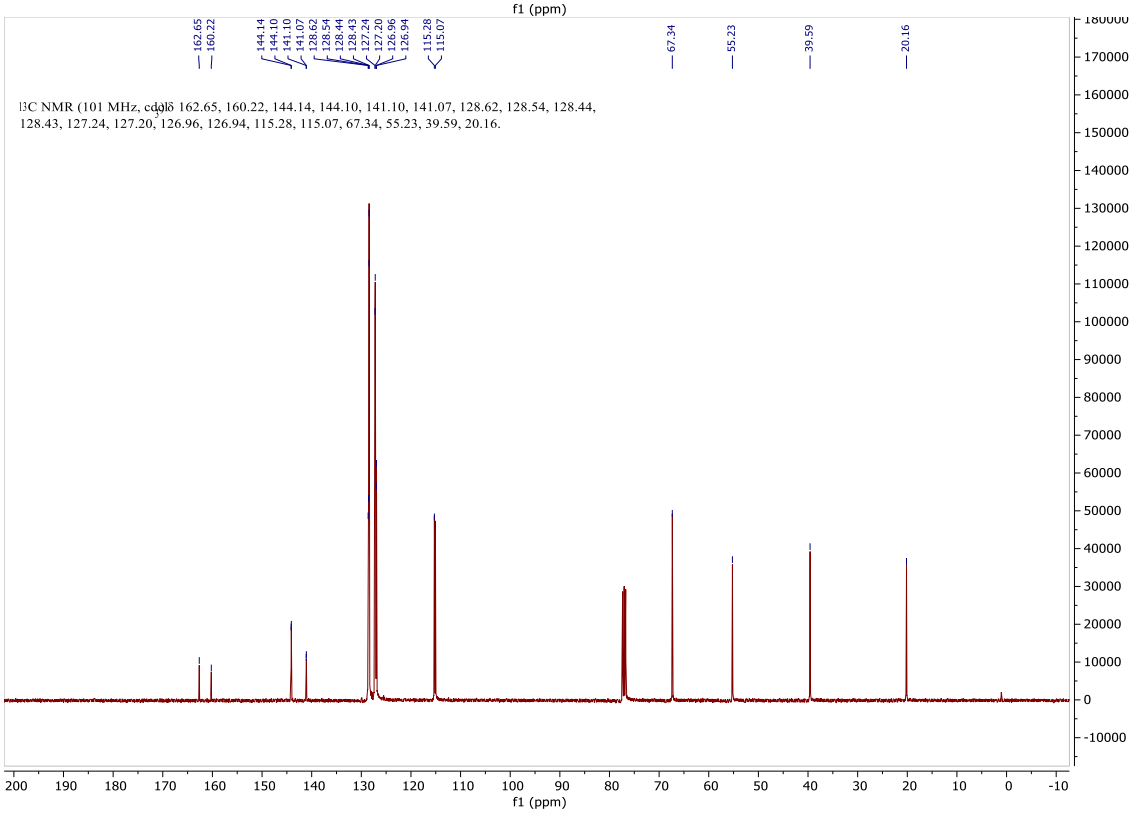

^{13}C NMR (101 MHz, cdcl$_3$) δ 162.65, 160.22, 144.14, 144.10, 141.10, 141.07, 128.62, 128.54, 128.44, 128.43, 127.24, 127.20, 126.96, 126.94, 115.28, 115.07, 67.34, 55.23, 39.59, 20.16.

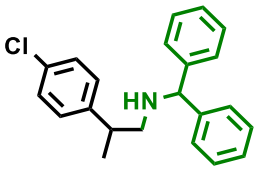
Cl
HN

5-6c

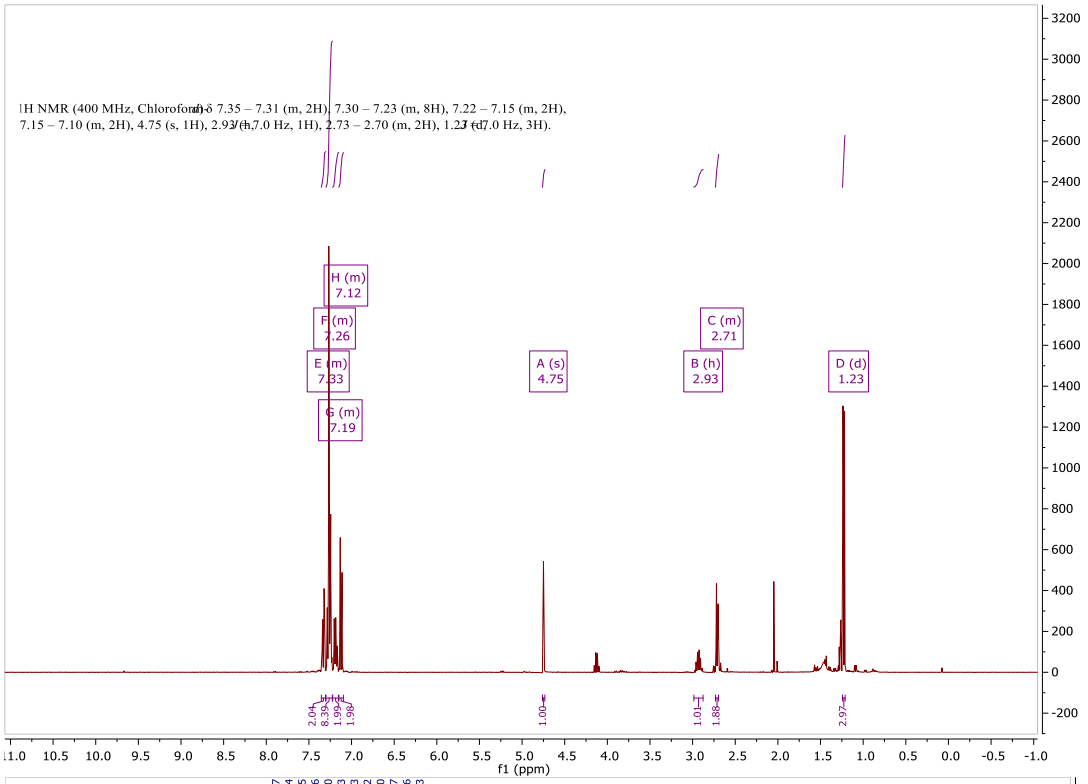
1H NMR (400 MHz, Chloroform-d) δ 7.35 – 7.31 (m, 2H), 7.30 – 7.23 (m, 8H), 7.22 – 7.15 (m, 2H), 7.15 – 7.10 (m, 2H), 4.75 (s, 1H), 2.93 (h, J = 7.0 Hz, 1H), 2.73 – 2.70 (m, 2H), 1.23 (d, J = 7.0 Hz, 3H).
H (m) 7.12
F (m) 7.26
E (m) 7.33
G (m) 7.19
A (s) 4.75
C (m) 2.71
B (h) 2.93
D (d) 1.23
f1 (ppm)

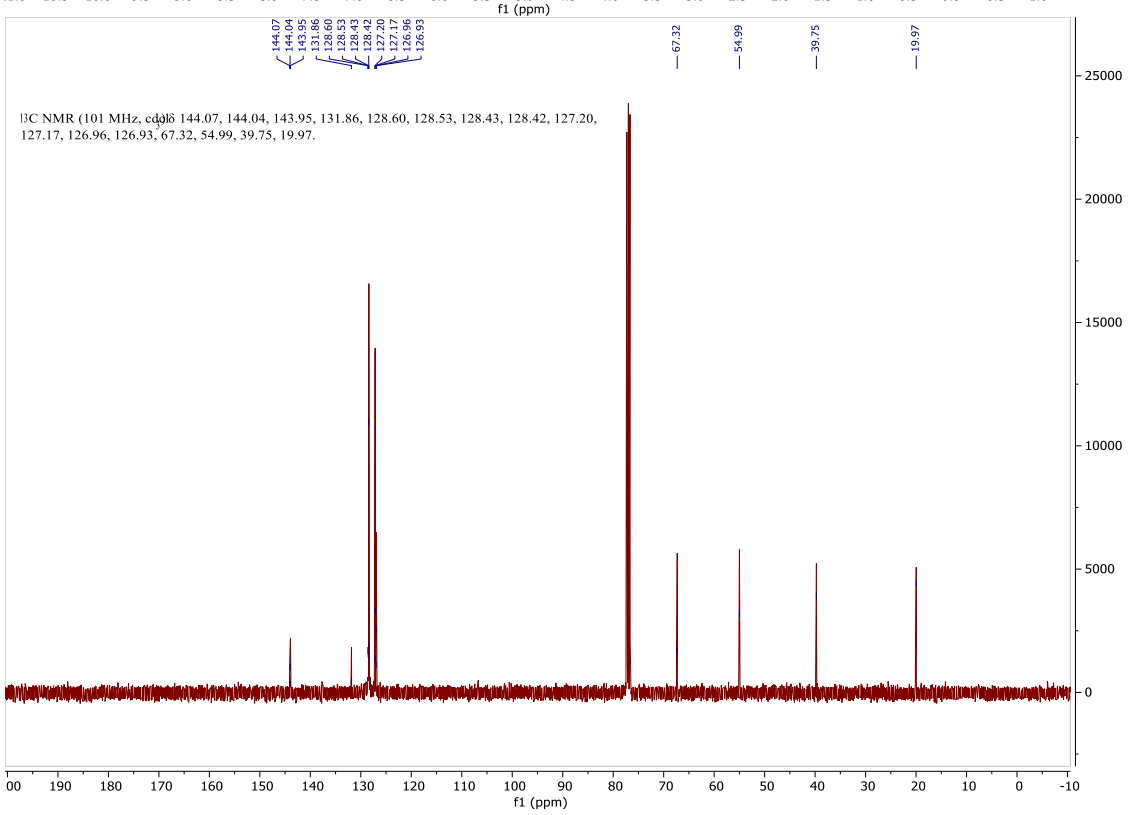
13C NMR (101 MHz, cdcl3) δ 144.07, 144.04, 143.95, 131.86, 128.60, 128.53, 128.43, 128.42, 127.20, 127.17, 126.96, 126.93, 67.32, 54.99, 39.75, 19.97.
144.07
144.04
143.95
131.86
128.60
128.53
128.43
128.42
127.20
127.17
126.96
126.93
67.32
54.99
39.75
19.97
f1 (ppm)

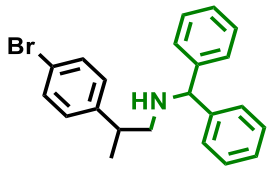

5-6d

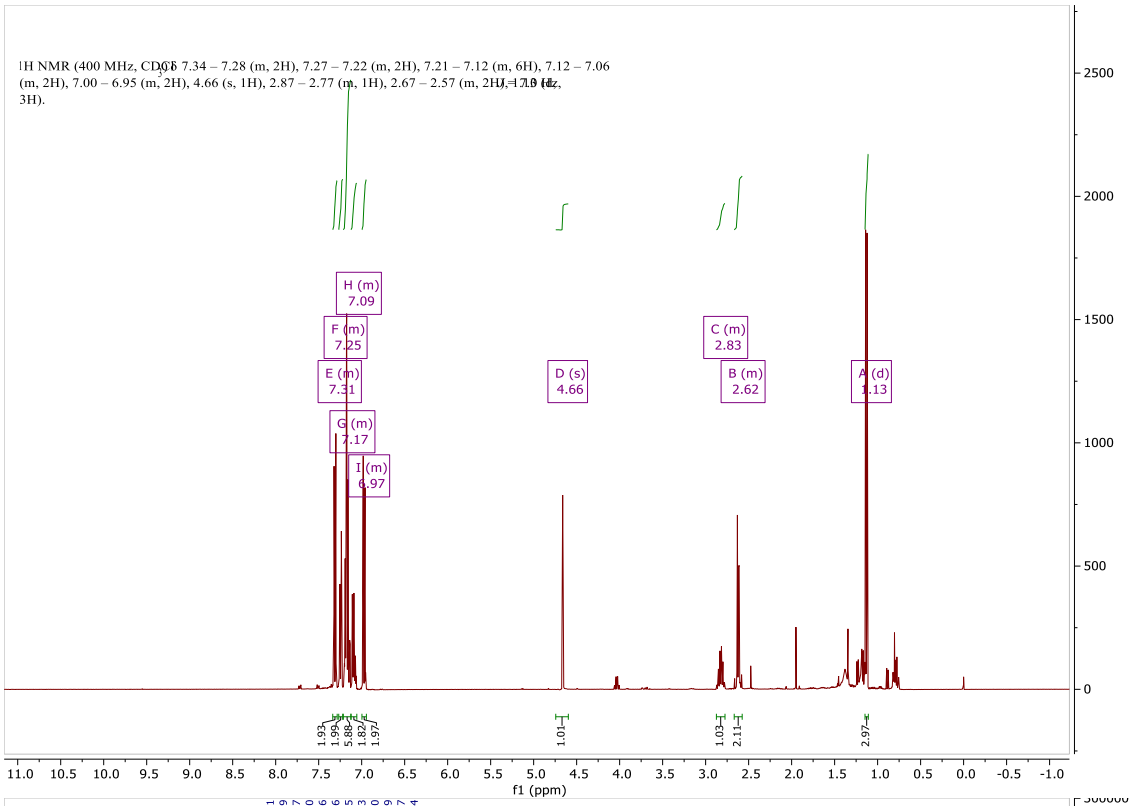

^{1}H NMR (400 MHz, $CDCl_3$) δ 7.34 – 7.28 (m, 2H), 7.27 – 7.22 (m, 2H), 7.21 – 7.12 (m, 6H), 7.12 – 7.06 (m, 2H), 7.00 – 6.95 (m, 2H), 4.66 (s, 1H), 2.87 – 2.77 (m, 1H), 2.67 – 2.57 (m, 2H), 1.13 (d, J = 7.0 Hz, 3H).

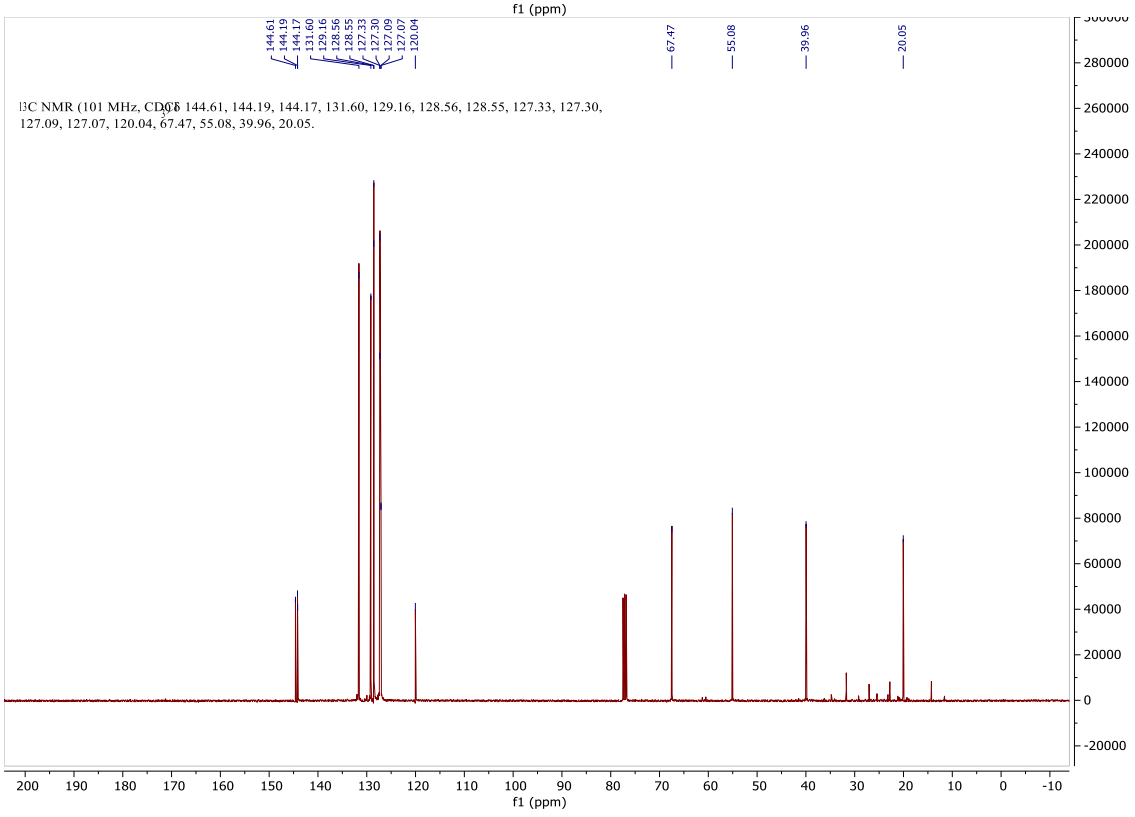

^{13}C NMR (101 MHz, $CDCl_3$) δ 144.61, 144.19, 144.17, 131.60, 129.16, 128.56, 128.55, 127.33, 127.30, 127.09, 127.07, 120.04, 67.47, 55.08, 39.96, 20.05.

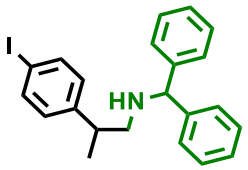

5-6e

^{1}H NMR (400 MHz, Chloroform-*d*) δ 7.65 – 7.56 (m, 2H), 7.36 – 7.29 (m, 2H), 7.28 – 7.21 (m, 6H), 7.21 – 7.12 (m, 2H), 6.98 – 6.90 (m, 2H), 4.74 (s, 1H), 2.89 (td, *J* = 6.9 Hz, 1H), 2.74 – 2.66 (m, 2H), 1.45 (s, 1H), 1.21 (d, *J* = 6.9 Hz, 3H).

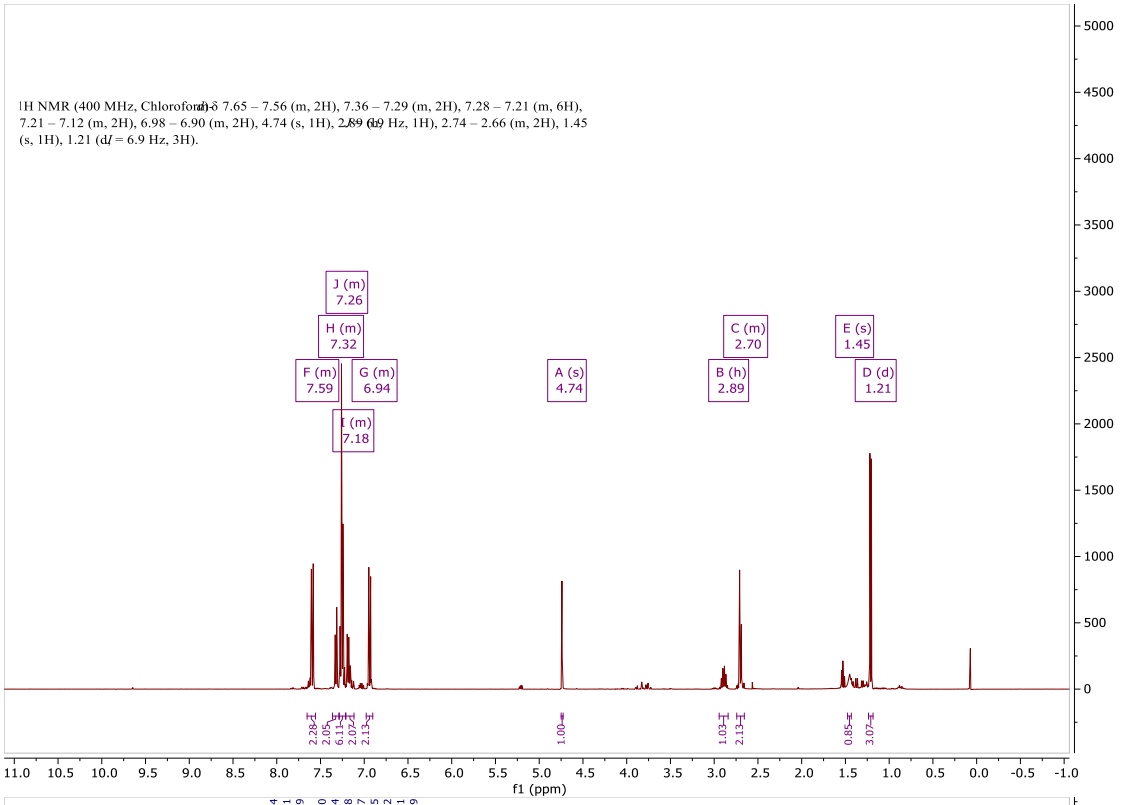

^{13}C NMR (101 MHz, cdcl$_3$) δ 145.34, 144.21, 144.19, 137.60, 129.54, 128.58, 128.57, 127.35, 127.32, 127.11, 127.09, 91.45, 67.48, 55.05, 40.06, 20.02.

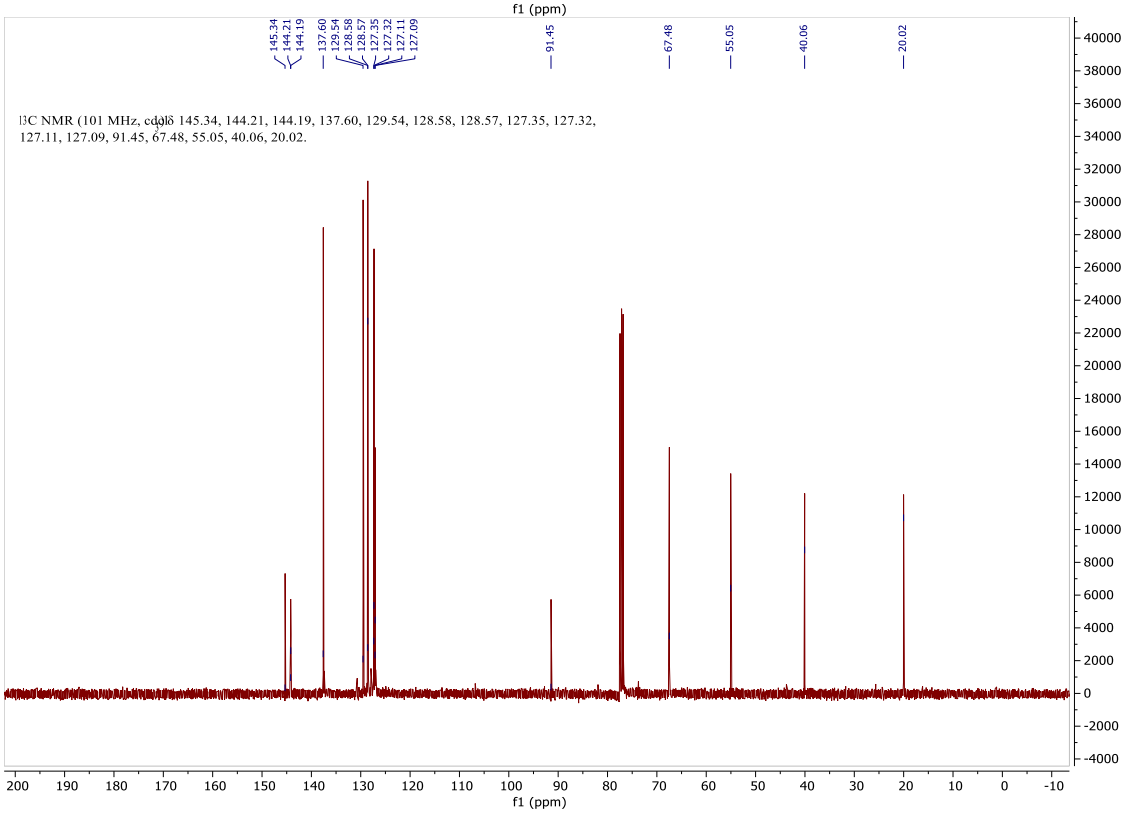

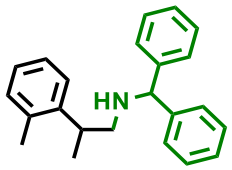
HN

5-6f

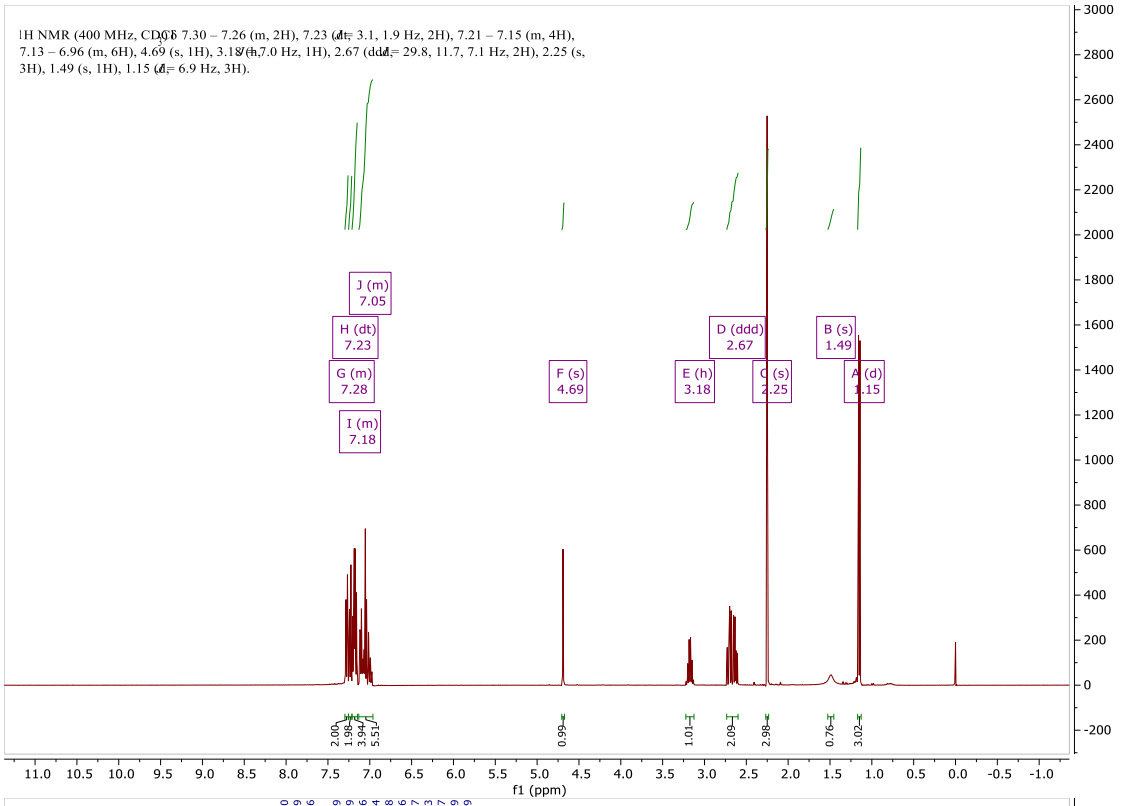
J (m)
7.05
H (dt)
7.23
G (m)
7.28
I (m)
7.18
F (s)
4.69
E (h)
3.18
D (ddd)
2.67
C (s)
2.25
B (s)
1.49
A (d)
1.15
f1 (ppm)

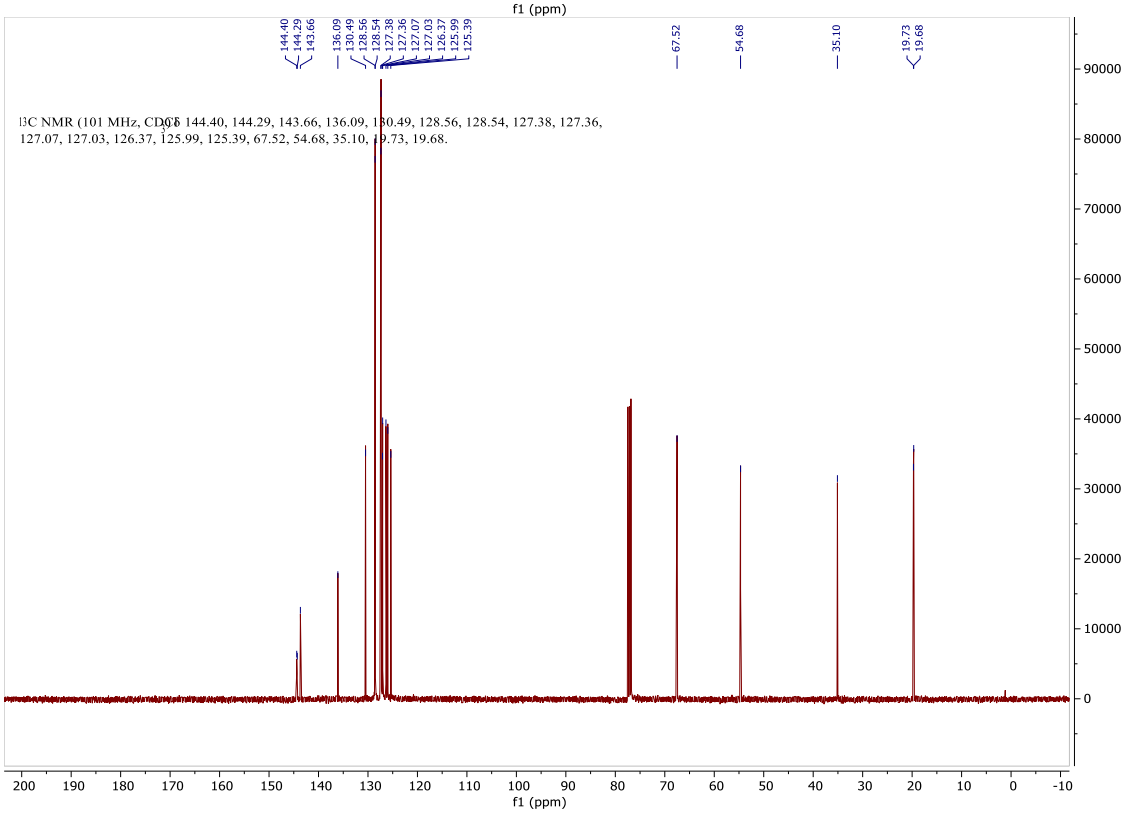
144.40
144.29
143.66
136.09
130.49
128.56
128.54
127.38
127.36
127.07
127.03
126.37
125.99
125.39
67.52
54.68
35.10
19.73
19.68
f1 (ppm)

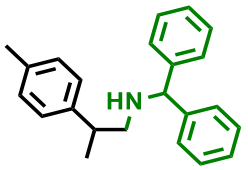

5-6g

^{1}H NMR (400 MHz, Chloroform-*d*) δ 7.34 (qd, *J* = 2.3, 1.2 Hz, 2H), 7.30 – 7.23 (m, 7H), 7.20 – 7.15 (m, 2H), 7.08 (d, *J* = 8.8 Hz, 4H), 4.76 (s, 1H), 2.94 (h, *J* = 7.0 Hz, 1H), 2.71 (t, *J* = 6.0 Hz, 2H), 2.31 (d, *J* = 6.1 Hz, 3H), 1.23 (d, *J* = 7.0 Hz, 3H).

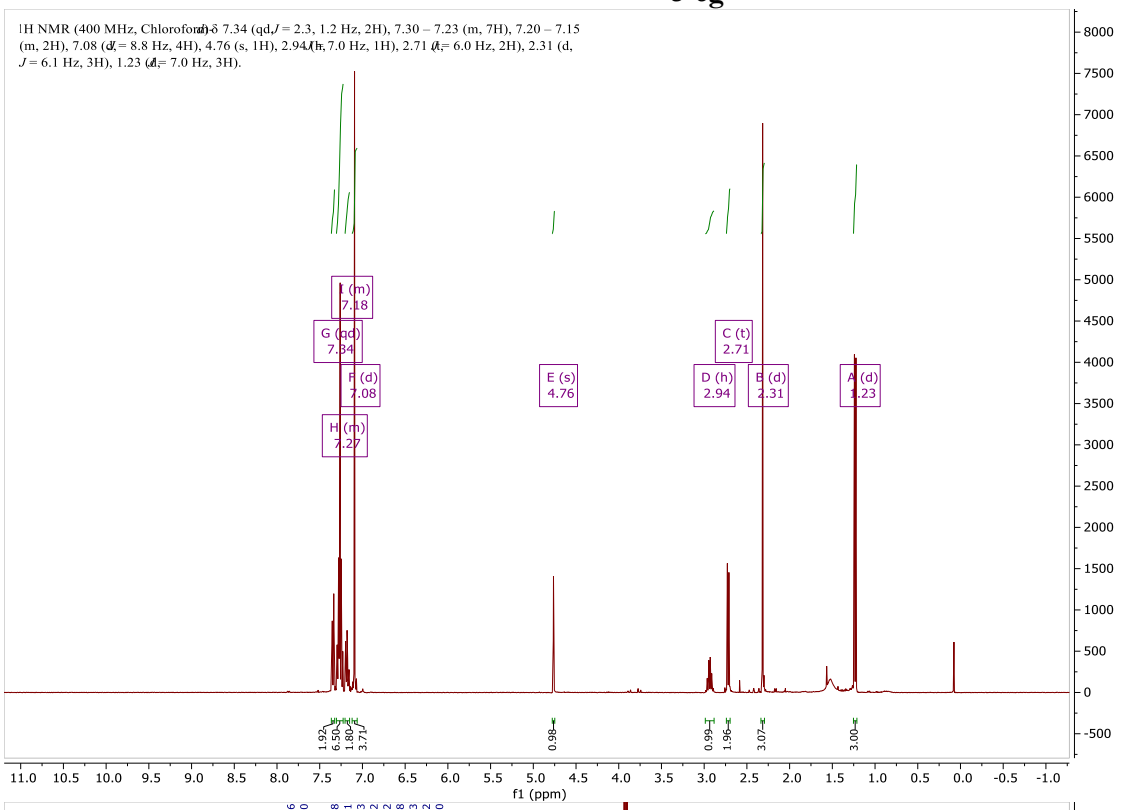

^{13}C NMR (101 MHz, CDCl$_3$) δ 144.36, 142.50, 135.88, 129.31, 128.53, 128.52, 127.42, 127.38, 127.23, 127.02, 127.00, 67.46, 55.35, 39.86, 21.15, 20.34.

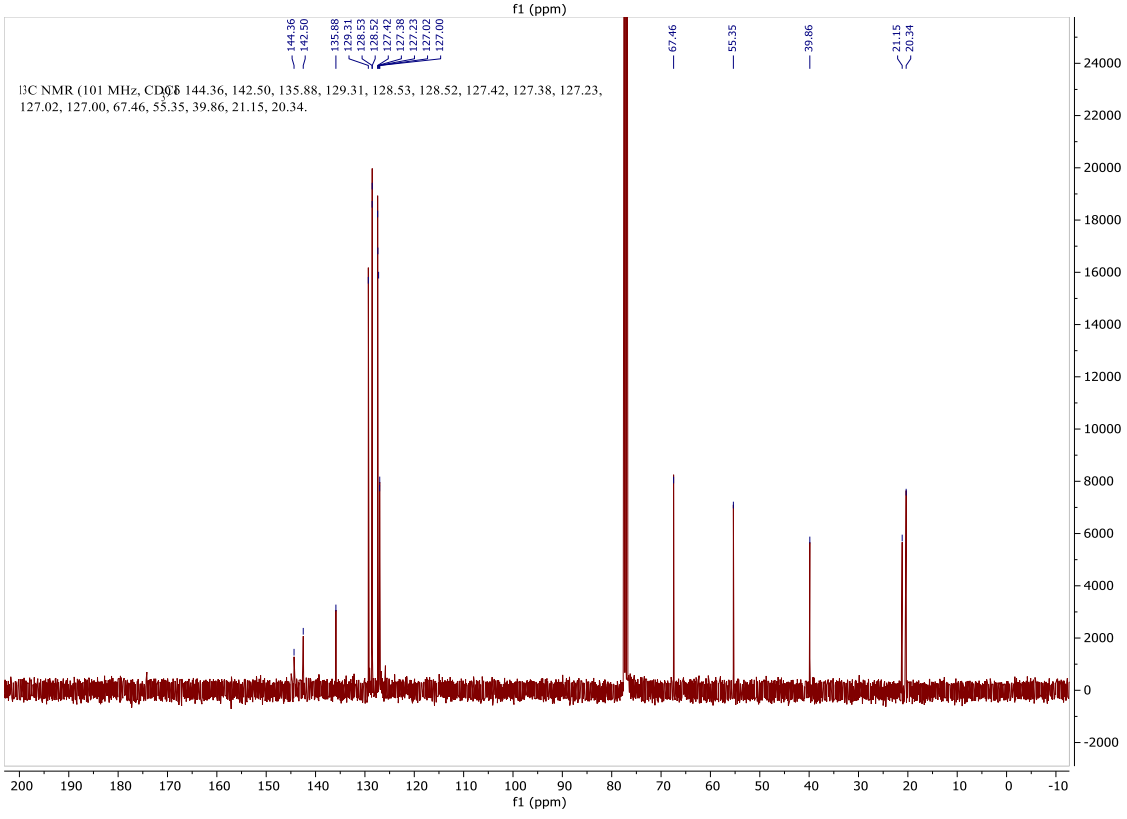

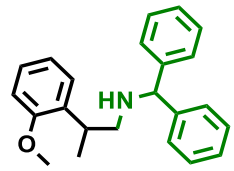
HN
O

5-6h

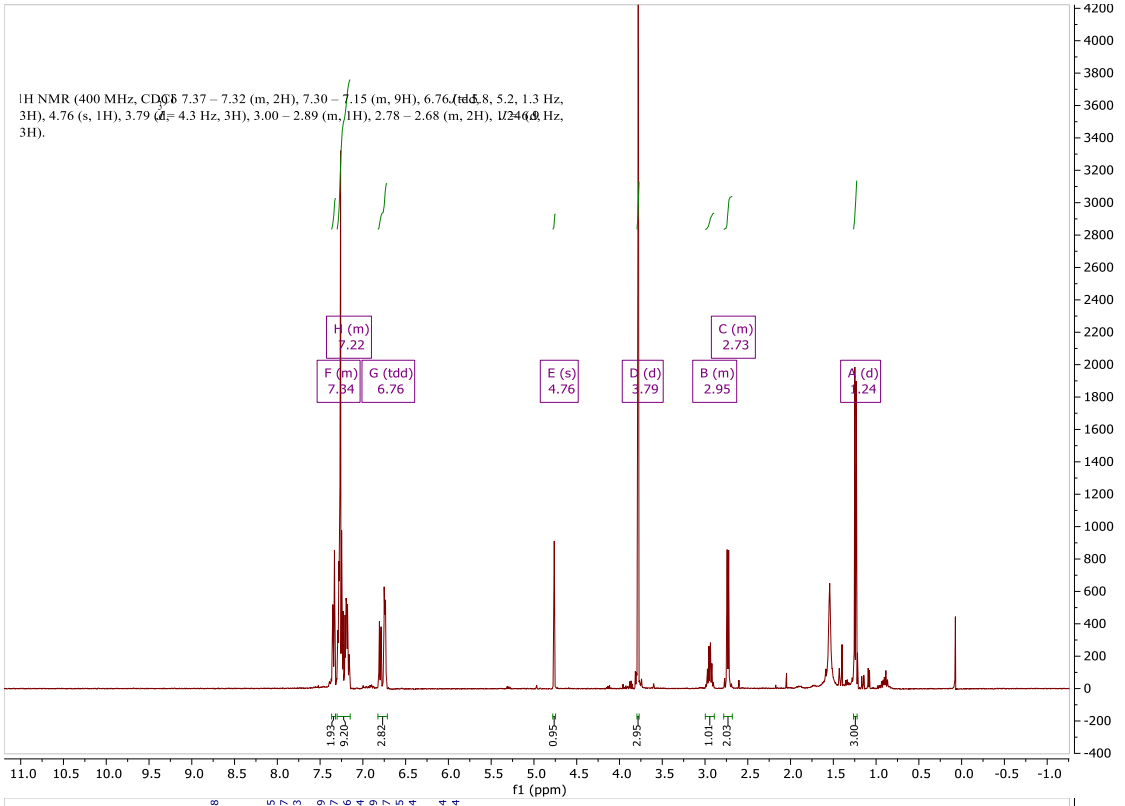
1H NMR (400 MHz, CDCl3) δ 7.37 – 7.32 (m, 2H), 7.30 – 7.15 (m, 9H), 6.76 (tdd, J = 7.8, 5.2, 1.3 Hz, 3H), 4.76 (s, 1H), 3.79 (d, J = 4.3 Hz, 3H), 3.00 – 2.89 (m, 1H), 2.78 – 2.68 (m, 2H), 1.24 (d, J = 6.0 Hz, 3H).
H (m) 7.22
F (m) 7.34
G (tdd) 6.76
E (s) 4.76
D (d) 3.79
C (m) 2.73
B (m) 2.95
A (d) 1.24
1.93
9.20
2.82
0.95
2.95
1.01
2.03
3.00
f1 (ppm)

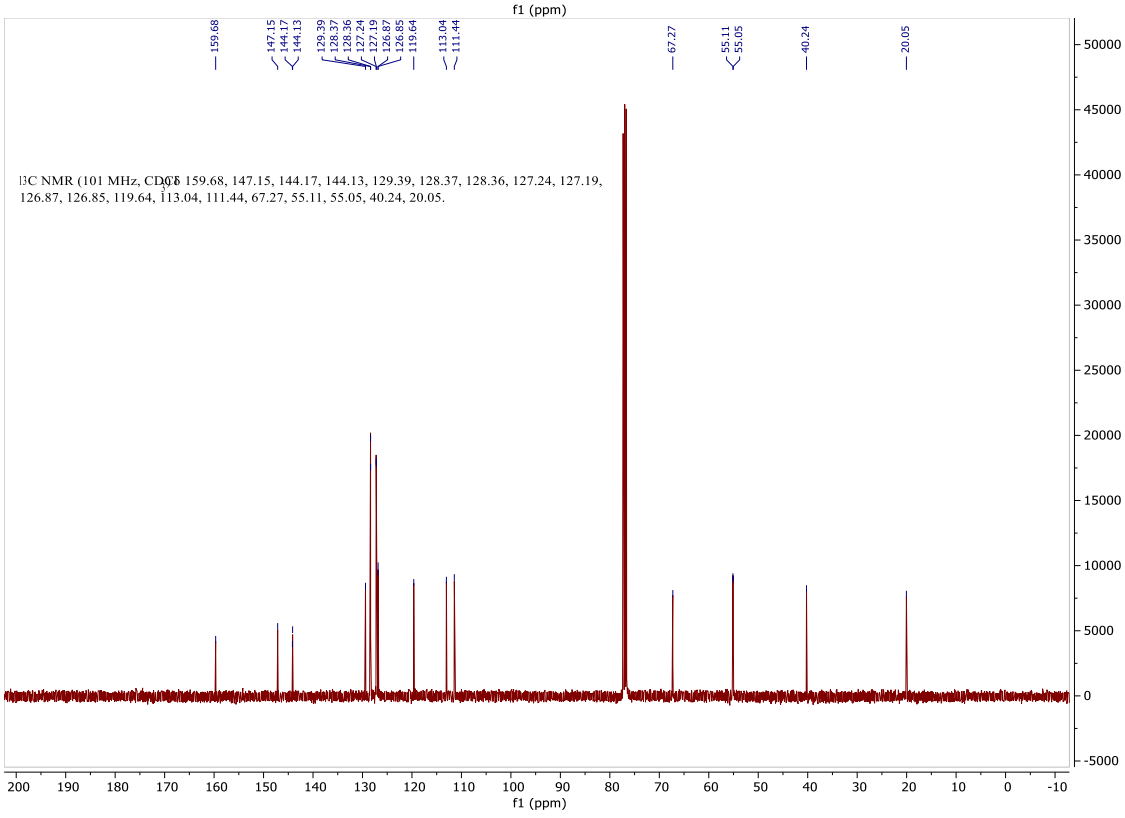
159.68
147.15
144.17
144.13
129.39
128.37
128.36
127.24
127.19
126.87
126.85
119.64
113.04
111.44
67.27
55.11
55.05
40.24
20.05
13C NMR (101 MHz, CDCl3) δ 159.68, 147.15, 144.17, 144.13, 129.39, 128.37, 128.36, 127.24, 127.19, 126.87, 126.85, 119.64, 113.04, 111.44, 67.27, 55.11, 55.05, 40.24, 20.05.
f1 (ppm)

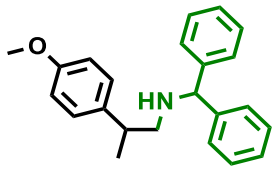

5-6i

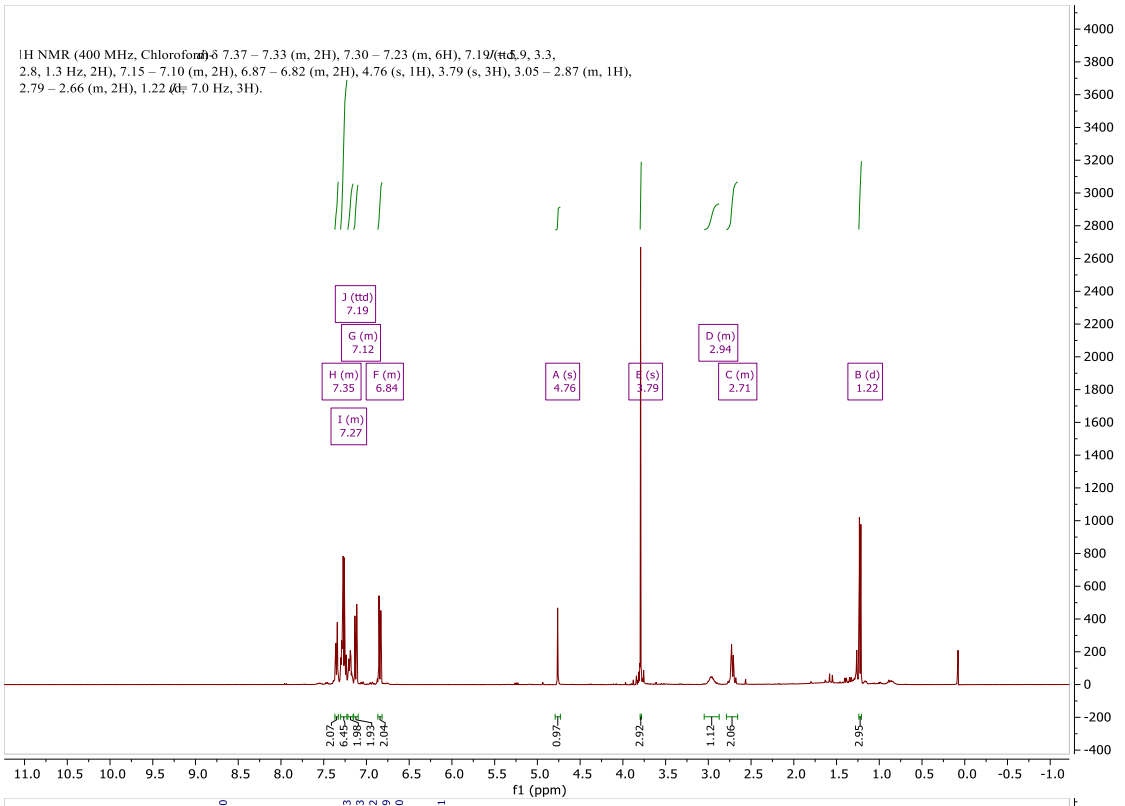
1H NMR (400 MHz, Chloroform-d) δ 7.37 – 7.33 (m, 2H), 7.30 – 7.23 (m, 6H), 7.19 (ttd, J = 7.5, 5.9, 3.3, 2.8, 1.3 Hz, 2H), 7.15 – 7.10 (m, 2H), 6.87 – 6.82 (m, 2H), 4.76 (s, 1H), 3.79 (s, 3H), 3.05 – 2.87 (m, 1H), 2.79 – 2.66 (m, 2H), 1.22 (d, J = 7.0 Hz, 3H).
J (ttd) 7.19
G (m) 7.12
H (m) 7.35
F (m) 6.84
I (m) 7.27
A (s) 4.76
E (s) 3.79
D (m) 2.94
C (m) 2.71
B (d) 1.22
2.07
6.45
1.98
1.93
2.04
0.97
2.92
1.12
2.06
2.95
f1 (ppm)

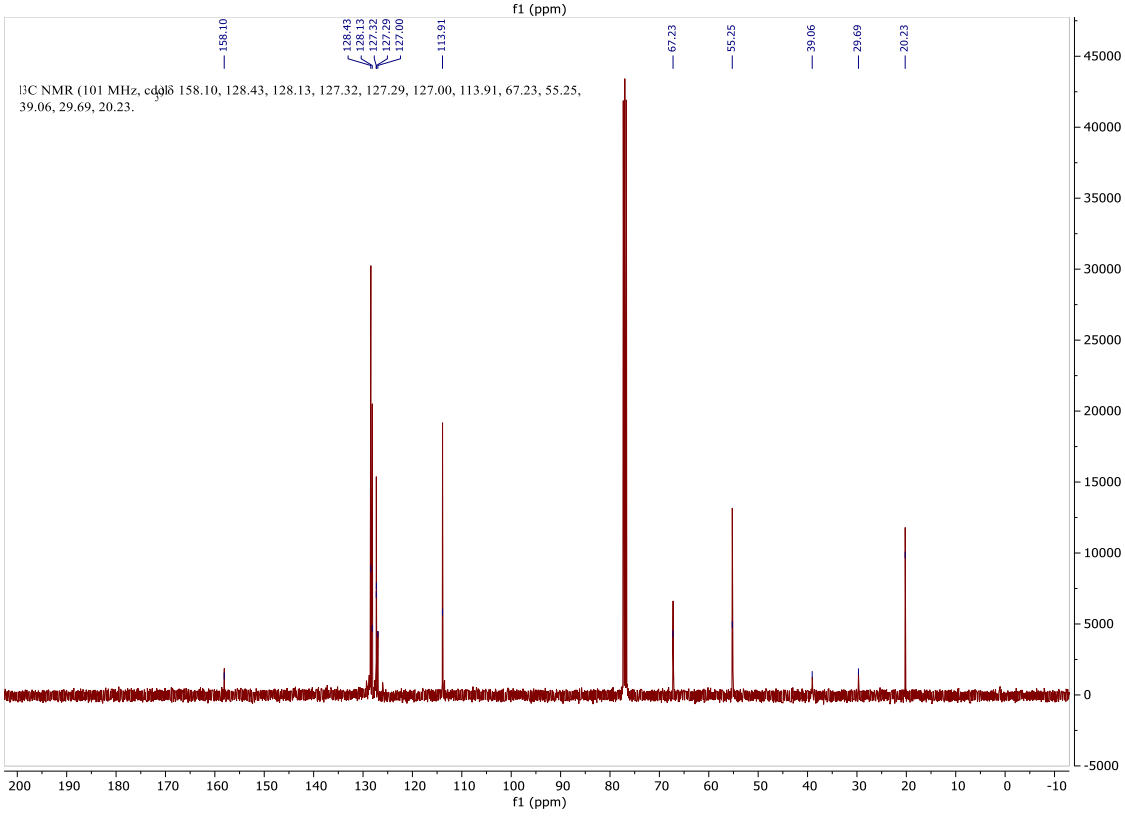
13C NMR (101 MHz, cdcl3) δ 158.10, 128.43, 128.13, 127.32, 127.29, 127.00, 113.91, 67.23, 55.25, 39.06, 29.69, 20.23.
158.10
128.43
128.13
127.32
127.29
127.00
113.91
67.23
55.25
39.06
29.69
20.23
f1 (ppm)

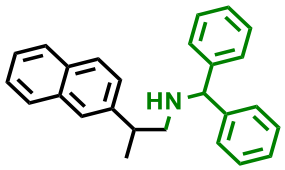
HN

5-6j

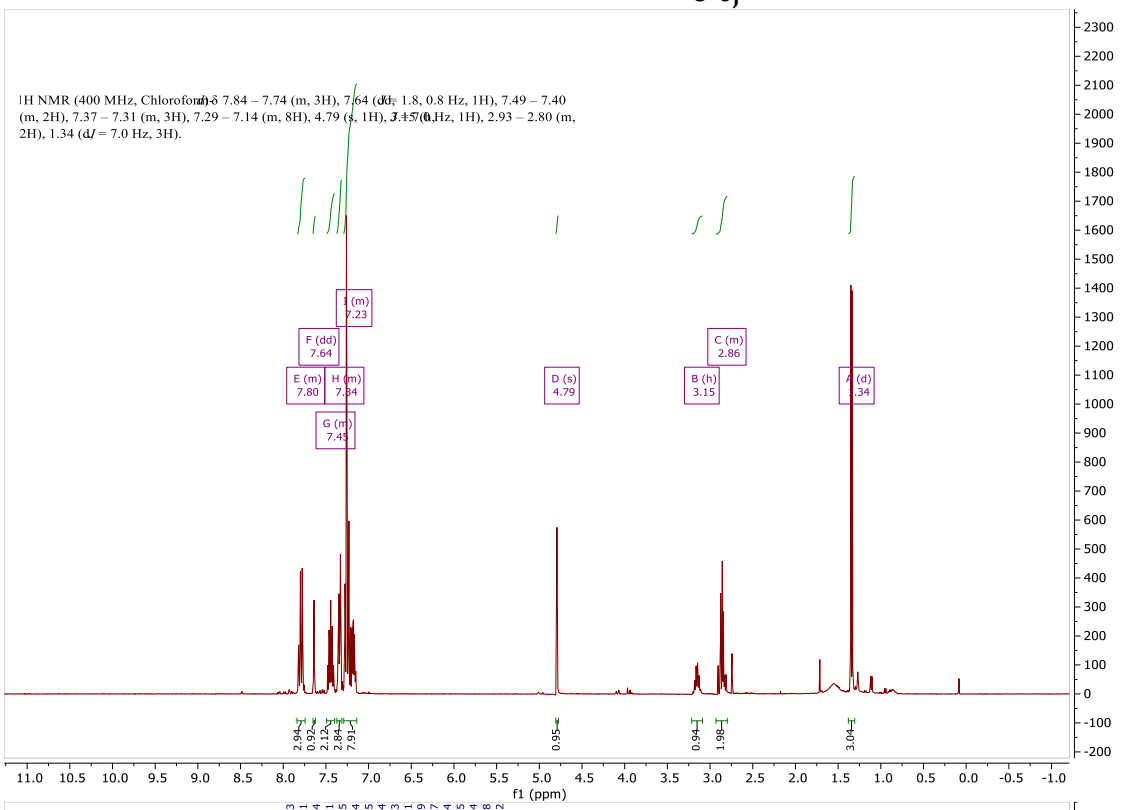
1H NMR (400 MHz, Chloroform-d) δ 7.84 – 7.74 (m, 3H), 7.64 (dd, J = 1.8, 0.8 Hz, 1H), 7.49 – 7.40 (m, 2H), 7.37 – 7.31 (m, 3H), 7.29 – 7.14 (m, 8H), 4.79 (s, 1H), 3.15 (h, J = 7.0 Hz, 1H), 2.93 – 2.80 (m, 2H), 1.34 (d, J = 7.0 Hz, 3H).
I (m) 7.23
F (dd) 7.64
E (m) 7.80
H (m) 7.84
G (m) 7.45
D (s) 4.79
C (m) 2.86
B (h) 3.15
A (d) 1.34
f1 (ppm)

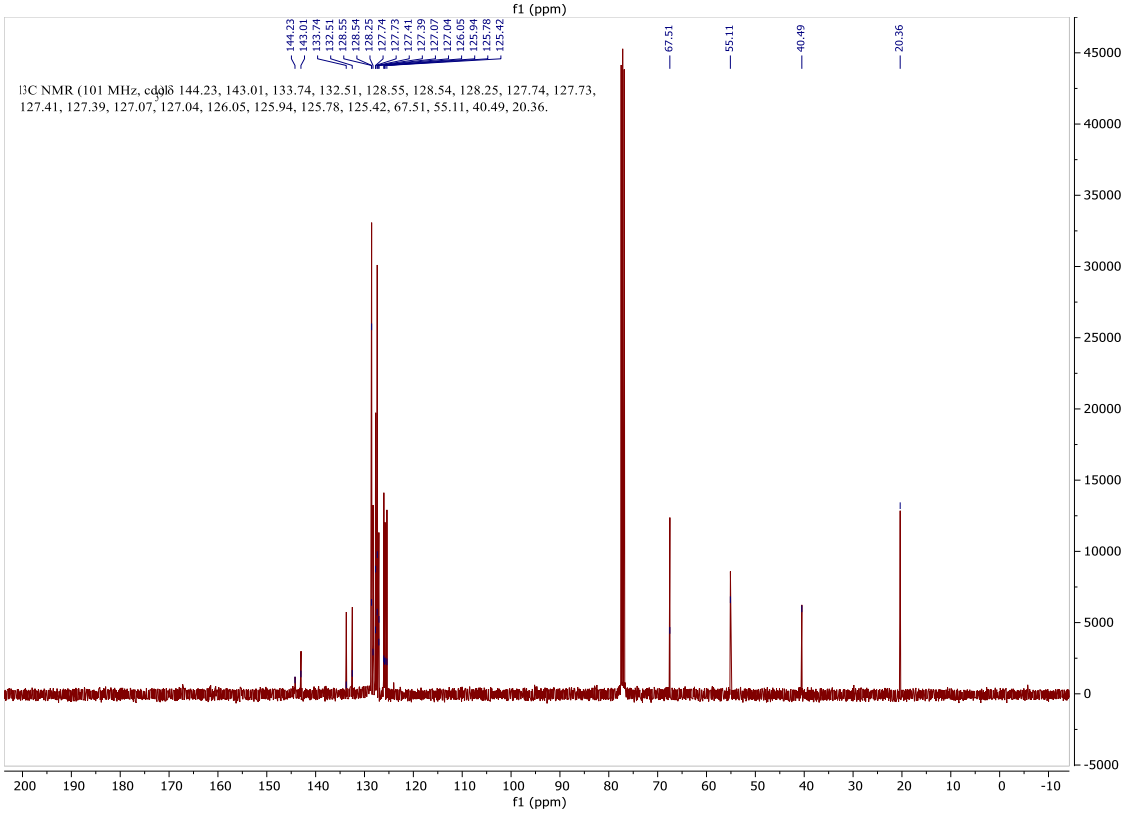
13C NMR (101 MHz, cdcl3) δ 144.23, 143.01, 133.74, 132.51, 128.55, 128.54, 128.25, 127.74, 127.73, 127.41, 127.39, 127.07, 127.04, 126.05, 125.94, 125.78, 125.42, 67.51, 55.11, 40.49, 20.36.
f1 (ppm)

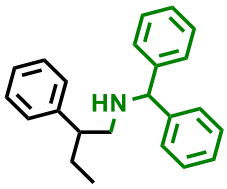

5-6k

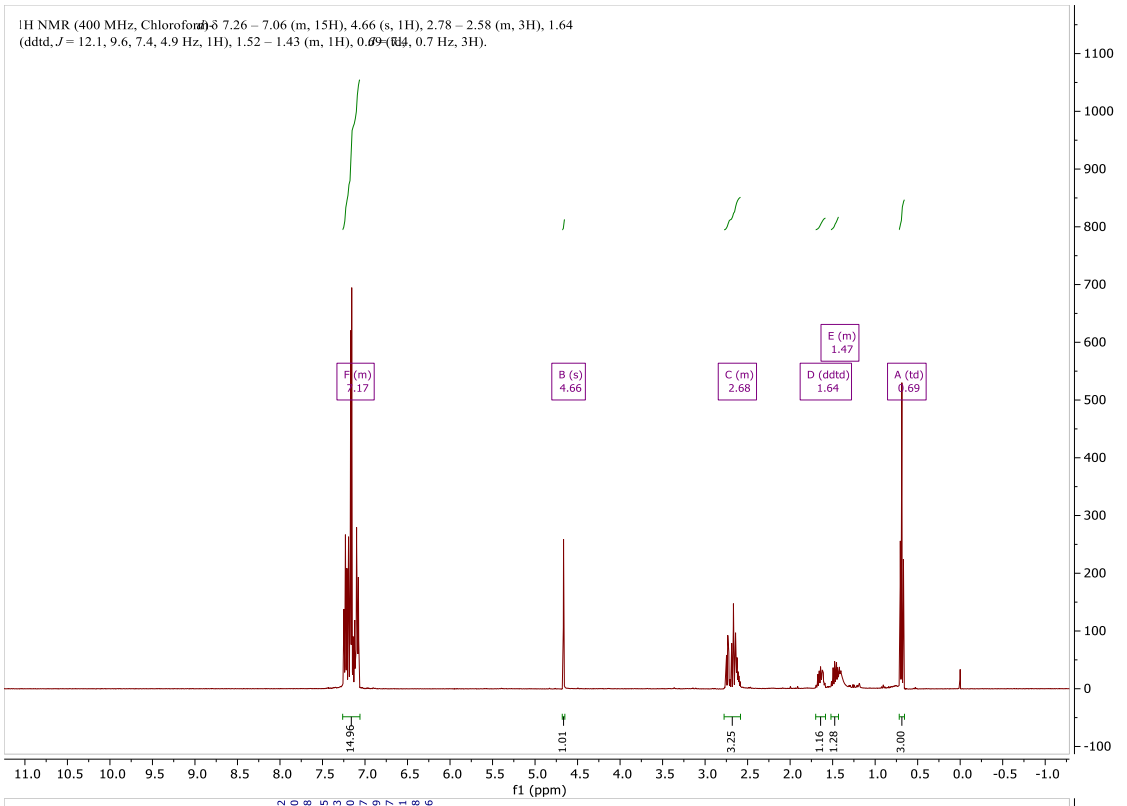

^{1}H NMR (400 MHz, Chloroform-d) δ 7.26 – 7.06 (m, 15H), 4.66 (s, 1H), 2.78 – 2.58 (m, 3H), 1.64 (ddtd, J = 12.1, 9.6, 7.4, 4.9 Hz, 1H), 1.52 – 1.43 (m, 1H), 0.69 (td, 0.7 Hz, 3H).

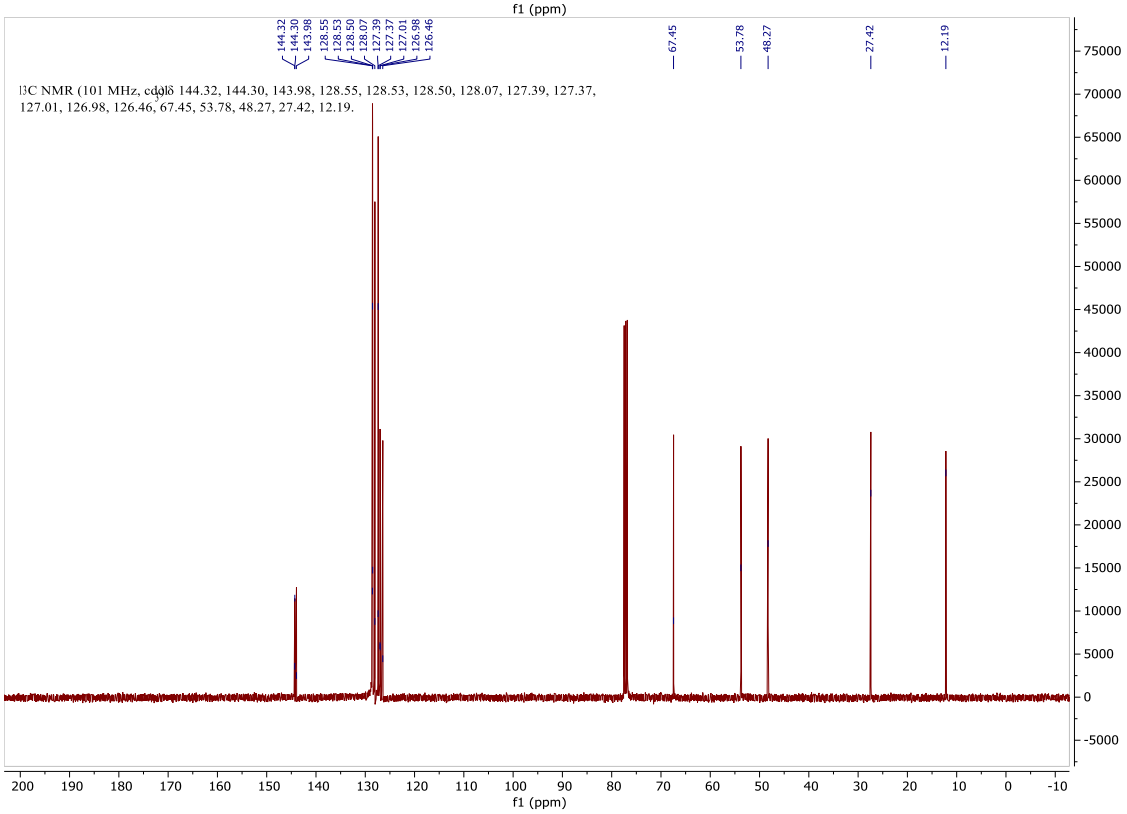

^{13}C NMR (101 MHz, cdcl$_3$) δ 144.32, 144.30, 143.98, 128.55, 128.53, 128.50, 128.07, 127.39, 127.37, 127.01, 126.98, 126.46, 67.45, 53.78, 48.27, 27.42, 12.19.

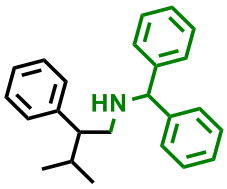
HN

5-61

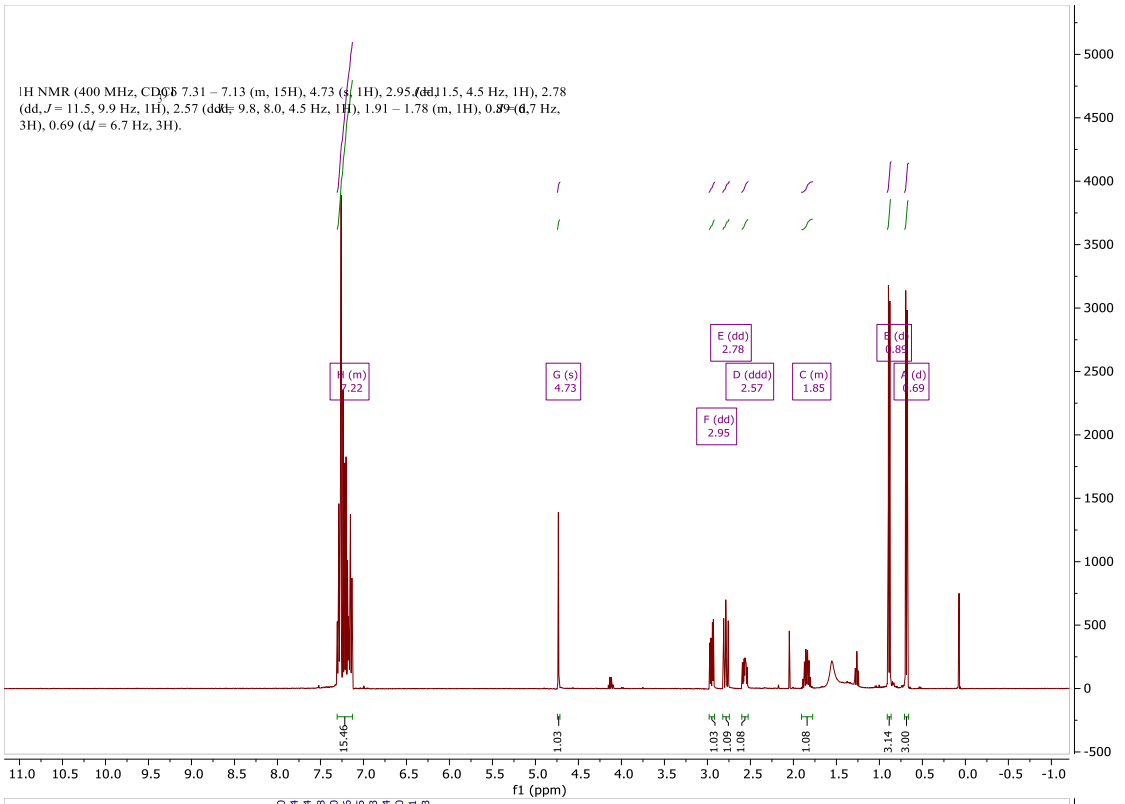
1H NMR (400 MHz, CDCl3) δ 7.31 – 7.13 (m, 15H), 4.73 (s, 1H), 2.95 (dd, J = 11.5, 4.5 Hz, 1H), 2.78 (dd, J = 11.5, 9.9 Hz, 1H), 2.57 (ddd, J = 9.8, 8.0, 4.5 Hz, 1H), 1.91 – 1.78 (m, 1H), 0.89 (d, J = 6.7 Hz, 3H), 0.69 (d, J = 6.7 Hz, 3H).
H (m) 7.22
G (s) 4.73
E (dd) 2.78
D (ddd) 2.57
F (dd) 2.95
C (m) 1.85
A (d) 0.69
15.46
1.03
1.03
1.09
1.08
1.08
3.14
3.00
f1 (ppm)

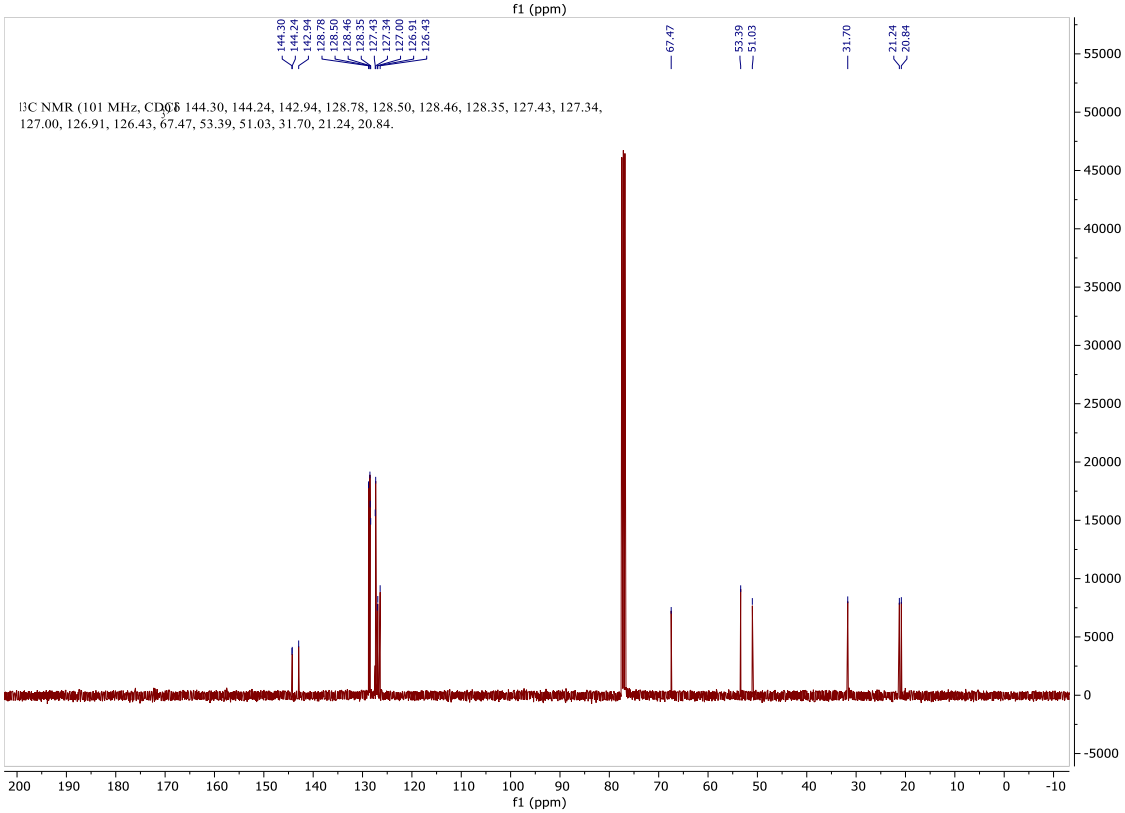
13C NMR (101 MHz, CDCl3) δ 144.30, 144.24, 142.94, 128.78, 128.50, 128.46, 128.35, 127.43, 127.34, 127.00, 126.91, 126.43, 67.47, 53.39, 51.03, 31.70, 21.24, 20.84.
144.30
144.24
142.94
128.78
128.50
128.46
128.35
127.43
127.34
127.00
126.91
126.43
67.47
53.39
51.03
31.70
21.24
20.84
f1 (ppm)

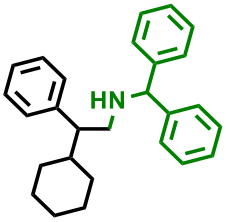

5-6m

^{1}H NMR (400 MHz, Chloroform-*d*) δ 7.22 – 7.03 (m, 15H), 4.64 (s, 1H), 2.89 (dd, *J* = 11.5, 4.4 Hz, 1H), 2.70 (dd, *J* = 11.4, 10.0 Hz, 1H), 2.54 (ddd, *J* = 9.9, 7.9, 4.4 Hz, 1H), 1.72 – 1.54 (m, 2H), 1.49 (ddt, *J* = 10.4, 7.7, 3.8 Hz, 2H), 1.40 (ddt, *J* = 11.3, 7.8, 3.3 Hz, 1H), 1.35 – 1.24 (m, 2H), 1.15 – 0.92 (m, 3H), 0.87 – 0.75 (m, 1H), 0.67 (qd, *J* = 12.2, 3.2 Hz, 1H).

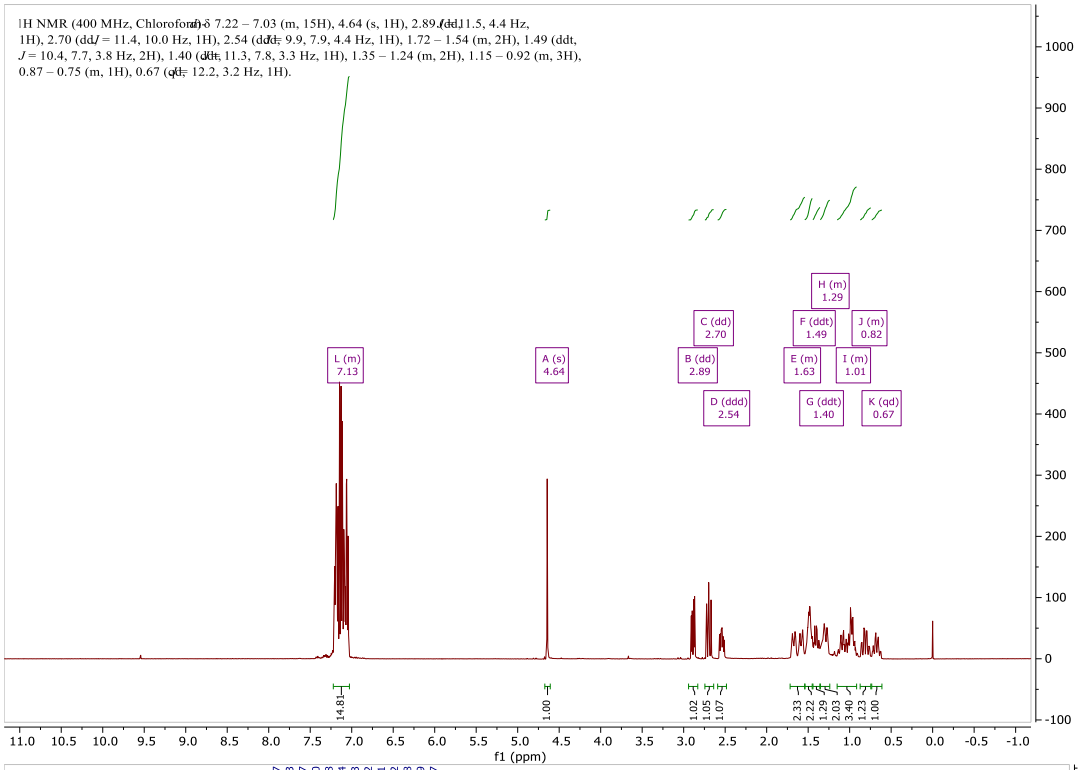

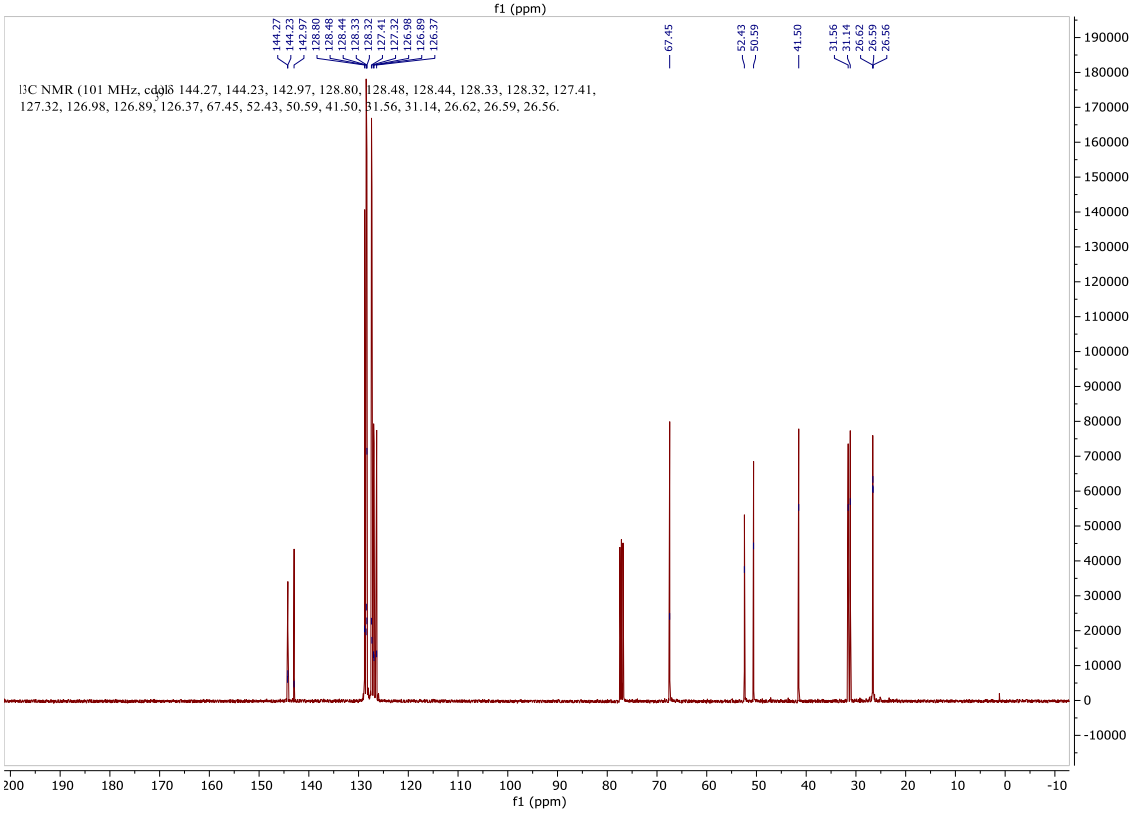

^{13}C NMR (101 MHz, cdcl$_3$) δ 144.27, 144.23, 142.97, 128.80, 128.48, 128.44, 128.33, 128.32, 127.41, 127.32, 126.98, 126.89, 126.37, 67.45, 52.43, 50.59, 41.50, 31.56, 31.14, 26.62, 26.59, 26.56.

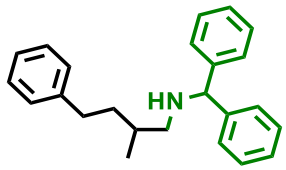
HN

5-6n

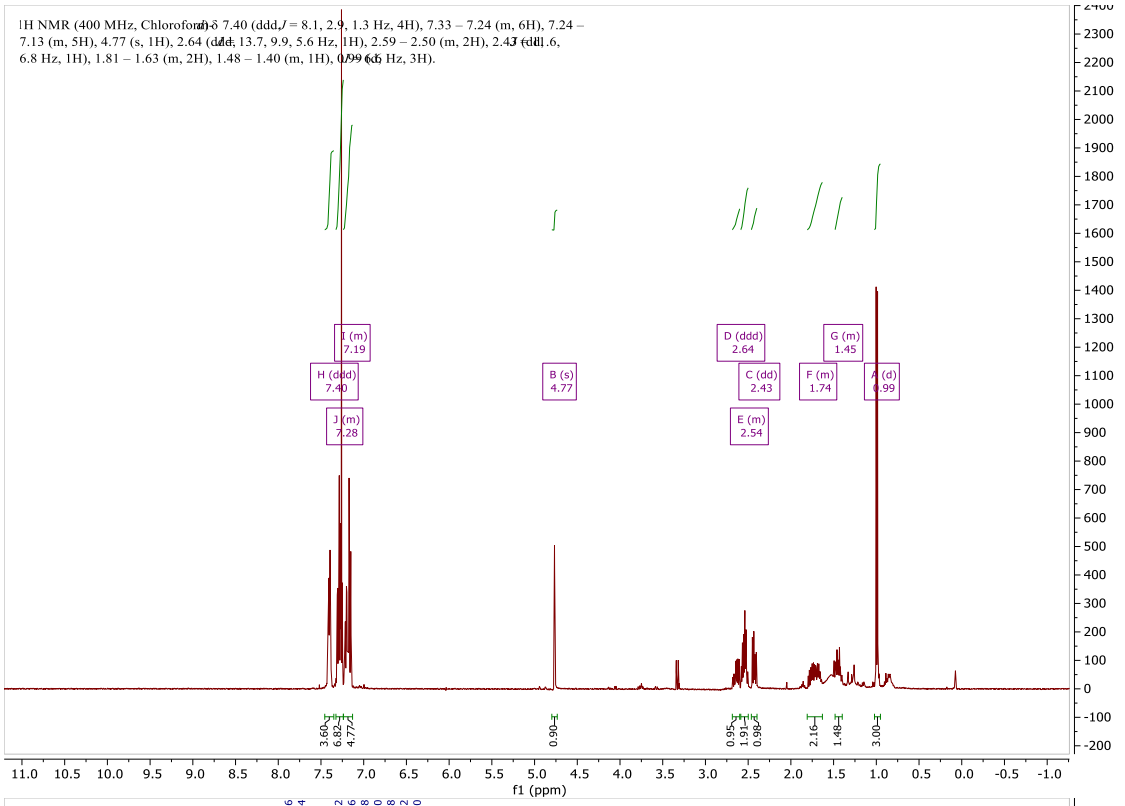
I (m)
7.19
H (ddd)
7.40
J (m)
7.28
B (s)
4.77
D (ddd)
2.64
C (dd)
2.43
E (m)
2.54
G (m)
1.45
F (m)
1.74
A (d)
0.99
f1 (ppm)

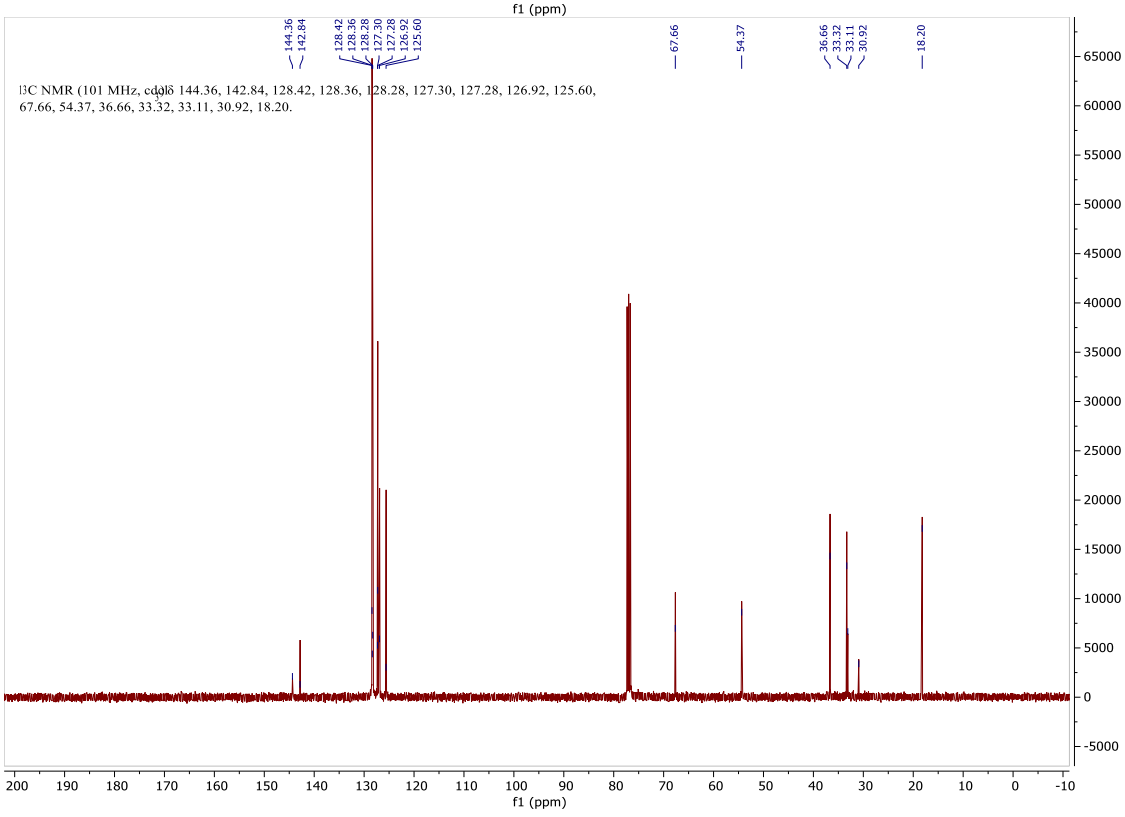
144.36
142.84
128.42
128.36
128.28
127.30
127.28
126.92
125.60
67.66
54.37
36.66
33.32
33.11
30.92
18.20
f1 (ppm)

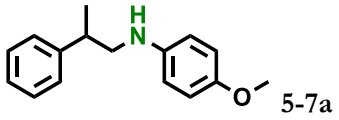

5-7a

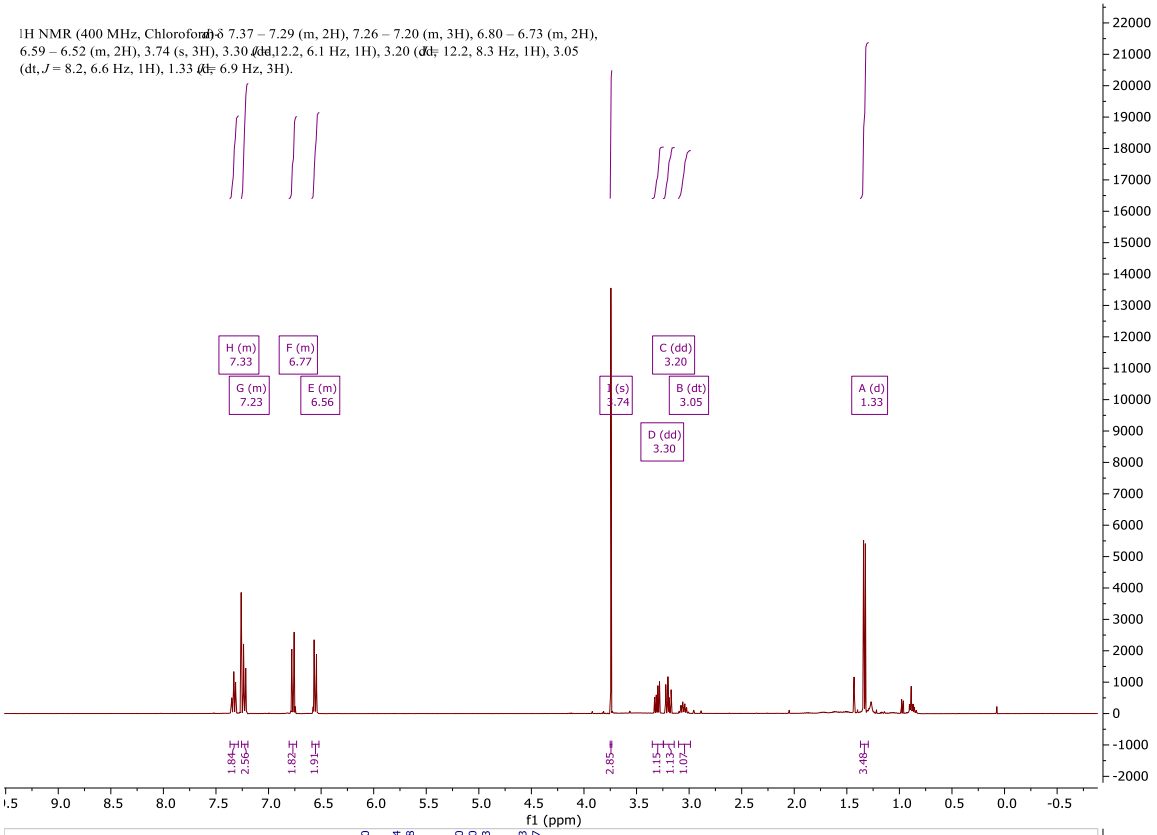

^{1}H NMR (400 MHz, Chloroform-d) δ 7.37 – 7.29 (m, 2H), 7.26 – 7.20 (m, 3H), 6.80 – 6.73 (m, 2H), 6.59 – 6.52 (m, 2H), 3.74 (s, 3H), 3.30 (dd, J = 12.2, 6.1 Hz, 1H), 3.20 (dd, J = 12.2, 8.3 Hz, 1H), 3.05 (dt, J = 8.2, 6.6 Hz, 1H), 1.33 (d, J = 6.9 Hz, 3H).

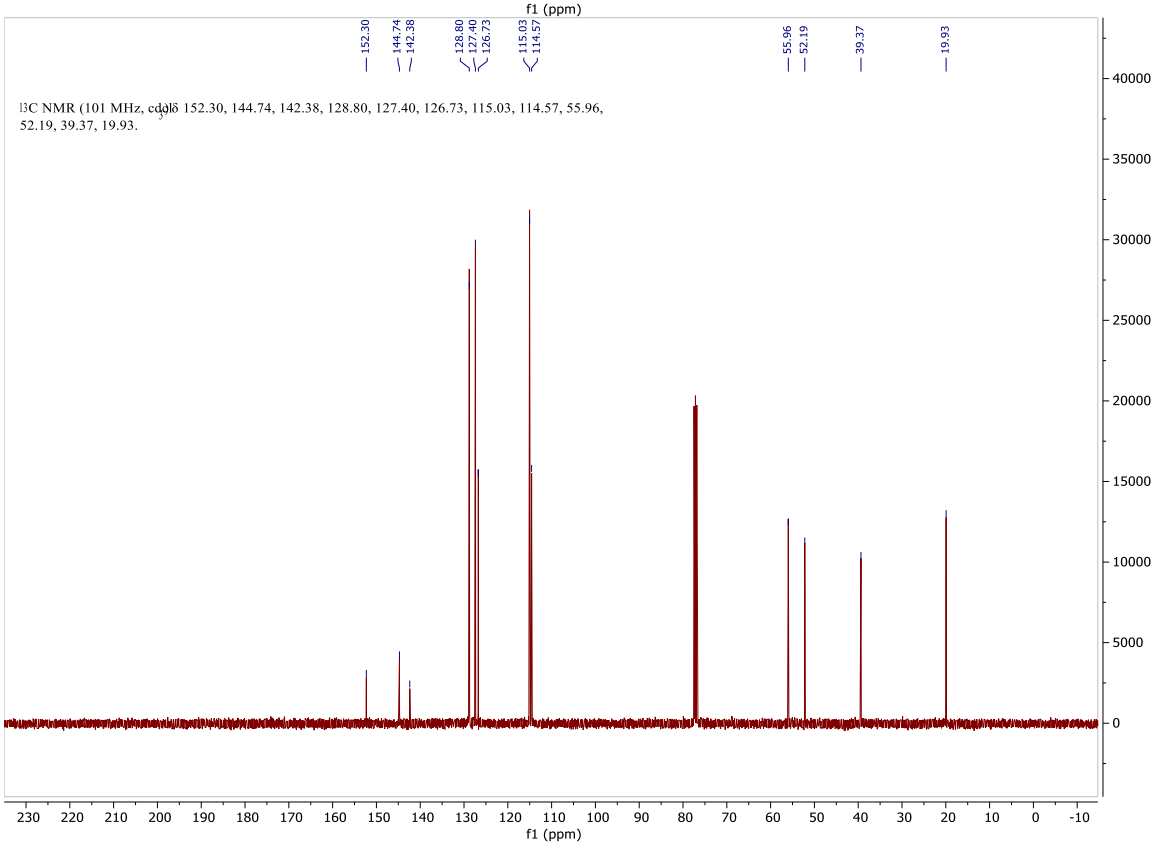

^{13}C NMR (101 MHz, $CDCl_3$) δ 152.30, 144.74, 142.38, 128.80, 127.40, 126.73, 115.03, 114.57, 55.96, 52.19, 39.37, 19.93.

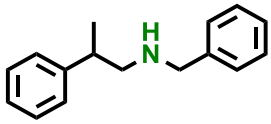

5-8a

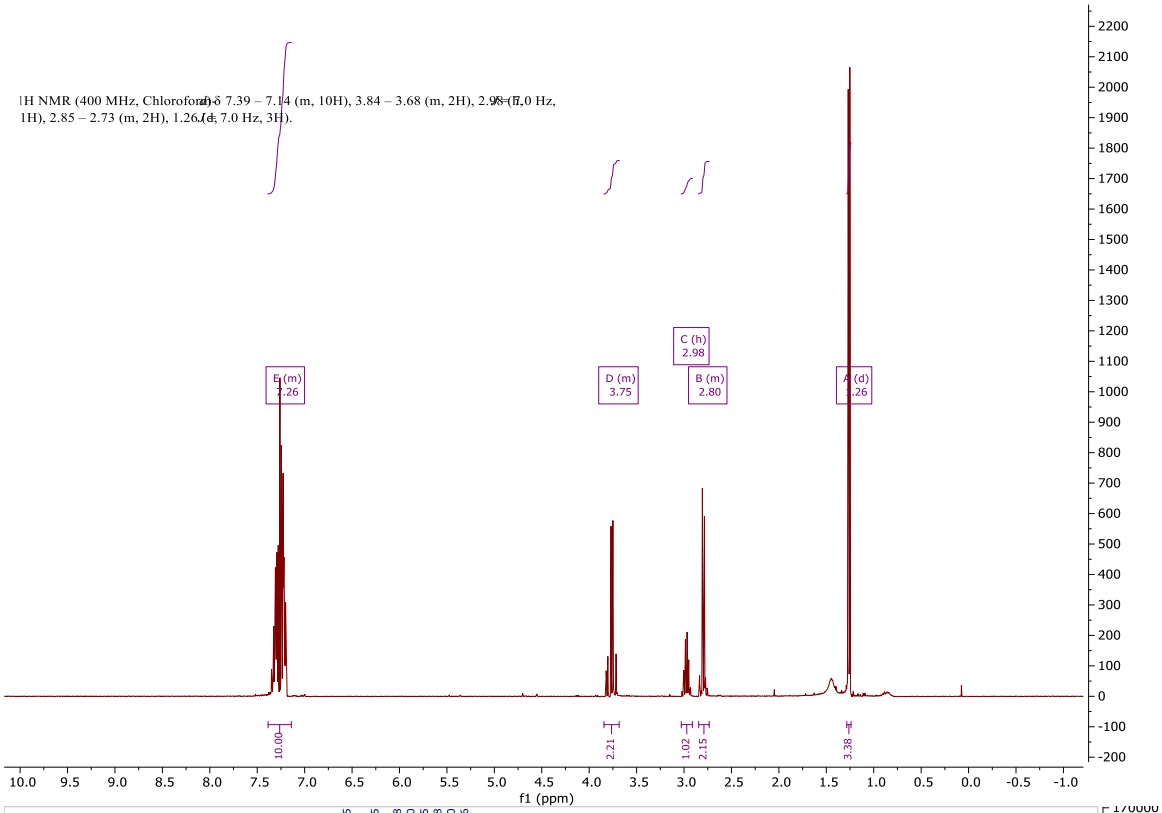

^{1}H NMR (400 MHz, Chloroform-*d*) δ 7.39 – 7.14 (m, 10H), 3.84 – 3.68 (m, 2H), 2.98 (h, *J* = 7.0 Hz, 1H), 2.85 – 2.73 (m, 2H), 1.26 (d, *J* = 7.0 Hz, 3H).

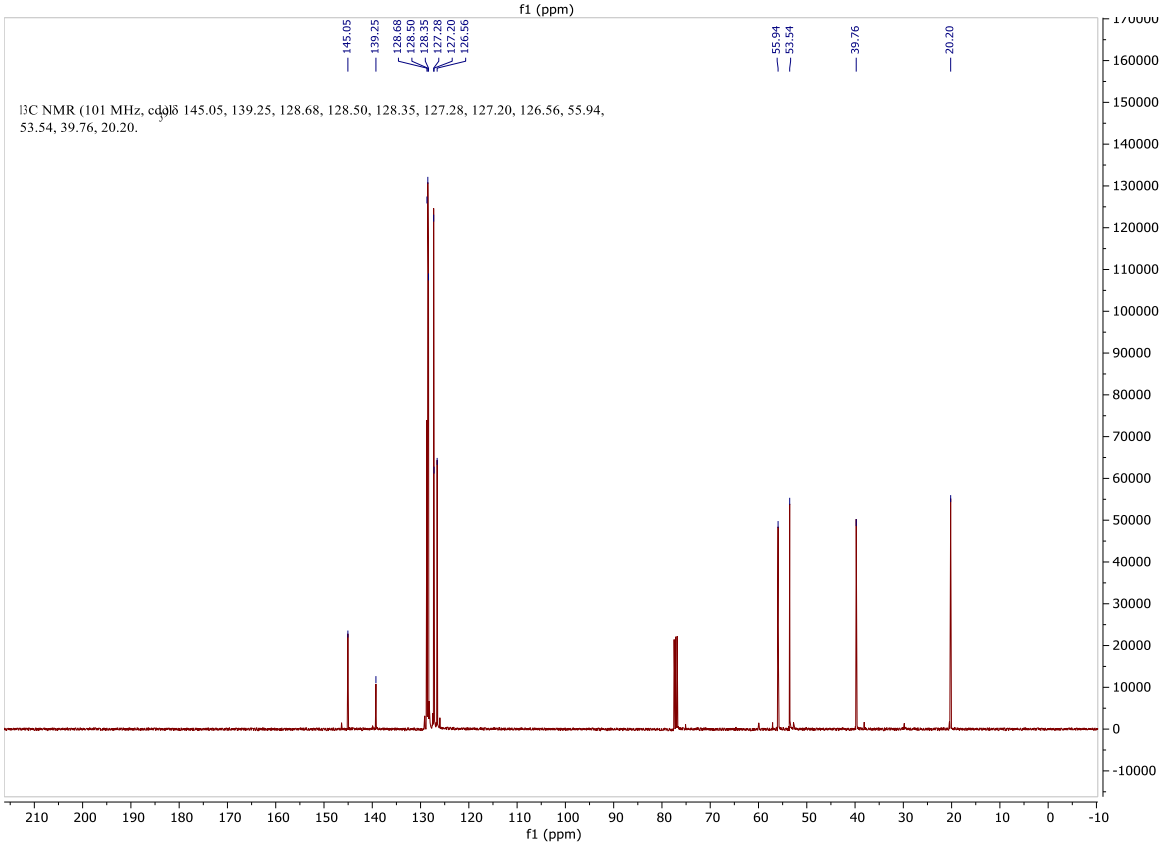

^{13}C NMR (101 MHz, cdcl$_3$) δ 145.05, 139.25, 128.68, 128.50, 128.35, 127.28, 127.20, 126.56, 55.94, 53.54, 39.76, 20.20.

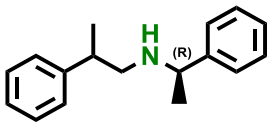

5-9a

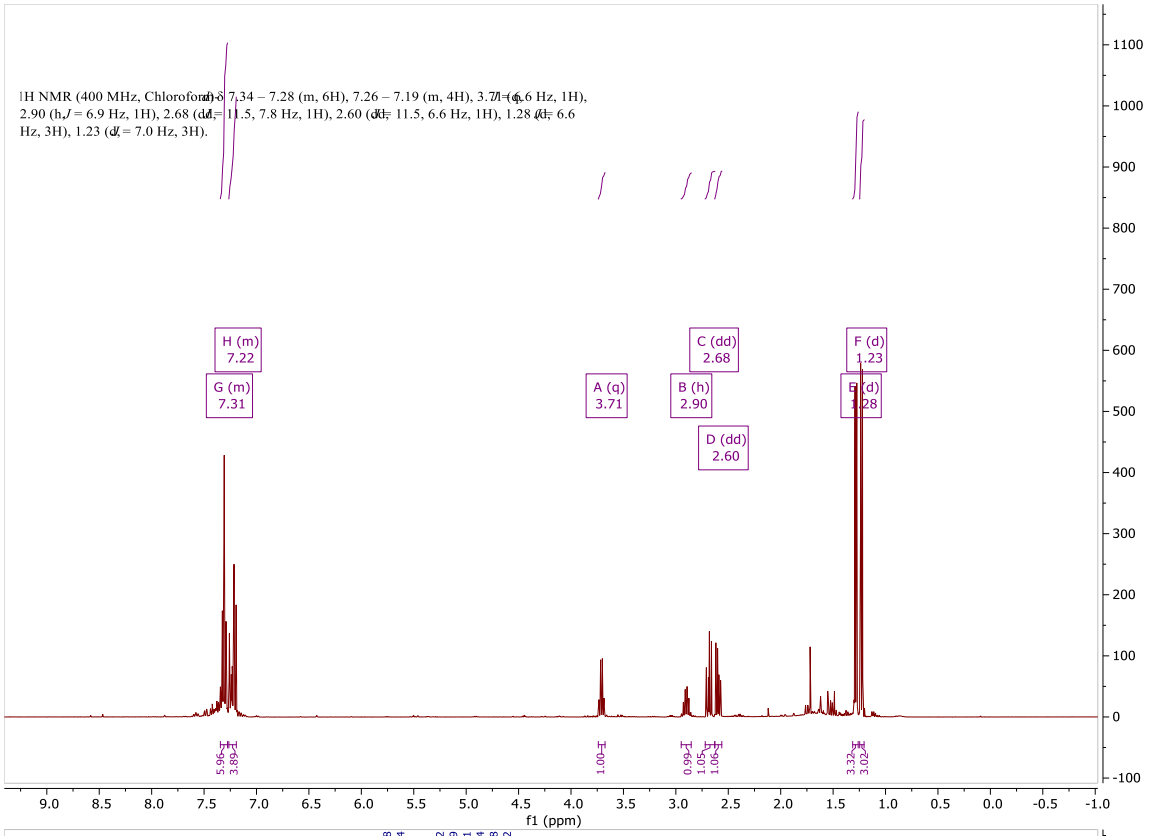
1H NMR (400 MHz, Chloroform-d) δ 7.34 – 7.28 (m, 6H), 7.26 – 7.19 (m, 4H), 3.71 (q, J = 6.6 Hz, 1H), 2.90 (h, J = 6.9 Hz, 1H), 2.68 (dd, J = 13.5, 7.8 Hz, 1H), 2.60 (dd, J = 13.5, 6.6 Hz, 1H), 1.28 (d, J = 6.6 Hz, 3H), 1.23 (d, J = 7.0 Hz, 3H).
H (m) 7.22
G (m) 7.31
A (q) 3.71
B (h) 2.90
C (dd) 2.68
D (dd) 2.60
F (d) 1.23
E (d) 1.28
5.96
3.89
1.00
0.99
1.05
1.06
3.32
3.02
f1 (ppm)

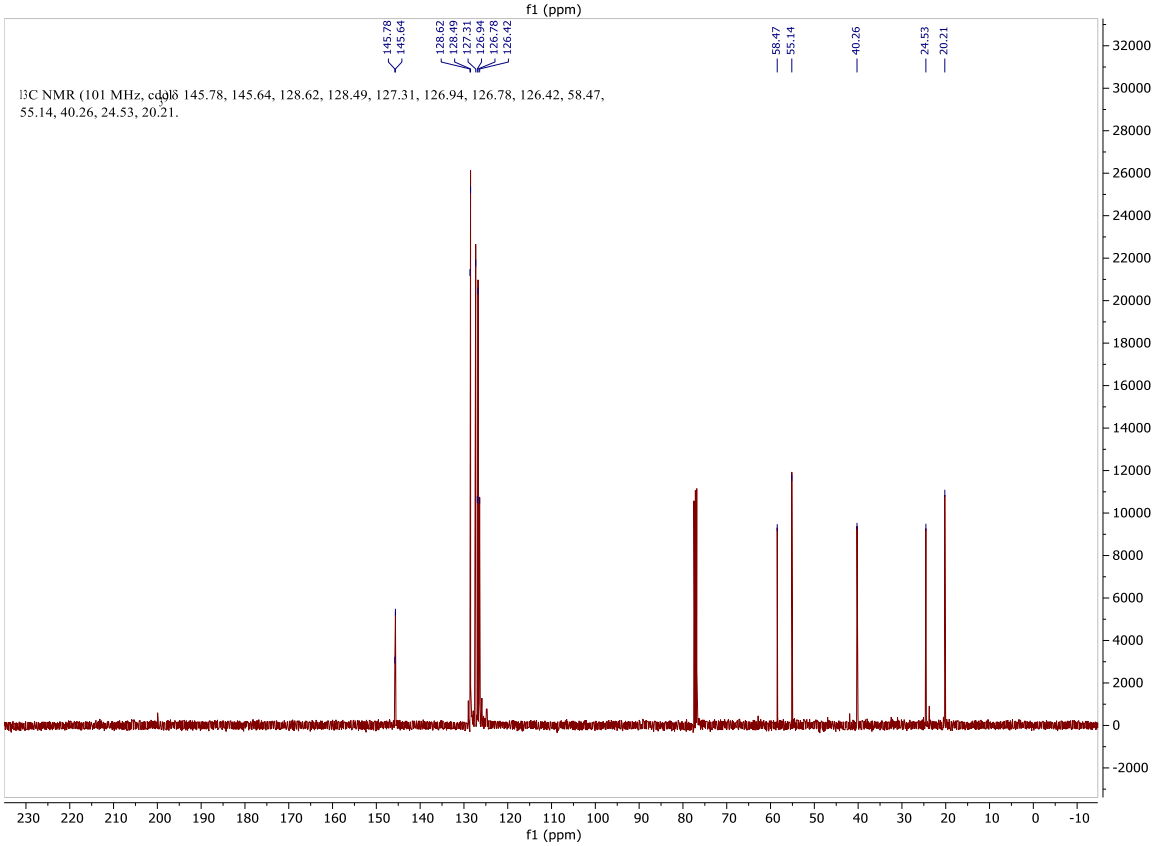
13C NMR (101 MHz, cdcl3) δ 145.78, 145.64, 128.62, 128.49, 127.31, 126.94, 126.78, 126.42, 58.47, 55.14, 40.26, 24.53, 20.21.
145.78
145.64
128.62
128.49
127.31
126.94
126.78
126.42
58.47
55.14
40.26
24.53
20.21
f1 (ppm)

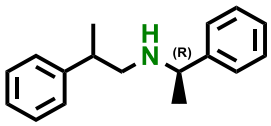
H
N
(R)

5-9a'

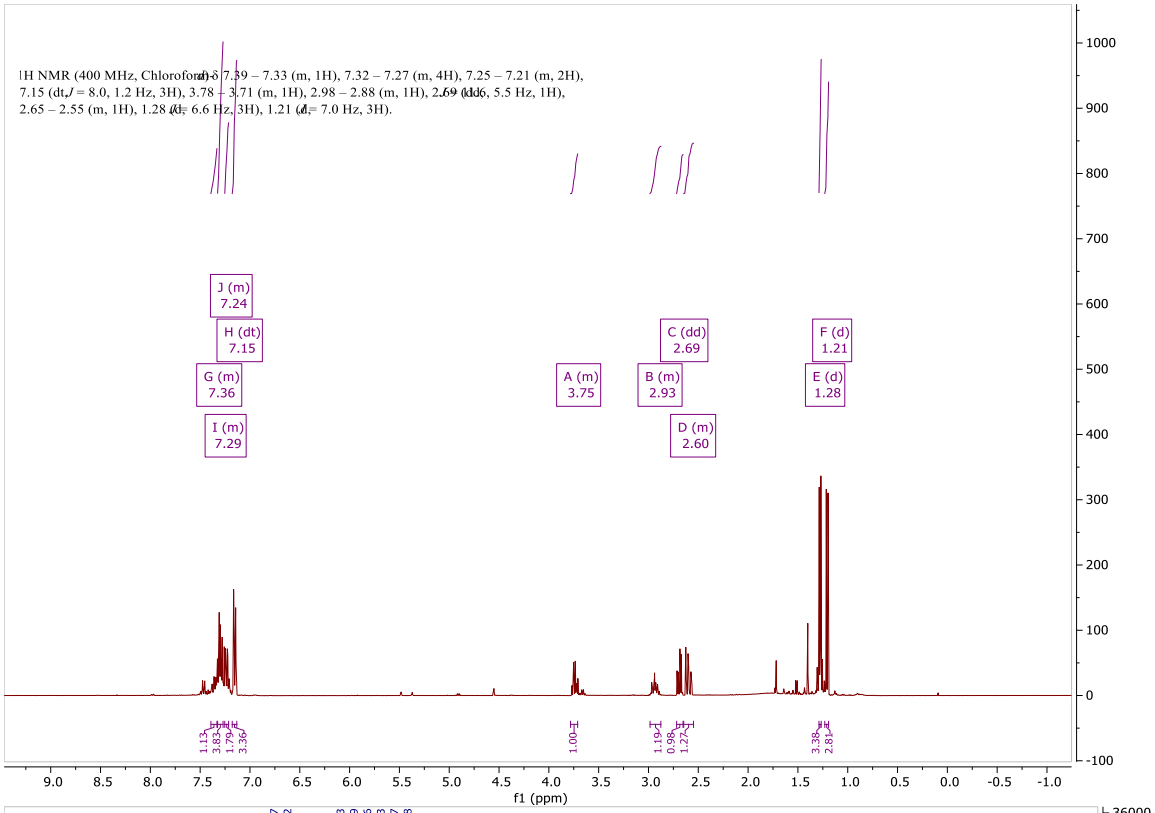
J (m) 7.24
H (dt) 7.15
G (m) 7.36
I (m) 7.29
A (m) 3.75
C (dd) 2.69
B (m) 2.93
D (m) 2.60
F (d) 1.21
E (d) 1.28
1.13
3.83
1.79
3.36
1.00
1.19
0.98
1.27
3.38
2.81
f1 (ppm)

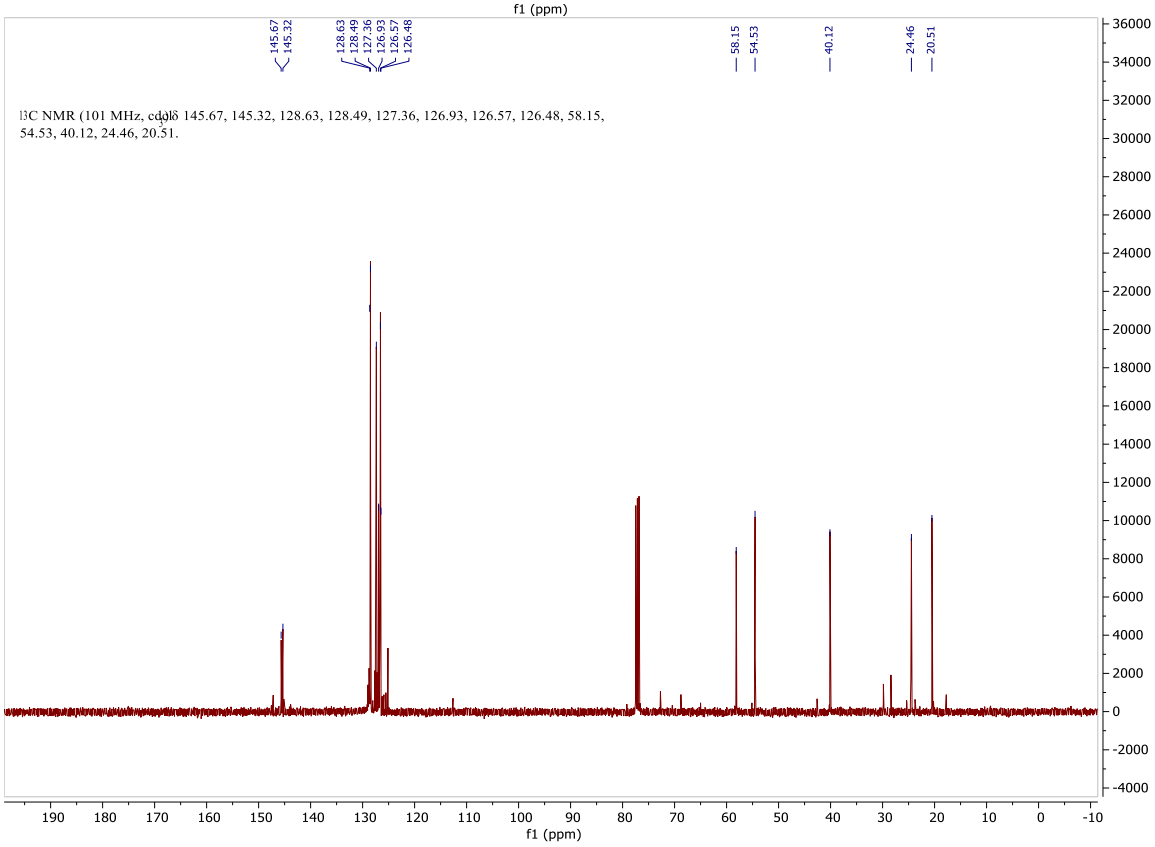
145.67
145.32
128.63
128.49
127.36
126.93
126.57
126.48
58.15
54.53
40.12
24.46
20.51
f1 (ppm)

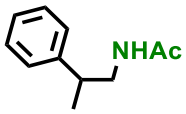

5-10

^{1}H NMR (400 MHz, Chloroform-d) δ 7.29 – 7.21 (m, 2H), 7.21 – 7.16 (m, 1H), 7.14 – 7.10 (m, 2H), 5.30 (s, 1H), 3.56 (ddd, J = 13.2, 7.1, 5.9 Hz, 1H), 3.14 (ddd, J = 13.5, 8.8, 4.8 Hz, 1H), 2.91 – 2.80 (m, 1H), 1.81 (s, 3H), 1.20 (d, J = 7.0 Hz, 4H).

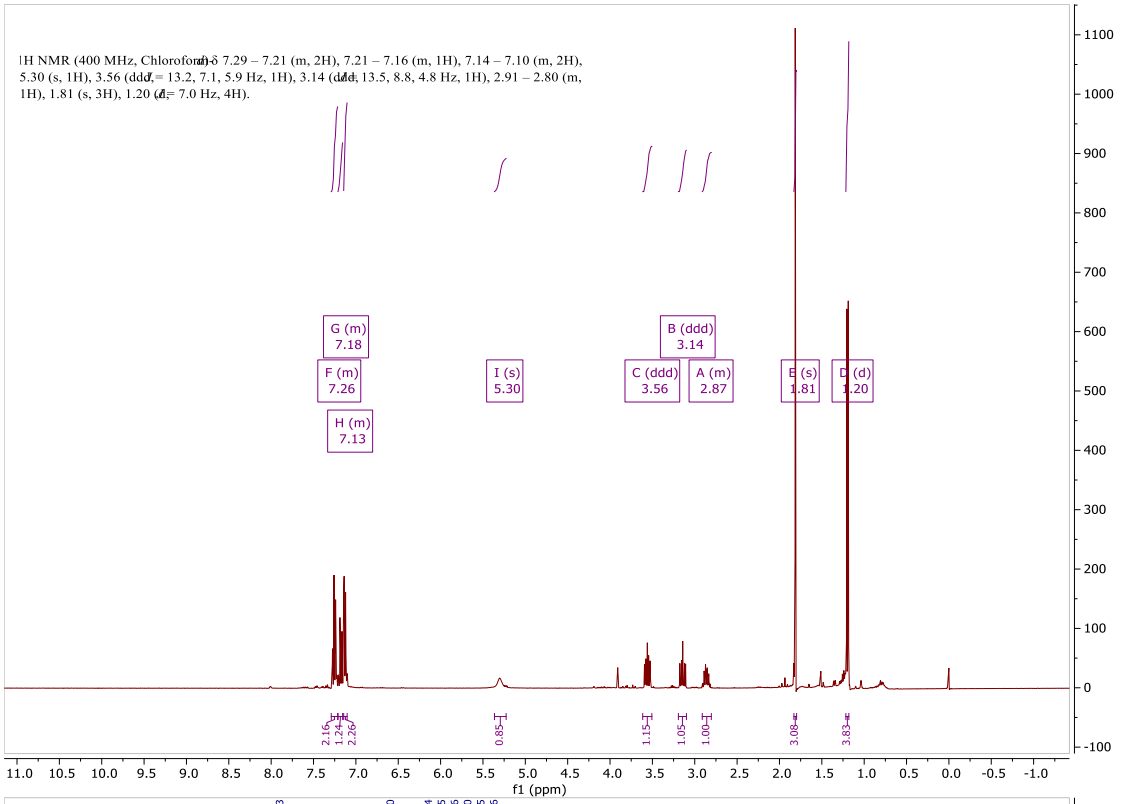

^{13}C NMR (101 MHz, $CDCl_3$) δ 170.13, 144.20, 129.04, 128.85, 128.56, 127.30, 126.85, 126.16, 46.25, 39.83, 23.41, 19.58.

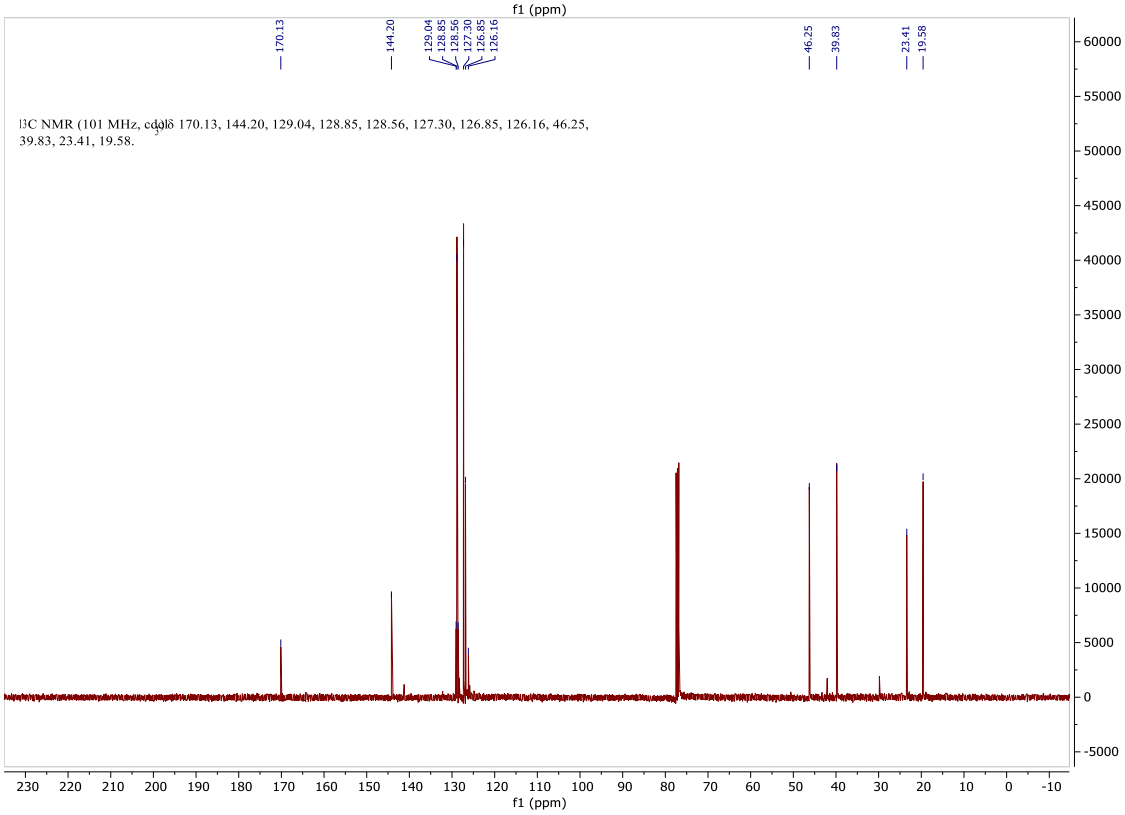

Chapter 6

Iridium-Catalyzed Isomerization of *N*-Sulfonyl Aziridines to Allyl Amines

Isomerization processes such as thermal rearrangements and catalytic isomerizations are of great synthetic interest due to their perfect atom economy, which makes them ideal transformations from the point of view of sustainability.[1] Terminal olefins,[2] allylic amines[3] and allylic alcohols[4] are the most common substrates for catalytic isomerization reactions using metal complexes.[5] Epoxides are also excellent substrates for isomerization. The rearrangement of epoxides to carbonyls, referred to as the Meinwald rearrangement,[6] can be promoted by Lewis acids such as $BF_3{\cdot}Et_2O$, lithium salts or iridium chloride.[7] More recently, Mazet and co-workers uncovered the use of Pd and Ir hydride complexes as efficient catalysts for the isomerization of epoxides.[8,9] The aza-version of the Meinwald rearrangement, however, has received little attention.[10] In 2002, Nakayama et al. described the BF_3-promoted aza-pinacol rearrangement of various *N*-tosyl aziridines to give the corresponding *N*-tosyl imines.[11] Later on, in 2003, Ney and co-workers reported a palladium-catalyzed isomerization of monosubstituted *N*-tosyl aziridines to sulfonyl ketimines.[12]

The ring strain, the facility of preparation, and the utility of the potential products make aziridines the ideal substrates to study new catalytic isomerization reactions. In the previous Chapter 6, the selective isomerization of epoxides to carbonyl compounds was achieved using Crabtree's catalyst with H_2 activation. Encouraged by these promising results, we were prompted to expand the chemical space of this useful transformation using the same iridium catalyst (Scheme 6.1). Herein, we describe the isomerization of 2,2-disubstituted *N*-sulfonyl aziridines to allylic amines catalyzed by the Crabtree's catalyst. The process provides an efficient synthetic strategy for the preparation of many valuable compounds since allyl amines are versatile intermediates[13] in addition to being fragments of several biologically active compounds.[14,15]

Scheme 6.1. Reaction scheme for the selective isomerization of epoxides and *N*-sulfonyl aziridines.

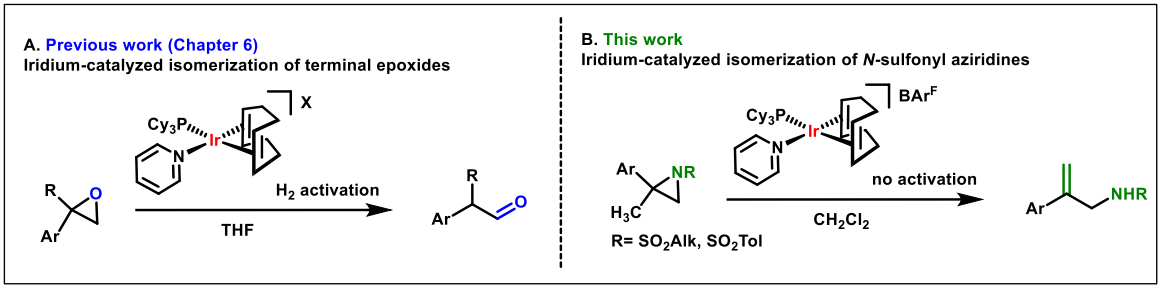

We selected 2-methyl-2-phenyl-1-tosylaziridine **6-1a**, as model substrate since it can be easily prepared from acetophenone by simple Wittig olefination and subsequent aziridination. Aziridine **6-1a** can, in principle, isomerize to allyl amine **6-2a**, to imine **6-3a**, in a similar way to the Meinwald rearrangement of epoxides, or to enamine **6-4a** (Table 6.1).

We started with the common catalysts used in the Meinwald rearrangement, namely $BF_3{\cdot}Et_2O$ and $IrCl_3$. In both cases, a 1:1 mixture of allyl amine (**6-2a**) and imine (**6-3a**) was obtained in moderate yield (Table 6.1, entries 1, 2). Of note, enamine **6-4a** was not detected. In our efforts to promote the reaction selectively, our next attempt involved the use of Crabtree's catalyst **6-5a** (PF_6 salt).[16] This commercial Ir-P,N complex is a well-known hydrogenation catalyst.[17] The CH_2Cl_2 solution of the catalyst was activated by hydrogenation for few minutes and degassed as described for allylic alcohols.[4f,g] Allylic amine was obtained in good selectivity with respect to the imine (6:1) after 3 h of reaction, using only 1 mol % of **6-5a** (Table 6.1, entry 3). The reaction was performed in a glove-box to avoid the formation of substantial amounts of *N*-tosyl-1-amino-2-phenylpropan-2-ol caused by aziridine ring-opening by moisture. We further improved the yield and selectivity using Pfaltz's version of Crabtree's catalyst (**6-5b,** BAr^F salt)[18] (Table 6.1, entry 4) and toluene as a solvent (Table 6.1, entry 5).

Table 6.1. Optimization of the isomerization of **6-1a.** The reactions were performed in a sealed vial, using 0.34 mmol of **6-1a** in CH_2Cl_2 [0.25 M], at room temperature.

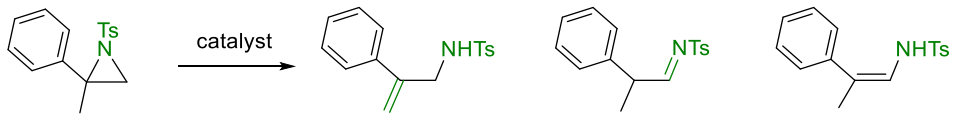

6-1a **6-2a** **6-3a** **6-4a**

entry	conditions	Yield (%)[b]	isomer ratio **6-2a/6-3a/6-4a**[a]
1	$BF_3{\cdot}Et_2O$ (10 mol %), 10 min	43	1:1:0
2	$IrCl_3{\cdot}xH_2O$ (5 mol %), 3 h	40	1:1:0
3[c]	**6-5a** (1 mol %),[e] 3 h, H_2 activation	71	6:1:0
4[c]	**6-5b** (1 mol %),[f] 3 h, H_2 activation	76	10:1:0
5[c,d]	**6-5b** (1 mol %), [f] 3 h, H_2 activation	81	95:5:0
6	**6-5b** (1 mol %),[f] 3 h, no activation	85	99:1:0

[a] Measured by ^1H NMR. [b] Isolated yield of **6-2a**. [c] The reaction was carried out in a pressure tube and prepared in a glove-box, charged with 1 bar of H_2 and then degassed (x3) with N_2. [d] Toluene was used as solvent. [e] $[Ir(cod)(PCy_3)(Py)]PF_6$ (**6-5a**). [f] $[Ir(cod)(PCy3)(Py)]$ BAr^F (**6-5b**).

Unexpectedly, during the optimization, control experiments revealed that the isomerization proceeded even without H_2-activation of the catalyst. Stirring the CH_2Cl_2 solution of aziridine **6-1a** with catalyst **6-5b** at room temperature allowed the isomerization to allyl amine **6-2a** with complete regioselectivity and excellent yield (Table 6.1, entry 6). Moreover, the use of the glove-box was no longer necessary. To the best of our knowledge, this is the first example in which Crabtree's catalyst has been used without activation either by hydrogen or temperature. These conditions are much simpler in terms of practicality and scalability than the ones that involve activation of the catalyst.

Table 6.2. Scope of the iridium-catalyzed isomerization of *N*-sulfonyl aziridines.[a]

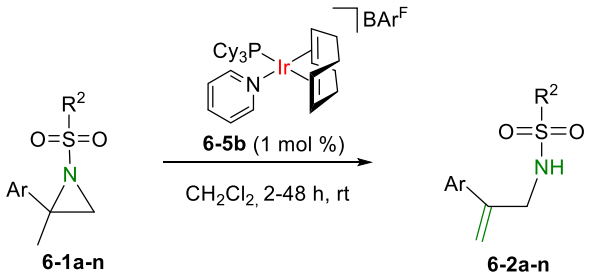

entry		Ar	R^2	conv. (**6-2/6-3**)[b]	Yield (%)[c]
1	**6-1a**	Ph	*p*-Tol	>99 (99:1)	87[f]
2[d]	**6-1b**	*p*-Cl-Ph	*p*-Tol	>99 (91:9)	82
3[e]	**6-1c**	*m*-Cl-Ph	*p*-Tol	>99 (98:2)	80
4[e]	**6-1d**	*o*-Cl-Ph	*p*-Tol	>99 (87:13)	68
5	**6-1e**	*p*-MePh	*p*-Tol	>99 (92:8)	76
6	**6-1f**	2-naphthyl	*p*-Tol	>99 (98:2)	79
7	**6-1g**	*o*-MeO-Ph	*p*-Tol	>99 (81:19)	72
8	**6-1h**	*p*-F-Ph	*p*-Tol	>99 (93:7)	79
9	**6-1i**	*m*-F-Ph	*p*-Tol	>99 (97:3)	82
10[e]	**6-1j**	*p*-CF_3-Ph	*p*-Tol	>99 (93:7)	67
11[e]	**6-1k**	*p*-NO_2-Ph	*p*-Tol	>99 (90:10)	69
12[e]	**6-1l**	*p*-I-Ph	^{i}Pr	>99 (96:4)	82
13[d]	**6-1m**	*p*-Br-Ph	^{i}Pr	>99 (98:2)	78
14[d]	**6-1n**	Ph	Me	>99 (99:1)	96

[a] The reaction was performed in a sealed vial, using 0.33 mmol of substrate. [b] Determined by ^{1}H NMR. [c] Isolated yield after column chromatography. [d] 3 mol % of **6-5b** was used. [e] The reaction was carried out using 3 mol % of **6-5b** and heating up to 40 ºC. [f] 1 gram of **6-1a** and 0.5 mol % of **6-5b** were used.

To test the scope of the reaction a collection of 2-aryl-2-methyl *N*-sulfonyl aziridines were treated with catalyst **6-5b** under the optimal conditions. Without activation of the catalyst, aziridines **6-(1a-n)** transposed selectively to the allyl amines **6-(2a-n)** in good yields (Table 6.2). Electron-donating (EDG) and electron-withdrawing (EWG) groups in the aryl ring were well tolerated, although the reactivity of aziridines with the EWGs was clearly lower. Harsher reaction conditions (3 mol % catalyst loading) were required in some cases (Table 6.2, entries 2, 4, 13 and 14). For stronger EWG (Table 6.2, entries 3, and 10-12), in addition, the temperature was increased to 40 ºC. The reaction took place in a similar manner when the p-toluenesulfonyl group was replaced by propanesulfonyl or methanesulfonyl (Table 6.2, entries 12, 13 and 14, respectively).

To further expand the scope of this transformation the methyl substituent in the aziridine was also modified. When the methyl was replaced by ethyl the reaction took place affording a mixture of *E*- and *Z*-allyl amines **6-2o** (Scheme 6.2A)**.** When the methyl was replaced by phenyl, the γ-elimination could not be achieved so the corresponding enamine (**6-2p**) was obtained instead (Scheme 6.2B).

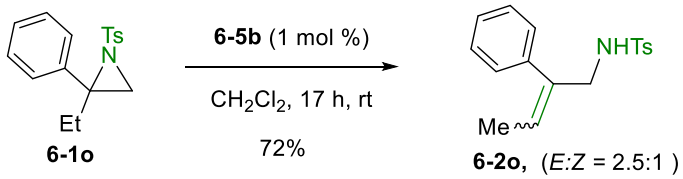

Scheme 6.2A. Isomerization of *N*-tosyl 2-ethyl-2-phenyl aziridine (**6-1o**)

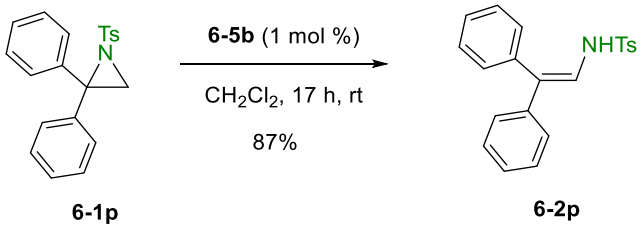

Scheme 6.2B. Isomerization of 2,2-diphenyl-1-tosylaziridine (**6-1p**).

The synthetic applications of these allylic amines are numerous. Simple replacement of the tosyl group by a methyl in **6-2a** and **6-2o** afforded compounds that have been reported to be precursors of several potent herbicides.[14] Some propargyl derivatives of **6-2a** showed activity against monoamine oxidases, which are involved in Parkinson's disease (PD).[15]

Moreover, the rich chemistry of the allyl amines can be applied to the synthesis of azepanes, 3-pyrrolidin-2-ones and 2,5-dihydropirroles among others.[13]

The novelty of the transformation led us to perform a mechanistic study. First, given that the catalyst was used without activation by hydrogen, we sought to determine the real catalytic species involved. Of the three ligands of Crabtree's catalyst we hypothesized that pyridine would be the most labile. To test this notion, we added deuterated pyridine to a solution of **6-5b** in CD_2Cl_2. The signals of the free pyridine were easily detected by ^1H NMR (Fig. 6.1). Moreover, we checked by ^1H NMR spectroscopy that if pyridine is used as additive, the reaction does not take place, leading to catalyst deactivation (Fig. 6.2).

Fig. 6.1. Key experiment for checking ligand lability using ^1H NMR.

(a) ^1H NMR spectrum of **6-4b** and mesitylene as internal standard. The signals of each ligand (pyridine, cyclooctadiene and tricyclohexylphosphine) were assigned.

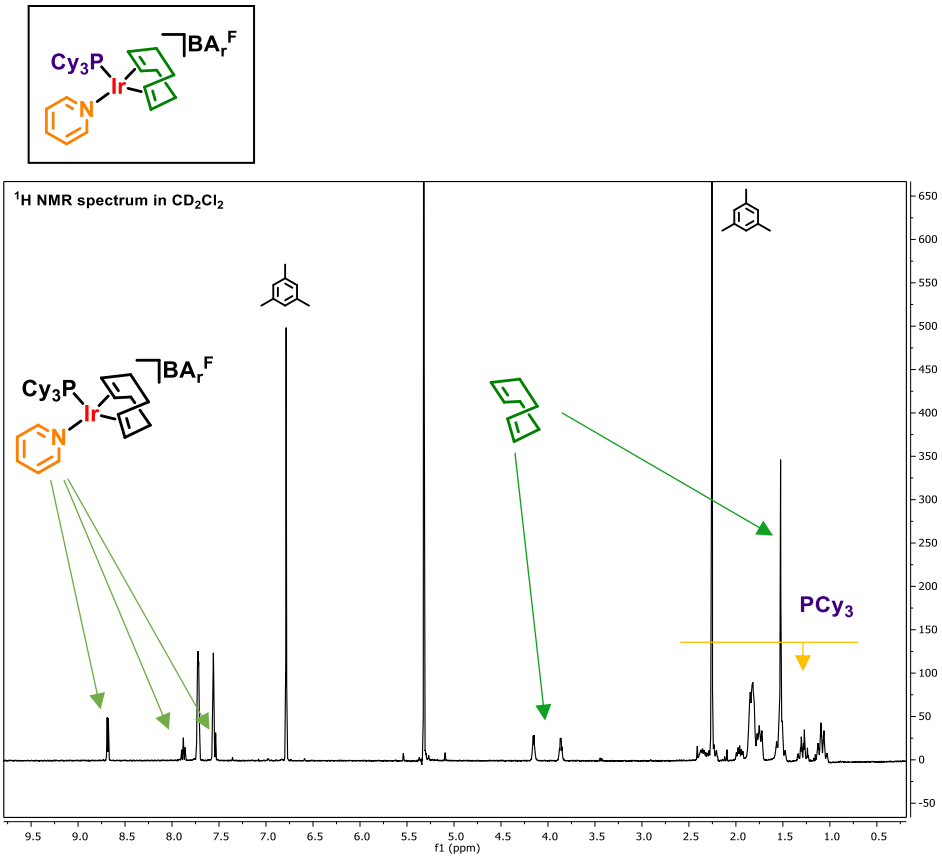

(b) To the same NMR tube, 5 equiv. of deuterated pyridine were added. After few minutes, the signals of the free pyridine were clearly observed proving a fast exchange between pyridines. A 95% of decoordination was measured by ^{1}H NMR using mesitylene as internal standard. Both cyclooctadiene and tricyclohexylphosphine remained coordinated, proving that pyridine is the most labile ligand.

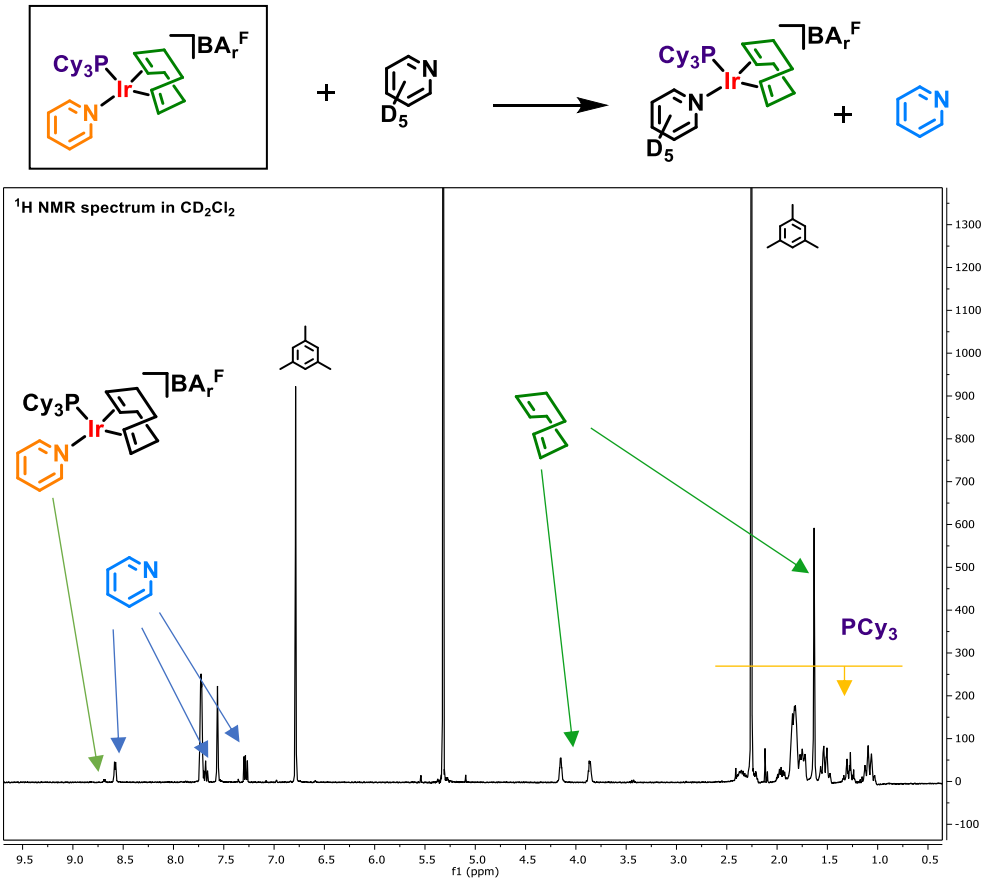

Fig. 6.2. Key experiment for checking catalyst deactivation using ^{1}H NMR.

(a) 10 mg of Crabtree's catalyst **6-4b** in 0.75 mL of CD_2Cl_2.

(b) 5 equiv. of pyridine were added to the (a) NMR tube.

(c) 38 mg (1.0 equiv.) of aziridine **6-1a** in CD_2Cl_2.

(d) To the solution of **6-1a** (c) was added the solution (b) –which represents 5 mol % of catalyst loading. After 3 hours of reaction, the reaction had not taken place, whilst with the absence of pyridine, the conversion was complete.

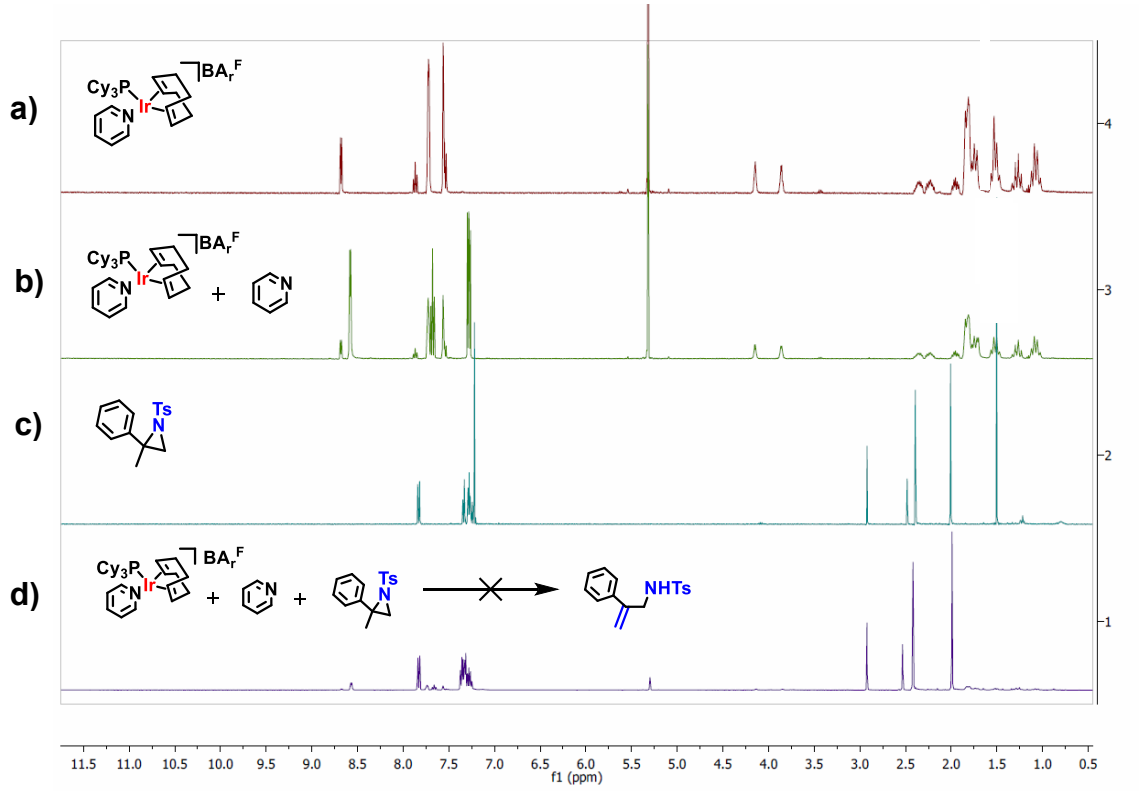

DFT calculations also confirmed that pyridine was the most labile ligand. In this regard, the calculated ΔG of dissociation in dichloromethane for the three ligands was 7.3 kcal mol^{-1} (py), 21.2 kcal mol^{-1} (PCy_3) and 34.5 kcal mol^{-1} (cod) (B3LYP-D3 calculations, see Computational details in the Experimental Part). In a second experiment, pyridine was added to a solution of **6-1a** and 5 mol % of **6-5b** in CD_2Cl_2 In this case, the reaction did not occur thereby indicating that the catalyst was fully inactivated by the excess of pyridine. Therefore, $[Ir(PCy_3)(cod)]^+$, which is generated with a low energy cost, was identified as the catalytically active species.

The DFT study of the reaction mechanism indicated that it starts by approaching aziridine **6-1a** to this unsaturated species, leading to intermediate **I** (Scheme 6.3). Several orientations were checked for this initial approach. In this initial species aziridine was not coordinated to the iridium center (Ir···N = 3.24 Å), thereby revealing the low donating capacity of the *N*-aziridine lone pair. Starting from intermediate **I,** aziridine ring opening followed by metal-assisted tautomerization was expected to yield the product.

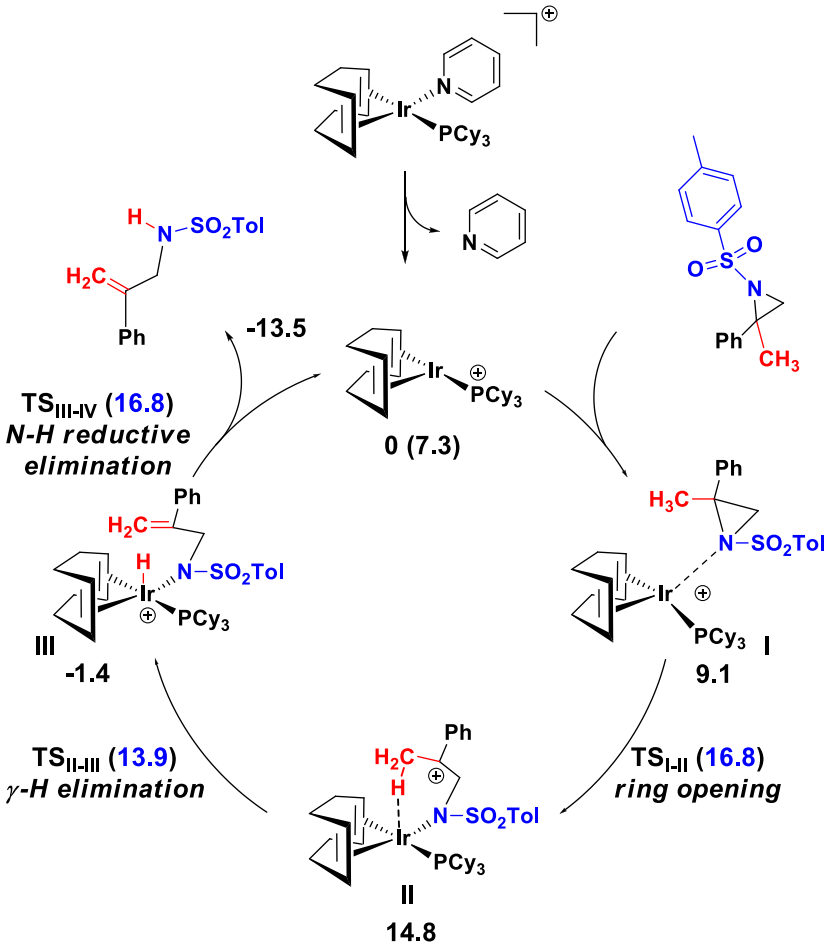

Scheme 6.3. DFT computed mechanism (B3LYP-D3 in CH_2Cl_2) for the isomerization of aziridine **6-1a** to allyl amine **6-2a**; the numbers are relative Gibbs energies in kcal mol^{-1}, taking as zero-energy the separated catalytically active species $[Ir(PCy_3)(cod)]^+$ and aziridine substrate **6-1a**. The ΔG of dissociation of pyridine is 7.3 kcal mol^{-1}. Relative energies of transition states are indicated in blue.

Ring–opening occurred from **I** with a low barrier of 9.5 kcal mol^{-1} (**TS_{I-II},** 16.8 kcal mol^{-1}, Scheme 6.3) and gave rise to the carbocation intermediate **II**. In addition to the breaking of the N-C bond of the ring, this step also involved coordination of the nitrogen to the Ir. We used a localized orbital approach to analyze the electronic rearrangements in the ring-opening step (see computational details).[19] This analysis showed the movement of the N-C

bonding pair toward the nitrogen, concomitant with the formation of a Ir-N bond from the N lone pair, with a positive charge remaining in C_α. It also showed that the phenyl substituent at C_β stabilizes the carbocation thus playing a key role in the ring-opening step, Accordingly, in **II** the C_β-C_{Ph} bond had a partial character of double bond (C_β- C_{Ph} = 1.43 Å Wiberg bond order = 1.24). Indeed, for the 2,3-Me,Ph disubstituted aziridine intermediate **II** was found at 23.4 kcal mol^{-1}, largely above the 14.8 kcal mol^{-1} of the 2,2-disubstituted substrate.

We have computed the pathways leading to the formation of secondary products for substrate **6-1a** (imine **6-3a** and enamine **6-4a**). The α-H elimination entails an extra rotational barrier of 4.4 kcal mol^{-1}, sufficient to govern the selectivity toward allyl amine formation.

The metal-mediated tautomerization that occurred after ring-opening could yield three different products (Table 6.1), depending on the hydrogen that migrates. Migration from a C_γ-H (those in the Me substituent) to the nitrogen gave the allyl amine, while migration of C_α-H led to the imine or the enamine. In **II,** a C_γ-H bond, placed above the Ir, was involved in an agostic interaction with the metal (Ir···H-C_γ = 2.18 Å). This agostic C_γ-H bond was already activated (1.15 Å) for the γ-H elimination, which was practically barrierless (**TS_{II-III},** 13.9 kcal mol^{-1}, Figure 6.3).[20] The readiness of the C_γ-H bond in **II** to participate in the H elimination step accounts for the selectivity toward the allyl amine product.

The γ-H elimination step led to a notably stable amido hydride intermediate **III** (-1.4 kcal mol^{-1}, Scheme 6.3). In the final step of the isomerization N-H reductive elimination from **III** (**TS_{III-IV},** 16.8 kcal mol^{-1}, Figure 6.3) formed the N-H bond and released the allyl amine product **6-3a**. The reductive elimination of the N-H bond entailed the highest barrier along the catalytic cycle (18.2 kcal mol^{-1}). Computational studies of homogenous reductive elimination of N-H bonds are much more scarce that those of C-H bonds.[21] Our transition state for this step has an interesting feature in that it can be described as an ion-pair, in which the aziridine nitrogen is completely dissociated (Ir···N = 3.12 Å, NPA charge of the N-fragment = -0.67) and ready to pick-up a proton from the cationic iridium moiety. Finally, the replacement of the allyl amine product by a reactant molecule closed the catalytic cycle.

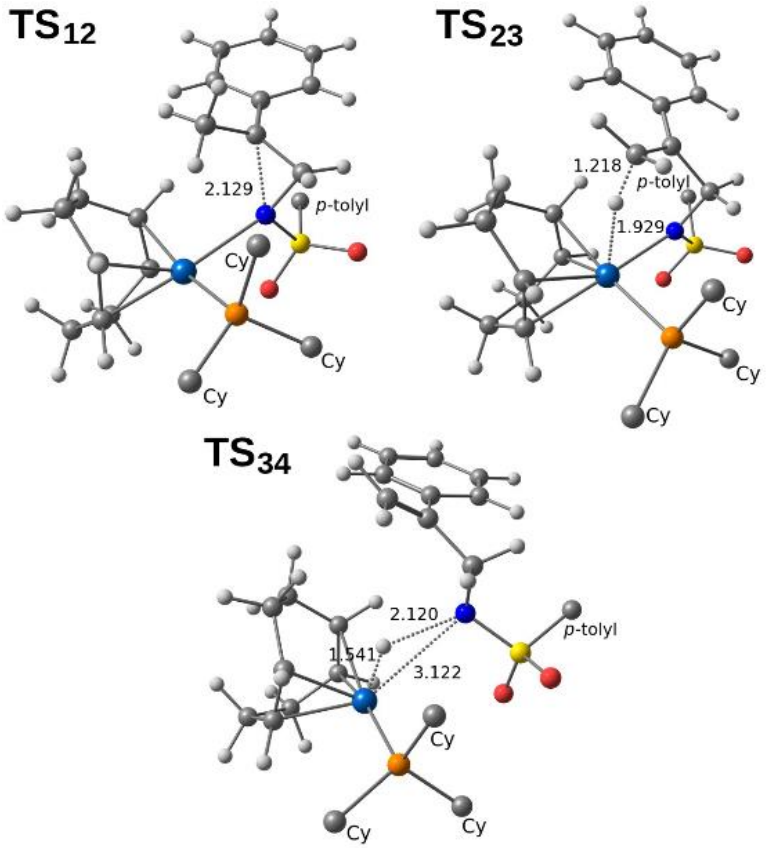

Figure 6.3. Optimized geometries for: ring opening, $\mathbf{TS_{I\text{-}II}}$, γ-H elimination, $\mathbf{TS_{II\text{-}III}}$ and N-H reductive elimination, $\mathbf{TS_{III\text{-}IV}}$. The most important distances are also reported in Å. Hydrogen atoms have been omitted for clarity.

In summary, here, we have described the selective isomerization of *N*-sulfonyl 2,2-disubstituted aziridines to *N*-sulfonyl allyl amines using the readily available Crabtree's catalyst. Of note, activation with hydrogen was not required and the reaction was performed in mild conditions and with low catalyst loading (usually 1 mol %). The catalytic species as well as a detailed reaction mechanism were studied by DFT-calculations. This novel transformation provides a new strategy for the synthesis of complex amines.

References

(1) (a) Trost, B. M. Atom Economy—A Challenge for Organic Synthesis: Homogeneous Catalysis Leads the Way. *Angew. Chem., Int. Ed.* **1995**, *34*, 259–281. (b) Wender, P. A.; Verma, V. A.; Paxton, T. J.; Pillow, T. H. Function-Oriented Synthesis, Step Economy, and Drug Design. *Acc. Chem. Res.* **2008**, *41*, 40–49.

(2) (a) S. Akutagawa, Isomerization of Carbon-Carbon Double Bonds. In *Comprehensive Asymmetric Catalysis*, *Vol. 2* (Eds.: E. Jacobsen, A. Pfaltz, H. Yamamoto), Springer: Berlin, 1999. (b) Romano, C.; Mazet, C. Multicatalytic Stereoselective Synthesis of Highly Substituted Alkenes by Sequential Isomerization/Cross-Coupling Reactions. *J. Am. Chem. Soc.* **2018**, *140*, 4743–4750.

(3) (a) Akutagawa, S. Enantioselective Isomerization of Allylamine to Enamine: Practical Asymmetric Synthesis of (-)-Menthol by Rh-BINAP Catalysts. *Top. Catal.* **1998**, *4*, 271–274. (b) Inoue, S. ichi; Sato, T.; Noyori, R.; Inoue, S.-ichi; Takaya, H.; Tani, K.; Otsuka, S. Mechanism of the Asymmetric Isomerization of Allylamines to Enamines Catalyzed by 2,2'-Bis(diphenylphosphino)-1,1'-binaphthyl-Rhodium Complexes. *J. Am. Chem. Soc.* **1990**, *112*, 4897–4905. (c) Cabré, A.; Khaizourane, H.; Garçon, M.; Verdaguer, X.; Riera, A.: Total Synthesis of (*R*)-Sarkomycin Methyl Ester via Regioselective Intermolecular Pauson–Khand Reaction and Iridium-Catalyzed Asymmetric Isomerization. *Org. Lett.* **2018**, *20*, 3953-3957.

(4) (a) Van Der Drift, R. C.; Bouwman, E.; Drent, E. Homogeneously Catalysed Isomerisation of Allylic Alcohols to Carbonyl Compounds. *J. Organomet. Chem.* **2002**, *650*, 1–24. (b) Mantilli, L.; Mazet, C. Platinum Metals in the Catalytic Asymmetric Isomerization of Allylic Alcohols. *Chem. Lett.* **2011**, *40*, 341–344. (c) Lorenzo-Luis, P.; Romerosa, A.; Serrano-Ruiz, M. Catalytic Isomerization of Allylic Alcohols in Water. *ACS Catal.* **2012**, *2*, 1079–1086. (d) Ahlsten, N.; Bartoszewicz, A.; Martín-Matute, B. Allylic Alcohols as Synthetic Enolate Equivalents: Isomerisation and Tandem Reactions Catalysed by Transition Metal Complexes. *Dalton Trans.* **2012**, *41*, 1660. (e) Cahard, D.; Gaillard, S.; Renaud, J. L. Asymmetric Isomerization of Allylic Alcohols. *Tetrahedron Lett.* **2015**, *56*, 6159–6169. (f) Li, H.; Mazet, C. Iridium-Catalyzed Selective Isomerization of Primary Allylic Alcohols. *Acc. Chem. Res.* **2016**, *49*, 1232–1241. (g) Li, J. Q.; Peters, B.; Andersson, P. G. Highly Enantioselective Asymmetric Isomerization of Primary Allylic Alcohols with an Iridium-N,P Complex. *Chem. Eur. J.* **2011**, *17*, 11143–11145.

(5) Larionov, E.; Li, H.; Mazet, C. Well-Defined Transition Metal Hydrides in Catalytic Isomerizations. *Chem. Commun.* **2014**, *50*, 9816–9826.

(6) Meinwald, J.; Labana, S. S.; Chadha, M. S. Peracid Reactions. III. The Oxidation of Bicyclo [2.2.1]Heptadiene. *J. Am. Chem. Soc.* **1963**, *85*, 582–585.

(7) Karamé, I.; Tommasino, M. L.; Lemaire, M. Iridium-Catalyzed Alternative of the Meinwald Rearrangement. *Tetrahedron Lett.* **2003**, *44*, 7687–7689.

(8) Vyas, D. J.; Larionov, E.; Besnard, C.; Guénée, L.; Mazet, C. Isomerization of Terminal Epoxides by a [Pd-H] Catalyst: A Combined Experimental and Theoretical Mechanistic Study. *J. Am. Chem. Soc.* **2013**, *135*, 6177–6183

(9) Humbert, N.; Vyas, D. J.; Besnard, C.; Mazet, C. An Air-Stable Cationic Iridium Hydride as a Highly Active and General Catalyst for the Isomerization of Terminal Epoxides. *Chem. Commun.* **2014**, *50*, 1–4.

(10) Zhang, Z. Da; Scheffold, R. Asymmetric Catalysis by Vitamin B12: The Isomerization of Achiral Aziridines to Optically Active Allylic Amines. *Helv. Chim. Acta* **1993**, *76*, 2602–2615.

(11) Sugihara, Y.; Iimura, S.; Nakayama, J. Aza-Pinacol Rearrangement : Acid-Catalyzed Rearrangement of Aziridines to Imines. *Chem. Commun.* **2002**, 134–135.

(12) Wolfe, J. P.; Ney, J. E. A New, Mild Synthesis of N-Sulfonyl Ketimines via the Palladium-Catalyzed Isomerization of Aziridines. *Org. Lett.* **2003**, *5*, 4607–4610.

(13) (a) Kiyokawa, K.; Kojima, T.; Hishikawa, Y.; Minakata, S. Iodine-Catalyzed Decarboxylative Amidation of B,γ-Unsaturated Carboxylic Acids with Chloramine Salts Leading to Allylic Amides. *Chem. Eur. J.* **2015**, *21*, 15548–15552. (b)Verendel, J. J.; Zhou, T.; Li, J. Q.; Paptchikhine, A.; Lebedev, O.; Andersson, P. G. Highly Flexible Synthesis of Chiral Azacycles via Iridium-Catalyzed Hydrogenation. *J. Am. Chem. Soc.* **2010**, *132*, 8880–8881. (c) Feng, J.; Wang, Y.; Li, Q.; Jiang, R.; Tang, Y. Facile Synthesis of Pyrroles via Rh(II)-Catalyzed Transannulation of 1-Tosyl-1,2,3-Triazoles with Silyl or Alkyl Enol Ethers. *Tetrahedron Lett.* **2014**, *55*, 6455–6458. (d) Meng, K.; Xia, J.; Wang, Y.; Zhang, X.; Yang, G.; Zhang, W. Ir/BiphPHOX-Catalyzed Asymmetric Hydrogenation of 3-Substituted 2,5-Dihydropyrroles and 2,5-Dihydrothiophene 1,1-Dioxides. *Org. Chem. Front.* **2017**, *4*, 1601–1605. (e) Deka, M. J.; Indukuri, K.; Sultana, S.; Borah, M.; Saikia, A. K. Synthesis of Five-, Six-, and Seven-Membered 1,3- and 1,4-Heterocyclic Compounds via Intramolecular Hydroalkoxylation/Hydrothioalkoxylation of Alkenols/Thioalkenols. *J. Org. Chem.* **2015**, *80*, 4349–4359. (f) Xia, Y.; Wang, J.; Dong, G. Distal-Bond-Selective C−C Activation of Ring-Fused Cyclopentanones: An Efficient Access to Spiroindanones. *Angew. Chem., Int. Ed.* **2017**, *56*, 2376–2380. (g) Groome, N. M.; Elboray, E. E.; Inman, M. W.; Dondas, H. A.; Phillips, R. M.; Kilner, C.; Grigg, R. Carbophilic 3-Component Cascades: Access to Complex Bioactive Cyclopropyl Diindolylmethanes. *Chem. Eur. J.* **2013**, *19*, 2180–2184. (h) Nishikata, T.; Nagashima, H. NAlkylation of Tosylamides Using Esters as Primary and Tertiary Alkyl Sources: Mediated by Hydrosilanes Activated by a Ruthenium Catalyst. *Angew. Chem., Int. Ed.* **2012**, *51*, 5363–5366.

(14) (a) Souto, J. A.; Zian, D.; Muñiz, K. Iodine(III)-Mediated Intermolecular Allylic Amination under Metal-Free Conditions. *J. Am. Chem. Soc.* **2012**, *134*, 7242–7245. (b) Jakihara, T.; Shike, T.; Ikeda, O.; Watanabe, H.; Takematsu, T.; Yoneyama, K. Preparation of benzenesulfonamide derivatives as herbicides. EP326170A1, 1989.

(15) Huleatt, P. B.; Khoo, M. L.; Chua, Y. Y.; Tan, T. W.; Liew, R. S.; Balogh, B.; Deme, R.; Gölöncsér, F.; Magyar, K.; Sheela, D. P.; Ho, H. K.; Sperlágh, B.; Mátyus, P.; Chai, C. L. L. Novel Arylalkenylpropargylamines as Neuroprotective, Potent, and Selective Monoamine Oxidase B Inhibitors for the Treatment of Parkinson's Disease. *J. Med. Chem.* **2015**, *58*, 1400–1419.

(16) (a) Crabtree, R. H.; Felkin, H.; Morris, G. E. Cationic Iridium Diolefin Complexes as Alkene Hydrogenation Catalysts and the Isolation of Some Related Hydrido Complexes. *J. Organomet. Chem.* **1977**, *141*, 205–215. (b) Crabtree, R. Iridium Compounds in Catalysis. *Acc. Chem. Res.* **1979**, *12*, 331–337.

(17) Verendel, J. J.; Pàmies, O.; Diéguez, M.; Andersson, P. G. Asymmetric Hydrogenation of Olefinss Using Chiral Crabtree-Type Catalysts: Scope and Limitations. *Chem. Soc. Rev.* **2014**, *114*, 2130–2169.

(18) Wüstenberg, B.; Pfaltz, A. Homogeneous Hydrogenation of Tri- and Tetrasubstituted Olefins: Comparison of Iridium-Phospinooxazoline [Ir-PHOX] Complexes and Crabtree Catalysts with Hexafluorophosphate (PF_6) and tetrakis[3,5-Bis(trifluoromethyl) Phenyl]borate (BArF) as Counterions. *Adv. Synth. Catal.* **2008**, *350*, 174–178.

(19) (a) Vidossich, P.; Lledós, A. Computing the Arrows of Chemical Reactions. *ChemTexts* **2017**, *3*, 17. (b) Vidossich, P.; Lledós, A. The Use of Localised Orbitals for the Bonding and Mechanistic Analysis of Organometallic Compounds. *Dalton Trans.* **2014**, *43*, 11145–11151.

(20) **TS$_{II-III}$** is optimized as a transition state in the potential energy surface, but it is placed slightly below intermediate **II** when thermal and entropic corrections are added to build up the Gibbs energy profile.

(21) (a) Wang, D. Y.; Choliy, Y.; Haibach, M. C.; Hartwig, J. F.; Krogh-Jespersen, K.; Goldman, A. S. Assessment of the Electronic Factors Determining the Thermodynamics Of "oxidative Addition" of C-H and N-H Bonds to Ir(I) Complexes. *J. Am. Chem. Soc.* **2016**, *138*, 149–163. (b) Takemoto, S.; Yamazaki, Y.; Yamano, T.; Mashima, D.; Matsuzaka, H. *J. Am. Chem. Soc.* **2012**, *134*, 17027–17035.

Experimental Part

General procedures and materials

Unless otherwise indicated, materials were obtained from commercial suppliers and used without further purification. All reactions that required anhydrous conditions were performed in dried glassware under a dry nitrogen atmosphere. Anhydrous and degassed dichloromethane and THF were taken from a solvent purification system (SPS PS-MD-3). Solvents were removed under reduced pressure with a rotary evaporator. Silica gel chromatography was performed using an automated chromatography system (PuriFlash® 430, Interchim).

Instrumentation

NMR spectroscopy: ^{1}H and ^{13}C were recorded on the NMR spectrometers of the *Centres Científics i Tecnològics de la Universitat de Barcelona*. The employed spectrometers were a Varian Mercury 400 MHz. Chemical shifts (δ) were referenced to internal solvent resonances and reported relative to TMS (tetramethylsilane). The coupling constants (*J*) are reported in Hertz (Hz). The following abbreviations are used to define multiplicities: s (singlet), d (doublet), t (triplet), q (quartet), dd (doublet of doublets), ddd (doublet of doublet of doublets), ddd (doublet of doublet of triplets), dddd (doublet of doublet of doublet of doublets), dt (doublet of triplets), td (triplet of doublets), ddq (doublet of doublet of quartets), dtd (doublet of triplet of doublets), dq (doublet of quartets), tt (triplet of triplets), qt (quartet of triplets), m (multiplet), br s (broad signal).

High Resolution Mass Spectrometry: High resolution ESI-MS spectra were recorded in an LC/MSD-TOF G1969A (Agilent Technologies) of the *Centres Científics i Tecnològics de la Universitat de Barcelona.*

IR spectroscopy: IR spectra were measured in a Thermo Nicolet 6700 FT-IR spectrometer using an ATR system, of the Department of Organic Chemistry in the Universitat de Barcelona.

Experimental procedures and characterization

General synthetic scheme

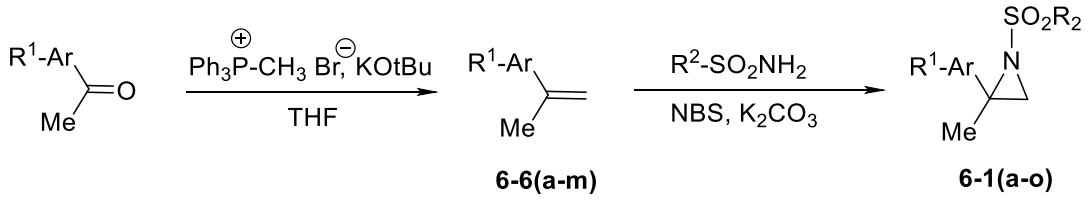

6-6(a-m) **6-1(a-o)**

General procedure for the preparation of alkenes

To a suspension of methyl triphenylphosphonium bromide (1.2 equiv.) in anhydrous THF (1.6 mL/mmol) at 0 ºC was added. KOtBu (1.2 equiv.) and the resulting yellow suspension was stirred 45 min at 0 ºC. To this suspension, a solution of ketone (1.0 equiv.) in THF (0.7 mL/mmol) was added dropwise and the resulting mixture was allowed to warm to r.t. and stirred for 16 hours. The reaction mixture was filtered over Celite®. The filtrate was concentrated under reduced pressure to yield an oil. Purification by column chromatography over silica gel using hexane as eluent afforded alkenes **6-6** as colorless oils.

General procedure for the preparation of 2,2-disubstituted aziridines

A round-bottom flask equipped with magnetic stirring was charged with the alkene (1.0 equiv.), CH_2Cl_2 (2.5 mL/mmol alkene), p-toluenesulfonamide or methanesulfonamide (1.0 equiv.) and $MnSO_4.H_2O$ (0.05 equiv.). *N*-Bromosuccinimide (NBS, 1.1 equiv.) was added, and the mixture was stirred at r.t. under N_2 for 17-24 hours. Then, K_2CO_3 (2.0 equiv.) was added and the mixture was stirred at r.t. for 1-4 hours. The resulting mixture was diluted with CH_2Cl_2 and H_2O, and the aqueous layer was extracted with CH_2Cl_2 (1x). The combined organic layer was dried over MgSO4, and the filtrate was concentrated. The crude was purified with column chromatography (EtOAc/hexanes, 2% Et_3N).

2-Methyl-2-phenyl-1-tosylaziridine (6-1a).

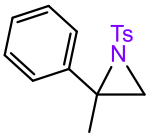

White solid (0.61 g, 43% yield). **^{1}H NMR** (400 MHz, $CDCl_3$) δ 7.90 – 7.85 (m, 2H), 7.41 – 7.36 (m, 2H), 7.35 – 7.27 (m, 5H), 2.96 (s, 1H), 2.52 (s, 1H), 2.43 (s, 3H), 2.05 (s, 3H). The analytical data for this compound were in excellent agreement with the reported data.[2]

2-(4-Chlorophenyl)-2-methyl-1-tosylaziridine (6-1b).

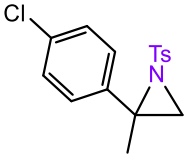

White solid (0.507 g, 32 % yield). **^{1}H NMR** (400 MHz, $CDCl_3$) δ 7.87 – 7.83 (m, 2H), 7.35 – 7.26 (m, 6H), 2.95 (s, 1H), 2.48 (s, 1H), 2.44 (s, 3H), 2.02 (s, 3H). The analytical data for this compound were in excellent agreement with the reported data.[2]

2-(3-Chlorophenyl)-2-methyl-1-tosylaziridine (6-1c).

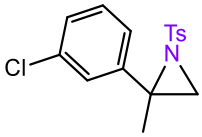

Pale yellow oil (0.714 g, 25% yield). **^{1}H NMR** (400 MHz, $CDCl_3$) δ 7.90 – 7.83 (m, 2H), 7.36 – 7.33 (m, 2H), 7.32 (h, J = 0.9 Hz, 1H), 7.28 – 7.21 (m, 3H), 2.96 (s, 1H), 2.50 – 2.46 (m, 1H), 2.44 (s, 3H), 2.04 (s, 3H). **^{13}C NMR** (101 MHz, $CDCl_3$) δ 144.33, 143.19, 137.65, 134.45, 129.89, 129.76, 128.12, 127.67, 126.95, 124.91, 51.03, 41.99, 21.77, 20.68. **HRMS** (ESI) calculated for $C_{16}H_{17}ClNO_2S$ 322.0663, found 322.0664 $[M+H]^+$. **IR** (ATR-FTIR) ν_{max} = 3021, 2928, 1592, 1320, 1158, 1085, 876, 750 cm^{-1}.

2-(2-Chlorophenyl)-2-methyl-1-tosylaziridine (6-1d).

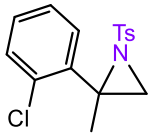

Colourless oil (0.49 g, 19 % yield). **^{1}H NMR** (400 MHz, $CDCl_3$) δ 7.93 – 7.88 (m, 2H), 7.62 – 7.57 (m, 1H), 7.35 – 7.31 (m, 2H), 7.31 – 7.18 (m, 3H), 3.06 (s, 1H), 2.50 (s, 1H), 2.43 (s, 3H), 2.04 (s, 3H). **^{13}C NMR** (101 MHz, $CDCl_3$) δ 144.26, 139.49, 137.77, 131.67, 130.69, 129.74, 129.49, 129.22, 127.69, 127.22, 51.97, 42.32, 21.76, 20.19. **HRMS** (ESI) calculated for $C_{16}H_{17}ClNO_2S$ 322.0663, found 322.0661 $[M+H]^+$. **IR** (ATR-FTIR) ν_{max} = 1323, 1161, 879, 568 cm^{-1}.

2-Methyl-2-(p-tolyl)-1-tosylaziridine (6-1e).

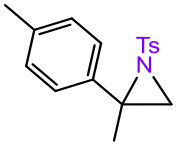

Colourless oil (0.86 g, 42 % yield). **^{1}H NMR** (400 MHz, $CDCl_3$) δ 7.88 – 7.82 (m, 2H), 7.34 – 7.26 (m, 4H), 7.15 – 7.10 (m, 2H), 2.93 (s, 1H), 2.53 (s, 1H), 2.43 (s, 3H), 2.32 (s, 3H), 2.02 (s, 3H). The analytical data for this compound were in excellent agreement with the reported data.[2]

2-Methyl-2-(naphthalen-2-yl)-1-tosylaziridine (6-1f).

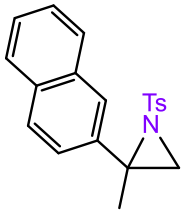

White solid (1.05 g, 48 % yield). **Mp**: 100 – 104 °C. **^{1}H NMR** (400 MHz, $CDCl_3$) δ 7.92 – 7.85 (m, 2H), 7.85 – 7.76 (m, 4H), 7.53 – 7.44 (m, 3H), 7.35 – 7.29 (m, 2H), 3.04 (s, 1H), 2.64 (s, 1H), 2.43 (s, 3H), 2.14 (s, 3H). **^{13}C NMR** (101 MHz, $CDCl_3$) δ 143.98, 138.32, 137.69, 132.98, 132.74, 129.52, 128.27, 127.95, 127.60, 127.52, 126.31, 126.20, 125.46, 124.46, 51.93, 41.83, 21.58, 20.92. **HRMS**

(ESI) calculated for $C_{20}H_{20}NO_2S$ 338.1209, found 332.1208 $[M+H]^+$. **IR** (ATR-FTIR) ν_{max} = 1321, 1160, 713, 571 cm^{-1}.

2-(2-Methoxyphenyl)-2-methyl-1-tosylaziridine (6-1g).

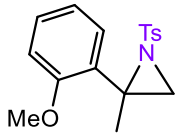

White solid (1.06 g, 56 % yield). **Mp**: 95 – 99 °C. **^{1}H NMR** (400 MHz, $CDCl_3$) δ 7.94 – 7.87 (m, 2H), 7.42 (dd, *J* = 7.5, 1.8 Hz, 1H), 7.34 – 7.30 (m, 2H), 7.26 – 7.21 (m, 1H), 6.91 (td, *J* = 7.5, 1.1 Hz, 1H), 6.82 (dd, *J* = 8.3, 1.0 Hz, 1H), 3.81 (s, 3H), 2.97 (s, 1H), 2.44 (s, 1H), 2.43 (s, 3H), 1.97 (s, 3H). **^{13}C NMR** (101 MHz, $CDCl_3$) δ 156.38, 143.91, 138.12, 129.92, 129.61, 129.49, 129.13, 127.67, 120.64, 110.53, 55.37, 51.06, 41.97, 21.73, 20.55. **HRMS** (ESI) calculated for $C_{17}H_{20}NO_3S$ 318.1158, found 318.1156 $[M+H]^+$. **IR** (ATR-FTIR) ν_{max} = 1651, 1320, 1161 cm^{-1}.

2-(4-Fluorophenyl)-2-methyl-1-tosylaziridine (6-1h).

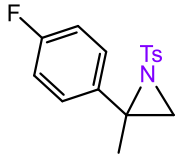

White solid (0.56 g, 41 % yield). **^{1}H NMR** (400 MHz, $CDCl_3$) δ 7.88 – 7.83 (m, 2H), 7.38 – 7.30 (m, 4H), 7.03 – 6.97 (m, 2H), 2.94 (s, 1H), 2.50 (s, 1H), 2.44 (s, 3H), 2.02 (s, 3H). The analytical data for this compound were in excellent agreement with the reported data.[2]

2-(3-Fluorophenyl)-2-methyl-1-tosylaziridine (6-1i).

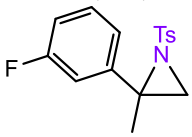

Colorless oil (0.57 g, 28 % yield). **^{1}H NMR** (400 MHz, $CDCl_3$) δ 7.93 – 7.82 (m, 2H), 7.37 – 7.31 (m, 2H), 7.30 – 7.25 (m, 1H), 7.17 (ddd, *J* = 7.7, 1.7, 1.0 Hz, 1H), 7.07 (ddd, *J* = 9.9, 2.6, 1.7 Hz, 1H), 6.96 (tdd, *J* = 8.4, 2.6, 1.0 Hz, 1H), 2.97 (s, 1H), 2.47 (s, 1H), 2.44 (s, 3H), 2.05 (s, 3H). **^{13}C NMR** (101 MHz, $CDCl_3$) δ 164.07, 161.63, 144.31, 143.73 (d, *J* = 7.4 Hz), 137.71, 130.16 (d, *J* = 8.2 Hz), 129.75, 127.66, 122.25 (d, *J* = 3.0 Hz), 114.88 (d, *J* = 21.1 Hz), 113.73, 42.18, 21.77, 20.55. **HRMS** (ESI) calculated for $C_{16}H_{17}FNO_2S$ 306.0959, found 306.0957 $[M+H]^+$. **IR** (ATR-FTIR) ν_{max} = 1588, 1320, 714 cm^{-1}.

2-Methyl-1-tosyl-2-(4-(trifluoromethyl)phenyl)aziridine (6-1j).

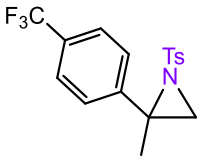

Colourless oil (0.37 g, 20 % yield). **^{1}H NMR** (400 MHz, $CDCl_3$) δ 7.87 (d, *J* = 7.9 Hz, 2H), 7.61 – 7.48 (m, 4H), 7.33 (d, *J* = 7.9 Hz, 2H), 2.99 (s, 1H), 2.49 (s, 1H), 2.44 (s, 3H), 2.06 (s, 3H). The analytical data for this compound were in excellent agreement with the reported data.[2]

2-Methyl-2-(4-nitrophenyl)-1-tosylaziridine (6-1k).

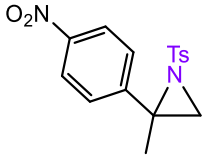

Colourless oil (0.39 g, 19 % yield). **^{1}H NMR** (400 MHz, $CDCl_3$) δ 8.22 – 8.15 (m, 2H), 7.89 – 7.86 (m, 2H), 7.59 – 7.54 (m, 2H), 7.38 – 7.33 (m, 2H), 3.02 (s, 1H), 2.49 (s, 1H), 2.45 (s, 3H), 2.09 (s, 3H). **^{13}C NMR** (101 MHz, $CDCl_3$) δ 148.17, 147.54, 144.62, 137.41, 129.86, 127.78, 127.68, 123.90, 50.68, 42.12, 21.79, 20.38. **HRMS** (ESI) calculated for $C_{16}H_{17}N_2O_4S$ 333.0904, found 333.0901 $[M+H]^+$. **IR** (ATR-FTIR) ν_{max} = 1602, 1520, 1348, 1161, 711 cm^{-1}.

2-(4-Iodophenyl)-1-(isopropylsulfonyl)-2-methylaziridine (6-1l).

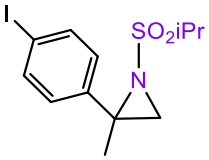

Colourless oil (0.23 g, 26% yield). **^{1}H NMR** (400 MHz, $CDCl_3$) δ 7.71 – 7.65 (m, 2H), 7.18 – 7.12 (m, 2H), 3.34 (p, *J* = 6.8 Hz, 1H), 2.91 (s, 1H), 2.49 (s, 1H), 1.97 (s, 3H), 1.47 (d, *J* = 6.9 Hz, 6H). **^{13}C NMR** (101 MHz, $CDCl_3$) δ 141.01, 137.54, 128.40, 93.33, 55.78, 48.80, 42.75, 20.70, 16.41. **HRMS** (ESI) calculated for $C_{12}H_{17}INO_2S$ 366.0019, found 366.0023 $[M+H]^+$. **IR** (ATR-FTIR) ν_{max} = 3022, 2983, 2929, 2876, 1486, 1310, 1142, 1119, 1099, 1004, 873, 820, 737 cm^{-1}.

2-(4-Bromophenyl)-1-(isopropylsulfonyl)-2-methylaziridine (6-1m).

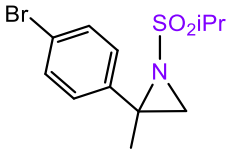

Colorless oil (0,39 g, 45% yield). **^{1}H NMR** (400 MHz, $CDCl_3$) δ 7.49 – 7.44 (m, 2H), 7.30 – 7.26 (m, 2H), 3.33 (h, *J* = 6.8 Hz, 1H), 2.91 (s, 1H), 2.49 (s, 1H), 1.97 (s, 3H), 1.47 (d, *J* = 6.9 Hz, 6H). **^{13}C NMR** (101 MHz, $CDCl_3$) δ 140.48, 131.73, 128.34, 121.90, 55.94, 48.88, 42.96, 20.93, 16.73, 16.58. **HRMS** (ESI) calculated for $C_{12}H_{17}BrNO_2S$ 318.0158, found 318.0162 $[M+H]^+$. **IR** (ATR-FTIR) ν_{max} = 3003, 2896, 1490, 1308, 1066 cm^{-1}.

2-Methyl-1-(methylsulfonyl)-2-phenylaziridine (6-1n)

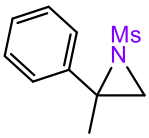

Colourless oil (0.78 g, 55 % yield). **^{1}H NMR** (400 MHz, $CDCl_3$) δ 7.44 – 7.39 (m, 2H), 7.38-7.33 (m, 2H), 7.31-7.27 (m, 1H), 3.13 (s, 3H), 2.94 (s, 1H), 2.61 (s, 1H), 1.99 (s, 3H). **^{13}C NMR** (101 MHz, $CDCl_3$) δ140.88, 128.49, 127.87, 126.45, 51.09, 42.32, 41.97, 20.88. . **HRMS** (ESI) calculated for $C_{10}H_{14}NO_2S$ 212.074, found 212.0739 $[M+H]^+$. **IR** (ATR-FTIR) ν_{max} = 1314, 1143, 749, 701 cm^{-1}.

2-Ethyl-2-phenyl-1-tosylaziridine (6-1o).

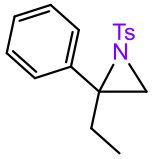

Colourless oil (0.55 g, 30 % yield). **^{1}H NMR** (400 MHz, $CDCl_3$) δ 7.86 – 7.79 (m, 2H), 7.36 – 7.29 (m, 7H), 2.82 (s, 1H), 2.65 (d, *J* = 1.0 Hz, 1H), 2.42 (s, 3H), 2.31 – 2.22 (m, 2H), 0.95 (t, *J* = 7.4 Hz, 3H). The analytical data for this compound were in excellent agreement with the reported data.[2]

2,2-Diphenyl-1-tosylaziridine (6-1p)

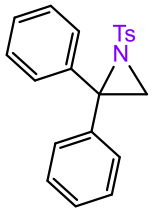

White solid (1.0 g, 64 % yield). **^{1}H NMR** (400 MHz, $CDCl_3$) δ 7.75 – 7.68 (m, 2H), 7.41 – 7.35 (m, 4H), 7.32 – 7.24 (m, 8H), 3.08 (s, 2H), 2.42 (s, 3H). The analytical data for this compound were in excellent agreement with the reported data.[1]

General procedure (GP) for the iridium-catalyzed isomerization of aziridines

Glass vials equipped with PTFE-coated stirring-bars were charged with the corresponding *N*-sulfonyl aziridine (0.33 mmol, 1.0 equiv) and Crabtree's catalyst **6-5b** (1-3 mol %). The vial was purged with N_2 and anhydrous CH_2Cl_2 ([0.25M]) was added. The reaction mixture was stirred 2-48 hours at room temperature (otherwise indicated). After concentrated under vacuum, the crude was purified by flash column chromatography (hexanes : ethyl acetate, 3:1) to afford the corresponding product.

4-Methyl-*N*-(2-phenylallyl)benzenesulfonamide (6-2a)

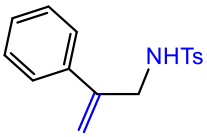

White solid (80 mg, 85%) was obtained following GP, leaving the reaction stirring for 3 hours. **^{1}H NMR** (400 MHz, $CDCl_3$) δ 7.67 – 7.63 (m, 2H), 7.24 – 7.20 (m, 5H), 7.18 – 7.15 (m, 2H), 5.31 (t, *J* = 0.8 Hz, 1H), 5.14 (td, *J* = 1.4, 0.7 Hz, 1H), 4.39 – 4.31 (m, 1H), 3.94 (ddt, *J* = 6.2, 1.4, 0.8 Hz, 2H), 2.38 (s, 3H). The analytical data for this compound were in excellent agreement with the reported data.[2]

***N*-(2-(4-Chlorophenyl)allyl)-4-methylbenzenesulfonamide (6-2b).**

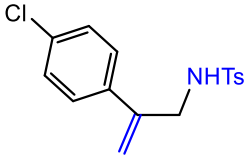

[1] Vyas, R.; Gao, G.-Y.; Harden, J.D.; Zhang, X.P. *J. Org. Chem.* **2004**, *6* (12), 1907.
[2] Liu, Y.; Che, C.-M. *Chem. Eur. J.* **2010**, *16*, 10494.

White solid (87 mg, 82%) was obtained following GP, using 3 mol % of **6-5b** and leaving the reaction stirring for 17 hours. **^{1}H NMR** (400 MHz, $CDCl_3$)) δ 7.73 – 7.68 (m, 2H), 7.30 (dq, *J* = 7.9, 0.6 Hz, 2H), 7.24 (d, *J* = 2.1 Hz, 2H), 7.20 – 7.16 (m, 2H), 5.38 (t, *J* = 0.6 Hz, 1H), 5.23 (q, *J* = 1.3 Hz, 1H), 4.37 (t, *J* = 6.3 Hz, 1H), 3.99 – 3.95 (m, 2H), 2.45 (s, 3H). The analytical data for this compound were in excellent agreement with the reported data.[8]

_N_-(2-(3-Chlorophenyl)allyl)-4-methylbenzenesulfonamide (6-2c).

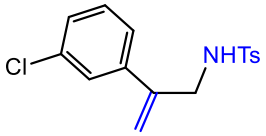

White solid (85 mg, 80%) was obtained following GP, using 3 mol % of **6-5b** and leaving the reaction stirring for 48 hours at 40 °C. **Mp**: 89 – 92 °C. **^{1}H NMR** (400 MHz, $CDCl_3$) δ 7.73 – 7.67 (m, 2H), 7.30 – 7.26 (m, 2H), 7.26 – 7.18 (m, 2H), 7.13 (td, *J* = 3.0, 1.6 Hz, 2H), 5.37 (s, 1H), 5.26 (d, *J* = 1.4 Hz, 1H), 4.66 (t, *J* = 6.2 Hz, 1H), 3.99 – 3.94 (m, 2H), 2.44 (s, 3H). **^{13}C NMR** (101 MHz, $CDCl_3$) δ 143.77, 142.00, 139.92, 136.80, 134.60, 129.88, 129.85, 128.27, 127.33, 126.44, 124.35, 116.65, 47.03, 21.70. **HRMS** (ESI) calculated for $C_{16}H_{17}ClNO_2S$ 322.0663, found 322.0665 $[M+H]^+$. **IR** (ATR-FTIR) ν_{max} = 3270, 2919, 1588, 1561, 1419, 1323, 1158 cm^{-1}.

_N_-(2-(2-Chlorophenyl)allyl)-4-methylbenzenesulfonamide (6-2d).

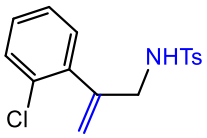

Colorless oil (72 mg, 68%) was obtained following GP, using 3 mol % of **6-5b** and leaving the reaction stirring for 48 hours at 40 °C. **^{1}H NMR** (400 MHz, $CDCl_3$) δ 7.69 – 7.65 (m, 2H), 7.32 – 7.27 (m, 2H), 7.26 – 7.23 (m, 1H), 7.22 – 7.16 (m, 2H), 7.04 – 7.00 (m, 1H), 5.45 – 5.41 (m, 1H), 5.12 (q, *J* = 1.0 Hz, 1H), 4.45 (d, *J* = 6.7 Hz, 1H), 3.95 (dt, *J* = 6.4, 1.3 Hz, 2H), 2.42 (s, 3H). **^{13}C NMR** (101 MHz, $CDCl_3$) δ 143.42, 138.42, 136.86, 132.10, 130.81, 129.61, 129.56, 129.06, 127.08, 126.81, 118.11, 47.50, 21.51. **HRMS** (ESI) calculated for $C_{16}H_{17}ClNO_2S$ 322.0663, found 322.0663 $[M+H]^+$. **IR** (ATR-FTIR) ν_{max} = 3284, 3017, 1330, 1222 cm^{-1}.

4-Methyl-_N_-(2-(p-tolyl)allyl)benzenesulfonamide (6-2e)

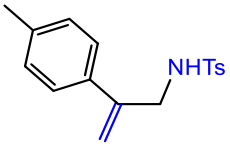

Colorless oil (75 mg, 76%) was obtained following GP, leaving the reaction stirring for 2 hours. **^{1}H NMR** (400 MHz, $CDCl_3$) δ 7.78 – 7.68 (m, 2H), 7.33 – 7.28 (m, 2H), 7.16 – 7.08 (m, 4H), 5.37 – 5.30 (m, 1H), 5.14 (q, *J* = 1.1 Hz, 1H), 4.47 (t, *J* = 6.1 Hz, 1H), 4.04 – 3.95 (m, 2H), 2.44 (s, 3H), 2.33 (s, 3H). The analytical data for this compound were in excellent agreement with the reported data.[8]

4-Methyl-_N_-(2-(naphthalen-2-yl)allyl)benzenesulfonamide (6-2f)

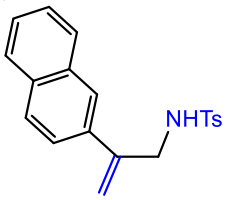

Colorless oil (88 mg, 79%) was obtained following GP, leaving the reaction stirring for 3 hours. **^{1}H NMR** (400 MHz, $CDCl_3$) δ 7.82 – 7.78 (m, 1H), 7.75 (d, *J* = 8.7 Hz, 1H), 7.73 – 7.69 (m, 3H), 7.61 – 7.59 (m, 1H), 7.49 – 7.46 (m, 2H), 7.40 (dd, *J* = 8.6, 1.9 Hz, 1H), 7.29 – 7.26 (m, 2H), 5.52 (d, *J* =

0.7 Hz, 1H), 5.31 (q, *J* = 1.2 Hz, 1H), 4.46 (t, *J* = 6.2 Hz, 1H), 4.13 (dq, *J* = 6.1, 0.6 Hz, 2H), 2.44 (s, 3H). The analytical data for this compound were in excellent agreement with the reported data.[8]

_N_-(2-(2-Methoxyphenyl)allyl)-4-methylbenzenesulfonamide (6-2g)

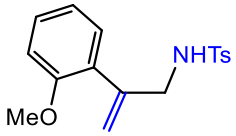

Colorless oil (75 mg, 72%) was obtained following GP, leaving the reaction stirring for 3 hours. **^{1}H NMR** (400 MHz, $CDCl_3$) δ 7.67 – 7.60 (m, 2H), 7.27 – 7.21 (m, 3H), 6.92 (dd, *J* = 7.5, 1.9 Hz, 1H), 6.84 (td, *J* = 7.4, 1.1 Hz, 1H), 6.79 (dd, *J* = 8.2, 1.0 Hz, 1H), 5.24 (q, *J* = 1.4 Hz, 1H), 5.10 (q, *J* = 0.9 Hz, 1H), 4.62 (t, *J* = 6.2 Hz, 1H), 4.00 (ddd, *J* = 6.2, 1.4, 0.8 Hz, 2H), 3.71 (s, 3H), 2.42 (s, 3H). **^{13}C NMR** (101 MHz, $CDCl_3$) δ 156.23, 143.77, 143.08, 137.12, 130.47, 129.46, 129.31, 128.34, 127.14, 120.83, 116.95, 110.58, 55.30, 47.68, 21.49. **HRMS** (ESI) calculated for $C_{17}H_{20}NO_3S$ 318.1158, found 318.1155 $[M+H]^+$. **IR** (ATR-FTIR) ν_{max} = 3018, 2960, 2930, 1490, 1325, 1094, 813 cm^{-1}.

_N_-(2-(4-Fluorophenyl)allyl)-4-methylbenzenesulfonamide (6-2h)

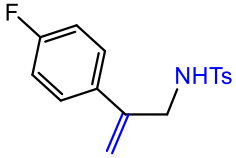

Colorless oil (79 mg, 79%) was obtained following GP, leaving the reaction stirring for 6 hours. **^{1}H NMR** (400 MHz, $CDCl_3$) δ 7.76 – 7.67 (m, 2H), 7.32 – 7.28 (m, 1H), 7.25 – 7.19 (m, 2H), 7.03 – 6.92 (m, 2H), 5.37 – 5.28 (m, 3H), 5.19 (dd, *J* = 1.3, 0.7 Hz, 1H), 4.36 (t, *J* = 5.9 Hz, 1H), 3.97 (ddd, *J* = 6.2, 1.4, 0.6 Hz, 2H), 2.45 (s, 3H). The analytical data for this compound were in excellent agreement with the reported data.[3]

_N_-(2-(3-Fluorophenyl)allyl)-4-methylbenzenesulfonamide (6-2i).

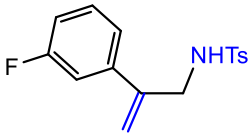

Colorless oil (82 mg, 82%) was obtained following GP, leaving the reaction stirring for 24 hours. **^{1}H NMR** (400 MHz, $CDCl_3$) δ 7.74 – 7.69 (m, 2H), 7.32 – 7.27 (m, 2H), 7.26 – 7.22 (m, 1H), 7.05 – 7.02 (m, 1H), 6.97 (tdd, *J* = 8.3, 2.6, 1.0 Hz, 1H), 6.88 – 6.84 (m, 1H), 5.40 (t, *J* = 0.7 Hz, 1H), 5.26 (d, *J* = 1.4 Hz, 1H), 4.47 (t, *J* = 6.2 Hz, 1H), 3.98 (ddd, *J* = 6.3, 1.4, 0.7 Hz, 2H), 2.44 (s, 3H). **^{13}C NMR** (101 MHz, $CDCl_3$) δ 164.02, 161.58, 143.63, 141.88 (d, *J* = 2.2 Hz), 140.15 (d, *J* = 6.7 Hz), 136.63, 130.00 (d, *J* = 8.4 Hz), 129.69, 127.19, 121.69 (d, *J* = 2.8 Hz), 116.32, 114.95 (d, *J* = 21.2 Hz), 113.08 (d, *J* = 22.3 Hz), 46.88, 21.51. **^{19}F NMR** (376 MHz, cdcl$_3$) δ -112.75 (ddd, *J* = 10.3, 8.5, 6.0 Hz). **HRMS** (ESI) calculated for $C_{16}H_{17}FNO_2S$ 306.0959, found 306.0955 $[M+H]^+$. **IR** (ATR-FTIR) ν_{max} = 3279, 3022, 1582, 1324, 1092 cm^{-1}.

4-Methyl-_N_-(2-(4-(trifluoromethyl)phenyl)allyl)benzenesulfonamide (6-2j)

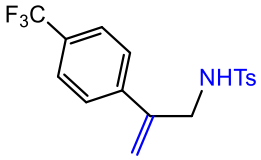

White solid (78 mg, 67%) was obtained following GP, using 3 mol % of **6-5b** and leaving the reaction stirring for 48 hours at 40 ºC. **^{1}H NMR** (400 MHz, $CDCl_3$) δ 7.72 – 7.66 (m, 2H), 7.55 – 7.50 (m,

[3] Kiyokawa, K.; Kojima, T.; Hishikawa, Y.; Minakata, S. *Chem. Eur. J.* **2015**, *21*, 15548.

2H), 7.40 – 7.32 (m, 2H), 7.31 – 7.23 (m, 2H), 5.47 – 5.41 (m, 1H), 5.32 (d, *J* = 1.4 Hz, 1H), 4.73 (t, *J* = 6.3 Hz, 1H), 4.00 (dq, *J* = 6.3, 0.7 Hz, 2H), 2.43 (s, 3H). The analytical data for this compound were in excellent agreement with the reported data.[10]

4-Methyl-*N*-(2-(4-nitrophenyl)allyl)benzenesulfonamide (6-2k).

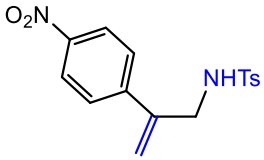

Colorless oil (75 mg, 69%) was obtained following GP, using 3 mol % of **6-5b** and leaving the reaction stirring for 36 hours at 40 ºC. **^{1}H NMR** (400 MHz, $CDCl_3$) δ 8.17 – 8.11 (m, 2H), 7.73 – 7.69 (m, 2H), 7.48 – 7.42 (m, 2H), 7.33 – 7.29 (m, 2H), 5.56 (s, 1H), 5.43 (t, *J* = 1.4 Hz, 1H), 4.55 (t, *J* = 6.3 Hz, 1H), 4.05 – 4.00 (m, 2H), 2.45 (s, 3H). **^{13}C NMR** (101 MHz, $CDCl_3$) δ 144.26, 143.87, 141.52, 136.56, 129.78, 127.15, 126.97, 123.73, 118.88, 46.87, 21.53. **HRMS** (ESI) calculated for $C_{16}H_{17}N_2O_4S$ 333.0904, found 333.0901 $[M+H]^+$. **IR** (ATR-FTIR) ν_{max} = 3021, 2914, 2847, 1735, 1601, 1518, 1343, 1158, 855, 749 cm^{-1}.

***N*-(2-(4-Iodophenyl)allyl)propane-2-sulfonamide (6-2l).**

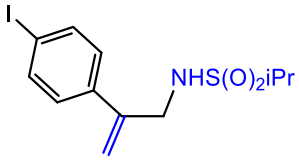

White solid (99 mg, 82%) was obtained following GP, using 3 mol % of **6-5b** and leaving the reaction stirring for 17 hours at 40 ºC. **Mp**: 83 – 86 ºC. **^{1}H NMR** (400 MHz, $CDCl_3$) δ 7.72 – 7.66 (m, 2H), 7.18 – 7.13 (m, 2H), 5.48 (d, *J* = 0.8 Hz, 1H), 5.37 (d, *J* = 1.4 Hz, 1H), 4.20 (d, *J* = 6.2 Hz, 1H), 4.17 – 4.13 (m, 2H), 3.11 (h, *J* = 6.8 Hz, 1H), 1.32 (d, *J* = 6.8 Hz, 6H). **^{13}C NMR** (101 MHz, $CDCl_3$) δ 143.40, 137.93, 137.73, 128.14, 115.64, 94.12, 54.10, 47.19, 16.70. **HRMS** (ESI) calculated for $C_{12}H_{17}INO_2S$ 366.0019, found 366.0024 $[M+H]^+$. **IR** (ATR-FTIR) ν_{max} = 3284, 2989, 1315, 1215, 1137, 748 cm^{-1}.

***N*-(2-(4-Bromophenyl)allyl)propane-2-sulfonamide (6-2m)**

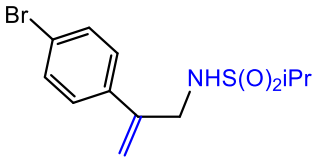

Colorless oil (82 mg, 78%) was obtained following GP, using 3 mol % of **6-5b** and leaving the reaction stirring for 17 hours. **^{1}H NMR** (400 MHz, $CDCl_3$) δ 7.51 – 7.47 (m, 2H), 7.30 – 7.27 (m, 2H), 5.48 (d, *J* = 0.8 Hz, 1H), 5.38 (d, *J* = 1.4 Hz, 1H), 4.25 (t, *J* = 6.2 Hz, 1H), 4.15 (d, *J* = 6.0 Hz, 2H), 3.12 (hept, *J* = 6.9 Hz, 1H), 1.31 (d, *J* = 6.8 Hz, 6H). **^{13}C NMR** (101 MHz, $CDCl_3$) δ 143.29, 137.14, 131.94, 127.95, 122.51, 115.60, 54.08, 47.25, 16.69. **HRMS** (ESI) calculated for $C_{12}H_{17}BrNO_2S$ 318.0158, found 318.0157 $[M+H]^+$. **IR** (ATR-FTIR) ν_{max} = 3279, 2977, 2936, 2874, 2251, 1489, 1314 cm^{-1}.

***N*-(2-Phenylallyl)methanesulfonamide (6-2n)**

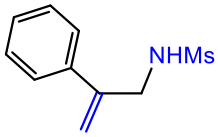

White solid (67 mg, 96%) was obtained following GP, using 3 mol % of **6-5b** and leaving the reaction stirring for 17 hours. **^{1}H NMR** (400 MHz, $CDCl_3$) δ 7.43 – 7.30 (m, 5H), 5.49 (q, *J* = 0.7 Hz, 1H), 5.36 (td, *J* = 1.3, 0.7 Hz, 1H), 4.57 (s, 1H), 4.21 (d, *J* = 4.3 Hz, 2H), 2.88 (s, 3H). **^{13}C NMR** (101 MHz, $CDCl_3$) δ 143.83, 138.09, 128.91, 128.55, 126.32, 126.30, 115.32, 47.17, 41.20. The analytical data for this compound were in excellent agreement with the reported data.[9]

4-Methyl-*N*-(3-methyl-2-phenylbut-2-en-1-yl)benzenesulfonamide (6-2o)

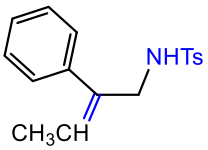

Colorless oil –as a mixture of 2.5:1 *E:Z* allylic amines- (71 mg, 72%) was obtained following GP, leaving the reaction stirring for 17 hours. **^{1}H NMR** (400 MHz, $CDCl_3$) δ 7.72 – 7.66 (m, 2H), 7.63 (dd, *J* = 8.5, 2.0 Hz, 2H), 7.36 – 7.20 (m, 13H), 7.13 – 7.07 (m, 2H), 6.96 (dt, *J* = 7.6, 1.3 Hz, 1H), 5.86 (q, *J* = 7.0 Hz, 1H), 5.76 – 5.65 (m, 1H), 4.35 (d, *J* = 4.7 Hz, 1H), 4.32 (d, *J* = 5.7 Hz, 1H), 4.03 (d, *J* = 5.6 Hz, 2H), 3.84 (dp, *J* = 6.2, 1.2 Hz, 2H), 2.45 (s, 3H), 2.43 (s, 2H), 1.72 (d, *J* = 7.0 Hz, 4H), 1.52 (dt, *J* = 6.9, 1.2 Hz, 3H). The analytical data for this compound were in excellent agreement with the reported data.[10]

***N*-(2,2-Diphenylvinyl)-4-methylbenzenesulfonamide (6-2p)**

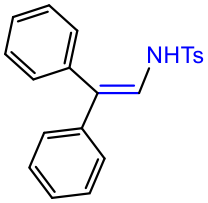

White solid (100 mg, 87%) was obtained following GP, leaving the reaction stirring for 17 hours. **^{1}H NMR** (400 MHz, $CDCl_3$) δ 7.75 – 7.70 (m, 2H), 7.34 (dddd, *J* = 6.8, 2.8, 1.7, 1.0 Hz, 5H), 7.26 – 7.20 (m, 3H), 7.13 – 7.08 (m, 2H), 6.94 – 6.90 (m, 2H), 6.80 (d, *J* = 11.6 Hz, 1H), 6.26 (d, *J* = 11.6 Hz, 1H), 2.45 (s, 3H). The analytical data for this compound were in excellent agreement with the reported data.[4]

Miscellaneous

Methylation of *N*-Sulfonyl Allylic Amines. General procedure.

The corresponding *N*-sulfonyl allylic amine (0.4 mmol, 1.0 equiv.) was solved in anhydrous DMF into a round-bottom flask previously purged with N_2. The reaction was stirred at 0 ºC. Then, a solution of NaH (60% dispersion in mineral oil, 1.0 equiv.) in anhydrous DMF was added via syringe or cannula. The reaction mixture was stirred at 0 ºC during 30 minutes. Then, CH_3I (2.0 equiv.) was added dropwise. The solution was stirred overnight at room temperature. Afterwards, the reaction was quenched with a saturated solution of NH_4Cl and extracted (x3) with diethyl ether. The organic phases were washed with brine (x1) and dried over magnesium sulfate. After evaporation under vacuum, the crude was purified by column chromatography (70:30 Hexanes:EtOAc).

[4] Selander, N.; Worrell, B. T.; Chuprakov, S.; Velaparthi, S.; Fokin, V. V. *J. Am. Chem. Soc.* **2012**, *134* (36), 14670.

_N_-methyl-_N_-(2-phenylallyl)methanesulfonamide (6-3a)

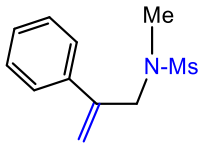

Colourless oil (70 mg, 76% yield). **^{1}H NMR** (400 MHz, $CDCl_3$) δ 7.50 – 7.44 (m, 2H), 7.39 – 7.28 (m, 3H), 5.53 (q, *J* = 0.8 Hz, 1H), 5.32 (q, *J* = 0.9 Hz, 1H), 4.22 (dd, *J* = 1.3, 0.7 Hz, 2H), 2.77 – 2.74 (m, 3H), 2.69 (d, *J* = 0.7 Hz, 3H). **^{13}C NMR** (101 MHz, $CDCl_3$) δ 142.93, 138.35, 128.65, 128.38, 126.66, 116.59, 54.12, 36.06, 33.99. **HRMS** (ESI) calculated for $C_{11}H_{16}NO_2S$ 226.0896, found 226.0897 $[M+H]^+$. **IR** (ATR-FTIR) ν_{max} = 3025, 1324, 1151, 913, 794, 780, 704 cm^{-1}.

_N_,4-dimethyl-_N_-(2-phenylallyl)benzenesulfonamide (6-3n)

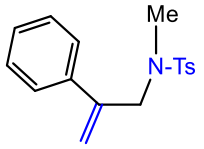

White solid (89 mg, 74% yield). **^{1}H NMR** (400 MHz, $CDCl_3$) δ 7.71 – 7.65 (m, 2H), 7.53 – 7.48 (m, 2H), 7.37 – 7.27 (m, 5H), 5.52 (d, *J* = 0.9 Hz, 1H), 5.22 (q, *J* = 1.2 Hz, 1H), 4.02 (d, *J* = 1.1 Hz, 2H), 2.58 (s, 3H), 2.44 (s, 3H). The analytical data for this compound were in excellent agreement with the reported data.[5]

***tert*-Butyl methyl(2-phenylallyl)carbamate (6-4a)**

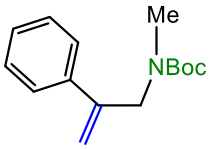

Sodium metal (69 mg, 3 mmol) was added at room temperature to a solution of naphthalene (197 mg, 1.5 mmol) in THF (4 mL). After stirring 30 minutes, this solution was added to a solution of sulfonamide **6-5a** (105 mg, 0.348 mmol) in THF (2 mL) at -78 ºC. After 10 min, few drops of saturated aqueous NH_4Cl were carefully added. The reaction mixture was allowed to warm to room temperature and Boc_2O (84 mg, 1.2 equiv.) were added under nitrogen. The reaction was stirred overnight. The solution was then concentrated under reduced pressure and purified by column chromatography (85:15 Hexanes:AcOEt) to afford **6-4a.**

Colourless oil (61 mg, 71% yield). **^{1}H NMR** (400 MHz, $CDCl_3$) δ 7.48 – 7.27 (m, 5H), 5.41 (br d, *J* = 25.8 Hz, 1H), 5.14 – 5.07 (m, 1H), 4.35 – 4.20 (m, 2H), 2.83 – 2.69 (m, 3H), 1.44 (s, 9H). The analytical data for this compound were in excellent agreement with the reported data.[6]

[5] Souto, J. A.; Zian, D.; Muñiz, K. *J. Am. Chem. Soc.* **2012**, *134*, 7242.
[6] Olofsson, K.; Sahlin, H.; Larhed, M.; Hallberg, A. *J. Org. Chem.* **2001**, *66*, 544.

Computational Details

Potential Energy Surface exploration

Theoretical calculations were performed at DFT level of theory using Gaussian09 software.[1] The structures of all the intermediates and transition states were optimized in dichloromethane solvent (DCM, ε= 8.93) with the SMD continuum model[2] using the B3LYP functional[3] combined with the Grimme's D3 correction for dispersion.[4] Basis set BS1 was used for the optimizations. BS1 includes the 6-31G(d,p) basis set for the main group elements,[5] and the scalar relativistic Stuttgart-Dresden SDD pseudopotential and its associated double-ζ basis set,[6] complemented with a set of *f* polarization functions,[7] for the iridum atom. Frequency calculations were carried out for all the optimized geometries in order to characterize the stationary points as either minima or transition states. It was confirmed that transition states connect with the corresponding intermediates by usual intrinsic reaction coordinate (IRC) calculations and subsequent optimization to minima.

Gibbs energies in DCM were calculated at 298.15 K adding to the potential energies in DCM, obtained with single point calculations at the BS1 optimized geometries using an extended basis set (BS2), the thermal and entropic corrections obtained with BS1. BS2 consists in the 6-311++G(2d,p) basis set for the main group elements[7] and the quadruple-ζ def2-QZVP basis set for Ir.[8] A correction of 1.9 kcal mol^{-1} was applied to all Gibbs values to change the standard state from the gas phase (1 atm) to solution (1 M) at 298.15 K.[9]

Basis set calibration

Rzepa and co-workers recommended TZVP basis set to ensure that basis set superposition errors become insignificant.[10] To calibrate the basis set we employed to build up the Gibbs energy profiles (BS2), discarding basis set superposition errors, single point calculations for the reference structures and TSs of the pathways forming the allyl amine products (Figure 6.S1) were performed using the TZVP basis set for the main group elements, [11] combined with def2-QZVP basis set for Ir.

The results obtained with both basis sets, summarized in table 6.S1, are very similar: the largest discrepancy found in the relative Gibbs energies is 0.7 kcal mol^{-1}, making us confident about the reliability of the BS2 energies.

Table 6.S1: Comparison of Gibbs energy for TSs of the pathways forming the allyl amine (Figure 6.S1) computed using 6-311++G(2d,p) or TZVP basis sets for the main group elements, combined with def2-QZVP basis set for Ir.

Species	**G(a.u.)[a]**		**ΔG(kcal mol^{-1})[a,b]**	
	6-311++G(2d,p)	TZVP	6-311++G(2d,p)	TZVP
6-1a	-1223.345109	-1223.344063	--	--
Ir_COD_PCy3_Py	-1463.383581	-1463.420583	--	--
TS_{I-II}	-2686.698790	-2686.735626	16.8	16.2
TS_{II-III}	-2686.703471	-2686.739159	13.8	14.0
TS_{III-IV}	-2686.698874	-2686.733547	16.8	17.5
TS_{I-II}[b]	-2686.700686	-2686.736883	15.7	15.4
TS_{II-III}[b]	-2686.702254	-2686.737890	14.7	14.8
TS_{III-IV}[b]	-2686.692768	-2686.727617	20.7	21.3

[a] Quadruple-ζ def2-QZVP basis set for Ir. [b] A correction of 1.9 kcal mol^{-1} was applied to all Gibbs values to change the standard state from the gas phase (1 atm) to solution (1 M) at 298.15 K.

Localized Orbital Analysis

A localized orbital analysis was performed as described below to pinpoint electron rearrangements in the ring-opening step. [12] Orbital localization of canonical Density Functional Theory orbitals was performed with the CP2K code (www.cp2k.org). The PBE exchange-correlation functional was used.[13] The Quickstep algorithm was used to solve the electronic structure problem,[14] employing a double-ζ plus polarization (DZVP) basis set to represent the valence orbitals and plane waves for the electron density (300 Ry cutoff). Goedecker-Teter-Hutter (GTH) type pseudopotentials were used for valence-core interactions.[15] Models were treated as isolated in a cubic box of 30 Å edge.

Gibbs Energy Profiles

Conformational analysis of the initial intermediate

Since the reaction takes place starting from an R/S racemic mixture of substrate **6-1a**, a preliminary analysis of this species was carried out. Considering that the reaction involves a γ-C-H elimination, after the ring opening and the *N*-coordination is needed a favorable methyl orientation toward the metal. In fact, as discussed in the main text, the agostic interaction in intermediate **II** is a key factor for the reaction selectivity. About the possible isomers and conformations of substrate **6-1a** in intermediate **I,** the convenient methyl orientation is provided only when the Me and the nitrogen lone pair are located on the same side of the plane defined by the aziridine ring (see ***(S)*-6-1a_Me** and ***(R)*- 6-1a_Me** in Scheme 6.S1).

Scheme 6.S1. Schematic representation of the four isomers of substrate **6-1a** and its related coordination modes to the catalyst $[Ir(PCy_3)(cod)]^+$. **6-(*R*)-1a** and **6-(*S*)-1a** are labelled with the suffix Me or Ph considering the group oriented on the lone pair side of the plane defined by the aziridine ring. The atoms and bonds involved in the steps leading to the γ-C-H elimination are reported in red dotted lines. Transition state energy reported in kcal mol^{-1}.

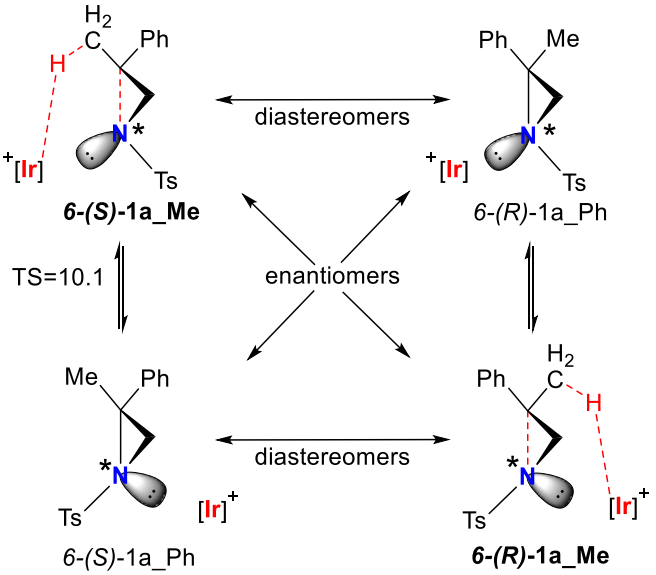

This arrangement is possible for both R and S enantiomers considering the fluxional nitrogen inversion with a computed relative low energetic barrier of 10.1 kcal mol^{-1}. Keeping this conclusions and the experimental selectivity in mind, the study of the catalytic cycle was performed starting from the two conformations of the initial intermediate with the Me substituent in the metal side (**6-(*R*)-1a_Me** and **6-(*S*)-1a_Me**, intermediates **I** and **I^B**, respectively). The results are discussed in the next section (see Figure 6.S1).

For sake of completeness the ring-opening transition state was also computed starting from the 6-*(S)*-1a-Ph coordination mode obtaining the highest value among all the computed points (21.2 kcal mol-1, **TS$_{I\text{-}II}^C$**).

Isomerization of *(R)*- and *(S)*-aziridine to allylamine 6-2a

It can be noted that the reaction takes place starting from an R/S racemic mixture of substrate **6-1a**. The relative Gibbs energies commented in the main text (Scheme 6.3) correspond to the reaction of the **6-*(R)*-1a** enantiomer. The catalytic cycle was also studied starting from the **6-(*S*)-1a**. With this enantiomer the reaction takes place in the opposite side of the plane defined by the metal, the two alkene bonds of the cod ligand and the P and N atoms of the PCy_3 and aziridine ligands, respectively. A comparison of the two reaction profiles is shown in Figure 6.S1. The computed pathway for **6-(*S*)-1a** shows intermediates and transition states (structures **B** in Figure 6.S1) analogues to those found for the reaction of the (*R*)-aziridine. Despite their general a bit higher energy values than for **6-*(R)*-1a**, the computed transition states are low enough to consider it a feasible pathway for **6-*(S)*-1a**. Therefore, the proposed mechanism is operative for both enantiomers of aziridine **6-1a**.

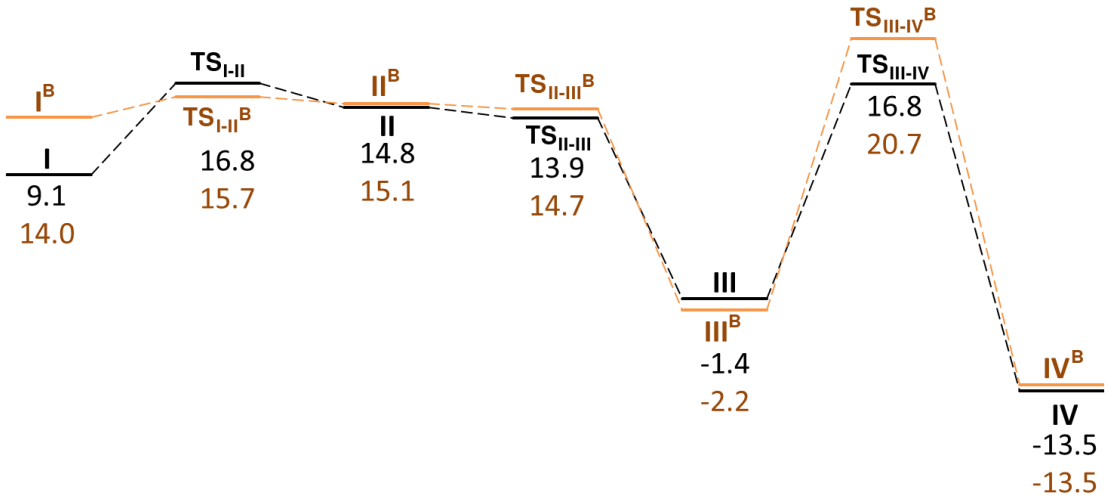

Figure 6.S1. Comparison of the two Gibbs energy profiles in DCM for the isomerization process of *(R)*-aziridine **6-1a** (in black) and its enantiomer *(S)*-aziridine (in orange) to allyl amine. Energy values reported in kcal mol^{-1}. The separated catalytically active species $[Ir(PCy_3)(cod)]^+$ and aziridine substrate **6-1a** are taken as zero-energy.

Formation of the secondary products (imine 6-3a and enamine 6-4a)

For sake of completeness, the pathways leading to the formation of the secondary products were computed for substrate **6-1a**. The discussed pathways and transition states are reported in Figure 6.S2. All the structures are reported in the Cartesian coordinates section.

The first part of the pathway (ring opening) is shared with the allyl amine formation. In fact, is the C-H elimination taking place after the ring opening which, depending on the hydrogen involved, defines the selectivity of the process. The direct elimination of the C_γ-H (those in the Me substituent), via $\mathbf{TS_{I\text{-}II}}$, followed by migration to the nitrogen, yields the allyl amine as described in the main text, while C_α-H elimination open the possibility to imine or enamine generation. To make this possible, on intermediate **II** rotation of the aziridine C_α-C_β bond and conformational rearrangement is needed to approach the C_α-H to the free Ir axial position. The transition state associated to this preparatory step ($\mathbf{TS_{II\text{-}III}^C}$) is located at 19.1 kcal mol^{-1}. This additional rotational barrier of 4.4 kcal mol^{-1} is sufficient to govern the selectivity toward allyl amine formation. Achieved the favorable conformation, the C_α-H elimination, via $\mathbf{TS_{IV\text{-}V}^C}$, located at 15.5 kcal mol^{-1} (with a relative barrier of 0.3 kcal mol^{-1}) leads to the formation of intermediate $\mathbf{V^C}$, at -9.3 kcal mol^{-1}, the lowest intermediate of all the computed pathways. The last step shows an additional bifurcation which defines the imine or enamine formation, depending on the hydrogen migration that closes the catalytic cycle. Transition state, $\mathbf{TS_{V\text{-}VI}^C}$, is involved in the C-H reductive elimination generating the N-C unsaturated bond of the imine, while, $\mathbf{TS_{V\text{-}VI}^D}$, produces the N-H reductive elimination leading to the formation of the C-C double bond of the enamine. $\mathbf{TS_{V\text{-}VI}^C}$ entails the highest energy barrier (21.0 kcal mol^{-1}). $\mathbf{TS_{V\text{-}VI}^D}$

lies at 8.6 kcal mol^{-1} and as **TS_{III-IV}** it can be described as an ion-pair, in which the aziridine nitrogen is completely dissociated (Ir···N = 3.228 Å).

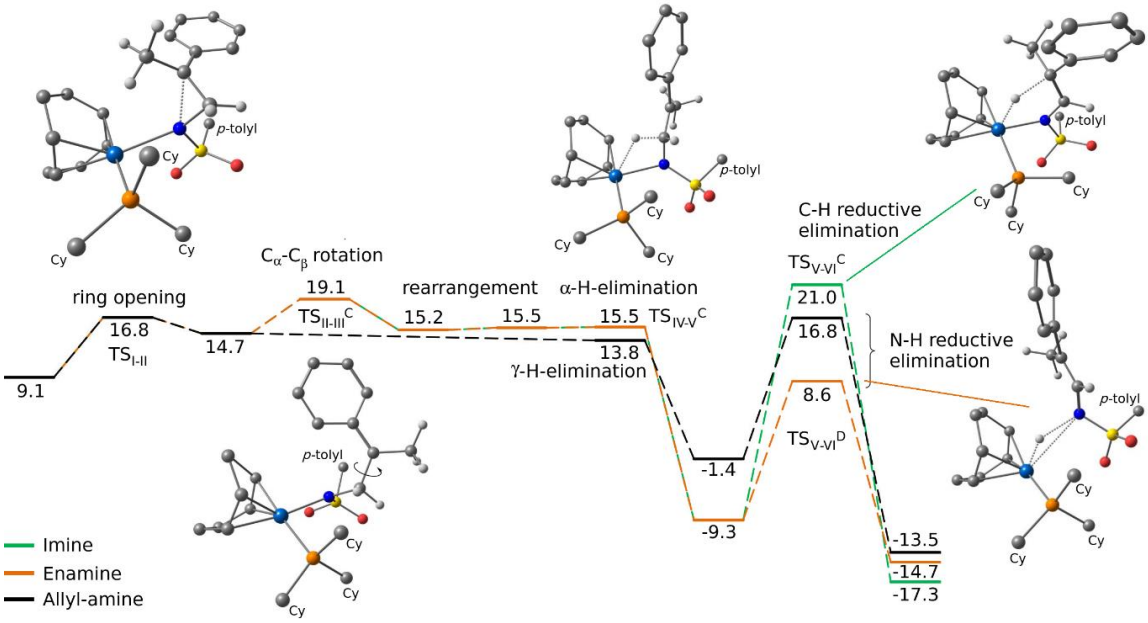

Figure 6.S2. Comparison of the three Gibbs energy profiles in DCM for the isomerization process of **6-1a** leading to the formation of allylamine **6-2a** (in black), imine **6-3a** (in green) and enamine **6-4a** (in orange). Energy values reported in kcal mol^{-1}. The separated catalytically active species [Ir(PCy$_3$)(cod)]$^+$ and aziridine substrate **6-1a** are taken as zero-energy.

<u>Localized MOs analysis of the ring-opening step.</u>

We have applied an orbital localization procedure to investigate the electronic rearrangements along the ring-opening step, starting from intermediate **I** and leading, through transition state **TS_{12}** to intermediate **II**. Specifically, after orbital localization,[12] we computed the centroids of charge of each localized orbital along structures arising from IRC calculations connecting **TS_{12}** with reactive and product (intermediates **I** and **II**, respectively). This procedure allows to visualize "where" electrons are and "who" they belong to. Furthermore, the displacement of orbital centroids along the reaction allows drawing the "curly arrows" commonly used in chemical reaction schemes.[16]

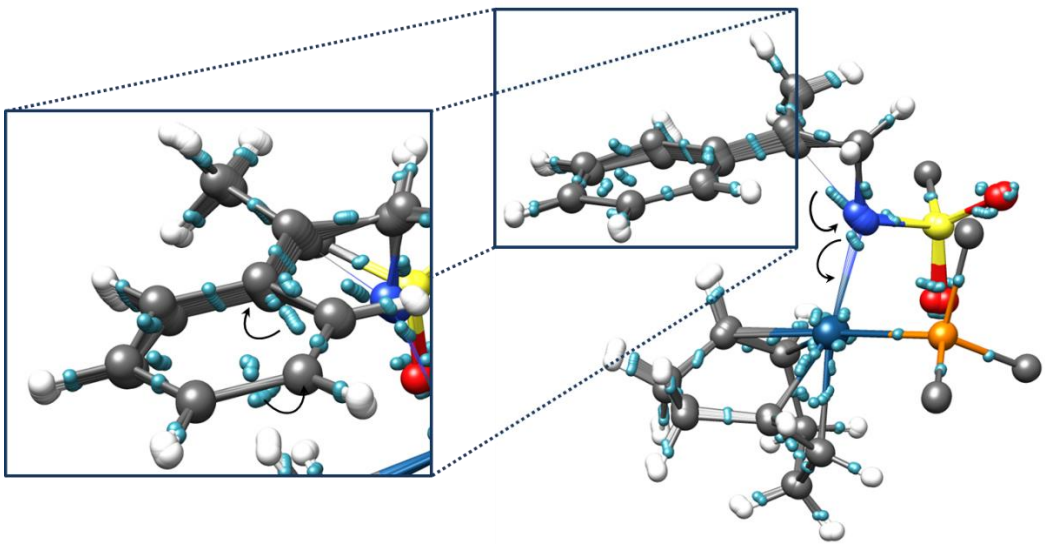

Figure 6.S3. Superposition of the structures from the IRC relative to the ring opening step. The centroids of the localized MOs, representing the electron pairs, are represented in blue. The thin line highlights the N-C bond breaking while the curve arrows describe the electron pair movements.

Tracking the displacement of the orbital centroids along the IRC, clearly show how the bonding electron pair of the C-N bond which is being broken in the ring-opening step is hopping to the nitrogen, at the same time that the N lone pair is forming a dative bond with the iridium atom (Figure 6.S3). The positive charge that appears on the β-carbon atom is stabilized by resonance with the π electrons of the phenyl ring.

The "curly arrow" description arising from this LMO analysis is in depicted in the Scheme:

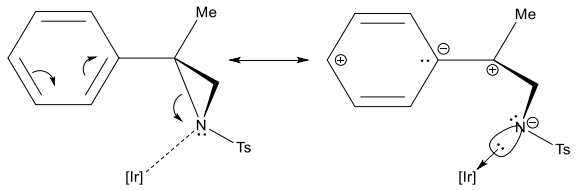

We have computed the Wiberg bond indices (WBI) for the three species involved in the ring-opening step (intermediates **I** and **II** and **TS$_{I-II}$**). The obtained values are collected in Table 6.S2. They agree with the above description from LMO centroids and point out the importance of the resonace stabilization in the ring-opening step.

Table 6.S2: Wiberg bond indices in the Natural Atomic Orbital basis set, for selected bonds along the ring-opening step.

Bond	I	TS$_{I-II}$	II
C-N	0.86	0.50	0.14
Ir-N	0.08	0.29	0.42
C-C$_{Ph}$	1.00	1.13	1.24

Cartesian coordinates and absolute E and G energies of the optimized structures

The cartesian coordinates are published online Organic Letters. They can be found in the Supporting Information file, which is available free of charge on the ACS Publications website at DOI: 10.1021/acs.orglett.8b02450

^{1}H NMR and ^{13}C NMR spectra

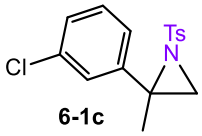

6-1c

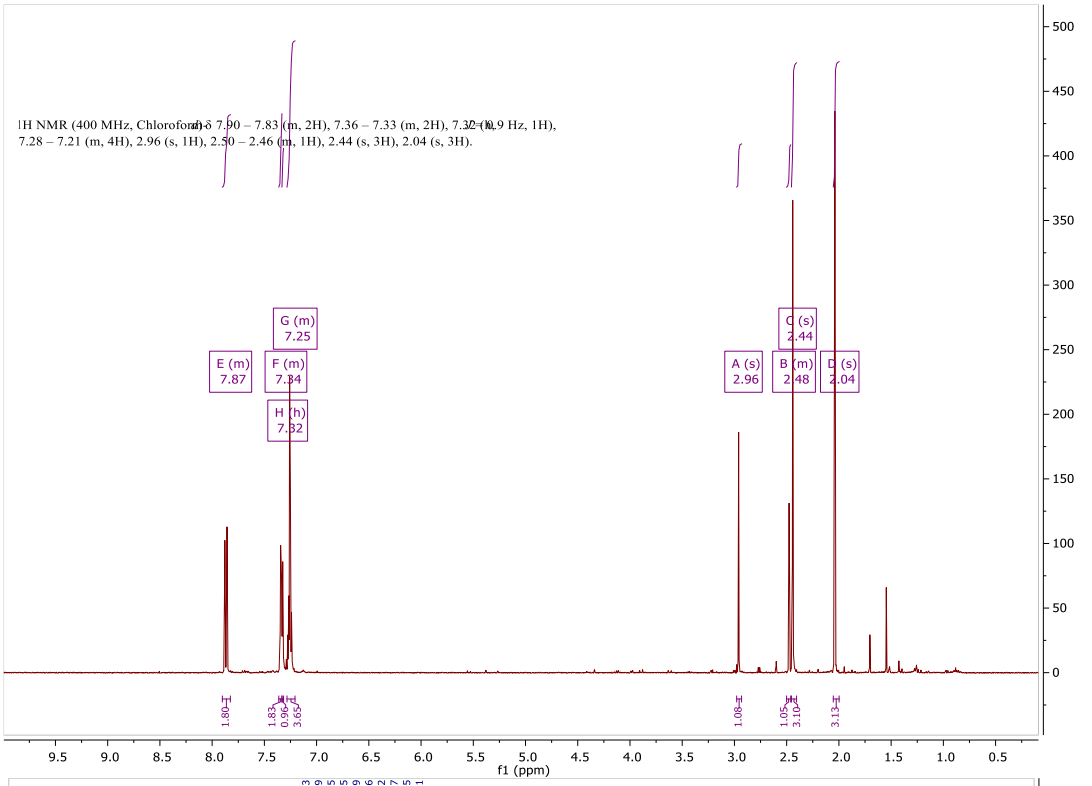

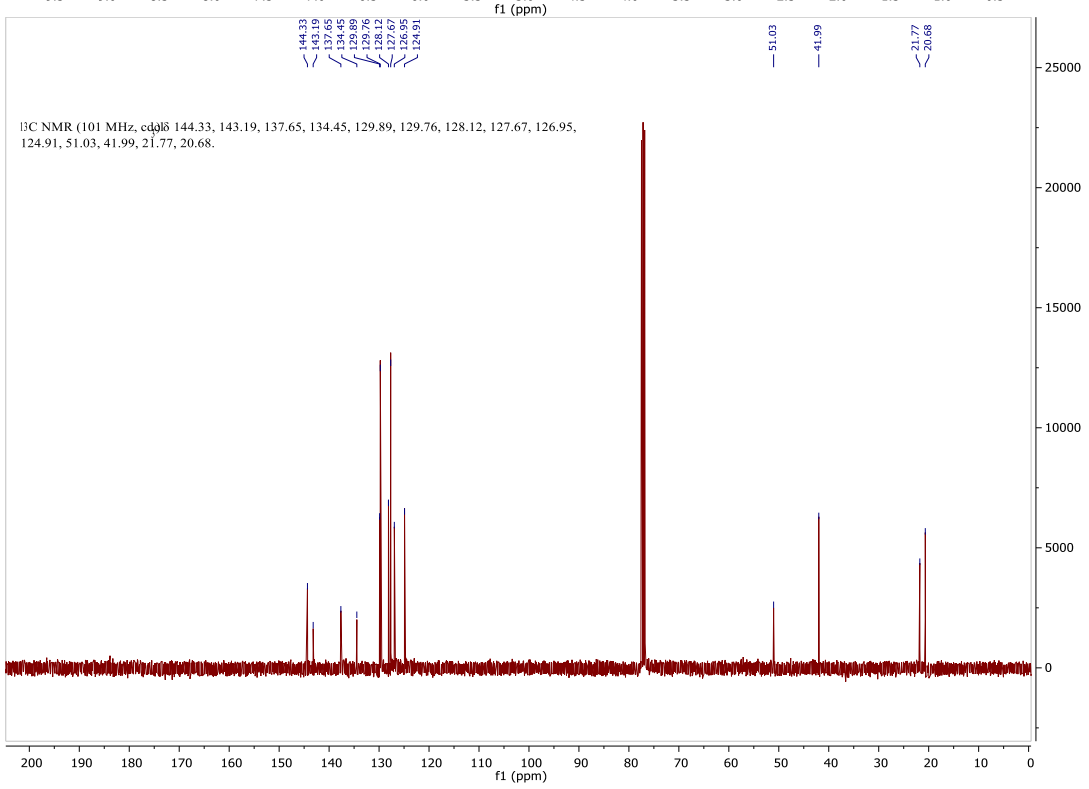

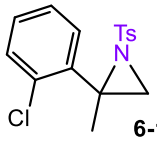
Ts
N
Cl

6-1d

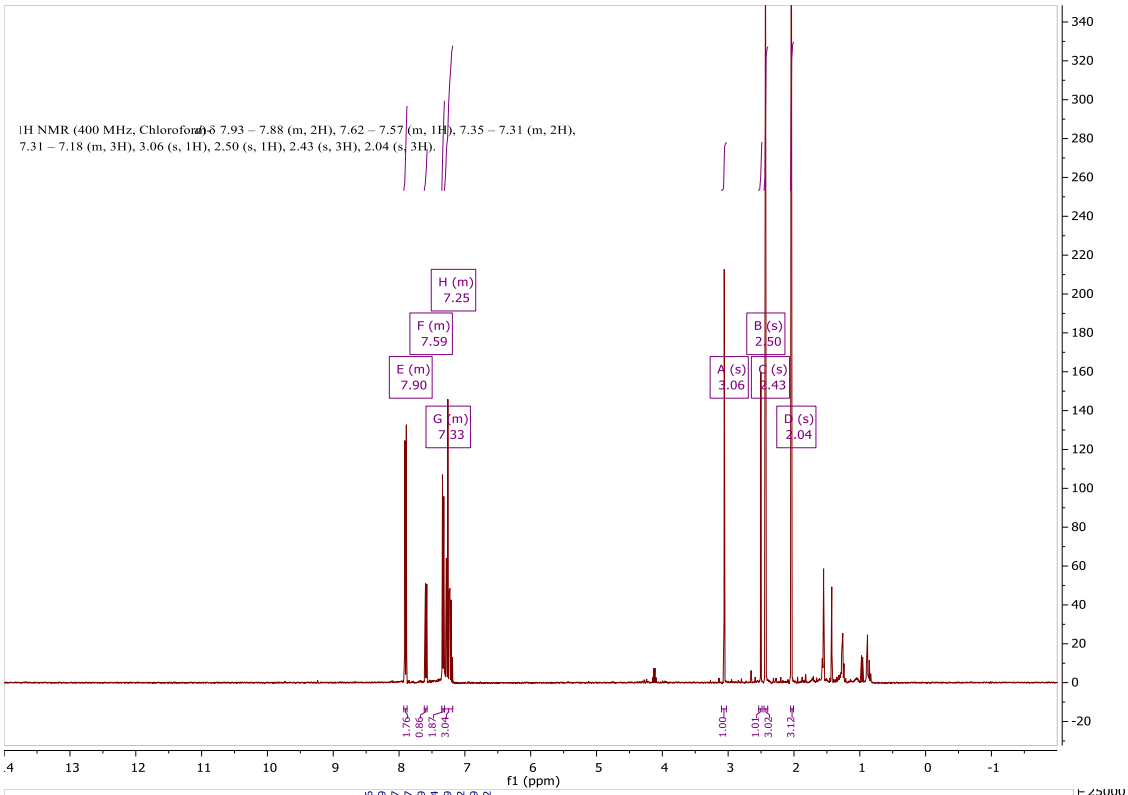
1H NMR (400 MHz, Chloroform-d) δ 7.93 – 7.88 (m, 2H), 7.62 – 7.57 (m, 1H), 7.35 – 7.31 (m, 2H), 7.31 – 7.18 (m, 3H), 3.06 (s, 1H), 2.50 (s, 1H), 2.43 (s, 3H), 2.04 (s, 3H).
H (m) 7.25
F (m) 7.59
E (m) 7.90
G (m) 7.33
B (s) 2.50
A (s) 3.06
C (s) 2.43
D (s) 2.04
1.76
0.86
1.82
3.04
1.00
1.01
3.02
3.12
f1 (ppm)

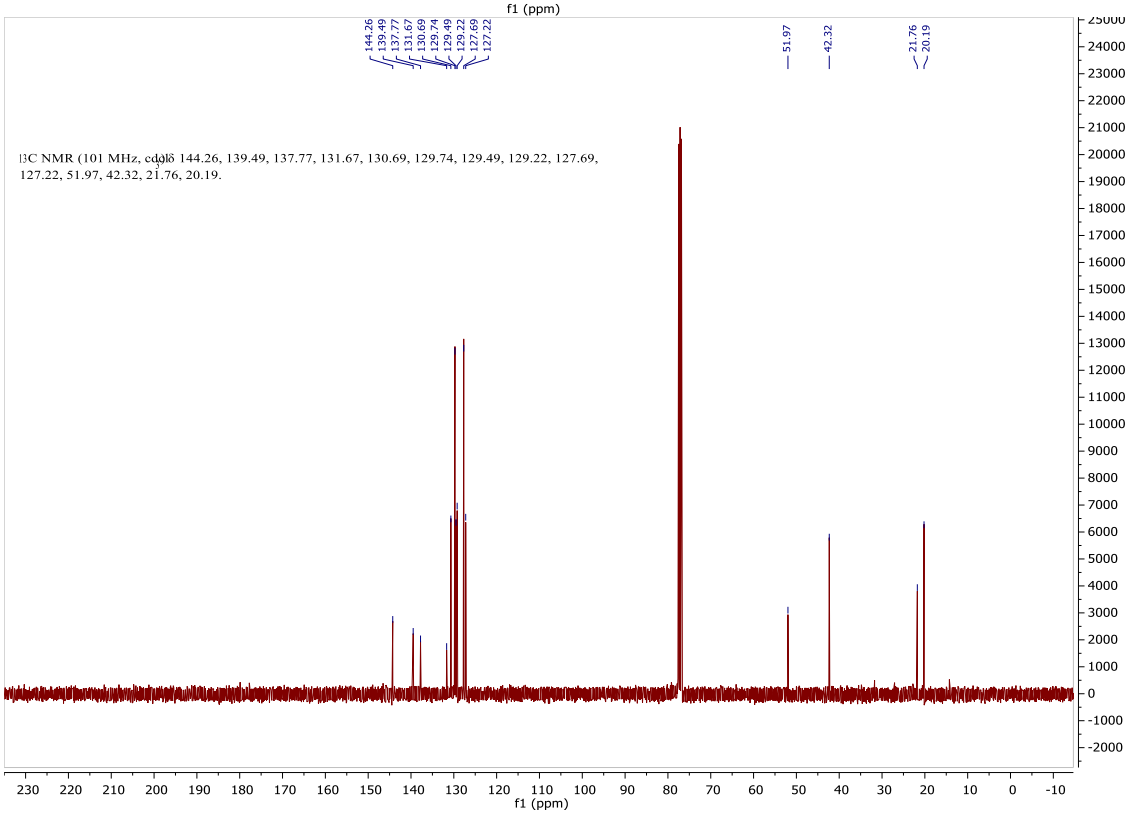
144.26
139.49
137.77
131.67
130.69
129.74
129.49
129.22
127.69
127.22
51.97
42.32
21.76
20.19
13C NMR (101 MHz, cdcl3) δ 144.26, 139.49, 137.77, 131.67, 130.69, 129.74, 129.49, 129.22, 127.69, 127.22, 51.97, 42.32, 21.76, 20.19.
f1 (ppm)

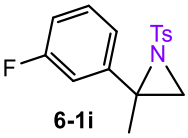

6-1i

^{1}H NMR (400 MHz, Chloroform-*d*) δ 7.90 – 7.84 (m, 2H), 7.36 – 7.32 (m, 2H), 7.32 – 7.27 (m, 1H), 7.16 (ddd, *J* = 7.7, 1.7, 1.0 Hz, 1H), 7.07 (ddd, *J* = 9.9, 2.6, 1.7 Hz, 1H), 7.01 – 6.93 (m, 1H), 2.97 (s, 1H), 2.47 (s, 1H), 2.44 (s, 3H), 2.05 (s, 3H).

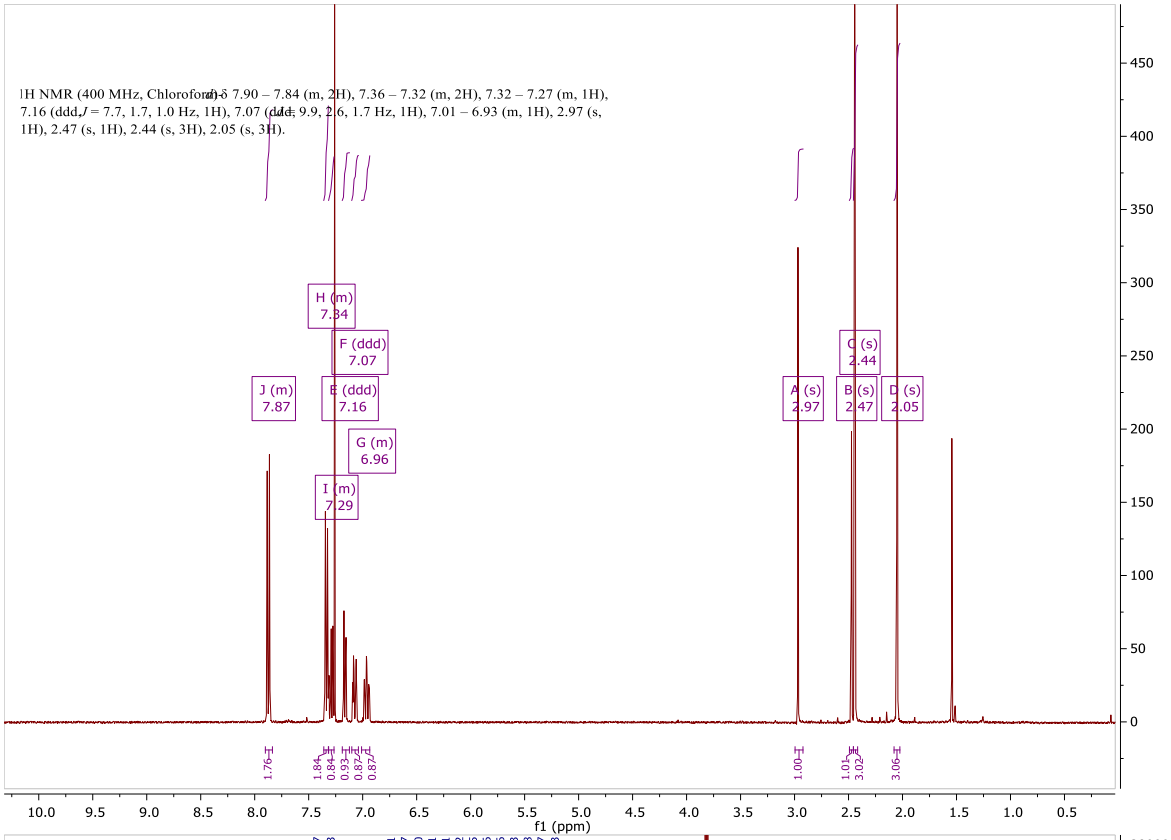

^{13}C NMR (101 MHz, Chloroform-*d*) δ 164.07, 161.63, 144.31, 143.73 (d, *J* = 7.4 Hz), 137.71, 130.16 (d, *J* = 8.2 Hz), 129.75, 127.66, 122.25 (d, *J* = 3.0 Hz), 114.88 (d, *J* = 21.1 Hz), 113.73, 42.18, 21.77, 20.55.

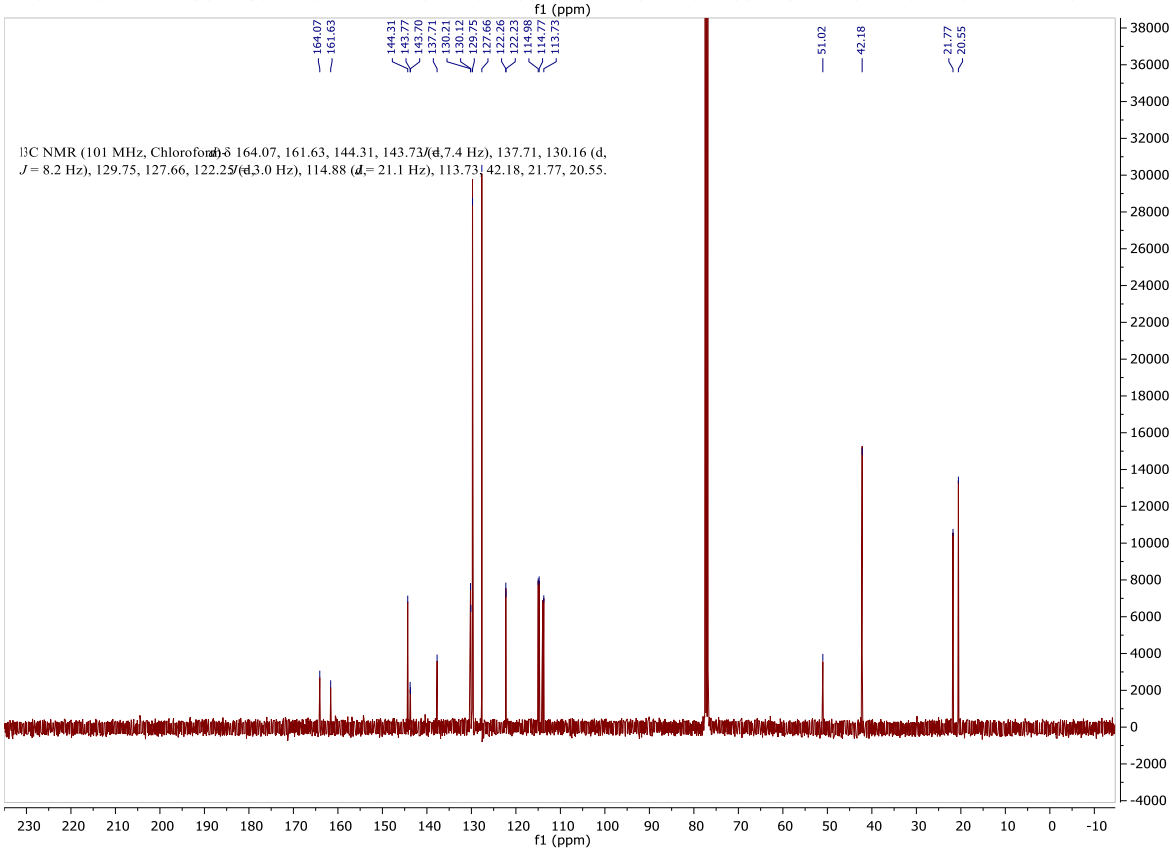

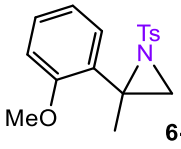
Ts
N
MeO

6-1g

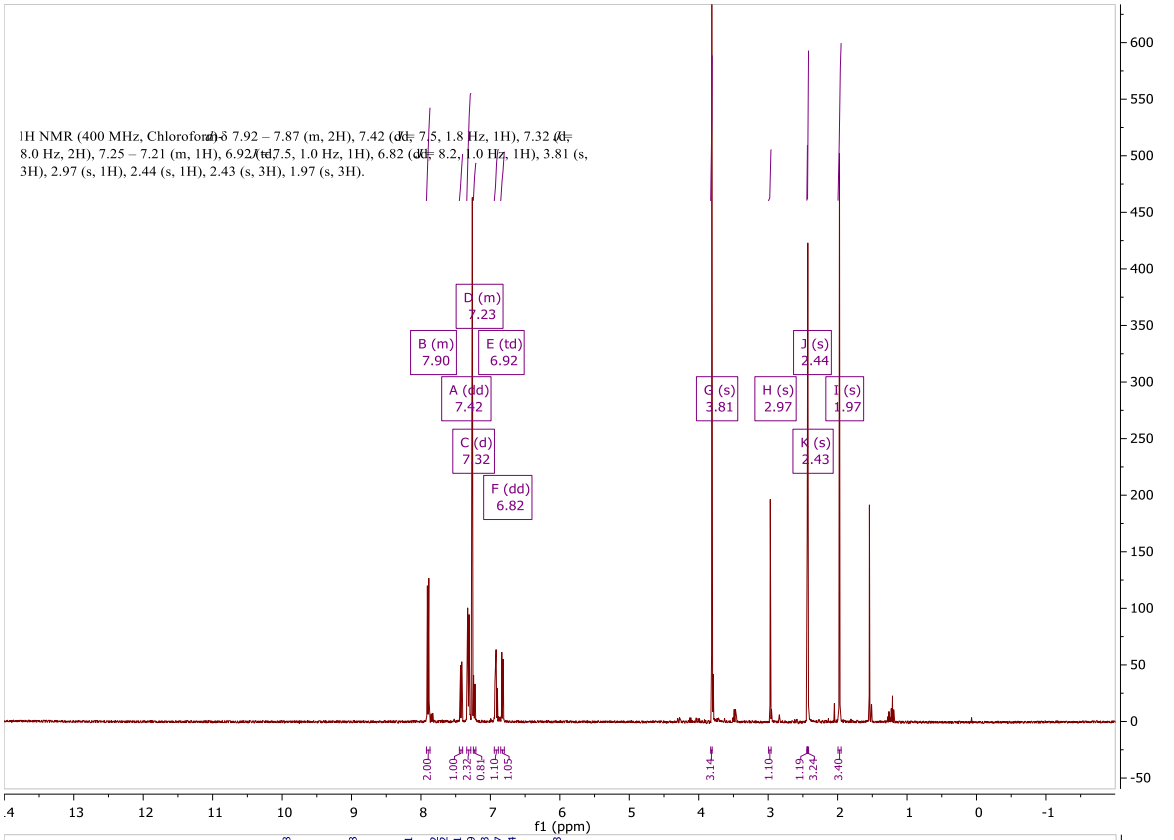
1H NMR (400 MHz, Chloroform-d) δ 7.92 – 7.87 (m, 2H), 7.42 (dd, J = 7.5, 1.8 Hz, 1H), 7.32 (d, J = 8.0 Hz, 2H), 7.25 – 7.21 (m, 1H), 6.92 (td, J = 7.5, 1.0 Hz, 1H), 6.82 (dd, J = 8.2, 1.0 Hz, 1H), 3.81 (s, 3H), 2.97 (s, 1H), 2.44 (s, 1H), 2.43 (s, 3H), 1.97 (s, 3H).
D (m) 7.23
B (m) 7.90
E (td) 6.92
A (dd) 7.42
C (d) 7.32
F (dd) 6.82
G (s) 3.81
H (s) 2.97
J (s) 2.44
K (s) 2.43
I (s) 1.97
2.00
1.00
2.32
0.81
1.10
1.05
3.14
1.10
1.19
3.24
3.40
f1 (ppm)

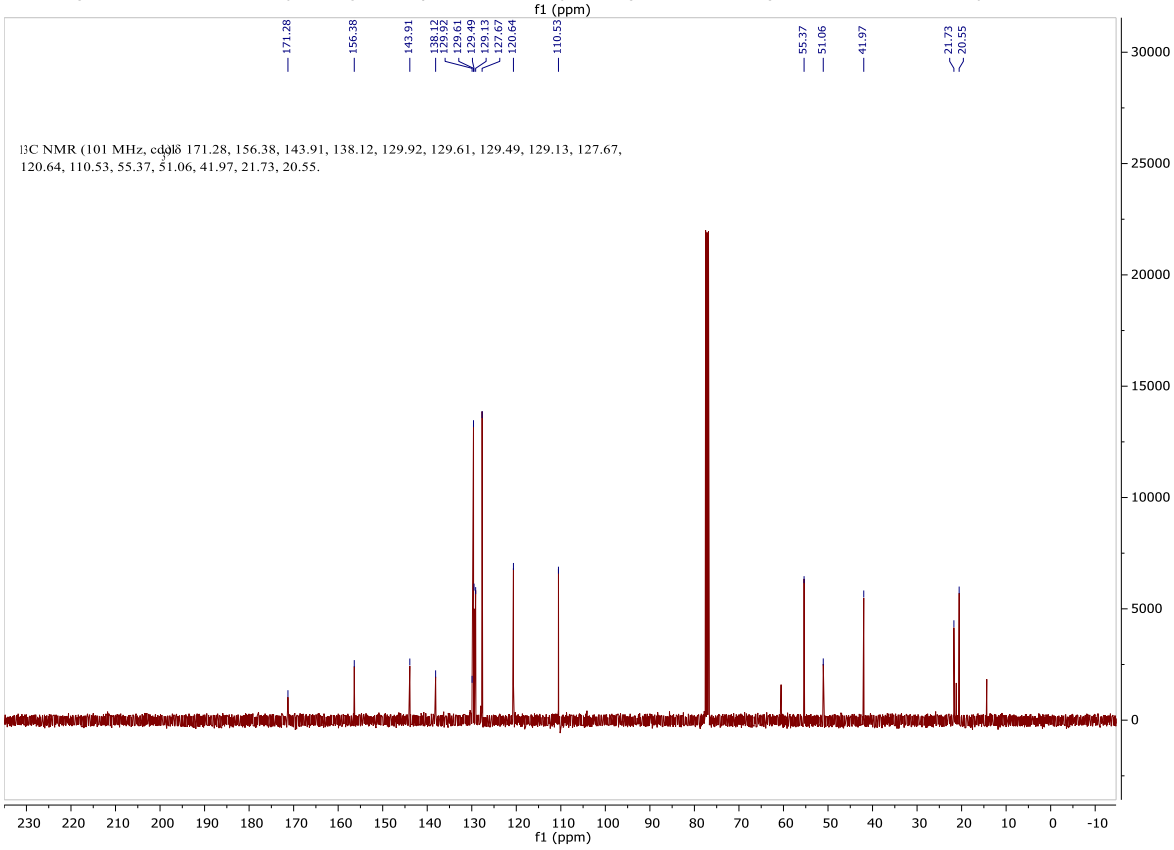
171.28
156.38
143.91
138.12
129.92
129.61
129.49
129.13
127.67
120.64
110.53
55.37
51.06
41.97
21.73
20.55
13C NMR (101 MHz, cdcl3) δ 171.28, 156.38, 143.91, 138.12, 129.92, 129.61, 129.49, 129.13, 127.67, 120.64, 110.53, 55.37, 51.06, 41.97, 21.73, 20.55.
f1 (ppm)

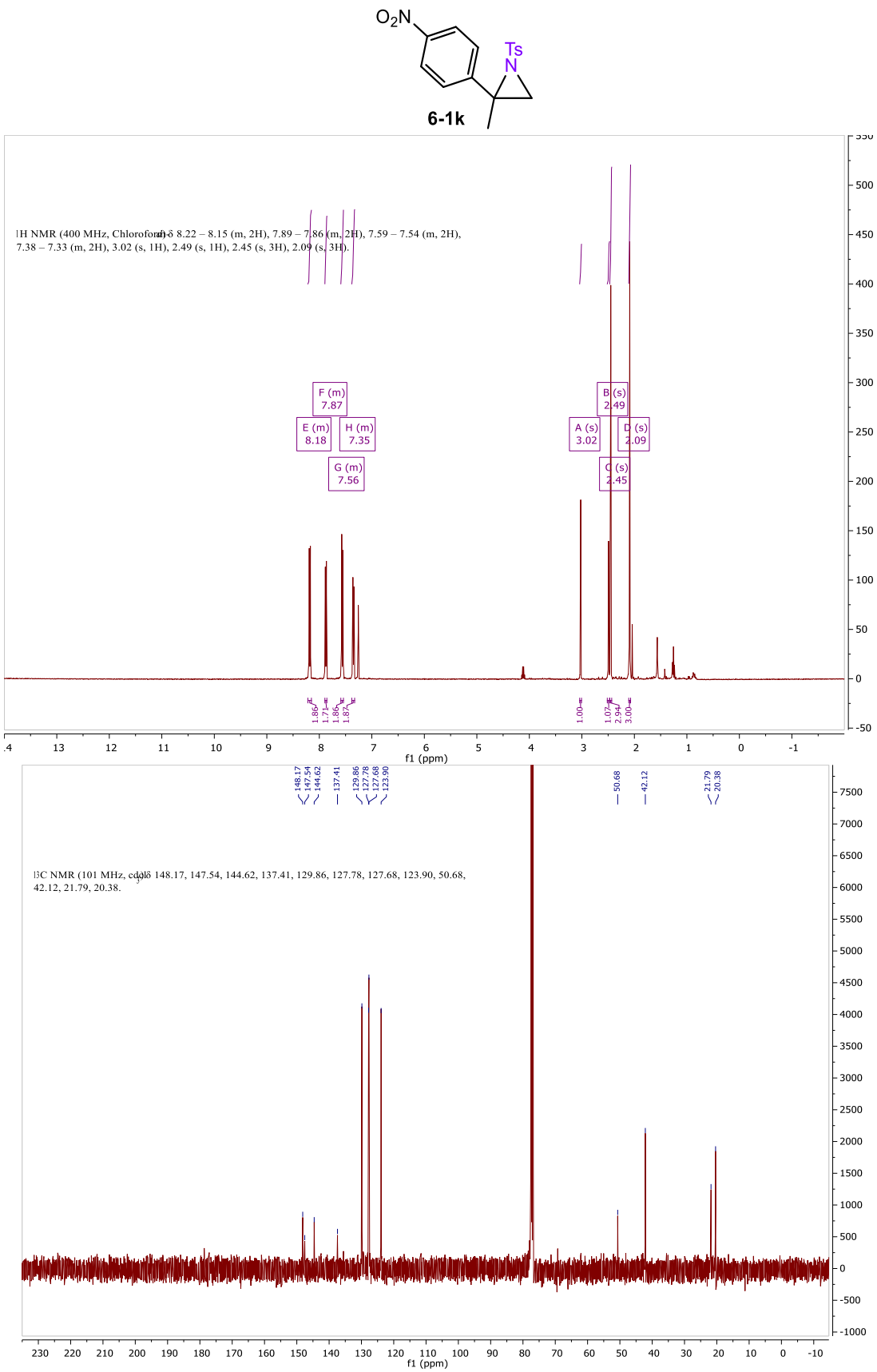
O2N
Ts
N
6-1k
1H NMR (400 MHz, Chloroform-d) δ 8.22 – 8.15 (m, 2H), 7.89 – 7.86 (m, 2H), 7.59 – 7.54 (m, 2H), 7.38 – 7.33 (m, 2H), 3.02 (s, 1H), 2.49 (s, 1H), 2.45 (s, 3H), 2.09 (s, 3H).
F (m) 7.87
E (m) 8.18
H (m) 7.35
G (m) 7.56
B (s) 2.49
A (s) 3.02
D (s) 2.09
C (s) 2.45
1.86
1.71
1.86
1.87
1.00
1.07
2.94
3.00
f1 (ppm)
13C NMR (101 MHz, cdcl3) δ 148.17, 147.54, 144.62, 137.41, 129.86, 127.78, 127.68, 123.90, 50.68, 42.12, 21.79, 20.38.
148.17
147.54
144.62
137.41
129.86
127.78
127.68
123.90
50.68
42.12
21.79
20.38
f1 (ppm)

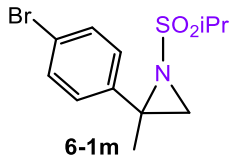
Br
SO2iPr
N

6-1m

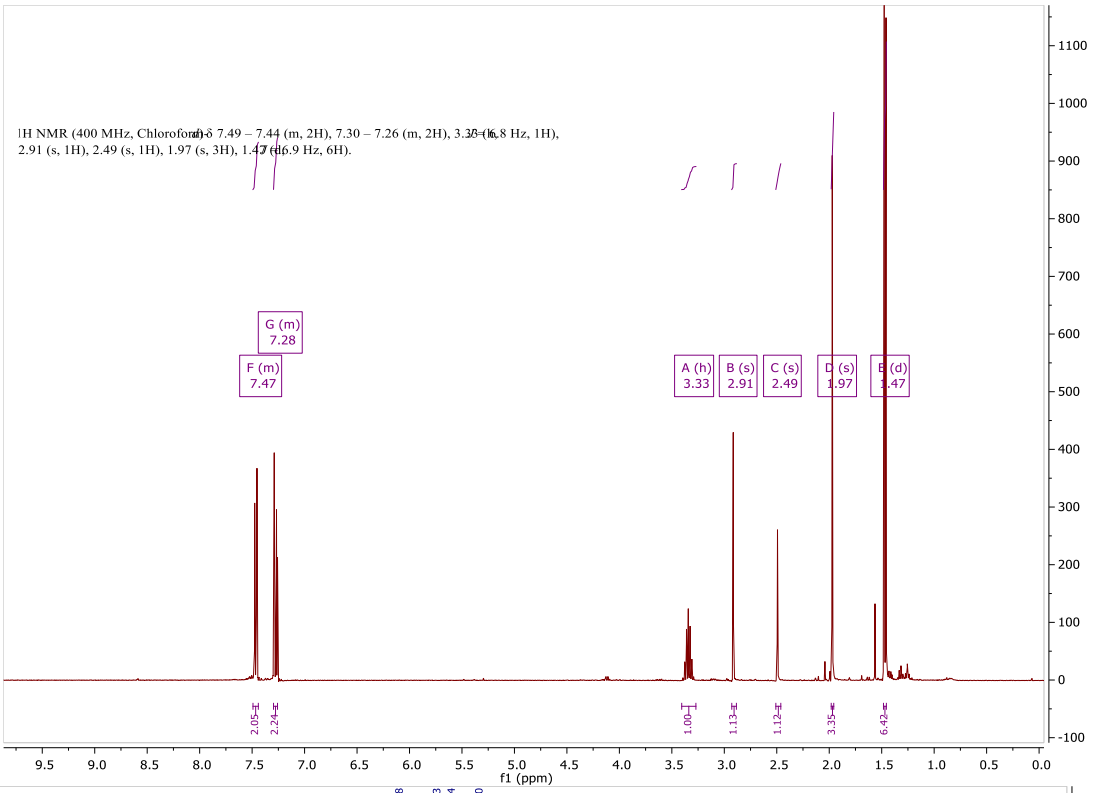
1H NMR (400 MHz, Chloroform-d) δ 7.49 – 7.44 (m, 2H), 7.30 – 7.26 (m, 2H), 3.33 (h, J = 6.8 Hz, 1H), 2.91 (s, 1H), 2.49 (s, 1H), 1.97 (s, 3H), 1.47 (d, J = 6.9 Hz, 6H).
G (m) 7.28
F (m) 7.47
A (h) 3.33
B (s) 2.91
C (s) 2.49
D (s) 1.97
E (d) 1.47
2.05
2.24
1.00
1.13
1.12
3.35
6.42
f1 (ppm)

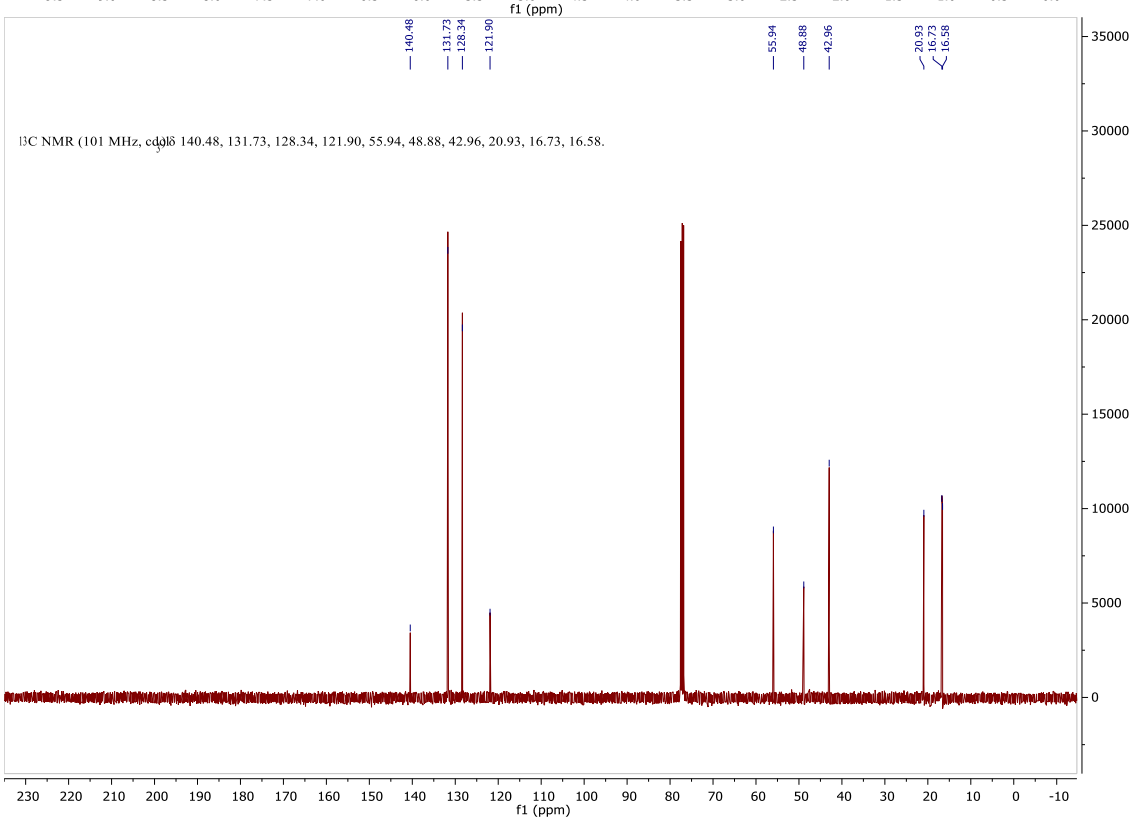
13C NMR (101 MHz, cdcl3) δ 140.48, 131.73, 128.34, 121.90, 55.94, 48.88, 42.96, 20.93, 16.73, 16.58.
140.48
131.73
128.34
121.90
55.94
48.88
42.96
20.93
16.73
16.58
f1 (ppm)

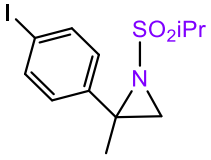
I
SO2iPr
N

6-1l

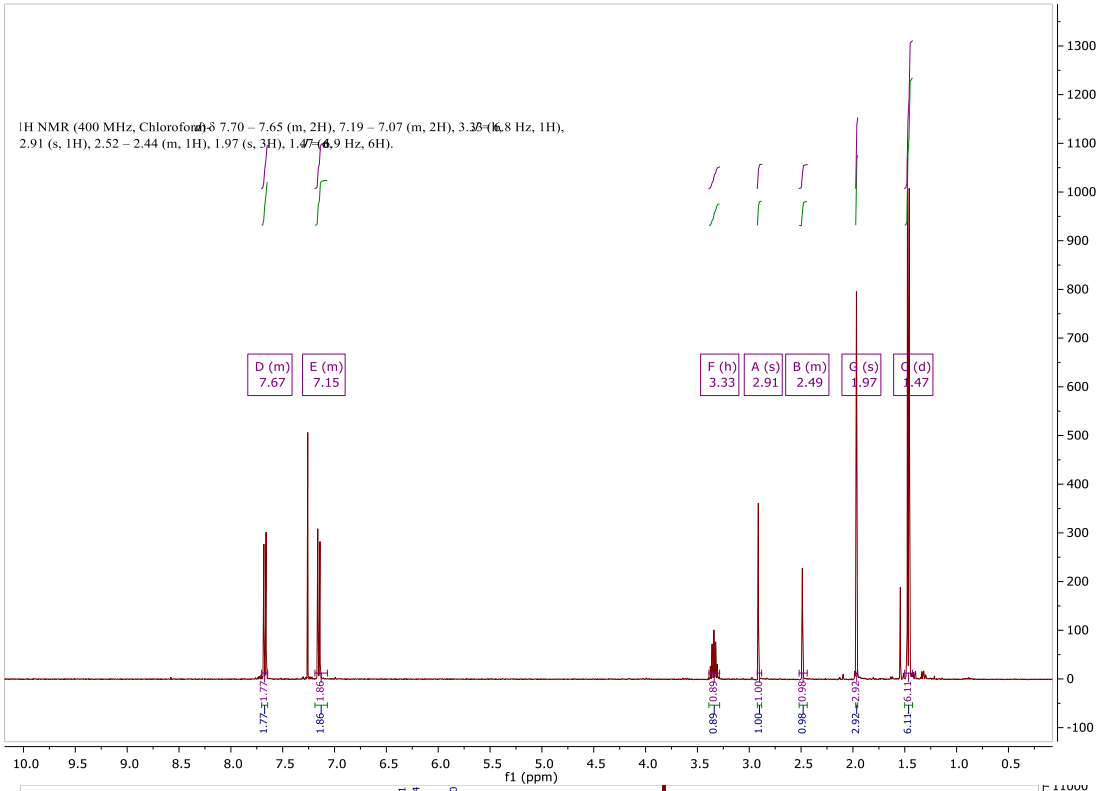
1H NMR (400 MHz, Chloroform-d) δ 7.70 – 7.65 (m, 2H), 7.19 – 7.07 (m, 2H), 3.33 (h, 6.8 Hz, 1H), 2.91 (s, 1H), 2.52 – 2.44 (m, 1H), 1.97 (s, 3H), 1.47 (d, 6.9 Hz, 6H).
D (m) 7.67
E (m) 7.15
F (h) 3.33
A (s) 2.91
B (m) 2.49
C (s) 1.97
G (d) 1.47
f1 (ppm)

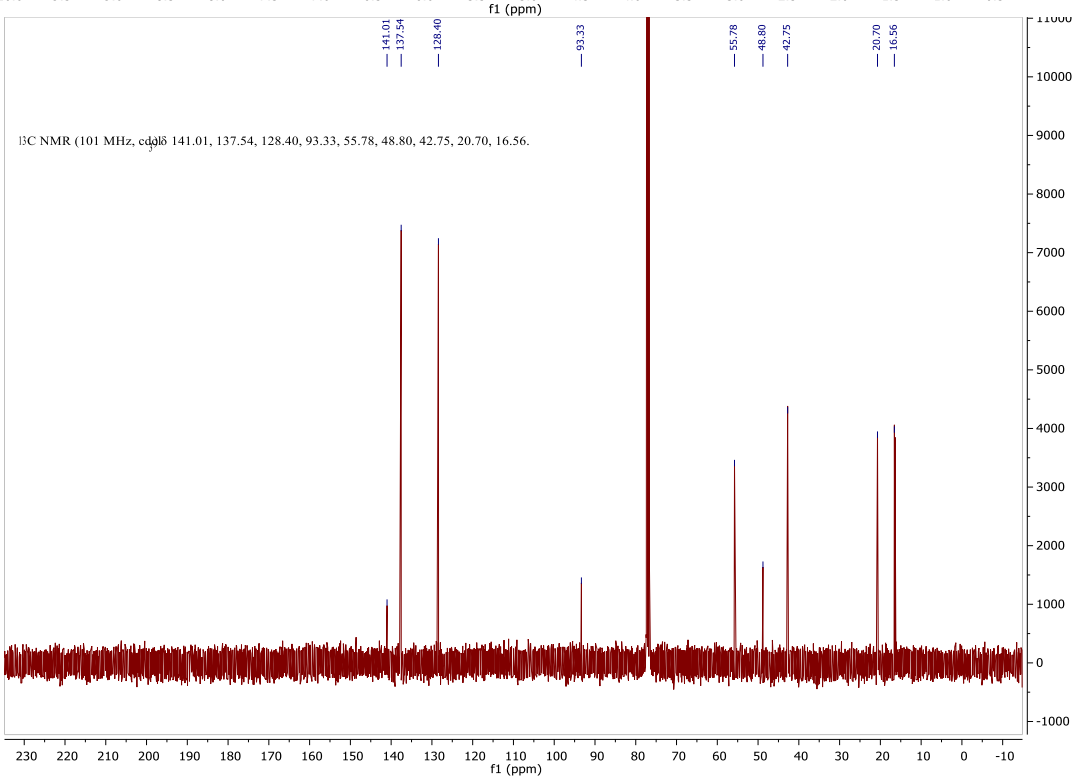
13C NMR (101 MHz, cdcl3) δ 141.01, 137.54, 128.40, 93.33, 55.78, 48.80, 42.75, 20.70, 16.56.
141.01
137.54
128.40
93.33
55.78
48.80
42.75
20.70
16.56
f1 (ppm)

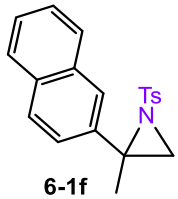
Ts
N

6-1f

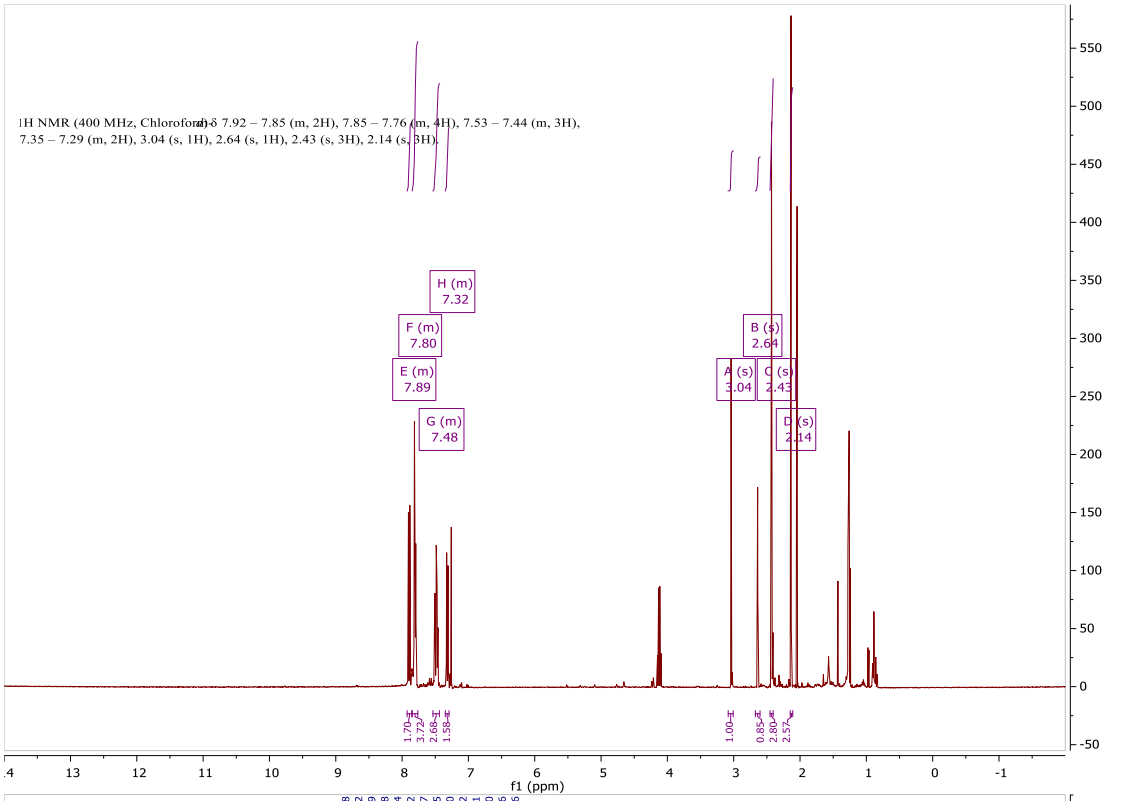
1H NMR (400 MHz, Chloroform-d) δ 7.92 – 7.85 (m, 2H), 7.85 – 7.76 (m, 4H), 7.53 – 7.44 (m, 3H), 7.35 – 7.29 (m, 2H), 3.04 (s, 1H), 2.64 (s, 1H), 2.43 (s, 3H), 2.14 (s, 3H).
H (m) 7.32
F (m) 7.80
E (m) 7.89
G (m) 7.48
B (s) 2.64
A (s) 3.04
C (s) 2.43
D (s) 2.14
f1 (ppm)

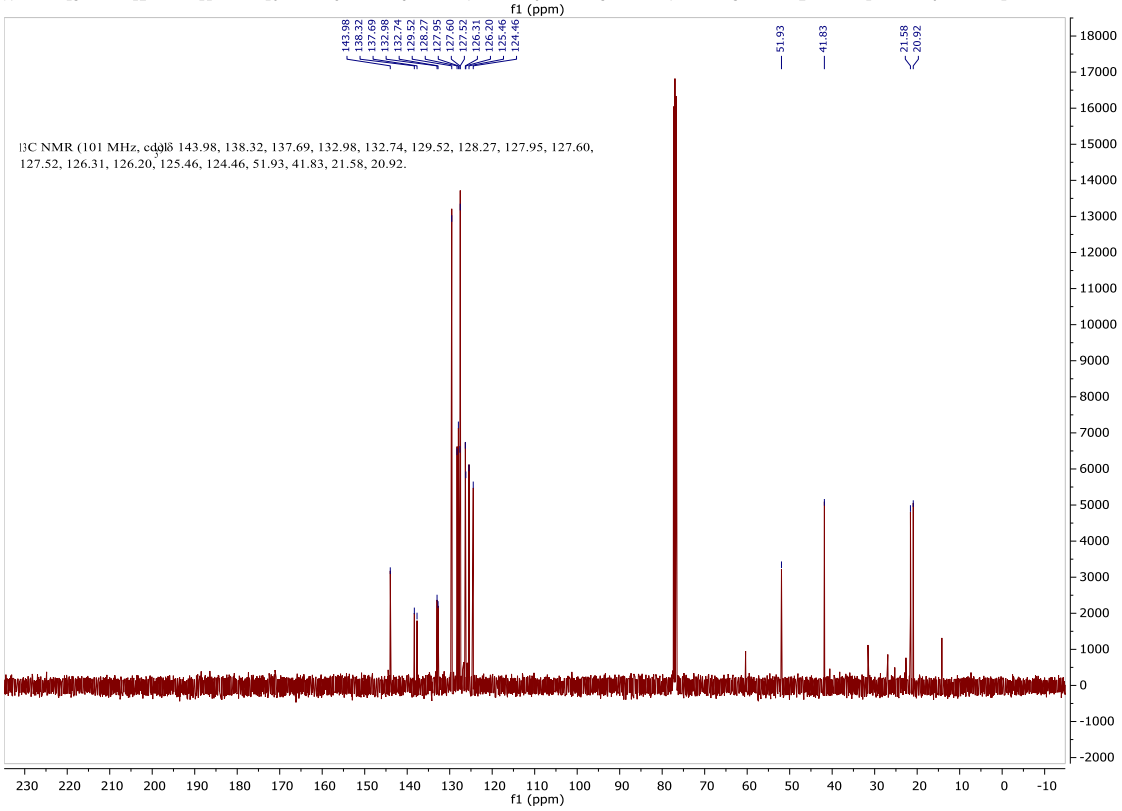
13C NMR (101 MHz, cdcl3) δ 143.98, 138.32, 137.69, 132.98, 132.74, 129.52, 128.27, 127.95, 127.60, 127.52, 126.31, 126.20, 125.46, 124.46, 51.93, 41.83, 21.58, 20.92.
143.98
138.32
137.69
132.98
132.74
129.52
128.27
127.95
127.60
127.52
126.31
126.20
125.46
124.46
51.93
41.83
21.58
20.92
f1 (ppm)

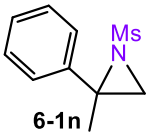
Ms
N

6-1n

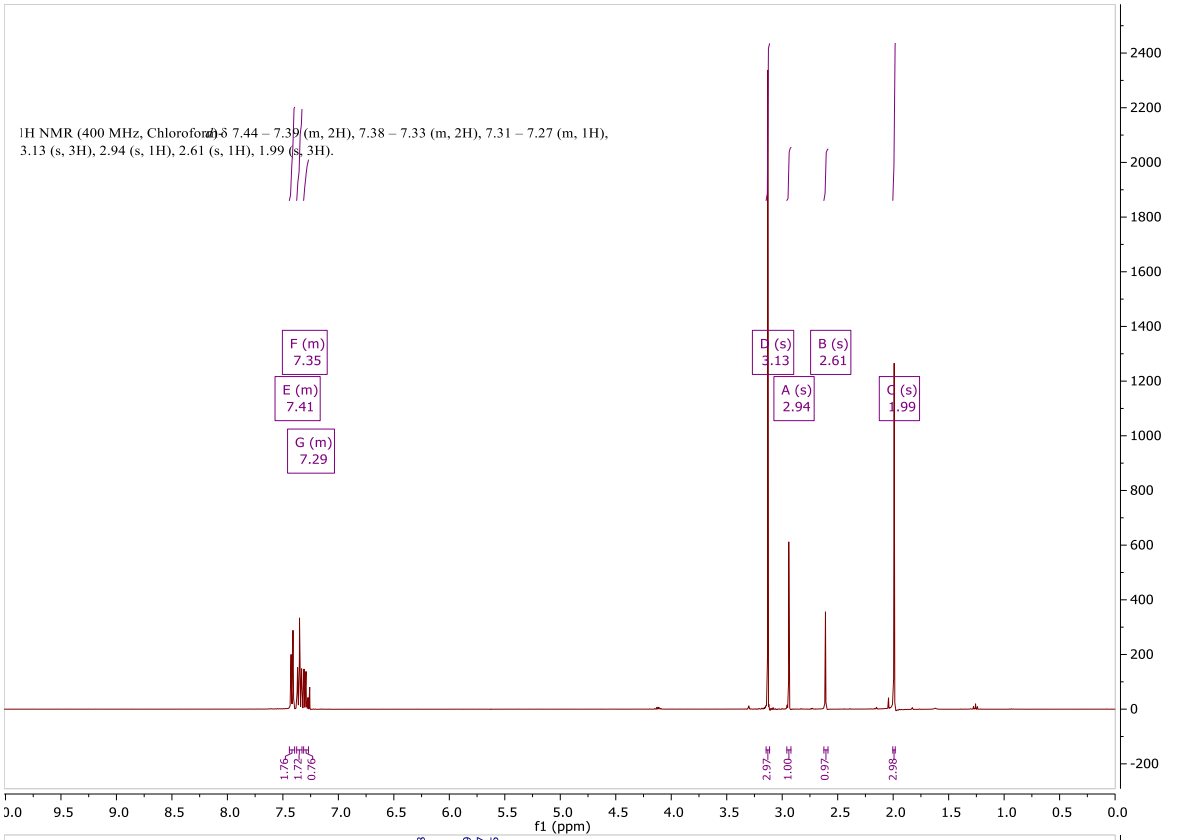
1H NMR (400 MHz, Chloroform-d) δ 7.44 – 7.39 (m, 2H), 7.38 – 7.33 (m, 2H), 7.31 – 7.27 (m, 1H), 3.13 (s, 3H), 2.94 (s, 1H), 2.61 (s, 1H), 1.99 (s, 3H).
F (m) 7.35
E (m) 7.41
G (m) 7.29
D (s) 3.13
B (s) 2.61
A (s) 2.94
C (s) 1.99
f1 (ppm)

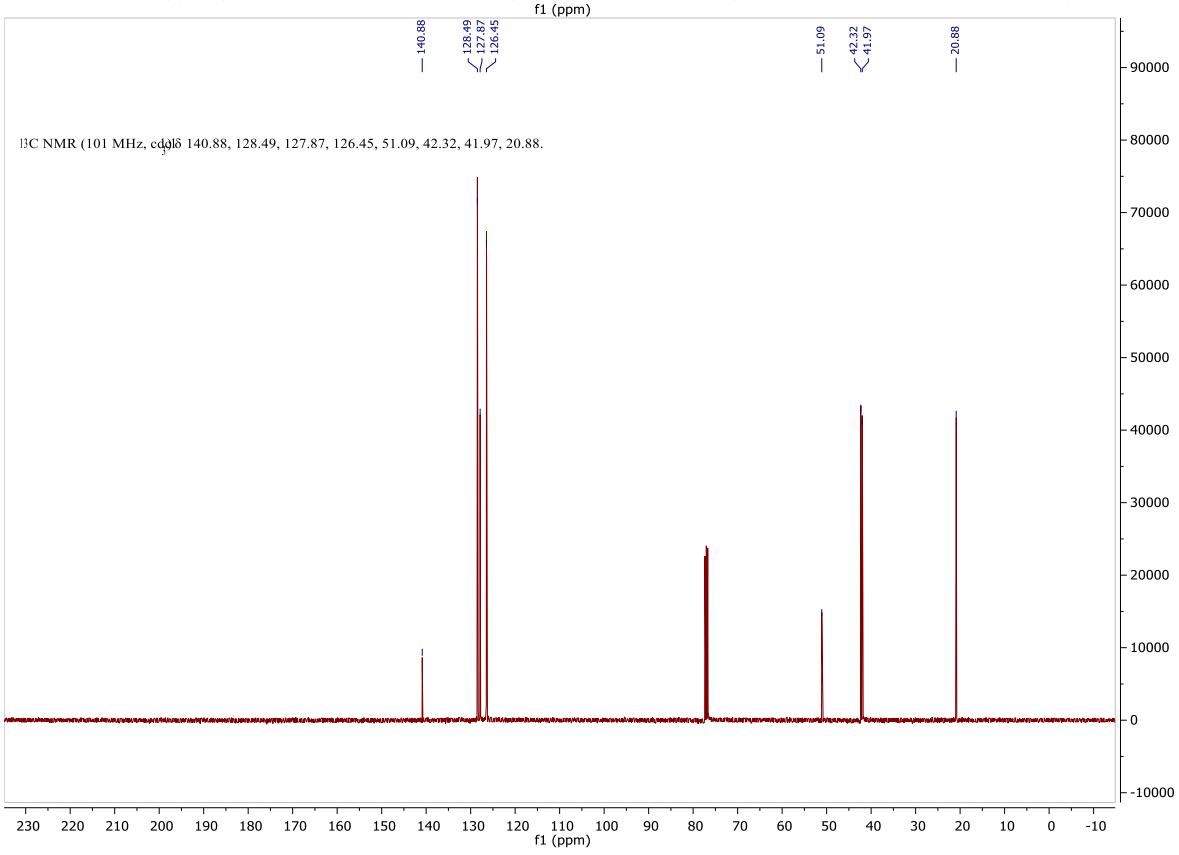
13C NMR (101 MHz, cdcl3) δ 140.88, 128.49, 127.87, 126.45, 51.09, 42.32, 41.97, 20.88.
140.88
128.49
127.87
126.45
51.09
42.32
41.97
20.88
f1 (ppm)

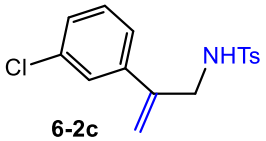
Cl
NHTs

6-2c

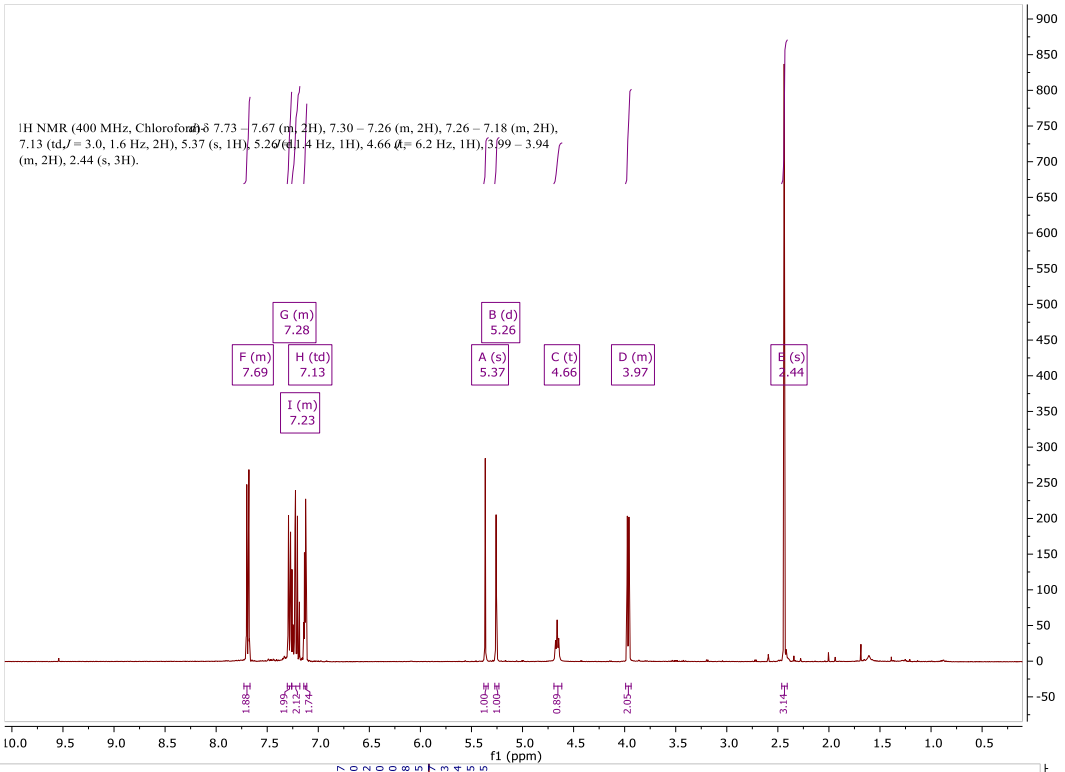
1H NMR (400 MHz, Chloroform-d) δ 7.73 – 7.67 (m, 2H), 7.30 – 7.26 (m, 2H), 7.26 – 7.18 (m, 2H), 7.13 (td, J = 3.0, 1.6 Hz, 2H), 5.37 (s, 1H), 5.26 (d, J = 1.4 Hz, 1H), 4.66 (t, J = 6.2 Hz, 1H), 3.99 – 3.94 (m, 2H), 2.44 (s, 3H).
G (m) 7.28
B (d) 5.26
F (m) 7.69
H (td) 7.13
A (s) 5.37
C (t) 4.66
D (m) 3.97
E (s) 2.44
I (m) 7.23
f1 (ppm)

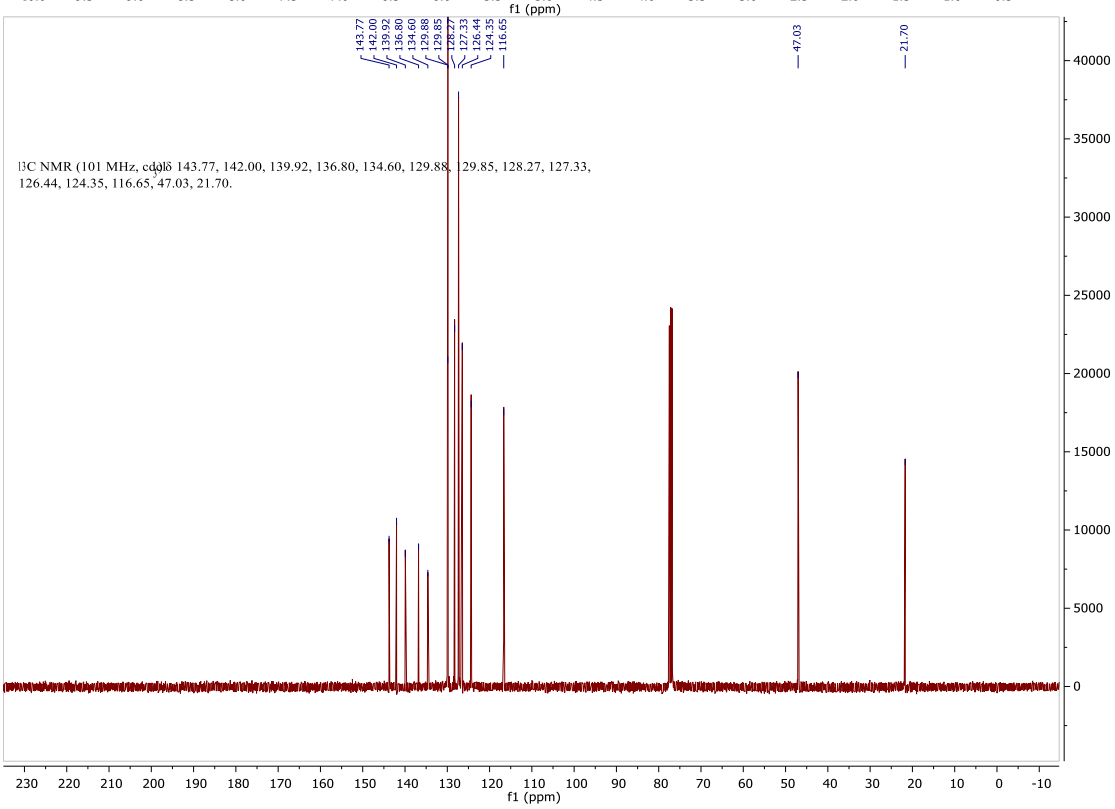
13C NMR (101 MHz, cdcl3) δ 143.77, 142.00, 139.92, 136.80, 134.60, 129.88, 129.85, 128.27, 127.33, 126.44, 124.35, 116.65, 47.03, 21.70.
143.77
142.00
139.92
136.80
134.60
129.88
129.85
128.27
127.33
126.44
124.35
116.65
47.03
21.70
f1 (ppm)

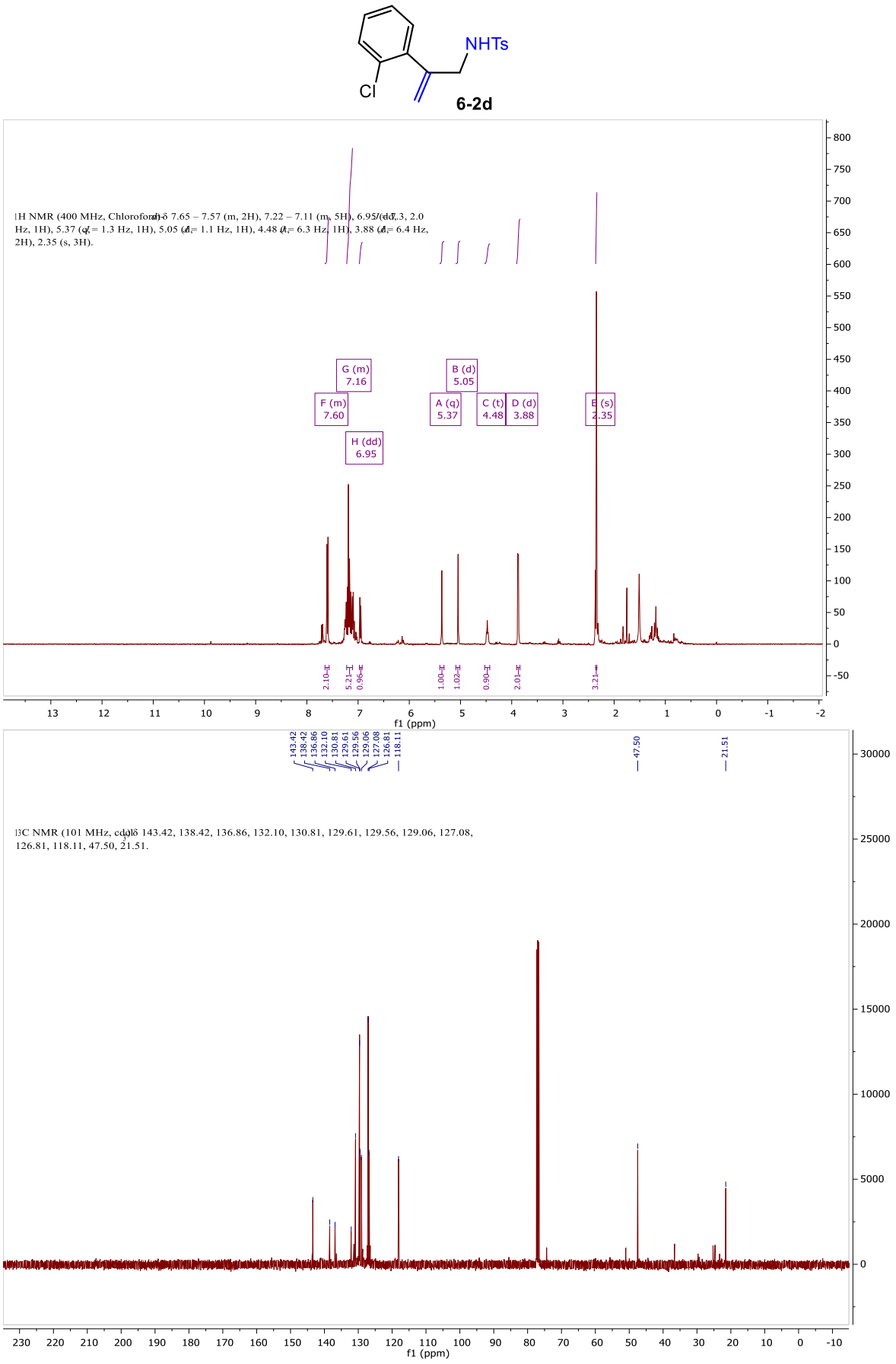
NHTs
Cl
6-2d
1H NMR (400 MHz, Chloroform-d) δ 7.65 – 7.57 (m, 2H), 7.22 – 7.11 (m, 5H), 6.95 (dd, J = 7.3, 2.0 Hz, 1H), 5.37 (q, J = 1.3 Hz, 1H), 5.05 (d, J = 1.1 Hz, 1H), 4.48 (t, J = 6.3 Hz, 1H), 3.88 (d, J = 6.4 Hz, 2H), 2.35 (s, 3H).
G (m) 7.16
B (d) 5.05
F (m) 7.60
A (q) 5.37
C (t) 4.48
D (d) 3.88
E (s) 2.35
H (dd) 6.95
2.10
5.21
0.96
1.00
1.02
0.90
2.01
3.21
f1 (ppm)
143.42
138.42
136.86
132.10
130.81
129.61
129.56
129.06
127.08
126.81
118.11
47.50
21.51
13C NMR (101 MHz, cdcl3) δ 143.42, 138.42, 136.86, 132.10, 130.81, 129.61, 129.56, 129.06, 127.08, 126.81, 118.11, 47.50, 21.51.
f1 (ppm)

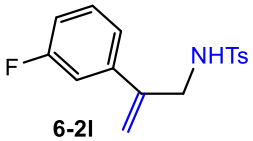
F
NHTs

6-2l

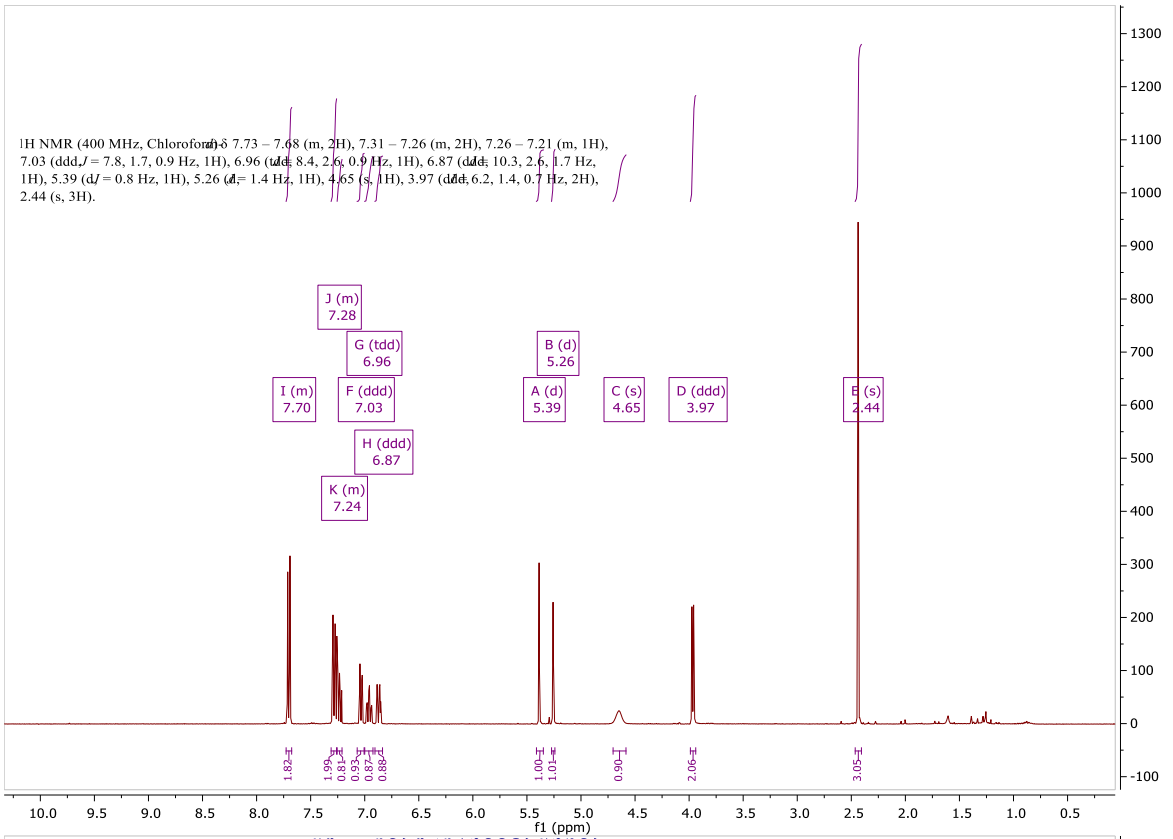
1H NMR (400 MHz, Chloroform-d) δ 7.73 – 7.68 (m, 2H), 7.31 – 7.26 (m, 2H), 7.26 – 7.21 (m, 1H), 7.03 (ddd, J = 7.8, 1.7, 0.9 Hz, 1H), 6.96 (tdd, J = 8.4, 2.6, 0.9 Hz, 1H), 6.87 (ddd, J = 10.3, 2.6, 1.7 Hz, 1H), 5.39 (d, J = 0.8 Hz, 1H), 5.26 (d, J = 1.4 Hz, 1H), 4.65 (s, 1H), 3.97 (ddt, J = 6.2, 1.4, 0.7 Hz, 2H), 2.44 (s, 3H).
J (m) 7.28
G (tdd) 6.96
B (d) 5.26
I (m) 7.70
F (ddd) 7.03
A (d) 5.39
C (s) 4.65
D (ddd) 3.97
E (s) 2.44
H (ddd) 6.87
K (m) 7.24
1.82
1.99
0.81
0.93
0.87
0.88
1.00
1.01
0.90
2.06
3.05
f1 (ppm)

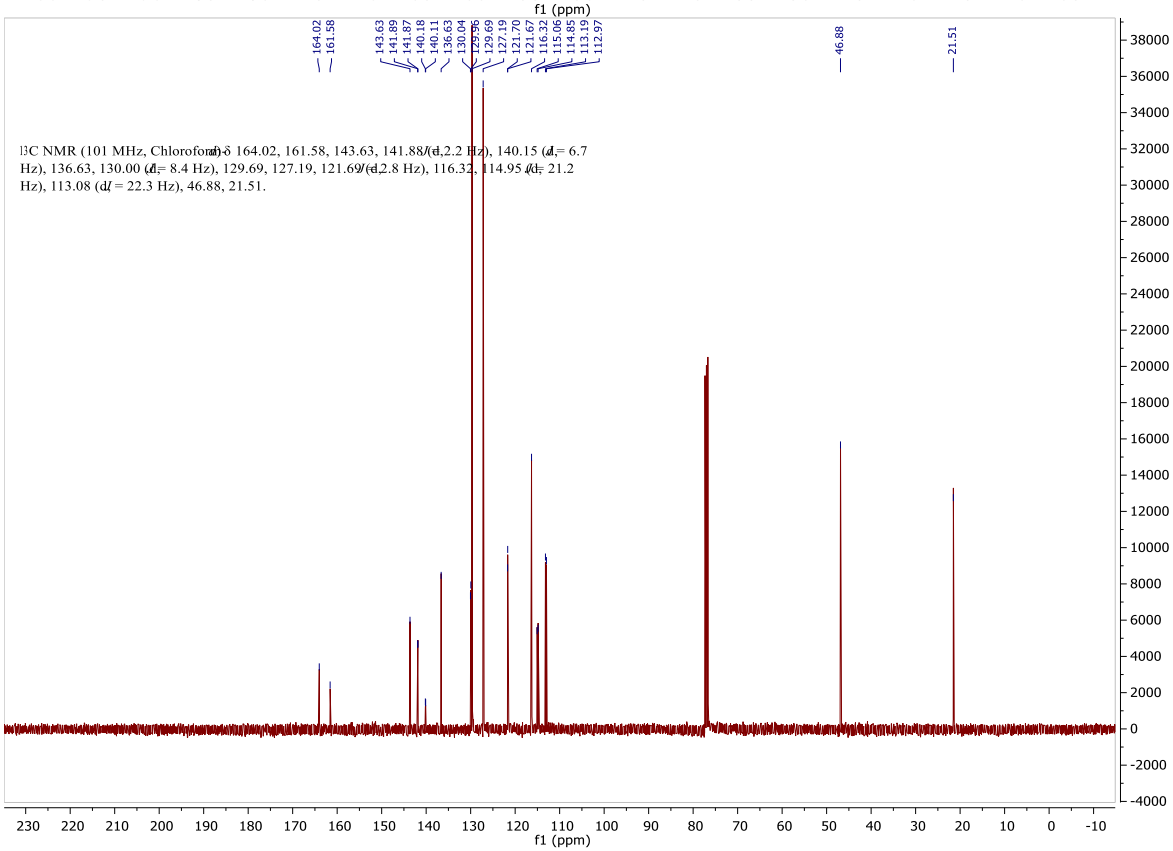
164.02
161.58
143.63
141.89
141.87
140.18
140.11
136.63
130.04
129.96
129.69
127.19
121.70
121.67
116.32
115.06
114.85
113.19
112.97
46.88
21.51
13C NMR (101 MHz, Chloroform-d) δ 164.02, 161.58, 143.63, 141.88 (d, J = 2.2 Hz), 140.15 (d, J = 6.7 Hz), 136.63, 130.00 (d, J = 8.4 Hz), 129.69, 127.19, 121.69 (d, J = 2.8 Hz), 116.32, 114.95 (d, J = 21.2 Hz), 113.08 (d, J = 22.3 Hz), 46.88, 21.51.
f1 (ppm)

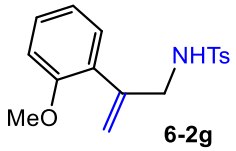

6-2g

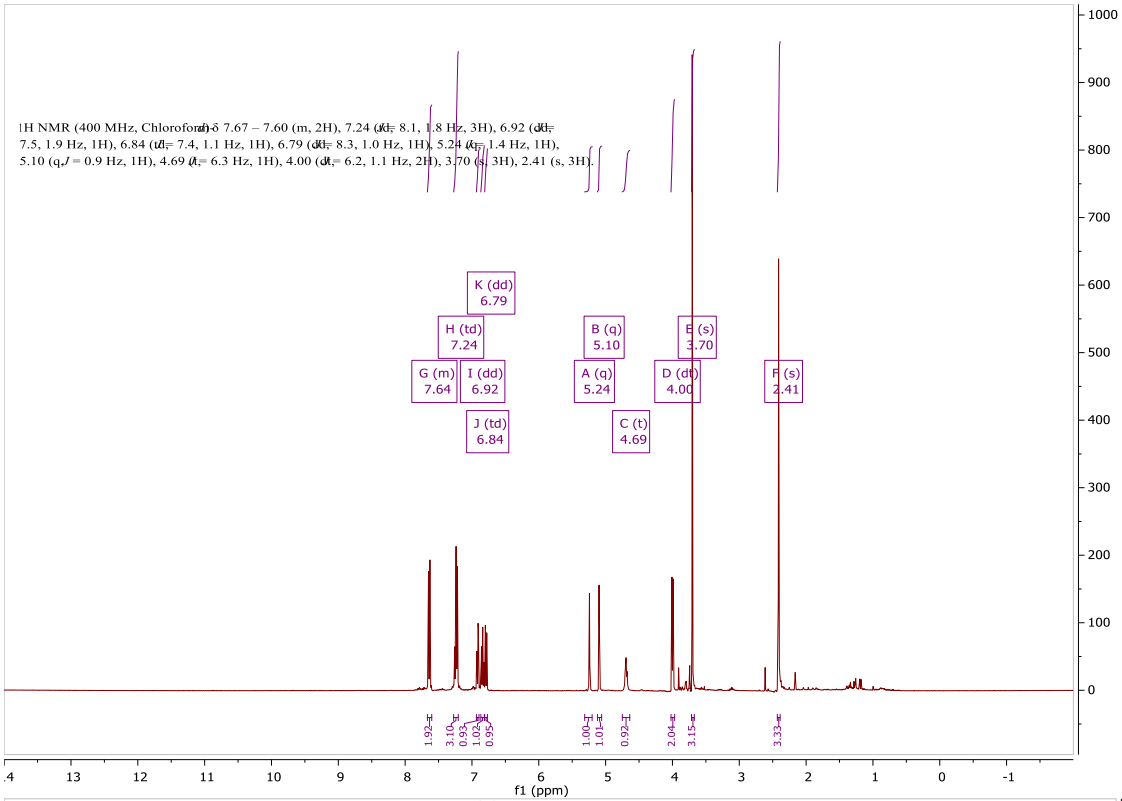

^{1}H NMR (400 MHz, Chloroform-*d*) δ 7.67 – 7.60 (m, 2H), 7.24 (dd, *J* = 8.1, 1.8 Hz, 3H), 6.92 (dd, *J* = 7.5, 1.9 Hz, 1H), 6.84 (td, *J* = 7.4, 1.1 Hz, 1H), 6.79 (dd, *J* = 8.3, 1.0 Hz, 1H), 5.24 (q, *J* = 1.4 Hz, 1H), 5.10 (q, *J* = 0.9 Hz, 1H), 4.69 (t, *J* = 6.3 Hz, 1H), 4.00 (dd, *J* = 6.2, 1.1 Hz, 2H), 3.70 (s, 3H), 2.41 (s, 3H).

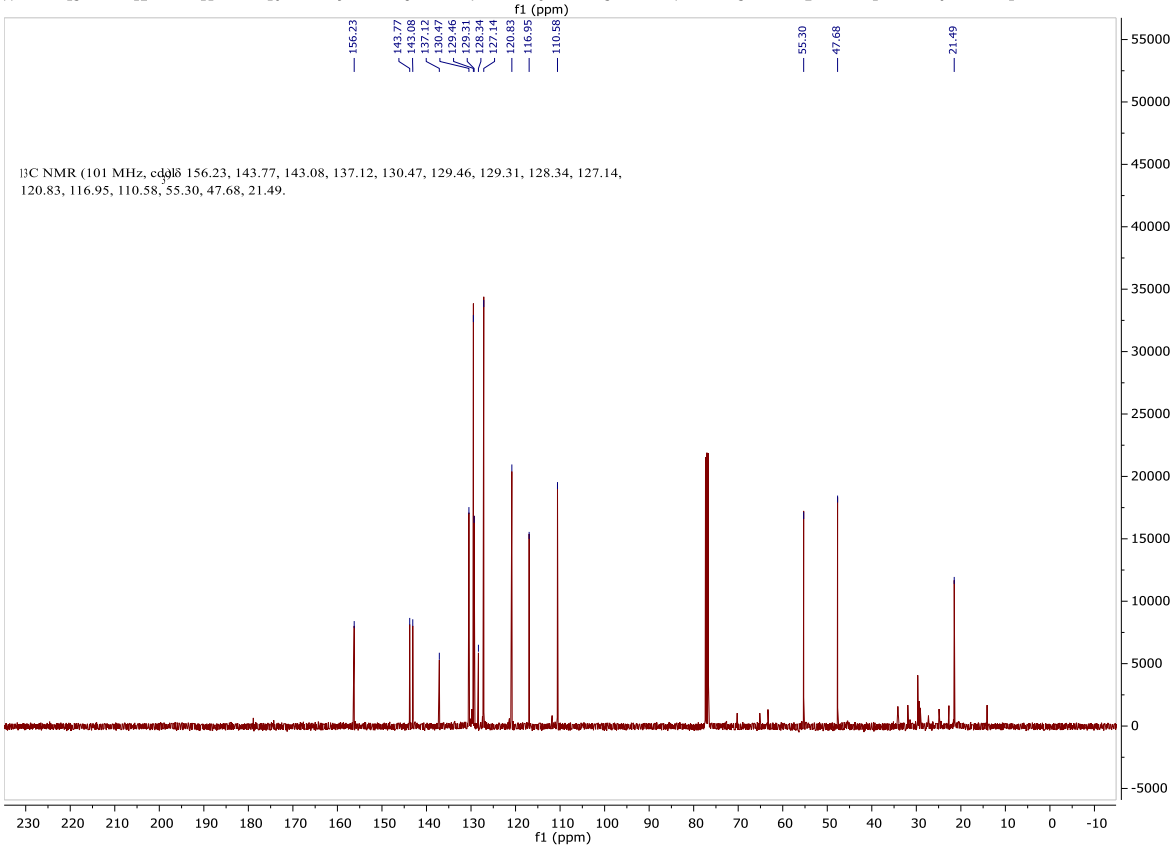

^{13}C NMR (101 MHz, cdcl$_3$) δ 156.23, 143.77, 143.08, 137.12, 130.47, 129.46, 129.31, 128.34, 127.14, 120.83, 116.95, 110.58, 55.30, 47.68, 21.49.

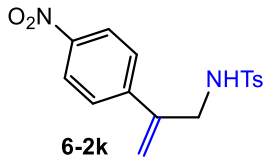
O2N
NHTs

6-2k

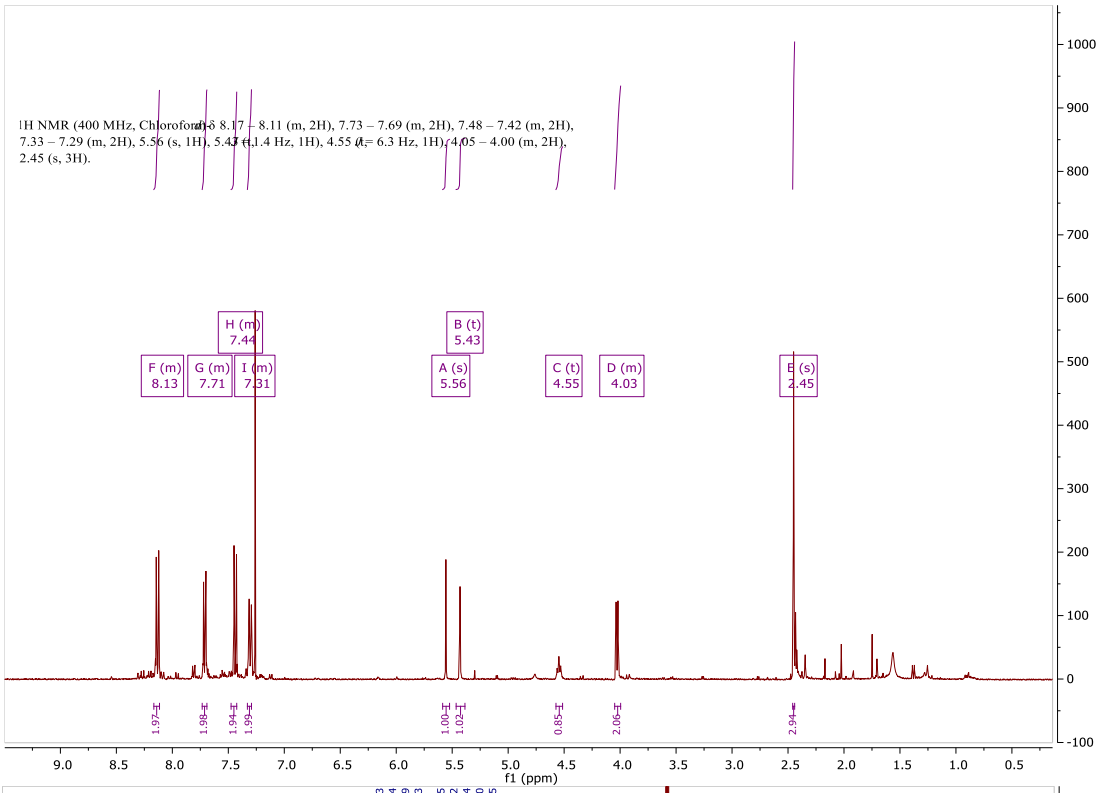
1H NMR (400 MHz, Chloroform-d) δ 8.17 – 8.11 (m, 2H), 7.73 – 7.69 (m, 2H), 7.48 – 7.42 (m, 2H), 7.33 – 7.29 (m, 2H), 5.56 (s, 1H), 5.43 (t, J = 1.4 Hz, 1H), 4.55 (t, J = 6.3 Hz, 1H), 4.05 – 4.00 (m, 2H), 2.45 (s, 3H).
H (m) 7.44
B (t) 5.43
F (m) 8.13
G (m) 7.71
I (m) 7.31
A (s) 5.56
C (t) 4.55
D (m) 4.03
E (s) 2.45
1.97
1.98
1.94
1.99
1.00
1.02
0.85
2.06
2.94
f1 (ppm)

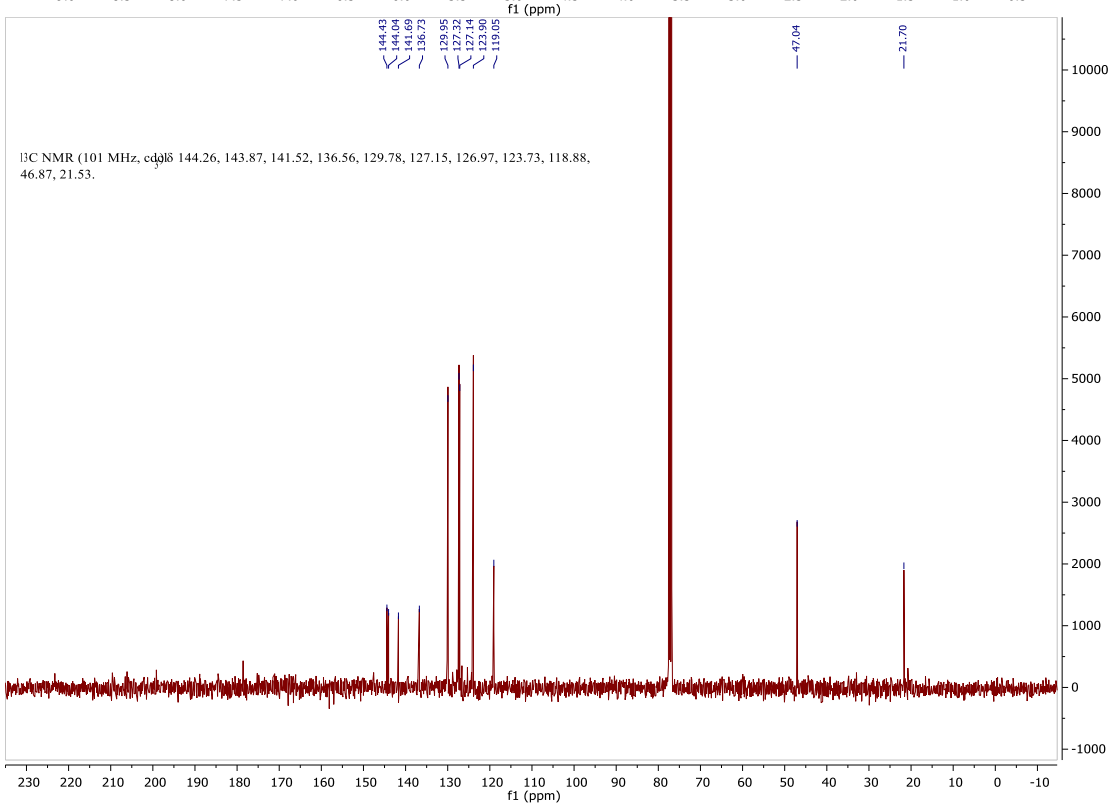
13C NMR (101 MHz, cdcl3) δ 144.26, 143.87, 141.52, 136.56, 129.78, 127.15, 126.97, 123.73, 118.88, 46.87, 21.53.
144.43
144.04
141.69
136.73
129.95
127.32
127.14
123.90
119.05
47.04
21.70
f1 (ppm)

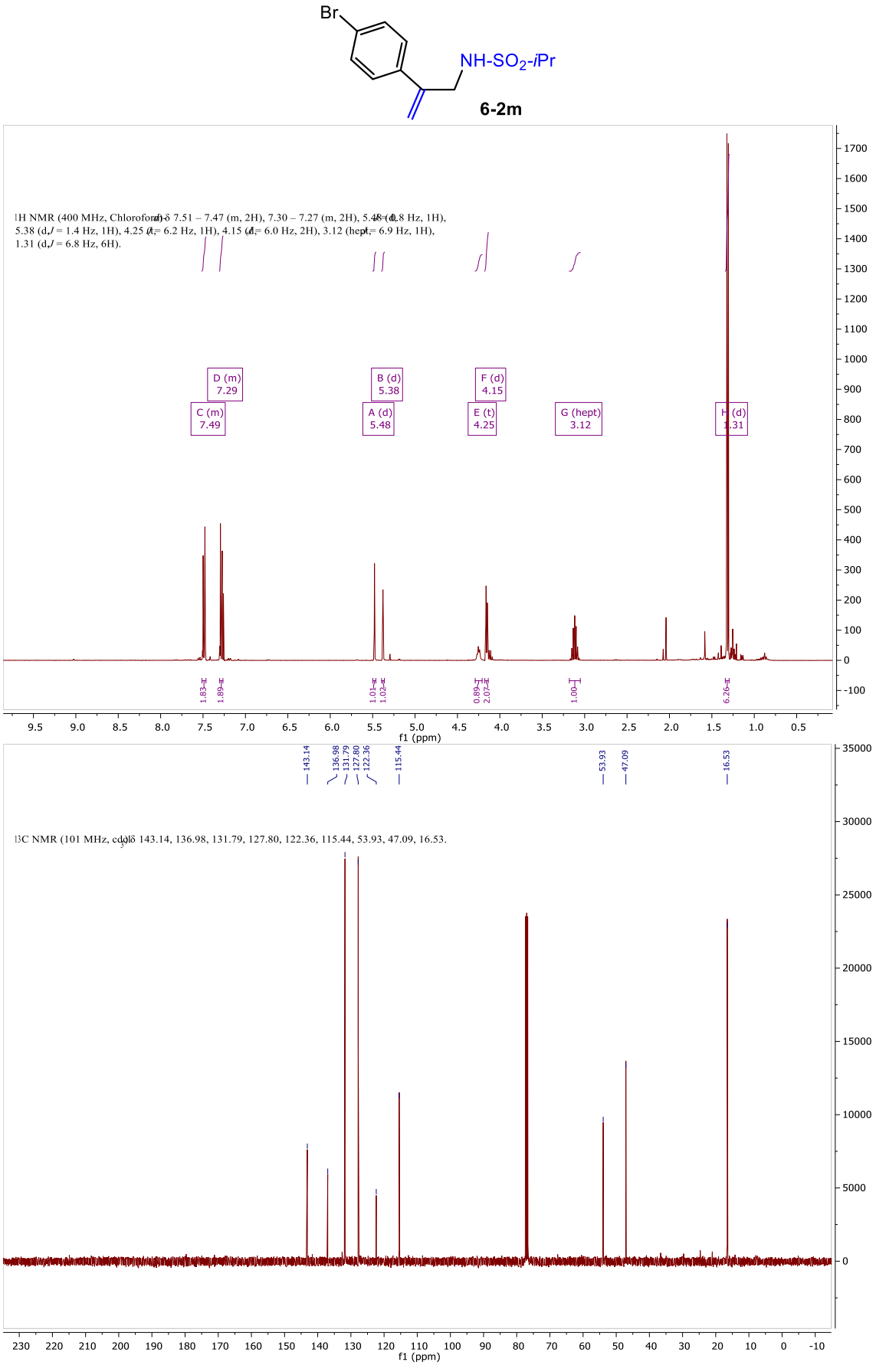
Br
NH-SO2-iPr
6-2m
1H NMR (400 MHz, Chloroform-d) δ 7.51 – 7.47 (m, 2H), 7.30 – 7.27 (m, 2H), 5.48 (d, J = 6.8 Hz, 1H), 5.38 (d, J = 1.4 Hz, 1H), 4.25 (t, J = 6.2 Hz, 1H), 4.15 (d, J = 6.0 Hz, 2H), 3.12 (hept, J = 6.9 Hz, 1H), 1.31 (d, J = 6.8 Hz, 6H).
D (m) 7.29
C (m) 7.49
B (d) 5.38
A (d) 5.48
F (d) 4.15
E (t) 4.25
G (hept) 3.12
H (d) 1.31
1.83
1.89
1.01
1.02
0.89
2.07
1.00
6.26
f1 (ppm)
143.14
136.98
131.79
127.80
122.36
115.44
53.93
47.09
16.53
13C NMR (101 MHz, cdcl3) δ 143.14, 136.98, 131.79, 127.80, 122.36, 115.44, 53.93, 47.09, 16.53.
f1 (ppm)

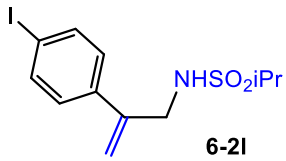

6-2l

^{1}H NMR (400 MHz, Chloroform-*d*) δ 7.71 – 7.66 (m, 2H), 7.17 – 7.13 (m, 2H), 5.48 (d, *J* = 6.7 Hz, 1H), 5.37 (q, *J* = 1.1 Hz, 1H), 4.25 (t, *J* = 6.2 Hz, 1H), 4.18 – 4.13 (m, 2H), 3.12 (hept, *J* = 6.8 Hz, 1H), 1.31 (d, *J* = 6.8 Hz, 6H).

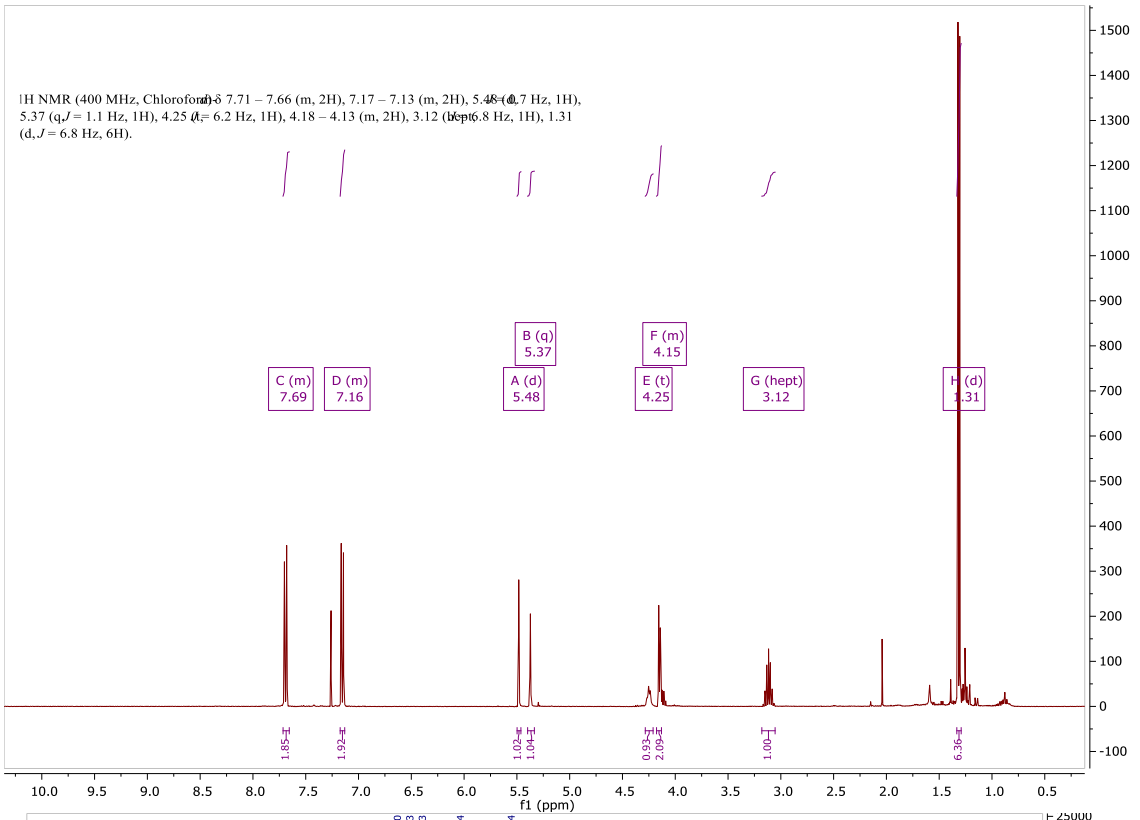

^{13}C NMR (101 MHz, cdcl$_3$) δ 143.40, 137.93, 137.73, 128.14, 115.64, 94.12, 54.10, 47.19, 16.70.

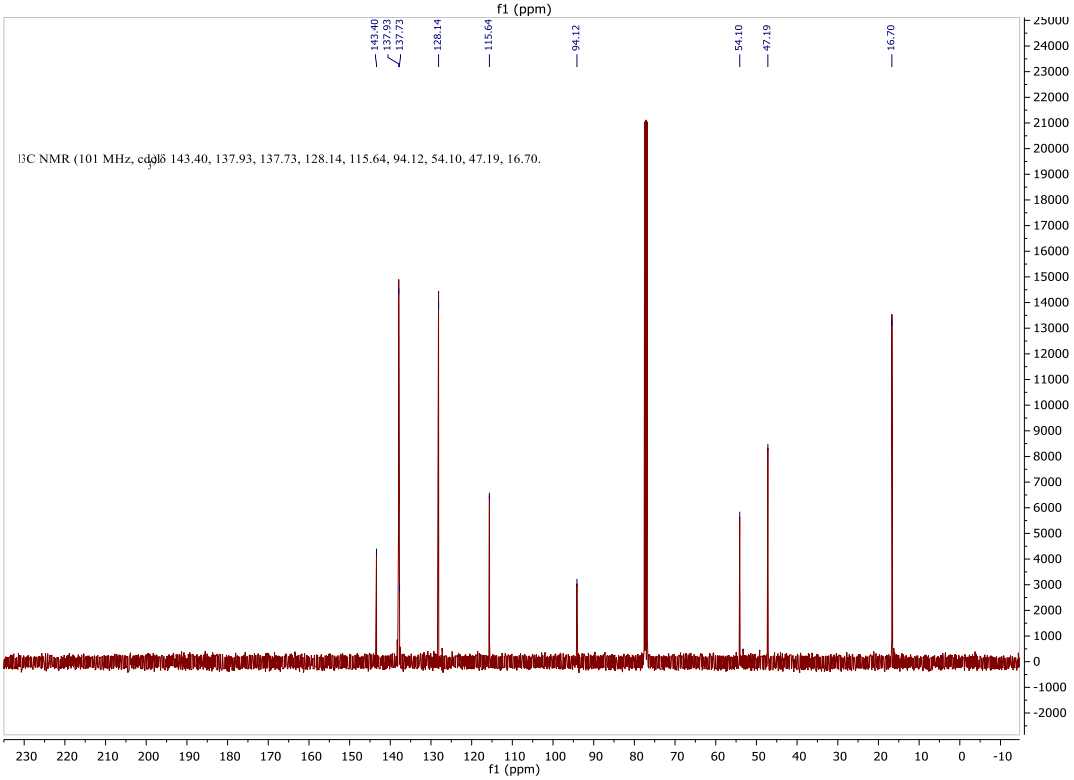

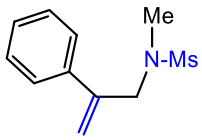

6-3a

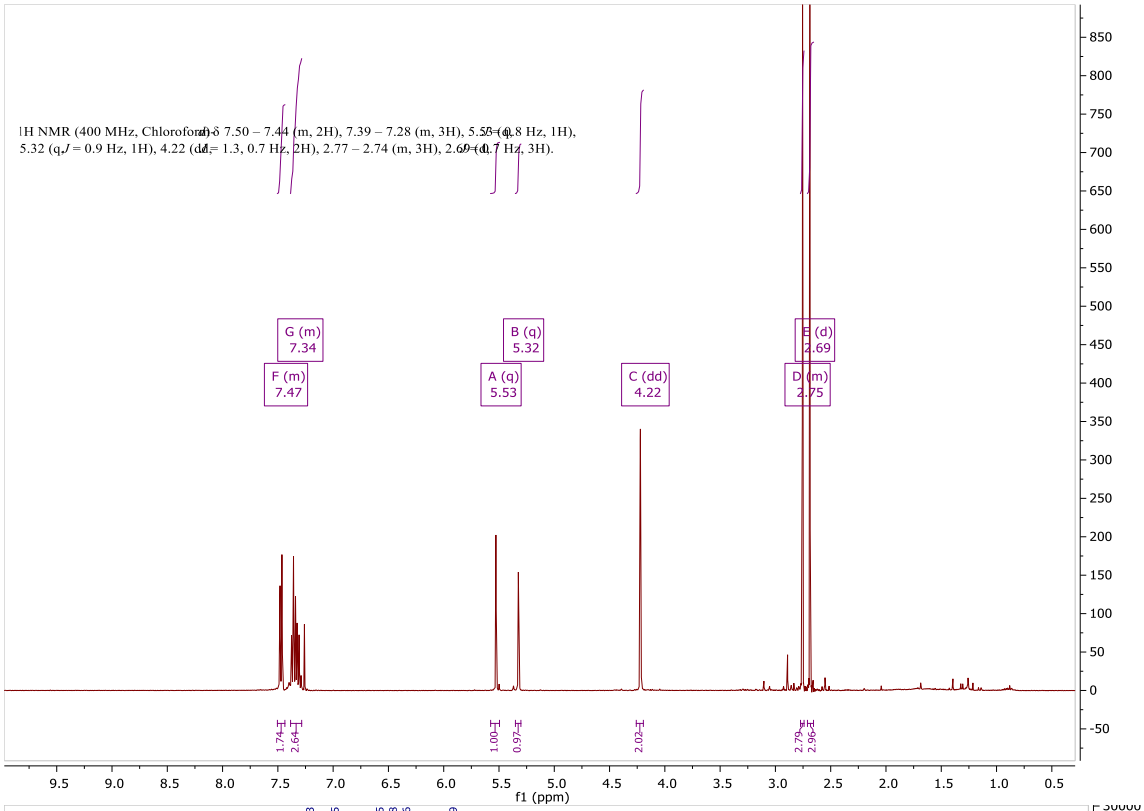

^{1}H NMR (400 MHz, Chloroform-d) δ 7.50 – 7.44 (m, 2H), 7.39 – 7.28 (m, 3H), 5.53 (q, J = 0.8 Hz, 1H), 5.32 (q, J = 0.9 Hz, 1H), 4.22 (dd, J = 1.3, 0.7 Hz, 2H), 2.77 – 2.74 (m, 3H), 2.69 (d, J = 0.7 Hz, 3H).

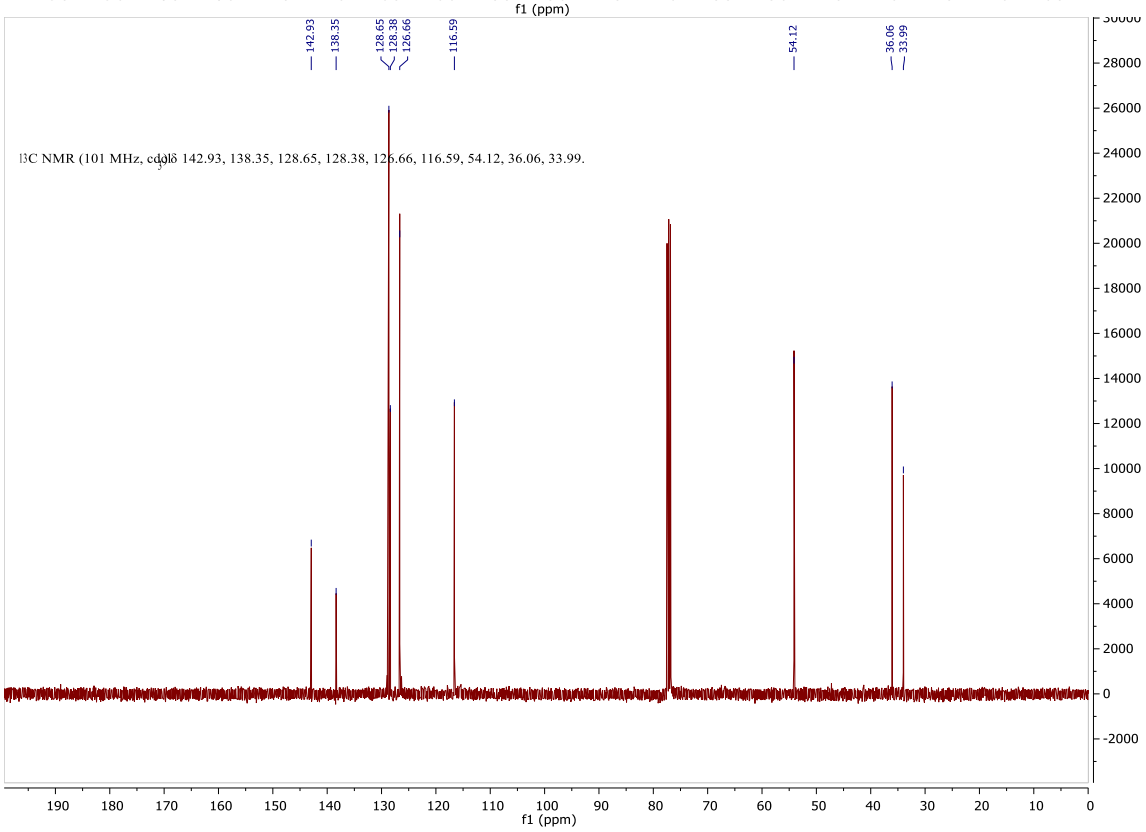

^{13}C NMR (101 MHz, cdcl$_3$) δ 142.93, 138.35, 128.65, 128.38, 126.66, 116.59, 54.12, 36.06, 33.99.

Chapter 7

Catalytic Regioselective Isomerization of 2,2-Disubstituted Oxetanes to Homoallylic Alcohols

Oxetanes are present in numerous drugs and natural products, such as Taxol (Paclitaxel), a well-known antitumoral.[1] They have found significant application in medicinal chemistry[2] since the introduction of an oxetane fragment usually has positive effects in terms of solubility and metabolic stability.[2,3] More recently, 3-substituted oxetanes have been used in polymer chemistry as monomers[4] or cross-linkers,[5] and in opto-electronic devices.[6,7]

The development of new and efficient methods for the preparation of oxetanes has enhanced their role as versatile building blocks in synthetic chemistry.[8,9] Although the ring strain energy of oxetanes (106 kJ·mol^{-1}) is only slightly lower than epoxides (112 kJ·mol^{-1}), they have been scarcely used compared to epoxides. One of the reasons is that 3-substituted oxetanes show a significantly lower electrophilicity than epoxides so they usually have to be activated by Lewis acids.[8,10]

Despite of their lower reactivity than epoxides, significant chemistry of 3-substituted oxetanes has been developed focusing on ring-opening reactions[8a,11], including asymmetric versions,[10] and ring-expansion reactions.[12] On the other hand, 2,2-disubstituted oxetanes are more reactive than the 3-substituted ones due to their facile ring-opening. However, they are also more sensitive to hydrolysis and polymerization. The main reactivity of 2,2-disubstituted oxetanes include reductive ring-opening by titanium[13] or iron[14] complexes, ring expansion[15] to five-membered cyclic ethers and perhydrolysis[16] (Figure 7.1). The oxetanes have also been used as a lithiation directing groups in aromatic rings.[12,17]

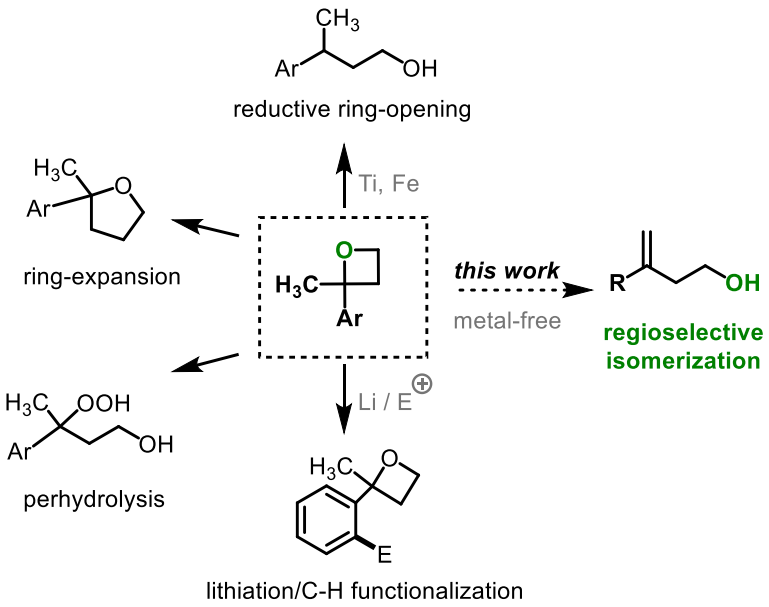

Figure 7.1. Reactivity of 2,2-disubstituted oxetanes.

Our group has recently explored the metal-catalyzed isomerization of strained heterocyclic compounds (Figure 7.2). Particularly, we reported the selective iridium-catalyzed isomerization of *N*-sulfonyl aziridines to allylic amines using Crabtree's catalyst (**7-1**) under very mild conditions and without external activation (Chapter 6 of this doctoral thesis).[20] Similarly, the conversion of epoxides into aldehydes[18] was achieved by hydrogen activation of reagent **7-1** (Chapter 5 of this doctoral thesis).[21] Inspired on these selective transformations, we wondered if 2,2-disubstituted oxetanes would be selectively isomerized when using the appropriate catalyst.

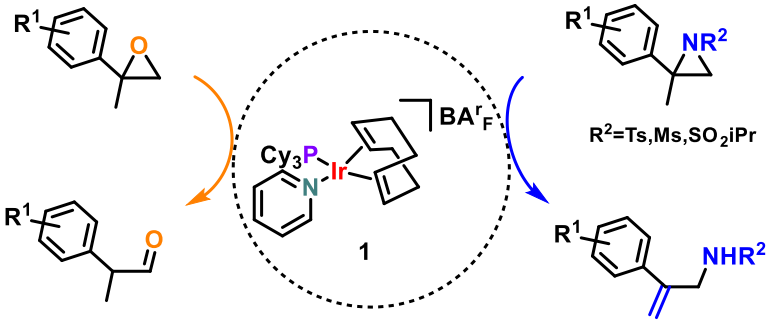

Figure 7.2. Selective isomerization of heterocyclic compounds catalyzed by Crabtree's catalyst, **7-1**.

In contrast with the regioselective isomerization of epoxides[18] (also called Meinwald rearrangement) the regioselective isomerization of oxetanes still remains a challenge and, to the best of our knowledge, no synthetic protocols been described to date. Most probably, the easy polymerization of 2-substituted oxetanes in acidic conditions has hampered their synthetic use.

Herein, we report a new catalytic reaction that affords homoallylic alcohols from 2,2-oxetanes in high selectivity using very low loading of tris(pentafluorophenyl)borane, $B(C_6F_5)_3$, as Lewis acid. The subsequent asymmetric hydrogenation allows the preparation of enantioenriched γ-substituted alcohols. Since the preparation 2,2-disubstituted oxetanes using the Corey-Chaykovski reaction[19] is straightforward and environmentally friendly, we believe that the new sequence emerges as a breakthrough in the synthesis of chiral alcohols from ketones.

Our preliminary studies began with the synthesis of 2-phenyl-2-methyloxetane **7-2a**, which was obtained from acetophenone via double Corey-Chaykovsky reaction[19] with good

yields without the need of further purification (see the Supporting Information). With **7-2a** in hand, the isomerization reaction was performed using several catalysts at 5 mol % loading at room temperature, as shown in Table 1. First, we tested Crabtree's catalyst **7-1** as it gave satisfactory results when using *N*-sulfonyl aziridines[20] and epoxides.[21] However, we observed that, without any external activation, conversion was very low (entry 1, Table 7.1) being the only product that could be quantified the homoallylic alcohol **7-3a**. Activation of the catalyst with H_2 to form an Ir-H,H as the catalytic active species led to polymerization (entry 2, Table 7.1). These disappointing results led us to study a wide range of Lewis-acids. Again, $ZnCl_2$ gave rise to polymerization (entry 3). When moving to milder, inorganic Lewis acids such as $InCl_3$, $IrCl_3$ or $AlCl_3$, **7-3a** was the major product but the mass balance of the reaction was poor, probably due to polymerization (entries 4-6, Table 7.1). At that point, we turned our attention to organic Lewis-acids. First, $BF_3{\cdot}Et_2O$ was tested. Full conversion was observed, although the selectivity of the reaction was null: an equimolar mixture of **7-3a: 7-(*E*)-4a: 7-(*Z*)-4a** (entry 7, Table 7.1) was afforded. We then tested a bulky Lewis acid namely $B(C_6F_5)_3$.[22] Gratifyingly, the reaction in dichloromethane afforded the homoallylic alcohol with excellent yield (82 %) and selectivity (**7-3a**: **7-4a**: 98:2, entry 8, Table 7.1). With this result in hand, we performed a solvent screening. EtOAc, THF and toluene gave excellent conversion and selectivity but the yield was not enhanced (entries 9-11, Table 7.1). Acetonitrile gave very low conversion (entry 12). The temperature effect was also evaluated and the reaction was performed at 0 ºC in dichloromethane (entry 13). However, any difference with the reaction performed at room temperature was observed. Finally, we reduced the catalyst loading to 0.5 mol %, and the reaction time to 2 h, thus demonstrating the outstanding catalytic activity of $B(C_6F_5)_3$ (entry 14, Table 7.1). In addition, a gram scale reaction was carried out, affording **3a** with an excellent 84% yield (entry 15).

Table 7.1. Screening of conditions for the isomerization of **7-2a**

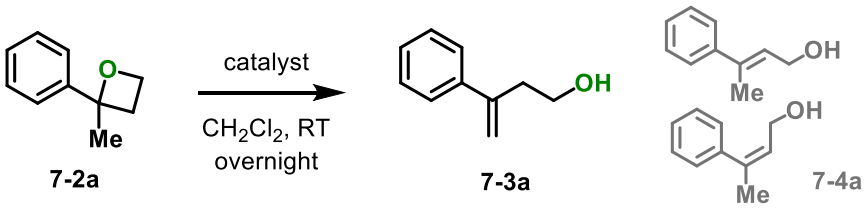

Entry	Catalyst	Solvent	Ratio 7-3a: 7-4a[a]	Conv. (%)[a]	Yield 7-3a (%)[b]
1	**7-1**	DCM	-	35	25
2[c]	**7-1**	DCM	-	>99	0 [d]
3	$ZnCl_2$	DCM	-	>99	0 [d]
4	$InCl_3$	DCM	4:1	50	39
5	$IrCl_3$	DCM	4:1	>99	34
6	$AlCl_3$	DCM	5:1	>99	51
7	$BF_3{\cdot}Et_2O$	DCM	1:2	>99	30
8	$B(C_6F_5)_3$	DCM	98:2	>99	82
9	$B(C_6F_5)_3$	EtOAc	96:4	>99	70
10	$B(C_6F_5)_3$	THF	98:2	>99	67
11[e]	$B(C_6F_5)_3$	Toluene	98:2	>99	79
12	$B(C_6F_5)_3$	MeCN	-	33	21
13[e]	$B(C_6F_5)_3$	DCM	98:2	>99	80
14[f]	$B(C_6F_5)_3$	DCM	98:2	>99	82, 78[g]
15[h]	$B(C_6F_5)_3$	DCM	98:2	>99	84

The reaction was performed in a sealed vial with 0.1 mmol of **7-2a,** [0.1 M] and using 5 mol % of catalyst loading. [a] Determined by ^{1}H NMR spectroscopy. [b] ^{1}H NMR yield using mesitylene as internal standard. [c] The reaction was performed in a pressure tube, using H_2 for catalyst activation and, after 1 min, the vessel was fully degassed. [d] Polymerization occurred. [e] The reaction was performed at 0 °C. [f] 0.5 mol% of catalyst was employed, and the reaction was left stirring for 2 h. [g] Isolated yield, at 0.8 mmol scale. [h] Isolated yield performing the reaction at gram scale, using 0.5 mol% of $B(C_6F_5)_3$.

With the optimal conditions in hand, we explored the substrate scope (Table 7.2). The aryl group was modified with a range of functionalities. A fluorine atom in *para*- and *ortho*-position was well tolerated (entries 1 and 2, Table 7.2), affording **7-3a** and **7-3b** with complete regioselectivity. In the latter case, the yield was moderate probably due to dimerization of the substrate. A substrate with stronger electron-withdrawing group such as *p*-CF_3 (entry 3, Table 7.2) afforded the homoallylic alcohol **7-3d** with high selectivity, albeit in moderate yield. *Para*-substituted halogen substituents such as *p*–Cl, *p*–Br and *p*-I showed excellent selectivity affording the homoallylic alcohols **7-3e**, **7-3g** and **7-3h** in high yield (entries 4-7, Table 7.2).

In the case of *m*–Cl (**7-2f**), the yield was high (84%, entry 5, Table 7.2), but up to 5% of the allylic alcohols **7-4** were also formed. We then moved on to test the effect of the electron-donating group in the aryl substituent. A methyl group was introduced in both *para*- and *ortho*-position (entries 8 and 9, Table 7.2). In both cases, the selectivity of the isomerization reaction decreased compared to EWG groups, although **7-3i** and **7-3j** were still obtained in good yields. Alternatively, a methoxy group in the *meta*-position enhanced the selectivity ratio **7-3:7-4** up to 98%, affording **7-3k** with an excellent 92% yield (entry 10, Table 7.2). In contrast, bulky group in *para*-position (*p-i*Bu) diminished the selectivity, although **7-3l** was afforded in synthetically useful yield (entry 11, Table 7.2). The naphthyl group was also studied, affording **7-3m** in excellent selectivity (92:8) and 83% yield (entry 12, Table 2). Interestingly, the reactivity was not limited to 2-aryl oxetanes. The dialkyl compound 2-cyclohexyl-2-methyl oxetane **7-2n** (entry 13, Table 2) afforded a 7:3 mixture of the expected product **7-3n** and the tetrasubstituted allyl alcohol in 56% yield *(*see the Experimental Part).

To prove the versatility of this reaction, we also modified the methyl group to other alkyl groups, such as an ethyl (**7-2o**) or benzyl group (**7-2p**). The corresponding trisubstituted homoallylic alcohols **7-3o** and **7-3p** were formed in good yields, with high *E* selectivity with respect to *Z* (Scheme 7.1). Also, bicyclic oxetane **7-2q**, synthesized from α-tetralone, proved highly reactive, exclusively affording homoallylic alcohol **7-3q** in 84% isolated yield (Scheme 1). Finally, the applicability of this methodology is exemplified by the synthesis of estrone derivative **7-3r**, which potential novel precursor for the development of further bioactive compounds. For this purpose, starting from estrone 3-methyl ether, the corresponding oxetane **7-2r** was synthesized in high yield affording a mixture of diastereomers (see the Supporting Information) which was directly treated with 0.5 mol% of $B(C_6F_5)_3$. After 5 h, the homoallylic alcohol **7-3r** was obtained with a 78% yield. The synthesis of this novel compound shows a new derivatization pathway for steroids and related compounds.

Table 7.2. Study of the substrate scope.

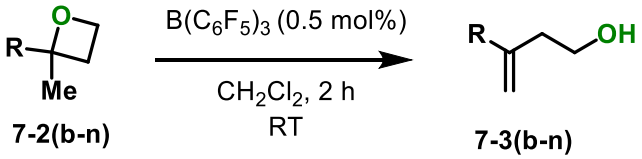

7-2(b-n) → 7-3(b-n)

Entry		R	Ratio 7-3: 7-4[a]	Conv. (%)[a]	Yield 7-3 (%)[b]
1	**7-2b**	*p*-F-C_6H_4-	>99	>99	77
2[c]	**7-2c**	*o*-F-C_6H_4-	>99	>99	57
3	**7-2d**	*p*-CF_3-C_6H_4-	99:1	>99	54
4	**7-2e**	*p*-Cl-C_6H_4-	>99	>99	95
5	**7-2f**	*m*-Cl-C_6H_4-	95:5	>99	84
6	**7-2g**	*p*-Br-C_6H_4-	>99	>99	86
7[c]	**7-2h**	*p*-I-C_6H_4-)	>99	>99	70
8	**7-2i**	*p*-Me-C_6H_4-	96:4	>99	79
9	**7-2j**	*o*-Me-C_6H_4-	91:9	>99	63
10	**7-2k**	*m*-OMe-C_6H_4-	98:2	>99	92
11	**7-2l**	*p*-*i*Bu-C_6H_4-	88:12	>99	70
12	**7-2m**	2-Naphthyl	92:8	>99	83
13	**7-2n**	cyclohexyl	>99	>99	56[d]

The reaction was performed in a sealed vial using 0.4 mmol of **7-2** and 0.5 mol % of catalyst loading. [a] Determined by ^{1}H NMR spectroscopy from the crude. [b] Isolated yield. [c] 1 mol% of catalyst was used, leaving the reaction stirring overnight. [d] A mixture homoallylic alcohols (7:3) was also obtained. (see the experimental part).

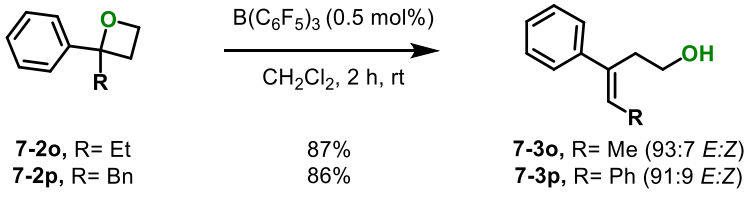

7-2o, R= Et; **7-2p**, R= Bn — 87%; 86% — **7-3o**, R= Me (93:7 *E*:*Z*); **7-3p**, R= Ph (91:9 *E*:*Z*)

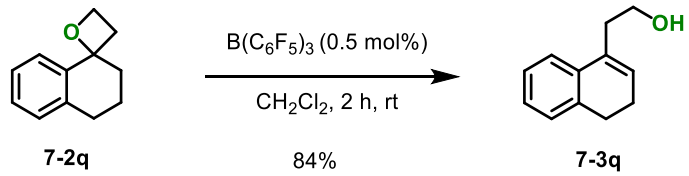

7-2q — 84% — **7-3q**

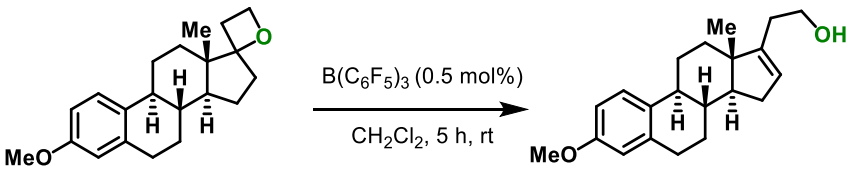

7-2r — 78% — **7-3r**

Scheme 7.1. Substrate scope with other alkyl substituents.

The novelty of the transformation led us to perform a mechanistic study. Our previous studies of iridium-catalyzed isomerization of *N*-sulfonyl aziridines and epoxides (Scheme1) disclosed a two-steps mechanism in which the initial ring-opening step is followed by metal-assisted tautomerization.[20,21] The selectivity of the process depends on the C-H hydrogen involved in the tautomerization. However, the metal-free nature of the oxetane isomerization raises new questions regarding the hydrogen migration step, in particular regarding the identity of the agent assisting the H-migration and how the selectivity homoallylic alcohol (**7-3**)/allylic alcohol (**7-4**) is defined. Indeed, the results obtained using the two borane reagents [$BF_3{\cdot}Et_2O$ and $B(C_6F_5)_3$] differ markedly. While the former yields an equimolar mixture of both products, the latter is highly selective toward the homoallylic product (Table 7.1). To answer these questions, here we studied the isomerization mechanism of 2-phenyl-2-methyloxetane **7-2a** catalyzed by both $BF_3{\cdot}Et_2O$ and $B(C_6F_5)_3$ Lewis acids. To this end, DFT calculations applying the B3LYP-D3 functional and treating the DCM solvent with the SMD continuum model (see Computational Details in the Experimental Part).

As $BF_3{\cdot}Et_2O$ gave similar yields of both products, we started the mechanistic study using this Lewis acid reagent. The computed catalytic cycle is shown in Scheme **7-2a**. The corresponding Gibbs energy profile can be found at the Supporting Information (Figure 7.S3). The formation of the Lewis-adduct **7-2a**·BF_3 (**I**) requires the previous displacement of Et_2O by **7-2a**, which takes places by means of a SN_2 substitution process demanding 12.7 kcal·mol^{-1}. Coordination of boron to the O-oxetane activates the C-O bond for ring opening, that only requires an activation barrier of 4.0 kcal·mol^{-1} (**TS$_{I\text{-}II}$**) and leads to the zwitterionic intermediate **II** (-4.9 kcal·mol^{-1}). At this point, the catalytic cycle can follow two different pathways depending on the proton that migrates to the oxygen: proton transfer from methyl group brings the homoallylic alcohol **7-3a**, while if it happens from the $C_\beta H_2$ group the allylic products **7-(*E*,*Z*)-4a** are formed. The process leading to **7-3a** has been characterized as a low barrier (8.3 kcal·mol^{-1}) intramolecular proton transfer involving a six-member ring transition state, **TS$_{II\text{-}IV}$**. On the contrary, the formation of the allylic products **7-4a** via an intramolecular mechanism, involving a four-member ring transition state, can be discarded as it presents a Gibbs energy barrier of 22.8 kcal·mol^{-1} (see the computational details), incompatible with the experimental detection of equimolar amounts of **7-3a** and **7-4a** products (Table 7.1). Therefore, we investigated the possible role of all the bases present in the reaction medium in assisting the proton migration from the $C_\beta H_2$ group to the oxygen.

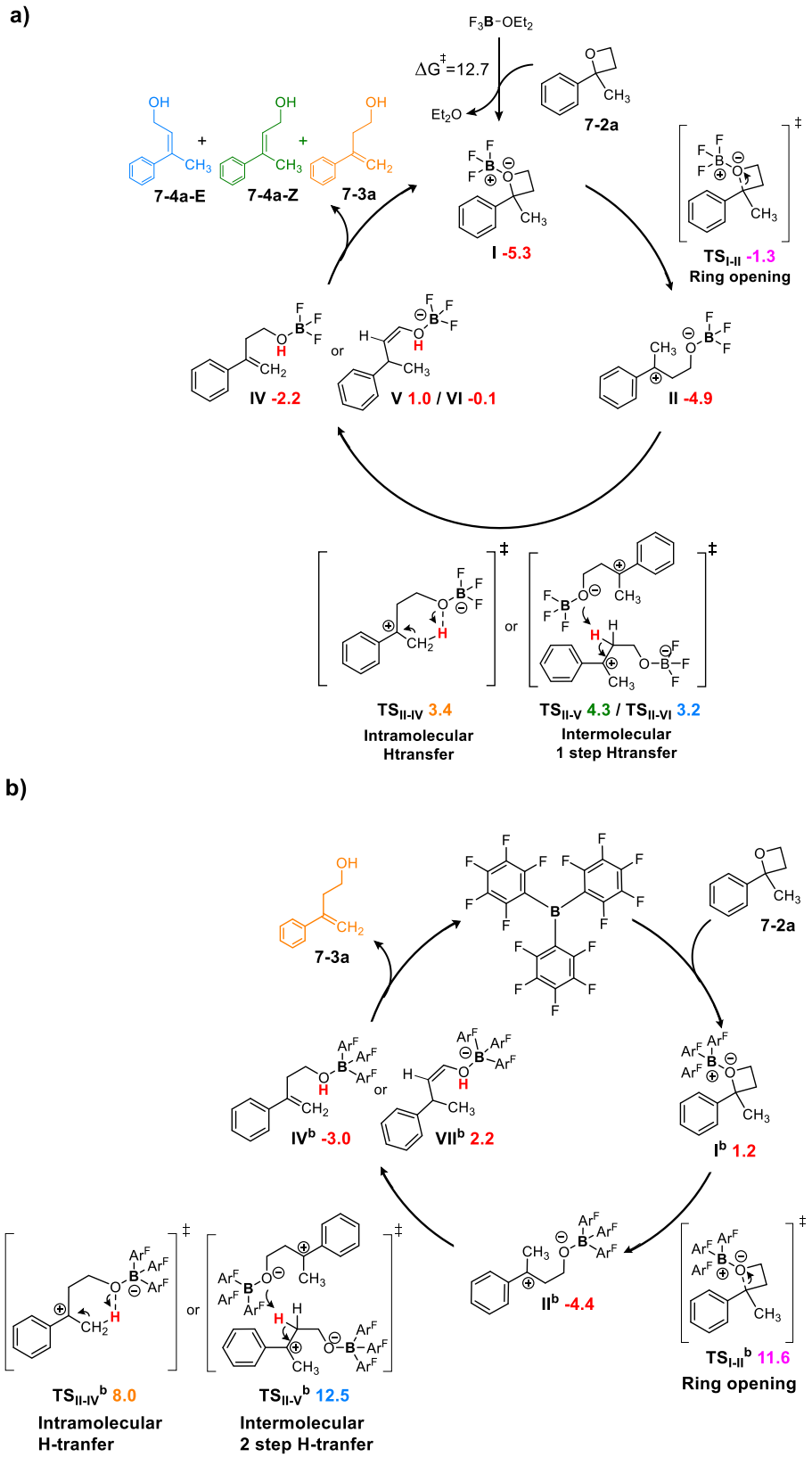

Scheme 7.2. DFT computed mechanism (B3LYP-D3 in DCM) for the isomerization of oxetane **7-2a** to homoallylic **7-3a** and allylic **7-(*E*)-4a** and **7-(*Z*)-4a** alcohols catalyzed by a) $BF_3{\cdot}Et_2O$ and b) $B(C_6F_5)_3$. Relative Gibbs energies (in red) in kcal·mol^{-1} are referred to the separated species; transition state energies are shown in purple, for the ring opening step and orange, blue or green for the proton transfer process entailing the formation of **7-3a**, **7-(*E*)-4a** and **7-(*Z*)-4a**, respectively.

Three O-bases were tested in the intermolecular base-assisted H transfer: the ether oxygen of Et_2O, that of oxetane substrate **7-2a**, and the negatively charged oxygen of intermediate **II**. Base-assisted transition states involving the three species have been computed leading to an energy ordering for the Gibbs energy barrier from **II** that follows the expected basicity order: O-**II** (8.1 kcal·mol^{-1}) < O-**2a** (13.6 kcal·mol^{-1}) < O-Et_2O (15.6 kcal·mol^{-1}) (see the Supporting Information). The favored intermolecular **II**-assisted TS bringing **4a** comes from a head-to-tail adduct of two unities of intermediate **II** (Figure 7.3a).

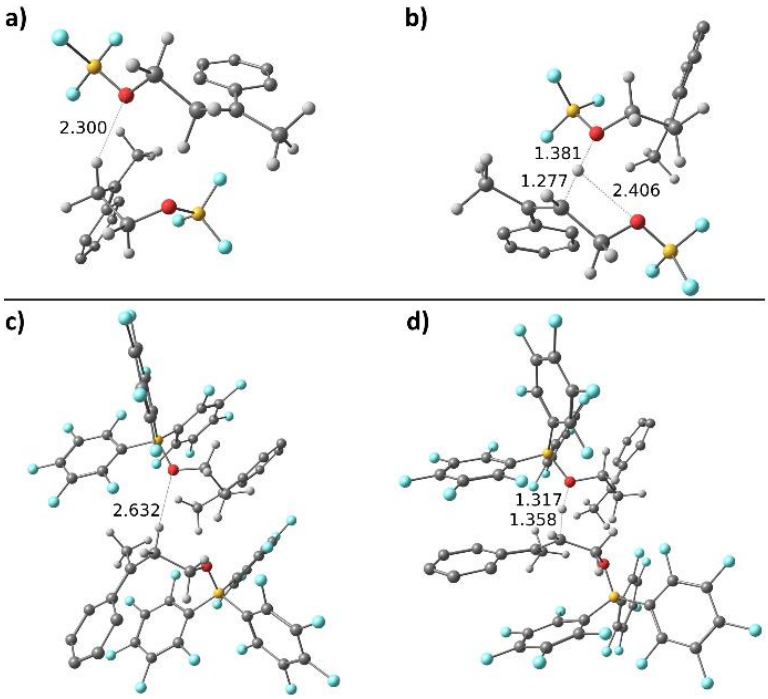

Figure 7.3. Optimized geometries for: a) adduct of two unities of intermediate II; b) concerted intermolecular proton migration transition state, $TS_{II\text{-}VI}$; c) adduct of two unities of intermediate II^b, and d) first step of the proton migration transition state, $TS_{II\text{-}V}{}^b$. The most important distances are also reported in Å. Hydrogen atoms of Ph groups have been omitted for clarity.

The proton migration has been characterized as a concerted mechanism in which the C_β-H proton, picked by the oxygen of one unity of intermediate **II**, is directly transferred to the oxygen of the second unity to form the allylic alcohol (Figure 7.3b). Both pro-(*E*), $\mathbf{TS_{III\text{-}V}}$ and pro-(*Z*), $\mathbf{TS_{III\text{-}VI}}$, show barriers (8.1 and 9.2 kcal·mol^{-1}, respectively) very close to $\mathbf{TS_{II\text{-}IV}}$ (8.3 kcal·mol^{-1}). Taking these data into account, from a micro-kinetics analysis carried out with COPASI software, a 1.0:1.8 mixture of **7-3a**: **7-4a** is predicted, highlighting no selectivity of the catalyst (for further details see the computational details).

When using $B(C_6F_5)_3$ (Scheme 7.2b and Gibbs energy profile at the experimental part, Figure 7.S2) no previous substitution is required. According with the lower Lewis acidity of $B(C_6F_5)_3$ respect to BF_3, its interaction with the O-oxetane is weaker and a bit higher barrier (11.6 kcal·mol^{-1}, **$TS_{I\text{-}II}^{b}$)** is required in the ring-opening step that leads to the zwitterionic intermediate **II^{b}** at -4.4 kcal·mol^{-1}. From **II^{b}** the homoallylic alcohol **7-3a** is obtained through an intramolecular H-transfer involving a 6-member ring transition state **$TS_{II\text{-}IV}^{b}$**, requiring a Gibbs energy barrier of 12.4 kcal·mol^{-1}. As for BF_3, the formation of the allylic products via an intramolecular mechanism, entailing a four-member ring transition state, implies high activation energy (21.3 kcal·mol^{-1}, see the Supporting Information). Regarding the base-assisted mechanism, the same basicity trend than for BF_3 reaction has been observed: the **II**-assisted process is favored over the **7-2a**-assisted proton transfer, with barriers of 16.9 and 18.5 kcal·mol^{-1}, respectively. In contrast to the process with the BF_3 catalyst, the proton migration needs two different steps: first, with an activation barrier of 16.9 kcal·mol^{-1}, the C_β-H proton is transferred to the oxygen of the second unity of intermediate **II^{b}** (**$TS_{III\text{-}V}^{b}$**); then, in a practically barrierless process, involving a relative reorientation of the two subunits, the proton migrates to form the allylic product **7-4a** (see the computational details). Contrary to what happen for the case of BF_3 catalyzed isomerization, **$TS_{III\text{-}V}^{b}$** has an energy barrier higher enough with respect the transition state **$TS_{II\text{-}IV}^{b}$ (**4.5 kcal·mol^{-1}) to assure a practically complete selectivity in favor of the homoallylic alcohol product **7-3a**, in line with the experimental results. The reasons behind the different performances of the two catalysts can be found on the steric hindrance introduced by the aryl rings of $B(C_6F_5)_3$ that destabilizes the proton migration step by placing the oxygen atom that will accept the proton further away (Figure 7.3c).

Last, to showcase the applicability of the novel synthetic protocol, we performed the enantioselective hydrogenation of the resulting homoallylic alcohols to give enantioenriched alcohols. Alcohols with an stereogenic center in γ-position constitute an important chemical motif, present in a wide range of natural products, pharmaceuticals, and fine chemicals of perfume industry.[23] Enantioenriched γ-methyl alcohols are also versatile building blocks that are used as synthetic intermediates in the synthesis of complex molecules.[3] For instance, (-)-citronellol is an intermediate for the production of rose oxide.[24]

Focusing on catalytic processes, the asymmetric isomerization and/or hydrogenation of primary allylic alcohols have emerged as promising alternatives to synthesize γ-methyl chiral

alcohols, where iridium-P,N complexes have come to dominate the field.[25] However, the catalytic isomerization[25a,b] of γ-methyl allylic alcohols suffer from very low conversion and moderate enantioselectivities, whereas the asymmetric hydrogenation[25c,d] requires harsh conditions (very high H_2 pressure) to avoid undesired isomerization byproducts.

Moreover, the preparation of the starting allylic alcohols have the disadvantage of a not efficient preparation. First, their synthesis usually require two steps with poor atom economy: an olefination reaction (Horner–Wadsworth–Emmons -HWE-, or similar), and ester reduction (usually with reactive hydrides).[11] Second, even more important, the usual poor selectivity of the HWE with ketones leads to the formation of mixtures of *E* and *Z* allylic alcohols that require complicated chromatographic separations (Scheme 7.3). For this reason, we believe that the strategy presented in this work constitutes a breakthrough to obtain chiral alcohols from cheap and abundant ketones in a greener 3-step synthetic approach. Therefore, we moved to perform the asymmetric hydrogenation of homoallylic alcohols **7-3**, which can be considered minimally functionalized olefins.[26]

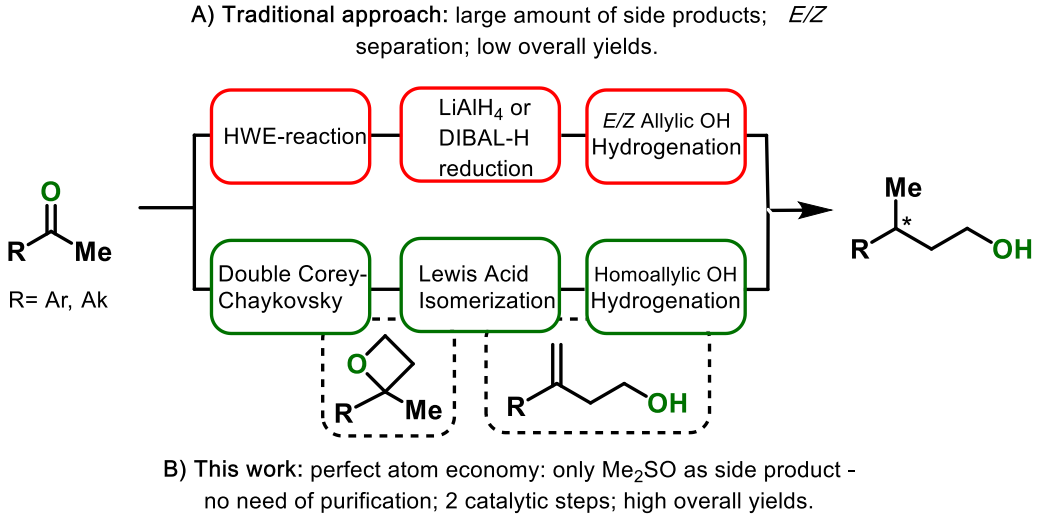

Scheme 7.3. Comparison of this work with the traditional approach.

During the last decade our group has developed several modular P stereogenic chiral ligands[27] that have proved to be excellent precursors of chiral catalysts. Although our iridium-P,N MaxPHOX[28] family of catalysts have been successfully applied to the asymmetric hydrogenation of cyclic enamides, [29] aryl and alkyl imines[30,31] and minimally functionalized olefins,[32] including 2-aryl *N*-allyl phthalimides[33], we found that in this

particular case, using **7-3a** as model substrate, [((4*S*,5*S*)-Cy$_2$-Ubaphox)Ir(COD)]BAr$^F{}_4$ **7-6**,[34] gave the best results.

Table 7.3. Iridium-catalyzed asymmetric hydrogenations of homoallylic alcohols.

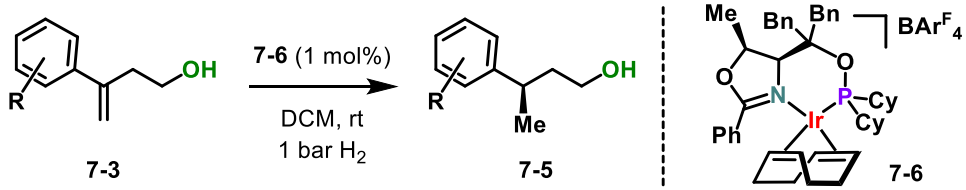

Entry		R	Product	Conv. (%) [a]	ee (%) [b]
1	**7-3a**	H	**7-5a**	>99	90
2	**7-3c**	*o*-F	**7-5c**	>99	94
3	**7-3e**	*p*-Cl	**7-5e**	>99	92
4	**7-3i**	*p*-Me	**7-5i**	>99	90
5	**7-3k**	*m*-OMe	**7-5k**	>99	94

The reaction was performed in a pressure reactor using 1 mol% of catalyst **7-6** and left stirring overnight. [a] Determined by ^{1}H NMR spectroscopy from the crude. [b] Measured by chiral HPLC.

Using 1 mol % of this commercially available catalyst **7-6** developed by Pfaltz and co-workers in dichloromethane under 1 bar of H_2 pressure, **7-5a** was obtained in 91% ee (entry 1, Table 7.3). The scope of this reaction was expanded to other homoallylic alcohols prepared from the corresponding oxetanes **7-2**. Both electron-withdrawing substituents such as *o*-F, (**7-3c**, entry 2) and *p*-Cl (**7-3e**, entry 3) and electron-donating substituents such as *p*-Me (**7-3i**, entry 4) and *m*-OMe (**7-3k**, entry 5) gave full conversions and excellent enantioselectivities (up to 94% ee).

In conclusion, we have reported a highly regioselective isomerization of 2,2-disubstituted oxetanes using $B(C_6F_5)_3$ as catalyst, using extremely mild conditions (0.5 mol% of catalyst loading and very short reaction times). DFT calculations shed light on the reaction mechanism and account for the high selectivity toward the homoallylic alcohol product displayed by the $B(C_6F_5)_3$ catalyst. This novel selective isomerization of oxetanes can be used as key step in multiple synthetic organic transformations. As a leading example, we have disclosed a highly efficient 3-step protocol towards the enantioselective synthesis of γ-aryl butanols starting from abundant inexpensive acetophenone derivatives. First, a double Corey-Chaykovksy reaction, which only generates dimethyl sulfoxide as by-product, is carried out. Then, and without further purification, the selective isomerization of the

resulting oxetanes takes place followed by iridium-catalyzed asymmetric hydrogenation (Figure 7.3). These last two steps, which are catalytic, accomplishes a greener, more sustainable and efficient approach to the enantioselective synthesis of valuable alcohols. Moreover, the applicability of the isomerization reaction was further demonstrated by the isomerization of spiranic oxetanes and the preparation of a new estrone-derivative.

References

[1] (a) M. C. Wani, H. L. Taylor, M. E. Wall, P. Coggon, A. T. Mcphail, *J. Am. Chem. Soc.* **1971**, *93*, 2325–2327. (b) M. Wang, B. Cornett, J. Nettles, D. C. Liotta, J. P. Snyder, *J. Org. Chem.* **2000**, *65*, 1059–1068.

[2] (a) J. A. Burkhard, G. Wuitschik, M. Rogers-Evans, K. Müller, E. M. Carreira, *Angew. Chem. Int. Ed.* **2010**, *49*, 9052–9067. (b) G. Wuitschik, E. M. Carreira, B. Wagner, H. Fischer, I. Parrilla, F. Schuler, M. Rogers-Evans, K. Müller, *J. Med. Chem.* **2010**, *53*, 3227–3246. (c) G. Wuitschik, M. Rogers-Evans, K. Müller, H. Fischer, B. Wagner, F. Schuler, L. Polonchuk, E. M. Carreira, *Angew. Chem. Int. Ed.* **2006**, *45*, 7736–7739. (d) M. McLaughlin, R. Yazaki, T. C. Fessard, E. M. Carreira, *Org. Lett.* **2014**, *16*, 4070–4073.

[3] (a) J. A. Burkhard, G. Wuitschik, J. M. Plancher, M. Rogers-Evans, E. M. Carreira, *Org. Lett.* **2013**, *15*, 4312–4315. (b) A. F. Stepan, K. Karki, W. S. McDonald, P. H. Dorff, J. K. Dutra, K. J. Dirico, A. Won, C. Subramanyam, I. V. Efremov, C. J. O'Donnell, et al., *J. Med. Chem.* **2011**, *54*, 7772–7783.

[4] J. V. Crivello, *J. Polym. Sci. Part A Polym. Chem.* **2014**, *52*, 2934–2946.

[5] B. Ghosh, M. W. Urban, *Science* **2009**, 323, 1458-1460.

[6] H. Kudo, T. Nishikubo, *J. Polym. Sci. Part A: Polym. Chem.* **2007**, *45*, 709–726

[7] T. Soga, H. Kudo, T. Nishikubo, S. Sato, *Polym. J.* **2008**, *40*, 832–836.

[8] (a) J. A. Bull, R. A. Croft, O. A. Davis, R. Doran, K. F. Morgan, *Chem. Rev.* **2016**, *116*, 12150–12233. (b) O. A. Davis, J. A. Bull, *Angew. Chem. Int. Ed.* **2014**, *53*, 14230–14234. (c) O. A. Davis, R. A. Croft, J. A. Bull, *Chem. Commun.* **2015**, *51*, 15446–15449. For enantioselective synthesis of oxetanes, see: (d) T. Sone, G. Lu, S. Matsunaga, M. Shibasaki, *Angew. Chem. Int. Ed.* **2009**, *48*, 1677–1680.

[9] S. Ahmad, M. Yousaf, A. Mansha, N. Rasool, A. F. Zahoor, F. Hafeez, S. M. A. Rizvi, *Synth. Commun.* **2016**, *46*, 1397–1416.

[10] (a) Z. Wang, Z. Chen, J. Sun, *Org. Biomol. Chem.* **2014**, *12*, 6028–6032. (b) Z. Wang, Z. Chen, J. Sun, *Angew. Chem. Int. Ed.* **2013**, *52*, 6685–6688. (c) Z. Chen, Z. Wang, J. Sun, *Chem. Eur. J.* **2013**, *19*, 8426–8430. (d) R. N. Loy, E. N. Jacobsen, *J. Am. Chem. Soc.* **2009**, *131*, 2786-2787.

[11] R. A. Croft, J. J. Mousseau, C. Choi, J. A. Bull, *Chem. Eur. J.* **2016**, *22*, 16271–16276.

[12] For the ring expansion of oxetanes to carbonates, see: (a) C. J. Whiteoak, E. Martin, M. M. Belmonte, J. Benet-Buchholz, A. W. Kleij, *Adv. Synth. Catal.* **2012**, *354*, 469–476. (b) J. Rintjema, A. W. Kleij, *Synth.* **2016**, *48*, 3863–3878. (c) W. Guo, V. Laserna, J. Rintjema, A. W. Kleij, *Adv. Synth. Catal.* **2016**, *358*, 1602–1607. (d) J. Rintjema, W. Guo, E. Martin, E. C. Escudero-Adán, A. W. Kleij, *Chem. Eur. J.* **2015**, *21*, 10754–10762. For another recent ring-expansion example of 3-substituted oxetanes, see: S. Jana, Z. Yang, C. Pei, X. Xu, R. M. Koenigs, *Chem. Sci.* **2019**, DOI 10.1039/c9sc04069b.

[13] (a) A. Gansäuer, N. Ndene, T. Lauterbach, J. Justicia, I. Winkler, C. Mück-Lichtenfeld, S. Grimme, *Tetrahedron* **2008**, *64*, 11839–11845. (b) N. Takekoshi, K. Miyashita, N. Shoji, S. Okamoto, *Adv. Synth. Catal.* **2013**, *355*, 2151–2157.

[14] Y. K. Sugiyama, S. Heigozono, S. Okamoto, *Org. Lett.* **2014**, *16*, 6278–6281.

[15] (a) E. D. Butova, A. V. Barabash, A. A. Petrova, C. M. Kleiner, P. R. Schreiner, A. A. Fokin, *J. Org. Chem.* **2010**, *75*, 6229–6235. (b) C. Gronnier, S. Kramer, Y. Odabachian, F. Gagosz, *J. Am. Chem. Soc.* **2012**, *134*, 828–831. (c) D. J. Mack, L. A. Batory, J. T. Njardarson, *Org. Lett.* **2012**, *14*, 378–381. (d) C. Larksarp, H. Alper, *J. Org. Chem.* **1999**, *64*, 4152–4158. (e) S. K. Pawar, D. Vasu, R.-S. Liu, *Adv. Synth. Catal.* **2014**, *356*, 2411-2416.

[16] (a) P. H. Dussault, T. K. Trullinger, F. Noor-e-Ain, *Org. Lett.* **2002**, *4*, 4591–4593. (b) W. B. Han, Y. Wu, *Org. Lett.* **2014**, *16*, 5706–5709.

[17] (a) D. I. Coppi, A. Salomone, F. M. Perna, V. Capriati, *Angew. Chem. Int. Ed.* **2012**, *51*, 7532–7536. (b) D. I. Coppi, A. Salomone, F. M. Perna, V. Capriati, *Chem. Commun.* **2011**, *47*, 9918–9920.

[18] J. Meinwald, S. S. Labana, M. S. Chadha, *J. Am. Chem. Soc.* **1963**, *85*, 582–585.

[19] K. Okuma, Y. Tanaka, S. Kaji, H. Ohta, *J. Org. Chem.* **1983**, *48*, 5133–5134.

[20] A. Cabré, G. Sciortino, G. Ujaque, X. Verdaguer, A. Lledós, A. Riera, *Org. Lett.* **2018**, *20*, 5747–5751.

[21] A. Cabré, J. Cabezas-Giménez, G. Sciortino, G. Ujaque, X. Verdaguer, A. Lledós, A. Riera, *Adv. Synth. Catal.* **2019**, 3624–3631.

[22] For the use of $B(C_6F_5)_3$ in stereoselective rearrangement of epoxides, see: (a) K. Ishihara, N. Hanaki, H. Yamamoto, *Synlett* **1995**, *1995*, 721-722. (b) M. R. Tiddens, R. J. M. Klein Gebbink, M. Otte, *Org. Lett.* **2016**, *18*, 3714–3717.

[23] L. A. Saudan, *Acc. Chem. Res.* **2007**, *40*, 1309–1319.

[24] P. L. Alsters, W. Jary, V. Nardello-Rataj, J. M. Aubry, *Org. Process Res. Dev.* **2010**, *14*, 259–262.

[25] (a) H. Li, C. Mazet, *Acc. Chem. Res.* **2016**, *49*, 1232–1241. (b) J. Q. Li, B. Peters, P. G. Andersson, *Chem. Eur. J.* **2011**, *17*, 11143–11145. (c) M. Bernasconi, V. Ramella, P. Tosatti, A. Pfaltz, *Chem. Eur. J.* **2014**, *20*, 2440–2444. (d) J. Q. Li, J. Liu, S. Krajangsri, N. Chumnanvej, T. Singh, P. G. Andersson, *ACS Catal.* **2016**, *6*, DOI 10.1021/acscatal.6b02456.

[26] (a) J. J. Verendel, O. Pàmies, M. Diéguez, P. G. Andersson, *Chem. Rev.* **2014**, *114*, 2130–2169. (b) S. J. Roseblade, A. Pfaltz, *Acc. Chem. Res.* **2007**, *40*, 1402–1411. (c) D. H. Woodmansee, A. Pfaltz, *Chem. Commun.* **2011**, *47*, 7912–7916. (d) C. Margarita, P. G. Andersson, *J. Am. Chem. Soc.* **2017**, *139*, 1346–1356. (e) A. Cabré, X. Verdaguer, A. Riera, *Adv. Synth. Catal.***2019**, *361*, 4196–4200.

[27] (a) M. Revés, C. Ferrer, T. León, S. Doran, P. Etayo, A. Vidal-Ferran, A. Riera, X. Verdaguer, *Angew. Chem. Int. Ed.* **2010**, *49*, 9452–9455. (b) T. León, A. Riera, X. Verdaguer, *J. Am. Chem. Soc.* **2011**, *133*, 5740–5743. (c) E. Cristõbal-Lecina, P. Etayo, S. Doran, M. Revés, P. Martín-Gago, A. Grabulosa, A. R. Costantino, A. Vidal-Ferran, A. Riera, X. Verdaguer, *Adv. Synth. Catal.* **2014**, *356*, 795–804. (d) T. Leon, M. Parera, A. Roglans, A. Riera, X. Verdaguer, *Angew. Chem. Int. Ed.* **2012**, *51*, 6951–6955. (e) A. Prades, S. Núñez-Pertíñez, A. Riera, X. Verdaguer, *Chem. Commun.* **2017**, *53*, 4605–4608.

[28] S. Orgué, A. Flores-Gaspar, M. Biosca, O. Pàmies, M. Diéguez, A. Riera, X. Verdaguer, *Chem. Commun.* **2015**, *51*, 17548–17551.

[29] E. Salomó, S. Orgué, A. Riera, X. Verdaguer, *Angew. Chem. Int. Ed.* **2016**, *55*, 7988–7992.

[30] E. Salomó, P. Rojo, P. Hernández-Lladó, A. Riera, X. Verdaguer, *J. Org. Chem.* **2018**, *83*, 4618–4627.

[31] E. Salomó, A. Gallen, G. Sciortino, G. Ujaque, A. Grabulosa, A. Lledós, A. Riera, X. Verdaguer, *J. Am. Chem. Soc.* **2018**, *140*, 16967–16970.

[32] M. Biosca, E. Salomó, P. De La Cruz-Sánchez, A. Riera, X. Verdaguer, O. Pàmies, M. Diéguez, *Org. Lett.* **2019**, *21*, 807–811.

[33] A. Cabré, E. Romagnoli, P. Martínez-Balart, X. Verdaguer, A. Riera, *Org. Lett.* **2019**, DOI 10.1021/acs.orglett.9b03865.

[34] F. Menges, A. Pfaltz, *Adv. Synth. Catal.* **2002**, *344*, 40–41.

Experimental Part

General procedures and materials

Unless otherwise indicated, materials were obtained from commercial suppliers and used without further purification. All reactions that required anhydrous conditions were performed in dried glassware under a dry nitrogen atmosphere. Dichloromethane and THF were degassed and anhydrised with a solvent purification system (SPS PS-MD-3). Anhydrous dichloroethane and DMF were used from Sigma Aldrich. Solvents were removed under reduced pressure with a rotary evaporator. Silica gel chromatography was performed using an automated chromatography system (PuriFlash® 430, Interchim).

Instrumentation

NMR spectroscopy: ^{1}H and ^{13}C were recorded on the NMR spectrometers of the *Centres Científics i Tecnològics de la Universitat de Barcelona*. The employed spectrometers were a Varian Mercury 400 MHz. Chemical shifts (δ) were referenced to internal solvent resonances and reported relative to TMS (tetramethylsilane). The coupling constants (*J*) are reported in Hertz (Hz). The following abbreviations are used to define multiplicities: s (singlet), d (doublet), t (triplet), q (quartet), dd (doublet of doublets), ddd (doublet of doublet of doublets), ddd (doublet of doublet of triplets), dddd (doublet of doublet of doublet of doublets), dt (doublet of triplets), td (triplet of doublets), ddq (doublet of doublet of quartets), dtd (doublet of triplet of doublets), dq (doublet of quartets), tt (triplet of triplets), qt (quartet of triplets), m (multiplet), br s (broad signal).

High Resolution Mass Spectrometry: High resolution ESI-MS spectra were recorded in an LC/MSD-TOF G1969A (Agilent Technologies) of the *Centres Científics i Tecnològics de la Universitat de Barcelona.*

IR spectroscopy: IR spectra were measured in a Thermo Nicolet 6700 FT-IR spectrometer using an ATR system, of the Department of Organic Chemistry in the Universitat de Barcelona.

Optical rotations were measured at room temperature (25°C) using a Jasco P-2000 iRM- 800 polarimeter. Concentration is expressed in g/100 mL. The cell sized 10 cm long and had 1 mL of capacity, measuring λ was 589 nm, which corresponds to a sodium lamp.

Melting points were determined using a Büchi melting point apparatus and were not corrected.

Preparation of substrates.[1]

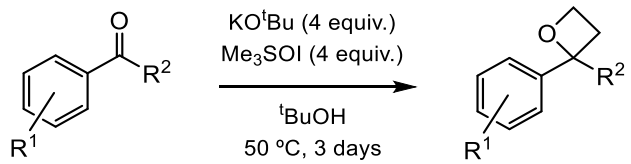

General Procedure (GP1): In an oven dried round bottom flask, trimethylsulfoxonium iodide (5.0 equiv.) was weighted and dissolved in *t*-BuOH (7.9 mL / mmol). *t*-BuOK (5.0 equiv.) was added to the reaction mixture in 4 portions and stirred at 50 °C for 30 min. resulting a white suspension. Afterwards, a solution of the correspondent ketone (1.0 equiv.) in *t*-BuOH (2.0 mL / mmol) was added dropwise. The reaction mixture was heated gradually to 70 °C and stirred for 3 days (or until the reaction went to completion after TLC monitoring). Once the reaction was completed, water was added to the reaction mixture and the two resulting layers were separated and the aqueous phase was extracted with hexanes (x3). Organic layers were combined, dried over anhydrous $MgSO_4$ and concentrated to dryness under vacuum. Purity of the obtained product was checked by ^{1}H-NMR spectroscopy. The obtained product was used without further purification.

For the synthesis of the following compounds, 1 g of ketone was used as starting material for all cases.

2-methyl-2-phenyloxetane, 7-2a

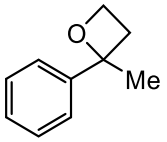

Following GP1, **7-2a** was obtained as pale yellow oil (1.1 g, 89% yield). **^{1}H-NMR** (400 MHz, $CDCl_3$) δ 7.49 – 7.32 (m, 4H), 7.29 – 7.23 (m, 1H), 4.63 (dt, *J* = 8.7, 6.3 Hz, 1H), 4.53 (ddd, *J* = 8.9, 6.9, 5.9 Hz, 1H), 2.78 (qdd, *J* = 10.9, 8.7, 6.8 Hz, 2H), 1.74 (s, 3H). The analytical data for this compound were in excellent agreement with the reported data.[1]

2-(4-fluorophenyl)-2-methyloxetane, 7-2b

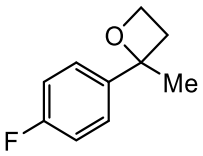

Following GP1, **7-2b** was obtained as pale yellow oil (1.18 g, 98% yield). **^{1}H NMR** (400 MHz $CDCl_3$) δ 7.45 – 7.31 (m, 2H), 7.12 – 6.94 (m, 2H), 4.63 (dddd, *J* = 8.6, 6.4, 5.9, 0.4 Hz, 1H), 4.55 – 4.45 (m, 1H), 2.87 – 2.67 (m, 2H), 1.72 (s, 3H). The analytical data for this compound were in excellent agreement with the reported data.[2]

2-(2-fluorophenyl)-2-methyloxetane, 7-2c

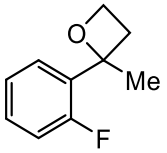

Following GP1, **7-2c** was obtained as pale yellow oil (0.71 g, 71% yield). **^{1}H NMR** (400 MHz, $CDCl_3$) δ 7.57 (ddd, *J* = 8.0, 7.6, 2.0 Hz, 1H), 7.27 – 7.20 (m, 1H), 7.15 (tdd, *J* = 7.5, 1.3, 0.4 Hz, 1H), 7.03 – 6.97 (m, 1H), 4.62 (dddd, *J* = 8.6, 6.4, 5.9, 0.4 Hz, 1H), 4.50 (dddd, *J* = 8.7, 7.1, 5.8, 0.4 Hz, 1H), 2.91 – 2.76 (m, 2H), 1.75 – 1.72 (m, 3H). **^{13}C NMR** (101 MHz, $CDCl_3$) δ 157.33, 134.96 (d, *J* = 13.9 Hz),

[1] Okuma, K.; Tanaka, Y.; Kaji, S.; Ohta, H. *J. Org. Chem.* **1983**, *48* (25), 5133–5134.
[2] Sone, T.; Lu, G.; Matsunaga, S.; Shibasaki, M. *Angew. Chem. Int. Ed.* **2009**, *48* (9), 1677-1680.

128.44 (d, *J* = 7.9 Hz), 125.80 (d, *J* = 4.5 Hz), 123.85 (d, *J* = 3.4 Hz), 115.41 (d, *J* = 21.3 Hz), 84.87, 65.29, 34.87, 29.54. **^{19}F NMR** (376 MHz, $CDCl_3$) δ -116.70 – -117.33 (m). **IR (ATR-FTIR)** νmax = 2969, 2874, 1486, 1439, 1210 cm^{-1}.

2-methyl-2-(4-(trifluoromethyl)phenyl)oxetane, 7-2d

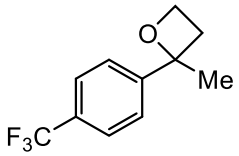

Following GP1, **7-2d** was obtained as pale yellow solid (0.97 g, 84% yield). **^{1}H NMR** (400 MHz, $CDCl_3$) δ 7.66 – 7.59 (m, 2H), 7.52 – 7.48 (m, 2H), 4.64 (ddd, *J* = 8.7, 6.5, 6.1 Hz, 1H), 4.52 (ddd, *J* = 8.8, 7.0, 6.1 Hz, 1H), 2.86 (ddd, *J* = 10.9, 8.7, 6.9 Hz, 1H), 2.72 (ddd, *J* = 10.8, 8.8, 6.5 Hz, 1H), 1.73 (s, 3H). The analytical data for this compound were in excellent agreement with the reported data.[3]

2-(4-chlorophenyl)-2-methyloxetane, 7-2e

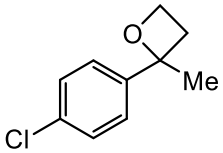

Following GP1, **7-2e** was obtained as pale yellow oil (1.12 g, 95% yield). **^{1}H-NMR** (400 MHz, $CDCl_3$) δ 7.26 (d, *J* = 0.4 Hz, 4H), 4.55 (ddd, *J* = 8.7, 6.5, 6.0 Hz, 1H), 4.47 – 4.40 (m, 1H), 2.74 (ddd, *J* = 10.7, 8.7, 6.9 Hz, 1H), 2.62 (ddd, *J* = 10.7, 8.8, 6.6 Hz, 1H), 1.64 (s, 3H). The analytical data for this compound were in excellent agreement with the reported data.[2]

2-(3-chlorophenyl)-2-methyloxetane, 7-2f

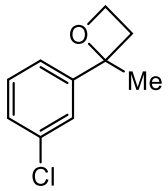

Following GP1, **7-2f** was obtained as pale yellow oil (0.98 g, 83% yield). **^{1}H-NMR** (400 MHz, $CDCl_3$) δ 7.41 – 7.39 (m, 1H), 7.32 – 7.26 (m, 2H), 7.25 – 7.21 (m, 1H), 4.66 – 4.59 (m, 1H), 4.52 (ddd, *J* = 8.8, 6.9, 5.9 Hz, 1H), 2.81 (ddd, *J* = 10.8, 8.7, 6.9 Hz, 1H), 2.71 (ddd, *J* = 10.8, 8.8, 6.6 Hz, 1H), 1.71 (s, 3H). The analytical data for this compound were in excellent agreement with the reported data.[3]

2-(4-bromophenyl)-2-methyloxetane, 7-2g

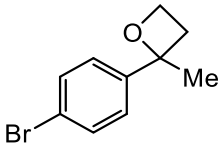

Following GP1, **7-2g** was obtained as pale yellow oil (0.91 g, 80% yield). **^{1}H NMR** (400 MHz, $CDCl_3$) δ 7.49 (dt, *J* = 9.1, 2.1 Hz, 2H), 7.29 – 7.26 (m, 2H), 4.62 (dt, *J* = 8.2, 6.4 Hz, 1H), 4.51 (dt, *J* = 8.6, 6.7 Hz, 1H), 2.81 (ddd, *J* = 10.3, 8.7, 6.9 Hz, 1H), 2.69 (ddd, *J* = 10.5, 8.7, 6.6 Hz, 1H), 1.70 (s, 3H). The analytical data for this compound were in excellent agreement with the reported data.[4]

[3] Coppi, D. I.; Salomone, A.; Perna, F. M.; Capriati, V. *Angew. Chem. Int. Ed.* **2012**, *51*, 7532-7536.
[4] Gansäuer, A.; Ndene, N.; Lauterbach, T.; Justicia, J.; Winkler, I.; Mück-Lichtenfeld, C.; Grimme, S. *Tetrahedron* **2008**, *64* (52), 11839–11845.

2-(4-iodophenyl)-2-methyloxetane, 7-2h

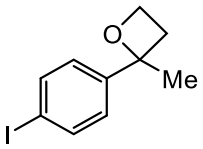

Following GP1, **7-2h** was obtained as pale yellow oil (0.8 g, 72% yield). **^{1}H NMR** (400 MHz, $CDCl_3$) δ 7.73 – 7.67 (m, 2H), 7.18 – 7.12 (m, 2H), 4.62 (ddd, *J* = 8.7, 6.5, 6.0 Hz, 1H), 4.51 (ddd, *J* = 8.8, 6.9, 6.0 Hz, 1H), 2.81 (ddd, *J* = 10.7, 8.7, 6.9 Hz, 1H), 2.73 – 2.65 (m, 1H), 1.71 (s, 3H). **^{13}C NMR** (101 MHz, $CDCl_3$) δ 148.07, 137.43, 125.97, 92.16, 86.39, 64.67, 35.66, 30.61. **HRMS (ESI)** calculated for $C_{10}H_{12}IO$ 274.9927, found 274.9932 $[M+H]^+$. **IR (ATR-FTIR)** νmax = 2963, 2879, 1482, 1390 cm^{-1}.

2-methyl-2-(p-tolyl)oxetane, 7-2i

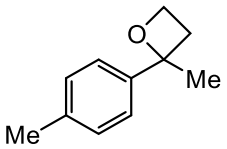

Following GP1, **2i** was obtained as pale yellow oil (0.95 g, 79% yield). **^{1}H-NMR** (400 MHz, $CDCl_3$) δ 7.33 – 7.28 (m, 2H), 7.22 – 7.17 (m, 2H), 4.63 (ddd, *J* = 8.6, 6.7, 5.9 Hz, 1H), 4.53 (ddd, *J* = 8.8, 7.0, 5.9 Hz, 1H), 2.84 – 2.69 (m, 2H), 2.37 (s, 3H), 1.73 (s, 3H). **^{13}C NMR** (101 MHz, CDCl3) δ 145.39, 136.39, 129.02, 123.72, 86.76, 64.66, 35.79, 30.84, 21.20. **HRMS (ESI)** calculated for $C_{11}H_{15}O$ 163.1117, found 163.1122 $[M+H]^+$. **IR (ATR-FTIR)** νmax = 2967, 2922, 2878, 1513, 1442, 1081 cm^{-1}.

2-methyl-2-(o-tolyl)oxetane, 7-2j

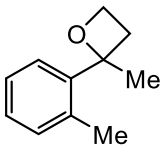

Following GP1, **2j** was obtained as pale yellow oil (1.05 g, 87% yield). **^{1}H NMR** (400 MHz, $CDCl_3$) δ 7.31 – 7.27 (m, 2H), 7.18 (ddt, *J* = 7.8, 1.3, 0.6 Hz, 2H), 4.62 (dddd, *J* = 8.6, 6.5, 5.9, 0.4 Hz, 1H), 4.52 (dddd, *J* = 8.8, 6.9, 5.9, 0.4 Hz, 1H), 2.82 – 2.68 (m, 2H), 2.35 (s, 3H), 1.72 (s, 3H). The analytical data for this compound were in excellent agreement with the reported data.[3]

2-(3-methoxyphenyl)-2-methyloxetane, 7-2k

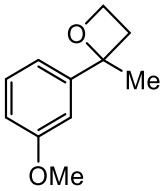

Following GP1, **7-2k** was obtained as pale yellow oil (1.11 g, 94% yield). **^{1}H-NMR** (400 MHz, $CDCl_3$) δ 7.32 – 7.26 (m, 1H), 6.99 (dd, *J* = 2.6, 1.6 Hz, 1H), 6.93 (ddd, *J* = 7.6, 1.6, 0.9 Hz, 1H), 6.80 (ddd, *J* = 8.2, 2.6, 1.0 Hz, 1H), 4.62 (ddd, *J* = 8.7, 6.6, 5.9 Hz, 1H), 4.52 (ddd, *J* = 8.7, 6.9, 5.9 Hz, 1H), 3.82 (s, 3H), 2.84 – 2.68 (m, 2H), 1.74 – 1.70 (m, 3H). **^{13}C NMR** (101 MHz, $CDCl_3$) δ 159.76, 150.16, 129.48, 116.07, 112.21, 109.51, 86.71, 64.70, 55.39, 35.72, 30.84. **HRMS (ESI)** calculated for $C_{11}H_{15}O_2$ 179.1067, found 179.1067 $[M+H]^+$. **IR (ATR-FTIR)** ν max = 2959, 2885, 2356, 1582, 1288, 1044 cm^{-1}.

2-(4-isobutylphenyl)-2-methyloxetane, 7-2l

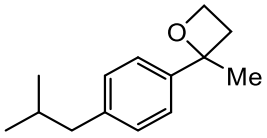

Following GP1, **7-2l** was obtained as pale yellow oil (0.97 g, 84% yield). **^{1}H NMR** (400 MHz, $CDCl_3$) δ 7.31 – 7.27 (m, 2H), 7.17 – 7.12 (m, 2H), 4.63 (td, *J* = 7.9, 6.1 Hz, 1H), 4.53 (td, *J* = 8.0, 6.1 Hz, 1H), 2.76 (ddd, *J* = 8.8, 7.2, 2.0 Hz, 2H), 2.47 (d, *J* = 7.1 Hz, 2H), 1.86 (dq, *J* = 13.5, 6.7 Hz, 1H), 1.73 (s, 3H), 0.91 (d, *J* = 6.6 Hz, 6H). **^{13}C NMR** (101 MHz, $CDCl_3$) δ 145.56, 140.23, 129.07, 123.53, 86.79, 64.67, 45.23, 35.76, 31.39, 30.78, 30.39, 22.56. **HRMS (ESI)** calculated for $C_{14}H_{21}O$ 205.1587, found 205.1594 $[M+H]^+$. **IR (ATR-FTIR)** ν max = 2954, 2922, 2869, 2357, 2330, 1365 cm^{-1}.

2-methyl-2-(naphthalen-2-yl)oxetane, 7-2m

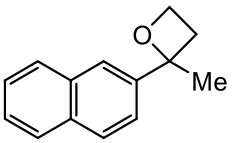

Following GP1, **7-2m** was obtained as pale yellow solid (0.89 g, 76% yield). **^{1}H NMR** (400 MHz, $CDCl_3$) δ 7.91 – 7.80 (m, 4H), 7.53 – 7.40 (m, 3H), 4.75 – 4.62 (m, 1H), 4.59 (ddd, *J* = 8.8, 6.9, 5.9 Hz, 1H), 2.85 (dddd, *J* = 24.1, 10.7, 8.6, 6.8 Hz, 2H), 1.82 (s, 3H). The analytical data for this compound were in excellent agreement with the reported data.[2]

2-cyclohexyl-2-methyloxetane, 7-2n

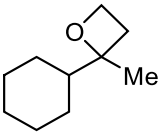

Following GP1, **7-2n** was obtained as colorless oil (0.75 g, 61% yield). **^{1}H-NMR** (400 MHz, $CDCl_3$) δ 4.50 (dddd, *J* = 8.8, 7.0, 6.1, 0.6 Hz, 1H), 4.42 – 4.32 (m, 1H), 2.47 (ddd, *J* = 10.8, 9.1, 7.0 Hz, 1H), 2.21 (dddt, *J* = 11.1, 8.8, 6.4, 0.6 Hz, 1H), 1.78 (dt, *J* = 18.0, 7.1 Hz, 6H), 1.34 (d, *J* = 0.6 Hz, 3H), 1.19 – 1.13 (m, 3H), 0.97 – 0.87 (m, 2H). The analytical data for this compound were in excellent agreement with the reported data.[2]

2-ethyl-2-phenyloxetane, 7-2o

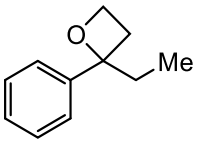

Following GP1, **7-2o** was obtained as pale yellow oil (0.93 g, 77% yield). **^{1}H NMR** (400 MHz, $CDCl_3$) δ 7.44 – 7.31 (m, 4H), 7.29 – 7.24 (m, 1H), 4.56 (dddd, *J* = 21.6, 8.9, 6.8, 5.9 Hz, 2H), 2.85 (ddd, *J* = 10.6, 8.8, 7.0 Hz, 1H), 2.70 (ddd, *J* = 10.6, 8.9, 6.5 Hz, 1H), 2.13 – 2.01 (m, 1H), 1.94 (dq, *J* = 13.8, 7.4 Hz, 1H), 0.85 (t, *J* = 7.4 Hz, 3H). **^{13}C NMR** (101 MHz, $CDCl_3$) δ 146.94, 128.14, 126.62, 124.29, 89.36, 65.06, 36.11, 33.47, 7.59. The analytical data for this compound were in excellent agreement with the reported data.[1]

2-benzyl-2-phenyloxetane, 7-2p

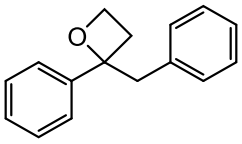

Following GP1, **7-2p** was obtained as pale yellow oil (0.89 g, 78% yield). **^{1}H-NMR** (400 MHz, $CDCl_3$) δ 7.36 – 7.30 (m, 2H), 7.27 – 7.19 (m, 6H), 7.14 (dd, *J* = 7.5, 2.0 Hz, 2H), 4.40 (ddd, *J* = 8.9, 6.8, 5.7 Hz, 1H), 4.24 (ddd, *J* = 8.9, 6.5, 5.7 Hz, 1H), 3.13 (s, 2H), 2.86 (ddd, *J* = 10.8, 8.8, 6.8 Hz, 1H), 2.69 (ddd, *J* = 10.8, 8.9, 6.6 Hz, 1H). **^{13}C NMR** (101 MHz, $CDCl_3$) δ 147.24, 136.78, 130.73, 128.09, 127.98, 126.76, 126.56, 124.32, 88.68, 64.93, 49.61, 32.72. The analytical data for this compound were in excellent agreement with the reported data.[5]

[5] Coppi, D. I.; Salomone, A.; Perna, F. M.; Capriati, V. *Chem. Commun.* **2011**, *47* (35), 9918–9920.

3,4-dihydro-2H-spiro[naphthalene-1,2'-oxetane], 7-2q

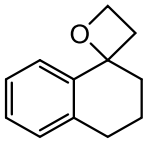

Following GP1, **7-2q** was obtained as pale yellow oil (0.9 g, 76% yield). **^{1}H-NMR** (400 MHz, $CDCl_3$) δ 7.91 (ddd, *J* = 7.9, 1.4, 0.5 Hz, 1H), 7.30 (dddt, *J* = 8.0, 7.3, 1.5, 0.8 Hz, 1H), 7.19 (td, *J* = 7.5, 1.4 Hz, 1H), 7.05 (ddq, *J* = 7.6, 1.4, 0.8 Hz, 1H), 4.76 – 4.65 (m, 2H), 2.86 – 2.72 (m, 3H), 2.63 (ddd, *J* = 11.1, 8.5, 6.3 Hz, 1H), 2.35 (dddd, *J* = 12.7, 6.6, 2.8, 1.0 Hz, 1H), 2.10 (dddd, *J* = 12.7, 11.5, 3.0, 0.8 Hz, 1H), 1.99 – 1.89 (m, 1H), 1.82 – 1.68 (m, 1H). The analytical data for this compound were in excellent agreement with the reported data.[4]

(8R,9S,13S,14S)-3-methoxy-13-methyl-6,7,8,9,11,12,13,14,15,16-decahydrospiro[cyclopenta[a]phenan-threne-17,2'-oxetane], 7-2r

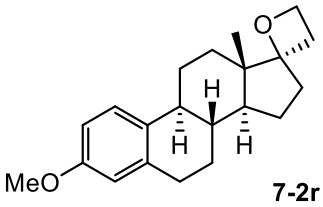

7-2r

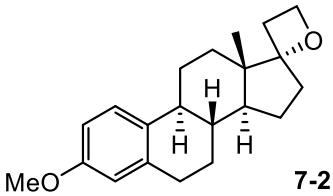

7-2r'

7-2r was synthesized according to a literature procedure.[6] S,S-dimethyl-N-(4-tolylsuflonyl)sulfoximine (1.26 g, 5.1 mmol, 3.3 equiv.) was added through a solid addition funnel (under N_2 flow) into a 2-necked 25 mL rounded-bottom flask equipped with a nitrogen inlet containing sodium hydride 60% mineral oil (183 mg, 3.0 equiv.) and a stirring bar. Anhydrous DMSO (5 mL) was syringed into the flask to give a yellow frothing mixture. After a few minutes a dull green colour developed which then was converted into a yellow colored solution. After 10 h of vigorous stirring at 35 ºC, the mixture was clear indicating complete formation of the anion. A solution of Estrone 3-methyl ether (440 mg, 1.55 mmol, 1.0 equiv.) in anhydrous DMSO (2 mL) was added and the reaction was heated to 48 ºC for 18 h. Afterwards, the reaction was cooled, diluted with saturated NaCl (50 mL) and extracted with ether (4 x 25 mL). The combined organic extracts were washed with brine, dried over MgSO4, filtered and concentrated in vacuo to a volume of few millilitres. Then, petroleum ether was added to precipitate the soluble salts, and the mixture was filtered through a small plug of celite. The eluate was evaporated under vacuum to afford **7-2r**, which was used for the isomerization reaction without further purification. ^{1}H NMR data showed that the product was a 2:1 ratio of diastereomeric oxetanes **7-2r** : **7-2r'**, respectively. **7-2r**: Yellow sticky solid (0.3 g, 62% yield).

^{1}H-NMR (400 MHz, $CDCl_3$) δ 7.25 – 7.20 (m, 1H), 6.70 (dt, *J* = 8.6, 2.3 Hz, 1H), 6.62 (d, *J* = 2.8 Hz, 1H), 4.43 (ddt, *J* = 15.4, 8.9, 6.1 Hz, 1H), 4.38 – 4.25 (m, 1H), 3.76 (t, *J* = 0.8 Hz, 3H), 2.83 (ddd, *J* = 10.8, 8.6, 6.1 Hz, 2H), 2.47 – 2.27 (m, 2H), 2.24 – 2.13 (m, 1H), 2.09 – 2.05 (m, 1H), 1.99 – 1.93 (m, 1H), 1.90 – 1.84 (m, 1H), 1.80 – 1.65 (m, 2H), 1.55 – 1.48 (m, 1H), 1.41 – 1.34 (m, 2H), 1.26 (d, *J* = 1.8 Hz, 3H), 1.10 (ddd, *J* = 11.9, 10.5, 7.5 Hz, 1H), 0.90 – 0.82 (m, 3H). **^{13}C NMR** (101 MHz, $CDCl_3$) δ 157.54, 157.48*, 138.11*, 138.00, 132.88*, 132.55, 126.45, 113.86, 113.84*, 111.58, 111.52*, 97.13*, 96.60, 64.94, 64.30, 55.23, 47.42*, 47.32, 46.23, 44.93, 43.80, 43.53*, 39.48, 39.43*, 37.88*, 37.82, 32.31, 31.07, 29.99*, 29.94, 29.80, 27.75, 27.27, 26.44, 26.18, 26.05, 23.52, 22.89, 22.79, 14.22, 13.24, 11.92. (The carbons with an asterisk correspond to the minor diastereoisomer). **HRMS (ESI)** calculated for $C_{21}H_{29}O_2$ 313.2162, found 313.2153 $[M+H]^+$. **IR (ATR-FTIR)** ν max = 2926, 2874, 2242, 1608, 1499, 1454, 1280, 1256, 1238, 1034 cm^{-1}.

[6] Welch, S. C.; Prakasa Rao, A. S. C.; Lyon, J. T.; Assercq, J.-M. *J. Am. Chem. Soc.* **1983**, *105*, 252-257.

$B(C_6F_5)_3$-Catalyzed Isomerization of 2,2-Disubstituted Oxetanes

General procedure (GP2)

An oven dried vial with a stirring bean was taken into a GloveBox. $B(C_6F_5)_3$ (0.005 equiv. 0.5 mol%, otherwise indicated). was weighted in the vial. The vial was taken out of the GloveBox and the corresponding oxetane (0.4 mmol, 1.0 equiv.) dissolved in anhydrous dichloromethane ([0.1 M]) was added. The reaction mixture was stirred at room temperature for 2 hours (otherwise indicated). Afterwards, the reaction was quenched by adding water and the two phases were separated. The aqueous layer was extracted with dichloromethane (x2) and the organic layers were combined, dried over anhydrous $MgSO_4$ and the solvent was evaporated to dryness under reduced pressure. The product was further purified by flash column chromatography using hexanes/EtOAc as eluent (90:10 and increasing polarities).

3-phenylbut-3-en-1-ol, 7-3a

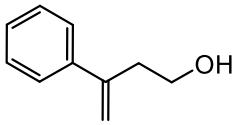

Following GP2, the desired product was obtained as an oil (45 mg, 78% yield). **^{1}H-NMR** (400 MHz, $CDCl_3$) δ 7.44 – 7.39 (m, 2H), 7.36 – 7.26 (m, 3H), 5.41 (d, *J* = 1.4 Hz, 1H), 5.17 – 5.15 (m, 1H), 3.72 (t, *J* = 6.4 Hz, 2H), 2.79 (td, *J* = 6.4, 1.2 Hz, 2H). The analytical data for this compound were in excellent agreement with the reported data.[7]

3-(4-fluorophenyl)but-3-en-1-ol, 7-3b

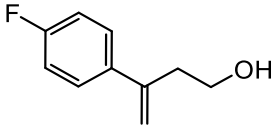

Following GP2, the desired product was obtained as an oil (50 mg, 77% yield). **^{1}H NMR** (400 MHz, $CDCl_3$) δ 7.41 – 7.36 (m, 2H), 7.05 – 7.00 (m, 2H), 5.36 (d, *J* = 1.2 Hz, 1H), 5.15 (q, *J* = 1.3 Hz, 1H), 3.72 (q, *J* = 6.2 Hz, 2H), 2.77 (td, *J* = 6.4, 1.2 Hz, 2H). The analytical data for this compound were in excellent agreement with the reported data.[7]

3-(2-fluorophenyl)but-3-en-1-ol, 7-3c

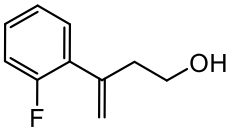

Following GP2, the desired product was obtained as an oil (37 mg, 57% yield). **^{1}H NMR** (400 MHz, $CDCl_3$) δ 7.26 (tdd, *J* = 7.1, 5.5, 1.7 Hz, 2H), 7.11 (td, *J* = 7.5, 1.2 Hz, 1H), 7.07 – 7.01 (m, 1H), 5.33 (t, *J* = 1.4 Hz, 1H), 5.30 – 5.27 (m, 1H), 3.67 (t, *J* = 6.3 Hz, 2H), 2.76 (tt, *J* = 6.4, 1.0 Hz, 2H). The analytical data for this compound were in excellent agreement with the reported data.[7]

3-(4-(trifluoromethyl)phenyl)but-3-en-1-ol, 7-3d

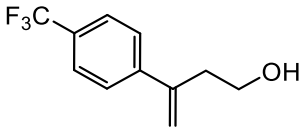

Following GP2, the desired product was obtained as an oil (46 mg, 54% yield). **^{1}H NMR** (400 MHz, $CDCl_3$) δ 7.59 (d, *J* = 8.3 Hz, 2H), 7.54 – 7.50 (m, 2H), 5.47 (d, *J* = 1.0 Hz, 1H), 5.27 (q, *J* = 1.2 Hz, 1H), 3.74 (t, *J* = 6.5 Hz, 2H), 2.80 (td, *J* = 6.4, 1.2 Hz, 2H). The analytical data for this compound were in excellent agreement with the reported data.[8]

---

[7] Mo, J.; Xu, L.; Ruan, J.; Liu, S.; Xiao, J. *Chem. Commun.* **2006**, *34*, 3591–3593.
[8] Ueki, Y.; Ito, H.; Usui, I.; Breit, B. *Chem. Eur. J.* **2011**, *17* (31), 8555–8558.

3-(4-chlorophenyl)but-3-en-1-ol , 7-3e

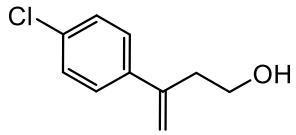

Following GP2, the desired product was obtained as an oil (68 mg, 95% yield). **^{1}H-NMR** (400 MHz, $CDCl_3$) δ 7.38 – 7.28 (m, 4H), 5.40 (d, *J* = 1.2 Hz, 1H), 5.18 (q, *J* = 1.2 Hz, 1H), 3.72 (q, *J* = 5.9 Hz, 2H), 2.76 (td, *J* = 6.4, 1.2 Hz, 2H). The analytical data for this compound were in excellent agreement with the reported data.[9]

3-(3-chlorophenyl)but-3-en-1-ol, 7-3f

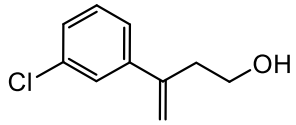

Following GP2, the desired product was obtained as an oil (60 mg, 84% yield). **^{1}H-NMR** (400 MHz, $CDCl_3$) δ 7.40 (q, *J* = 1.5 Hz, 1H), 7.31 – 7.26 (m, 3H), 5.42 (d, *J* = 1.1 Hz, 1H), 5.25 – 5.20 (m, 1H), 3.73 (q, *J* = 5.8 Hz, 2H), 2.76 (td, *J* = 6.6, 1.2 Hz, 2H). The analytical data for this compound were in excellent agreement with the reported data.[10]

¡3-(4-bromophenyl)but-3-en-1-ol, 7-3g

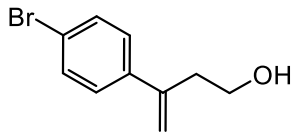

Following GP2, the desired product was obtained as an oil (76 mg, 86% yield). **^{1}H NMR** (400 MHz, $CDCl_3$) δ 7.48 – 7.44 (m, 2H), 7.31 – 7.27 (m, 2H), 5.41 (d, *J* = 1.2 Hz, 1H), 5.19 (q, *J* = 1.2 Hz, 1H), 3.72 (t, *J* = 5.5 Hz, 2H), 2.76 (td, *J* = 6.4, 1.2 Hz, 2H). The analytical data for this compound were in excellent agreement with the reported data.[11]

3-(4-iodophenyl)but-3-en-1-ol, 7-3h

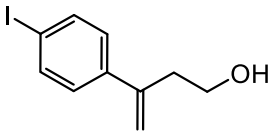

Following GP2, and using 1 mol% of catalyst and stirring the reaction for 17 hours, the desired product was obtained as an oil (75 mg, 70% yield). **^{1}H NMR** (400 MHz, $CDCl_3$) δ 7.70 – 7.63 (m, 2H), 7.18 – 7.13 (m, 2H), 5.41 (d, *J* = 1.2 Hz, 1H), 5.17 (q, *J* = 1.2 Hz, 1H), 3.72 (t, *J* = 6.4 Hz, 2H), 2.75 (td, *J* = 6.4, 1.2 Hz, 2H). **^{13}C NMR** (101 MHz, $CDCl_3$) δ 144.07, 140.11, 137.65, 128.15, 115.31, 93.34, 61.04, 38.43. **HRMS (ESI)** calculated for $C_{10}H_{12}IO$ 274.9927, found 274.9930 $[M+H]^+$. **IR (ATR-FTIR)** ν max = 3360, 2945, 1624, 1485, 1389 cm^{-1}.

3-(p-tolyl)but-3-en-1-ol, 7-3i

[9] Reetz, M. T.; Guo, H.; Ma, J.-A.; Goddard, R.; Mynott, R. J. *J. Am. Chem. Soc.* **2009**, *131,* 4136-4142.
[10] Brindle, C. S.; Yeung, C. S.; Jacobsen, E. N. *Chem. Sci.* **2013**, *4*, 2100-2104.
[11] Sultana, S.; Bondalpati, S.; Indukuri, K.; Gogoi, P.; Saha, P.; Saikia, A. K. *Tetrahedron Lett.,* **2013**, *54*, 1576–1578.

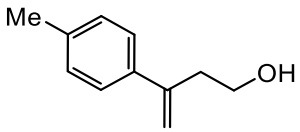

Following GP2, the desired product was obtained as an oil (50 mg,79% yield). **^{1}H-NMR** (400 MHz, $CDCl_3$) δ 7.32 (dt, *J* = 7.0, 2.1 Hz, 2H), 7.16 – 7.14 (m, 2H), 5.12 (q, *J* = 1.3 Hz, 1H), 3.72 (t, *J* = 6.4 Hz, 2H), 2.78 (td, *J* = 6.4, 1.2 Hz, 2H), 2.35 (s, 3H). The analytical data for this compound were in excellent agreement with the reported data.[7]

3-(o-tolyl)but-3-en-1-ol, 7-3j

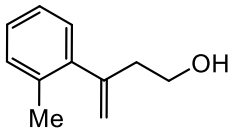

Following GP2, the desired product was obtained as an oil (40 mg, 63% yield). ^{1}H NMR (400 MHz, $CDCl_3$) δ 7.20 – 7.17 (m, 3H), 7.14 – 7.12 (m, 1H), 5.39 (d, *J* = 1.5 Hz, 1H), 5.12 (q, *J* = 1.3 Hz, 1H), 3.72 (td, *J* = 6.4, 0.5 Hz, 2H), 2.81 – 2.77 (m, 2H), 2.35 (s, 3H). The analytical data for this compound were in excellent agreement with the reported data.[9]

3-(3-methoxyphenyl)but-3-en-1-ol, 7-3k

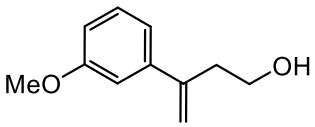

Following GP2, the desired product was obtained as an oil (64 mg, 92% yield). **^{1}H-NMR** (400 MHz, $CDCl_3$) δ 7.25 (d, *J* = 7.7 Hz, 1H), 7.01 (ddd, *J* = 7.7, 1.7, 0.9 Hz, 1H), 6.95 (dd, *J* = 2.6, 1.7 Hz, 1H), 6.84 (ddd, *J* = 8.2, 2.6, 0.9 Hz, 1H), 5.41 (d, *J* = 1.4 Hz, 1H), 5.17 (q, *J* = 1.3 Hz, 1H), 3.76 – 3.70 (m, 2H), 2.78 (td, *J* = 6.4, 1.2 Hz, 2H). The analytical data for this compound were in excellent agreement with the reported data.[7]

3-(4-isobutylphenyl)but-3-en-1-ol, 7-3l

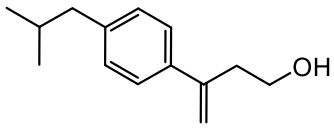

Following GP2, the desired product was obtained as an oil (56 mg, 70% yield). **^{1}H NMR** (400 MHz, $CDCl_3$) δ 7.35 – 7.31 (m, 2H), 7.13 – 7.09 (m, 2H), 5.41 (d, *J* = 1.4 Hz, 1H), 5.12 (q, *J* = 1.3 Hz, 1H), 3.73 (t, *J* = 6.4 Hz, 2H), 2.78 (td, *J* = 6.4, 1.1 Hz, 2H), 2.47 (d, *J* = 7.2 Hz, 3H), 1.85 (dq, *J* = 13.6, 6.8 Hz, 1H), 0.91 (d, *J* = 6.6 Hz, 7H). **^{13}C NMR** (101 MHz, $CDCl_3$) δ 144.69, 141.53, 137.71, 129.33, 125.94, 113.96, 61.18, 45.20, 38.70, 30.34, 22.53. **HRMS (ESI)** calculated for $C_{14}H_{21}O$ 205.1587, found 205.1590 $[M+H]^+$. **IR (ATR-FTIR)** ν max = 3353, 2947, 2911, 2859, 1690, 1525, 1348 cm^{-1}.

3-(naphthalen-2-yl)but-3-en-1-ol, 7-3m

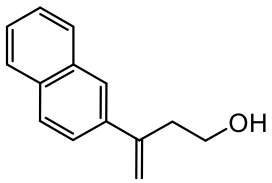

Following GP2, the desired product was obtained as an oil (64mg, 83% yield). **^{1}H NMR** (400 MHz, $CDCl_3$) δ 7.86 – 7.81 (m, 4H), 7.59 (dd, *J* = 8.6, 1.9 Hz, 1H), 7.49 – 7.45 (m, 2H), 5.57 (d, *J* = 1.3 Hz, 1H), 5.28 (d, *J* = 1.2 Hz, 1H), 3.79 (t, *J* = 6.5 Hz, 2H), 2.92 (td, *J* = 6.4, 1.2 Hz, 2H). The analytical data for this compound were in excellent agreement with the reported data.[7]

3-cyclohexylbut-3-en-1-ol, 7-3n

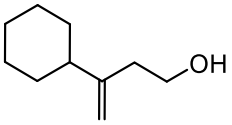

Following GP2, the desired product was obtained as an oil (34 mg, 56% ^{1}H NMR yield). Tetrasubstituted homoallylic alcohol was also formed as the minor product (ratio 7:3). **^{1}H-NMR** (400 MHz, $CDCl_3$) δ 4.87 (t, *J* = 1.3 Hz, 1H), 4.78 (q, *J* = 1.3 Hz, 1H), 3.71 (q, *J* = 6.1 Hz, 2H), 2.34 – 2.29 (m, 2H), 1.89 – 1.81 (m, 1H), 1.81 – 1.72 (m, 4H), 1.71 (d, *J* = 2.2 Hz, 1H), 1.42 (t, *J* = 5.8 Hz, 1H), 1.27 (d, *J* = 12.7 Hz, 2H), 1.24 – 1.19 (m, 1H), 1.16 (d, *J* = 11.6 Hz, 2H). The analytical data for this compound were in excellent agreement with the reported data.[12]

(*E*)-3-phenylpent-3-en-1-ol, 7-3o

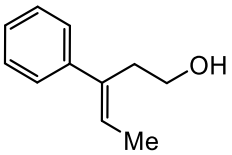

Following GP2, the desired product was obtained as an oil (mixture of *E:Z* 93:7; 55 mg, 87% yield). **^{1}H NMR** (400 MHz, $CDCl_3$) δ 7.34 – 7.30 (m, 4H), 7.25 – 7.21 (m, 1H), 5.92 (q, *J* = 6.9 Hz, 1H), 3.64 (t, *J* = 6.8 Hz, 2H), 2.83 (t, *J* = 6.8 Hz, 2H), 1.85 (d, *J* = 6.8 Hz, 3H). The analytical data for this compound were in excellent agreement with the reported data.[13]

(*E*)-3,4-diphenylbut-3-en-1-ol, 7-3p

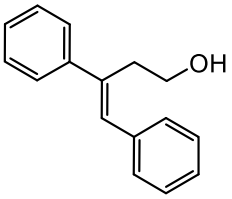

Following GP2, the desired product was obtained as an oil (mixture of *E:Z* 91:9; 75 mg, 86% yield). **^{1}H-NMR** (400 MHz, $CDCl_3$) δ 7.50 – 7.45 (m, 2H), 7.43 – 7.35 (m, 6H), 7.34 – 7.27 (m, 2H), 6.86 (s, 1H), 3.76 – 3.67 (m, 2H), 3.04 (td, *J* = 6.8, 0.8 Hz, 2H). The analytical data for this compound were in excellent agreement with the reported data.[14]

2-(3,4-dihydronaphthalen-1-yl)ethan-1-ol, 7-3q

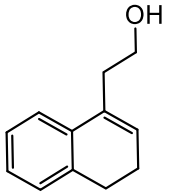

Following GP2, the desired product was obtained as an oil (57 mg, 84% yield). **^{1}H-NMR** (400 MHz, $CDCl_3$) δ 7.27 – 7.23 (m, 1H), 7.23 – 7.17 (m, 1H), 7.17 – 7.14 (m, 2H), 5.96 (td, *J* = 4.6, 2.2 Hz, 1H), 3.79 (t, *J* = 6.5 Hz, 2H), 2.79 – 2.72 (m, 4H), 2.29 (dddd, *J* = 10.3, 5.8, 2.6, 1.3 Hz, 2H). The analytical data for this compound were in excellent agreement with the reported data.[15]

2-((8S,9S,13S,14S)-3-methoxy-13-methyl-7,8,9,11,12,13,14,15-octahydro-6H-cyclopenta[a]phenanthren-17-yl)ethan-1-ol, 7-3r

[12] Fiorito, D.; Mazet, C. *ACS Catal.*, **2018**, *8*, 9382-9387.
[13] Denmark, S. E.; Pan, W. *Org. Lett.* **2001**, *3* (1), 61-64.
[14] Panteleev, J.; Huang, R. Y.; Lui, E. K. J.; Lautens, M. *Org. Lett.* **2011**, *13* (19), 5314-5317.
[15] Ferraz, H. M. C.; Silva, L. F. *Tetrahedron* **2001**, *57* (50), 9939-9949.

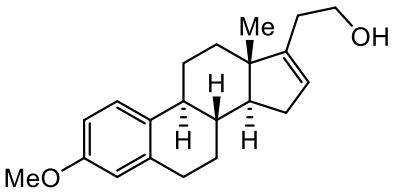

Following GP2, and leaving the reaction stirring 5 hours, the desired product was obtained as a white solid (70 mg, 78% yield). **m.p.** 73-76 ºC. **^{1}H-NMR** (400 MHz, $CDCl_3$) δ 7.25 – 7.17 (m, 1H), 6.71 (dd, *J* = 8.6, 2.8 Hz, 1H), 6.63 (dd, *J* = 7.4, 2.8 Hz, 1H), 5.46 (dt, *J* = 3.1, 1.7 Hz, 1H), 3.83 – 3.71 (m, 6H), 2.87 (ddt, *J* = 18.9, 11.5, 4.7 Hz, 2H), 2.38 – 2.17 (m, 4H), 1.97 – 1.75 (m, 3H), 1.68 – 1.58 (m, 3H), 1.47 – 1.35 (m, 2H), 0.80 (s, 3H). **^{13}C NMR** (101 MHz, $CDCl_3$) δ 157.42, 157.32*, 151.92, 138.21*, 138.00, 132.93, 132.77*, 126.59*, 125.98, 123.87, 113.85, 113.74*, 111.47*, 111.38, 62.05, 60.90, 56.19, 55.19, 48.66, 47.04, 44.36, 43.89, 43.58, 37.43, 35.56, 34.63, 34.52*, 32.25, 31.06, 30.77, 30.55*, 30.45, 30.08, 29.73, 28.79, 27.80, 27.59*, 26.45, 24.08, 15.87, 15.41. (The carbons with an asterisk correspond to the minor diastereoisomer). **HRMS (ESI)** calculated for $C_{21}H_{29}O_2$ 313.2162, found 313.2156 $[M+H]^+$. **IR (ATR-FTIR)** ν max = 3377, 2927, 2850, 1608, 1498, 1463, 1280, 1254, 1237 cm^{-1}.

Iridium-Catalyzed Asymmetric Hydrogenation of Homoallylic Alcohols

General procedure (GP3)

Glass vials equipped with PTFE-coated stir-bars were charged with the corresponding substrate (0.288 mmol, 1.0 equiv.). The corresponding catalyst [((4*S*,5*S*)-Cy$_2$-Ubaphox)Ir(COD)]BARF **7-6** was added (1 mol%) and dissolved with anhydrous DCM (1 mL/0.1 mmol substrate). They were placed into a low pressure reactor. Once sealed, the reactor was purged and charged with 1 bar of H_2 and left stirring overnight at room temperature. Afterwards, the crude was filtrated with a short plug of silica to afford the corresponding isolated product. The conversion was measured by ^{1}H NMR spectroscopy and the enantiomeric excess using chiral HPLC chromatography.

(*S*)-3-phenylbutan-1-ol, 7-5a

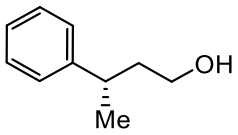

Following GP3, the desired product was obtained as an oil (full conversion, 90% ee). **$[\alpha]_D^{25}$:** +20.5 (c 0.5, $CHCl_3$), lit.[16] $[\alpha]_D^{23}$: -22.7 (c 0.5, $CHCl_3$, for *R* enantiomer with 94% ee). **^{1}H NMR** (400 MHz, $CDCl_3$) δ 7.33 – 7.27 (m, 2H), 7.23 – 7.17 (m, 3H), 3.64 – 3.49 (m, 2H), 2.89 (h, *J* = 7.1 Hz, 1H), 1.90 – 1.80 (m, 2H), 1.28 (d, *J* = 7.0 Hz, 3H). **HPLC**: CHIRALCEL ODH. Heptane/iPrOH 95:5, 0.5 mL/min, λ = 254 nm. $t_{(R)}$ = 23.2 min, $t_{(S)}$ = 26.8 min. The analytical data for this compound were in excellent agreement with the reported data.[16]

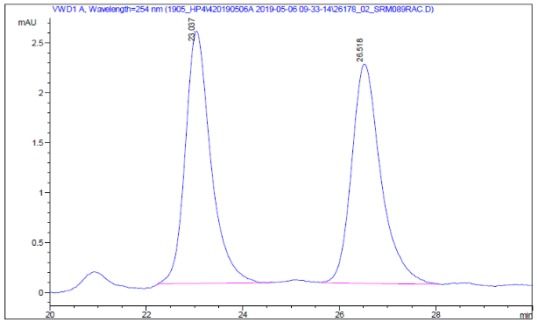

#	Meas. R	Pea	Width	Area	Height	Area %
1	23.037	MM	0.613	92.896	2.527	50.025
2	26.518	MM	0.704	92.804	2.198	49.975

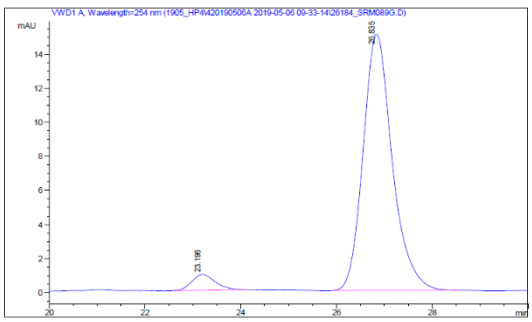

#	Meas. R	Pea	Width	Area	Height	Area %
1	23.196	MM	0.574	32.056	0.931	4.800
2	26.835	MM	0.705	635.837	15.041	95.200

[16] Zhou, Y.; Bandar, J. S.; Liu, R. Y.; Buchwald, S. L. *J. Am. Chem. Soc.* **2018**, *140* (2), 606-609.

(*S*)-3-(2-fluorophenyl)butan-1-ol, 7-5c

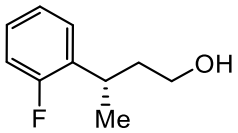

Following GP3, the desired product was obtained as an oil (full conversion, 94% ee). **$[\alpha]_D^{25}$:** +17.7 (c 0.4, $CHCl_3$), lit.[16] $[\alpha]_D^{23}$: -13.6 (c 0.5, $CHCl_3$, for *R* enantiomer with 95% ee). **^{1}H NMR** (400 MHz, $CDCl_3$) δ 7.25 – 7.20 (m, 1H), 7.17 (dddd, *J* = 8.1, 7.2, 5.2, 1.9 Hz, 1H), 7.09 (td, *J* = 7.5, 1.4 Hz, 1H), 7.01 (ddd, *J* = 10.7, 8.0, 1.4 Hz, 1H), 3.58 (qt, *J* = 10.8, 6.6 Hz, 2H), 3.25 (h, *J* = 7.2 Hz, 1H), 1.92 – 1.85 (m, 2H), 1.30 (dd, *J* = 7.0, 0.5 Hz, 3H). **HPLC**: CHIRALCEL ODH. Heptane/IPA 96:4, 0.5 mL/min, λ = 210 nm. $t_{(R)}$ = 24.8 min, $t_{(S)}$ = 27.8 min. The analytical data for this compound were in excellent agreement with the reported data.[16]

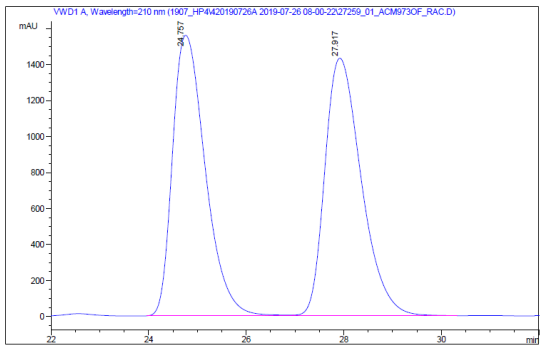

#	Meas. R	Pea	Width	Area	Height	Area %
1	24.757	MF	0.779	72865.703	1.560e3	49.494
2	27.917	FM	0.865	74354.703	1.432e3	50.506

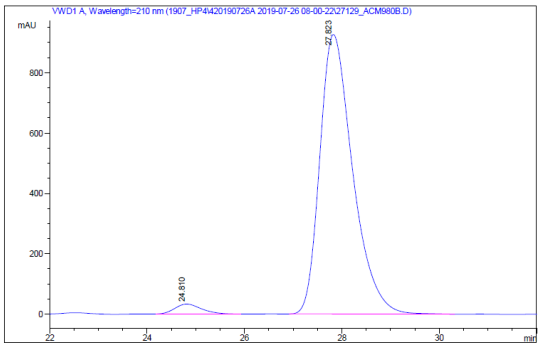

#	Meas. R	Pea	Width	Area	Height	Area %
1	24.810	MM	0.639	1273.587	33.231	2.842
2	27.823	MM	0.783	43545.590	926.393	97.158

(*S*)-3-(4-chlorophenyl)butan-1-ol, 7-5e

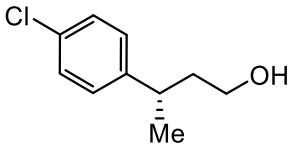

Following GP, the desired product was obtained as an oil (full conversion, 92% ee). **$[\alpha]_D^{25}$:** +18.4 (c 0.7, $CHCl_3$), lit.[16] $[\alpha]_D^{23}$: -30.9 (c 0.5, $CHCl_3$, for *R* enantiomer with 95% ee). **^{1}H NMR** (400 MHz, $CDCl_3$) δ 7.28 – 7.25 (m, 2H), 7.16 – 7.12 (m, 2H), 3.62 – 3.47 (m, 2H), 2.93 – 2.82 (m, 1H), 1.89 – 1.75 (m, 2H), 1.26 (d, *J* = 7.0 Hz, 3H). **HPLC**: Chiralcel OJ. Heptane/EtOH 98:2, 0.5 mL/min, λ = 210 nm. $t_{(S)}$ = 37.0 min, $t_{(R)}$ = 41.2 min. The analytical data for this compound were in excellent agreement with the reported data.[16]

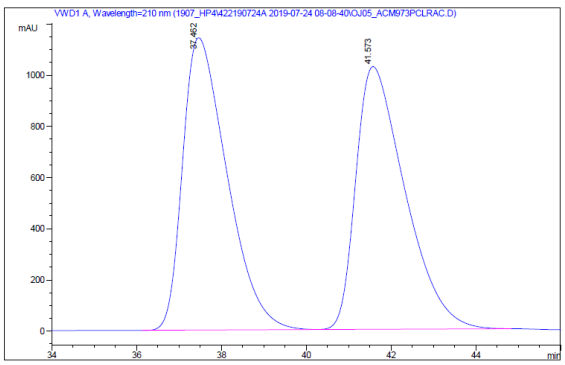

#	Meas. R	Pea	Width	Area	Height	Area %
1	37.462	VB	1.105	83193.742	1.143e3	50.122
2	41.573	BB	1.213	82789.562	1.027e3	49.878

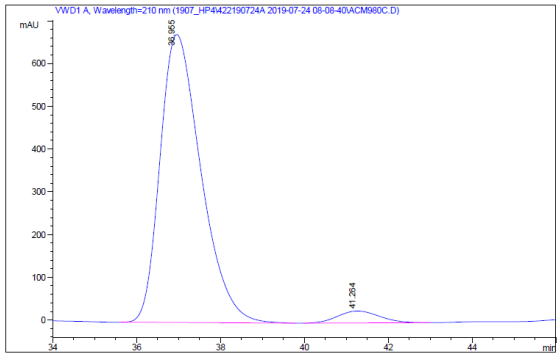

#	Meas. R	Pea	Width	Area	Height	Area %
1	36.955	MM	1.132	45763.762	674.048	95.925
2	41.264	MM	1.157	1944.230	27.996	4.075

(*S*)-3-(p-tolyl)butan-1-ol, 7-5i

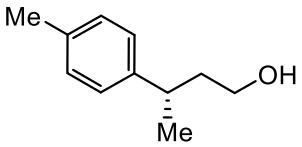

Following GP, the desired product was obtained as an oil (full conversion, 90% ee). **$[\alpha]_D^{25}$:** +13.7 (c 0.4, $CHCl_3$), lit.[17] $[\alpha]_D^{23}$: -24.1 (c 0.22, $CHCl_3$, for *R* enantiomer with 90% ee). **^{1}H NMR** (400 MHz, $CDCl_3$) 7.11 (d, *J* = 0.9 Hz, 4H), 3.56 (q, *J* = 7.8, 7.3 Hz, 2H), 2.85 (dt, *J* = 8.1, 6.9 Hz, 1H), 2.32 (s, 3H), 1.89 – 1.80 (m, 2H), 1.26 (d, *J* = 7.0 Hz, 4H). **HPLC**: CHIRALCEL OJ. Heptane/EtOH 95:5, 0.5 mL/min, λ = 210 nm. $t_{(S)}$ = 22.4 min, $t_{(R)}$ = 24.7 min. The analytical data for this compound were in excellent agreement with the reported data.[17]

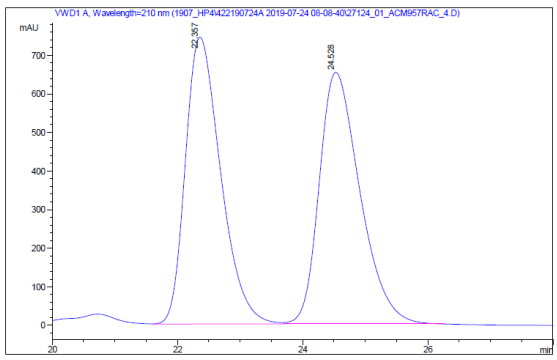

#	Meas. R	Pea	Width	Area	Height	Area %
1	22.357	MF	0.653	29140.732	743.262	49.724
2	24.528	FM	0.753	29463.850	651.971	50.276

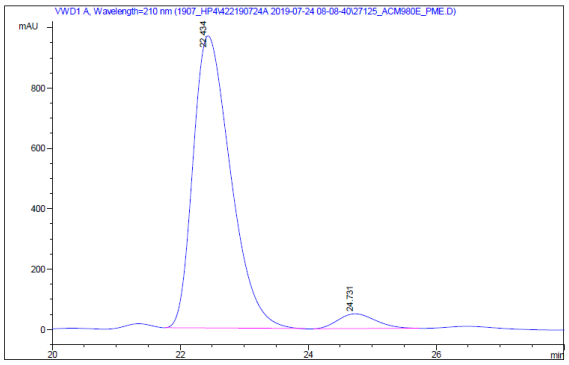

#	Meas. R	Pea	Width	Area	Height	Area %
1	22.434	MF	0.679	39455.824	968.185	95.127
2	24.731	MM	0.684	2021.209	49.284	4.873

(*S*)-3-(3-methoxyphenyl)butan-1-ol, 7-5k

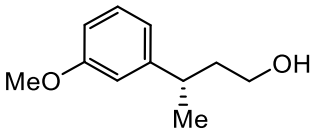

Following GP, the desired product was obtained as an oil (full conversion, 94% ee). **$[\alpha]_D^{25}$:** +15.0 (c 0.5, $CHCl_3$). The absolute stereochemistry was assigned as (*S*) by analogy. **^{1}H NMR** (400 MHz, $CDCl_3$) δ 7.23 (tdd, *J* = 7.8, 1.7, 0.8 Hz, 1H), 6.81 (dt, *J* = 7.7, 1.5 Hz, 1H), 6.78 – 6.72 (m, 2H), 3.81 (s, 3H), 3.57 (tdd, *J* = 9.5, 6.9, 3.8 Hz, 2H), 2.93 – 2.81 (m, 1H), 1.88 – 1.81 (m, 2H), 1.28 (dd, *J* = 7.0, 1.6 Hz, 3H). **HPLC**: CHIRALPAK IC. Heptane/iPrOH 96:4, 1.0 mL/min, λ = 210 nm. $t_{(R)}$ = 37.0 min, $t_{(S)}$ = 39.8 min. The analytical data for this compound were in excellent agreement with the reported data.[18]

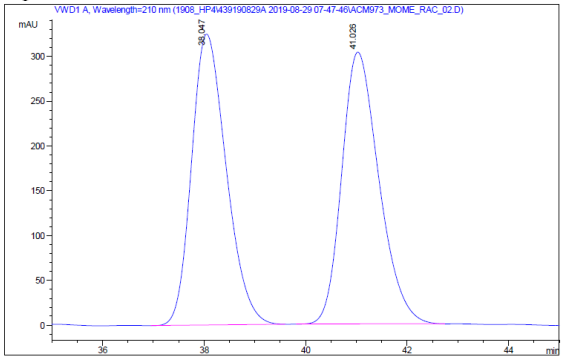

#	Meas. R	Pea	Width	Area	Height	Area %
1	38.047	VB	0.734	15429.838	324.665	49.927
2	41.026	BB	0.777	15475.159	303.468	50.073

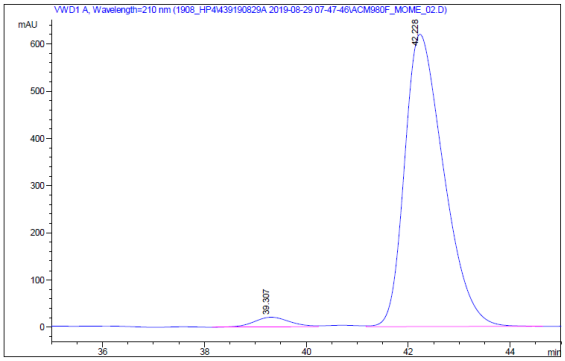

#	Meas. R	Pea	Width	Area	Height	Area %
1	39.307	VV	0.761	1038.221	20.869	3.047
2	42.228	VB	0.816	33031.969	619.145	96.953

[17] Chen, B.; Cao, P.; Liao, Y.; Wang, M.; Liao, J. *Org. Lett.* **2018**, *20* (5), 1346-1349.
[18] Dethe, D. H.; Boda, R.; Murhade, G. M. *Org. Chem. Front.* **2015**, *2* (6), 645-658.

Computational details

Theoretical mechanistic analysis was performed at DFT level of theory with Gaussian09 software.[1] The structures of all the intermediates and transition states were optimized in dichloromethane solvent using the B3LYP functional[2] combined with the Grimme's D3 correction for dispersion.[3] The SMD continuum model[4] was employed to model dichloromethane solvent (DCM, ε= 8.93). The 6-31G(d,p) basis-set[5] (BS1) was used for the optimizations. Vibrational frequencies were computed at the B3LYP-D3/BS1/SMD level of theory for all the stationary points, to characterize them as either minima or transition states. Connection of transition states with the corresponding minima was confirmed by intrinsic reaction coordinate (IRC) calculations and subsequent optimization to minima.
Final Gibbs energies at 298.15 K in DCM were obtained adding the thermal and entropic corrections obtained with BS1 to the electronic energy in DCM computed using the extended triple-ζ *def2*-TZVP basis-set[6] (BS2) at the BS1 optimized geometries. A correction of 1.9 kcal mol^{-1} was applied to all Gibbs energy values to change the standard state from the gas phase (1 atm) to solution phase (1 M) at 298.15 K.[7] In this way, all the energy values in the energy profiles are Gibbs energies in DCM solvent calculated using the formula:

$$G = E(BS2) + G(BS1) - E(BS1) + \Delta G^{1atm \rightarrow 1M}$$

Assessment of the proton migration mechanism for the formation of the allylic alcohol products

Using $BF_3 \cdot Et_2O$ as a catalyst screening of the possible pathways for the formation of the allylic alcohol products **7-*(E)*-4a** and **7-(*Z*)-4a** has been carried out. In the first instance proton migration via an intramolecular mechanism, involving a four-member ring transition state, has been computed. However, it can be discarded as it presents a Gibbs energy barrier of 23.8 kcal·mol^{-1}, incompatible with the experimental detection of equimolar amounts of both products. Then the three O-bases present in the reaction mixture, ethyl ether, substrate **7-2a** and zwitterionic intermediate **II**, have been evaluated for the assisted proton migration leading to **7-*(E)*-4a** and **7-(*Z*)-4a** products. Taking the lowest barrier for each case, the order of the Gibbs energy barrier from **II** for the base-assisted proton migration is: O-**II** (8.1 kcal·mol^{-1}) < O-**7-2a** (13.6 kcal·mol^{-1}) < O-Et_2O (15.6 kcal·mol^{-1}). The four computed TSs are shown in Figure S1.

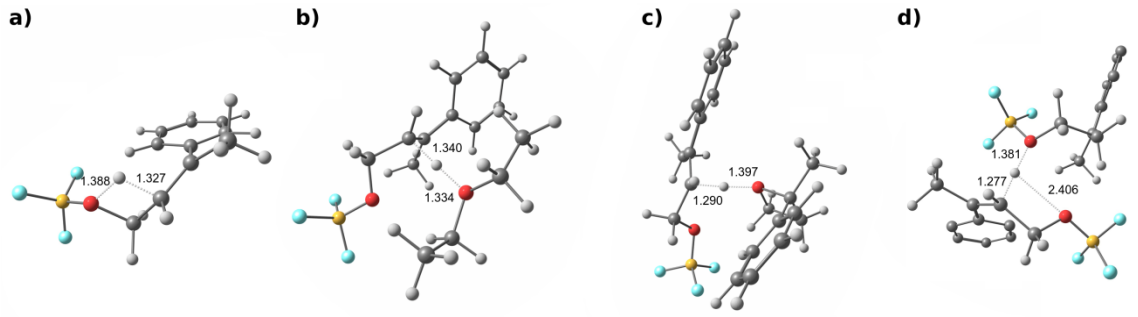

Figure 7.S1. Optimized geometries for transition states of the proton migration step leading to the formation of allylic species **7-*(E)*-4a**, catalyzed by BF_3-Et_2O: **a)** intramolecular four-member ring TS; **b)** intermolecular Et_2O-assisted TS; **c)** intermolecular oxetane **7-2a**-assisted TS, and **d)** intermolecular intermediate-**II** assisted TS. The most important distances are also reported in Å.

The same conclusions have been drawn analyzing the process catalyzed by $B(C_6F_5)_3$ for which the formation of the allylic product via an intramolecular mechanism, involving a four-member ring transition state, has a barrier of 21.3 kcal·mol^{-1}. Similarly, the Gibbs energy barrier from **II** follow the order O-**II** (16.9 kcal·mol^{-1}) < O-**7-2a** (18.5 kcal·mol^{-1}). The three computed TSs are shown in Figure S2.

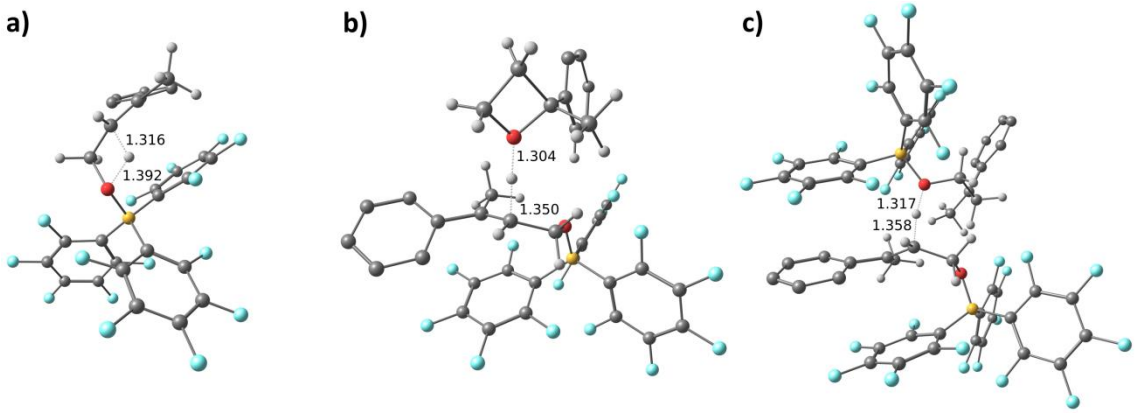

Figure 7.S2. Optimized geometries for transition states of the proton migration step leading to the formation of allylic species **7**-*(E)*-**4a**, catalyzed by $B(C_6F_5)_3$: **a)** intramolecular four-member ring TS; **b)** oxetane **7-2a**-assisted intermolecular TS, and **c)** intermediate **II**-assisted intermolecular TS. The most important distances are also reported in Å.

Gibbs energy profiles

*Isomerization of 2-phenyl-2-methyloxetane **7-2a** catalyzed by $BF_3{\cdot}Et_2O$.*

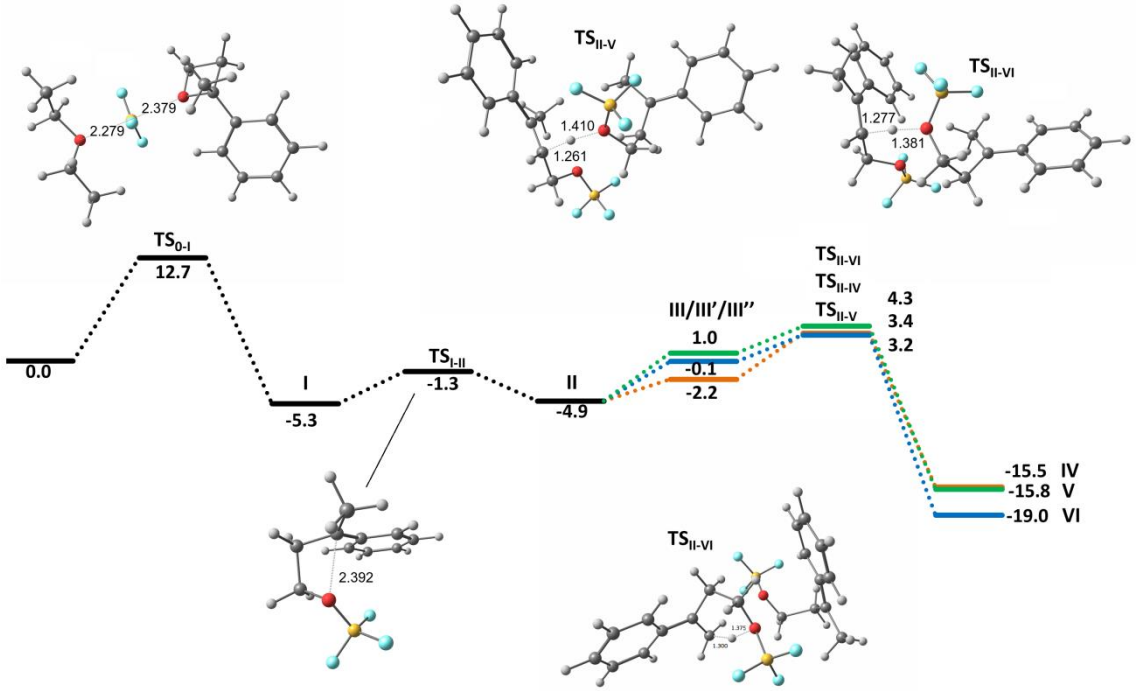

Figure 7.S3. DFT computed mechanism (B3LYP-D3 in DCM) for the isomerization of oxetane **7-2a** to homoallylic **7-3a** (orange path) and allylic **7-***(E)*-**4a** (blue path) and **7-**(*Z*)-**4a** (green path) alcohols catalyzed by $BF_3{\cdot}Et_2O$. Relative Gibbs energies in kcal·mol^{-1} are referred to the separated species. Orange, blue and green pathways are referred to the proton transfer process entailing the formation of **7-3a**, **7-*(E)*-4a** and **7-**(*Z*)-**4a**, respectively. Geometries of the transition states are also shown.

Isomerization of 2-phenyl-2-methyloxetane ***7-2a*** *catalyzed by* $B(C_6F_5)_3$.

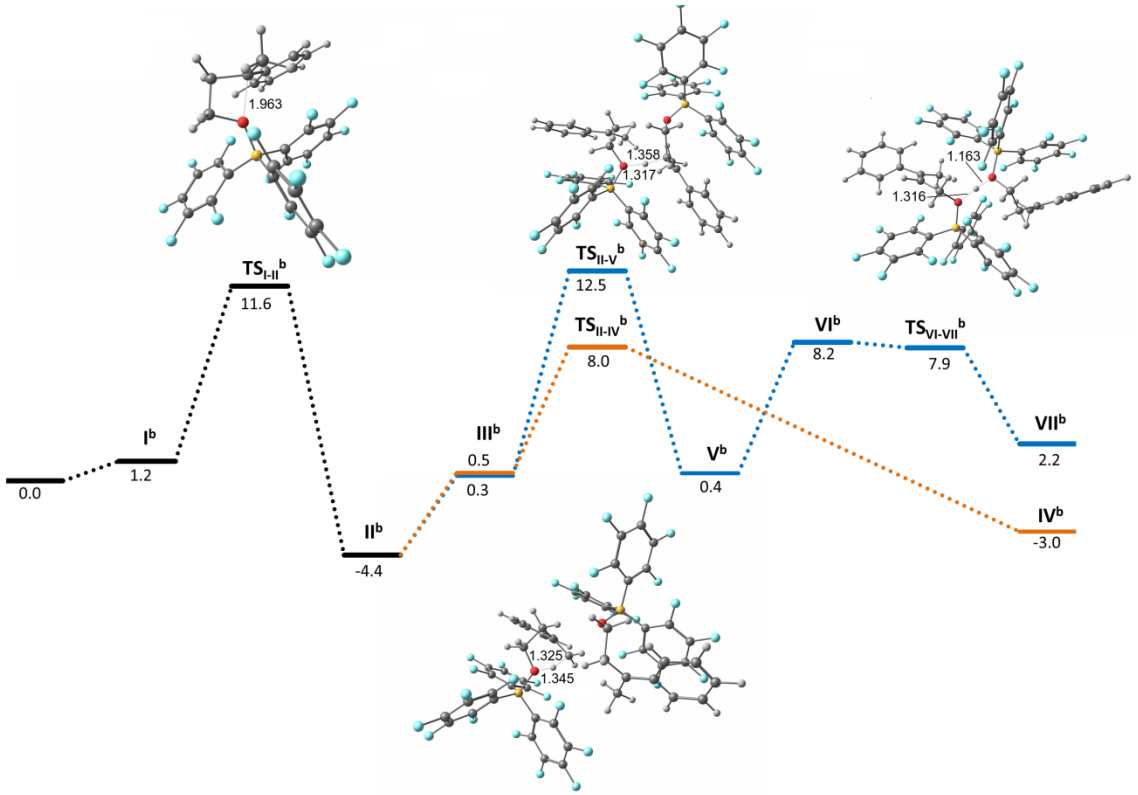

Figure 7.S4. DFT computed mechanism (B3LYP-D3 in DCM) for the isomerization of oxetane **7-2a** to homoallylic **7-3a** (orange path) and allylic **7-***(E)*-**4a** (blue path) alcohols catalyzed by $B(C_6F_5)_3$. Relative Gibbs energies in kcal·mol^{-1} are referred to the separated species. Geometries of the transition states are also shown.

Microkinetic Analysis

The validity of the DFT description of the reaction summarized in the Gibbs energy profiles of Figures 7.S3 and 7.S4 was assessed from microkinetic modeling[8] in which the evolution of concentrations through time is estimated from initial concentrations and rate constants of each reaction step computed as follows:

$$k = \frac{\kappa \cdot k_B \cdot T}{h} e^{\left(\frac{-\Delta G^{\ddagger}}{R \cdot T}\right)}$$

were k is the reaction rate constant, κ the transmission factor (assumed to be 1), k_B the Boltzman's constant, T the temperature, h the Plank's constant, $\Delta G^{\ddagger}$ computed Gibbs energy of activation and R the ideal gas constant. Microkinetics simulations have been performed with the COPASI software[9] considering initial concentrations of 10 mmol/mL for BF_3-Et_2O, $B(C_6H_5)_3$ and **7-2a**.

Isomerization of 2-phenyl-2-methyloxetane ***7-2a*** *catalyzed by* $BF_3{\cdot}Et_2O$.

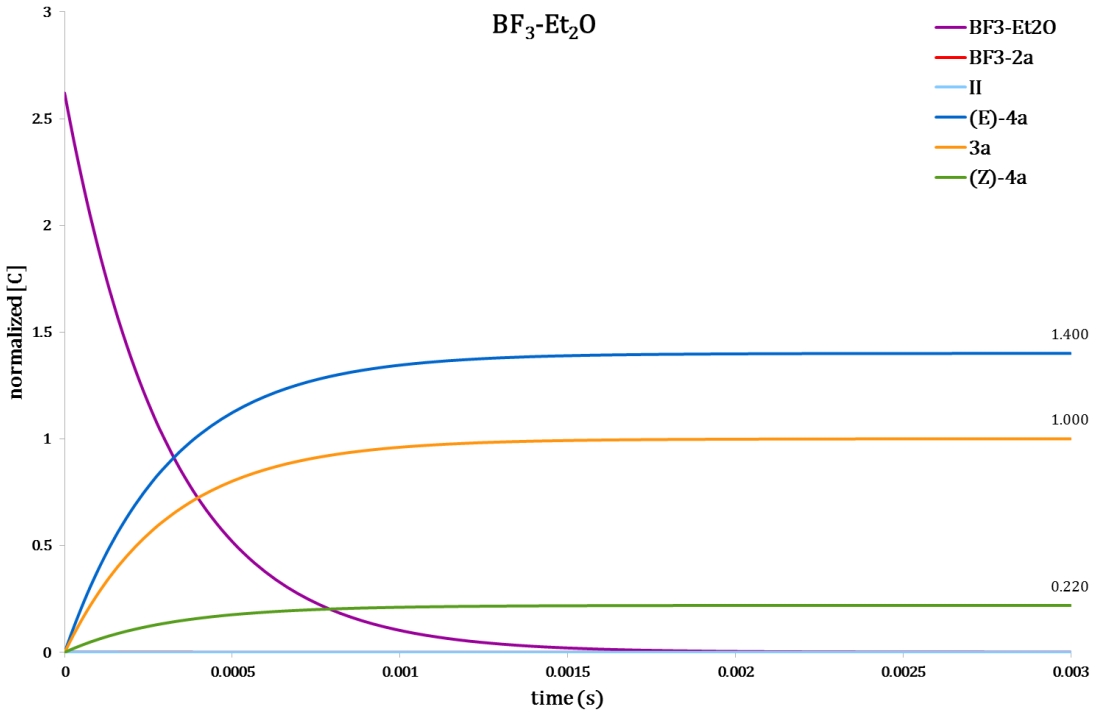

Figure 7.S5. Microkinetic model outcome with normalized concentrations (mmol/mL) of the species involved in the isomerization of ***7-2a*** catalyzed by BF_3-Et_2O over time (in seconds).

Isomerization of 2-phenyl-2-methyloxetane ***7-2a*** *catalyzed by* $B(C_6F_5)_3$.

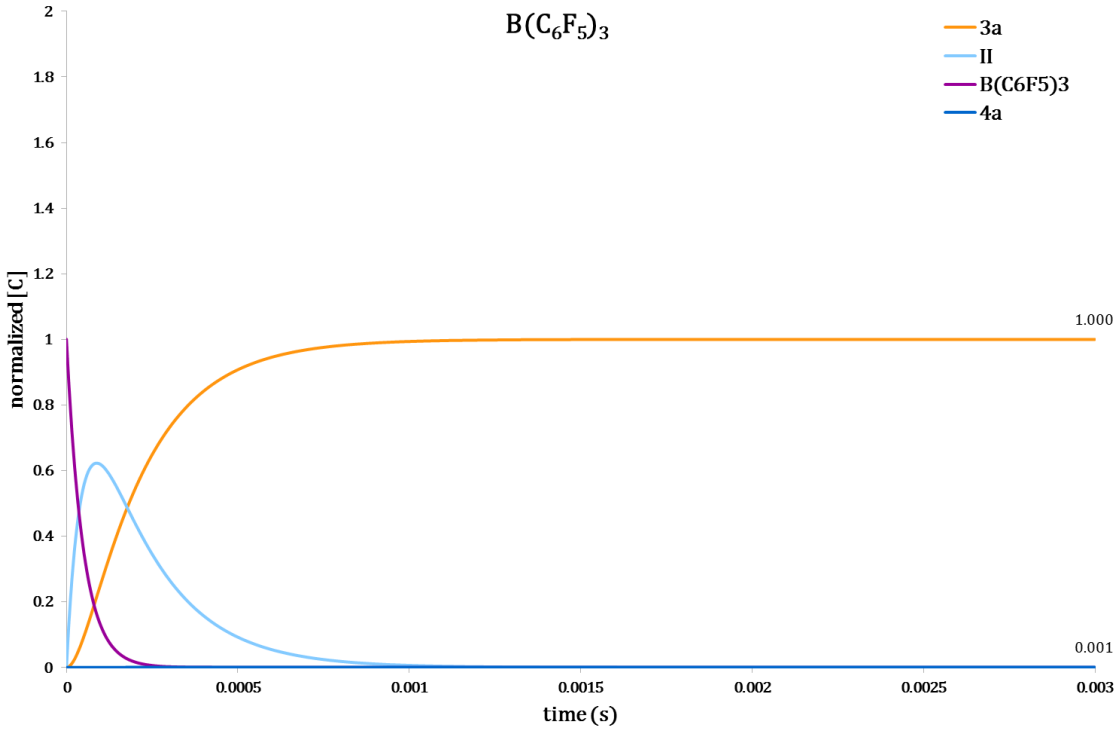

Figure 7.S6. Microkinetic model outcome with normalized concentrations (mmol/mL) of the species involved in the isomerization of ***7-2a*** catalyzed by $B(C_6F_5)_3$ over time (in seconds).

References of the computational part

(1) Gaussian 09 (Revision D.01): Frisch, M. J.; Trucks, G. W.; Schlegel, H. B.; Scuseria, G. E.; Robb, M. A.; Cheeseman, J. R.; Scalmani, G.; Barone, V.; Mennucci, B.; Petersson, G. A.; Nakatsuji, H.; Caricato, M.; Li, X.; Hratchian, H. P.; Izmaylov, A. F.; Bloino, J.; Zheng, G.; Sonnenberg, J. L.; Hada, M.; Ehara, M.; Toyota, K.; Fukuda, R.; Hasegawa, J.; Ishida, M.; Nakajima, T.; Honda, Y.; Kitao, O.; Nakai, H.; Vreven, T.; Montgomery, Jr., J. A.; Peralta, J. E.;Ogliaro, F.; Bearpark, M.; Heyd, J. J.; Brothers, E.; Kudin, K. N.; Staroverov, V. N.; Kobayashi, R.; Normand, J.; Raghavachari, K.; Rendell, A.; Burant, J. C.; Iyengar, S. S.; Tomasi, J.; Cossi, M.; Rega, N.; Millam, J. M.; Klene, M.; Knox, J. E.; Cross, J. B.; Bakken, V.; Adamo, C.; Jaramillo, J.; Gomperts, R.; Stratmann, R. E.; Yazyev, O.; Austin, A. J.; Cammi, R.; Pomelli, C.; Ochterski, J.W.; Martin, R. L.; Morokuma, K.; Zakrzewski, V. G.; Voth, G. A.; Salvador, P.; Dannenberg, J. J.; Dapprich, S.; Daniels, A. D.; Farkas, Ö.; Foresman, J. B.; Ortiz, J. V.; Cioslowski, J.; Fox, D. J., Gaussian, Inc., Wallingford CT, 2011.

(2) (a) Lee, C. T.; Yang, W. T.; Parr, R. G. *Phys. Rev. B* **1988**, *37*, 785-789. (b) Miehlich, B.; Savin, A.; Stoll, H.; Preuss, H. *Chem. Phys. Lett.* **1989**, *157*, 200-206. (c) Becke, A. D. *J. Chem. Phys.* **1993**, *98*, 5648-5652.

(3) Grimme, S.; Antony, J.; Ehrlich, S.; Krieg, H. *J. Chem. Phys.* **2010,** *132*, 154104.

(4) Marenich, S. A. V.; Cramer, C. J.; Truhlar, D. G. *J. Phys. Chem. B* **2009**, *113*, 6378-6396.

(5) Hehre, W. J.; Ditchfield, R.; Pople, J. A. *J. Chem. Phys.* **1972**, *56*, 2257-2261. b) Francl, M. M.; Pietro, W. J.; Hehre, W. J.; Binkley, J. S.; Gordon, M. S.; DeFrees, D. J.; Pople, J. A. *J. Chem. Phys.* **1982**, *77*, 3654-3665.

(6) Weigend, Ahlrichs, R. *Phys. Chem. Chem. Phys.* **2005**, *7*, 3297-3305.

(7) Bryantsev, V. S.; Diallo, M. S.; Goddard, W. A., III *J. Phys.Chem. B* **2008**, *112*, 9709-9719.

(8) Besora, M.; Maseras, F. *Wiley Interdiscip.Rev.: Comput. Mol. Sci.* **2018**, *8*, e1372.

(9) Hoops, S.; Sahle, S.; Gauges, R.; Lee, C.; Pahle, J.; Simus, N.; Singhal, M.; Xu, L.; Mendes, P.; Kummer, U. *Bioinformatics* **2006**, 22, 3067-3074.

^{1}H and ^{13}C NMR Spectra

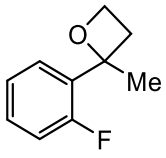

7-2c

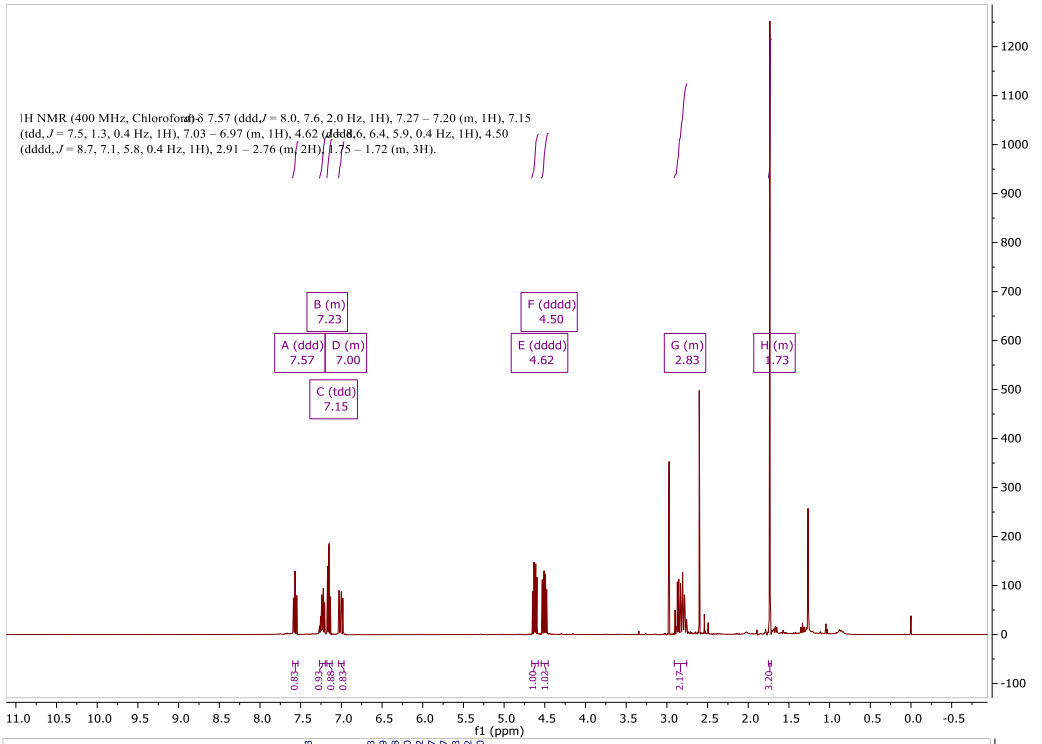

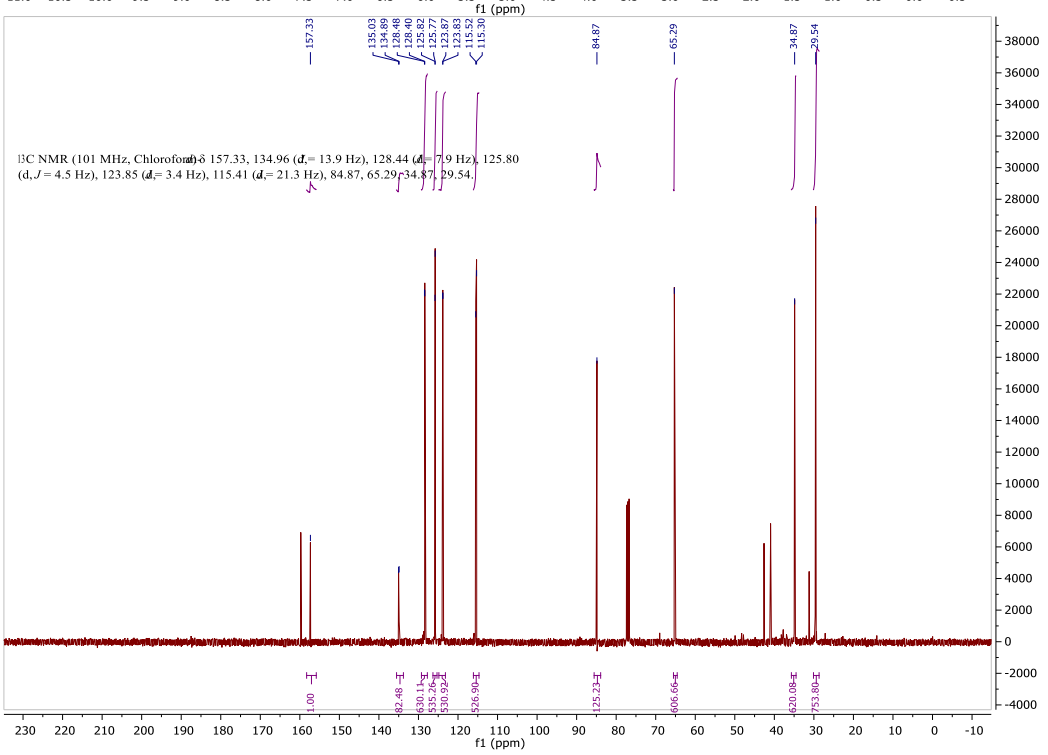

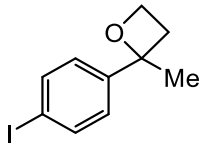
O
Me
I

7-2h

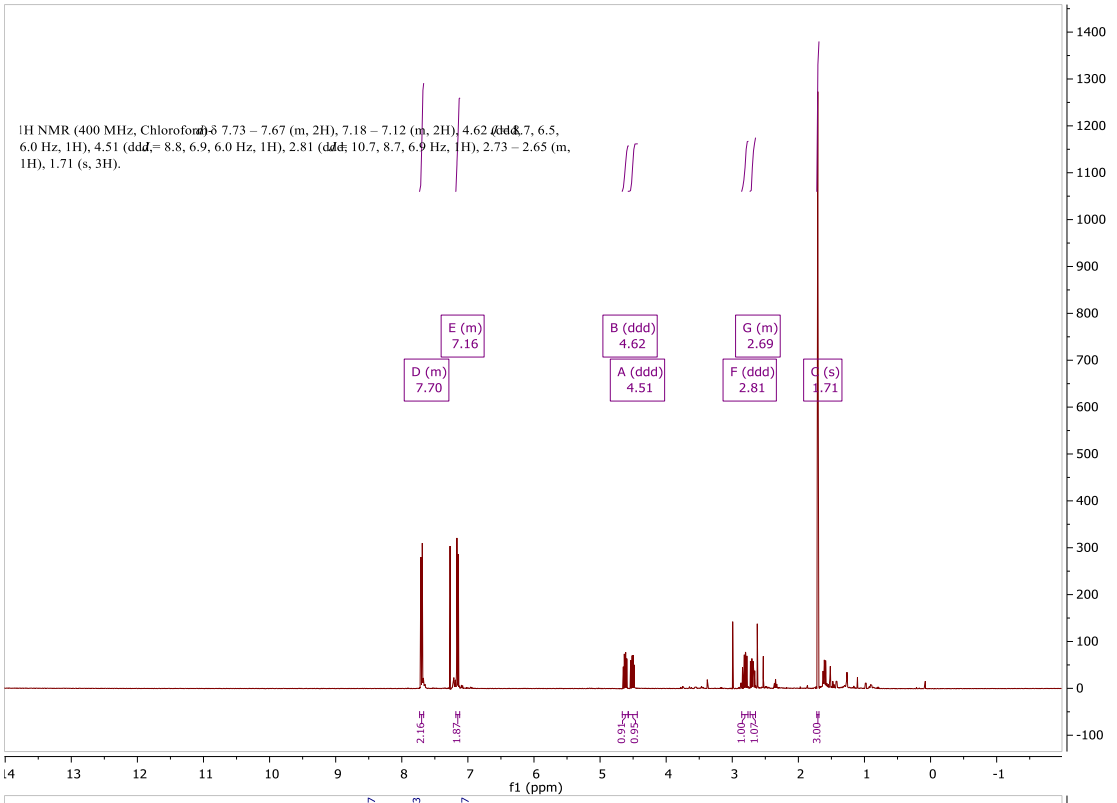
1H NMR (400 MHz, Chloroform-d) δ 7.73 – 7.67 (m, 2H), 7.18 – 7.12 (m, 2H), 4.62 (ddd, J = 8.7, 6.5, 6.0 Hz, 1H), 4.51 (ddd, J = 8.8, 6.9, 6.0 Hz, 1H), 2.81 (ddd, J = 10.7, 8.7, 6.9 Hz, 1H), 2.73 – 2.65 (m, 1H), 1.71 (s, 3H).
E (m) 7.16
D (m) 7.70
B (ddd) 4.62
A (ddd) 4.51
G (m) 2.69
F (ddd) 2.81
C (s) 1.71
2.16
1.87
0.91
0.95
1.00
1.02
3.00
f1 (ppm)

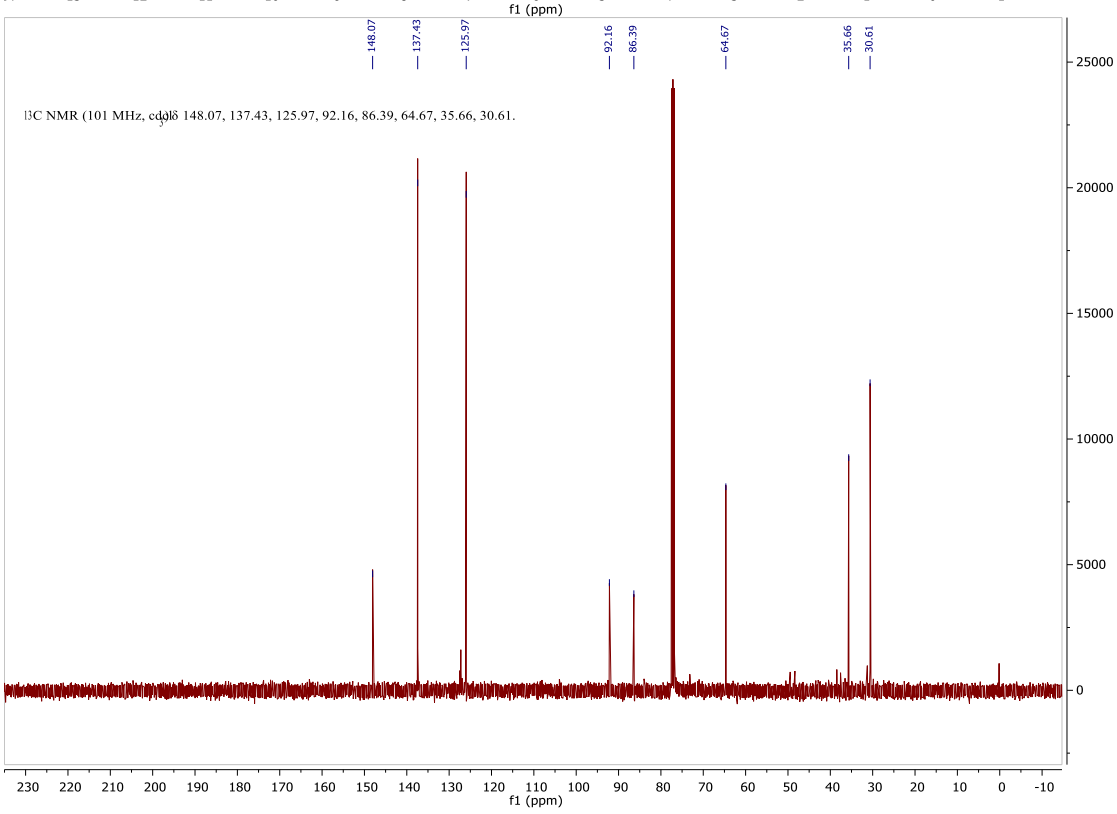
13C NMR (101 MHz, cdcl3) δ 148.07, 137.43, 125.97, 92.16, 86.39, 64.67, 35.66, 30.61.
148.07
137.43
125.97
92.16
86.39
64.67
35.66
30.61
f1 (ppm)

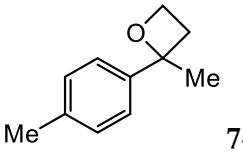

7-2i

^{1}H NMR (400 MHz, Chloroform-d) δ 7.33 – 7.28 (m, 2H), 7.22 – 7.17 (m, 2H), 4.63 (ddd, J = 8.6, 6.7, 5.9 Hz, 1H), 4.53 (ddd, J = 8.8, 7.0, 5.9 Hz, 1H), 2.84 – 2.69 (m, 2H), 2.37 (s, 3H), 1.73 (s, 3H).

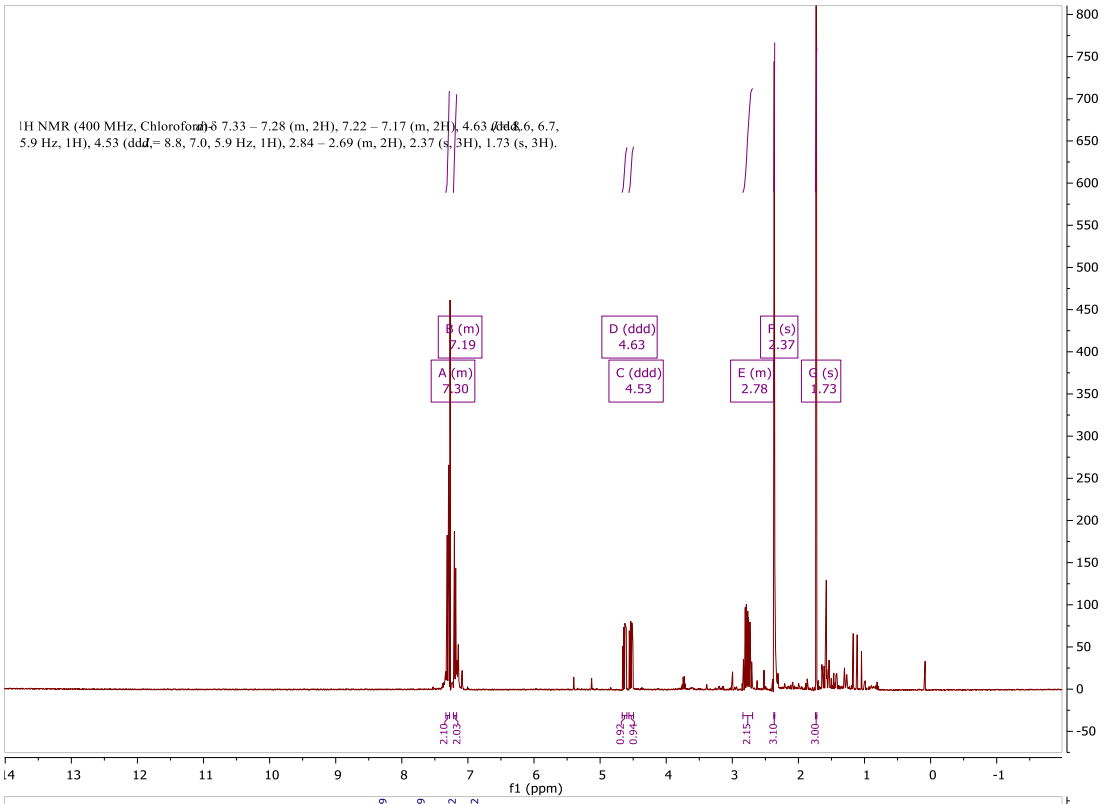

^{13}C NMR (101 MHz, cdcl$_3$) δ 145.39, 136.39, 129.02, 123.72, 86.76, 64.66, 35.79, 30.84, 21.20.

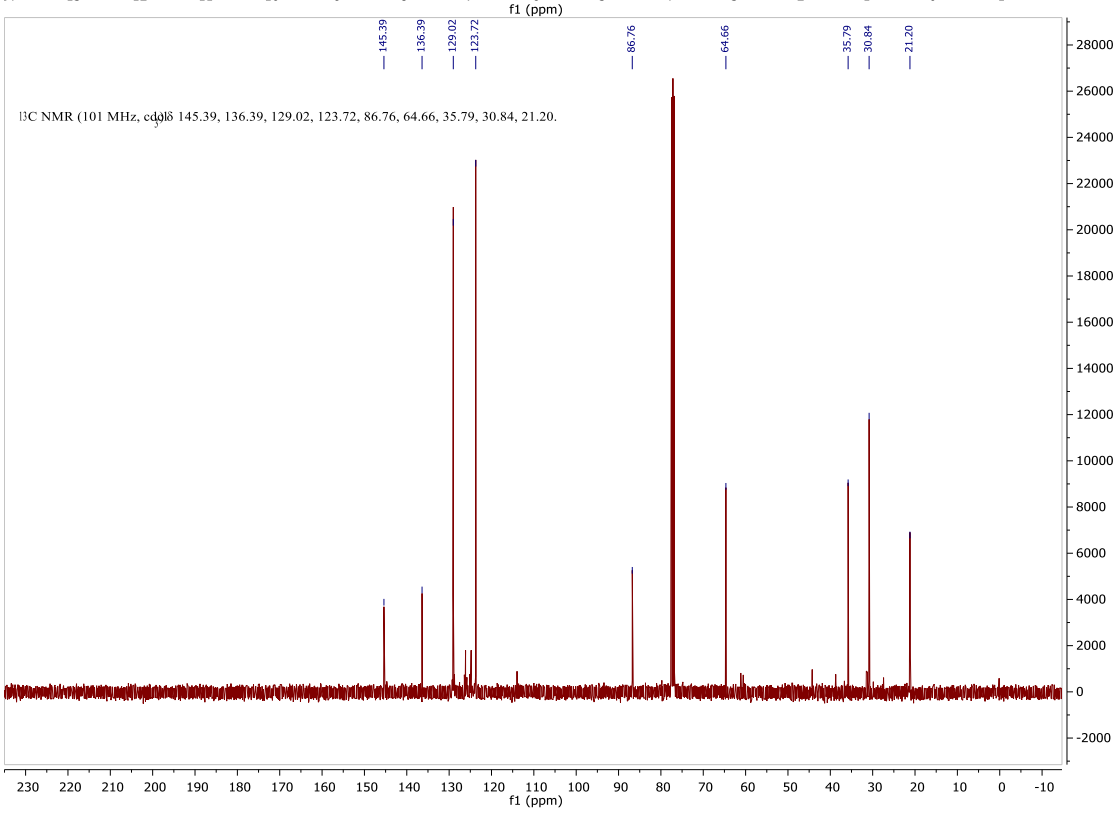

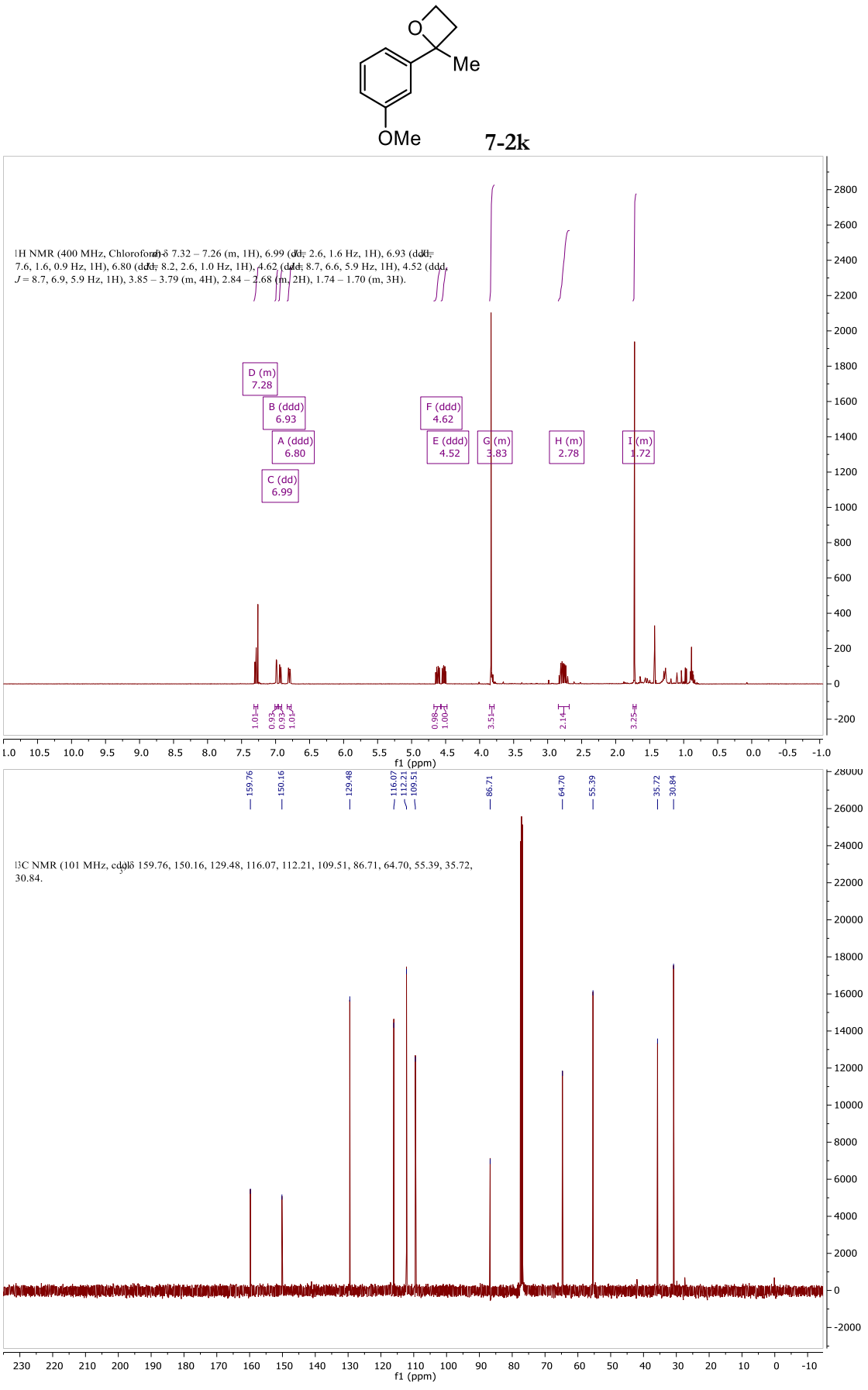
Me
OMe
7-2k
1H NMR (400 MHz, Chloroform-d) δ 7.32 – 7.26 (m, 1H), 6.99 (dd, J = 2.6, 1.6 Hz, 1H), 6.93 (ddd, J = 7.6, 1.6, 0.9 Hz, 1H), 6.80 (ddd, J = 8.2, 2.6, 1.0 Hz, 1H), 4.62 (ddd, J = 8.7, 6.6, 5.9 Hz, 1H), 4.52 (ddd, J = 8.7, 6.9, 5.9 Hz, 1H), 3.85 – 3.79 (m, 4H), 2.84 – 2.68 (m, 2H), 1.74 – 1.70 (m, 3H).
D (m) 7.28
B (ddd) 6.93
A (ddd) 6.80
C (dd) 6.99
F (ddd) 4.62
E (ddd) 4.52
G (m) 3.83
H (m) 2.78
I (m) 1.72
1.01
0.93
0.93
1.01
0.98
1.00
3.51
2.14
3.25
f1 (ppm)
13C NMR (101 MHz, cdcl3) δ 159.76, 150.16, 129.48, 116.07, 112.21, 109.51, 86.71, 64.70, 55.39, 35.72, 30.84.
159.76
150.16
129.48
116.07
112.21
109.51
86.71
64.70
55.39
35.72
30.84
f1 (ppm)

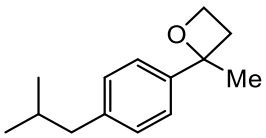

7-21

^{1}H NMR (400 MHz, Chloroform-*d*) δ 7.31 – 7.27 (m, 2H), 7.17 – 7.12 (m, 2H), 4.63 (td, *J* = 7.9, 6.1 Hz, 1H), 4.53 (td, *J* = 8.0, 6.1 Hz, 1H), 2.76 (ddd, *J* = 8.8, 7.2, 2.0 Hz, 2H), 2.47 (d, *J* = 7.1 Hz, 2H), 1.86 (dq, *J* = 13.5, 6.7 Hz, 1H), 1.73 (s, 3H), 0.91 (d, *J* = 6.6 Hz, 6H).

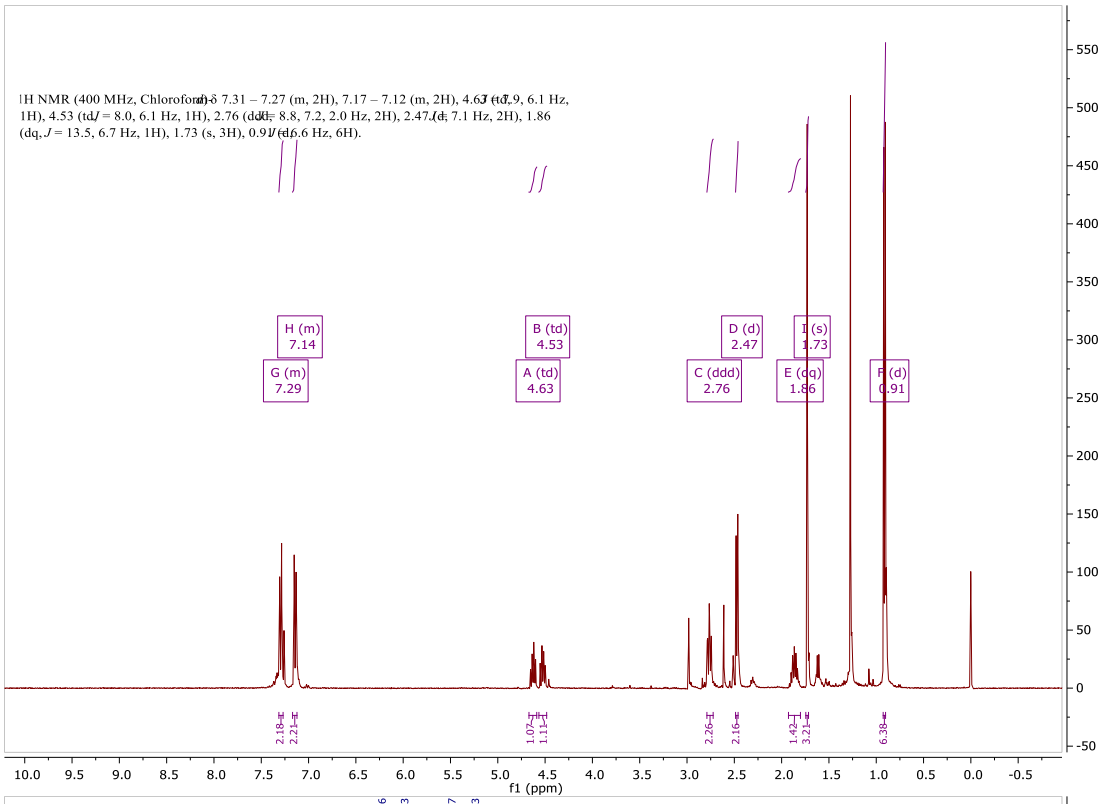

^{13}C NMR (101 MHz, cdcl$_3$) δ 145.56, 140.23, 129.07, 123.53, 86.79, 64.67, 45.23, 35.76, 31.39, 30.78, 30.39, 22.56.

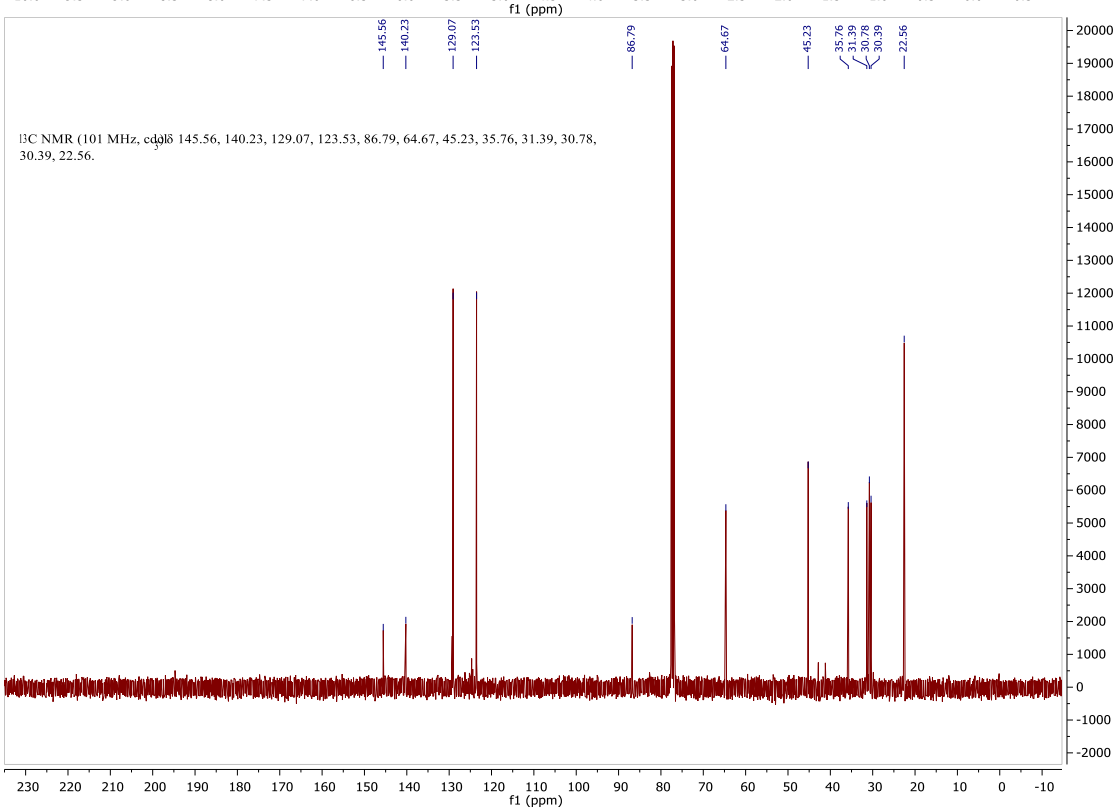

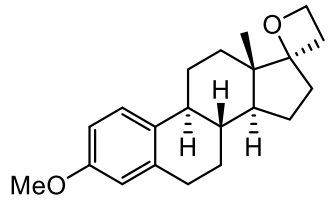

7-2r

^{1}H NMR (400 MHz, Chloroform-d) δ 7.25 – 7.20 (m, 1H), 6.70 (d, J = 8.6, 2.3 Hz, 1H), 6.62 (d, J = 2.8 Hz, 1H), 4.43 (ddt, J = 15.4, 8.9, 6.1 Hz, 1H), 4.38 – 4.25 (m, 1H), 3.76 (t, J = 8 Hz, 3H), 2.83 (ddd, J = 10.8, 8.6, 6.1 Hz, 2H), 2.47 – 2.27 (m, 2H), 2.24 – 2.13 (m, 1H), 2.09 – 2.05 (m, 1H), 1.99 – 1.93 (m, 1H), 1.90 – 1.84 (m, 1H), 1.80 – 1.65 (m, 2H), 1.55 – 1.48 (m, 1H), 1.41 – 1.34 (m, 2H), 1.26 (d, J = 1.8 Hz, 3H), 1.10 (ddd, J = 11.9, 10.5, 7.5 Hz, 1H), 0.90 – 0.82 (m, 3H).

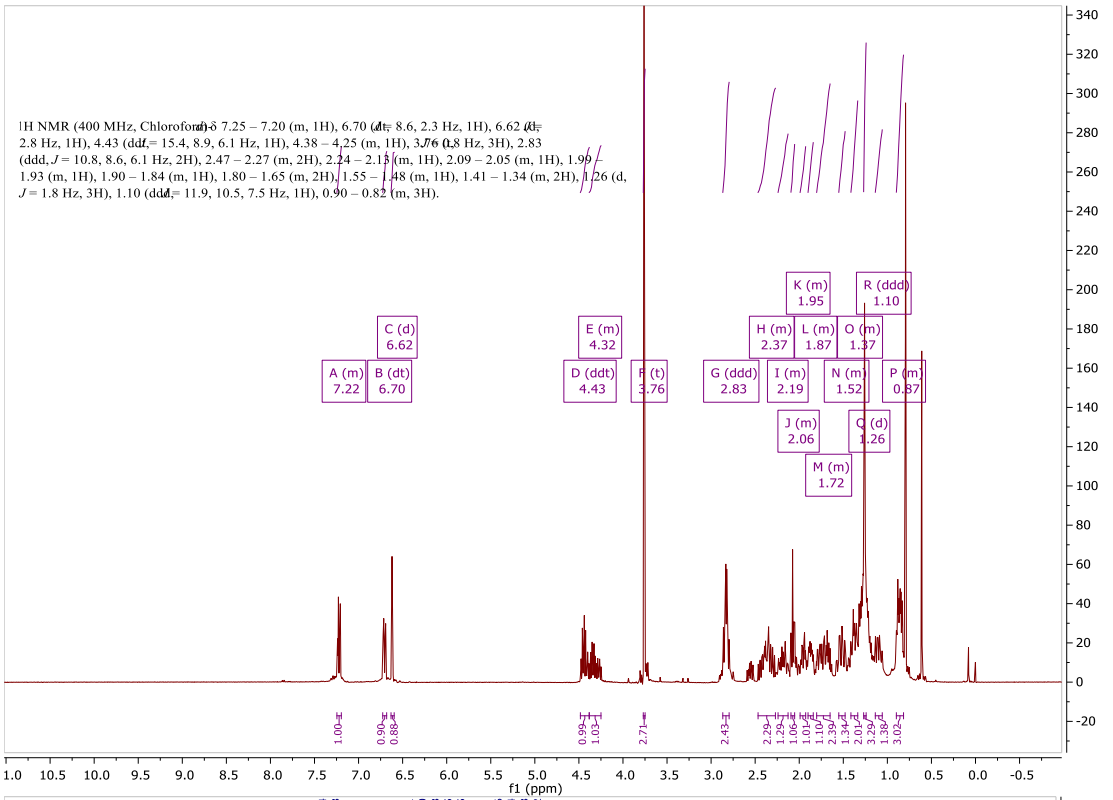

^{13}C NMR (101 MHz, cdcl$_3$) δ 157.54, 157.48, 138.11, 138.00, 132.88, 132.55, 126.45, 113.86, 113.84, 111.58, 111.52, 97.13, 96.60, 64.94, 64.30, 55.23, 47.42, 47.32, 46.23, 44.93, 43.80, 43.53, 39.48, 39.43, 37.88, 37.82, 32.31, 31.07, 29.99, 29.94, 29.80, 27.75, 27.27, 26.44, 26.18, 26.05, 23.52, 22.89, 22.79, 14.22, 13.24, 11.92.

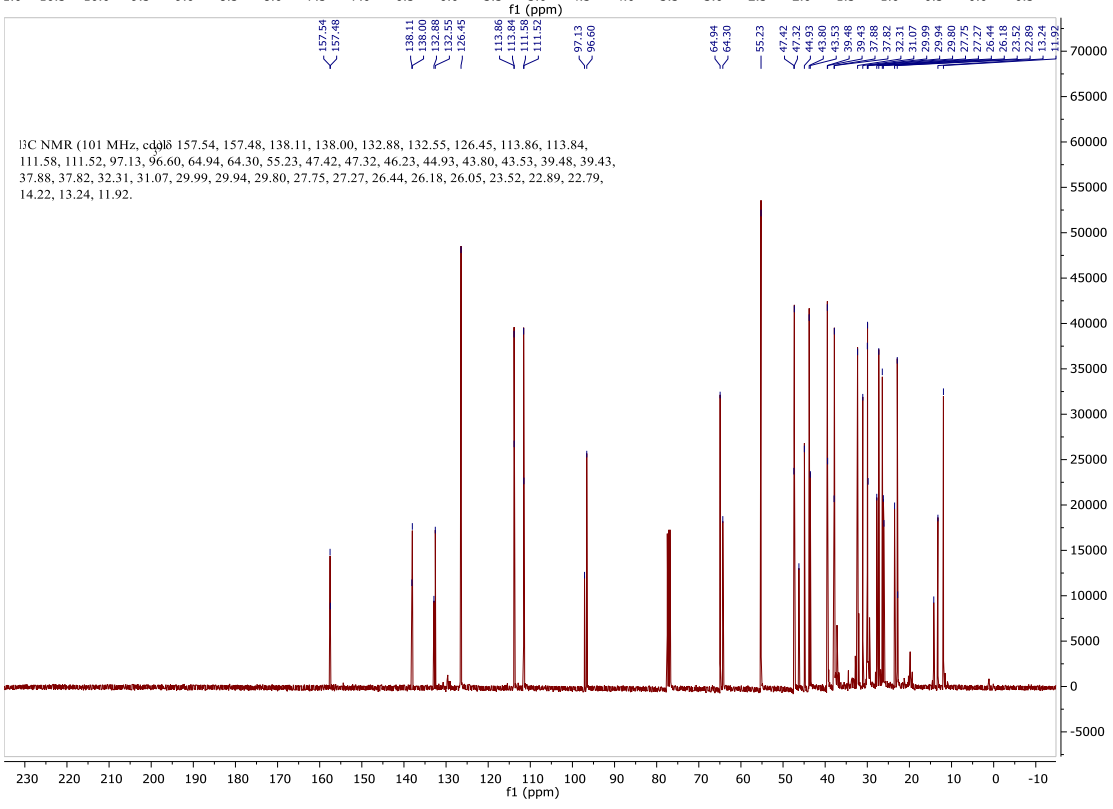

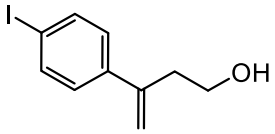
I
OH

7-3h

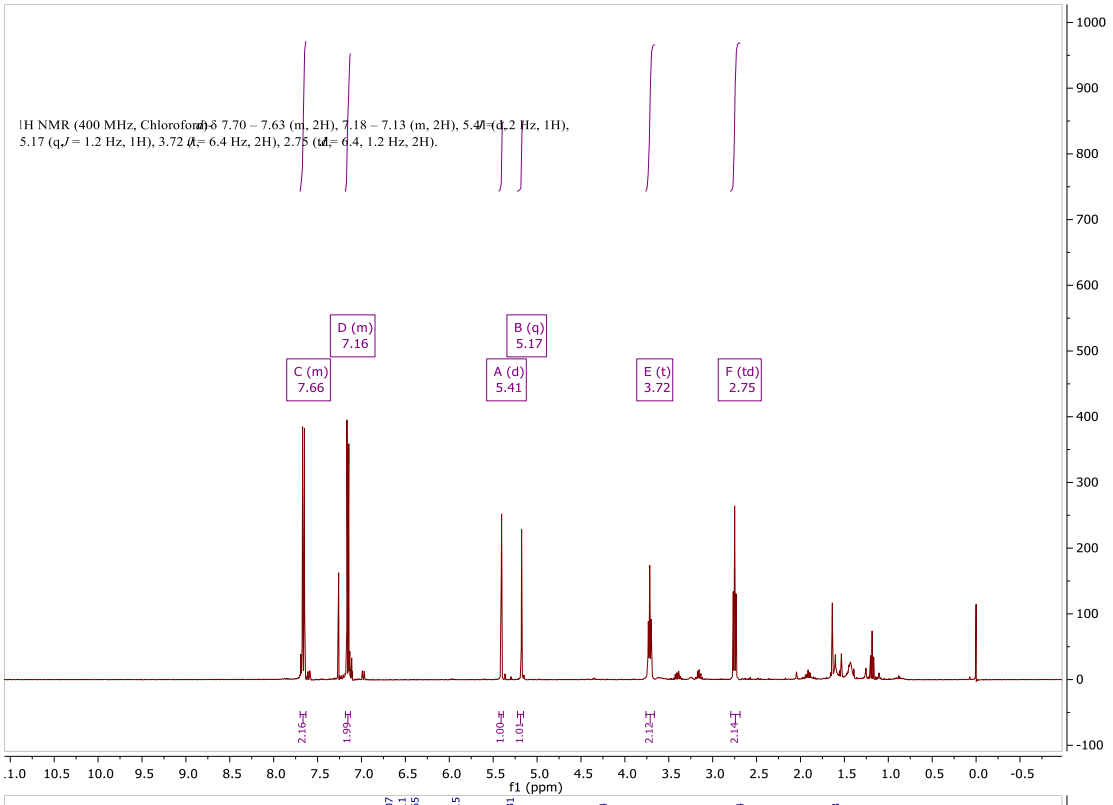
1H NMR (400 MHz, Chloroform-d) δ 7.70 – 7.63 (m, 2H), 7.18 – 7.13 (m, 2H), 5.41 (d, J = 1.2 Hz, 1H), 5.17 (q, J = 1.2 Hz, 1H), 3.72 (t, J = 6.4 Hz, 2H), 2.75 (td, J = 6.4, 1.2 Hz, 2H).
D (m) 7.16
B (q) 5.17
C (m) 7.66
A (d) 5.41
E (t) 3.72
F (td) 2.75
2.16
1.99
1.00
1.01
2.12
2.14
f1 (ppm)

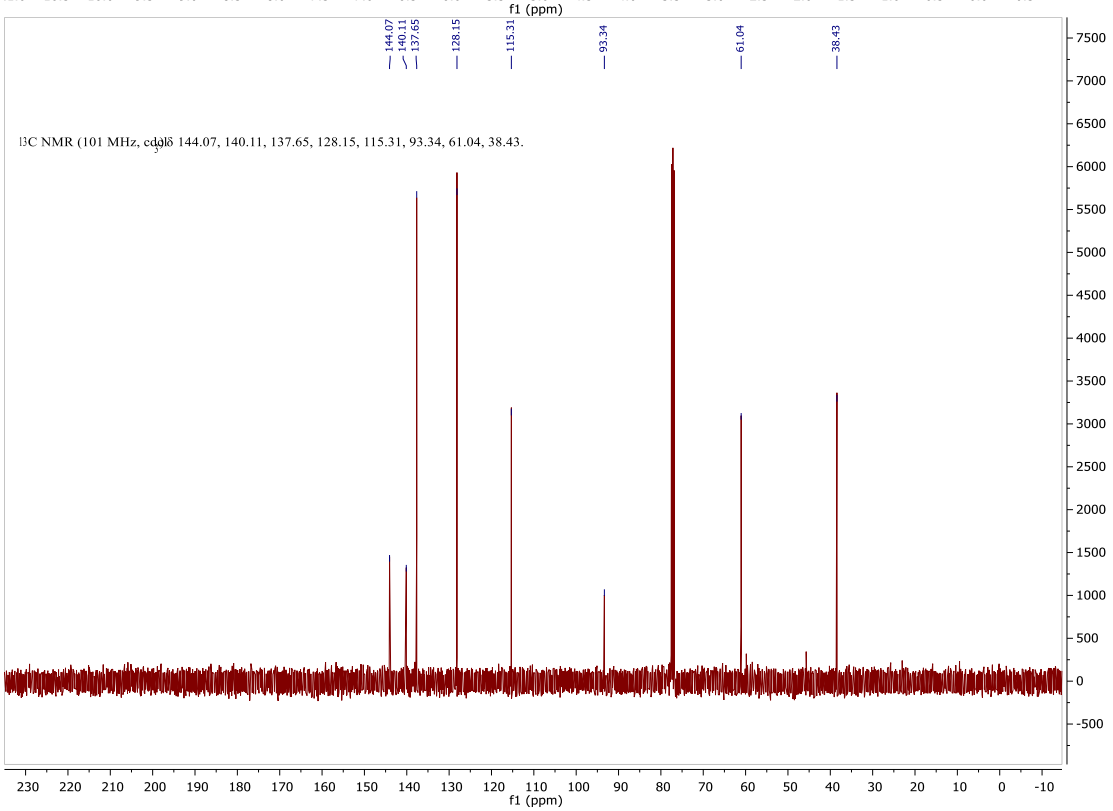
144.07
140.11
137.65
128.15
115.31
93.34
61.04
38.43
13C NMR (101 MHz, cdcl3) δ 144.07, 140.11, 137.65, 128.15, 115.31, 93.34, 61.04, 38.43.
f1 (ppm)

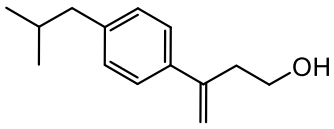

7-31

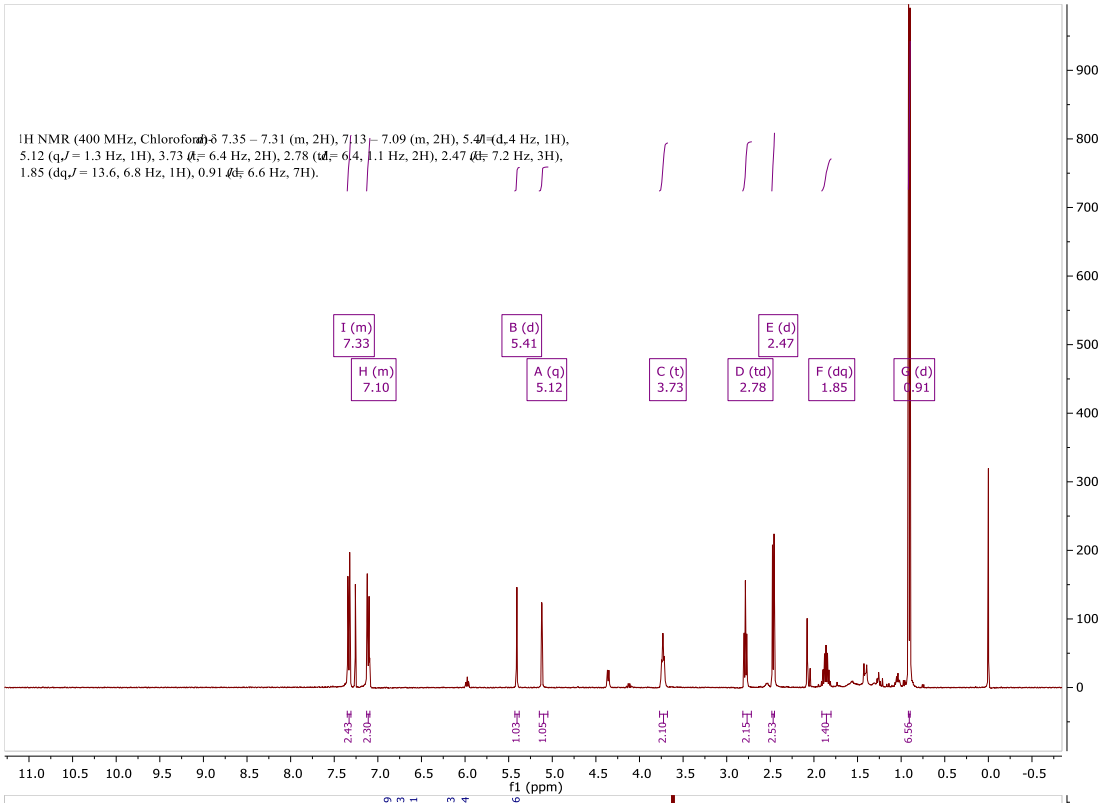

^{1}H NMR (400 MHz, Chloroform-*d*) δ 7.35 – 7.31 (m, 2H), 7.13 – 7.09 (m, 2H), 5.41 (d, *J* = 1.4 Hz, 1H), 5.12 (q, *J* = 1.3 Hz, 1H), 3.73 (t, *J* = 6.4 Hz, 2H), 2.78 (td, *J* = 6.4, 1.1 Hz, 2H), 2.47 (d, *J* = 7.2 Hz, 3H), 1.85 (dq, *J* = 13.6, 6.8 Hz, 1H), 0.91 (d, *J* = 6.6 Hz, 7H).

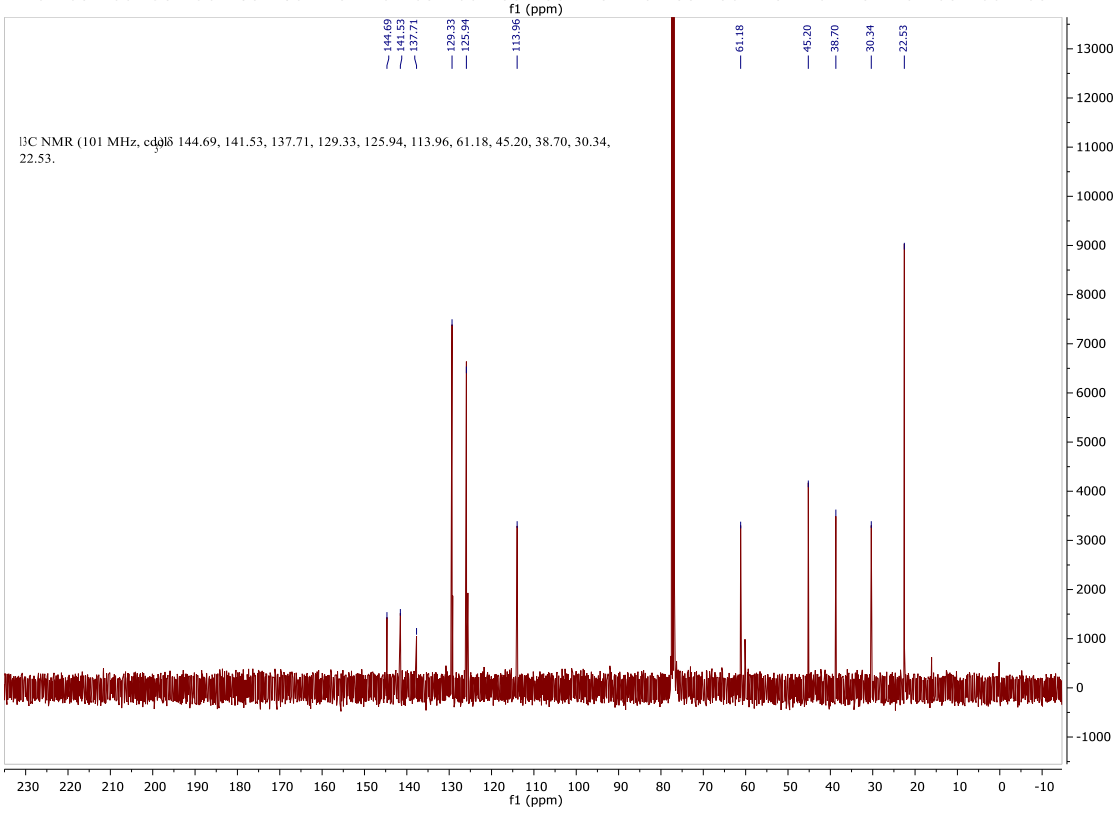

^{13}C NMR (101 MHz, cdcl$_3$) δ 144.69, 141.53, 137.71, 129.33, 125.94, 113.96, 61.18, 45.20, 38.70, 30.34, 22.53.

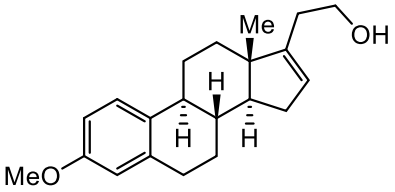
Me
OH
H
H
H
MeO

7-3r

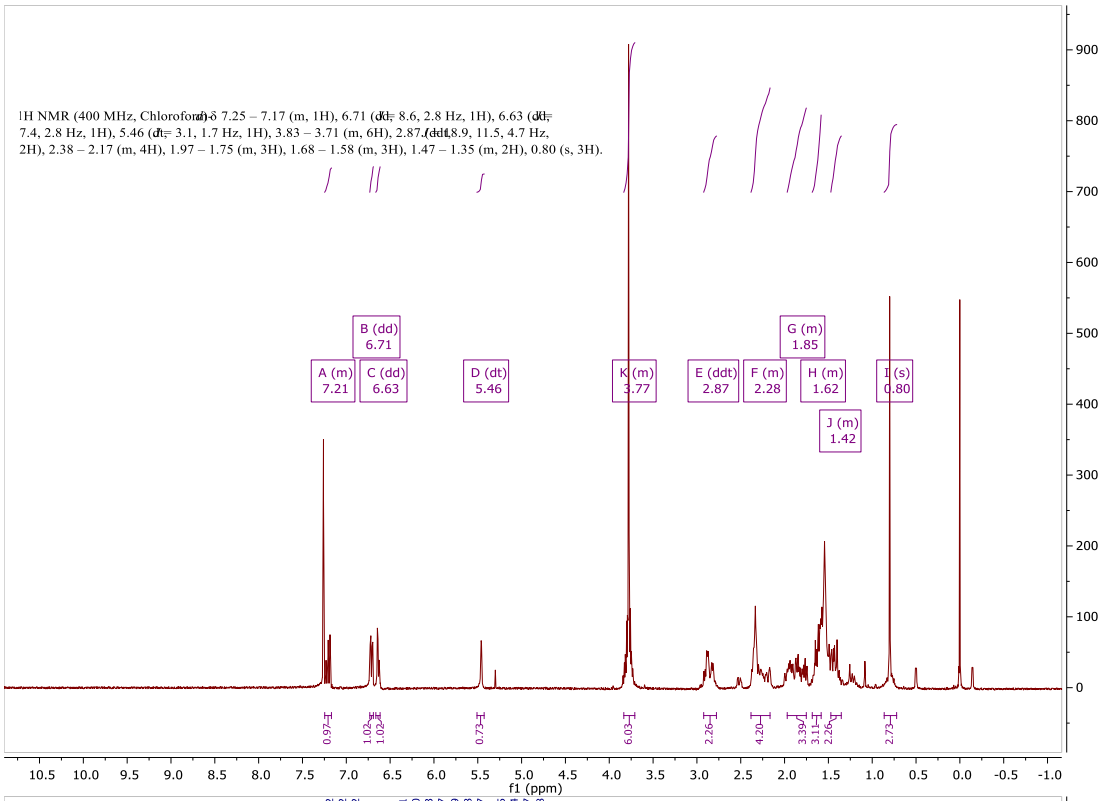
1H NMR (400 MHz, Chloroform-d) δ 7.25 – 7.17 (m, 1H), 6.71 (dd, J = 8.6, 2.8 Hz, 1H), 6.63 (dd, J = 7.4, 2.8 Hz, 1H), 5.46 (dt, J = 3.1, 1.7 Hz, 1H), 3.83 – 3.71 (m, 6H), 2.87 (ddt, J = 18.9, 11.5, 4.7 Hz, 2H), 2.38 – 2.17 (m, 4H), 1.97 – 1.75 (m, 3H), 1.68 – 1.58 (m, 3H), 1.47 – 1.35 (m, 2H), 0.80 (s, 3H).
B (dd) 6.71
A (m) 7.21
C (dd) 6.63
D (dt) 5.46
K (m) 3.77
E (ddt) 2.87
F (m) 2.28
G (m) 1.85
H (m) 1.62
I (s) 0.80
J (m) 1.42
f1 (ppm)

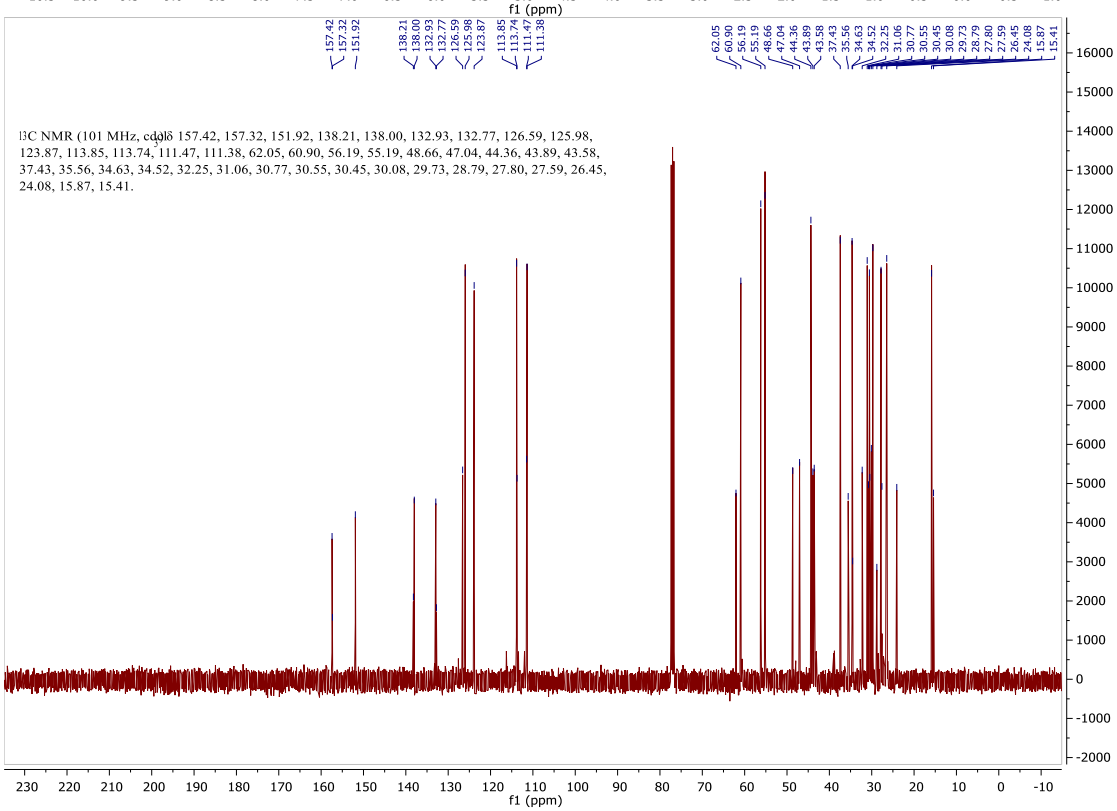
13C NMR (101 MHz, cdcl3) δ 157.42, 157.32, 151.92, 138.21, 138.00, 132.93, 132.77, 126.59, 125.98, 123.87, 113.85, 113.74, 111.47, 111.38, 62.05, 60.90, 56.19, 55.19, 48.66, 47.04, 44.36, 43.89, 43.58, 37.43, 35.56, 34.63, 34.52, 32.25, 31.06, 30.77, 30.55, 30.45, 30.08, 29.73, 28.79, 27.80, 27.59, 26.45, 24.08, 15.87, 15.41.
f1 (ppm)

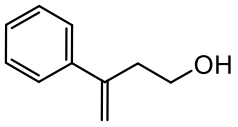
OH

7-3a

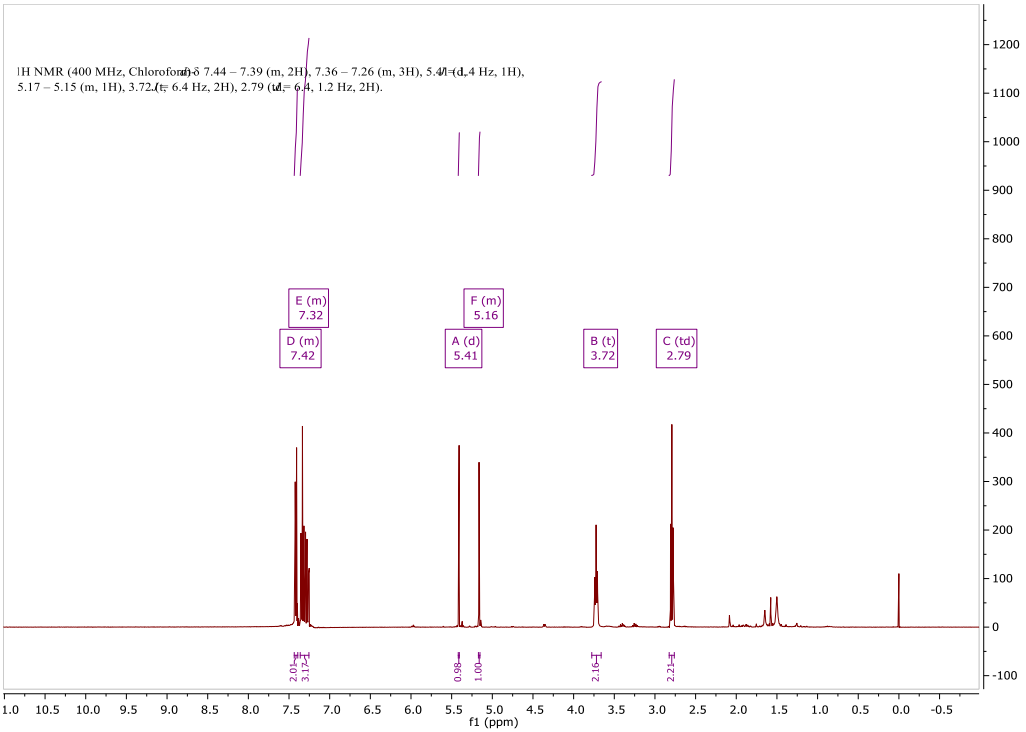
¹H NMR (400 MHz, Chloroform-d) δ 7.44 – 7.39 (m, 2H), 7.36 – 7.26 (m, 3H), 5.41 (d, J = 1.4 Hz, 1H), 5.17 – 5.15 (m, 1H), 3.72 (t, J = 6.4 Hz, 2H), 2.79 (td, J = 6.4, 1.2 Hz, 2H).
E (m) 7.32
D (m) 7.42
F (m) 5.16
A (d) 5.41
B (t) 3.72
C (td) 2.79
2.01
3.17
0.98
1.00
2.16
2.21
f1 (ppm)

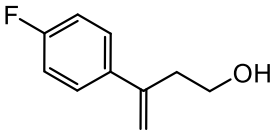
F
OH

7-3b

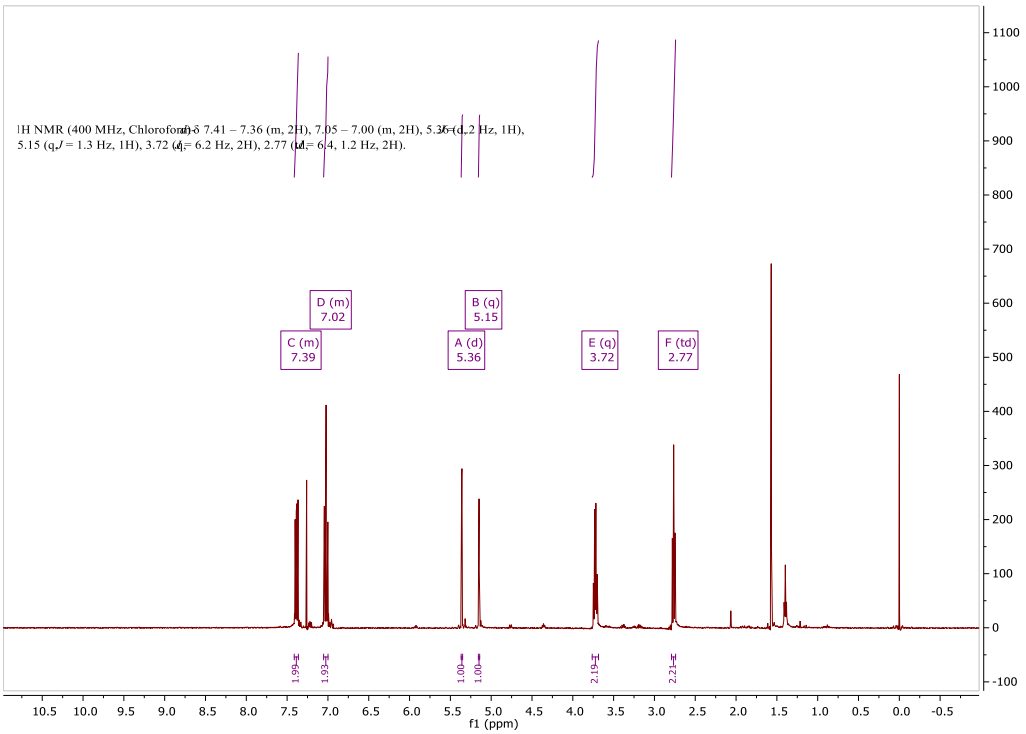
¹H NMR (400 MHz, Chloroform-d) δ 7.41 – 7.36 (m, 2H), 7.05 – 7.00 (m, 2H), 5.36 (d, J = 1.2 Hz, 1H), 5.15 (q, J = 1.3 Hz, 1H), 3.72 (t, J = 6.2 Hz, 2H), 2.77 (td, J = 6.4, 1.2 Hz, 2H).
D (m) 7.02
C (m) 7.39
B (q) 5.15
A (d) 5.36
E (q) 3.72
F (td) 2.77
1.99
1.93
1.00
1.00
2.19
2.21
f1 (ppm)

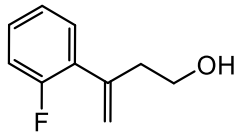
OH
F

7-3c

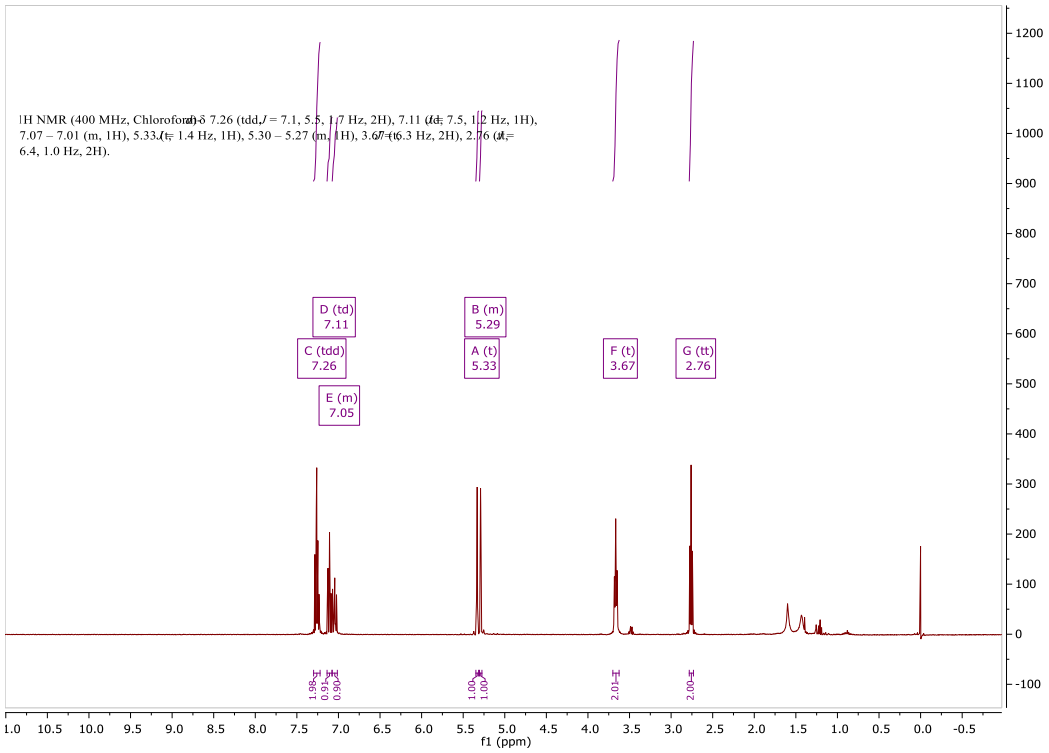
D (td) 7.11
B (m) 5.29
C (tdd) 7.26
A (t) 5.33
F (t) 3.67
G (tt) 2.76
E (m) 7.05
f1 (ppm)

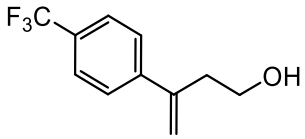
F3C
OH

7-3d

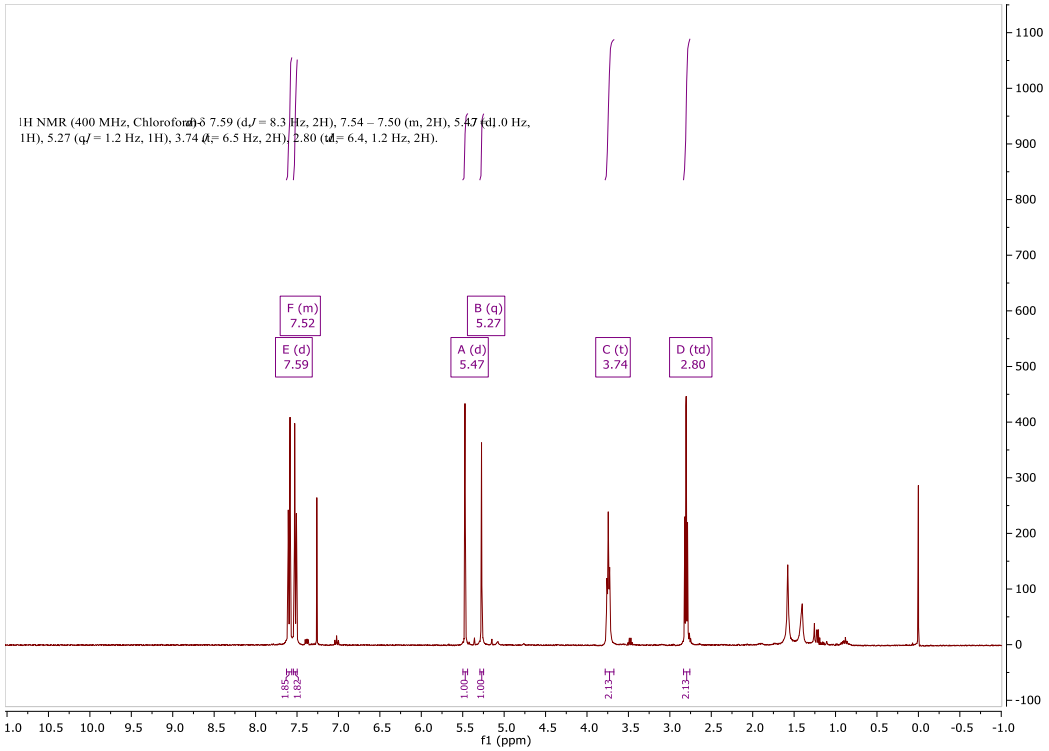
F (m) 7.52
B (q) 5.27
E (d) 7.59
A (d) 5.47
C (t) 3.74
D (td) 2.80
f1 (ppm)

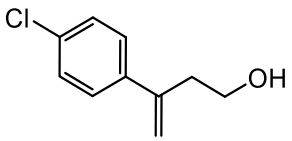

7-3e

^{1}H NMR (400 MHz, Chloroform-*d*) δ 7.37 – 7.33 (m, 2H), 7.33 – 7.28 (m, 2H), 5.40 (d, *J* = 1.2 Hz, 1H), 5.18 (q, *J* = 1.2 Hz, 1H), 3.72 (t, *J* = 8.0 Hz, 2H), 2.76 (td, *J* = 6.4, 1.2 Hz, 2H).

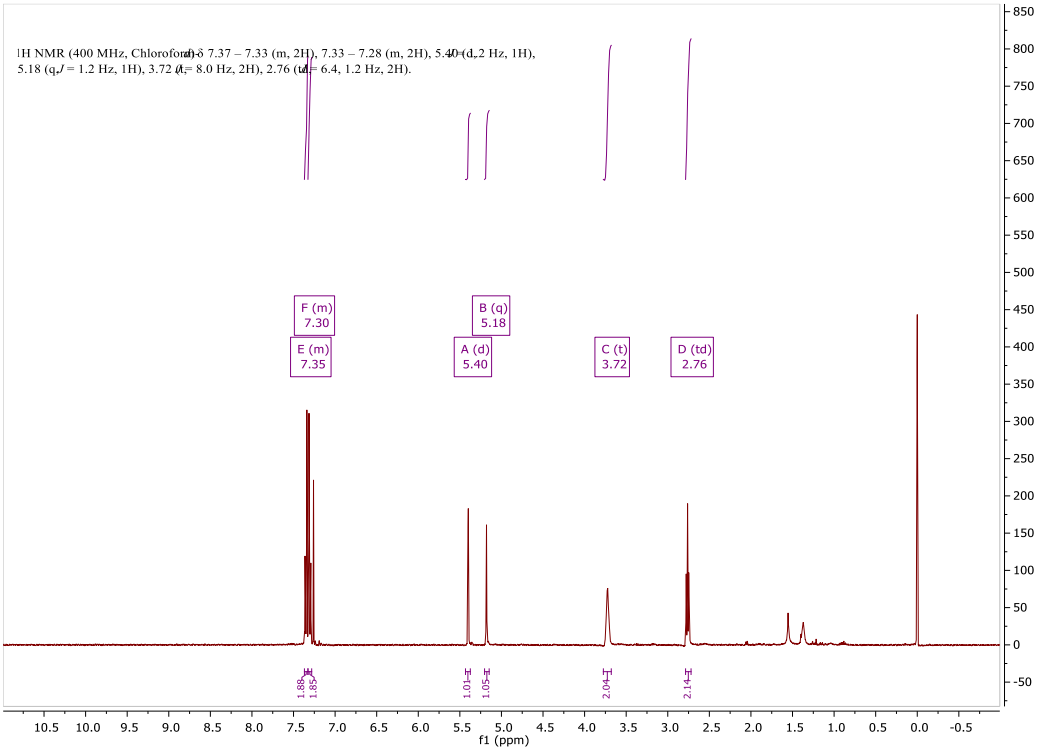

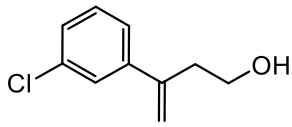

7-3f

^{1}H NMR (400 MHz, Chloroform-*d*) δ 7.40 (q, *J* = 1.5 Hz, 1H), 7.31 – 7.26 (m, 3H), 5.42 (d, *J* = 1.1 Hz, 1H), 5.25 – 5.20 (m, 1H), 3.73 (q, *J* = 5.8 Hz, 2H), 2.76 (td, *J* = 6.6, 1.2 Hz, 2H).

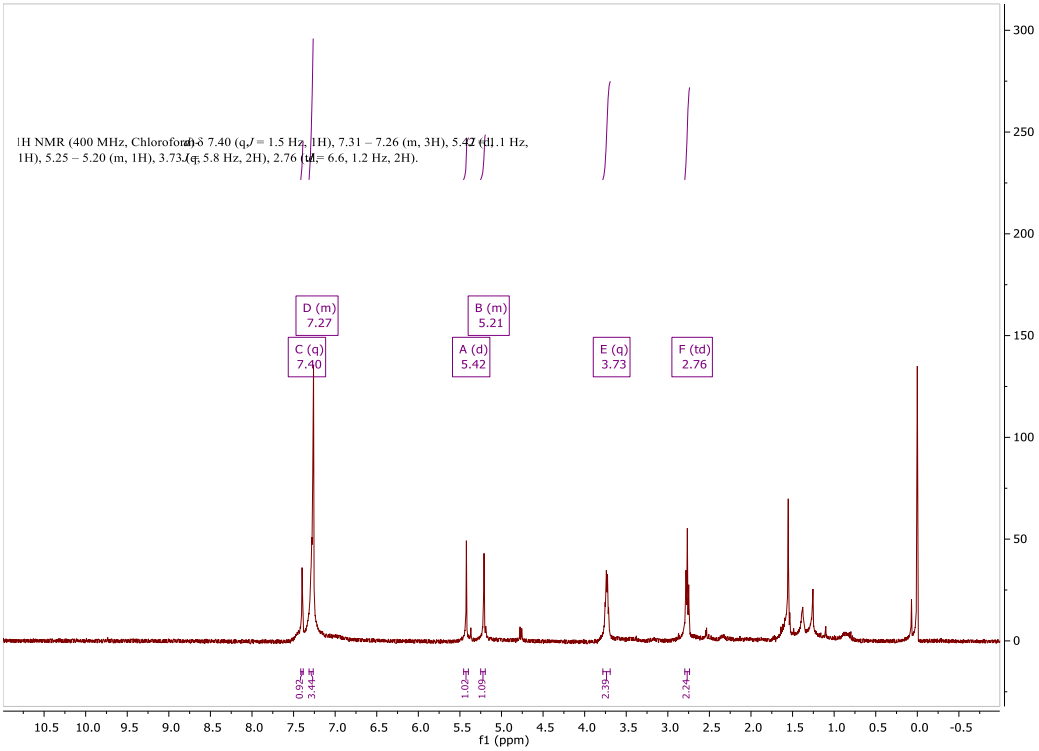

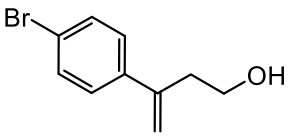
Br
OH

7-3g

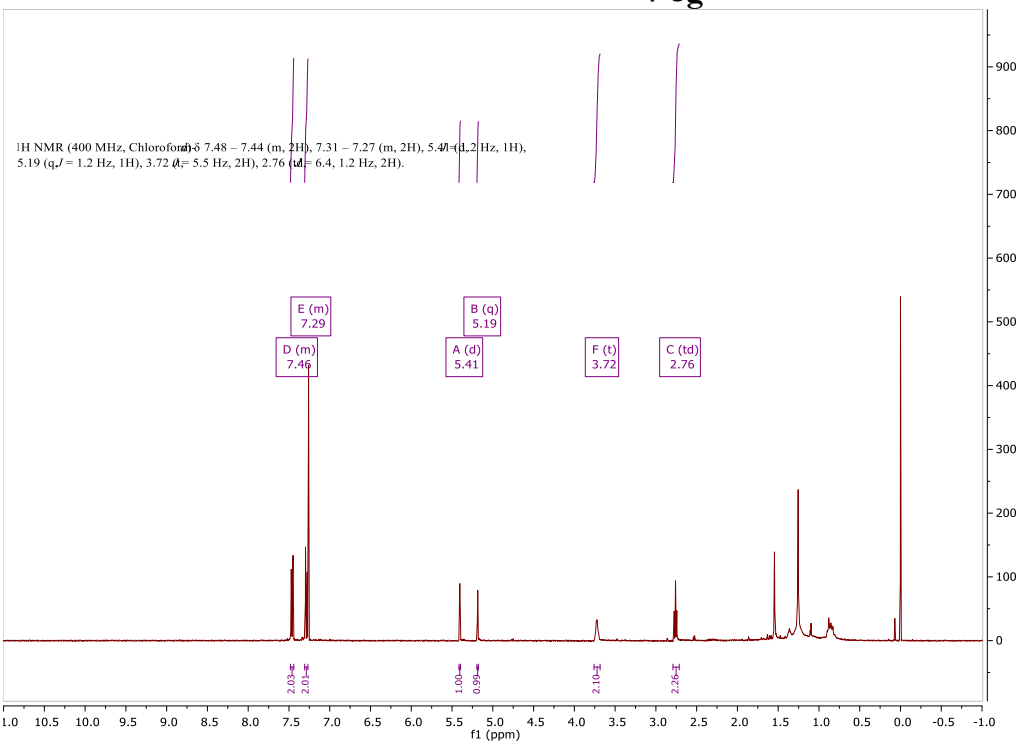
E (m)
7.29
B (q)
5.19
D (m)
7.46
A (d)
5.41
F (t)
3.72
C (td)
2.76
2.03
2.01
1.00
0.99
2.10
2.26
f1 (ppm)

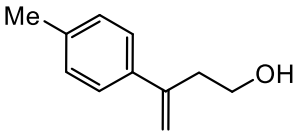
Me
OH

7-3i

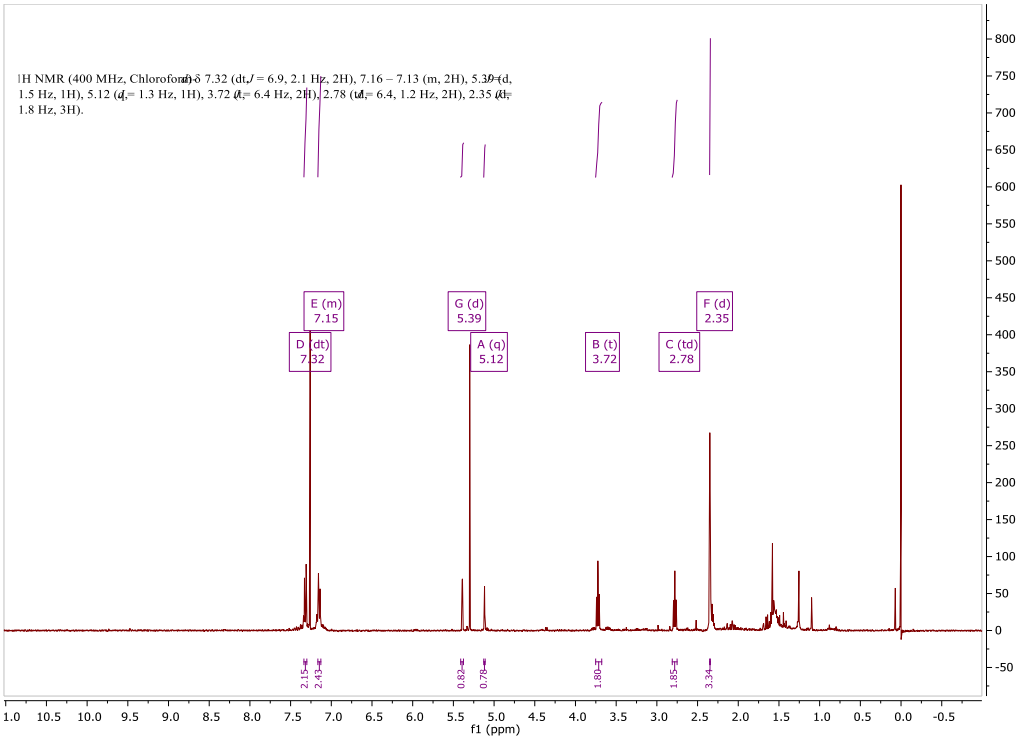
E (m)
7.15
G (d)
5.39
F (d)
2.35
D (dt)
7.32
A (q)
5.12
B (t)
3.72
C (td)
2.78
2.15
2.43
0.82
0.78
1.80
1.85
3.34
f1 (ppm)

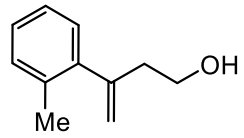
OH
Me

7-3j

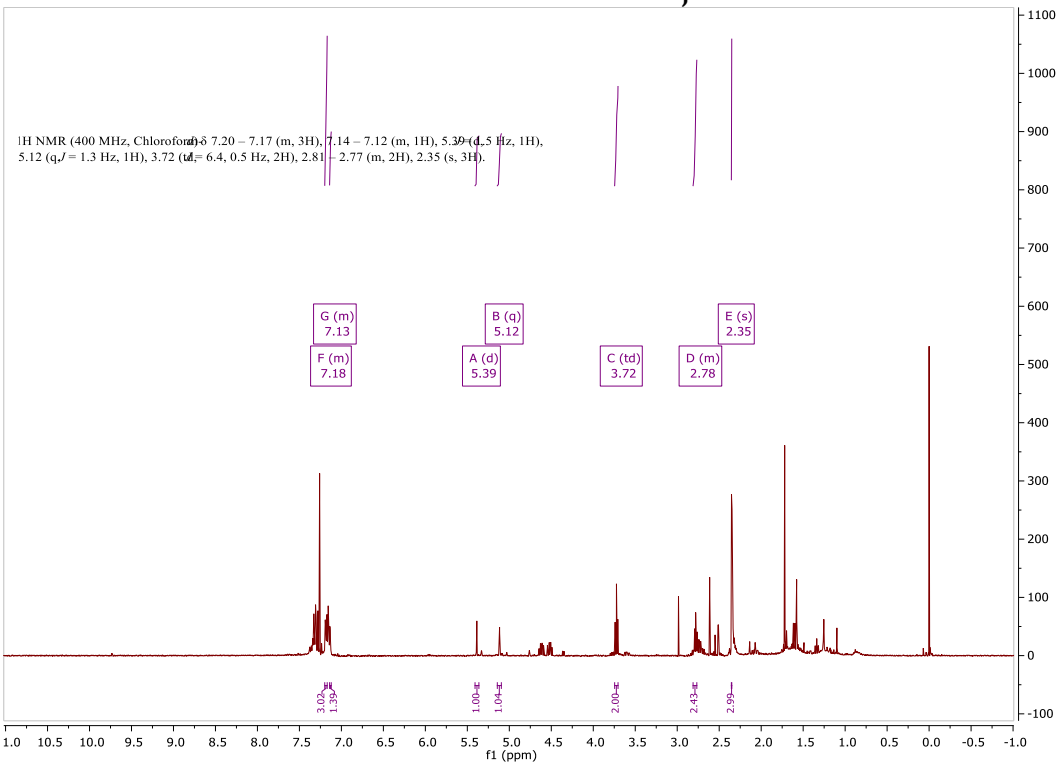
G (m) 7.13
F (m) 7.18
B (q) 5.12
A (d) 5.39
C (td) 3.72
D (m) 2.78
E (s) 2.35
f1 (ppm)

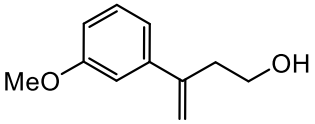
MeO
OH

7-3k

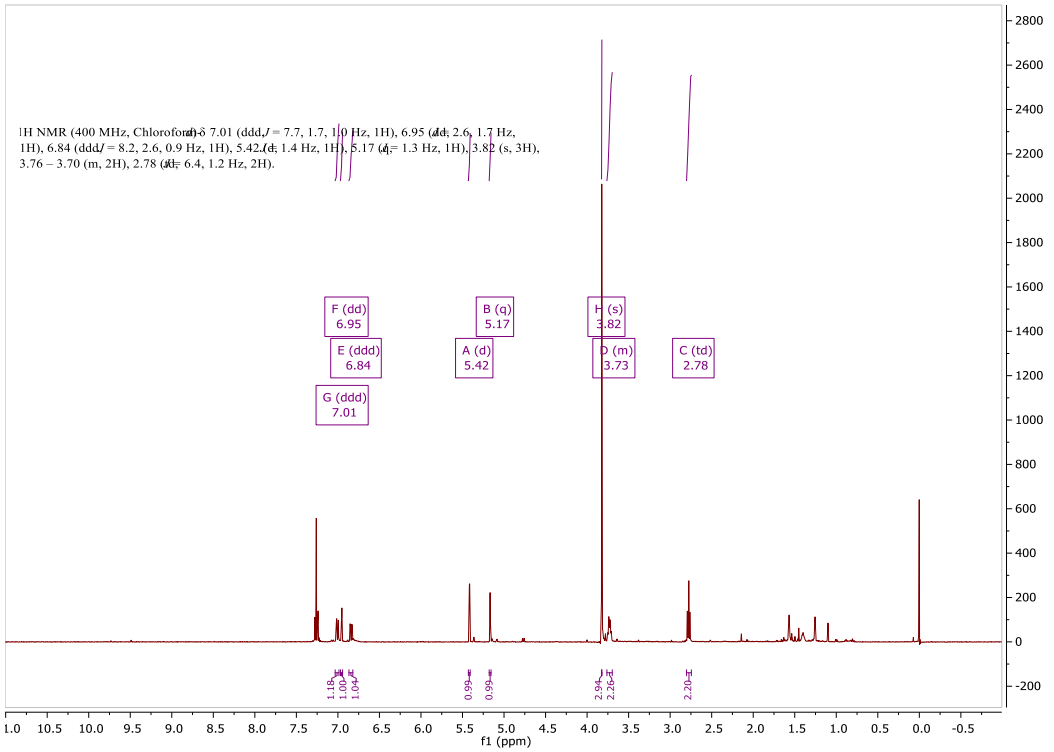
F (dd) 6.95
E (ddd) 6.84
G (ddd) 7.01
B (q) 5.17
A (d) 5.42
H (s) 3.82
D (m) 3.73
C (td) 2.78
f1 (ppm)

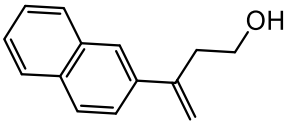
OH

7-3m

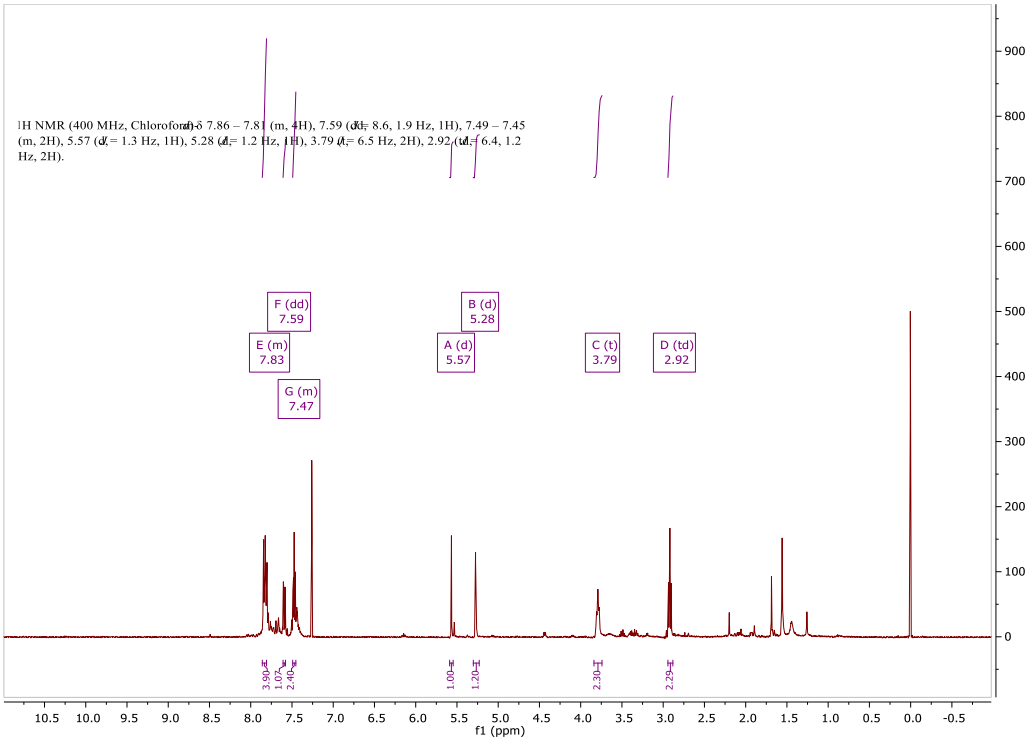
¹H NMR (400 MHz, Chloroform-d) δ 7.86 – 7.81 (m, 4H), 7.59 (dd, J = 8.6, 1.9 Hz, 1H), 7.49 – 7.45 (m, 2H), 5.57 (d, J = 1.3 Hz, 1H), 5.28 (d, J = 1.2 Hz, 1H), 3.79 (t, J = 6.5 Hz, 2H), 2.92 (td, J = 6.4, 1.2 Hz, 2H).
F (dd) 7.59
E (m) 7.83
G (m) 7.47
B (d) 5.28
A (d) 5.57
C (t) 3.79
D (td) 2.92
3.90
1.07
2.40
1.00
1.20
2.30
2.29
f1 (ppm)

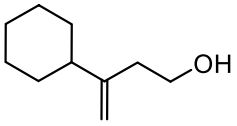
OH

7-3n

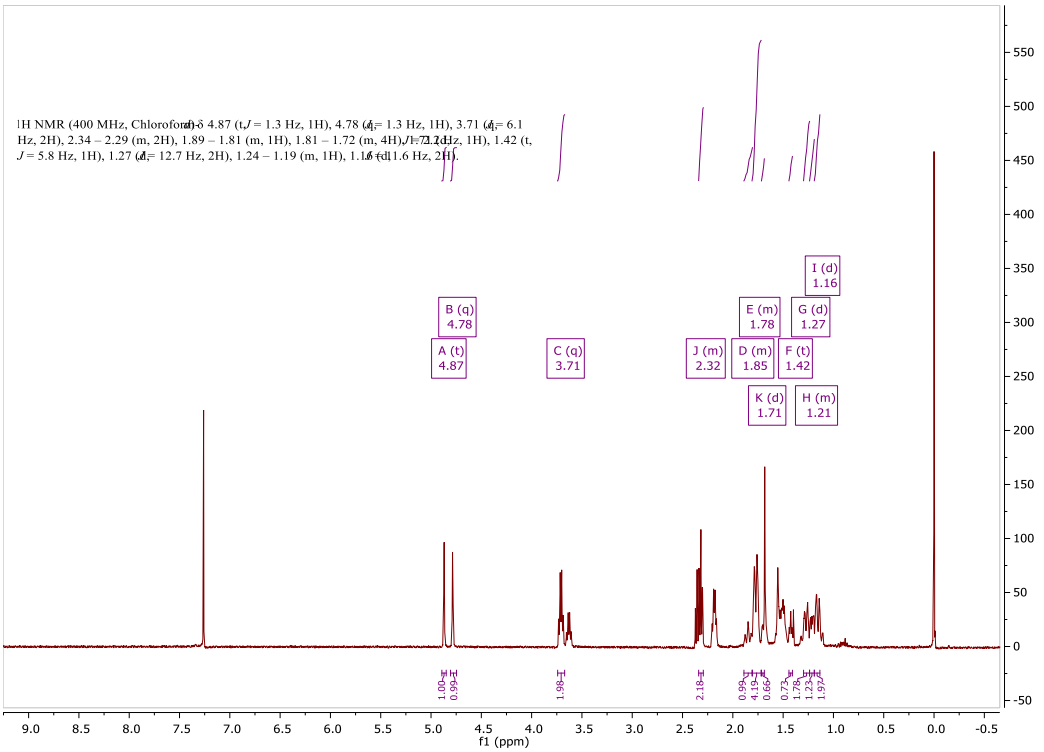
¹H NMR (400 MHz, Chloroform-d) δ 4.87 (t, J = 1.3 Hz, 1H), 4.78 (d, J = 1.3 Hz, 1H), 3.71 (d, J = 6.1 Hz, 2H), 2.34 – 2.29 (m, 2H), 1.89 – 1.81 (m, 1H), 1.81 – 1.72 (m, 4H), 1.72 (d, J = 1.2 Hz, 1H), 1.42 (t, J = 5.8 Hz, 1H), 1.27 (d, J = 12.7 Hz, 2H), 1.24 – 1.19 (m, 1H), 1.16 (d, J = 11.6 Hz, 2H).
I (d) 1.16
B (q) 4.78
E (m) 1.78
G (d) 1.27
A (t) 4.87
C (q) 3.71
J (m) 2.32
D (m) 1.85
F (t) 1.42
K (d) 1.71
H (m) 1.21
1.00
0.99
1.98
2.18
0.99
4.19
0.66
0.73
1.78
1.23
1.97
f1 (ppm)

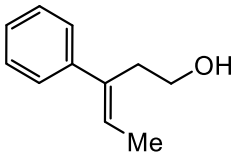
OH
Me

7-3o

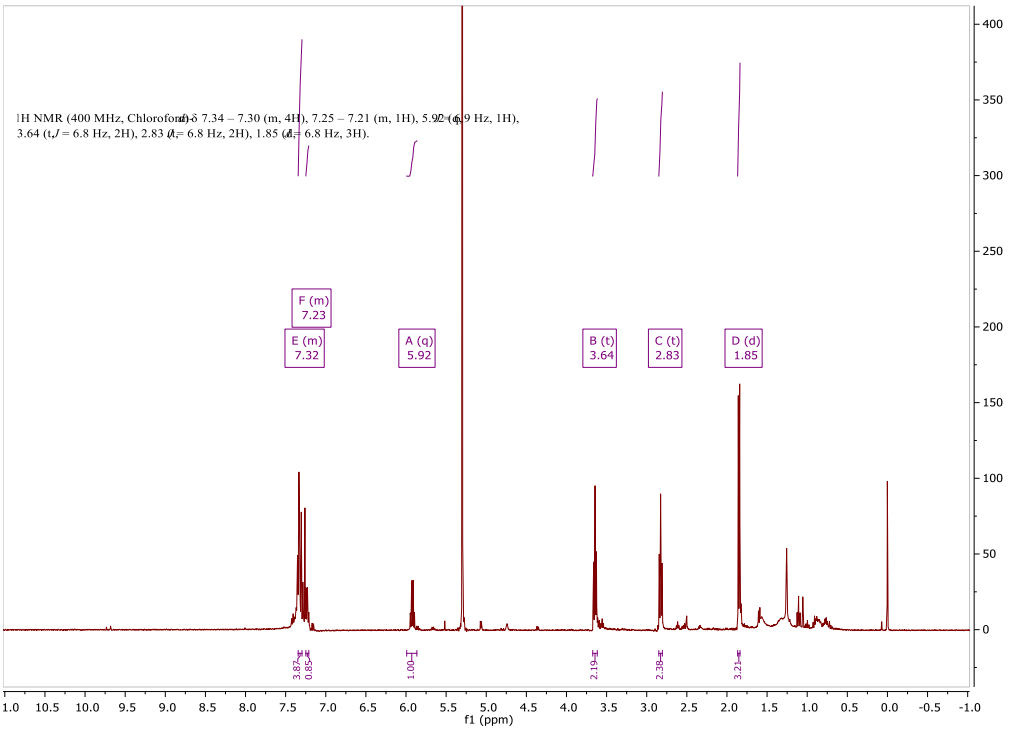
F (m) 7.23
E (m) 7.32
A (q) 5.92
B (t) 3.64
C (t) 2.83
D (d) 1.85
f1 (ppm)

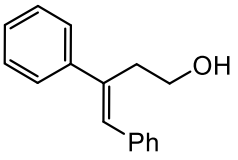
OH
Ph

7-3p

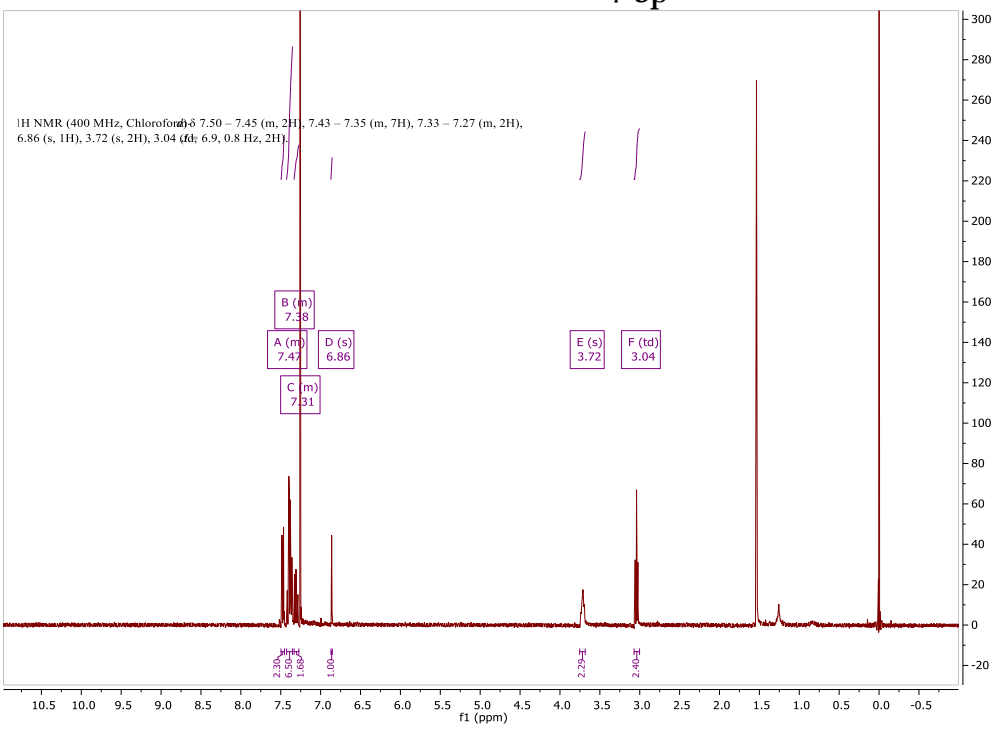
B (m) 7.38
A (m) 7.47
D (s) 6.86
C (m) 7.31
E (s) 3.72
F (td) 3.04
f1 (ppm)

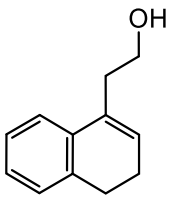
OH

7-3q

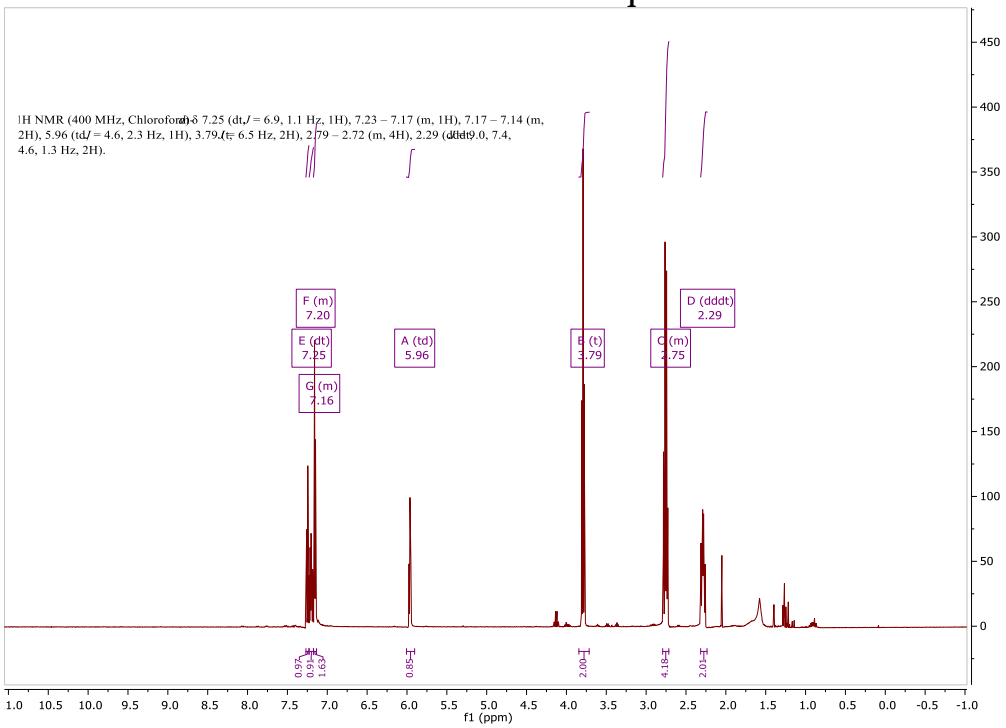
¹H NMR (400 MHz, Chloroform-d) δ 7.25 (dt, J = 6.9, 1.1 Hz, 1H), 7.23 – 7.17 (m, 1H), 7.17 – 7.14 (m, 2H), 5.96 (td, J = 4.6, 2.3 Hz, 1H), 3.79 (t, J = 6.5 Hz, 2H), 2.79 – 2.72 (m, 4H), 2.29 (dddt, J = 9.0, 7.4, 4.6, 1.3 Hz, 2H).
F (m) 7.20
E (dt) 7.25
G (m) 7.16
A (td) 5.96
B (t) 3.79
C (m) 2.75
D (dddt) 2.29
f1 (ppm)

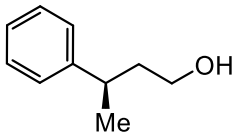
OH
Me

7-5a

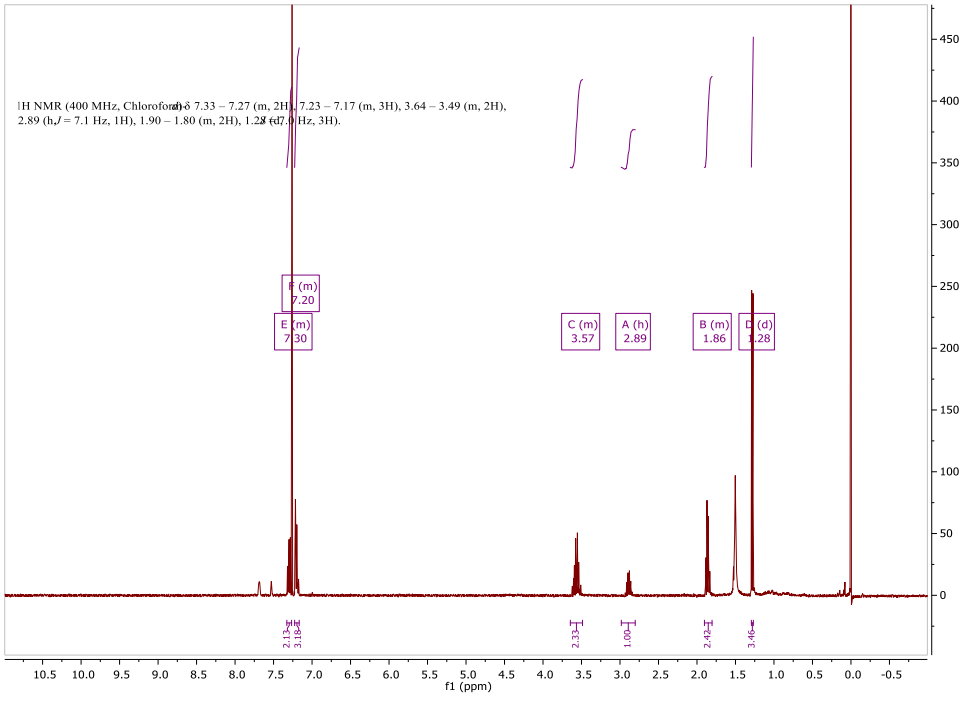
¹H NMR (400 MHz, Chloroform-d) δ 7.33 – 7.27 (m, 2H), 7.23 – 7.17 (m, 3H), 3.64 – 3.49 (m, 2H), 2.89 (h, J = 7.1 Hz, 1H), 1.90 – 1.80 (m, 2H), 1.28 (d, J = 7.0 Hz, 3H).
F (m) 7.20
E (m) 7.30
C (m) 3.57
A (h) 2.89
B (m) 1.86
D (d) 1.28
f1 (ppm)

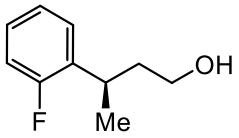
OH
F
Me

7-5c

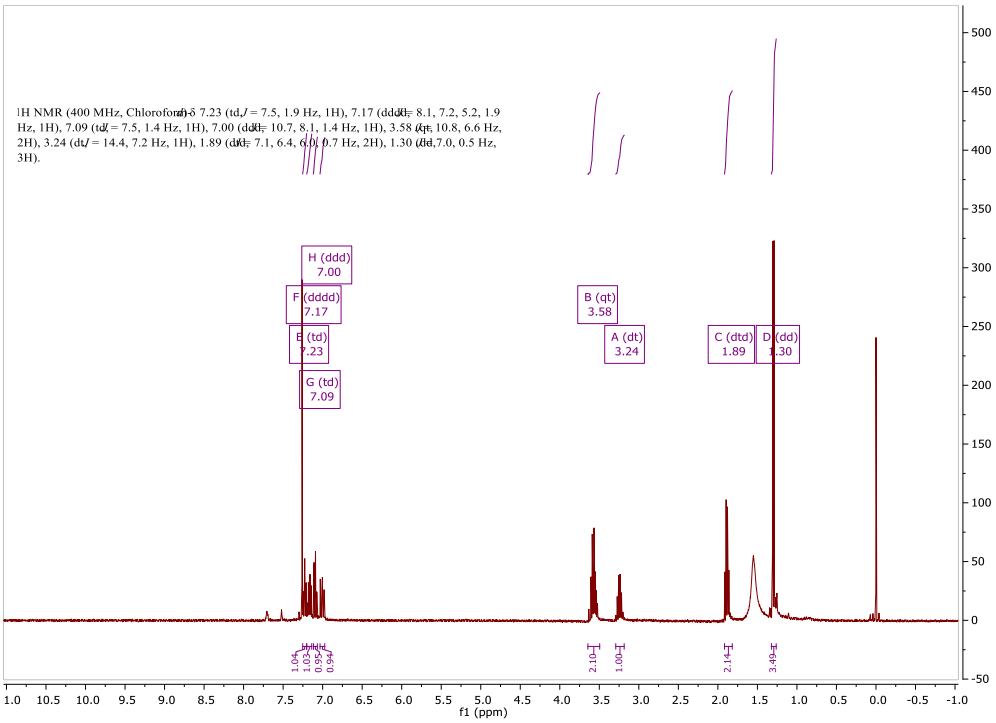
H (ddd) 7.00
F (dddd) 7.17
E (td) 7.23
G (td) 7.09
B (qt) 3.58
A (dt) 3.24
C (dtd) 1.89
D (dd) 1.30
f1 (ppm)

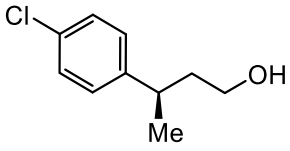
Cl
OH
Me

7-5e

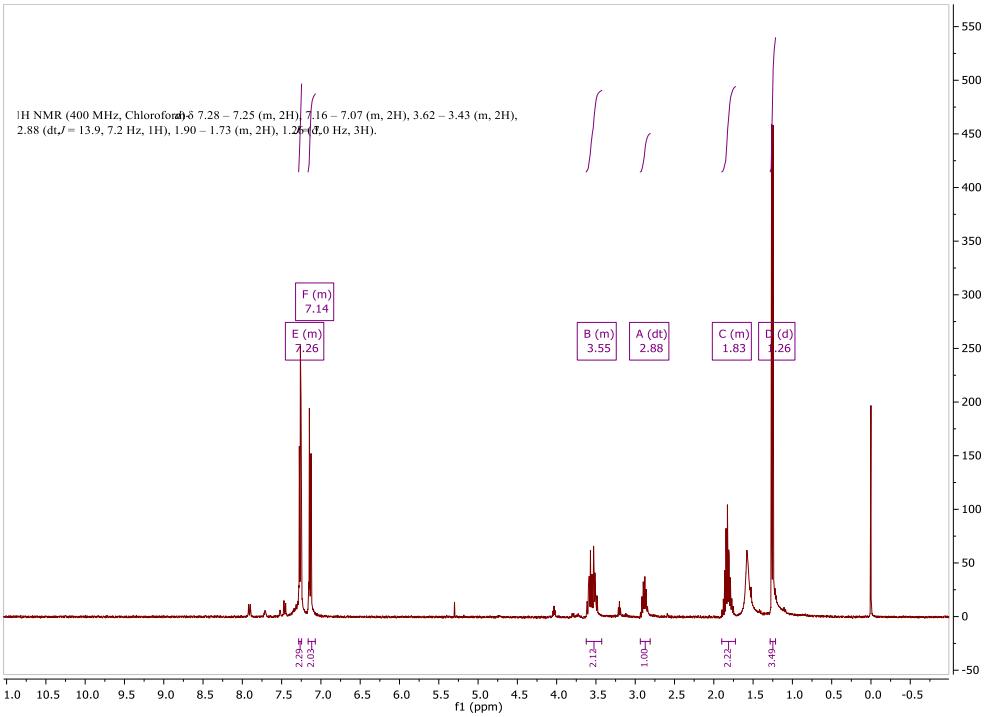
F (m) 7.14
E (m) 7.26
B (m) 3.55
A (dt) 2.88
C (m) 1.83
D (d) 1.26
f1 (ppm)

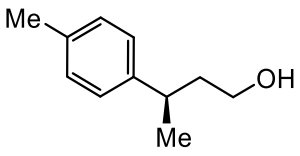
Me
OH
Me

7-5i

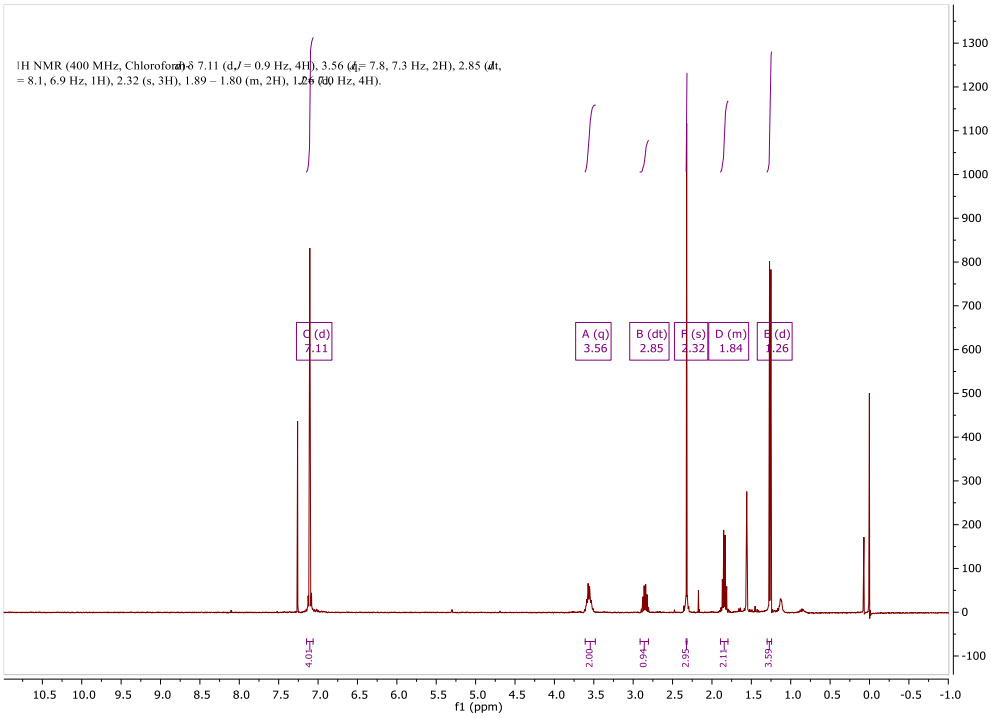
1H NMR (400 MHz, Chloroform-d) δ 7.11 (d, J = 0.9 Hz, 4H), 3.56 (dq, J = 7.8, 7.3 Hz, 2H), 2.85 (dt, J = 8.1, 6.9 Hz, 1H), 2.32 (s, 3H), 1.89 – 1.80 (m, 2H), 1.26 (d, J = 7.0 Hz, 4H).
C (d) 7.11
A (q) 3.56
B (dt) 2.85
F (s) 2.32
D (m) 1.84
E (d) 1.26
4.01
2.00
0.94
2.95
2.11
3.59
f1 (ppm)

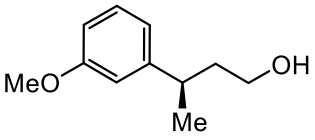
MeO
OH
Me

7-5k

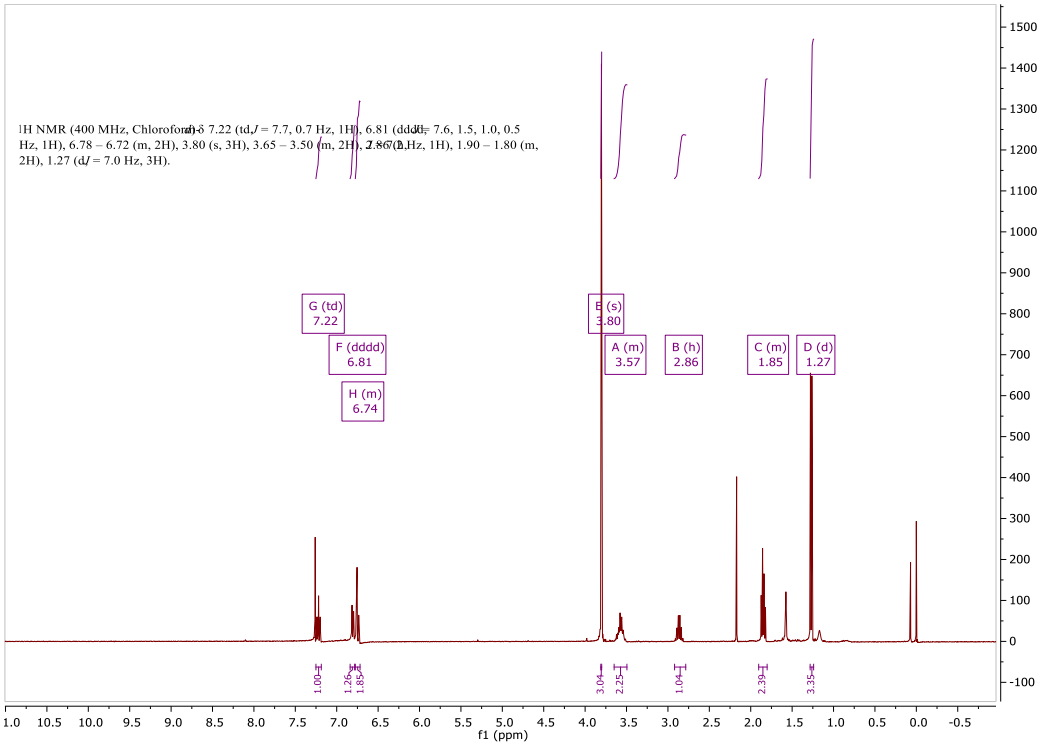
1H NMR (400 MHz, Chloroform-d) δ 7.22 (td, J = 7.7, 0.7 Hz, 1H), 6.81 (dddd, J = 7.6, 1.5, 1.0, 0.5 Hz, 1H), 6.78 – 6.72 (m, 2H), 3.80 (s, 3H), 3.65 – 3.50 (m, 2H), 2.86 (h, J = 7.0 Hz, 1H), 1.90 – 1.80 (m, 2H), 1.27 (d, J = 7.0 Hz, 3H).
G (td) 7.22
F (dddd) 6.81
H (m) 6.74
E (s) 3.80
A (m) 3.57
B (h) 2.86
C (m) 1.85
D (d) 1.27
1.00
1.26
1.85
3.04
2.25
1.04
2.39
3.35
f1 (ppm)

Chapter 8

Enantioselective Synthesis of β-Methyl Amines via Iridium-Catalyzed Asymmetric Hydrogenation of *N*-Sulfonyl Allyl Amines

Chiral amines are key structural features in natural products and fine chemicals.[1,2] Amines bearing a β-methyl stereogenic center are present in numerous bioactive compounds and pharmaceuticals.[3-5] Several examples of this type of drugs are shown in Figure 8.1. For example, Lorcaserin is a marketed anorectic for which a synthesis based on asymmetric hydrogenation have not been described to date.[3] Biarylpropylsulfonamides such as LY-404187 are potent positive allosteric modulators of 2-amino-3-(5-methyl-3-hydroxyisoxazol-4-yl)-propanoic acid (AMPA) receptors.[4] NPS-1392 is a potent stereoselective antagonist of the NMDA receptor.[5]

The asymmetric hydrogenation is one of the most important catalytic reactions in the preparation of pharmaceuticals due to its atom economy, low environmental impact and operational simplicity.[6] Ru or Rh catalysts, which usually bear chiral phosphines, can induce high enantioselectivity on substrates functionalized with a coordinating group.[7] However, when facing minimally functionalized olefins, these catalysts commonly show low reactivity and asymmetric induction. Conversely, Ir complexes bearing chiral P,N-ligands[8] can be used in the hydrogenation of poorly coordinative alkenes. Although several minimally functionalized olefins have been enantioselectively hydrogenated with Ir complexes,[9] the range of substrates available is still limited. In this context, reports of the asymmetric synthesis of β-methyl amines from 2-aryl allylamines are scarce. Zhang and co-workers developed a highly enantioselective method for the synthesis of β-methyl phthalimides based on the asymmetric hydrogenation of 2-alkyl allylphthalimides using a Ru-C_3-tunephos catalyst.[10] However, hydrogenation of the only example of 2-aryl allylphthalimide described in the paper took place with low enantiomeric excess (55% ee). The hydrogenation of *N*-acetamido 2-phenyl allylamine using a cationic Ru complex bearing the axially chiral ligand (-)-TMBTP gave an ee of 80%.[11] However, in this case, the hydrogenation occurred after partial isomerization to the enamide. Therefore, to the best of our knowledge, there are no precedents of Ir-catalyzed asymmetric hydrogenation of *N*-sulfonyl 2-aryl allylamines.

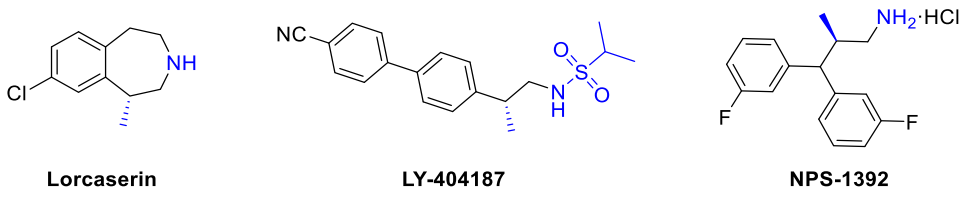

Lorcaserin **LY-404187** **NPS-1392**

Fig. 8.1. Examples of pharmaceutically active chiral β-methyl amines.

In theory, all compounds shown in Figure 8.1 can be prepared by asymmetric hydrogenation of a suitable allyl amine. However, the absence of appropriate methodologies might be explained by the lack of easy preparation procedures for 2-aryl allylamines. As described in the previous Chapter 7, our group recently uncovered a new isomerization reaction that provides *N*-sulfonyl 2-aryl allylamines **8-2** from *N*-sulfonyl aziridines **8-1** (Scheme 8.1).[12] The isomerization is catalyzed by the readily available Crabtree catalyst and takes place with low catalyst loading, high selectivity and mild reaction conditions.

Herein, we describe the Ir-catalyzed asymmetric hydrogenation of *N*-sulfonyl allylic amines **8-2** to chiral β-methyl amines **8-3** (Scheme 8.1; 16 examples). The commercial iridium-UbaPhox catalyst[13] developed by Pfaltz gave complete conversions and good to excellent enantioselectivities. The high functional group tolerance and the mild conditions employed in this novel catalytic process are remarkable. To showcase the applicability of this new enantioselective methodology, the asymmetric synthesis of several biologically active compounds is also described.

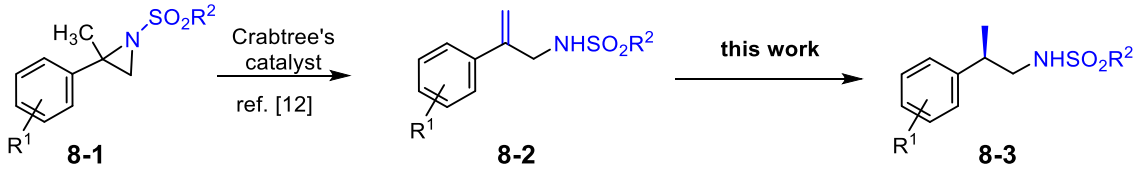

Scheme 8.1. Synthetic approach to chiral β-methylamines

Our studies first began with the asymmetric hydrogenation of **8-2a**, which was chosen as model substrate (Table 8.1). This compound was easily obtained by isomerization of the corresponding *N*-tosyl aziridine which, in turn was prepared from 1-methylstyrene. With **8-2a** in hand, several Rh- and Ir-catalysts were tested for their asymmetric hydrogenation. However, the best results were obtained using [((4*S*,5*S*)-Cy2-Ubaphox)Ir(COD)] BAr^F (**8-4**), the threonine-based Ir-P,N catalysts developed by Pfaltz.[13] The optimization of the reaction conditions is shown in Table 1. Methanol gave low conversion (Table 8.1, entry 1). Ethers such as THF, dioxane and diethyl ether gave complete conversions but moderate ee values (Table 8.1, entries 2-4). Ethyl acetate and dichloromethane gave better results, but dichloroethane (DCE) (Table 8.1, entry 7,) emerged as the best solvent for the reaction, with full conversion and 93% ee. A decrease in the temperature of the reaction (Table 8.1, entry 8) or an increase of hydrogen pressure (Table 8.1, entry 9) had a small effect in the asymmetric induction. Finally, the reaction was achieved with 1 mol % of catalyst loading

and 1 bar of hydrogen (Table 8.1, entry 10). Under these conditions the reaction reached completion in only 3 h.

Table 8.1. Solvent screening and optimization of the asymmetric hydrogenation of *N*-tosyl 2-phenyl allylamine **8-2a.**[a]

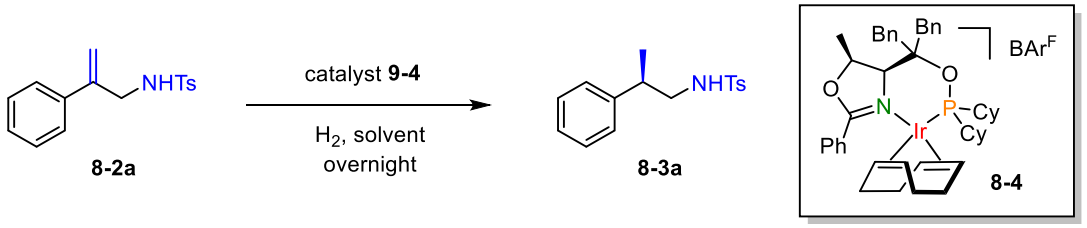

Entry	Cat. (mol %)	Solvent	P, T	Conv. (%)[b]	ee (%)[c]
1	5	MeOH	1 bar, rt	30	75 (*R*)
2	5	THF	1 bar, rt	>99	82 (*R*)
3	5	dioxane	1 bar, rt	>99	76 (*R*)
4	5	Et_2O	1 bar, rt	>99	74 (*R*)
5	5	EtOAc	1 bar, rt	>99	83 (*R*)
6	5	CH_2Cl_2	1 bar, rt	>99	88 (*R*)
7	5	DCE	1 bar, rt	>99	93 (*R*)
8	5	DCE	1 bar, 0ºC	>99	93 (*R*)
9	5	DCE	50 bar, rt	>99	91 (*R*)
10[d]	1	DCE	1 bar, rt	>99	93 (*R*)

[a] See Supporting Information for experimental details. Reactions were run in a pressure reactor at 1 bar of H_2 pressure. [b] Conversion was measured by ^{1}H NMR. [c] Enantiomeric excess was determined by chiral HPLC. [d] The reaction was completed after 3 h.

We also tested the one pot procedure treating aziridine **8-1a** with hydrogen (1-50 bar) in the presence of catalyst **8-4** (Fig. 8.2). Into a dry box, aziridine **8-1a** (0.05 mmol, 1.0 equiv.) and catalyst **8-4** (3 mol%) were weighted in borosilicate glass tube equipped with PTFE-coated stirring-bar and placed in a pressure reactor. Then, the corresponding anhydrous solvent was added (0.1 M). Once sealed, the pressure reactor was purged and charged with H_2 (1, 3 or 50 barG). The reaction was stirred 17 hours at room temperature. Afterwards, the crude was filtered through a short plug of silica to afford the corresponding isolated product. The conversion was measured by ^{1}H NMR spectroscopy and the enantiomeric excess was determined using HPLC chiral chromatography.

Fig. 8.2. Reaction scheme of the one-pot isomerization – asymmetric hydrogenation reaction. Graphic showing the enantiomeric excesses obtained.

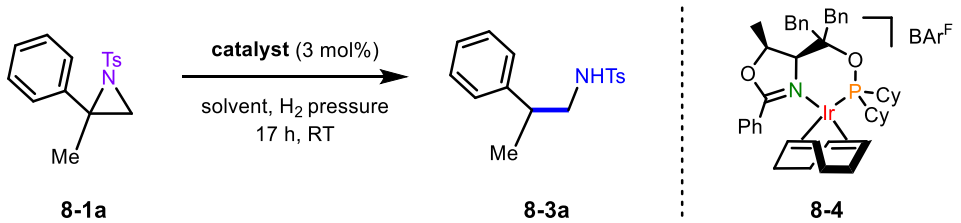

8-1a **8-3a** **8-4**

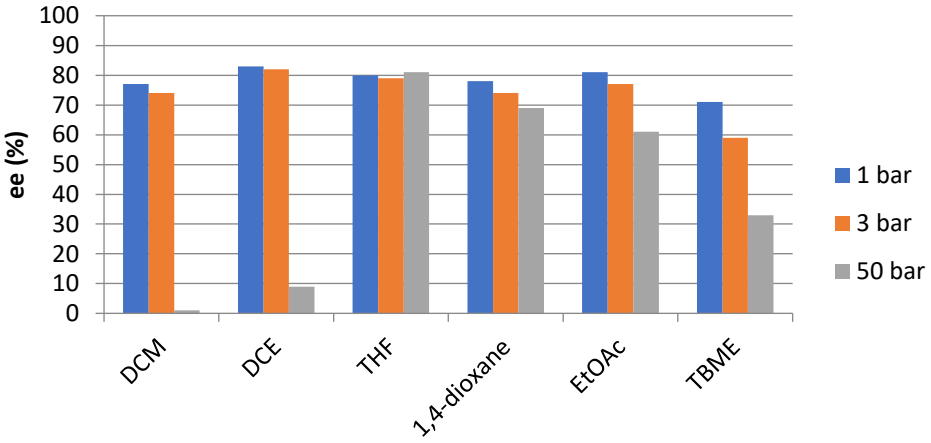

The one-pot strategy to afford chiral amines using *N*-sulfonyl aziridines as the starting substrate presents two main drawbacks:

- As seen in Fig. 8.1., the enantiomeric excesses are lower in comparison to the ones obtained using the 2-step synthetic procedure. This is due to the formation of (racemic) imine after the isomerization step. Albeit it is formed in low yield (between 3-7% depending on the reaction conditions), the asymmetric hydrogenation will be performed to both products, thus affording a unique chiral amine but with lower enantioselectivity. Therefore, the maximum ee (83%) was obtained when using DCE at 1 bar of H_2 pressure, which is 10 points lower than when performing the hydrogenation of pure allyl amine.
- Moreover, dry box is necessary to ensure the absence of air moisture. If not, amino alcohol is obtained due to the nucleophilic attack of water. The benzylic carbon, in presence of highly reactive Ir-H,H species, can rapidly catalyze the ring-opening of the aziridine and undesired byproduct is obtained. On the other hand, if the reaction is carried out in two steps, the isomerization reaction using Crabtree's catalyst can be performed outside the glovebox and without H_2 activation, thus resulting in a simpler synthetic protocol.

Therefore, although the *N*-tosyl 2-phenylpropanamine **8-3a** was obtained cleanly, the maximum enantiomeric excess that we could obtain was 83% ee. We believe that this was due to the uncomplete selectivity of the isomerization reaction. The presence of 3-7% of racemic imine drops the enantioselectivity of the overall reaction.

Next, we moved to evaluate the substrate scope. For this purpose, we applied the optimal conditions to a range of *N*-sulfonyl allylic amines. Up to 15 *N*-sulfonyl allylic amines were tested showing excellent reactivity and affording the chiral amines in high conversions and with good to excellent ee values (Table 8.2). We assumed that all products had *R* configuration by analogy with **8-3a**. The absolute configuration of **8-3a** had been stablished by derivatization of ethyl (*R*)-2-phenylpropanoate.[14] In all cases, except **8-2(d-e),** the sign of the rotation matched with **8-3a**. We believe that in all cases the sense of the induction is the same. Substrates presenting substituents in *ortho* position (Table 8.2, entries 3 and 6) and naphthalene (Table 8.2, entry 5) required an increase in catalyst loading (2 mol %) to assure full conversion. This novel catalytic transformation demonstrated high functional group tolerance when modifying the electronic character (electron-donor and electron-withdrawing substituents) in the aryl group.

The sulfonyl group was also modified, and we were pleased to see that when replacing the tosyl group by a methyl or isopropyl group, full conversion and excellent ee's were also achieved (Table 8.2, entries 10, 11, 12 and 13). Finally, *N*-methyl, *N*-sulfonyl allylic amines **8-2o** and **8-2p** were also hydrogenated affording the corresponding chiral amines with 94% of enantiomeric excess in both cases (Table 8.2, entries 14 and 15).

To check if the hydrogenation takes place after isomerization to the corresponding enamide, labeling studies were conducted. Allyl amine **8-2a** was hydrogenated with 1 bar of D_2 and 1 mol % of **8-4** in DCE. NMR analysis showed that the deuterium atoms were exclusively found at the methyl and benzylic positions. Applying the optimal conditions, we found after the screening, we were pleased to see that direct hydrogenation took place exclusively to the allylic bond. Therefore, we proved that the enantioselective hydrogenation –thus the asymmetric induction- takes place to the minimally functionalized olefin, and that no isomerization reaction towards the formation of enamide occurs, as seen in Figures 8.3A and 8.3B.

Table 8.2. Scope of Asymmetric Hydrogenation of *N*-Sulfonyl Allyl Amines

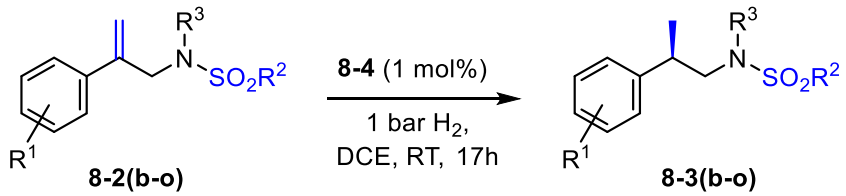

Entry		R¹	R²	R²	Conv. (%)[b]	ee (%)[c]
1	**8-2b**	*p*-Cl	*p*-tolyl	H	>99	85
2	**8-2c**	*m*-Cl	*p*-tolyl	H	>99	89
3[d]	**8-2d**	*o*-Cl	*p*-tolyl	H	>99	82
4	**8-2e**	*p*-Me	*p*-tolyl	H	>99	92
5[d]	**8-2f**	2-naphthyl	*p*-tolyl	H	>99	88
6[d]	**8-2g**	*o*-OMe	*p*-tolyl	H	>99	92
7	**8-2h**	p-F	*p*-tolyl	H	>99	91
8	**8-2i**	m-F	*p*-tolyl	H	>99	92
9	**8-2j**	*p*-CF_3	*p*-tolyl	H	>99	82
10	**8-2k**	*p*-Br	*i*Pr	H	>99	87
11	**8-2l**	*p*-I	*i*Pr	H	>99	88
12	**8-2m**	H	Me	H	>99	92
13	**8-2n**	*p*-*i*Bu	Me	H	>99	91
14	**8-2o**	H	Me	Me	>99	94
15	**8-2p**	H	*p*-tolyl	Me	>99	94

[a] All reactions were run in a pressure reactor at 1 bar of H_2 pressure. [b] Conversion was measured by ^1H NMR. [c] Enantiomeric ratio was determined by chiral HPLC. [d] 2 mol% of catalyst was used.

Fig. 8.3A. Labelled experiment to determine the reaction pathway using deuterium.

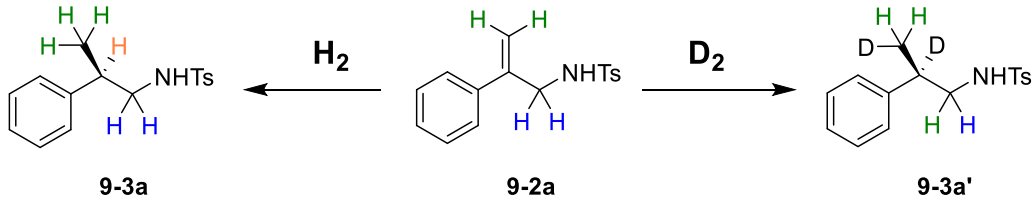

Fig. 8.3B. ^{1}H NMR spectra comparison of **8-3a** and **8-3a'**.

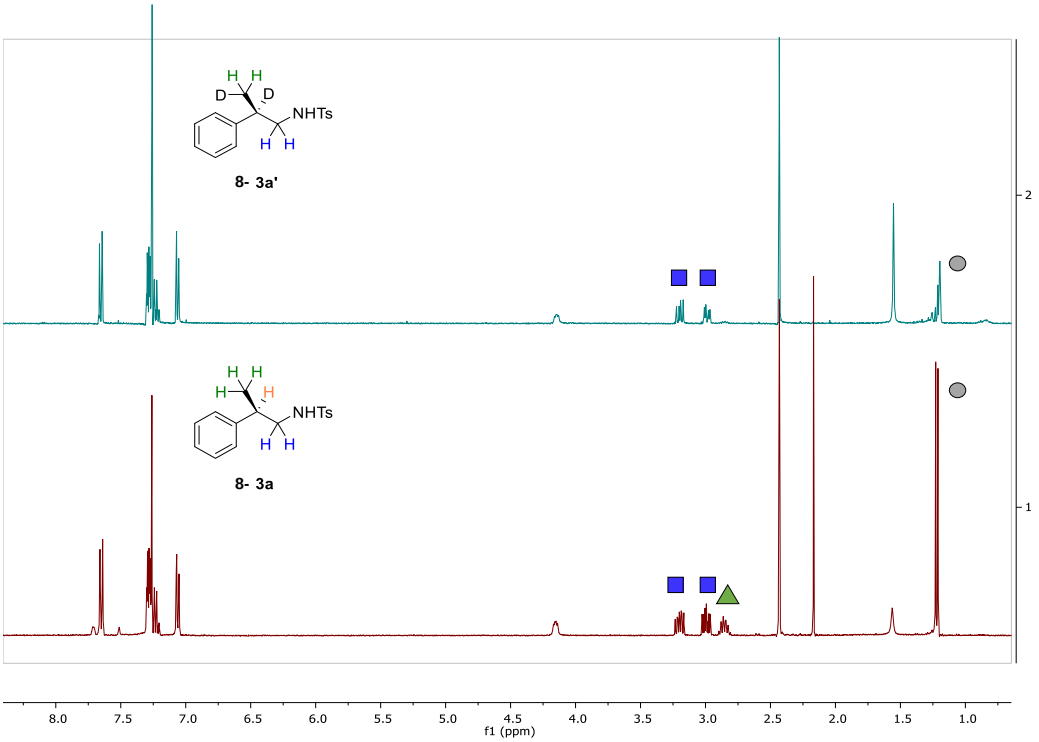

Many biologically active compounds have amines with a chiral methyl group in β - position. Compound **8-2a** is already a direct precursor of potassium channel inhibitors after simple tosyl deprotection and acylation [15,16]. The mesyl amine **8-2m** is also a key intermediate for the preparation of allosteric modulators of AMPA receptor.[16,17] However, to further showcase the applicability of our methodology, and encouraged by the relevance of these chiral β-methyl amines as fragments of biologically active compounds we envisioned easy access to LY-404187 and *(R)*-Lorcaserin. To obtain the biarylpropylsulfonamide LY-404187,[4] we designed a 3-step synthetic procedure starting from *N*-sulfonyl aziridine **8-1l**. The isomerization[12] of **8-1l** to **8-2l** and the subsequent asymmetric hydrogenation to **8-3l** took place in excellent yields. Finally, the chiral amine **8-3l** was converted to the final product by a Suzuki-Miyaura coupling. LY-404187, the potent potentiator of the AMPA receptor, was obtained as the only product with good yield and almost no loss of optical purity (Scheme 8.2).

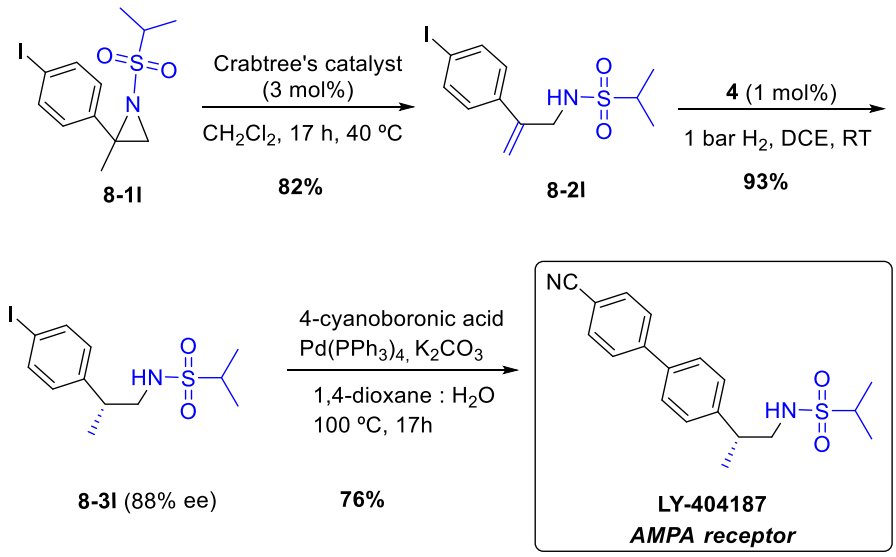

Scheme 8.2. Synthesis of LY-404187

The anorectic drug Lorcaserin has a tetrahydro-3-benzazepine skeleton, a common structural feature in many natural and pharmaceutical products. Lorcaserin has serotonergic properties and is currently used as a weight-loss drug. Several racemic syntheses of this compound have been reported. Only a few strategies for the enantioenriched form of this drug can be found in the literature, and most of them use kinetic resolution or stoichiometric reagents.[18] We envisioned to apply our novel catalytic asymmetric methodology (Scheme 8.3). *N*-sulfonyl aziridine **8-1c** was isomerized[12] and the corresponding allyl amine was hydrogenated to afford **8-3c** in good yield and 89% ee. Subsequent *N*-alkylation gave **9-5** in 68% yield. Regioselective Lewis acid-promoted intramolecular Friedel-Craft alkylation[18d] afforded the unsaturated 7-membered ring. Finally, enamine hydrogenation gave desired compound **8-6**, which is a direct precursor of Lorcaserin.[18d]

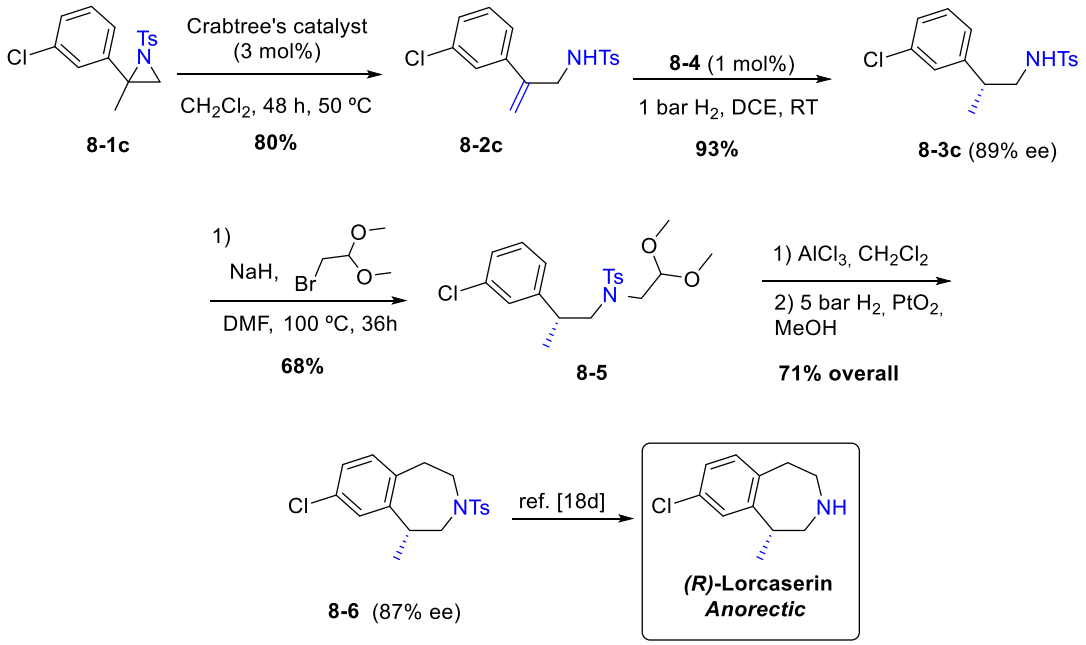

Scheme 8.3. Formal synthesis of (*R*)-Lorcaserin.

In summary, we have shown that commercially available complex Ir(UbaPHOX) (**8-4**) is an excellent catalyst for the challenging asymmetric hydrogenation of 2-aryl *N*-sulfonyl allylamines. The hydrogenation takes place at low hydrogen pressure (1 bar) and with only 1 mol % of catalyst in DCE at room temperature. Since the starting amines can be easily obtained by Ir-catalyzed isomerization of *N*-tosylaziridines, which in turn can be prepared from the corresponding styrenes, the overall sequence provides a straightforward and practical route to chiral amines bearing a methyl group in β position. These compounds are useful synthetic intermediates since they are, or can be transformed into, precursors of several biologically active compounds. As a synthetic application of this methodology, we have described the formal synthesis of enantioenriched (*R*)-Lorcaserin and LY-404187.

References

(1) a) G.-Q. Lin, J.-G. Zhang, J.-F. Cheng, Overview of chirality and chiral drugs. In *Chiral Drugs*, John Wiley & Sons, Inc., 2011; pp 3-28. b) Macrolide Antibiotics (Ed: S. Omura), Academic Press, Orlando, FL, **1984**.

(2) Chiral amines with β-stereogenic centres: a) H. M. L. Davies, A. Ni, *Chem. Commun.* **2006**, 3110-3112; b) R. N. Harris, R. S. Stabler, D. B. Repke, J. M. Kress, K. A. Walker, R. S. Martin, J. M. Brothers, M. Ilnicka, S. W. Lee, T. Mirzadegan, *Bioorg. Med. Chem. Lett.* **2010**, *20*, 3436–3440. c) P. Ramesh, D. Suman, K. Reddy, *Synthesis* **2018**, *50*, 211–226. d) G. M. Nicholas, T. F. Molinski, *Tetrahedron* **2000**, *56*, 2921.

(3) a) B. M. Smith, J. M. Smith, J. H. Tsai, J. A. Schultz, C. A. Gilson, S. A. Estrada, R. R. Chen, D. M. Park, E. B. Prieto, C. S. Gallardo, D. Sengupta, P. I. Dosa, J. A. Covel, A. Ren, R. R. Webb, N. R. A. Beeley, M. Martin, M. Morgan, S. Espitia, H. R. Saldana, C. Bjenning, K. T. Whelan, A. J. Grottick, F. Menzaghi, W. J. Thomsen, *J. Med. Chem.* **2008**, *51*, 305-313. b) D. Nikolic, P. P. Toth, A. Ferlita, V. Di Bartolo, G. Montalto, M. Banach, M. Rizzo, *Clin. Lipidol.* **2014**, *9*, 179–187. c) I. G. Smilovic, J. Cluzeau, F. Richter, S. Nerdinger, E. Schreiner, G. Laus, H. Schottenberger, *Bioorg. Med. Chem.* **2018**, *26*, 2686–2690. d)

(4) a) P. L. Ornstein, D. M. Zimmerman, M. B. Arnold, T. J. Bleisch, B. Cantrell, R. Simon, H. Zarrinmayeh, S. R. Baker, M. Gates, J. P. Tizzano, D. Bleakman, A. Mandelzys, K. R. Jarvie, K. Ho, M. Deverill, R. K. Kamboj, *J. Med. Chem.* **2000**, *43*, 4354-4358. b)M. Gates, A. Ogden, D. Bleakman, *Neuropharmacology* **2001**, *40*, 984–991. c) N. Jones, M. J. O'Neill, M. Tricklebank, V. Libri, S. C. R. Williams, *Psychopharmacology* **2005**, *180*, 743–751.

(5) S. T. Moe, S. M. Shimizu, D. L. Smith, B. C. Van Wagenen, E. G. DelMar, M. F. Balandrin, Y. Chien, J. L. Raszkiewicz, L. D. Artman, A. L. Mueller, E. Lobkovsky, J. Clardy, *Bioorganic & Medicinal Chemistry Letters* **1999**, *9*, 1915-1920.

(6) a) *Catalytic Asymmetric Synthesis*. (Ed.I. Ojima), Wiley-VCH: Weinheim, **2000**; b) *Applied Homogeneous Catalysis with Organometallic Compounds*, (Eds.: B. Cornils, W. A. Herrmann), Wiley-VCH: Weinheim, **2002**; c) *Asymmetric Catalysis on Industrial Scale: Challenges, Approaches and Solutions*. (Eds.: H. U. Blaser, E. Schmidt), Wiley-VCH: Weinheim, **2004**. d) J. M. Brown. in *Comprehensive Asymmetric Catalysis Vol. I*; (Eds: Jacobsen, E. N., Pfaltz, A., Yamamoto, Y.); Springer: Berlin, 1999. e) H.-U. Blaser, B. Pugin, F. Spindler, *Top. Organomet. Chem.* **2012**, *42*, 65-102. f) P. Etayo, A. Vidal-Ferran, *Chem. Soc. Rev.* **2013**, *42*, 728-754. g) Z. Zhang, N. A. Butt, W. Zhang, *Chem. Rev.* **2016**, *116*, 14769-14827. h) C. Margarita, P. G. Andersson, *J. Am. Chem. Soc.* **2017**, *139*, 1346-1356.

(7) E. Cristobal-Lecina, P. Etayo, S. Doran, M. Reves, P. Martin-Gago, A. Grabulosa, A. R. Costantino, A. Vidal-Ferran, A. Riera, X. Verdaguer, *Adv. Synth. Catal.* **2014**, *356*, 795-804.

(8) a) A. Pfaltz, J. Blankenstein, R. Hilgraf, E. Hörmann, S. McIntyre, F. Menges, M. Schönleber, S. P. Smidt, B. Wüstenberg, N. Zimmermann, *Adv. Synth. Catal.* **2003**, *345*, 33–43. b) J. J. Verendel, O. Pàmies, M. Diéguez, P. G. Andersson, *Chem. Rev.* **2014**, *114*, 2130–2169. c) M. A. Müller, S. Gruber, A. Pfaltz, *Adv. Synth. Catal.* **2018**, *360*, 1340–1345. d) W. J. Lu, Y. W. Chen, X. L. Hou, *Adv. Synth. Catal.* **2010**, *352*, 103–107. e) A. Trifonova, J. S. Diesen, C. J. Chapman, P. G. Andersson, *Org. Lett.* **2004**, *6*, 3825–3827. f) J. Q. Li, J. Liu, S. Krajangsri, N. Chumnanvej, T. Singh, P. G. Andersson, *ACS Catal.* **2016**, *6*, 8342–8349. g) E. Salomo, S. Orgue, A. Riera, X. Verdaguer, *Angew. Chem., Int. Ed.* **2016**, *55*, 7988-7992. h) E. Salomo, A.

Gallen, G. Sciortino, G. Ujaque, A. Grabulosa, A. Lledos, A. Riera, X. Verdaguer, *J. Am. Chem. Soc.* **2018**, *140*, 16967-16970.

(9) a) S. J. Roseblade, A. Pfaltz, *Acc. Chem. Res.* **2007**, *40*, 1402–1411. b) S. McIntyre, E. Hörmann, F. Menges, S. P. Smidt, A. Pfaltz, *Adv. Synth. Catal.* **2005**, *347*, 282–288. c) J. Mazuela, J. J. Verendel, M. Coll, B. Schäffner, A. Börner, P. G. Andersson, O. Pàmies, M. Diéguez, *J. Am. Chem. Soc.* **2009**, *131*, 12344–12353. d) O. Pàmies, P. G. Andersson, M. Diéguez, *Chem. - A Eur. J.* **2010**, *16*, 14232–14240. e) D. H. Woodmansee, A. Pfaltz, *Chem. Commun.* **2011**, *47*, 7912–7916. f) J. Mazuela, O. Pàmies, M. Diéguez, *ChemCatChem* **2013**, *5*, 2410–2417. g) M. Biosca, E. Salomo, P. de la Cruz-Sanchez, A. Riera, X. Verdaguer, O. Pamies, M. Dieguez, *Org. Lett.* **2019**, *21*, 807-811.

(10) C. J. Wang, X. Sun, X. Zhang, *Angew. Chem., Int. Ed.* **2005**, *44*, 4933–4935.

(11) D. P. Steinhuebel, S. W. Krska, A. Alorati, J. M. Baxter, K. Belyk, B. Bishop, M. Palucki, Y. Sun, I. W. Davies, *Org. Lett.* **2010**, *12*, 4201–4203.

(12) A. Cabre, G. Sciortino, G. Ujaque, X. Verdaguer, A. Lledos, A. Riera, *Org. Lett.* **2018**, *20*, 5747-5751.

(13) a) J. Blankenstein, A. Pfaltz, *Angew. Chem. Int. Ed.* **2001**, *40*, 4445–4447. b) F. Menges, A. Pfaltz, *Adv. Synth. Catal.* **2002**, *344*, 40–41.

(14) T. Nishikata, H. Nagashima, *Angew. Chem., Int. Ed.* **2012**, *51*, 5363–5366.

(15) B. H. Kaae, K. Harpsøe, J. S. Kastrup, A. C. Sanz, D. S. Pickering, B. Metzler, R. P. Clausen, M. Gajhede, P. Sauerberg, T. Liljefors, et al., *Chem. Biol.* **2007**, *14*, 1294–1303.

(16) J. Zhang, C. Liu, X. Wang, J. Chen, Z. Zhang, W. Zhang, *Chem. Commun.* **2018**, *54*, 6024–6027.

(17) T. Drapier, P. Geubelle, C. Bouckaert, L. Nielsen, S. Laulumaa, E. Goffin, S. Dilly, P. Francotte, J. Hanson, L. Pochet, J. S. Kastrup, B. Pirotte, *J. Med. Chem.* **2018**, *61*, 5279-5291.

(18) a) B. Xu, J. Su, J. Wang, G.-C. Zhou, *Aust. J. Chem.* **2016**, *69*, 770. b) A. Gini, J. Bamberger, J. Luis-Barrera, M. Zurro, R. Mas-Ballesté, J. Alemán, O. G. Mancheño, *Adv. Synth. Catal.* **2016**, *358*, 4049–4056. c) Q. Zhu, J. Wang, X. Bian, L. Zhang, P. Wei, Y. Xu, *Org. Process Res. Dev.* **2015**, *19*, 1263–1267. d) S. Gaj, J. Cluzeau, F. Richter, G. Laus, I. Gazic Smilovic, Lek Pharmaceuticals D. D., Slovenia. **2014**, WO2014173928A1.

Experimental Part

General procedures and materials

Unless otherwise indicated, materials were obtained from commercial suppliers and used without further purification. All reactions that required anhydrous conditions were performed in dried glassware under a dry nitrogen atmosphere. Dichloromethane and THF were degassed and dried with a solvent purification system (SPS PS-MD-3). Anhydrous dichloroethane and DMF were used from Sigma Aldrich. Solvents were removed under reduced pressure with a rotary evaporator. Silica gel chromatography was performed using an automated chromatography system (PuriFlash® 430, Interchim).

Instrumentation

NMR spectroscopy: ^{1}H and ^{13}C were recorded on the NMR spectrometers of the *Centres Científics i Tecnològics de la Universitat de Barcelona*. The employed spectrometers were a Varian Mercury 400 MHz. Chemical shifts (δ) were referenced to internal solvent resonances and reported relative to TMS (tetramethylsilane). The coupling constants (*J*) are reported in Hertz (Hz). The following abbreviations are used to define multiplicities: s (singlet), d (doublet), t (triplet), q (quartet), dd (doublet of doublets), ddd (doublet of doublet of doublets), dt (doublet of triplets), td (triplet of doublets), ddq (doublet of doublet of quartets), dtd (doublet of triplet of doublets), dq (doublet of quartets), tt (triplet of triplets), qt (quartet of triplets), m (multiplet), br s (broad signal).

High Resolution Mass Spectrometry: High resolution ESI-MS spectra were recorded in an LC/MSD-TOF G1969A (Agilent Technologies) of the *Centres Científics i Tecnològics de la Universitat de Barcelona.*

IR spectroscopy: IR spectra were measured in a Thermo Nicolet 6700 FT-IR spectrometer using an ATR system, of the Department of Organic Chemistry in the Universitat de Barcelona.

Optical rotations were measured at room temperature (25°C) using a Jasco P-2000 iRM- 800 polarimeter. Concentration is expressed in g/100 mL. The cell sized 10 cm long and had 1 mL of capacity, measuring λ was 589 nm, which corresponds to a sodium lamp.

Melting points were determined using a Büchi melting point apparatus and were not corrected.

Experimental procedures and characterization

Preparation of substrates

All substrates **8-2(a-p)** as well as their precursor **8-1(a-p)** were prepared according to the procedure described.[1]

All compounds were described in ref 1, except **8-1n** and **8-2n**.

Aziridination reaction. A round-bottom flask equipped with magnetic stirring was charged with the alkene (1.0 equiv.), CH_2Cl_2 (2.5 mL/mmol alkene), p-toluenesulfonamide or methanesulfonamide (1.0 equiv.) and $MnSO_4.H_2O$ (0.05 equiv.). *N*-Bromosuccinimide (NBS, 1.1 equiv.) was added, and the mixture was stirred at r.t. under N_2 for 17-24 hours. Then, K_2CO_3 (2.0 equiv.) was added and the mixture was stirred at r.t. for 1-4 hours. The resulting mixture was diluted with CH_2Cl_2 and H_2O, and the aqueous layer was extracted with CH_2Cl_2 (1x). The combined organic layer was dried over $MgSO_4$, and the filtrate was concentrated. The crude was purified with column chromatography (EtOAc/hexanes, 2% Et_3N).

2-(4-isobutylphenyl)-2-methyl-1-(methanesulfonyl)aziridine, 8-1n

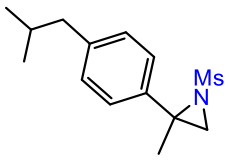

Following the described procedure,[1] starting from the corresponding alkene (1.16 g) compound **8-1n** was obtained as an oil (950 mg, 53% yield). **^{1}H NMR** (400 MHz, $CDCl_3$) δ 7.33 – 7.29 (m, 2H), 7.14 – 7.10 (m, 2H), 3.12 (s, 3H), 2.93 (s, 1H), 2.61 (s, 1H), 2.46 (d, J = 7.2 Hz, 2H), 1.98 (s, 3H), 1.84 (dp, J = 13.6, 6.7 Hz, 1H), 0.89 (dd, J = 6.6, 0.8 Hz, 6H). **^{13}C NMR** (101 MHz, $CDCl_3$) δ 141.63, 138.28, 129.34, 126.30, 51.19, 45.18, 42.48, 42.21, 30.32, 22.50, 21.02. **HRMS** (ESI) calculated for $C_{14}H_{22}NO_2S$ 268.1366, found 268.1366 $[M+H]^+$. **IR** (ATR-FTIR) ν_{max} = 3257, 2953, 2927, 2868, 1676, 1313, 1145 cm^{-1}.

Isomerization reaction. A glass vial equipped with PTFE-coated stirring-bar was charged with the corresponding *N*-sulfonyl 2,2-disubstituted aziridine (1.72 mmol) and Crabtree's catalyst was added (1 mol%). The vial was purged with N_2 and dissolved with specified anhydrous CH_2Cl_2 ([0.25M]). The reaction mixture was left stirring during 3-17 hours at the indicated temperature. After concentrated under vacuum, the crude was purified by flash column chromatography (hexanes: ethyl acetate, 3:1) to afford the corresponding isolated product.

***N*-(2-(4-isobutylphenyl)allyl)methanesulfonamide, 8-2n**

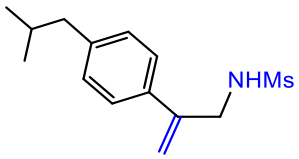

[1] A. Cabré, G. Sciortino, G. Ujaque, X. Verdaguer, A. Lledós, A. Riera, *Org. Lett.* **2018**, *20* (18), 5747.

Following the isomerization procedure,[1] starting from *N*-mesyl aziridine **8-1n** (460 mg) and using Crabtree's catalyst (1 mol%), compound **2n** was obtained as a white solid (363 mg, 79% yield). **m.p.** 69-72 ºC. **^{1}H NMR** (400 MHz, $CDCl_3$) δ 7.35 – 7.30 (m, 2H), 7.17 – 7.12 (m, 2H), 5.47 (q, *J* = 0.7 Hz, 1H), 5.31 (q, *J* = 1.2 Hz, 1H), 4.68 (t, *J* = 6.3 Hz, 1H), 4.19 (ddd, *J* = 6.2, 1.4, 0.7 Hz, 2H), 2.87 (s, 3H), 2.48 (d, *J* = 7.2 Hz, 2H), 1.93 – 1.81 (m, 1H), 0.91 (d, *J* = 6.6 Hz, 6H). **^{13}C NMR** (101 MHz, $CDCl_3$) δ 143.46, 142.14, 135.22, 129.48, 125.85, 114.31, 47.01, 45.02, 40.98, 30.15, 22.35. **HRMS** (ESI) calculated for $C_{14}H_{22}NO_2S$ 268.1366, found 268.1368 $[M+H]^+$. **IR** (ATR-FTIR) ν_{max} = 3277, 2958, 2932, 2866, 1410, 1303, 1144 cm^{-1}.

Iridium-catalysed asymmetric hydrogenation of *N*-sulfonyl allyl amines.

General procedure for asymmetric hydrogenation (GP)

Glass vials equipped with PTFE-coated stirring-bars were charged with the corresponding substrate (0.288 mmol, 1.0 equiv.). The corresponding catalyst **8-4** was added (1 mol %, otherwise indicated) and dissolved with anhydrous DCE (1 mL/0.1 mmol substrate). They were placed into a low-pressure reactor. Once sealed, the reactor was purged and charged with 1 bar of H_2 and left stirring overnight at room temperature. Afterwards, the crude was filtrated with a short plug of silica to afford the corresponding isolated product. The conversion was measured by ^{1}H NMR spectroscopy and the enantiomeric excess was determined using HPLC chiral chromatography. For reactions at small scale (0.288 mmol) with full conversion and only one product by NMR we describe quantitative yield. For larger scale reactions the product weight and isolated yield after flash column chromatography are given.

(*R*)-4-methyl-*N*-(2-phenylpropyl)benzenesulfonamide, 8-3a

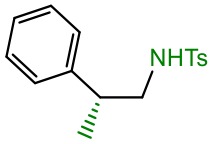

Following the GP and stirring for 3 hours, compound **8-3a** was obtained as a white solid (quant. by NMR, 93% ee). **$[\alpha]_D^{25}$**: +2.4 (c 1.2, $CHCl_3$). **^{1}H NMR** (400 MHz, $CDCl_3$) δ 7.69 – 7.62 (m, 2H), 7.31 – 7.26 (m, 4H), 7.25 – 7.20 (m, 1H), 7.10 – 7.02 (m, 2H), 4.15 (dd, *J* = 8.2, 4.5 Hz, 1H), 3.20 (ddd, *J* = 12.4, 8.2, 5.9 Hz, 1H), 2.99 (ddd, *J* = 12.4, 8.7, 4.5 Hz, 1H), 2.90 – 2.81 (m, 1H), 2.43 (s, 3H), 1.22 (d, *J* = 6.9 Hz, 3H). **^{13}C NMR** (101 MHz, $CDCl_3$) δ 143.48, 142.98, 137.04, 129.81, 128.97, 127.26, 127.18, 127.14, 49.76, 39.87, 21.65, 19.34. **HPLC**: CHIRALPAK IA. Heptane/iPrOH 50:50, 1.0 mL/min, λ = 210 nm. $t_{(R)}$ = 12.7 min, $t_{(S)}$ = 14.0 min. The analytical data for this compound were in excellent agreement with the reported data.[2]

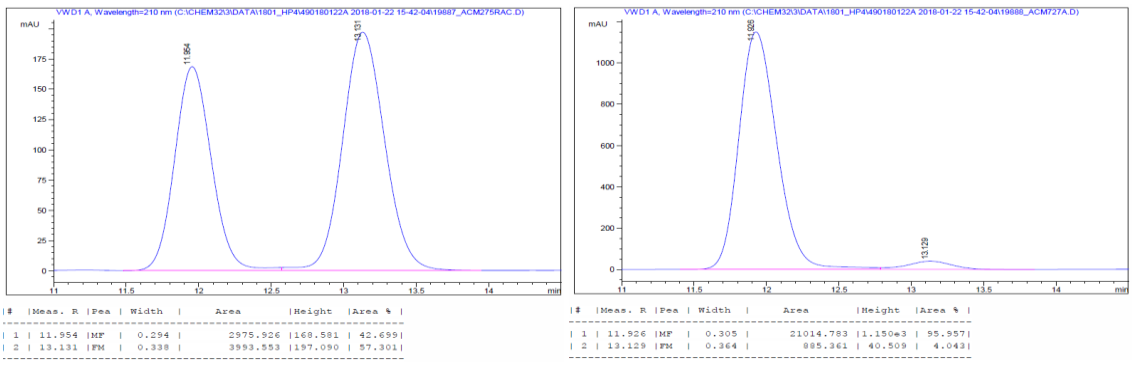

[2] T. Nishikata, H. Nagashima, *Angew. Chem. Int. Ed.* **2012**, *51* (22), 5363.

(*R*)-*N*-(2-(4-chlorophenyl)propyl)-4-methylbenzenesulfonamide, 8-3b

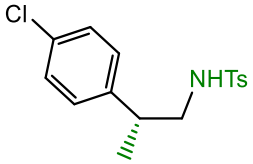

Following the GP, compound **8-3b** was obtained as a white solid (quant. by NMR, 85% ee). **m.p.** 99-102 ºC. **[α]$_D$**: +1.5 (c 1.0, $CHCl_3$). **^{1}H NMR** (400 MHz, $CDCl_3$) δ 7.67 – 7.60 (m, 2H), 7.29 – 7.25 (m, 2H), 7.22 – 7.17 (m, 2H), 7.02 – 6.96 (m, 2H), 4.62 – 4.53 (m, 1H), 3.13 (ddd, *J* = 12.6, 7.4, 6.2 Hz, 1H), 2.97 (ddd, *J* = 12.6, 8.3, 5.4 Hz, 1H), 2.90 – 2.77 (m, 1H), 2.42 (s, 3H), 1.19 (d, *J* = 6.9 Hz, 3H). **^{13}C NMR** (101 MHz, $CDCl_3$) δ 143.59, 141.57, 136.91, 132.74, 129.82, 128.97, 128.63, 127.11, 49.68, 39.42, 21.65, 19.20. **HRMS** (ESI) calculated for $C_{16}H_{19}ClNO_2S$ 324.082, found 324.0817 $[M+H]^+$. **IR** (ATR-FTIR) ν_{max} = 3457, 1493, 1322, 1157, 1012, 826 cm^{-1}. **HPLC**: CHIRALPAK IA. Heptane/EtOH-0.2% DEA 70:30, 0.5 mL/min, λ = 210 nm. $t_{(R)}$ = 13.3 min, $t_{(S)}$ = 14.9 min.

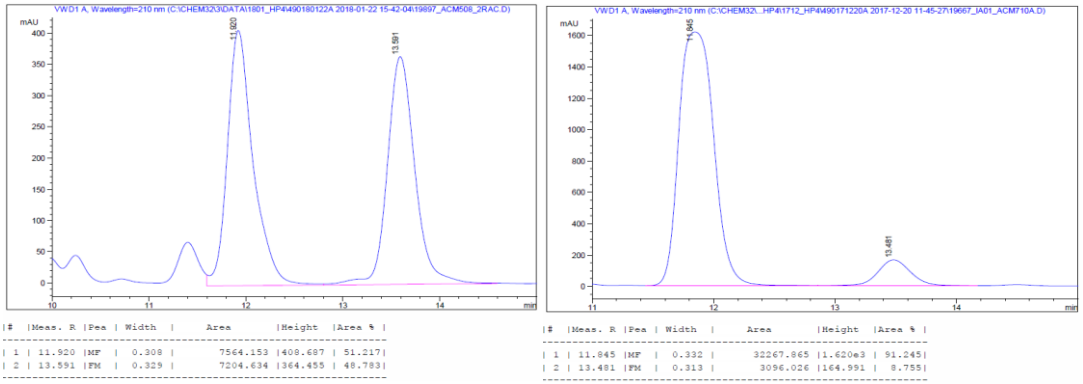

#	Meas. R	Pea	Width	Area	Height	Area %
1	11.920	MF	0.308	7564.153	408.687	51.217
2	13.591	FM	0.329	7204.634	364.455	48.783

#	Meas. R	Pea	Width	Area	Height	Area %
1	11.845	MF	0.332	32267.865	1.620e3	91.245
2	13.481	FM	0.313	3096.026	164.991	8.755

(*R*)-*N*-(2-(3-chlorophenyl)propyl)-4-methylbenzenesulfonamide, 8-3c

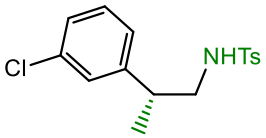

Following the GP, but using 225 mg (0.7 mmol) of **8-2c**, compound **8-3c** was obtained as an oil (230 mg, 97% isolated yield, 89% ee). **[α]$_D$**: +11.0 (c 1.0, $CHCl_3$). **^{1}H NMR** (400 MHz, $CDCl_3$) δ 7.67 – 7.63 (m, 2H), 7.33 – 7.23 (m, 2H), 7.22 – 7.17 (m, 2H), 7.00 – 6.94 (m, 2H), 4.37 – 4.28 (m, 1H), 3.17 (ddd, *J* = 12.7, 7.8, 6.0 Hz, 1H), 2.98 (ddd, *J* = 12.7, 8.5, 5.1 Hz, 1H), 2.88 – 2.78 (m, 1H), 2.43 (s, 3H), 1.20 (d, *J* = 6.9 Hz, 3H). **^{13}C NMR** (101 MHz, $CDCl_3$) δ 145.19, 143.67, 136.93, 134.76, 130.21, 129.89, 127.38, 127.32, 127.14, 125.60, 49.58, 39.79, 21.68, 19.20. **HRMS** (ESI) calculated for $C_{16}H_{19}ClNO_2S$ 324.082, found 324.0820 $[M+H]^+$. **IR** (ATR-FTIR) ν_{max} = 3359, 3061, 1324, 1159, 1092 cm^{-1}. **HPLC**: CHIRALCEL ODH. Heptane/iPrOH 92:8, 0.5 mL/min, λ = 210 nm. $t_{(R)}$ = 29.2 min, $t_{(S)}$ = 32.3 min.

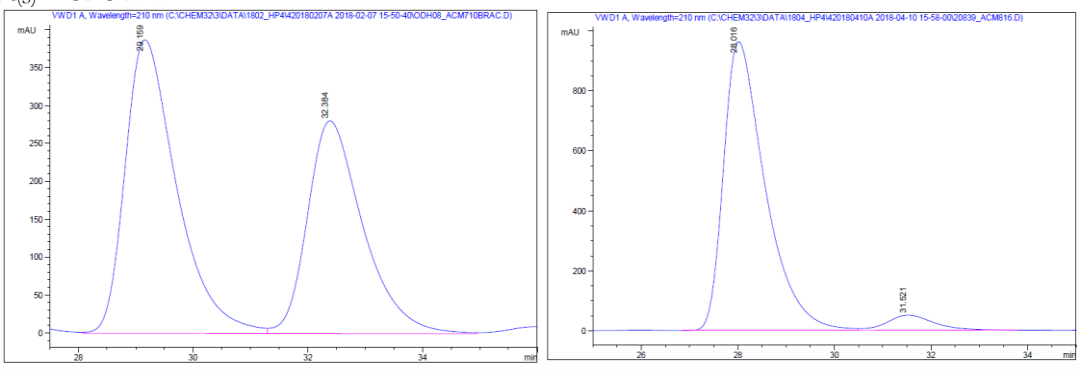

#	Meas. R	Pea	Width	Area	Height	Area %
1	29.159	BV	0.942	24297.252	387.859	56.153
2	32.384	VB	1.018	18972.271	281.048	43.847

#	Meas. R	Pea	Width	Area	Height	Area %
1	28.016	MF	0.998	57625.758	962.607	94.368
2	31.521	FM	1.129	3439.337	50.793	5.632

(*R*)-*N*-(2-(2-chlorophenyl)propyl)-4-methylbenzenesulfonamide, 8-3d

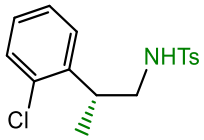

Following the GP and using 2 mol% of **8-4**, compound **8-3d** was obtained as an oil (quant. by NMR, 82% ee). **[α]D**: -4.06 (c 0.1, $CHCl_3$). **^{1}H NMR** (400 MHz, $CDCl_3$) δ 7.69 – 7.64 (m, 2H), 7.34 – 7.28 (m, 3H), 7.22 – 7.09 (m, 3H), 4.25 (t, *J* = 6.4 Hz, 1H), 3.44 (q, *J* = 6.9 Hz, 1H), 3.19 – 3.12 (m, 2H), 2.42 (s, 3H), 1.23 (d, *J* = 7.0 Hz, 3H). **^{13}C NMR** (101 MHz, $CDCl_3$) δ 143.43, 140.00, 136.73, 134.84, 129.89, 129.69, 127.98, 127.27, 127.20, 127.02, 48.11, 35.44, 21.49, 18.05. **HRMS** (ESI) calculated for $C_{16}H_{19}ClNO_2S$ 324.082, found 324.0802 $[M+H]^+$. **IR** (ATR-FTIR) ν_{max} = 3270, 2928, 1278, 1215, 1158, 1127 cm^{-1}. **HPLC**: CHIRALCEL OJ. Heptane/EtOH-0.2% DEA 90:10, 0.8 mL/min, λ = 210 nm. $t_{(S)}$ = 20.2 min, $t_{(R)}$ = 22.3 min.

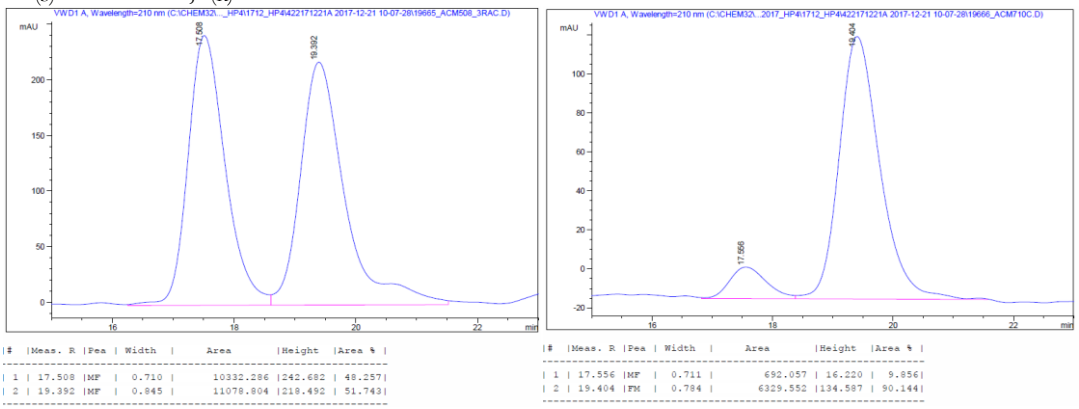

#	Meas. R	Pea	Width	Area	Height	Area %
1	17.508	MF	0.710	10332.286	242.682	48.257
2	19.392	MF	0.845	11078.804	218.492	51.743

#	Meas. R	Pea	Width	Area	Height	Area %
1	17.556	MF	0.711	692.057	16.220	9.856
2	19.404	FM	0.784	6329.552	134.587	90.144

(*R*)-4-methyl-*N*-(2-(p-tolyl)propyl)benzenesulfonamide, 8-3e

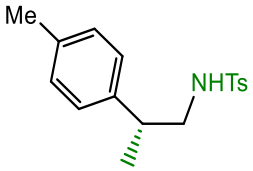

Following the GP, compound **8-3e** was obtained as an oil (quant. by NMR, 92% ee). **[α]D**: +6.35 (c 0.4, $CHCl_3$). **^{1}H NMR** (400 MHz, $CDCl_3$) δ 7.61 – 7.54 (m, 2H), 7.24 – 7.19 (m, 2H), 7.04 – 6.99 (m, 2H), 6.90 – 6.86 (m, 2H), 4.07 (dd, *J* = 8.5, 4.4 Hz, 1H), 3.11 (ddd, *J* = 12.4, 8.3, 5.9 Hz, 1H), 2.89 (ddd, *J* = 12.3, 8.7, 4.4 Hz, 1H), 2.80 – 2.67 (m, 1H), 2.36 (s, 4H), 2.25 (s, 3H), 1.13 (d, *J* = 6.9 Hz, 3H). **^{13}C NMR** (101 MHz, $CDCl_3$) δ 143.52, 139.82, 136.80, 129.96, 129.88, 129.81, 129.68, 127.20, 127.13, 49.79, 39.43, 21.67, 21.13, 19.45. **HRMS** (ESI) calculated for $C_{17}H_{22}NO_2S$ 304.1366, found 304.1352 $[M+H]^+$. **IR** (ATR-FTIR) ν_{max} = 3550, 1348, 1278, 1159, 1127 cm^{-1}. **HPLC**: CHIRALPAK IA. Heptane/EtOH-0.2% DEA 90:10, 0.5 mL/min, λ = 210 nm. $t_{(R)}$ = 23.9 min, $t_{(S)}$ = 26.8 min.

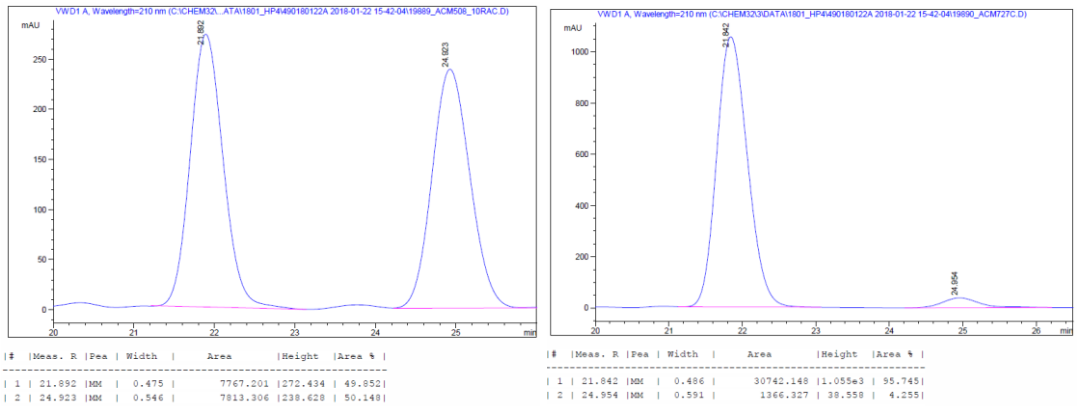

#	Meas. R	Pea	Width	Area	Height	Area %
1	21.892	MM	0.475	7767.201	272.434	49.852
2	24.923	MM	0.546	7813.306	238.628	50.148

#	Meas. R	Pea	Width	Area	Height	Area %
1	21.842	MM	0.486	30742.148	1.055e3	95.745
2	24.954	MM	0.591	1366.327	38.558	4.255

(*R*)-4-methyl-*N*-(2-(naphthalen-2-yl)propyl)benzenesulfonamide, 8-3f

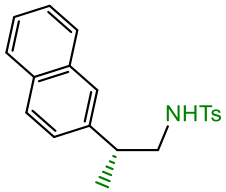

Following the GP and using 2 mol% of **8-4**, the desired product was obtained as a white solid (quant. by NMR, 88% ee). **[α]$_D$**: +1.94 (c 1.1, $CHCl_3$). **^{1}H NMR** (400 MHz, $CDCl_3$) δ 7.71 (ddd, *J* = 8.4, 5.1, 3.0 Hz, 3H), 7.67 – 7.62 (m, 2H), 7.55 – 7.50 (m, 2H), 7.40 – 7.35 (m, 3H), 7.21 – 7.18 (m, 1H), 7.14 – 7.08 (m, 3H), 4.28 (dd, *J* = 7.8, 4.7 Hz, 1H), 3.23 – 3.15 (m, 1H), 3.02 (ddd, *J* = 12.2, 8.6, 4.7 Hz, 1H), 2.98 – 2.89 (m, 1H), 2.32 (s, 3H), 1.22 (d, *J* = 6.8 Hz, 3H). **^{13}C NMR** (101 MHz, $CDCl_3$) δ 143.48, 140.32, 136.92, 133.57, 132.66, 129.82, 129.76, 128.75, 127.73, 127.13, 126.54, 126.38, 126.04, 125.89, 125.20, 124.00, 49.66, 39.99, 21.63, 19.32. **HRMS** (ESI) calculated for $C_{17}H_{19}F_3NO_2S$ 340.1366, found 340.1352 $[M+H]^+$. **IR** (ATR-FTIR) ν_{max} = 3279, 3025, 2932, 1278, 1215, 1158, 1128 cm^{-1}. **HPLC**: CHIRALCEL OJ. Heptane/EtOH-0.2% DEA 60:40, 0.5 mL/min, λ = 210 nm. $t_{(R)}$ = 26.3 min, $t_{(S)}$ = 30.0 min.

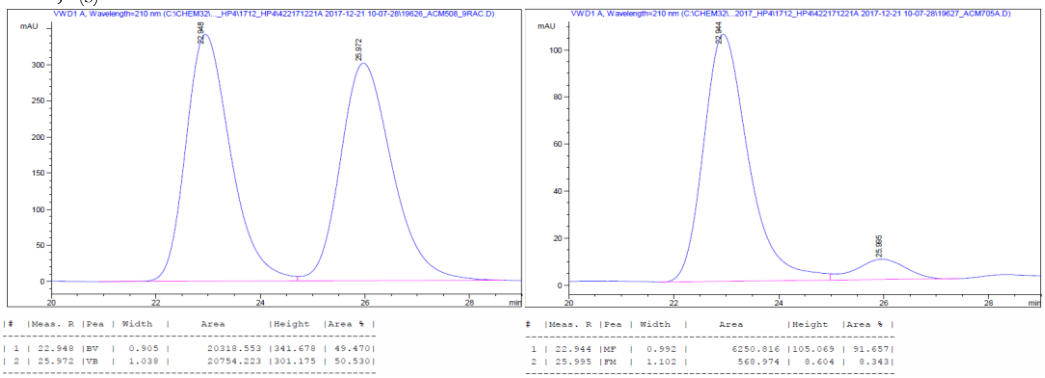

#	Meas. R	Pea	Width	Area	Height	Area %
1	22.948	BV	0.905	20318.553	341.678	49.470
2	25.972	VB	1.038	20754.223	301.175	50.530

#	Meas. R	Pea	Width	Area	Height	Area %
1	22.944	MF	0.992	6250.816	105.069	91.657
2	25.995	FM	1.102	568.974	8.604	8.343

(*R*)-*N*-(2-(2-methoxyphenyl)propyl)-4-methylbenzenesulfonamide, 8-3g

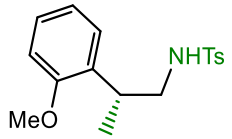

Following the GP and using 2 mol% of **8-4**, the desired product was obtained as a white solid (quant. by NMR, 92% ee). **m.p.** 109-112 °C. **[α]$_D$**: -8.7 (c 0.5, $CHCl_3$). **^{1}H NMR** (400 MHz, $CDCl_3$) δ 7.65 – 7.58 (m, 2H), 7.29 – 7.23 (m, 2H), 7.21 – 7.16 (m, 1H), 7.01 – 6.97 (m, 1H), 6.91 – 6.79 (m, 2H), 4.45 (t, *J* = 6.0 Hz, 1H), 3.74 (s, 3H), 3.37 – 3.23 (m, 1H), 3.19 – 3.04 (m, 2H), 2.41 (d, *J* = 0.8 Hz, 3H), 1.19 (d, *J* = 7.0 Hz, 3H). **^{13}C NMR** (101 MHz, $CDCl_3$) δ 157.03, 143.09, 136.87, 130.76, 129.53, 127.79, 127.18, 127.01, 120.87, 110.64, 55.24, 48.48, 32.65, 21.48, 17.77. **HRMS** (ESI) calculated for $C_{17}H_{22}NO_3S$ 320.1315, found 320.1313 $[M+H]^+$. **IR** (ATR-FTIR) ν_{max} = 3279, 3012, 2919, 1278, 1215, 1158, 1127 cm^{-1}. **HPLC**: CHIRALPAK IC. Heptane/iPrOH 80:20, 0.5 mL/min, λ = 210 nm. $t_{(S)}$ = 40.7 min, $t_{(R)}$ = 43.2 min.

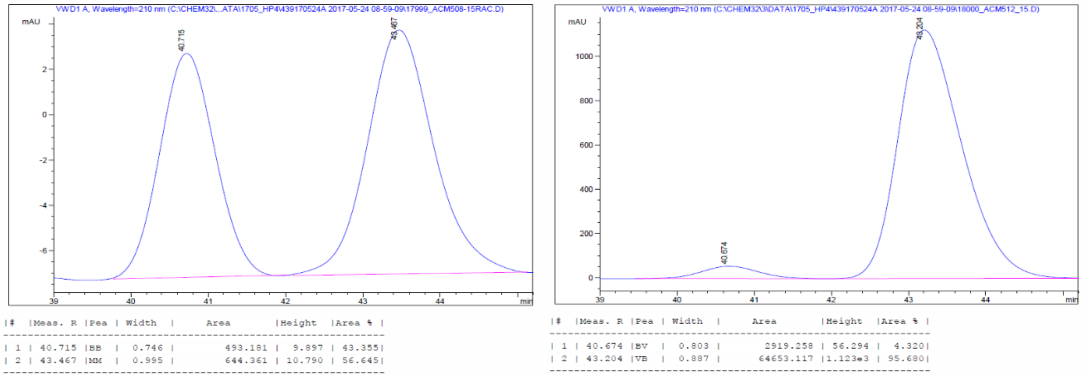

#	Meas. R	Pea	Width	Area	Height	Area %
1	40.715	BB	0.746	493.181	9.897	43.355
2	43.467	MM	0.995	644.361	10.790	56.645

#	Meas. R	Pea	Width	Area	Height	Area %
1	40.674	BV	0.803	2919.258	56.294	4.320
2	43.204	VB	0.887	64653.117	1.123e3	95.680

(*R*)-*N*-(2-(4-fluorophenyl)propyl)-4-methylbenzenesulfonamide, 8-3h

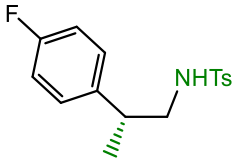

Following the GP, compound **8-3h** was obtained as a white solid (quant. by NMR, 91% ee). **m.p.** 81-84 ºC. **[α]$_D$**: +3.95 (c 1.4, $CHCl_3$). **^{1}H NMR** (400 MHz, $CDCl_3$) δ 7.68 – 7.61 (m, 2H), 7.30 – 7.24 (m, 2H), 7.06 – 6.99 (m, 2H), 6.96 – 6.90 (m, 2H), 4.49 (dd, *J* = 7.6, 5.1 Hz, 1H), 3.13 (ddd, *J* = 12.5, 7.6, 6.1 Hz, 1H), 2.96 (ddd, *J* = 12.5, 8.3, 5.1 Hz, 1H), 2.89 – 2.79 (m, 1H), 2.42 (s, 3H), 1.19 (d, *J* = 6.9 Hz, 3H). **^{13}C NMR** (101 MHz, $CDCl_3$) δ 162.93, 160.50, 143.47, 138.54 (d, *J* = 3.4 Hz), 129.69, 128.55 (d, *J* = 7.7 Hz), 126.99, 115.57 (d, *J* = 21.3 Hz), 49.68, 39.10, 21.49, 19.26. **^{19}F NMR** (376 MHz, cdcl$_3$) δ -62.43. **HRMS** (ESI) calculated for $C_{16}H_{19}FNO_2S$ 308.1115, found 308.111 $[M+H]^+$. **IR** (ATR-FTIR) ν_{max} = 3281, 3015, 1600, 1510, 1278, 1215, 1158, 1092 cm^{-1}. **HPLC**: CHIRALPAK IA. Heptane/EtOH-0.2% DEA 70:30, 0.5 mL/min, λ = 210 nm. $t_{(R)}$ = 12.8 min, $t_{(S)}$ = 14.4 min.

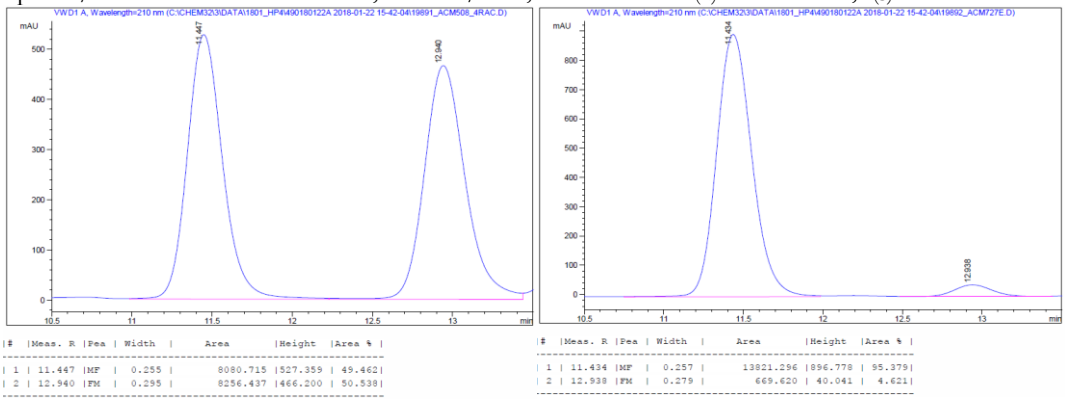

(*R*)-*N*-(2-(3-fluorophenyl)propyl)-4-methylbenzenesulfonamide, 8-3i

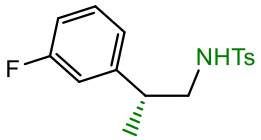

Following the GP, compound **8-3i** was obtained as an oil (quant. by NMR, 92% ee). **[α]$_D$**: +6.0 (c 1.7, $CHCl_3$). **^{1}H NMR** (400 MHz, $CDCl_3$) δ 7.62 – 7.54 (m, 2H), 7.24 – 7.14 (m, 4H), 6.84 (tdd, *J* = 8.4, 2.6, 1.0 Hz, 1H), 6.79 (dq, *J* = 7.7, 1.0 Hz, 1H), 6.68 – 6.62 (m, 1H), 4.12 (t, *J* = 6.5 Hz, 1H), 3.12 (ddd, *J* = 12.6, 8.0, 5.9 Hz, 1H), 2.96 – 2.86 (m, 1H), 2.80 (dq, *J* = 14.5, 6.8 Hz, 1H), 2.37 (s, 3H), 1.14 (d, *J* = 6.9 Hz, 3H). **^{13}C NMR** (101 MHz, $CDCl_3$) δ 164.23, 161.78, 145.62 (d, *J* = 6.8 Hz), 143.52, 136.73, 130.25 (d, *J* = 8.3 Hz), 129.71, 126.99, 122.91 (d, *J* = 2.8 Hz), 113.87 (dd, *J* = 21.1, 6.6 Hz), 49.45, 39.62, 21.49, 19.02. **^{19}F NMR** (376 MHz, $CDCl_3$) δ -62.43. **HRMS** (ESI) calculated for $C_{16}H_{19}FNO_2S$ 308.1115, found 308.1107 $[M+H]^+$. **IR** (ATR-FTIR) ν_{max} = 3278, 3025, 1278, 1215, 1157, 1093 cm^{-1}. **HPLC**: CHIRALPAK IA. Heptane/EtOH-0.2% DEA 90:10, 0.5 mL/min, λ = 210 nm. $t_{(S)}$ = 15.9 min, $t_{(R)}$ = 17.2 min.

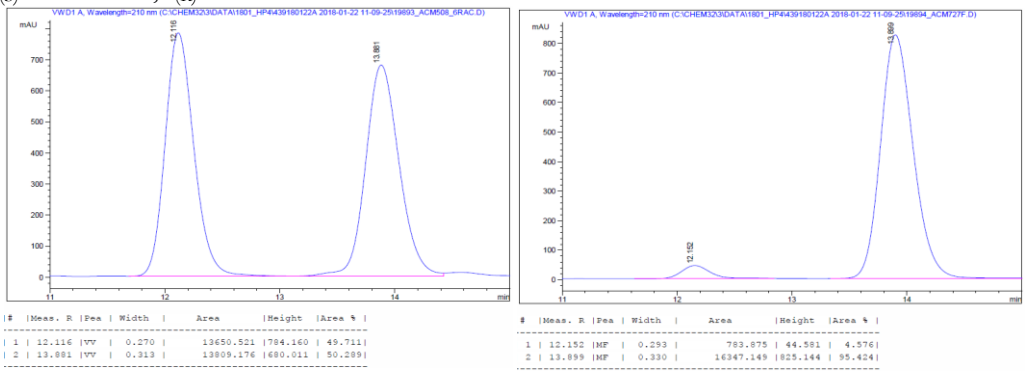

(*R*)-4-methyl-*N*-(2-(4-(trifluoromethyl)phenyl)propyl)benzenesulfonamide, 8-3j

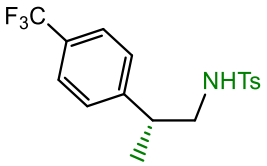

Following the GP, compound **8-3j** was obtained as an oil (quant. by NMR, 82% ee). **[α]D**: +5.2 (c 0.6, $CHCl_3$). **^{1}H NMR** (400 MHz, $CDCl_3$) δ 7.62 – 7.53 (m, 2H), 7.46 – 7.41 (m, 2H), 7.24 – 7.18 (m, 3H), 7.17 – 7.08 (m, 2H), 4.17 (dd, *J* = 7.5, 5.4 Hz, 1H), 3.14 (ddd, *J* = 12.6, 7.6, 5.9 Hz, 1H), 2.97 (ddd, *J* = 12.6, 8.4, 5.3 Hz, 1H), 2.88 (dt, *J* = 14.3, 6.9 Hz, 1H), 2.36 (s, 3H), 1.18 (d, *J* = 6.9 Hz, 4H). **^{13}C NMR** (101 MHz, $CDCl_3$) δ 147.25, 143.72, 136.91, 134.93, 134.90, 129.87, 127.70, 127.13, 125.83 (q, *J* = 3.7 Hz), 49.56, 40.01, 21.64, 19.10. **^{19}F NMR** (376 MHz, $CDCl_3$) δ -62.53. **HRMS** (ESI) calculated for $C_{17}H_{19}F_3NO_2S$ 358.1083, found 358.1083 $[M+H]^+$. **IR** (ATR-FTIR) ν_{max} = 3275, 2928, 1619, 1593, 1324, 1277, 1158, 1121, 1068 cm^{-1}. **HPLC**: CHIRALPAK IA. Heptane/EtOH-0.2% DEA 90:10, 0.5 mL/min, λ = 210 nm. $t_{(R)}$ = 24.2 min, $t_{(S)}$ = 26.3 min.

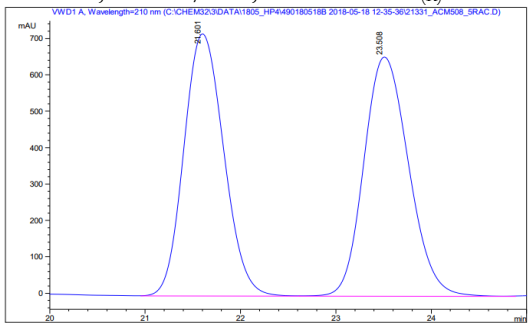

#	Meas. R	Pea	Width	Area	Height	Area %
1	21.601	MF	0.485	20963.480	720.247	49.372
2	23.508	FM	0.545	21497.047	657.386	50.628

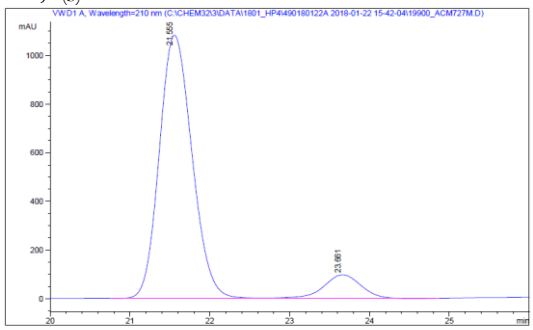

#	Meas. R	Pea	Width	Area	Height	Area %
1	21.555	MF	0.474	30756.965	1.082e3	90.716
2	23.661	FM	0.541	3147.891	96.964	9.284

(*R*)-*N*-(2-(4-bromophenyl)propyl)propane-2-sulfonamide, 8-3k

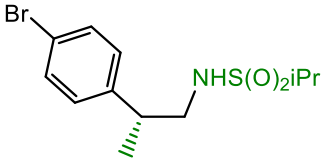

Following the GP, compound **8-3k** was obtained as an off-white solid (quant. by NMR, 87% ee). **m.p.** 95-97 °C. **[α]D**: +11.7 (c 0.1, $CHCl_3$). **^{1}H NMR** (400 MHz, $CDCl_3$) δ 7.50 – 7.41 (m, 2H), 7.15 – 7.06 (m, 2H), 3.87 (t, *J* = 6.5 Hz, 1H), 3.33 (ddd, *J* = 13.1, 7.8, 6.0 Hz, 1H), 3.19 (ddd, *J* = 13.1, 8.5, 5.1 Hz, 1H), 3.06 (p, *J* = 6.8 Hz, 1H), 2.99 – 2.89 (m, 1H), 1.30 (d, *J* = 6.8 Hz, 3H), 1.28 (dd, *J* = 6.9, 2.8 Hz, 6H). **^{13}C NMR** (101 MHz, $CDCl_3$) δ 142.23, 132.12, 129.17, 120.99, 53.71, 50.34, 40.62, 19.06, 16.77, 16.66. **HRMS** (ESI) calculated for $C_{12}H_{19}BrNO_2S$ 320.0314, found 320.0323 $[M+H]^+$. **IR** (ATR-FTIR) ν_{max} = 3288, 2970, 2927, 2360, 2341, 1487, 1311, 1277 cm^{-1}. **HPLC**: CHIRALPAK IC. Heptane/EtOH 95:5, 0.5 mL/min, λ = 210 nm. $t_{(S)}$ = 30.6 min, $t_{(R)}$ = 32.6 min.

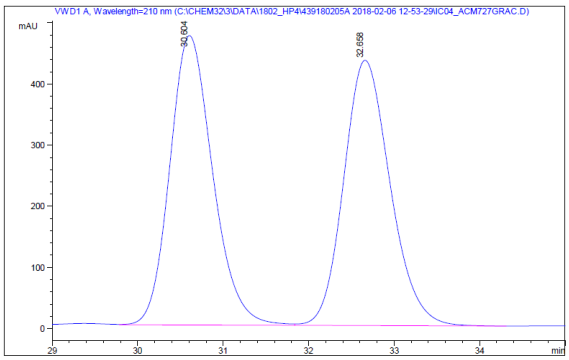

#	Meas. R	Pea	Width	Area	Height	Area %
1	30.604	VV	0.535	16524.609	473.338	50.168
2	32.658	VB	0.583	16414.107	433.963	49.832

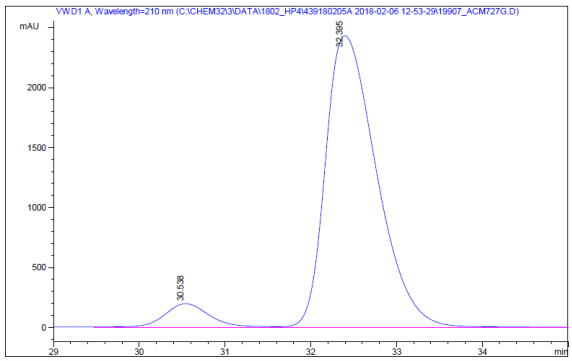

#	Meas. R	Pea	Width	Area	Height	Area %
1	30.538	VV	0.556	7213.232	197.401	6.709
2	32.395	VB	0.637	100296.156	2.431e3	93.291

(*R*)-*N*-(2-(4-iodophenyl)propyl)propane-2-sulfonamide, 8-3l

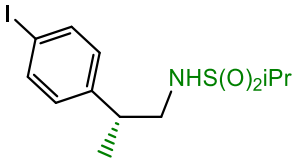

Following the GP, starting from **8-2l** (0.17 mmol) compound **8-3l** was obtained as a white solid (60 mg, 93% isolated yield, 88% ee). The reaction was performed at scale. **m.p.** 93-95 ºC **[α]D**: +20 (c 0.8, $CHCl_3$). **^{1}H NMR** (400 MHz, $CDCl_3$) δ 7.68 – 7.63 (m, 2H), 6.99 – 6.94 (m, 2H), 3.90 (t, *J* = 6.6 Hz, 1H), 3.32 (ddd, *J* = 13.1, 7.7, 6.0 Hz, 1H), 3.18 (ddd, *J* = 13.2, 8.4, 5.1 Hz, 1H), 3.05 (p, *J* = 6.8 Hz, 1H), 2.98 – 2.87 (m, 1H), 1.30 (d, *J* = 6.8 Hz, 3H), 1.27 (dd, *J* = 6.9, 1.4 Hz, 6H). **^{13}C NMR** (101 MHz, $CDCl_3$) δ 142.94, 138.08, 129.47, 92.37, 53.70, 50.29, 40.71, 19.01, 16.77, 16.66. **HRMS** (ESI) calculated for $C_{12}H_{19}INO_2S$ 368.0176, found 368.0183 $[M+H]^+$. **IR** (ATR-FTIR) ν_{max} = 3292, 2967, 1406, 1315. 1215, 1058, 748 cm^{-1}. **HPLC**: CHIRALPAK IA. Heptane/EtOH-0.2% DEA 70:30, 0.5 mL/min, λ = 210 nm. $t_{(R)}$ = 12.5 min, $t_{(S)}$ = 15.4 min.

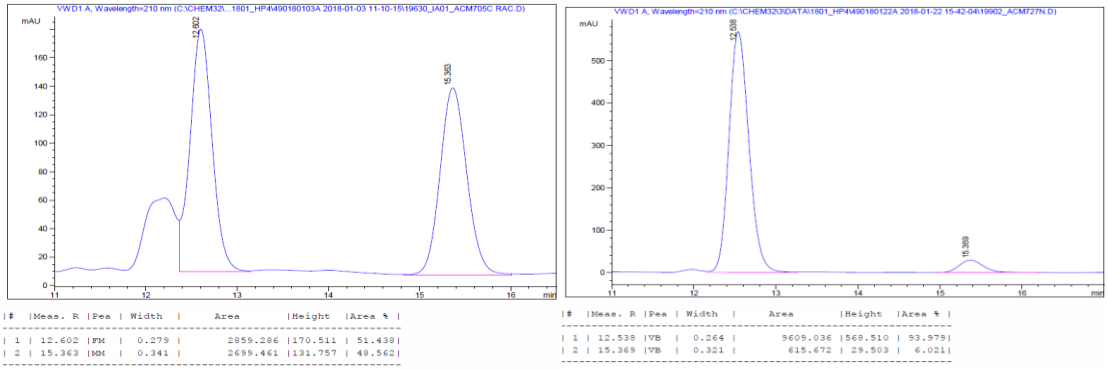

#	Meas. R	Pea	Width	Area	Height	Area %
1	12.602	FM	0.279	2859.286	170.511	51.438
2	15.363	MM	0.341	2699.461	131.757	48.562

#	Meas. R	Pea	Width	Area	Height	Area %
1	12.538	VB	0.264	9609.036	568.510	93.979
2	15.369	VB	0.321	615.672	29.503	6.021

(*R*)-*N*-(2-phenylpropyl)methanesulfonamide, 8-3m

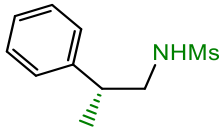

Following the GP, starting from **8-2m** (1.3 mmol), compound **8-3m** was obtained as an oil (268 mg, 96% isolated yield, 92% ee). **[α]D**: +13.2 (c 0.3, $CHCl_3$). **^{1}H NMR** (400 MHz, $CDCl_3$) δ 7.38 – 7.30 (m, 2H), 7.22 (tt, *J* = 5.9, 1.2 Hz, 3H), 4.09 (s, 1H), 3.37 (ddd, *J* = 13.2, 7.8, 5.7 Hz, 1H), 3.27 – 3.19 (m, 1H), 2.98 (dq, *J* = 8.7, 6.8 Hz, 1H), 2.79 (s, 3H), 1.31 (d, *J* = 7.0 Hz, 3H). **HPLC**: CHIRALCEL OJ. Heptane/EtOH-0.2% DEA 70:30, 0.5 mL/min, λ = 210 nm. $t_{(R)}$ = 15.3 min, $t_{(S)}$ = 16.7 min. The analytical data for this compound were in excellent agreement with the reported data. [3]

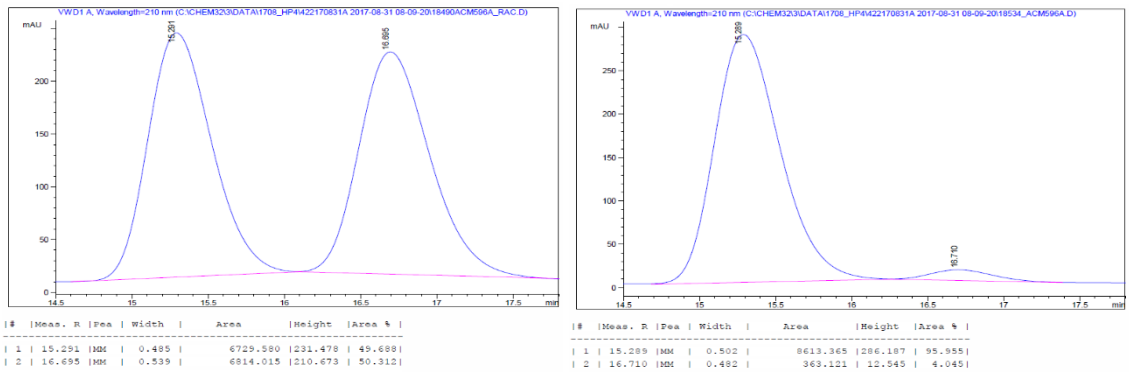

#	Meas. R	Pea	Width	Area	Height	Area %
1	15.291	MM	0.485	6729.580	231.478	49.688
2	16.695	MM	0.539	6814.015	210.673	50.312

#	Meas. R	Pea	Width	Area	Height	Area %
1	15.289	MM	0.502	8613.365	286.187	95.955
2	16.710	MM	0.482	363.121	12.545	4.045

[3] S. Manolov, S. Nikolova, I. Ivanov, *Molecules* **2013**, *18*, 1869.

(*R*)-*N*-(2-(4-isobutylphenyl)propyl)methanesulfonamide, 8-3n

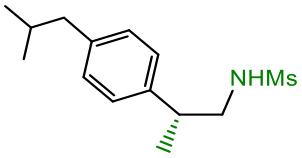

Following the GP, compound **8-3n** was obtained as a white solid (quant. by NMR, 91% ee). **m.p.** 53-55 ºC. **[α]$_D$**: +12.5 (c 0.1, $CHCl_3$). **^{1}H NMR** (400 MHz, $CDCl_3$) δ 7.11 (s, 4H), 4.09 (s, 1H), 3.35 (ddd, *J* = 12.8, 7.7, 5.7 Hz, 1H), 3.22 (ddd, *J* = 12.7, 8.7, 5.0 Hz, 1H), 2.99 – 2.89 (m, 1H), 2.77 (s, 3H), 2.45 (d, *J* = 7.2 Hz, 2H), 1.85 (dt, *J* = 13.5, 6.8 Hz, 1H), 1.30 (d, *J* = 7.0 Hz, 3H), 0.90 (d, *J* = 6.6 Hz, 6H). **^{13}C NMR** (101 MHz, $CDCl_3$) δ 140.81, 140.17, 129.81, 127.09, 50.19, 45.13, 40.43, 40.06, 30.34, 22.52, 19.21. **HRMS** (ESI) calculated for $C_{14}H_{24}NO_2S$ 270.1522, found 270.1522 $[M+H]^+$. **IR** (ATR-FTIR) ν_{max} = 3275, 2955, 2926, 2870, 1451, 1309, 1277, 1136, 1056 cm^{-1}. **HPLC**: CHIRALPAK IC. Heptane/EtOH-0.2% DEA 80:20, 0.5 mL/min, λ = 210 nm. $t_{(S)}$ = 18.0 min, $t_{(R)}$ = 20.0 min.

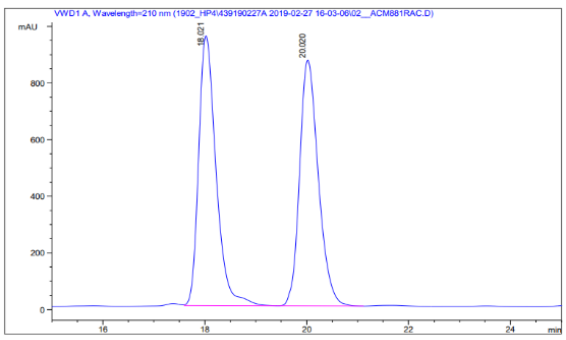

#	Meas. R	Pea	Width	Area	Height	Area %
1	18.021	MF	0.396	22632.143	953.078	50.500
2	20.020	FM	0.426	22184.176	868.275	49.500

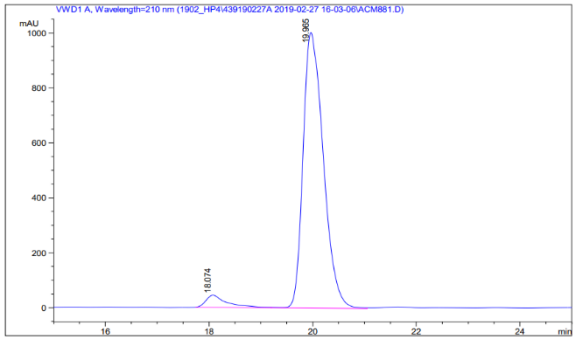

#	Meas. R	Pea	Width	Area	Height	Area %
1	18.074	MF	0.485	1303.854	44.836	4.559
2	19.965	FM	0.453	27294.123	1.004e3	95.441

(*R*)-*N*-methyl-N-(2-phenylpropyl)methanesulfonamide, 8-3o

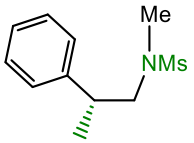

Following the GP, compound **8-3o** was obtained as an oil (quant. by NMR, 94% ee). **[α]$_D$**: +23.0 (c 0.4, $CHCl_3$). **^{1}H NMR** (400 MHz, $CDCl_3$)7.35 – 7.29 (m, 2H), 7.27 – 7.20 (m, 3H), 3.37 – 3.19 (m, 2H), 3.04 (h, *J* = 7.2 Hz, 1H), 2.76 (s, 3H), 2.55 (s, 3H), 1.31 (d, *J* = 7.0 Hz, 3H). **^{13}C NMR** (101 MHz, $CDCl_3$) δ 143.94, 128.78, 127.48, 126.99, 57.30, 39.01, 35.88, 35.18, 18.97. **HRMS** (ESI) calculated for $C_{11}H_{18}NO_2S$ 228.1053, found 228.1056 $[M+H]^+$. **IR** (ATR-FTIR) ν_{max} = 3018, 1326, 1215, 1146, 966, 700 cm^{-1}. **HPLC**: CHIRALCEL OJ. Heptane/EtOH-0.2% DEA 70:30, 0.5 mL/min, λ = 210 nm. $t_{(R)}$ = 24.7 min, $t_{(S)}$ = 30.9 min.

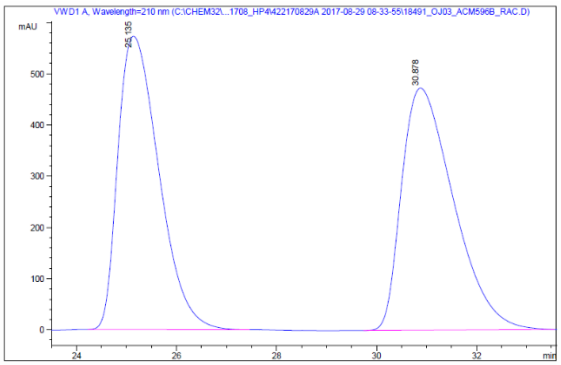

#	Meas. R	Pea	Width	Area	Height	Area %
1	25.135	MM	0.949	32609.719	572.766	48.831
2	30.878	MM	1.205	34171.387	472.603	51.169

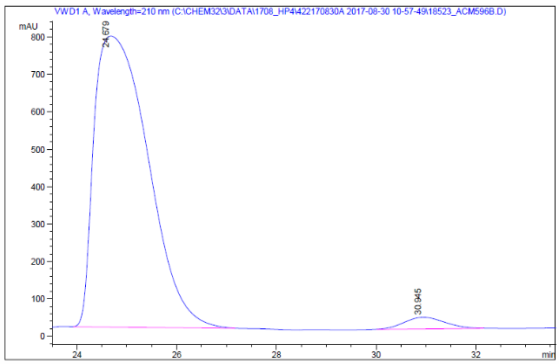

#	Meas. R	Pea	Width	Area	Height	Area %
1	24.679	MM	1.259	58787.285	778.253	97.026
2	30.945	MM	0.956	1801.652	31.418	2.974

(*R*)-*N*,4-dimethyl-N-(2-phenylpropyl)benzenesulfonamide, 8-3p

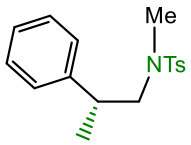

Following the GP, compound **8-3p** was obtained as an oil (quant. by NMR, 94% ee). **[α]$_D$**: +23.5 (c 0.5, $CHCl_3$). **^{1}H NMR** (400 MHz, $CDCl_3$) δ 7.63 – 7.59 (m, 2H), 7.33 – 7.23 (m, 5H), 7.23 – 7.19 (m, 2H), 3.29 (dd, *J* = 13.0, 8.4 Hz, 1H), 3.01 (dq, *J* = 8.5, 6.9 Hz, 1H), 2.91 (dd, *J* = 13.0, 6.6 Hz, 1H), 2.62 (s, 3H), 2.40 (s, 3H), 1.33 (d, *J* = 6.9 Hz, 3H). **^{13}C NMR** (101 MHz, $CDCl_3$) δ 143.99, 143.35, 134.75, 129.74, 128.71, 127.51, 127.42, 126.82, 57.42, 38.85, 35.61, 21.60, 18.95. **IR** (ATR-FTIR) ν_{max} = 3017, 2923, 1338, 1278, 1214, 1160, 700 cm^{-1}. **HRMS** (ESI) calculated for $C_{17}H_{22}NO_2S$ 304.1366, found 304.1367 $[M+H]^+$. **HPLC**: CHIRALCEL OJ. Heptane/EtOH-0.2% DEA 70:30, 0.5 mL/min, λ = 210 nm. $t_{(R)}$ = 20.0 min, $t_{(S)}$ = 24.1 min.

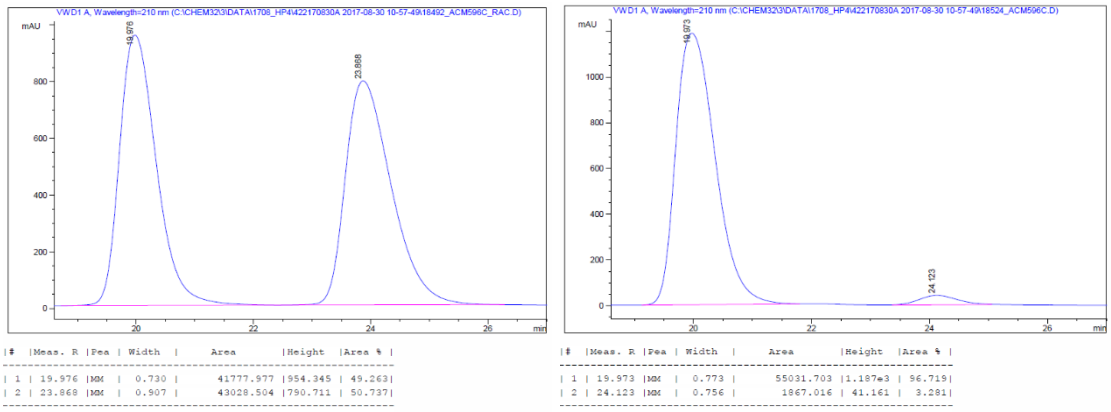

#	Meas. R	Pea	Width	Area	Height	Area %
1	19.976	MM	0.730	41777.977	954.345	49.263
2	23.868	MM	0.907	43028.504	790.711	50.737

#	Meas. R	Pea	Width	Area	Height	Area %
1	19.973	MM	0.773	55031.703	1.187e3	96.719
2	24.123	MM	0.756	1867.016	41.161	3.281

<u>Tosyl deprotection towards the synthesis of potassium channel inhibitor 8-S2.</u>

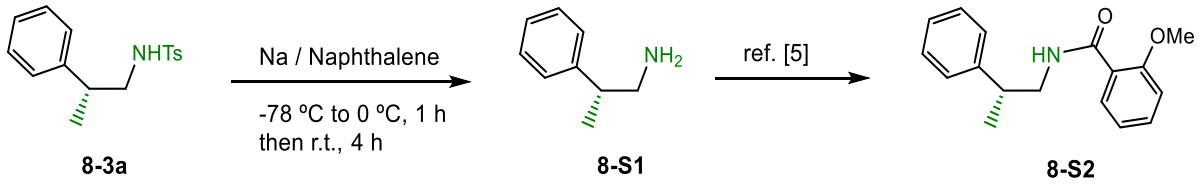

8-3a **8-S1** **8-S2**

Sodium metal (41 mg, 1.8 mmol) was added to room temperature to a solution of naphthalene (118 mg, 0.9 mmol) in THF (2.5 mL). The resulting dark green solution was stirred for 1 hour. Afterwards, this solution was added to a solution of sulfonamide **8-3a** (65 mg, 0.225 mmol) in THF (1.5 mL) at -78 °C. After 10 min, the mixture was cooled down to room temperature and left stirring for 4 hours, until TLC monitoring revealed full consumption of the starting material. Then, H_2O and EtOAc were added. The aqueous layer was separated and extracted with EtOAc (x2). The combined organic layers were washed with brine, dried over $MgSO_4$, filtered and concentrated to obtain a colorless oil **8-S1**. The analytical data for this compound were in excellent agreement with the reported data.[4] The crude can be used as direct precursor of **8-S2** following the experimental procedure described in the literature.[5]

[4] M. Szostak, B. Sautler, M. Spain, D. J. Procter, *Org. Lett.* **2014**, *16* (4), 1902.
[5] J. Zhang, C. Liu, X. Wang, J. Chen, Z. Zhang, W. Zhang, *Chem. Commun.* **2018**, *54*, 6024.

Synthesis of AMPA receptor LY-404187.

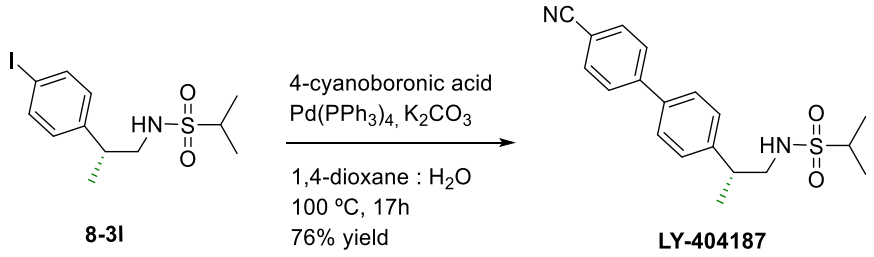

8-3l **LY-404187**

To a degassed solution of **8-2l** (60 mg, 0.17 mmol, 1.0 equiv.), 4-cyanophenylboronic acid (1.1 equiv.) and potassium carbonate (1.1 equiv.) in 1 mL of 75% dioxane/water was added 5 mg of tetrakis(triphenylphosphine)palladium (0) (5 mol%). The mixture was heated to 100 ºC for 16 hours, cooled to ambient temperature, diluted with water and extracted three times with diethyl ether. The combined organic phases were dried (MgSO4), filtered and concentrated in vacuo. Column chromatography (hexanes:EtOAc 60:40) afforded **LY-404187** as a pale yellow solid (44 mg, 76% isolated yield; 85% ee).[6]

m.p. 107-110 ºC **[α]D**: +16.1 (c 0.2, $CHCl_3$). **^{1}H NMR** (400 MHz, $CDCl_3$) δ 7.75 – 7.72 (m, 2H), 7.69 – 7.65 (m, 2H), 7.58 – 7.55 (m, 2H), 7.36 – 7.32 (m, 2H), 3.88 (t, *J* = 6.4 Hz, 1H), 3.39 (ddd, *J* = 13.1, 7.9, 5.9 Hz, 1H), 3.27 (ddd, *J* = 13.1, 8.5, 4.9 Hz, 1H), 3.14 – 2.99 (m, 2H), 1.33 (dd, *J* = 8.8, 6.9 Hz, 6H), 1.29 (d, *J* = 6.8 Hz, 3H). **^{13}C NMR** (101 MHz, $CDCl_3$) δ 145.10, 143.74, 138.00, 132.63, 128.07, 127.72, 127.56, 118.87, 110.95, 53.54, 50.24, 40.64, 19.01, 16.52. **IR** (ATR-FTIR) ν_{max} = 2954, 2919, 2848, 2359, 2341, 1315, 1135 cm^{-1}. **HRMS** (ESI) calculated for $C_{19}H_{26}N_2O_2S$ 343.1475, found 343.1478 $[M+H]^+$. **HPLC**: CHIRALCEL OJ. Heptane/EtOH-0.2% DEA 70:30, 0.5 mL/min, λ = 210 nm. $t_{(R)}$ = 31.1 min, $t_{(S)}$ = 34.3 min.

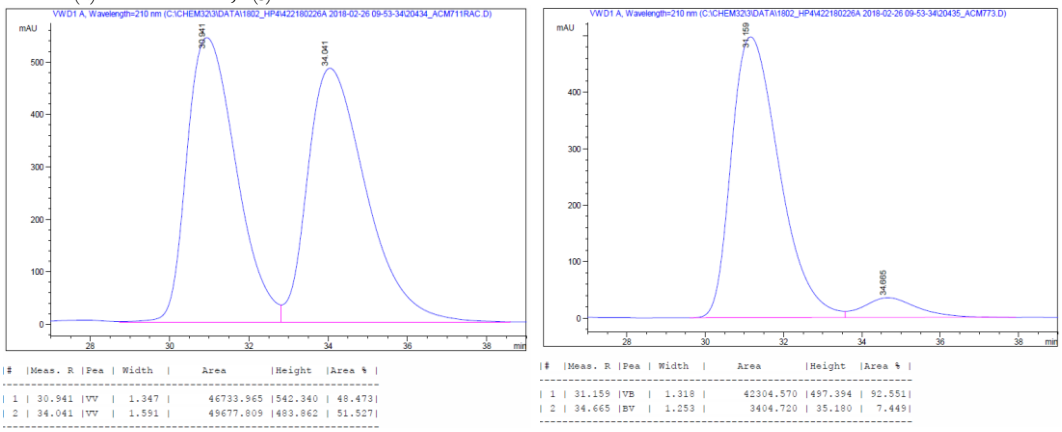

Formal synthesis of *(R)*-Lorcaserin.

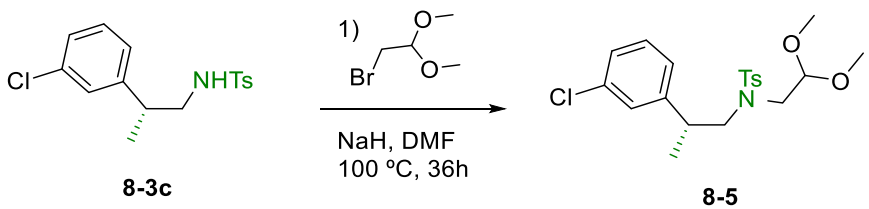

8-3c **8-5**

In a vacuum-dried flask, **8-2c** (238 mg, 0.736 mmol) and bromodimethoxymethane (0.27 ml, 1.5 equiv) were dissolved in anhydrous DMF (2.5 ml). Flask was cooled to 0 ºC followed by slow addition of NaH (80 mg, 2 equiv). Reflux was set, and flask was heated to 110 ºC for 36 hours. Reaction was

[6] Arnold, M. B.; Jones, W. D.; Zimmerman, D. M.. (Eli Lilly Co., USA). N-Substituted Sulfonamide Derivaties. US Patent 6,525,099, February 25, 2003. WO0006537.

quenched with NH_4Cl, H_2O and diluted with ethyl acetate. Organic layer was washed with brine, and water was removed with magnesium sulfate. Product was purified by silica gel column chromatography (hexanes : EtOAc 80:20) to afford **8-5** as a colorless oil (206 mg, 68 % yield).

[α]$_D$: +23.5 (c 1.9, $CHCl_3$). **^{1}H NMR** (400 MHz, $CDCl_3$) δ 7.66 – 7.61 (m, 2H), 7.30 – 7.25 (m, 2H), 7.20 – 7.14 (m, 2H), 7.06 – 7.03 (m, 2H), 4.42 (t, *J* = 5.2 Hz, 1H), 3.47 – 3.40 (m, 1H), 3.36 (s, 3H), 3.33 (s, 3H), 3.22 – 3.02 (m, 4H), 2.41 (s, 3H), 1.24 (d, *J* = 6.8 Hz, 3H). **^{13}C NMR** (101 MHz, $CDCl_3$) δ 146.33, 143.52, 136.77, 134.35, 129.90, 129.80, 127.79, 127.37, 126.84, 125.65, 104.74, 56.64, 55.43, 55.19, 50.91, 38.35, 21.64, 18.75. **IR** (ATR-FTIR) ν_{max} = 2367, 2336, 1339, 1157 cm^{-1}. **HRMS** (ESI) calculated for $C_{20}H_{24}ClNNaO_4S$ 432.1007, found 432.1001 $[M+Na]^+$.

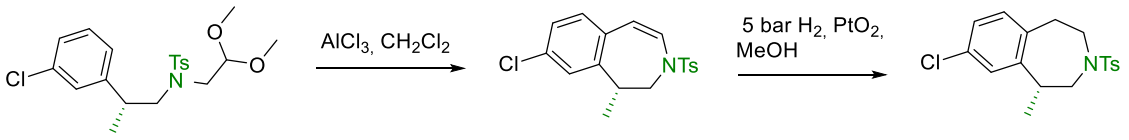

8-5 **8-S2** **8-6**

A solution of **8-5** (93 mg, 0.226 mmol) in dichloromethane (1.2 mL) was added to a suspension of $AlCl_3$ (110 mg, 4 equiv) in dichloromethane (1.8 mL) under nitrogen atmosphere. The reaction was stirred for 15 min at room temperature and then was cooled to 0 ºC. After quenching with 1M NaOH and H_2O, the phases were separated. The aqueous phase was extracted with CH_2Cl_2 (x3). The combined organic phases were dried over $MgSO_4$, filtered and solvent was removed by evaporation. The crude **8-S2** was used in the following step without further purification.

^{1}H NMR (400 MHz, $CDCl_3$) δ 7.73 – 7.69 (m, 2H), 7.33 – 7.29 (m, 2H), 7.10 (dd, *J* = 8.2, 2.2 Hz, 1H), 7.06 – 7.02 (m, 2H), 6.90 – 6.86 (m, 1H), 5.54 (d, *J* = 10.5 Hz, 1H), 4.05 (ddd, *J* = 13.1, 6.5, 1.7 Hz, 1H), 3.19 – 3.09 (m, 2H), 2.41 (s, 3H), 1.16 (d, *J* = 7.2 Hz, 3H).

8-S2 was dissolved in methanol (1 mL) and PtO_2 (8 mg) and few drops of HCl were added. The reaction mixture was stirred at room temperature in a pressure reactor, under 5 bar of hydrogen for 36 hours. After filtration through Celite® pad, the solvent was removed by evaporation under reduced pressure. The residue was dissolved in ethyl acetate, washed with water, dried over magnesium, filtered and evaporated to dryness. After purification by flash chromatography (hexanes : EtOAc, 85:15), the desired product **8-6** was afforded as sticky solid (56 mg, 71% yield; 87% ee).

[α]$_D$: +4.7 (c 0.4, $CHCl_3$) [reported for commercialized enantiopure (*R*)-Lorcaserin: [[α]$_D$: +17-24 (c 1.0, H_2O)]. **^{1}H NMR** (400 MHz, $CDCl_3$) δ 7.63 – 7.59 (m, 2H), 7.28 – 7.24 (m, 2H), 7.09 – 7.04 (m, 2H), 6.96 (d, *J* = 7.9 Hz, 1H), 3.36 – 3.15 (m, 4H), 3.14 – 3.04 (m, 2H), 2.97 – 2.90 (m, 1H), 2.39 (s, 3H), 1.39 (d, *J* = 7.1 Hz, 3H). **^{13}C NMR** (101 MHz, $CDCl_3$) δ 146.05, 143.29, 137.75, 135.35, 132.41, 131.31, 129.65, 127.08, 126.33, 53.51, 48.11, 39.99, 35.91, 21.45, 17.53. **IR** (ATR-FTIR) ν_{max} = 2952, 2920, 2848, 2249, 1163 cm^{-1}. **HRMS** (ESI) calculated for $C_{18}H_{21}ClNO_2S$ 350.0976, found 350.0969 $[M+H]^+$. **HPLC**: CHIRALCEL OJ. Heptane/EtOH 70:30, 0.5 mL/min, λ = 210 nm. $t_{(S)}$ = 18.0 min, $t_{(R)}$ = 24.1 min.

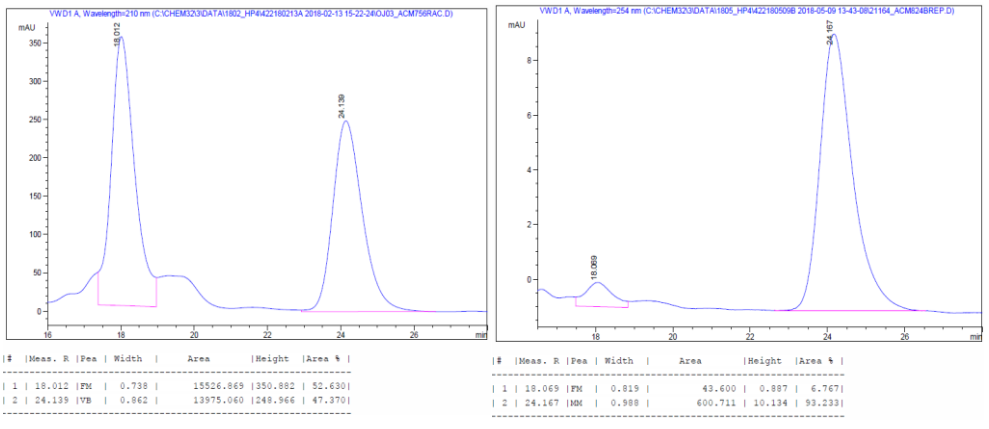

^{1}H NMR and ^{13}C NMR spectra

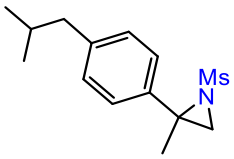

8-1n

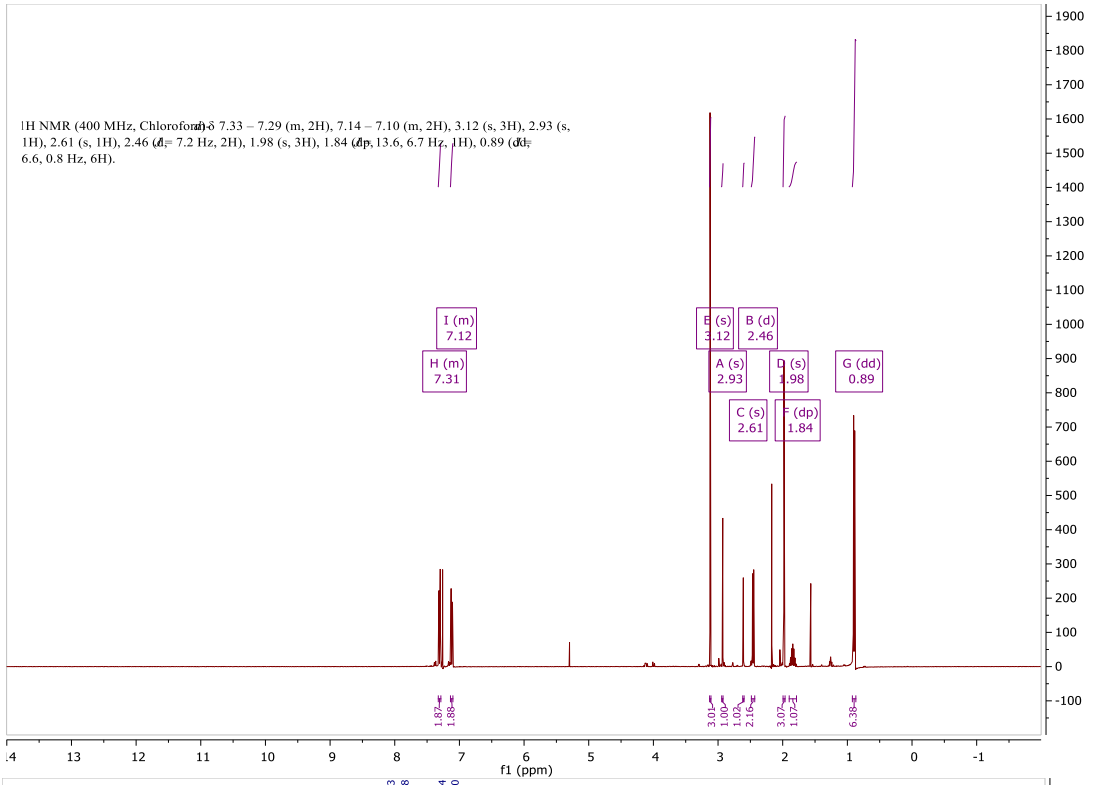

^{1}H NMR (400 MHz, Chloroform-d) δ 7.33 – 7.29 (m, 2H), 7.14 – 7.10 (m, 2H), 3.12 (s, 3H), 2.93 (s, 1H), 2.61 (s, 1H), 2.46 (d, J = 7.2 Hz, 2H), 1.98 (s, 3H), 1.84 (dp, J = 13.6, 6.7 Hz, 1H), 0.89 (dd, J = 6.6, 0.8 Hz, 6H).

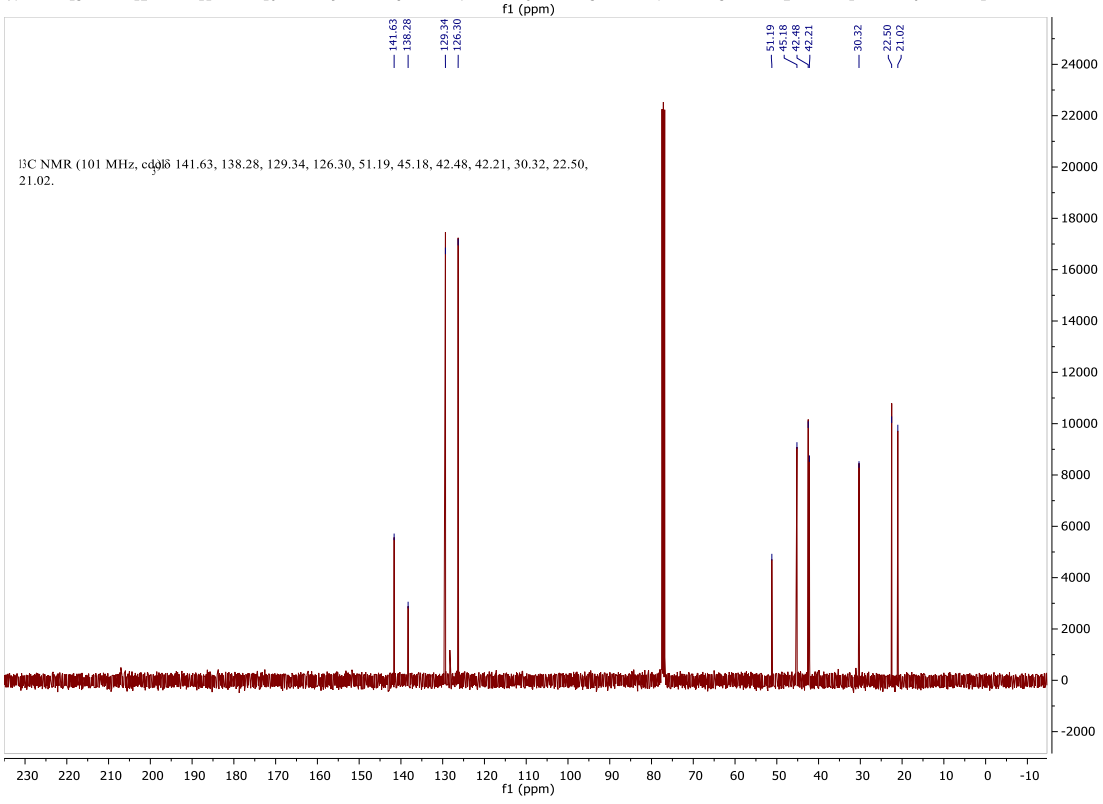

^{13}C NMR (101 MHz, cdcl$_3$) δ 141.63, 138.28, 129.34, 126.30, 51.19, 45.18, 42.48, 42.21, 30.32, 22.50, 21.02.

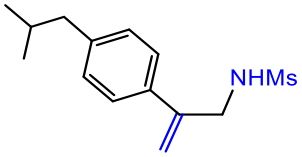

8-2n

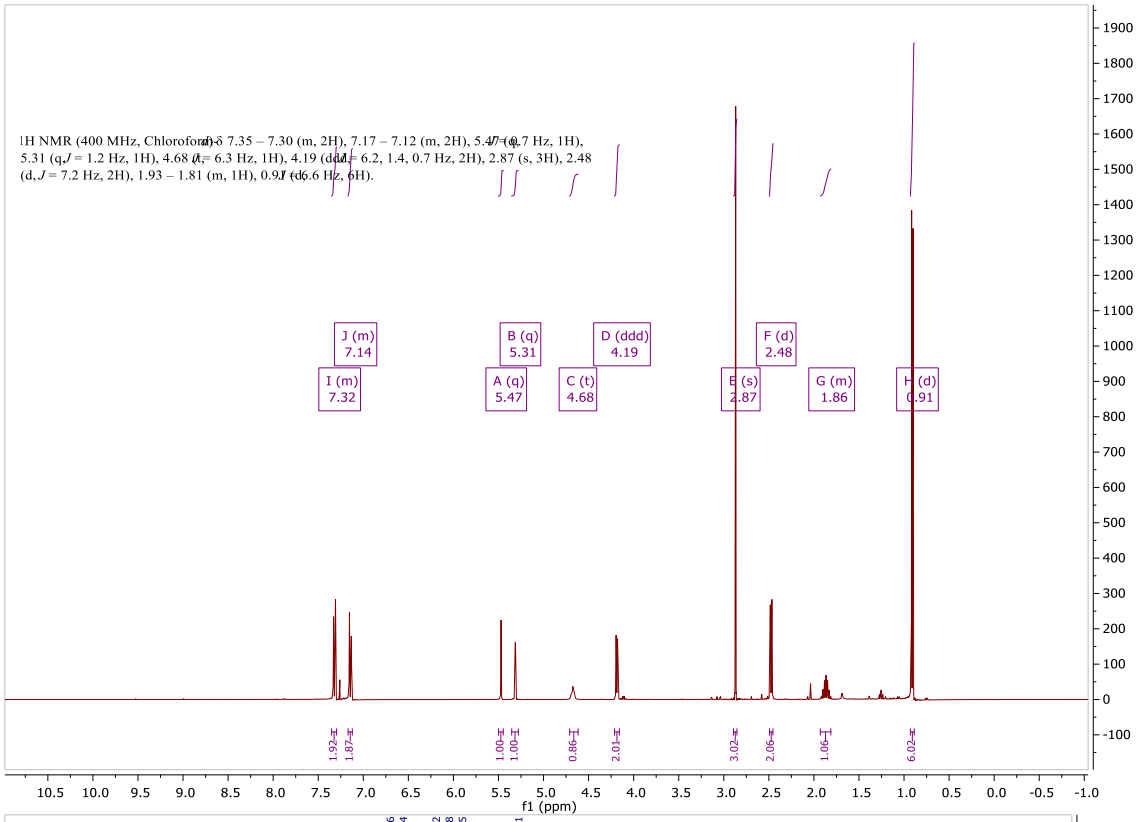

^{1}H NMR (400 MHz, Chloroform-*d*) δ 7.35 – 7.30 (m, 2H), 7.17 – 7.12 (m, 2H), 5.47 (q, *J* = 1.7 Hz, 1H), 5.31 (q, *J* = 1.2 Hz, 1H), 4.68 (t, *J* = 6.3 Hz, 1H), 4.19 (ddd, *J* = 6.2, 1.4, 0.7 Hz, 2H), 2.87 (s, 3H), 2.48 (d, *J* = 7.2 Hz, 2H), 1.93 – 1.81 (m, 1H), 0.91 (d, *J* = 6.6 Hz, 6H).

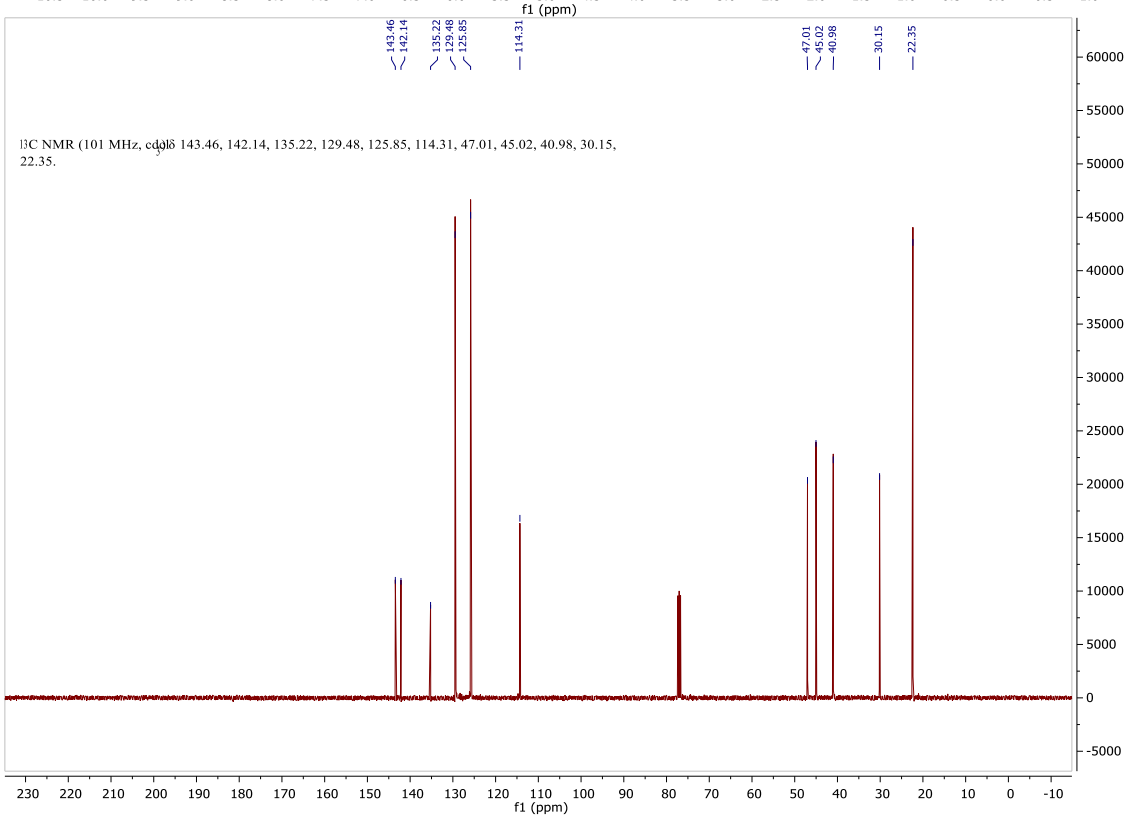

^{13}C NMR (101 MHz, cdcl$_3$) δ 143.46, 142.14, 135.22, 129.48, 125.85, 114.31, 47.01, 45.02, 40.98, 30.15, 22.35.

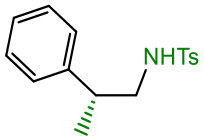
NHTs

8-3a

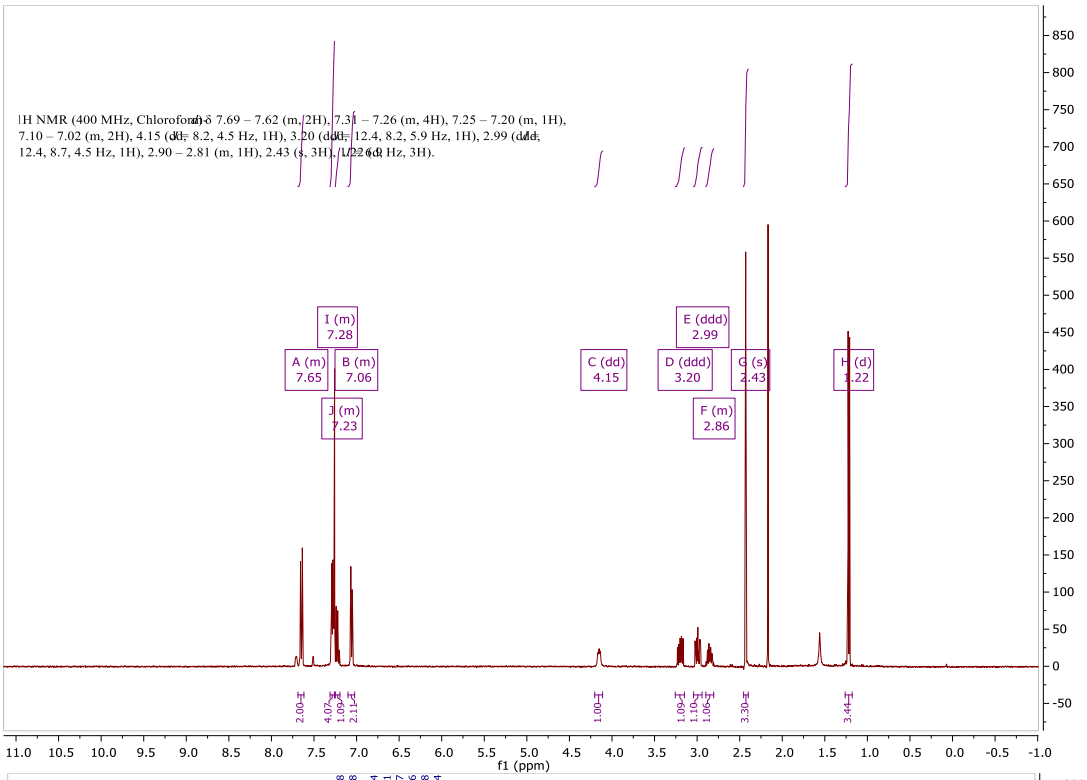
I (m)
7.28
A (m)
7.65
B (m)
7.06
J (m)
7.23
C (dd)
4.15
E (ddd)
2.99
D (ddd)
3.20
F (m)
2.86
G (s)
2.43
H (d)
1.22
2.00
4.07
1.09
2.11
1.00
1.09
1.10
1.06
3.30
3.44
f1 (ppm)

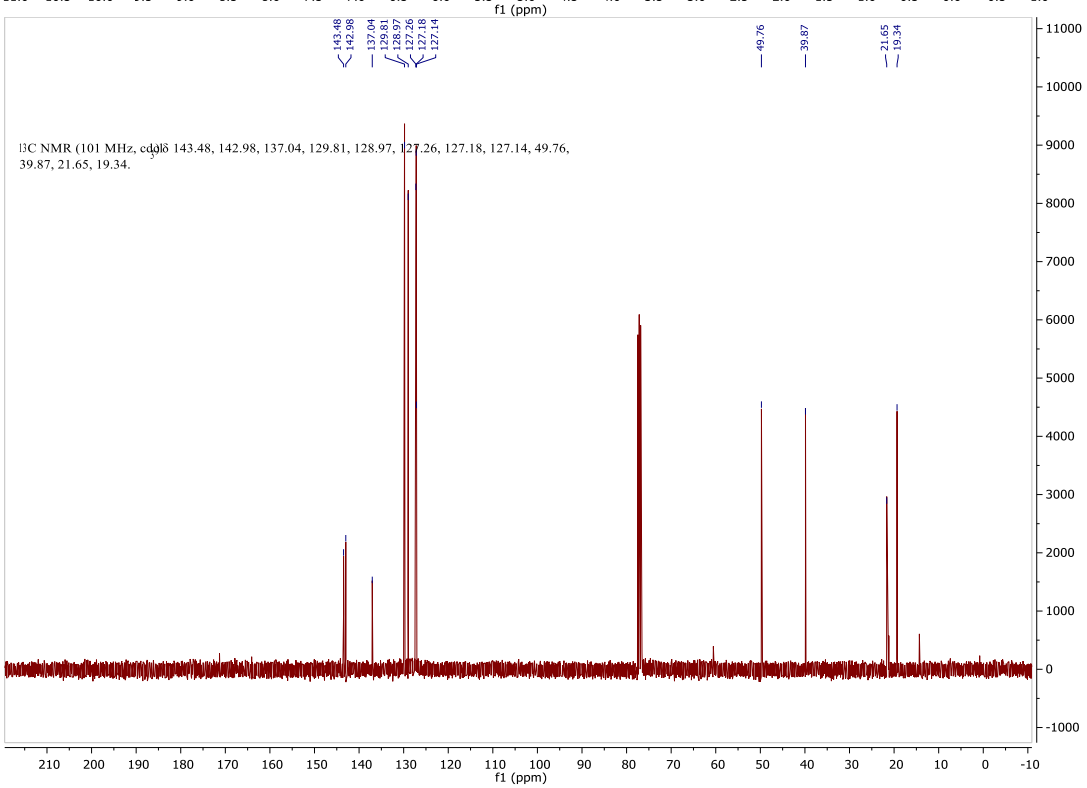
143.48
142.98
137.04
129.81
128.97
127.26
127.18
127.14
49.76
39.87
21.65
19.34
f1 (ppm)

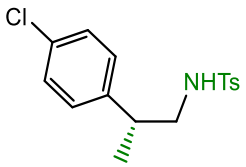

8-3b

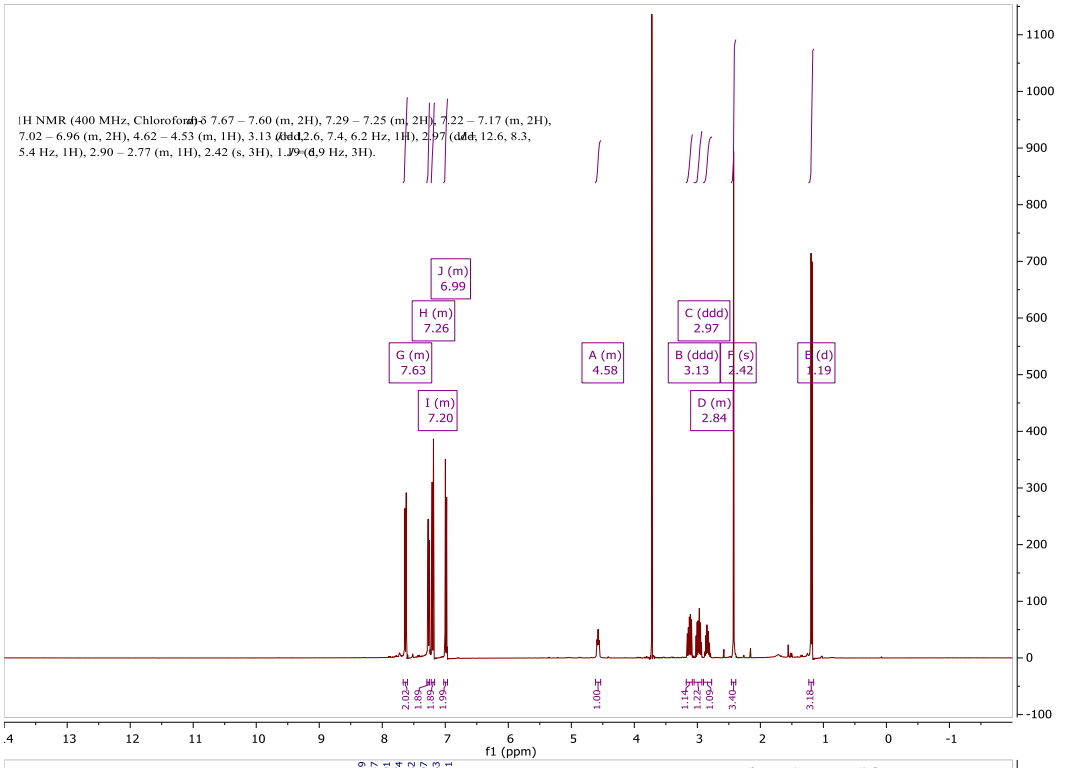

^{1}H NMR (400 MHz, Chloroform-d) δ 7.67 – 7.60 (m, 2H), 7.29 – 7.25 (m, 2H), 7.22 – 7.17 (m, 2H), 7.02 – 6.96 (m, 2H), 4.62 – 4.53 (m, 1H), 3.13 (ddd, J = 12.6, 7.4, 6.2 Hz, 1H), 2.97 (ddd, J = 12.6, 8.3, 5.4 Hz, 1H), 2.90 – 2.77 (m, 1H), 2.42 (s, 3H), 1.19 (d, J = 6.9 Hz, 3H).

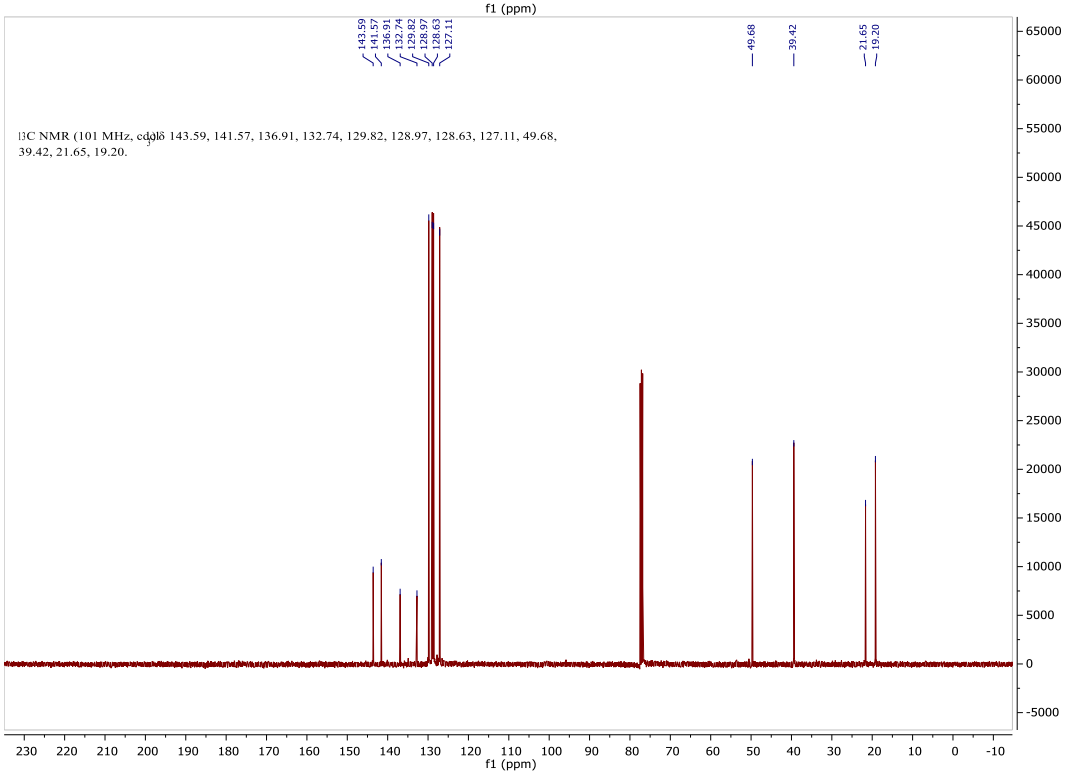

^{13}C NMR (101 MHz, cdcl$_3$) δ 143.59, 141.57, 136.91, 132.74, 129.82, 128.97, 128.63, 127.11, 49.68, 39.42, 21.65, 19.20.

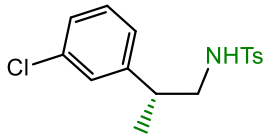

8-3c

^{1}H NMR (400 MHz, Chloroform-*d*) δ 7.68 – 7.62 (m, 2H), 7.31 – 7.25 (m, 2H), 7.20 (ddd, *J* = 8.4, 2.2 Hz, 2H), 6.97 (dd, *J* = 8.4, 2.2 Hz, 2H), 4.29 (t, *J* = 6.6 Hz, 1H), 3.18 (ddd, *J* = 12.7, 7.9, 6.0 Hz, 1H), 2.99 (ddd, *J* = 13.0, 8.5, 5.0 Hz, 1H), 2.84 (dt, *J* = 8.4, 6.5 Hz, 1H), 2.43 (s, 3H), 1.20 (d, *J* = 6.9 Hz, 3H).

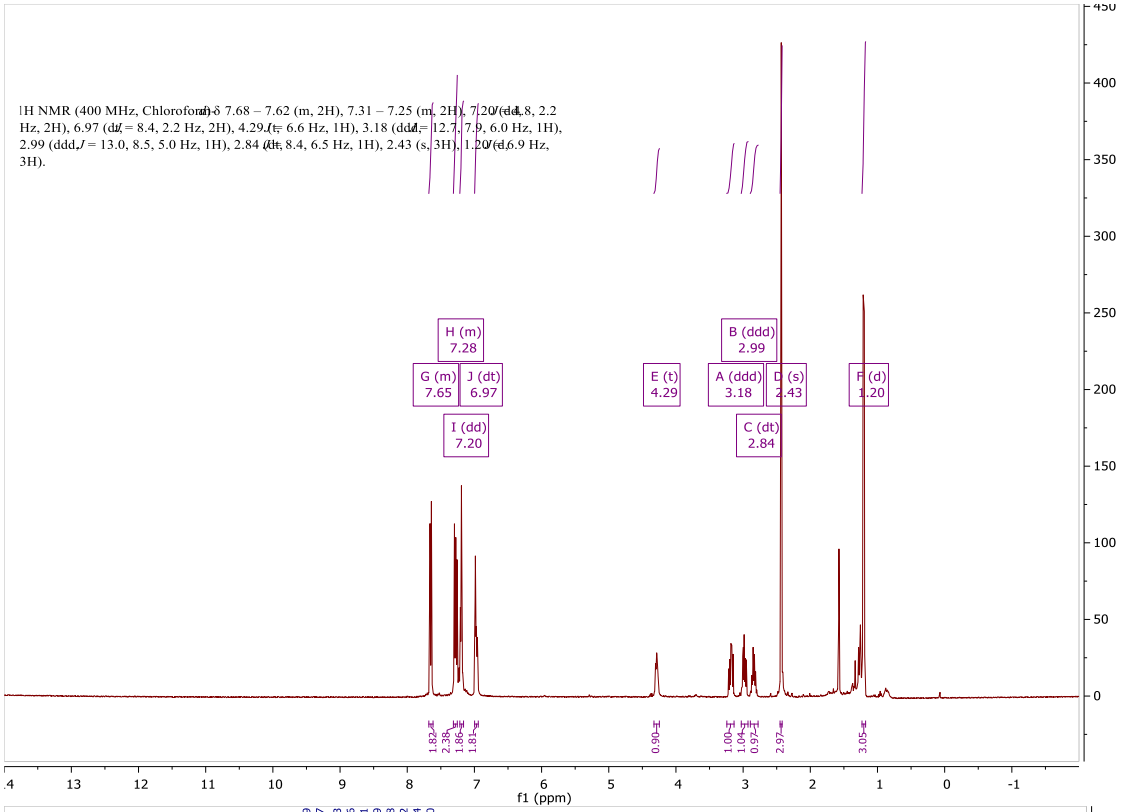

^{13}C NMR (101 MHz, cdcl) δ 145.19, 143.67, 136.93, 134.76, 130.21, 129.89, 127.38, 127.32, 127.14, 125.60, 49.58, 39.79, 21.68, 19.20.

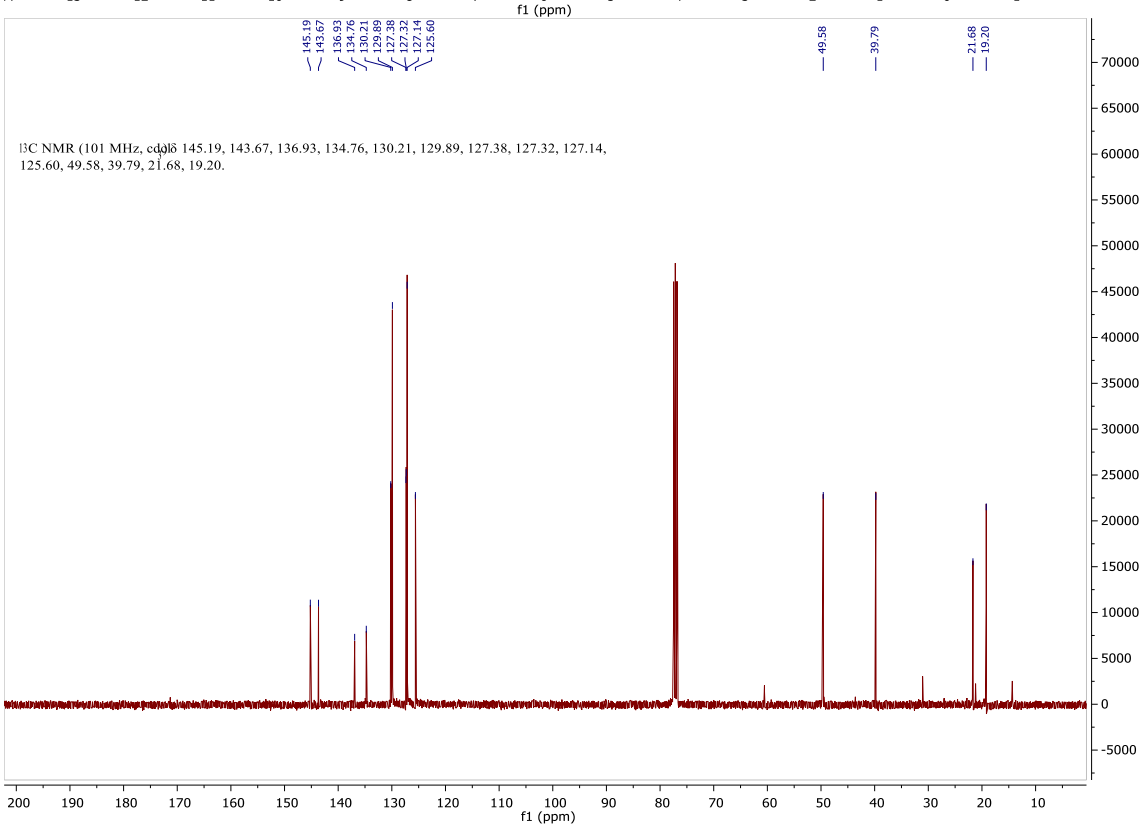

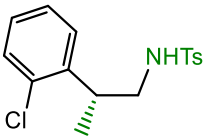
NHTs
Cl

8-3d

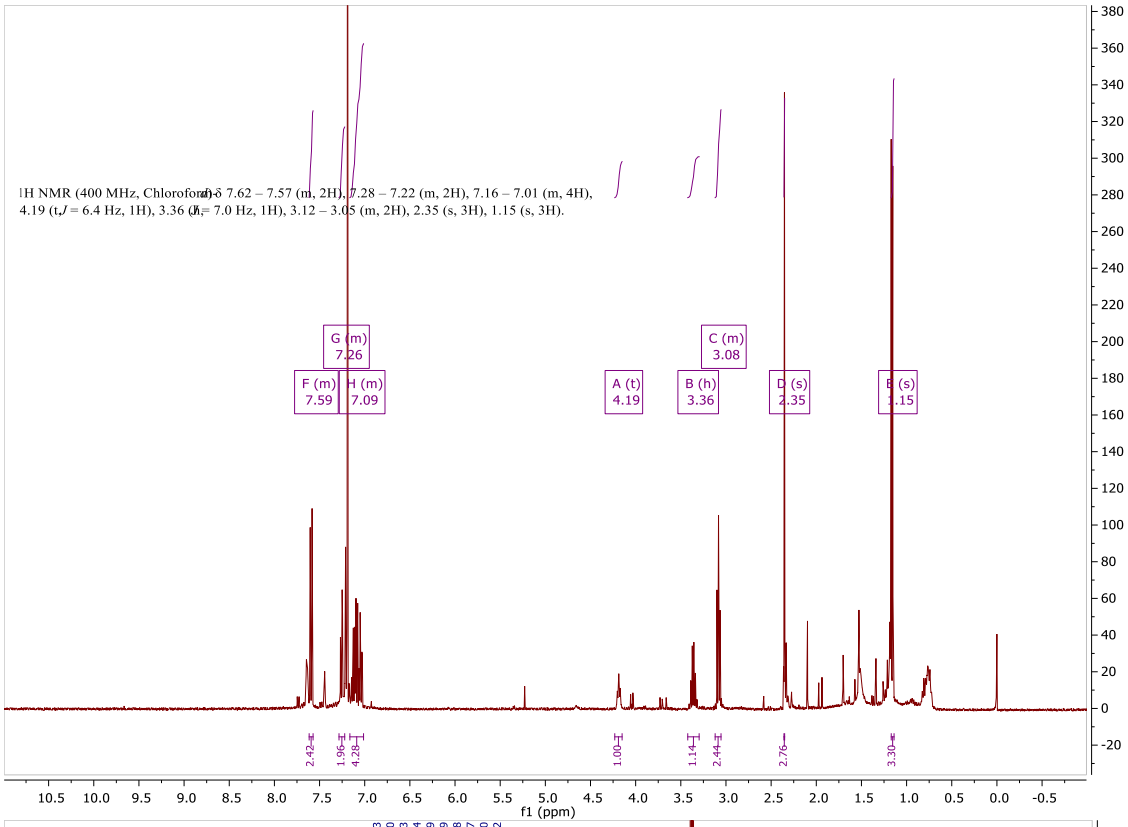
1H NMR (400 MHz, Chloroform-d) δ 7.62 – 7.57 (m, 2H), 7.28 – 7.22 (m, 2H), 7.16 – 7.01 (m, 4H), 4.19 (t, J = 6.4 Hz, 1H), 3.36 (d, J = 7.0 Hz, 1H), 3.12 – 3.05 (m, 2H), 2.35 (s, 3H), 1.15 (s, 3H).
G (m) 7.26
F (m) 7.59
H (m) 7.09
A (t) 4.19
C (m) 3.08
B (h) 3.36
D (s) 2.35
E (s) 1.15
2.42
1.96
4.28
1.00
1.14
2.44
2.76
3.30
f1 (ppm)

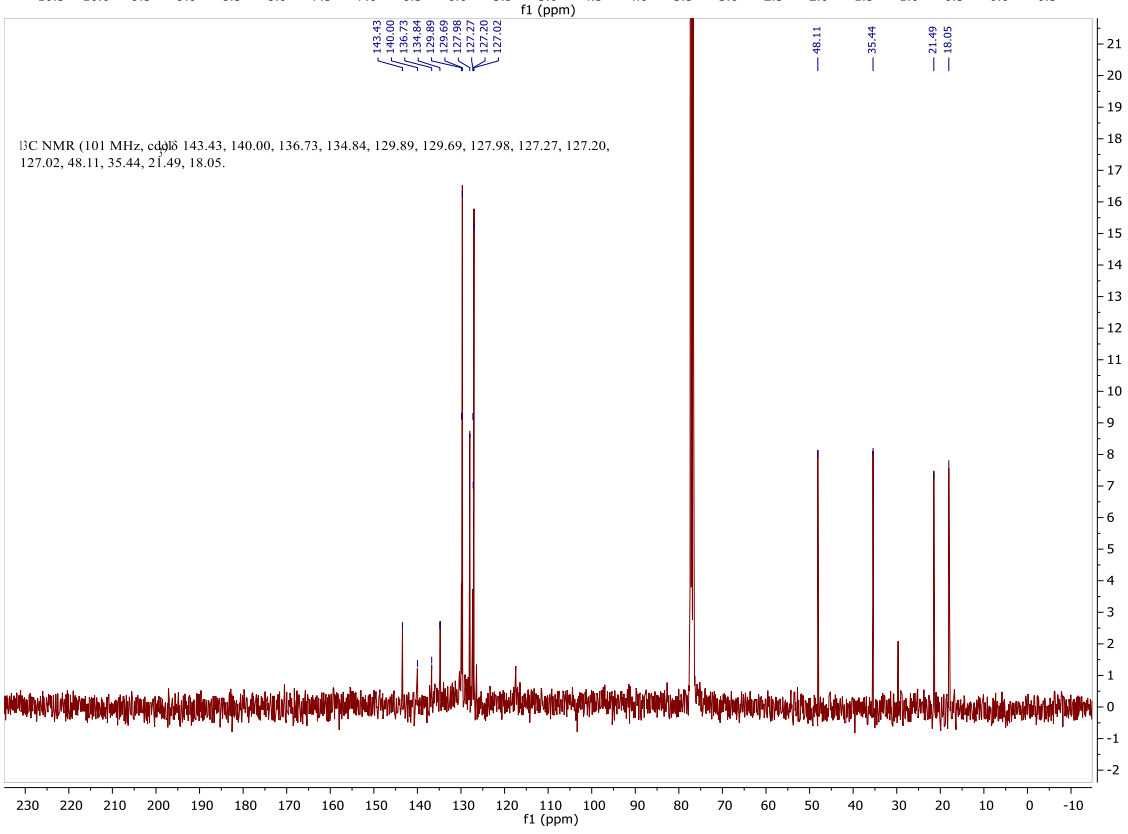
13C NMR (101 MHz, cdcl3) δ 143.43, 140.00, 136.73, 134.84, 129.89, 129.69, 127.98, 127.27, 127.20, 127.02, 48.11, 35.44, 21.49, 18.05.
143.43
140.00
136.73
134.84
129.89
129.69
127.98
127.27
127.20
127.02
48.11
35.44
21.49
18.05
f1 (ppm)

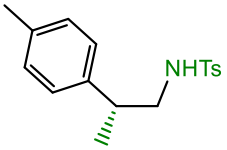
NHTs

8-3e

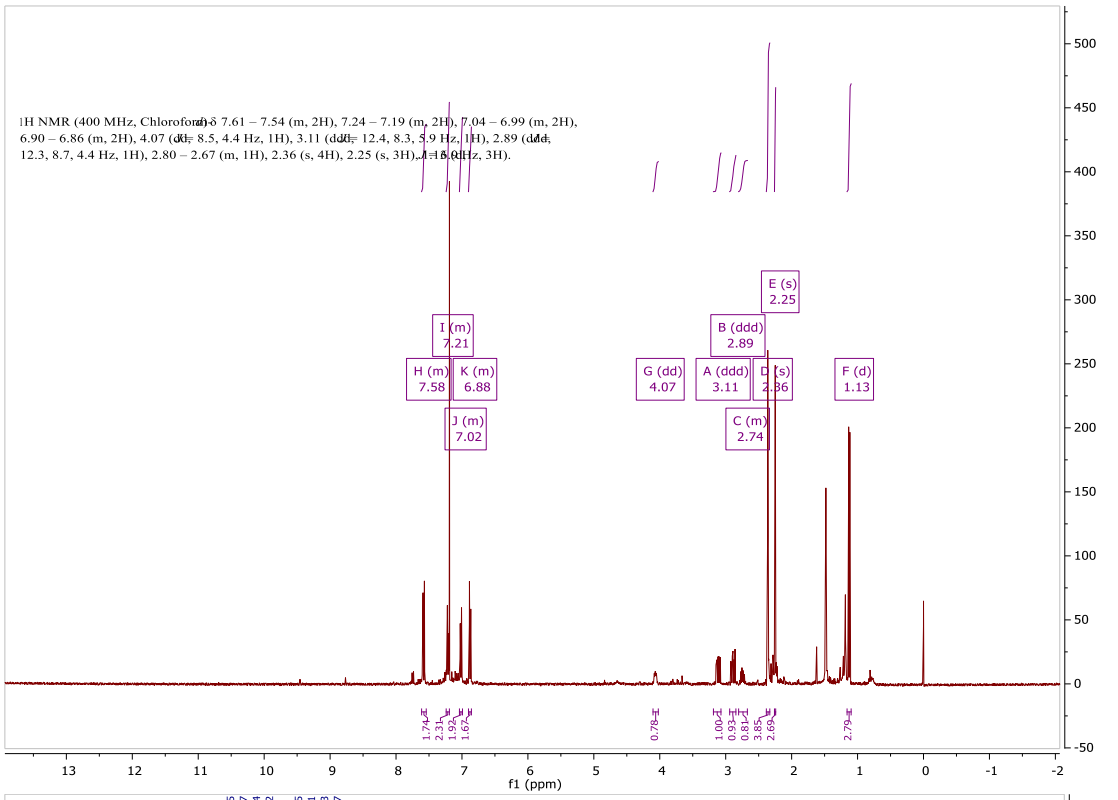
1H NMR (400 MHz, Chloroform-d) δ 7.61 – 7.54 (m, 2H), 7.24 – 7.19 (m, 2H), 7.04 – 6.99 (m, 2H), 6.90 – 6.86 (m, 2H), 4.07 (dd, J = 8.5, 4.4 Hz, 1H), 3.11 (ddd, J = 12.4, 8.3, 5.9 Hz, 1H), 2.89 (ddd, J = 12.3, 8.7, 4.4 Hz, 1H), 2.80 – 2.67 (m, 1H), 2.36 (s, 4H), 2.25 (s, 3H), 1.13 (d, J = 6.9 Hz, 3H).
I (m) 7.21
H (m) 7.58
K (m) 6.88
J (m) 7.02
G (dd) 4.07
B (ddd) 2.89
A (ddd) 3.11
E (s) 2.25
D (s) 2.36
C (m) 2.74
F (d) 1.13
f1 (ppm)

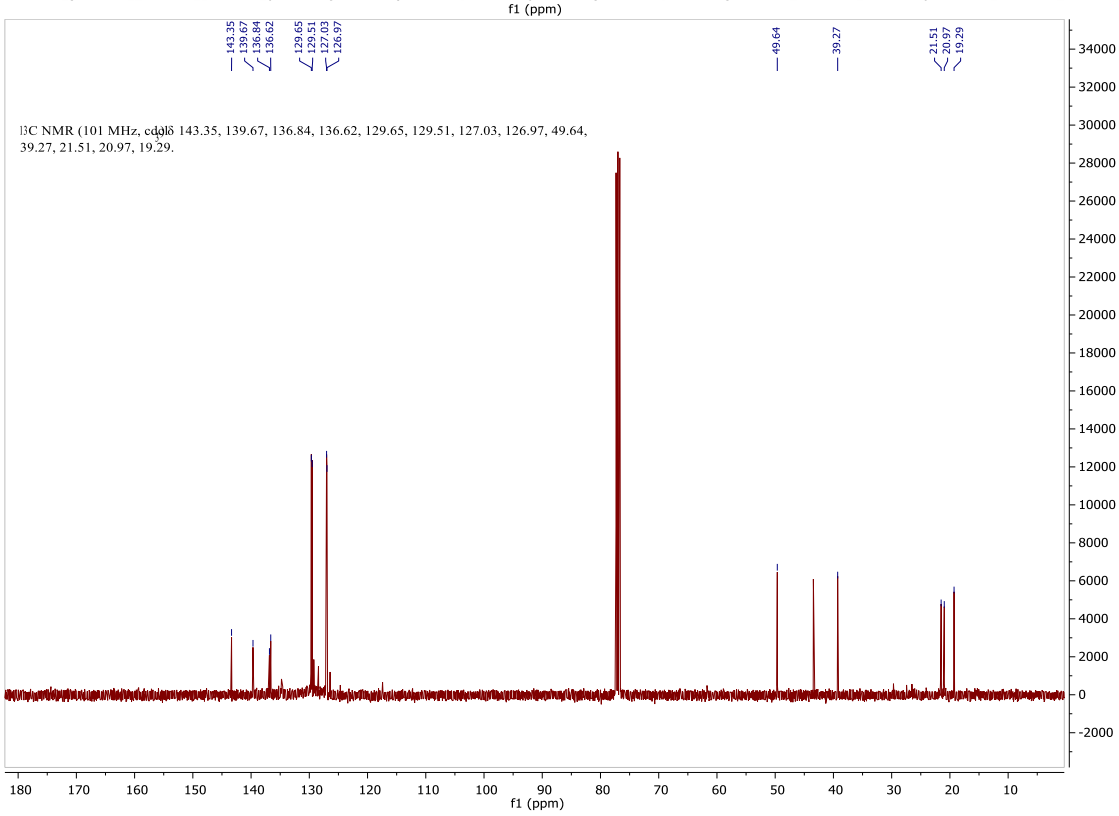
143.35
139.67
136.84
136.62
129.65
129.51
127.03
126.97
49.64
39.27
21.51
20.97
19.29
13C NMR (101 MHz, cdcl3) δ 143.35, 139.67, 136.84, 136.62, 129.65, 129.51, 127.03, 126.97, 49.64, 39.27, 21.51, 20.97, 19.29.
f1 (ppm)

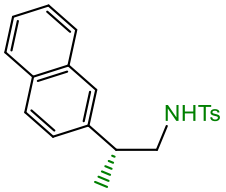
NHTs

8-3f

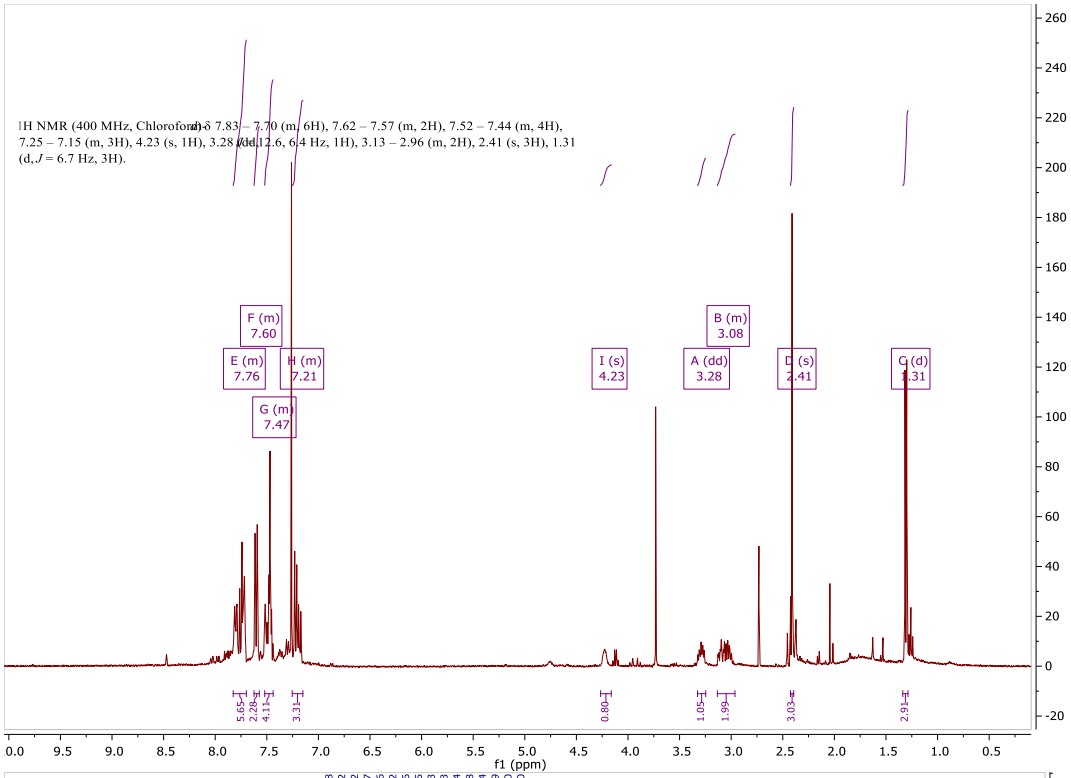
1H NMR (400 MHz, Chloroform-d) δ 7.83 – 7.70 (m, 6H), 7.62 – 7.57 (m, 2H), 7.52 – 7.44 (m, 4H), 7.25 – 7.15 (m, 3H), 4.23 (s, 1H), 3.28 (dd, J = 12.6, 6.4 Hz, 1H), 3.13 – 2.96 (m, 2H), 2.41 (s, 3H), 1.31 (d, J = 6.7 Hz, 3H).
F (m) 7.60
E (m) 7.76
H (m) 7.21
G (m) 7.47
I (s) 4.23
B (m) 3.08
A (dd) 3.28
D (s) 2.41
C (d) 1.31
f1 (ppm)

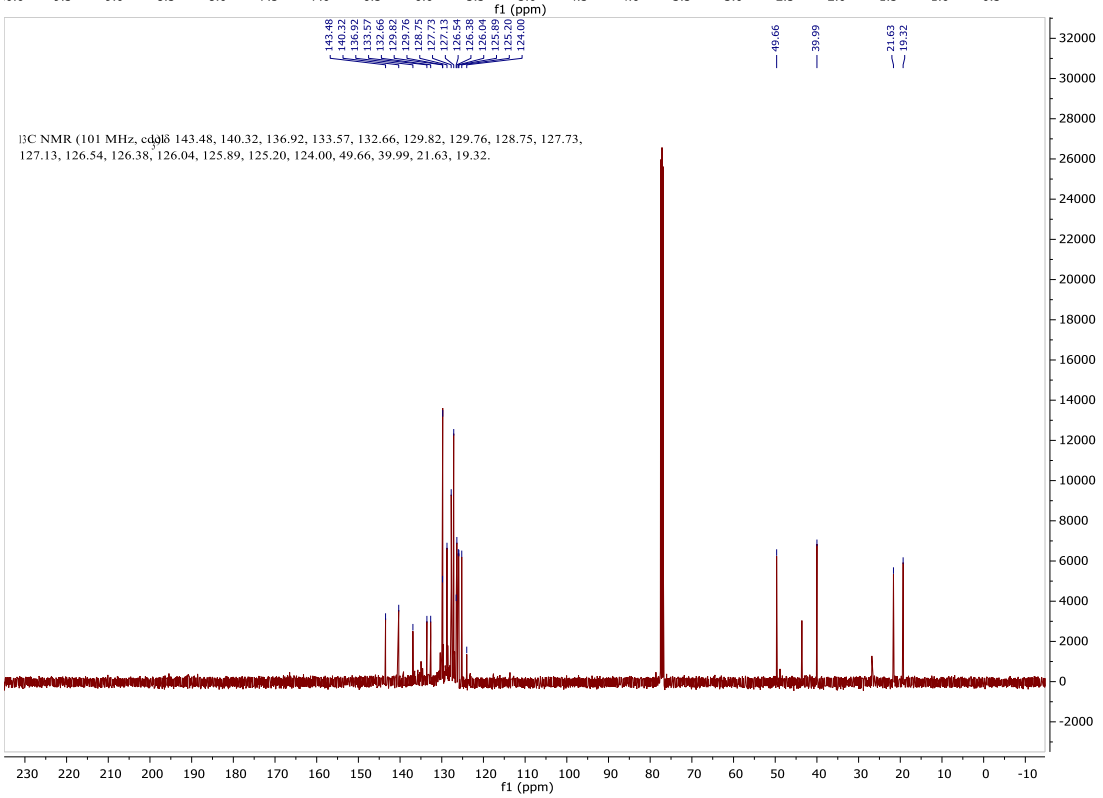
13C NMR (101 MHz, cdcl3) δ 143.48, 140.32, 136.92, 133.57, 132.66, 129.82, 129.76, 128.75, 127.73, 127.13, 126.54, 126.38, 126.04, 125.89, 125.20, 124.00, 49.66, 39.99, 21.63, 19.32.
f1 (ppm)

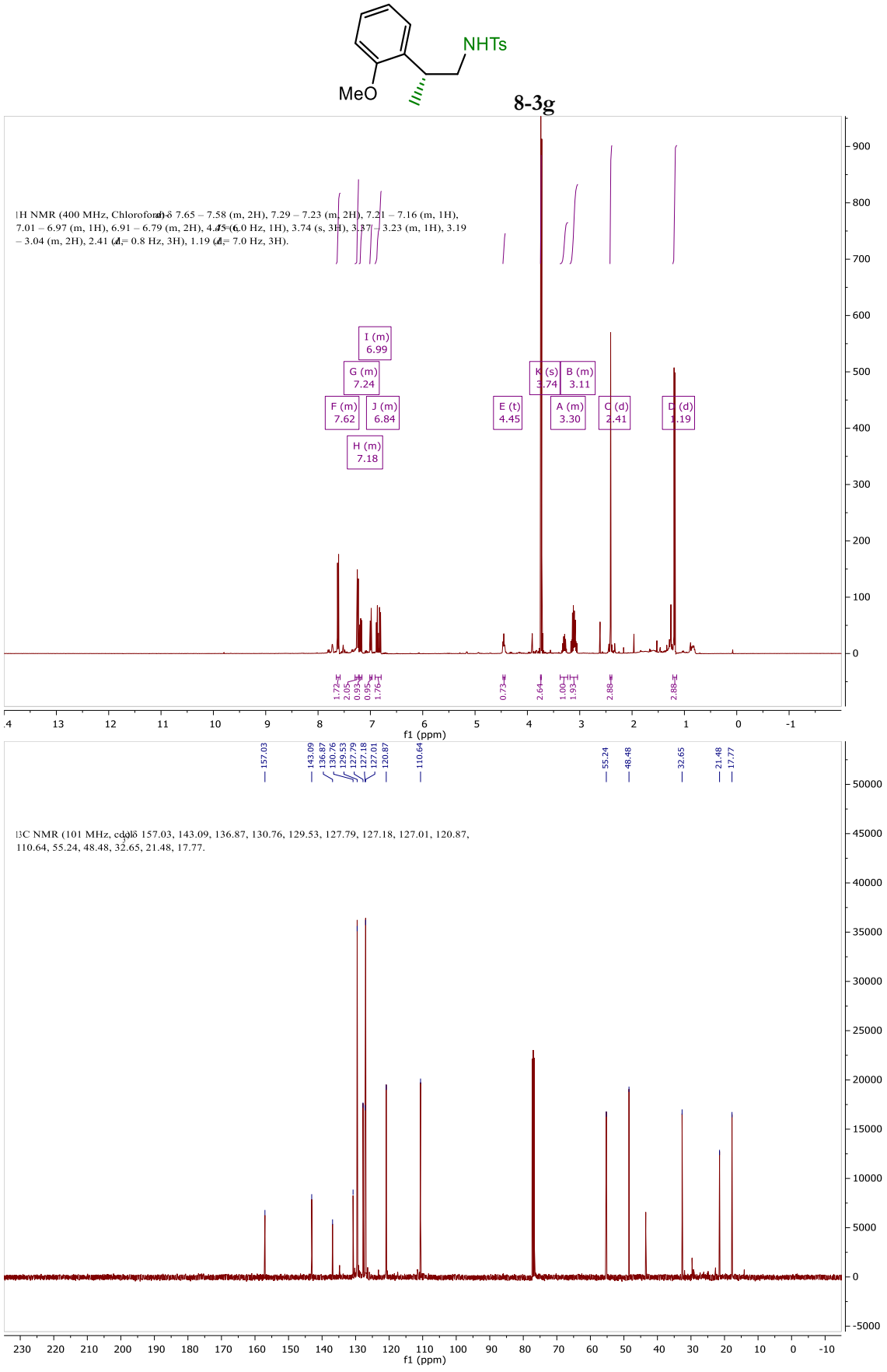
NHTs
MeO
8-3g
¹H NMR (400 MHz, Chloroform-d) δ 7.65 – 7.58 (m, 2H), 7.29 – 7.23 (m, 2H), 7.21 – 7.16 (m, 1H), 7.01 – 6.97 (m, 1H), 6.91 – 6.79 (m, 2H), 4.45 (t, J = 6.0 Hz, 1H), 3.74 (s, 3H), 3.37 – 3.23 (m, 1H), 3.19 – 3.04 (m, 2H), 2.41 (d, J = 0.8 Hz, 3H), 1.19 (d, J = 7.0 Hz, 3H).
I (m) 6.99
G (m) 7.24
F (m) 7.62
J (m) 6.84
H (m) 7.18
E (t) 4.45
K (s) 3.74
B (m) 3.11
A (m) 3.30
C (d) 2.41
D (d) 1.19
f1 (ppm)
¹³C NMR (101 MHz, cdcl3) δ 157.03, 143.09, 136.87, 130.76, 129.53, 127.79, 127.18, 127.01, 120.87, 110.64, 55.24, 48.48, 32.65, 21.48, 17.77.
f1 (ppm)

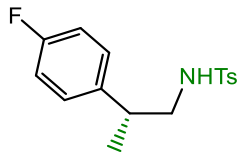

8-3h

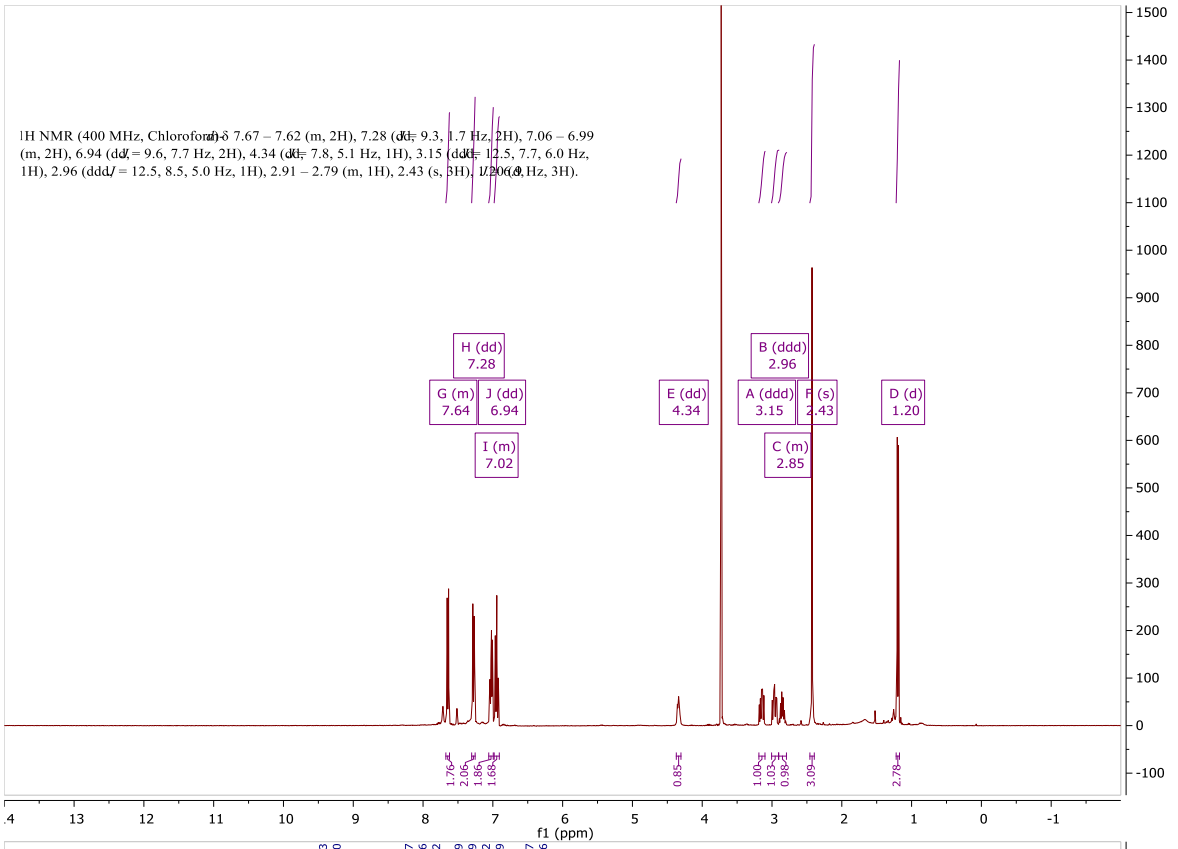

^{1}H NMR (400 MHz, Chloroform-*d*) δ 7.67 – 7.62 (m, 2H), 7.28 (dd, *J* = 9.3, 1.7 Hz, 2H), 7.06 – 6.99 (m, 2H), 6.94 (dd, *J* = 9.6, 7.7 Hz, 2H), 4.34 (dd, *J* = 7.8, 5.1 Hz, 1H), 3.15 (ddd, *J* = 12.5, 7.7, 6.0 Hz, 1H), 2.96 (ddd, *J* = 12.5, 8.5, 5.0 Hz, 1H), 2.91 – 2.79 (m, 1H), 2.43 (s, 3H), 1.20 (d, *J* = 6.9 Hz, 3H).

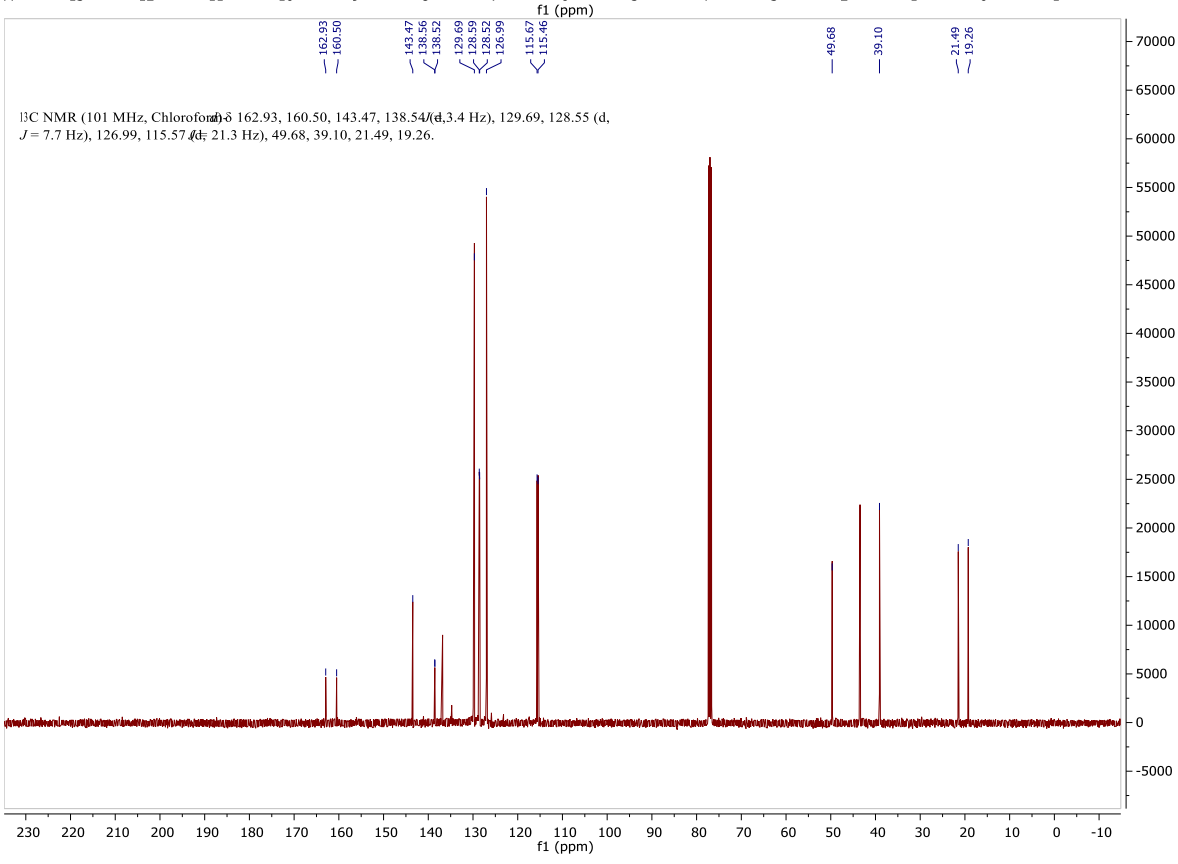

^{13}C NMR (101 MHz, Chloroform-*d*) δ 162.93, 160.50, 143.47, 138.54 (d, *J* = 3.4 Hz), 129.69, 128.55 (d, *J* = 7.7 Hz), 126.99, 115.57 (d, *J* = 21.3 Hz), 49.68, 39.10, 21.49, 19.26.

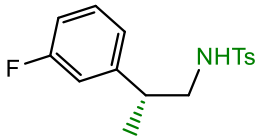
F
NHTs

8-3i

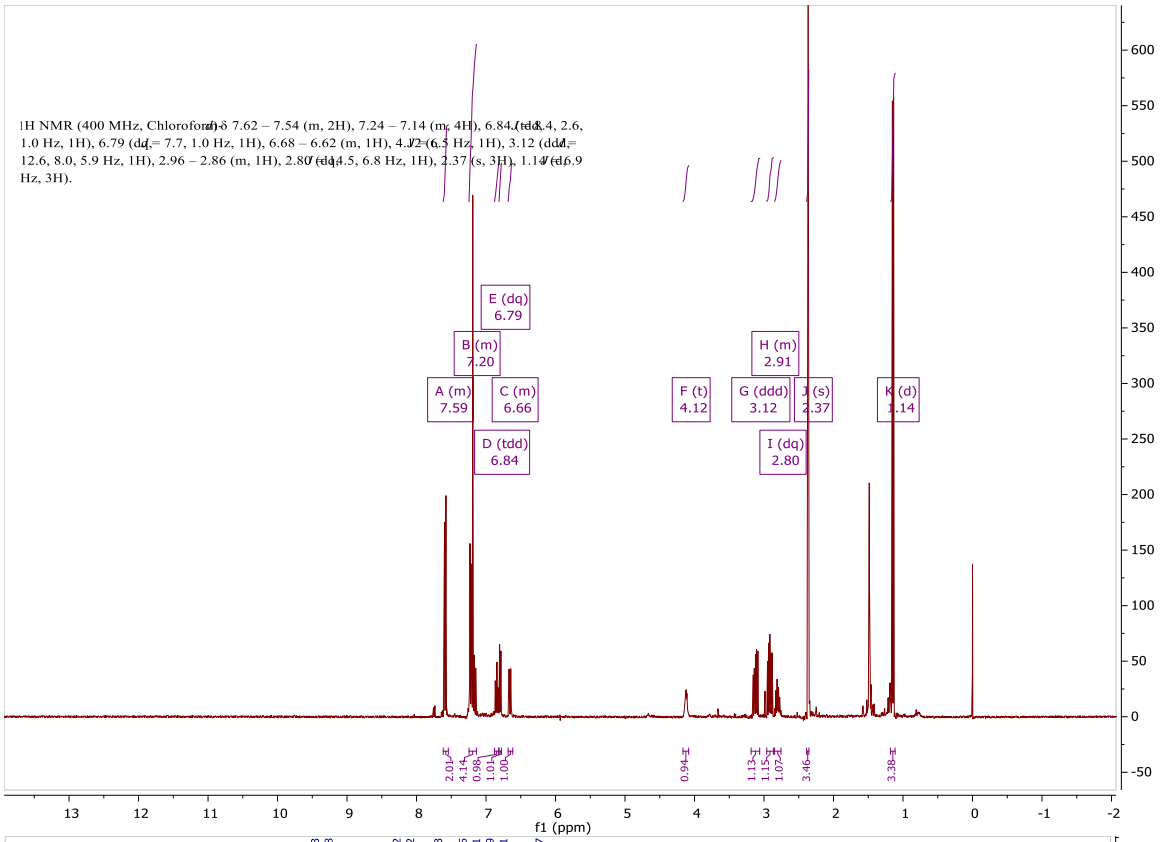
E (dq) 6.79
B (m) 7.20
H (m) 2.91
A (m) 7.59
C (m) 6.66
F (t) 4.12
G (ddd) 3.12
J (s) 2.37
K (d) 1.14
D (tdd) 6.84
I (dq) 2.80
f1 (ppm)

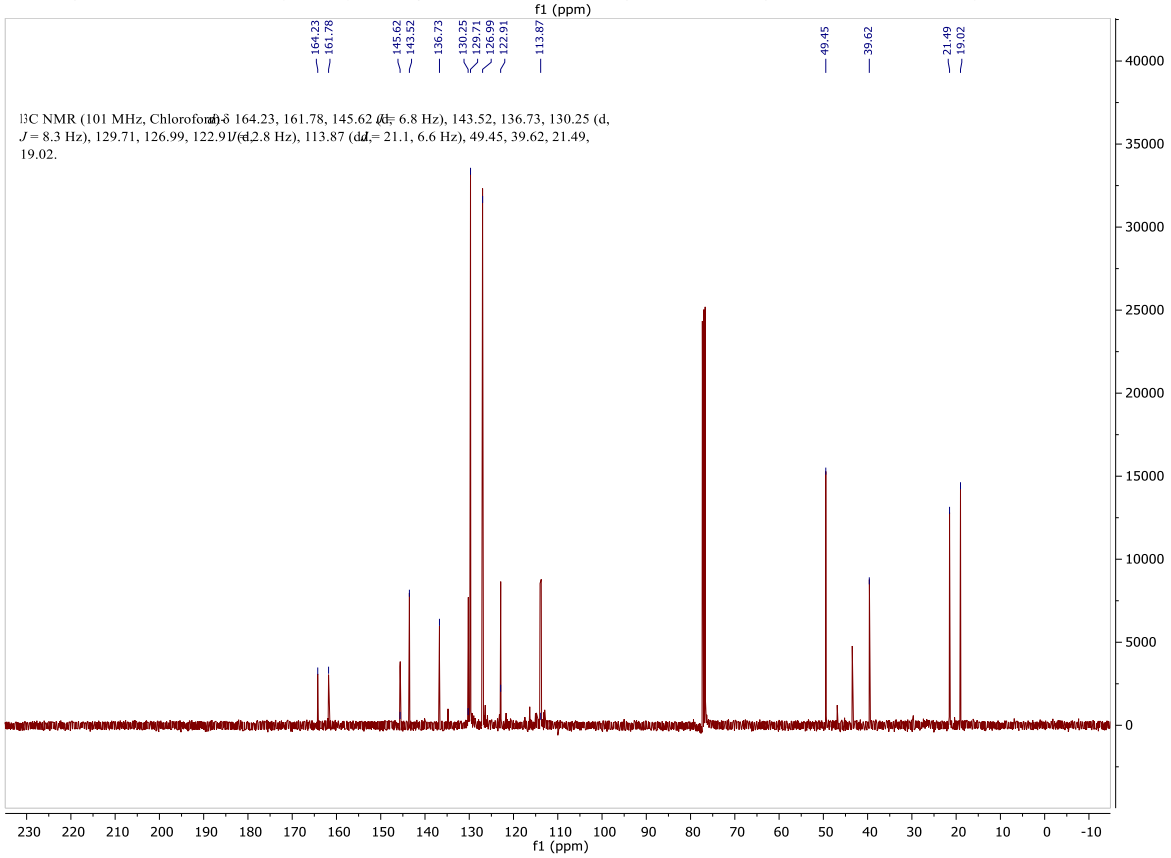
164.23
161.78
145.62
143.52
136.73
130.25
129.71
126.99
122.91
113.87
49.45
39.62
21.49
19.02
f1 (ppm)

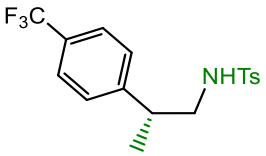
F3C
NHTs

8-3j

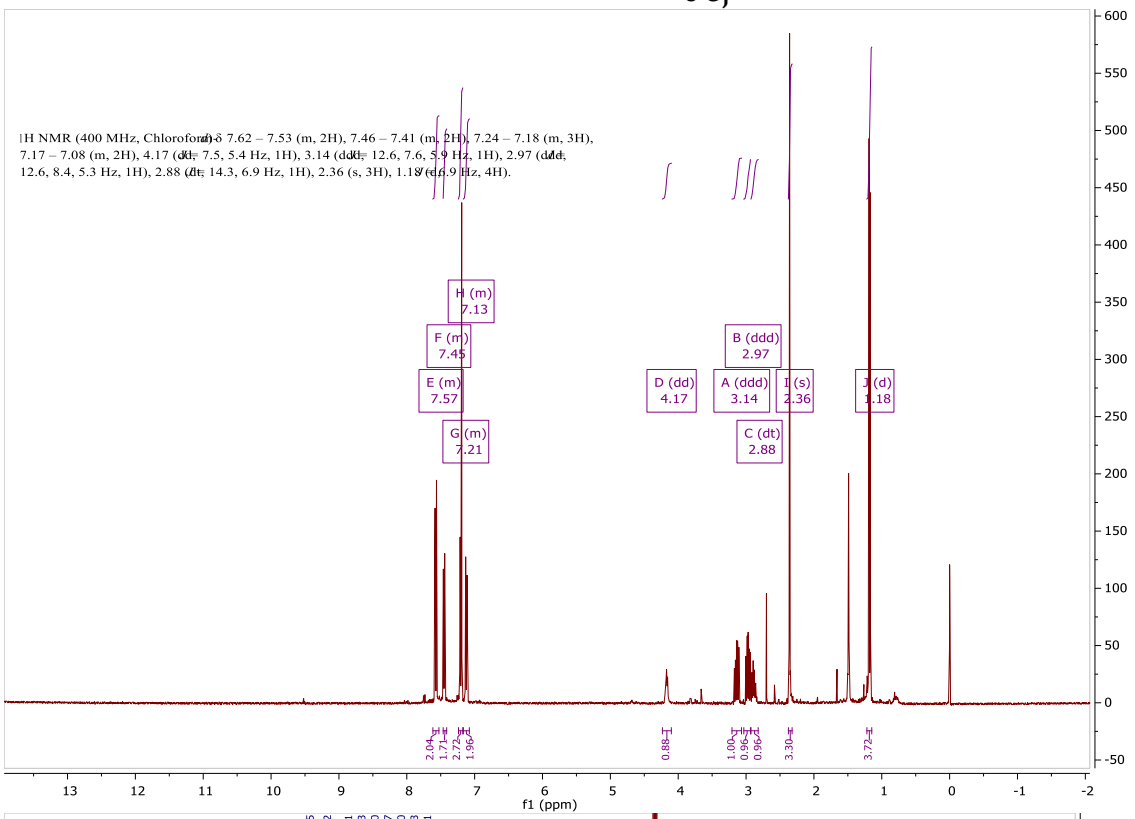
1H NMR (400 MHz, Chloroform-d) δ 7.62 – 7.53 (m, 2H), 7.46 – 7.41 (m, 2H), 7.24 – 7.18 (m, 3H), 7.17 – 7.08 (m, 2H), 4.17 (dd, J = 7.5, 5.4 Hz, 1H), 3.14 (ddd, J = 12.6, 7.6, 5.9 Hz, 1H), 2.97 (ddd, J = 12.6, 8.4, 5.3 Hz, 1H), 2.88 (dt, J = 14.3, 6.9 Hz, 1H), 2.36 (s, 3H), 1.18 (d, J = 6.9 Hz, 4H).
H (m) 7.13
F (m) 7.45
E (m) 7.57
G (m) 7.21
D (dd) 4.17
B (ddd) 2.97
A (ddd) 3.14
I (s) 2.36
J (d) 1.18
C (dt) 2.88
f1 (ppm)

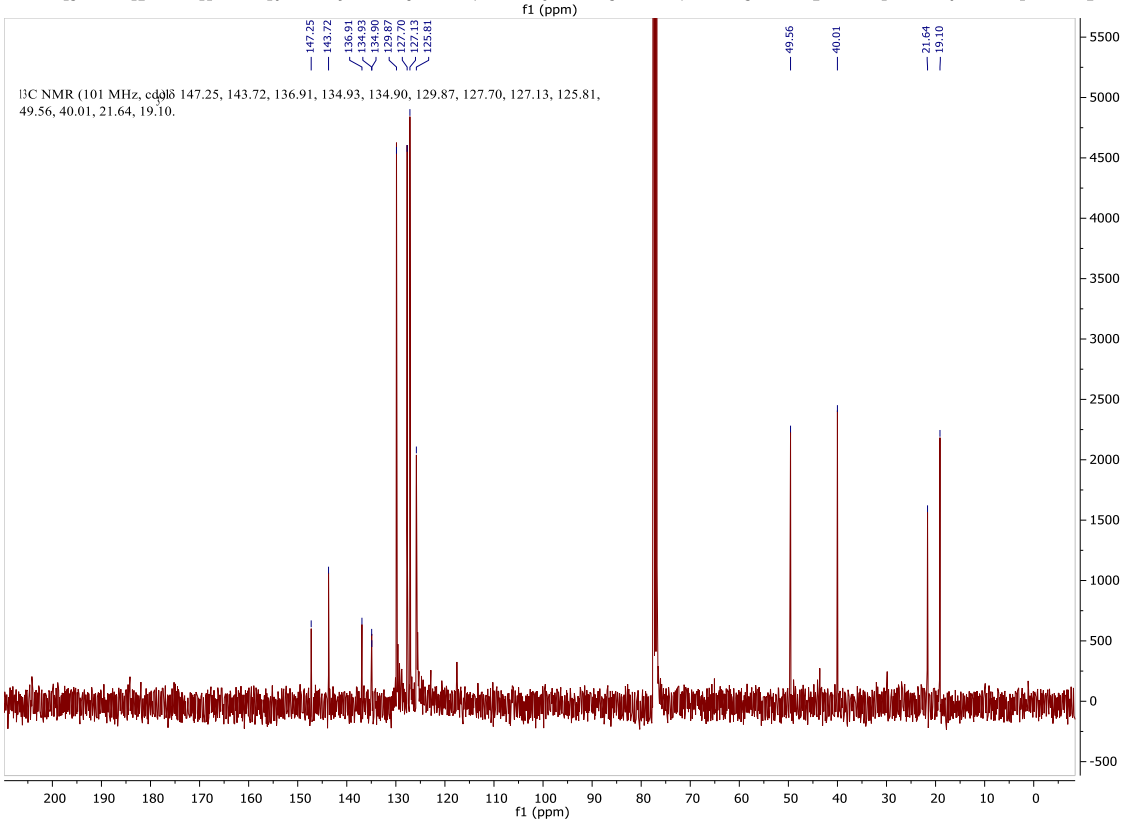
13C NMR (101 MHz, cdcl3) δ 147.25, 143.72, 136.91, 134.93, 134.90, 129.87, 127.70, 127.13, 125.81, 49.56, 40.01, 21.64, 19.10.
147.25
143.72
136.91
134.93
134.90
129.87
127.70
127.13
125.81
49.56
40.01
21.64
19.10
f1 (ppm)

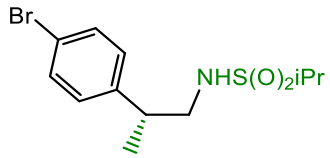
Br
NHS(O)2iPr

8-3k

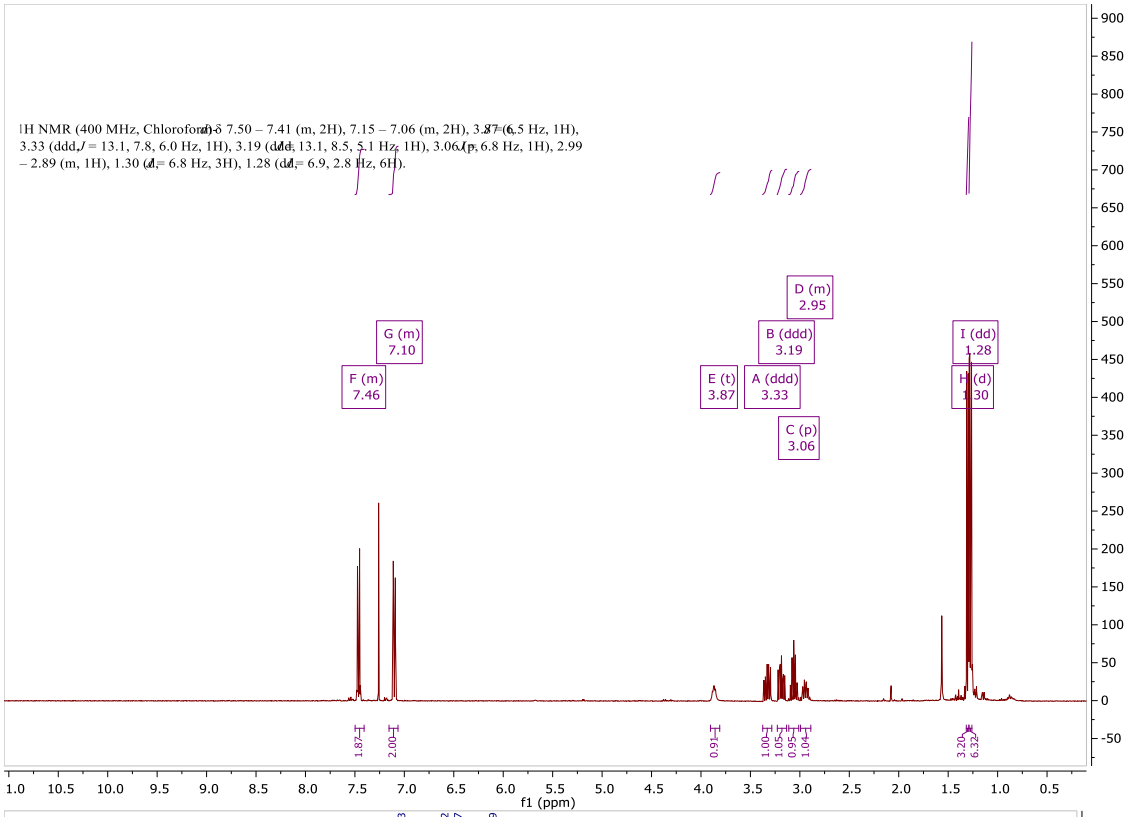
1H NMR (400 MHz, Chloroform-d) δ 7.50 – 7.41 (m, 2H), 7.15 – 7.06 (m, 2H), 3.87 (t, J = 6.5 Hz, 1H), 3.33 (ddd, J = 13.1, 7.8, 6.0 Hz, 1H), 3.19 (ddd, J = 13.1, 8.5, 5.1 Hz, 1H), 3.06 (p, J = 6.8 Hz, 1H), 2.99 – 2.89 (m, 1H), 1.30 (d, J = 6.8 Hz, 3H), 1.28 (dd, J = 6.9, 2.8 Hz, 6H).
D (m) 2.95
G (m) 7.10
B (ddd) 3.19
I (dd) 1.28
F (m) 7.46
E (t) 3.87
A (ddd) 3.33
H (d) 1.30
C (p) 3.06
1.87
2.00
0.91
1.00
1.05
0.95
1.04
3.20
6.32
f1 (ppm)

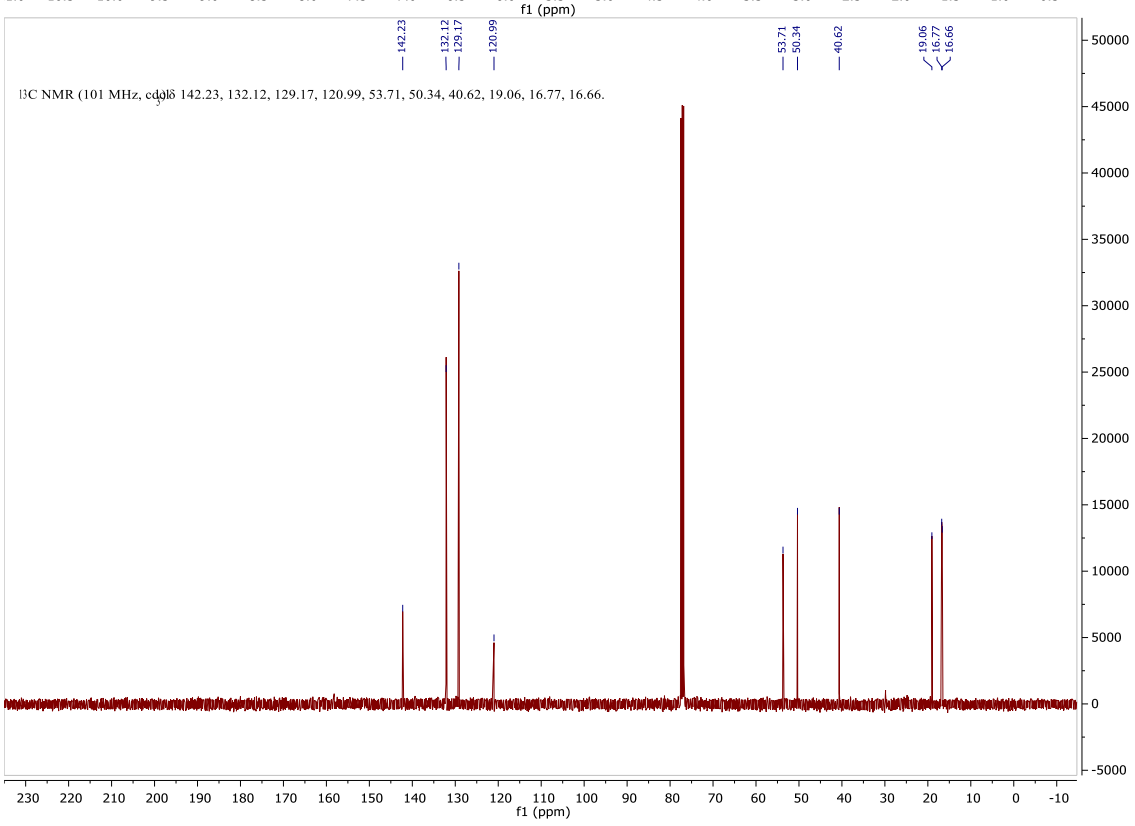
13C NMR (101 MHz, cdcl3) δ 142.23, 132.12, 129.17, 120.99, 53.71, 50.34, 40.62, 19.06, 16.77, 16.66.
142.23
132.12
129.17
120.99
53.71
50.34
40.62
19.06
16.77
16.66
f1 (ppm)

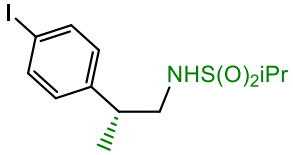
I
NHS(O)2iPr

8-31

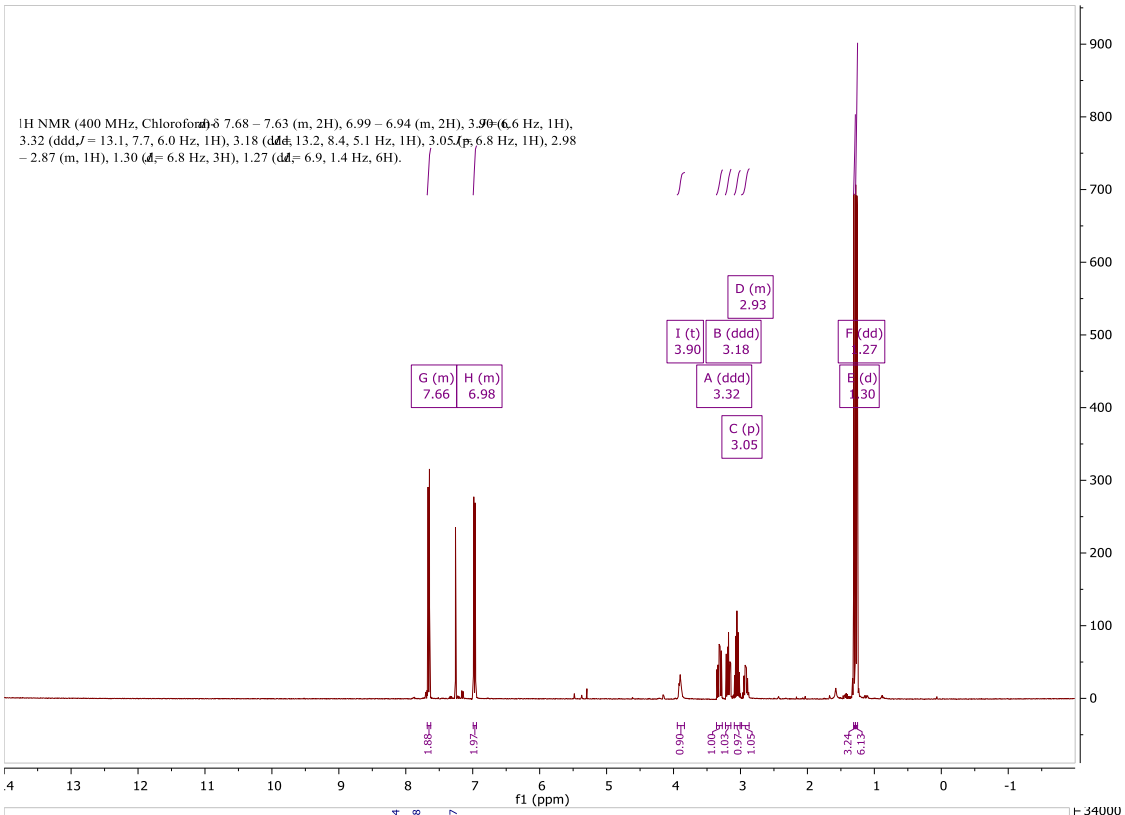
D (m)
2.93
I (t)
3.90
B (ddd)
3.18
F (dd)
3.27
G (m)
7.66
H (m)
6.98
A (ddd)
3.32
E (d)
1.30
C (p)
3.05
f1 (ppm)

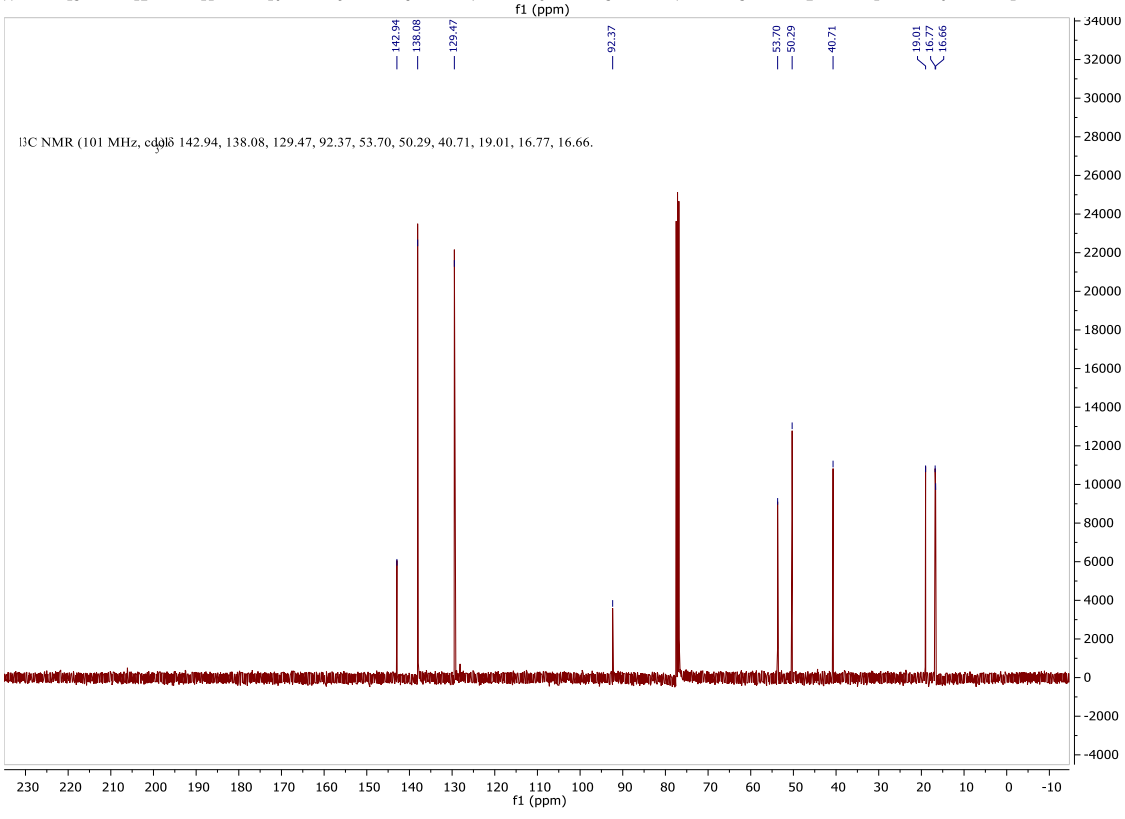
142.94
138.08
129.47
92.37
53.70
50.29
40.71
19.01
16.77
16.66
f1 (ppm)

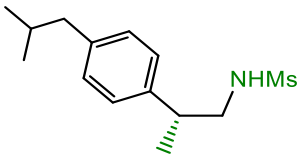

8-3n

^{1}H NMR (400 MHz, Chloroform-*d*) δ 7.11 (s, 4H), 4.09 (s, 1H), 3.35 (ddd, *J* = 12.8, 7.7, 5.7 Hz, 1H), 3.22 (ddd, *J* = 12.7, 8.7, 5.0 Hz, 1H), 2.99 – 2.89 (m, 1H), 2.77 (s, 3H), 2.45 (d, *J* = 7.2 Hz, 2H), 1.85 (dt, *J* = 13.5, 6.8 Hz, 1H), 1.30 (d, *J* = 7.0 Hz, 3H), 0.90 (d, *J* = 6.6 Hz, 6H).

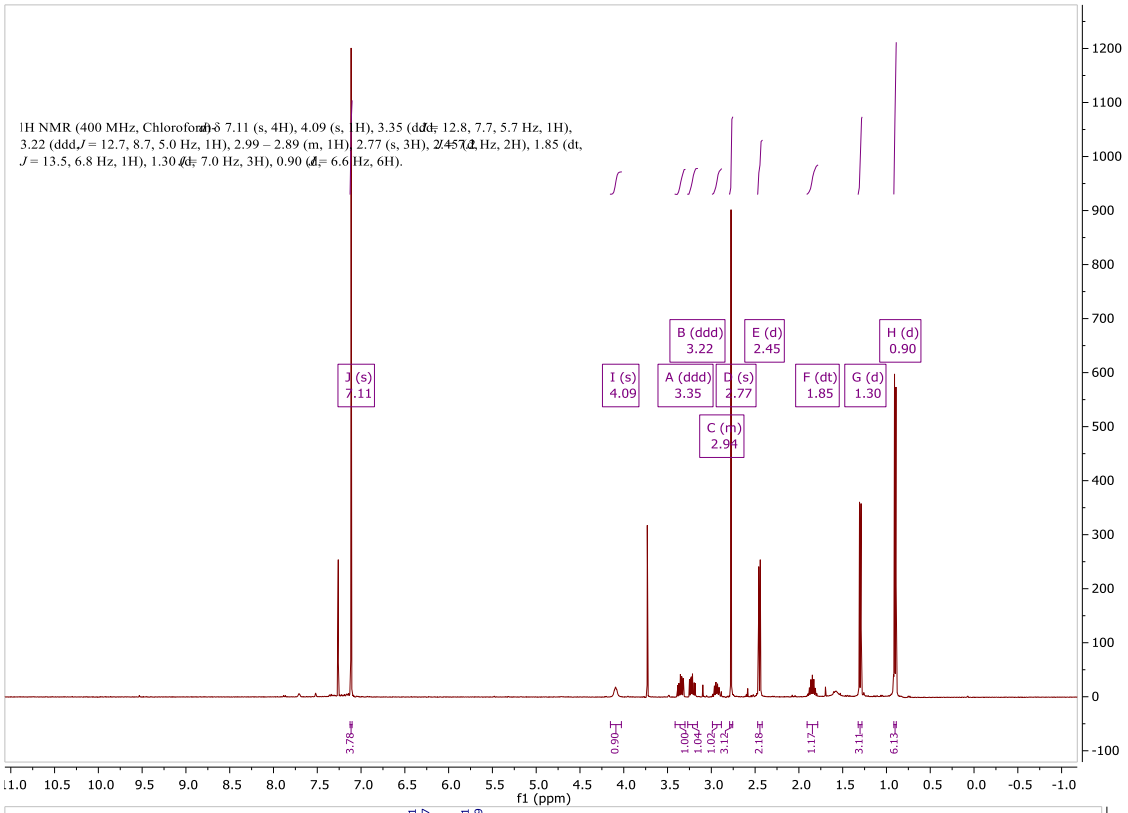

^{13}C NMR (101 MHz, cdcl$_3$) δ 140.81, 140.17, 129.81, 127.09, 50.19, 45.13, 40.43, 40.06, 30.34, 22.52, 19.21.

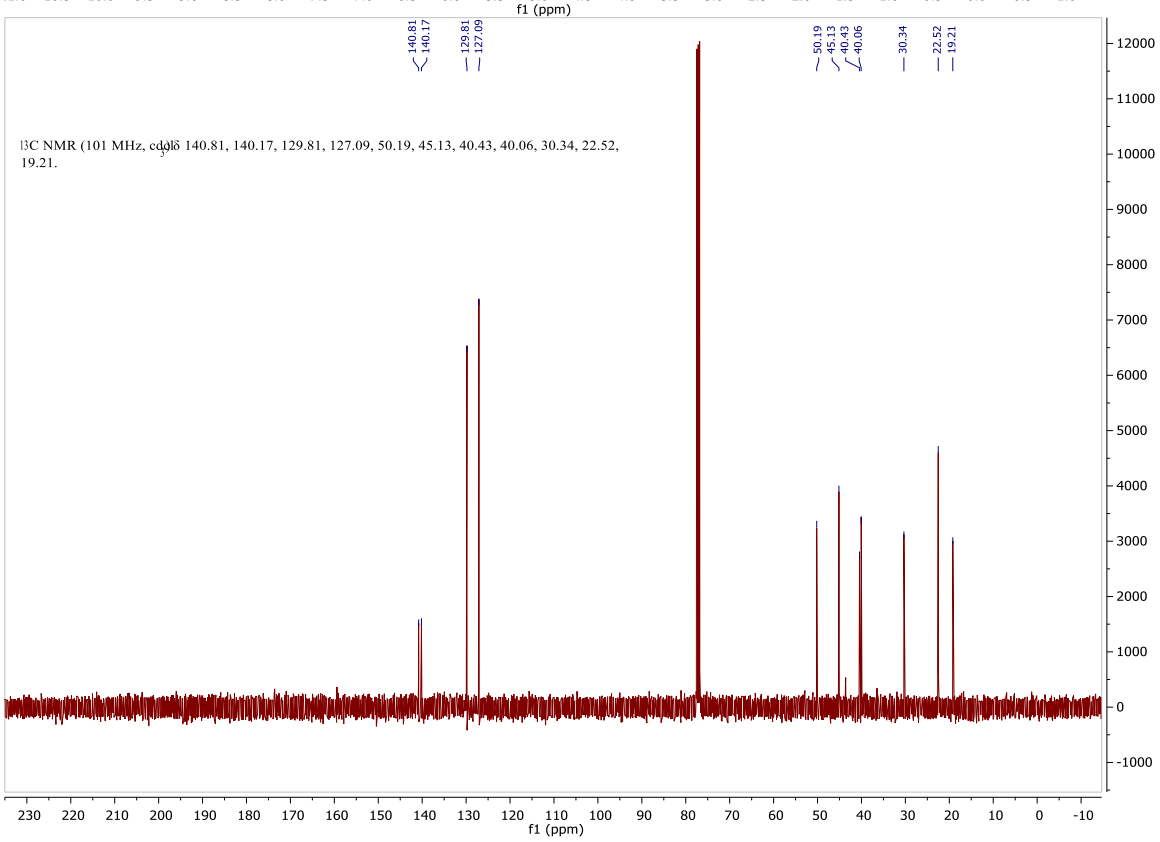

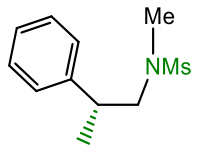

8-3o

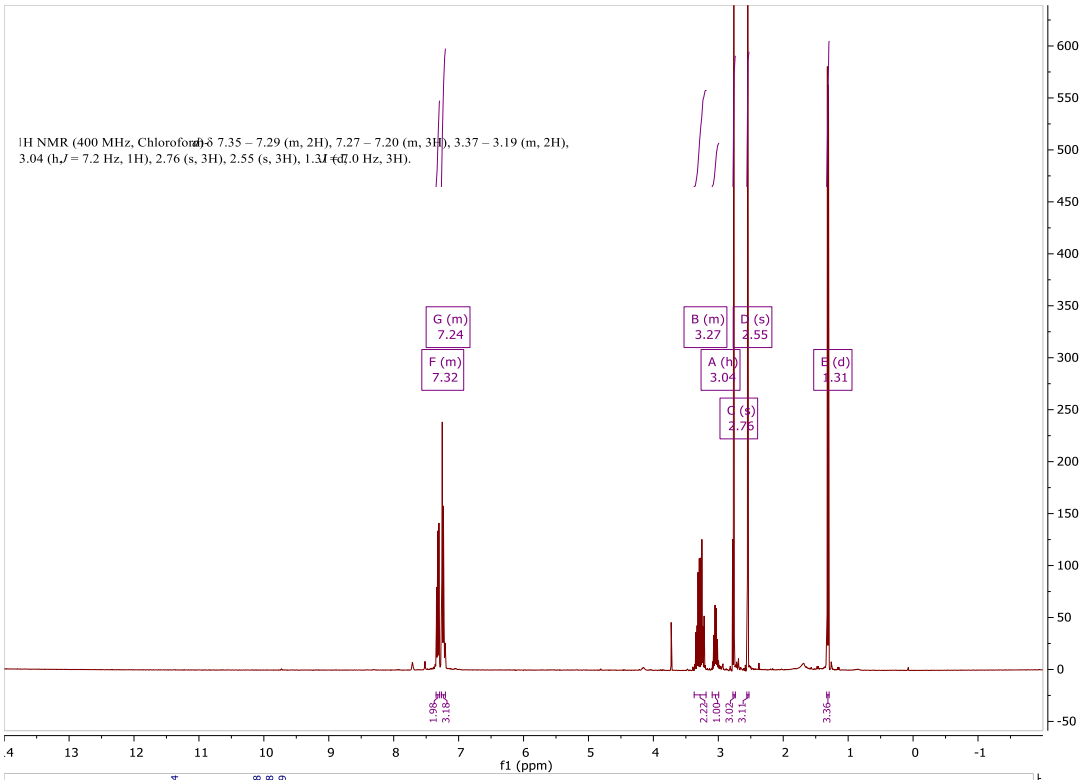

^{1}H NMR (400 MHz, Chloroform-*d*) δ 7.35 – 7.29 (m, 2H), 7.27 – 7.20 (m, 3H), 3.37 – 3.19 (m, 2H), 3.04 (h, *J* = 7.2 Hz, 1H), 2.76 (s, 3H), 2.55 (s, 3H), 1.31 (d, *J* = 7.0 Hz, 3H).

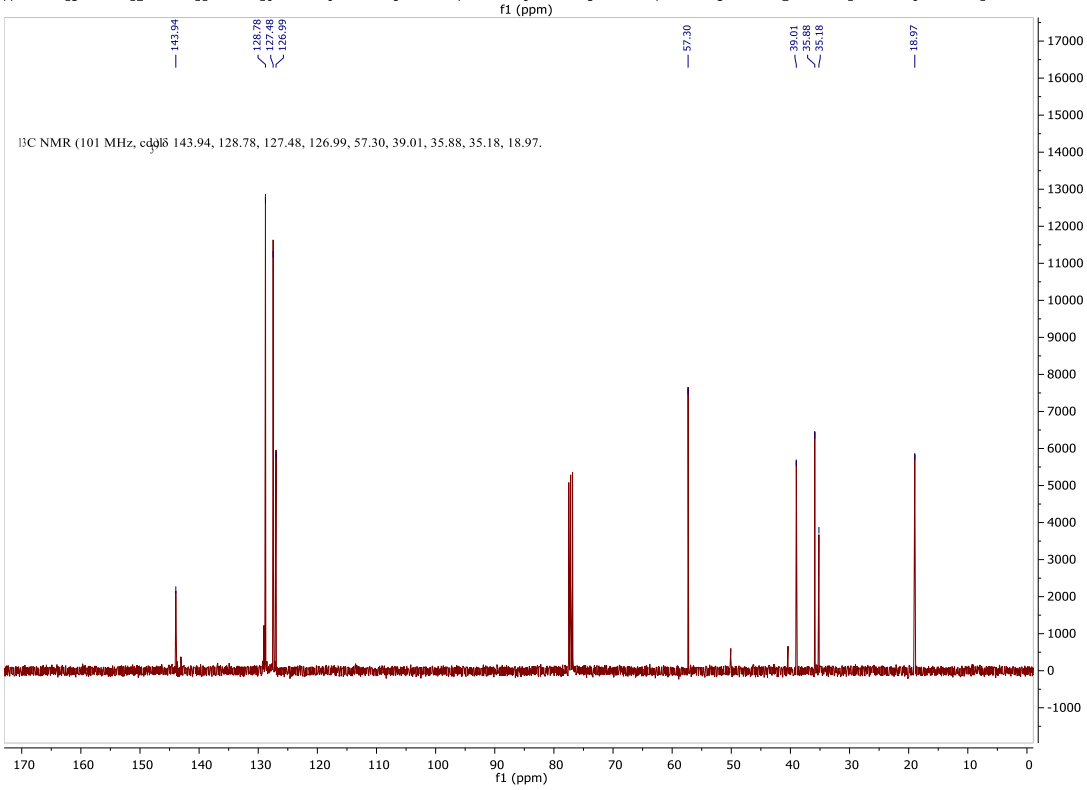

^{13}C NMR (101 MHz, cdcl$_3$) δ 143.94, 128.78, 127.48, 126.99, 57.30, 39.01, 35.88, 35.18, 18.97.

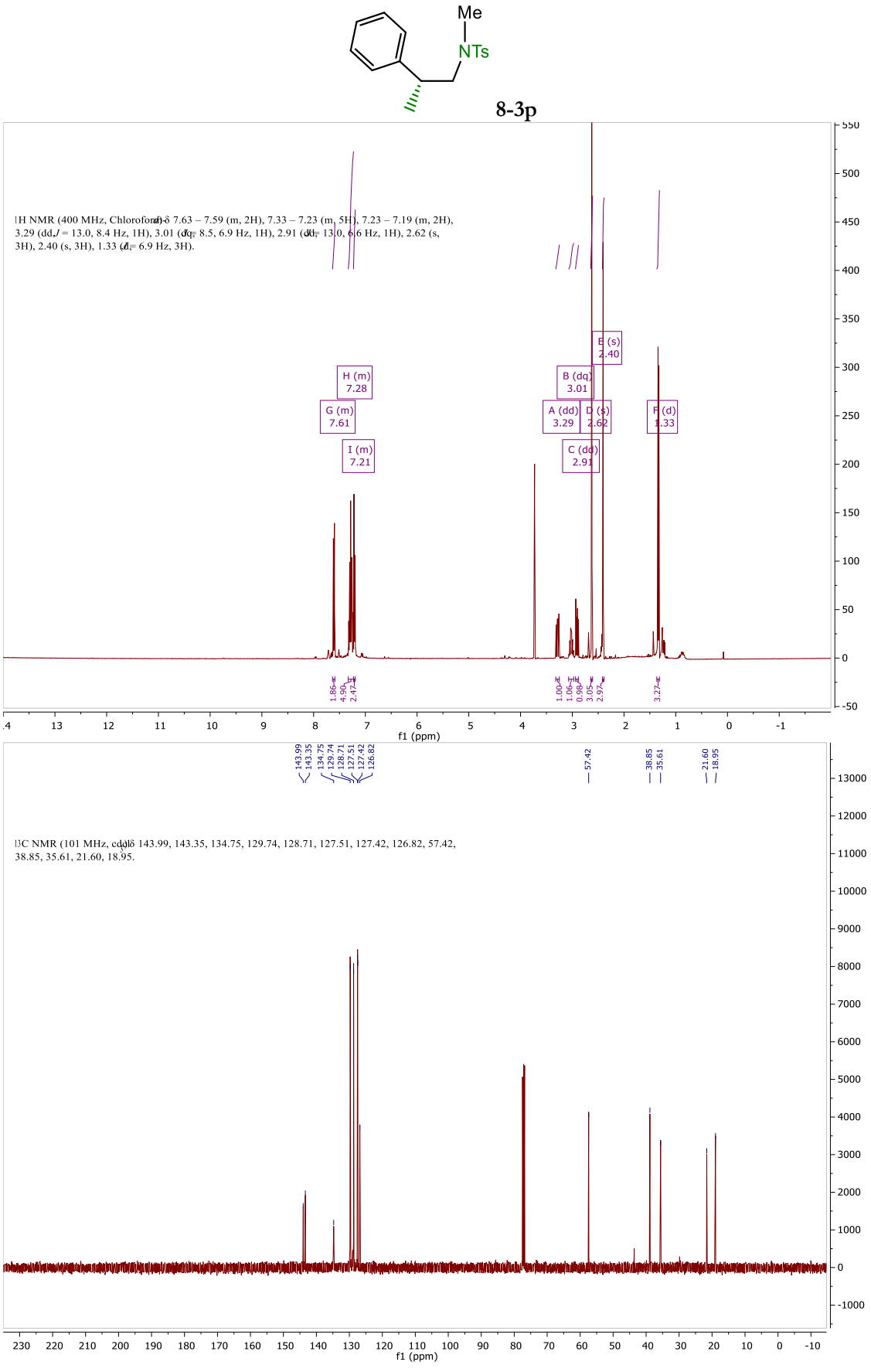
Me
NTs
8-3p
1H NMR (400 MHz, Chloroform-d) δ 7.63 – 7.59 (m, 2H), 7.33 – 7.23 (m, 5H), 7.23 – 7.19 (m, 2H), 3.29 (dd, J = 13.0, 8.4 Hz, 1H), 3.01 (dq, J = 8.5, 6.9 Hz, 1H), 2.91 (dd, J = 13.0, 6.6 Hz, 1H), 2.62 (s, 3H), 2.40 (s, 3H), 1.33 (d, J = 6.9 Hz, 3H).
H (m) 7.28
G (m) 7.61
I (m) 7.21
E (s) 2.40
B (dq) 3.01
A (dd) 3.29
D (s) 2.62
F (d) 1.33
C (dd) 2.91
1.86
4.90
2.47
1.00
1.06
0.98
3.05
2.97
3.27
f1 (ppm)
13C NMR (101 MHz, cdcl3) δ 143.99, 143.35, 134.75, 129.74, 128.71, 127.51, 127.42, 126.82, 57.42, 38.85, 35.61, 21.60, 18.95.
143.99
143.35
134.75
129.74
128.71
127.51
127.42
126.82
57.42
38.85
35.61
21.60
18.95
f1 (ppm)

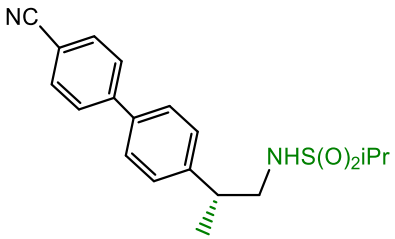
NC
NHS(O)2iPr

8-7

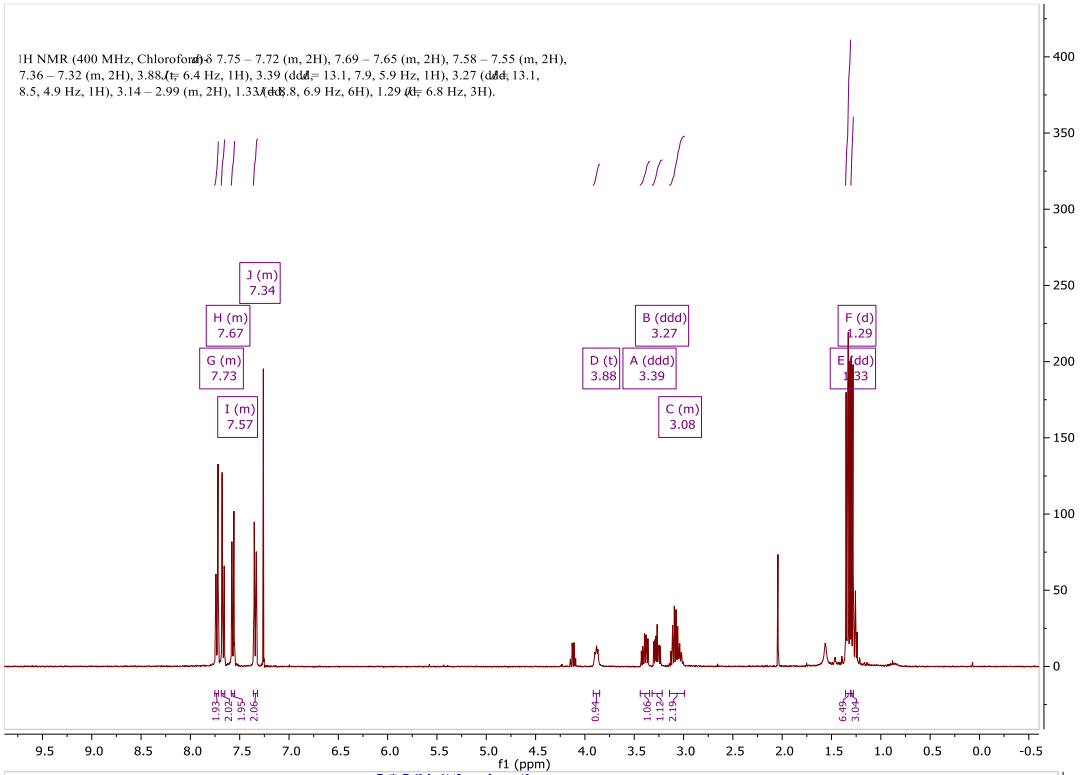
J (m) 7.34
H (m) 7.67
G (m) 7.73
I (m) 7.57
B (ddd) 3.27
D (t) 3.88
A (ddd) 3.39
C (m) 3.08
F (d) 1.29
E (dd) 3.33
f1 (ppm)

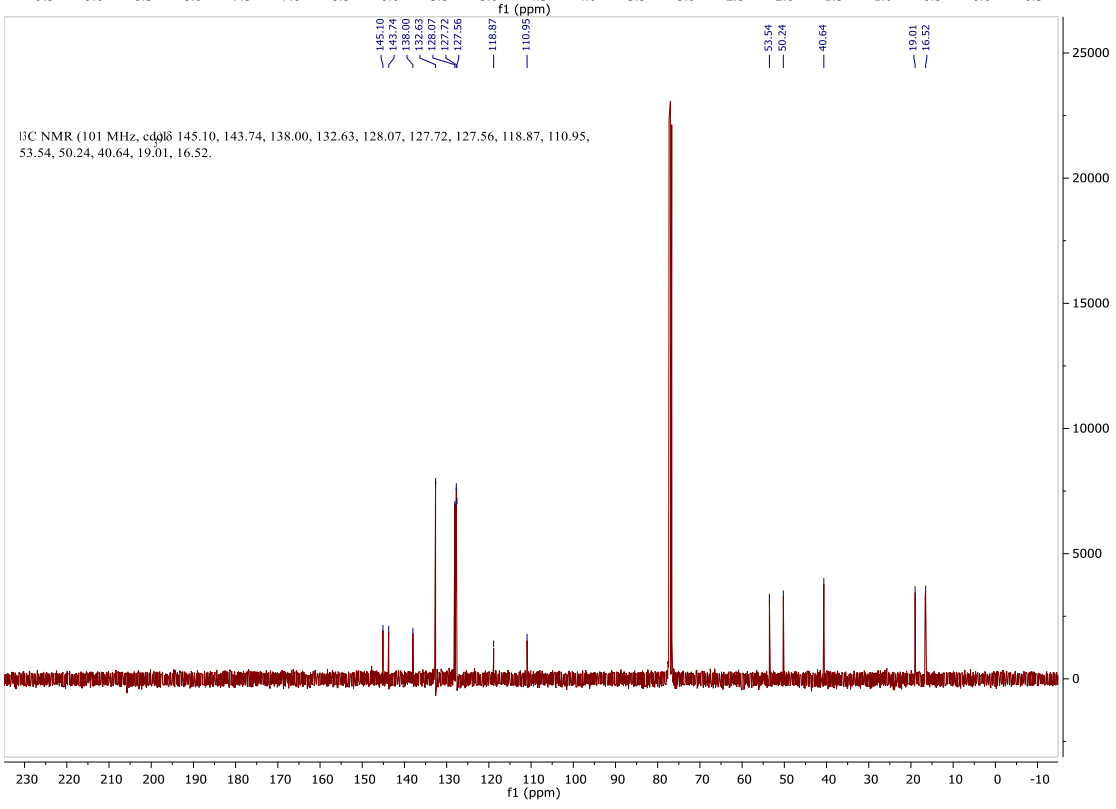
145.10
143.74
138.00
132.63
128.07
127.72
127.56
118.87
110.95
53.54
50.24
40.64
19.01
16.52
f1 (ppm)

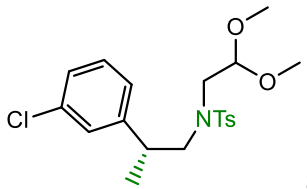
O
O
Cl
NTs

8-5

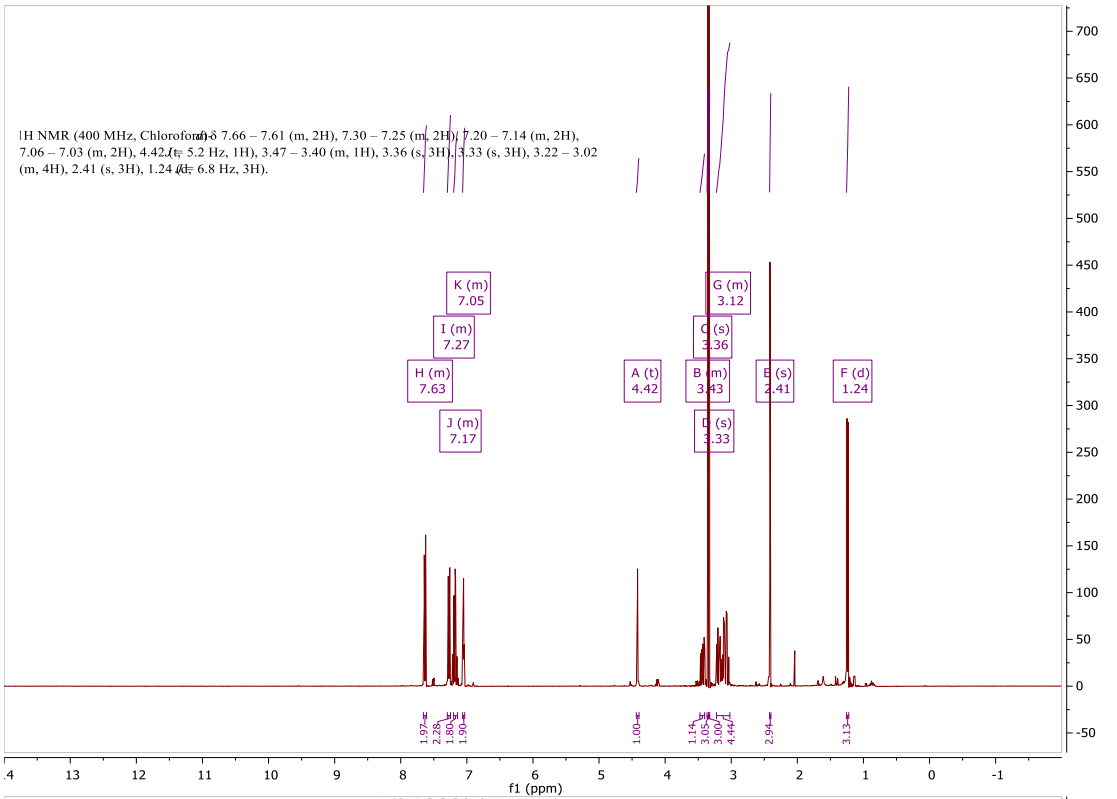
1H NMR (400 MHz, Chloroform-d) δ 7.66 – 7.61 (m, 2H), 7.30 – 7.25 (m, 2H), 7.20 – 7.14 (m, 2H), 7.06 – 7.03 (m, 2H), 4.42 (t, J = 5.2 Hz, 1H), 3.47 – 3.40 (m, 1H), 3.36 (s, 3H), 3.33 (s, 3H), 3.22 – 3.02 (m, 4H), 2.41 (s, 3H), 1.24 (d, J = 6.8 Hz, 3H).
K (m) 7.05
I (m) 7.27
H (m) 7.63
J (m) 7.17
A (t) 4.42
G (m) 3.12
C (s) 3.36
B (m) 3.43
D (s) 3.33
E (s) 2.41
F (d) 1.24
1.97
2.28
1.80
1.90
1.00
1.14
3.05
3.00
4.44
2.94
3.13
f1 (ppm)

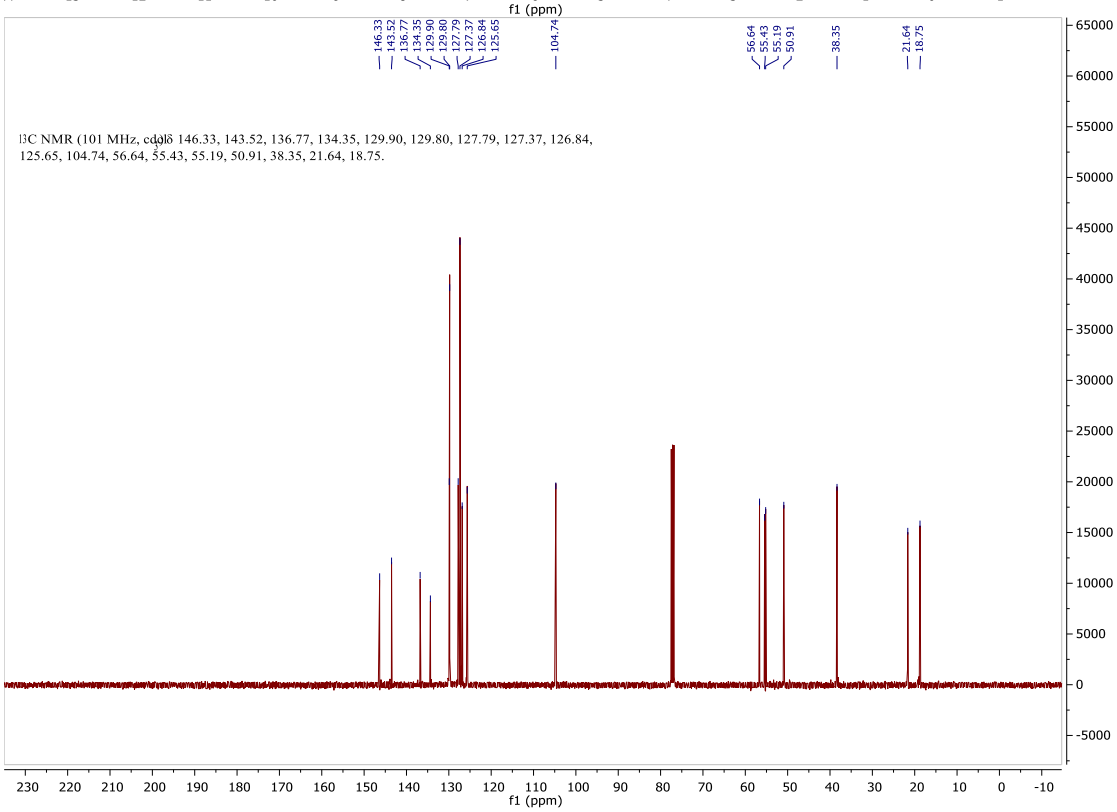
13C NMR (101 MHz, cdcl3) δ 146.33, 143.52, 136.77, 134.35, 129.90, 129.80, 127.79, 127.37, 126.84, 125.65, 104.74, 56.64, 55.43, 55.19, 50.91, 38.35, 21.64, 18.75.
146.33
143.52
136.77
134.35
129.90
129.80
127.79
127.37
126.84
125.65
104.74
56.64
55.43
55.19
50.91
38.35
21.64
18.75
f1 (ppm)

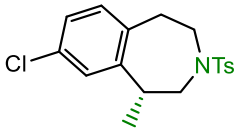
Cl
NTs

8-6

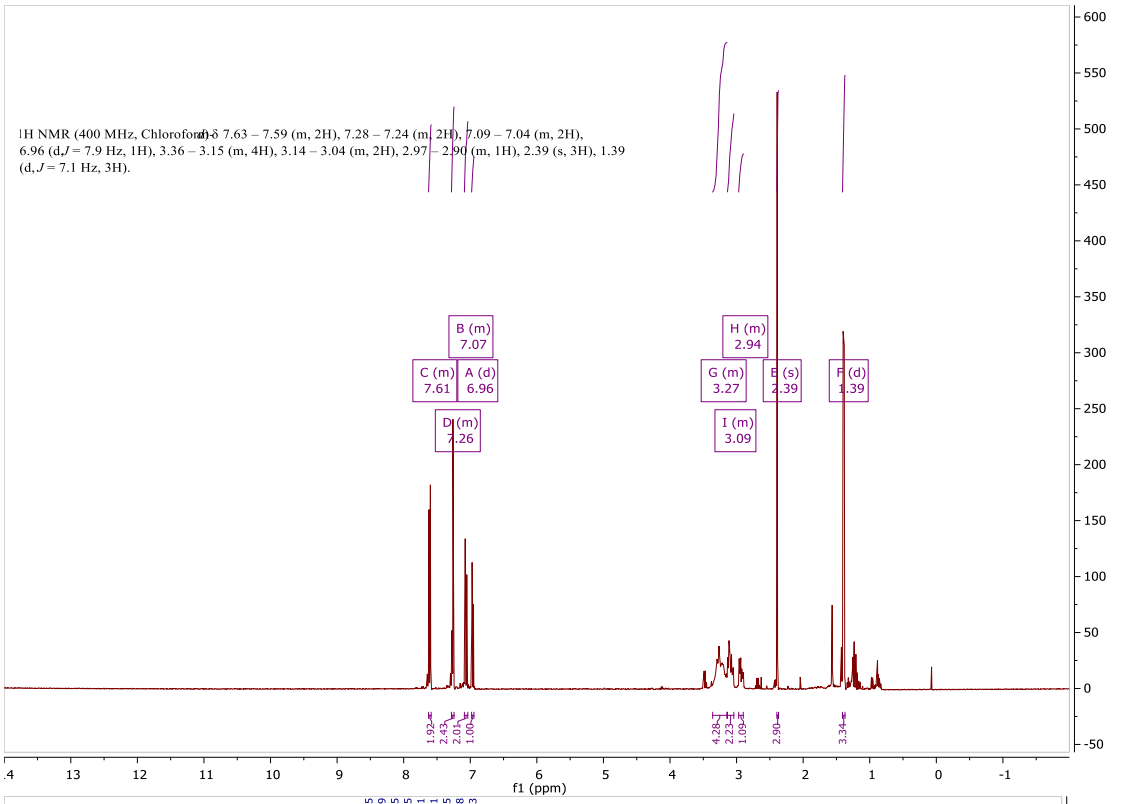
1H NMR (400 MHz, Chloroform-d) δ 7.63 – 7.59 (m, 2H), 7.28 – 7.24 (m, 2H), 7.09 – 7.04 (m, 2H), 6.96 (d, J = 7.9 Hz, 1H), 3.36 – 3.15 (m, 4H), 3.14 – 3.04 (m, 2H), 2.97 – 2.90 (m, 1H), 2.39 (s, 3H), 1.39 (d, J = 7.1 Hz, 3H).
B (m) 7.07
C (m) 7.61
A (d) 6.96
D (m) 7.26
H (m) 2.94
G (m) 3.27
E (s) 2.39
F (d) 1.39
I (m) 3.09
f1 (ppm)

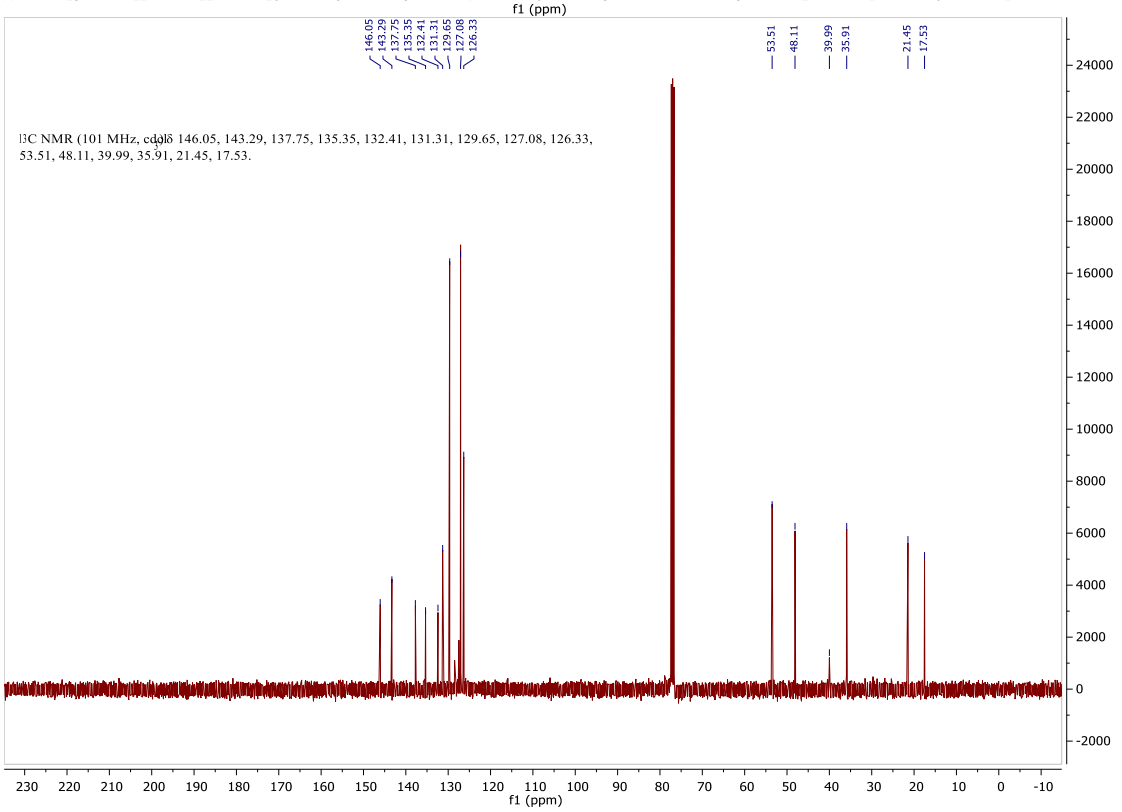
13C NMR (101 MHz, cdcl3) δ 146.05, 143.29, 137.75, 135.35, 132.41, 131.31, 129.65, 127.08, 126.33, 53.51, 48.11, 39.99, 35.91, 21.45, 17.53.
146.05
143.29
137.75
135.35
132.41
131.31
129.65
127.08
126.33
53.51
48.11
39.99
35.91
21.45
17.53
f1 (ppm)

Chapter 9

Highly Enantioselective Iridium-Catalyzed Hydrogenation of 2-Aryl Allyl Phthalimides

The biological activity of many pharmaceutical compounds and agrochemicals is intrinsically related to their absolute molecular configuration.[1] The asymmetric synthesis of chiral compounds is, therefore, an essential field in organic chemistry. In particular, chiral β-aryl propanamines are extremely interesting candidates as precursors of pharmaceuticals and active molecules.[2] For example, Lorcaserin, an anorectic drug that has been typically synthesized by chiral resolution;[3] OTS514, a marketed inhibitor of a serine-threonine kinase that is often overexpressed and transactivated in several types of cancer;[4] or LY-392098, a potent positive allosteric modulator of 2-amino-3-(5-methyl-3-hydroxyisoxazol-4-yl)-propanoic acid (AMPA) receptor.[5] Moreover, we can envision the synthesis of several drug intermediates such as 3-methylindolines in few steps from β-aryl propanamines (Figure 9.1).

Among the strategies to obtain enantioenriched β-aryl propanamines, catalytic asymmetric hydrogenation provides one of the most practical and powerful approaches due to its operational simplicity, high reactivity and atom economy.[6] However, most of the syntheses found in the literature are performed by means of chiral resolution or by using stoichiometric agents.[7] To the best of our knowledge, there are only few examples in which enantioenriched β-aryl propanamines can be obtained by metal-catalyzed enantioselective hydrogenation.[8] In 2005, Zhang and co-workers reported the asymmetric hydrogenation of 2-alkyl allyl phthalimides using a Ru-C_3-tunephos catalyst.[8a] However, the scope of this reaction was focused on alkyl groups and the single example of β-aryl allyl phthalimide gave only 55% ee of the corresponding β-methylpropanamine. More recently, our group reported the hydrogenation of *N*-sulfonyl allyl amines using the iridium complex of Pfaltz's catalyst Ubaphox.[8d]

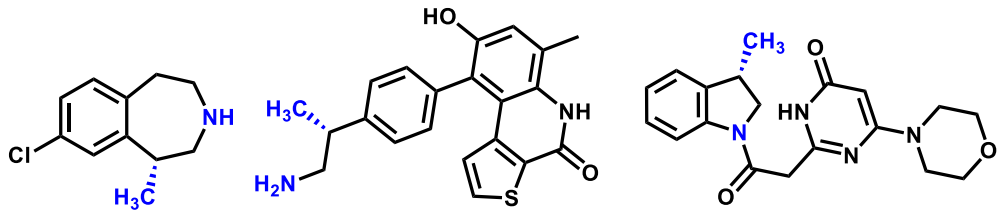

Figure 9.1. Examples of biologically active compounds containing a chiral β-methyl amine.

Iridium complexes bearing chiral P,N ligands[9] have been successfully applied in the asymmetric hydrogenation of a wide range of unfunctionalized or minimally functionalized

olefins.[10] Our group has developed several P-stereogenic chiral ligands.[11] Recently, we designed a family of P,N-ligands (MaxPHOX) that were coordinated to iridium.[12] These catalysts can be obtained from protected *tert*-butyl methyl phosphinous acid and commercially available amino acids and amino alcohols. These iridium complexes have three chiral centers, so up to four diastereoisomers (catalysts **9-(1-4)**, Figure 9.2) can be obtained. Moreover, the substituent of the oxazoline ring can be easily modified. This variety of structures facilitates the fine-tuning of the catalyst. This strategy has allowed us to find an excellent catalyst for the enantioselective hydrogenation of cyclic enamides[12a], *N*-aryl[12b] and *N*-alkyl[12c] imines. Moreover, these catalysts also proved to be extremely efficient in the isomerization of cyclic allyl carbamates, yielding high levels of enantioselectivity.[12d]

Here, we present the asymmetric hydrogenation of *N*-phthalimido 2-phenyl allyl amines using an Ir-MaxPHOX catalyst to obtain chiral β-methyl amines. It is worth noting that, in this occasion, the best catalyst of the family (**9-2c**) had not been described. To showcase the applicability of this reaction, the formal enantioselective synthesis of several biologically active compounds was performed.

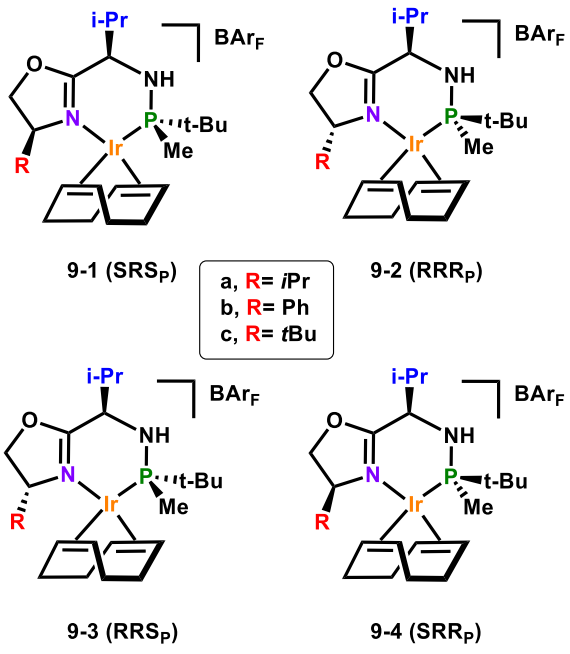

Figure 9.2. Ir-MaxPHOX family of catalysts.

On the basis of our studies, *N*-phthalimido 2-phenyl allyl amine (**9-5a**), which is easily synthesized in three steps from acetophenone *(see Supporting Info)*, was used as model

substrate. The family of Ir-MaxPHOX catalysts was then used for the asymmetric hydrogenation of **9-5a** to afford chiral amine **9-6a** (Table 9.1). The standard conditions of the reaction were as follows: dichloromethane as solvent, 1 bar of H_2 pressure and stirring overnight. The Ir-MaxPHOX catalysts with an isopropyl in the oxazoline ring **9-(1a-4a)** were first tested (Table 9.1, entries 1-4). All of them showed full conversion to **9-6a**. In particular, catalyst **9-2a** gave the best ee (64% ee, Table 9-1, entry 2). Of note is the huge difference between the catalysts in terms of chiral induction achieved by simply modifying the relative configuration of their chiral centers. We then modified the oxazoline substituent of **9-2** into an aromatic group, such as phenyl (**9-2b**) or bulkier group such as *tert*-butyl (**9-2c**). In the first case, the reactivity was not affected but the enantioselectivity was substantially improved (Table 9.1, entry 5). With **9-2c**, the enantiomeric excess was enhanced up to 90% without affecting the conversion (Table 9.1, entry 6). The synthesis of this ligand is described in the Supporting information.

Table 9.1. Catalyst screening and optimization of the asymmetric hydrogenation of 2-(2-phenylallyl)isoindoline-1,3-dione **9-5a**.[a]

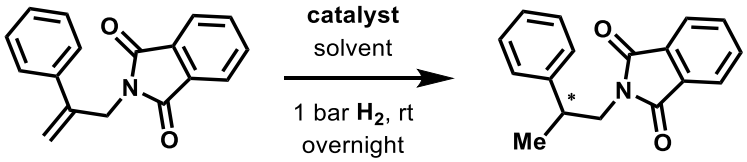

9-5a **9-6a**

entry	catalyst	loading	solvent	conv. (%)[b]	ee (%)[c]
1	**9-1a**	5 mol%	CH_2Cl_2	>99	6 (*S*)
2	**9-2a**	5 mol%	CH_2Cl_2	>99	64 (*R*)
3	**9-3a**	5 mol%	CH_2Cl_2	>99	20 (*S*)
4	**9-4a**	5 mol%	CH_2Cl_2	>99	32 (*R*)
5	**9-2b**	5 mol%	CH_2Cl_2	>99	69 (*R*)
6	**9-2c**	5 mol%	CH_2Cl_2	>99	90 (*R*)
7[d]	**9-2c**	5 mol%	CH_2Cl_2	>99	89 (*R*)
8	**9-2c**	1 mol%	CH_2Cl_2	>99	90 (*R*)
9	**9-2c**	1 mol%	EtOAc	60	89 (*R*)
10	**9-2c**	1 mol%	THF	5	n.d.
11[e]	**9-2c**	1 mol%	CH_2Cl_2	>99	**98** (*R*) (96)[f]

[a] See Supporting Information for experimental details. Reactions were run in a pressure reactor at 1 bar^G of H_2 pressure. [b] Determined by ^1H NMR. [c] Measured by chiral HPLC. [d] Reaction was performed at 50 bar of H_2. [e] Reaction was performed at −20 °C. [f] Isolated yield.

Then we studied the effect of the hydrogen pressure: when increased to 50 barG the enantioselectivity was not affected (Table 9.1, entry 7). Finally, catalyst loading was decreased to 1 mol % and a solvent screening was performed at 1 bar of H_2. With dichloromethane the conversion after 12 h was still complete (Table 9.1, entry 8); in contrast, with ethyl acetate or THF the reactivity decreased to 60% and 5%, respectively (Table 9.1, entries 9 and 10). Using dichloromethane the reaction temperature could be decreased to -20 ºC, affording **9-6a** with an excellent 98% ee and full conversion (Table 9.1, entry 11).

To further investigate the mechanism of this reaction we performed a key experiment using 1 bar of deuterium instead of hydrogen (Figure 9.3).

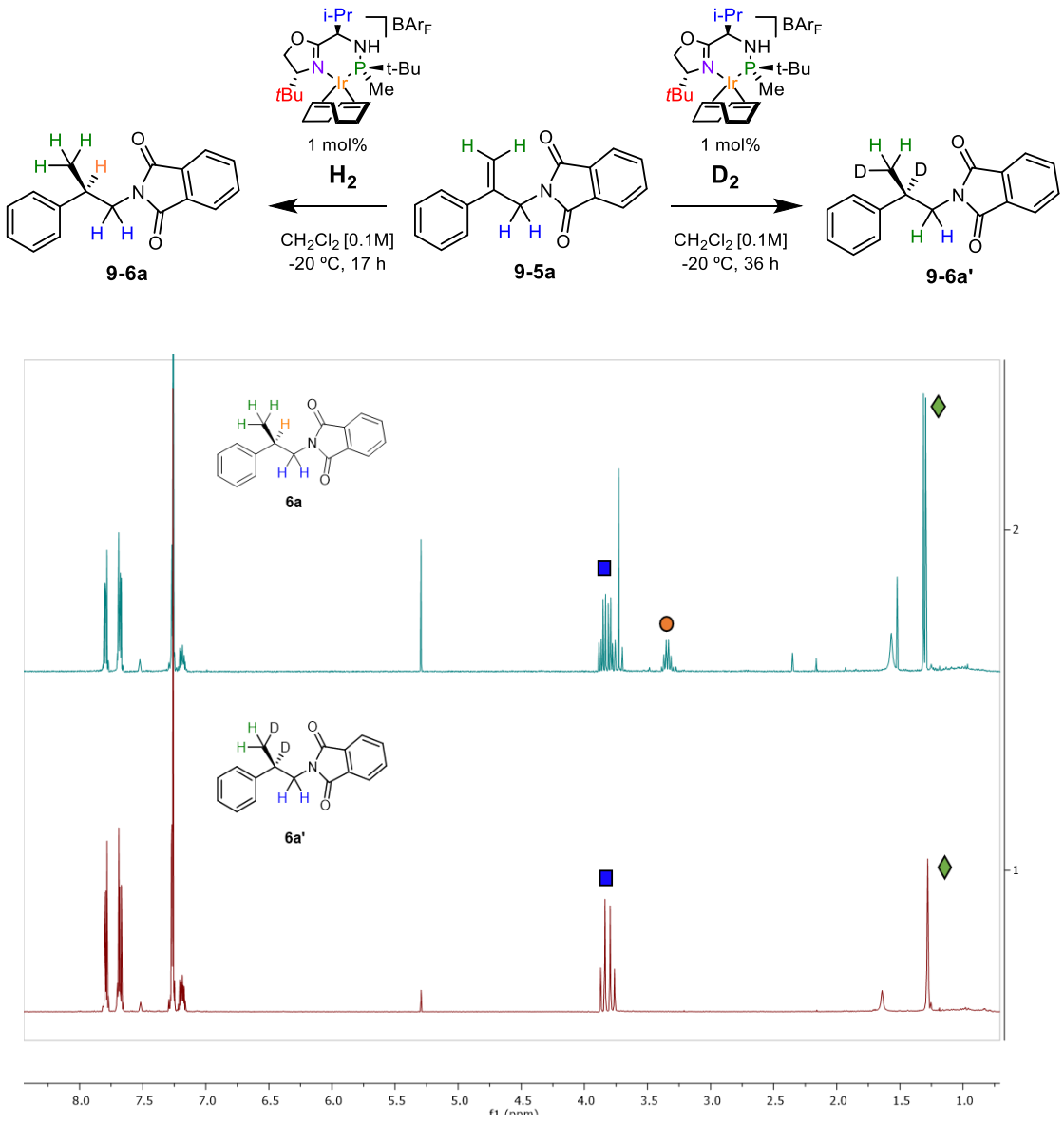

Fig. 9.3. ^{1}H NMR spectra of **9-6a** and **9-6a'**.

Applying the optimal conditions we found after the screening, we were pleased to see that direct hydrogenation took place exclusively to the allylic bond. Therefore, we proved that the enantioselective hydrogenation –thus the asymmetric induction- takes place to the minimally functionalized olefin, and that no isomerization reaction towards the formation of enamide occurs, as seen in Figure 9.3.

With the optimal conditions in hand, we studied the scope of the reaction (Scheme 9.1).

Scheme 9.1. Scope of the catalytic hydrogenation.[a]

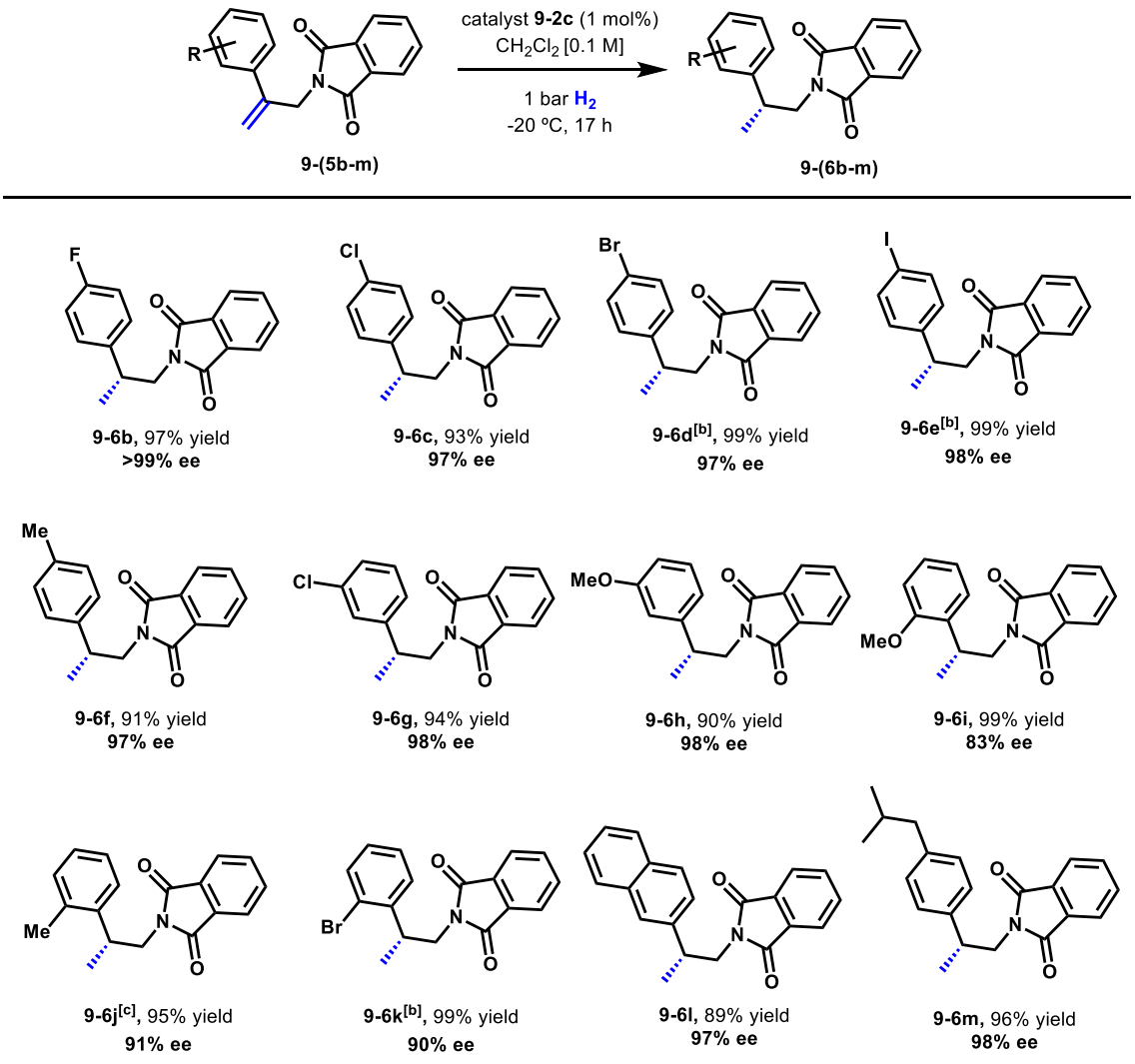

[a] See Supporting Information for experimental details. Reactions were run in a pressure reactor at 1 bar of H_2 pressure. The reaction showed full conversion for all the examples. Enantiomeric excess was measured by chiral HPLC. [b] 2 mol % of catalyst **9-2c** was used. [c] 3 mol % of catalyst **9-2c** was used.

As seen in Scheme 9.1, halide-substituted aryl groups were well-tolerated, with excellent enantioselectivities in all cases (**9-6b** to **9-6e**, Scheme 9.1). The catalyst loading for the substrates with bromine (**9-5d**) and iodine (**9-5e**) had to be increased to 2 mol% to ensure full conversion. Electron-donating substituents such as methyl (**9-6f**) or isobutyl (**9-6m**) gave 97% and 98% ee respectively (Scheme 9.1). We then expanded the substrates to *meta*-substituted aryl groups. Again, and using only 1 mol % of catalyst **9-2c**, chiral amines **9-6g** and **9-6h** were afforded with excellent enantioselectivities. The asymmetric hydrogenation *ortho*-substituted compounds (**9-(5i-k)**) also gave excellent enantiomeric excesses except in the case of the methoxy substituent (**9-6i**) that decreased to 83% ee. Finally, an allyl amine with another aryl substituent such as a naphthyl (**9-5l**) also afforded the corresponding amine **9-6l** in 97% ee.

To showcase the applicability of our methodology, here we disclose a novel, short and efficient synthesis of (*R*)-Lorcaserin, **9-8** (Scheme 9.2). We performed a gram scale enantioselective synthesis of **9-6g** applying our optimal conditions and decreasing the catalyst loading to 0.5 mol%. The compound **9-6g** was achieved with an excellent 98% ee without recrystallization. Next, we deprotected the phthalimido group with hydrazine in toluene to afford **9-7** in excellent yield (93 %). To the best of our knowledge, this is the most efficient catalytic enantioselective synthesis of intermediate **9-7**, a direct precursor of (*R*)-Lorcaserin (**9-8**).[13]

Scheme 9.2. Formal synthesis of (*R*)-Lorcaserin, **9-8**.

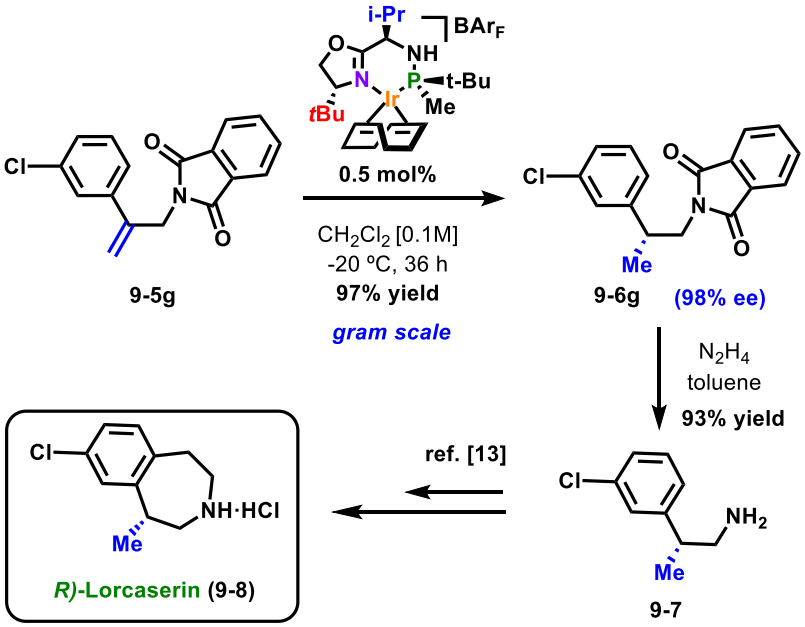

The importance of the methodology developed here can also be appreciated by using **9-6d** in the formal synthesis of OTS514 (**9-10**) (Scheme 9.3). The enantioenriched phathalimide **9-6d** was deprotected by ethanolamine at reflux and protected as *tert*-butyl carbamate. The resulting *N*-Boc amine **9-9** is a known precursor of **9-10**.[4a]

Scheme 9.3. Formal synthesis of OTS514, **9-10**.

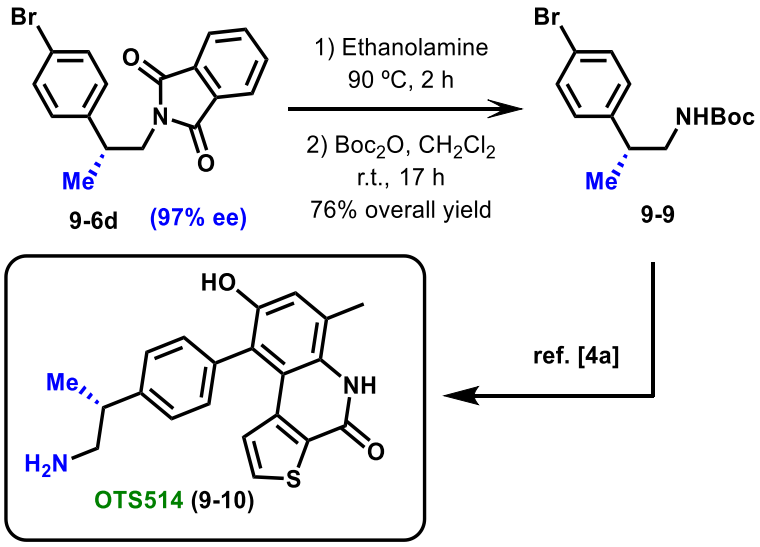

Finally, the chiral amines prepared here can be used in the synthesis of 3-methyl indolines.[14] These compounds are relevant precursors of a number of biologically active compounds and natural products such as Duocarmycins,[14a,15] the potent cytotoxic drug (+)-CC1065[14a,16] and the Akt/PBK phosphorylation inhibitor **9-12**,[17] currently in clinical phases. Thus, 3-methyl indoline **9-11** was readily prepared from amine **9-6k** (Scheme 9.4) by phthalimido deprotection followed by copper-catalyzed intramolecular Ullmann-type amination.[18]

Scheme 9-4. Enantioselective synthesis of 3-methyl indoline **9-11**.

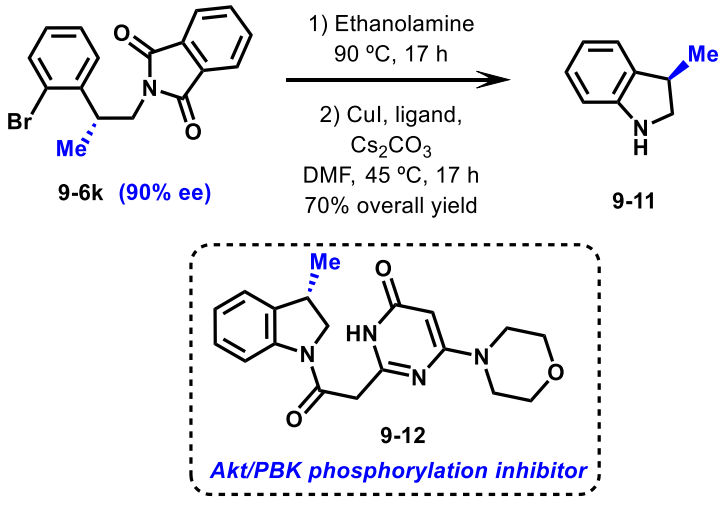

In summary, we have described a very efficient enantioselective synthesis of β-aryl propanamines by means of iridium-catalyzed asymmetric hydrogenation of *N*-phthalimido 2-aryl propanamines using the Ir-MaxPHOX complex **9-2c**. Excellent enantiomeric excess values were obtained for wide range of compounds (up to 13 examples) using low catalyst loading and low hydrogen pressure. Several direct synthetic applications of this novel and effective catalytic method have been disclosed such as a formal synthesis of (*R*)-Lorcaserin and OTS514, as well as a novel approach to enantiomerically enriched 3-methyl indolines.

References

(1) (a) Lin, G.-Q.; Zhang, J.-G.; Cheng, J.-F., Overview of chirality and chiral drugs. In Chiral Drugs, John Wiley & Sons, Inc.2011; pp 3-28. (b) Ferrer, C.; Verdaguer, X.; Riera, A., Recent advances in the metal-catalyzed stereoselective synthesis of biologically active molecules. In Catalytic Methods in Asymmetric Synthesis, John Wiley & Sons, Inc.2011; pp 625-670.

(2) (a) Omura, S. Macrolide Antibiotics, Academic Press, Orlando, FL, 1984. (b) Lazarevski, G.; Kobrehel, G.; Metelko, B.; Duddeck, H. Ring Opening Reactions of 6-Deoxy- 9-deoxo-9a-aza-9a-homoerythromycin A 6,9-Cyclic Imino Ether. *J. Antibiot.* **1996**, *49*, 1066-1069. (c) Nicholas, G. M.; Molinski, T. F. Structures of Cribochalines A and B, Branched-Chain Methoxylaminoalkyl Pyridines from the Micronesian Sponge, Cribochalina Sp. Absolute Configuration and Enantiomeric Purity of Related O-Methyl Oximes. *Tetrahedron* **2000**, *56*, 2921–2927. (d) Davies, H. M. L.; Ni, A. Enantioselective Synthesis of β-Amino Esters and Its Application to the Synthesis of the Enantiomers of the Antidepressant Venlafaxine. *Chem. Commun.* **2006**, 3110–3112. (e) Iii, R. N. H.; Stabler, R. S.; Repke, D. B.; Kress, J. M.; Walker, K. A.; Martin, R. S.; Brothers, J. M.; Ilnicka, M.; Lee, S. W.; Mirzadegan, T. Highly Potent , Non-Basic 5-HT 6 Ligands . Site Mutagenesis Evidence for a Second Binding Mode at 5-HT6 for Antagonism. *Bioorg. Med. Chem. Lett.* **2010**, *20* (11), 3436–3440. (f) Ramesh, P.; Suman, D. Asymmetric Synthetic Strategies of (*R*)-(–)-Baclofen : An Antispastic Drug. *Synlett* **2018**, 50, 211–226.

(3) For the chemistry and biology of Lorcaserin, see: (a) Smith, B. M.; Smith, J. M.; Tsai, J. H.; Schultz, J. A.; Gilson, C. A.; Estrada, S. A.; Chen, R. R.; Park, D. M.; Prieto, E. B.; Gallardo, C. S.; Sengupta, D.; Dosa, P. I.; Covel, J. A.; Ren, A.; Webb, R. R.; Beeley, N. R. A.; Martin, M.; Morgan, M.; Espitia, S.; Saldana, H. R.; Bjenning, C.; Whelan, K. T.; Grottick, A. J.; Menzaghi, F.; Thomsen, W. J. Discovery and Structure - Activity Relationship of (1R)-8-Chloro-2,3,4,5-Tetrahydro-1-Methyl-1H-3-Benzazpine (Lorcaserin), a Selective Serotonin 5-HT 2C Receptor Agonist for the Treatment of Obesity. *J. Med. Chem.* **2008**, *51*, 305–313. (b) Nikolic, D.; Toth, P. P.; Ferlita, A.; Bartolo, V. D.; Montalto, G.; Banach, M.; Rizzo, M. Novel anti-obesity drugs and plasma lipids. *Clinc. Lipidol.* **2014**, *9*, 179.

(4) (a) Nakamura, Y.; Matsuo, Y.; Hisada, S.; Walker, J. R.; Decornez, H.; Gurram, M. (OncoTherapy Science, Inc., Japan). Preparation of thieno[2,3-c]quinoline derivatives as PKB inhibitors for treating cancer. PCT/US2011/030278. October 6, **2011**. WO 2011/123419. (b) Park, J. H.; Chung, S.; Matsuo, Y.; Nakamura, Y. Development of Small Molecular Compounds Targeting Cancer Stem Cells. *Med. Chem. Commun.* **2017**, *8* (1), 73–80. (c) Park, J. H.; Inoue, H.; Kato, T.; Zewde, M.; Miyamoto, T.; Matsuo, Y.; Salgia, R.; Nakamura, Y. TOPK (T-LAK Cell-Originated Protein Kinase) Inhibitor Exhibits Growth Suppressive Effect on Small Cell Lung Cancer. *Cancer Sci.* **2017**, *108* (3), 488–496.

(5) (a) Li, X.; Tizzano, J. P.; Griffey, K.; Clay, M.; Lindstrom, T.; Skolnick, P. Antidepressant-like Actions of an AMPA Receptor Potentiator (LY392098). *Neuropharmacology* **2001**, *40* (8), 1028–1033. (b) Ornstein, P. L.; Zimmerman, D. M.; Arnold, M. B.; Bleisch, T. J.; Cantrell, B.; Simon, R.; Zarrinmayeh, H.; Baker, S. R.; Gates, M.; Tizzano, J. P. Biarylpropylsulfonamides as Novel, Potent Potentiators of 2-Amino-3-(5-Methyl-3-Hydroxyisoxazol-4-yl)-Propanoic Acid (AMPA) Receptors. *J. Med. Chem.* **2000**, *43*, 4354–4358. (c) Jones, N.; Neill, M. J. O.; Tricklebank, M.; Libri, V.; Williams, S. C. R. Examining the Neural Targets of the AMPA Receptor Potentiator LY404187 in the Rat Brain Using Pharmacological Magnetic Resonance Imaging. *Psychopharmacology* **2005**, *180*, 743–751.

(6) (a) *Catalytic Asymmetric Synthesis*, 2nd ed.; Ojima, I.; Ed.; Wiley-VCH: Weinheim, 2000. (b) *Applied Homogeneous Catalysis with Organometallic Compounds*, 2nd ed.; Cornils, B., Herrmann, W. A., Eds.; Wiley-VCH: Weinheim, 2002. (c) *Asymmetric Catalysis on Industrial Scale: Challenges, Approaches and*

Solutions. Blaser, H. U., Schmidt, E., Eds.; Wiley-VCH: Weinheim, 2004. (d) Noyori, R. Asymmetric Catalysis : Science and Opportunities. *Angew. Chem. Int. Ed.* **2002**, *41*, 2008-2022.

(7) Recent selected examples: (a) Chem, A. J.; Xu, B.; Su, C. J.; Wang, C. J.; Zhou, G. C. A Concise Synthesis of Racemic Lorcaserin. *Aust. J. Chem* **2016**, *69*, 770–774. (b) Gini, A.; Bamberger, J.; Luis-Barrera, J.; Zurro, M.; Mas-Ballesté, R.; Alemán, J.; Mancheño, O. G. Synthesis of 3-Benzazepines by Metal-Free Oxidative C–H Bond Functionalization–Ring Expansion Tandem Reaction. *Adv. Synth. Catal.* **2016**, *358* (24), 4049–4056. (c) Zhu, Q.; Wang, J.; Bian, X.; Zhang, L.; Wei, P.; Xu, Y. Novel Synthesis of Antiobesity Drug Lorcaserin Hydrochloride. *Org. Process Res. Dev.* **2015**, *19*, 6–10.

(8) (a) Wang, C.; Sun, X.; Zhang, X. Enantioselective Hydrogenation of Allylphthalimides: An Efficient Method for the Synthesis of β-Methyl Chiral Amines. *Angew. Chem. Int. Ed.* **2005**, *44*, 4933–4935. (b) Sun, X.; Zhou, L.; Li, W.; Zhang, X. Convenient Divergent Strategy for the Synthesis of TunePhos-Type Chiral Diphosphine Ligands and Their Applications in Highly Enantioselective Ru-Catalyzed Hydrogenations. *J. Org. Chem.* **2008**, *73* (3), 1143–1146. (c) Steinhuebel, D. P.; Krska, S. W.; Alorati, A.; Baxter, J. M.; Belyk, K.; Bishop, B.; Palucki, M.; Sun, Y.; Davies, I. W. Asymmetric Hydrogenation of Protected Allylic Amines. *Org. Lett.* **2010**, *12* (18), 4201–4203. (d) Cabre, A.; Verdaguer, X.; Riera, A., Enantioselective Synthesis of β-Methyl Amines via Iridium-Catalyzed Asymmetric Hydrogenation of *N*-Sulfonyl Allyl Amines. *Adv. Synth. Catal.* **2019,** *361*, 4196-4200.

(9) (a) Pfaltz, A.; Blankenstein, J.; Hilgraf, R.; Hörmann, E.; Mcintyre, S.; Menges, F.; Schönleber, M.; Smidt, S. P.; Bettina, W.; Zimmermann, N. Iridium-Catalyzed Enantioselective Hydrogenation of Olefins. *Adv. Synth. Catal.* **2003**, *345*, 33–43. (b) Verendel, J. J.; Pàmies, O.; Diéguez, M.; Andersson, P. G. Asymmetric Hydrogenation of Olefins Using Chiral Crabtree-Type Catalysts : Scope and Limitations. *Chem. Rev.* **2014**, *114*, 2130–2169. (c) Müller, M. A.; Gruber, S.; Pfaltz, A. Recovery and Recycling of Chiral Iridium (N,P Ligand) Catalysts from Hydrogenation Reactions. *Adv. Synth. Catal.* **2018**, *360* (7), 1340–1345. (d) Lu, W. J.; Chen, Y. W.; Hou, X. L. Highly Enantioselective Iridium-Catalyzed Hydrogenation of Trisubstituted Olefins, A,β-Unsaturated Ketones and Imines with Chiral Benzylic Substituted P,N Ligands. *Adv. Synth. Catal.* **2010**, *352* (1), 103–107. (e) Trifonova, A.; Diesen, J. S.; Chapman, C. J.; Andersson, P. G. Application of Phosphino-Oxazoline Ligands in Ir-Catalyzed Asymmetric Hydrogenation of Acyclic Aromatic N -Aryl Imines. *Org. Lett.* **2004**, *6* (21), 3825–3827. (f) Li, J.-Q.; Liu, J.; Krajangsri, S.; Chumnanvej, N.; Singh, T.; Andersson, P. G. Asymmetric Hydrogenation of Allylic Alcohols Using Ir–N,P-Complexes. *ACS Catal.* **2016**, *6* (12), 8342–8349.

(10) (a) Roseblade, S. J.; Pfaltz, A. Iridium-Catalyzed Asymmetric Hydrogenation of Olefins Initial Studies : An Unexpected Anion Effect. *Acc. Chem. Res.* **2007**, *40*, 1402–1411. (b) McIntyre, S.; Hörmann, E.; Menges, F.; Smidt, S. P.; Pfaltz, A. Iridium-Catalyzed Enantioselective Hydrogenation of Terminal Alkenes. *Adv. Synth. Catal.* **2005**, *347* (2–3), 282–288. (c) Mazuela, J.; Verendel, J. J.; Coll, M.; Bo, A.; Marcel, C. Iridium Phosphite - Oxazoline Catalysts for the Highly Enantioselective Hydrogenation of Terminal Alkenes. *J. Am. Chem. Soc.* **2009**, *131*, 12344–12353. (d) Pàmies, O.; Andersson, P. G. Asymmetric Hydrogenation of Minimally Functionalised Terminal Olefins : An Alternative Sustainable and Direct Strategy for Preparing Enantioenriched Hydrocarbons. *Chem. Eur. J.* **2010**, *16*, 14232–14240. (e) Woodmansee, D. H.; Pfaltz, A. Asymmetric Hydrogenation of Alkenes Lacking Coordinating Groups. *Chem. Commun.* **2011**, *47* (28), 7912–7916. (f) Mazuela, J.; Pàmies, O. Expanded Scope of the Asymmetric Hydrogenation of Minimally Functionalized Olefins Catalyzed by Iridium Complexes with Phosphite – Thiazoline Ligands. *ChemCatChem* **2013**, *5*, 2410–2417 (g) Patureau, F. W.; Worch, C.; Siegler, M. A.; Spek, A. L.; Bolm, C.; Reek, J. N. H., SIAPhos: Phosphorylated Sulfonimidamides and their Use in Iridium-Catalyzed Asymmetric Hydrogenations of Sterically Hindered Cyclic Enamides. *Adv. Synth. Catal.* **2012,** *354*, 59-64.

(11) (a) Cristóbal-Lecina, E.; Etayo, P.; Doran, S.; Revés, M.; Martín-Gago, P.; Grabulosa, A.; Costantino, A. R.; Vidal-Ferran, A.; Riera, A.; Verdaguer, X. MaxPHOS Ligand: PH/NH Tautomerism and Rhodium-Catalyzed Asymmetric Hydrogenations. *Adv. Synth. Catal.* **2014**, *356* (4), 795–804. (b) Orgué, S.; Flores-Gaspar, A.; Biosca, M.; Pàmies, O.; Diéguez, M.; Riera, A.; Verdaguer, X. Stereospecific SN2@P Reactions: Novel Access to Bulky P-Stereogenic Ligands. *Chem. Commun.* **2015**, *51* (99), 17548–17551. (c) Salomó, E.; Orgué, S.; Riera, A.; Verdaguer, X. Efficient Preparation of (S)- and (R)- Tert -Butylmethylphosphine-Borane: A Novel Entry to Important P-Stereogenic Ligands. *Synthesis* **2016**, *48* (16), 2659–2663. (d) Prades, A.; Núñez-Pertíñez, S.; Riera, A.; Verdaguer, X. P-Stereogenic Bisphosphines with a Hydrazine Backbone: From N-N Atropoisomerism to Double Nitrogen Inversion. *Chem. Commun.* **2017**, *53* (33), 4605–4608. (e) Salomó, E.; Prades, A.; Riera, A.; Verdaguer, X. Dialkylammonium tert-Butylmethylphosphinites: Stable Intermediates for the Synthesis of P-Stereogenic Ligands. *J. Org. Chem.* **2017**, *82* (13), 7065–7069. (f) Téllez, J.; Gallen, A.; Ferrer, J.; Lahoz, F. J.; García-Orduña, P.; Riera, A.; Verdaguer, X.; Carmona, D.; Grabulosa, A. Half-Sandwich Complexes of Ir(III), Rh(III) and Ru(II) with the MaxPhos Ligand: Metal Centred Chirality and Cyclometallation. *Dalt. Trans.* **2017**, *46* (45), 15865–15874. (g) Gallen, A.; Orgué, S.; Muller, G.; Escudero-Adán, E. C.; Riera, A.; Verdaguer, X.; Grabulosa, A. Synthesis and Coordination Chemistry of Enantiopure: *tert*-BuMeP(O)H. *Dalt. Trans.* **2018**, *47* (15), 5366–5379.

(12) (a) Salomó, E.; Orgué, S.; Riera, A.; Verdaguer, X. Highly Enantioselective Iridium-Catalyzed Hydrogenation of Cyclic Enamides. *Angew. Chem. Int. Ed.* **2016**, *55* (28), 7988–7992. (b) Salomó, E.; Rojo, P.; Hernández-Lladó, P.; Riera, A.; Verdaguer, X. P-Stereogenic and Non-P-Stereogenic Ir-MaxPHOX in the Asymmetric Hydrogenation of N -Aryl Imines. Isolation and X-Ray Analysis of Imine Iridacycles. *J. Org. Chem.* **2018**, *83* (8), 4618–4627. (c) Salomó, E.; Gallen, A.; Sciortino, G.; Ujaque, G.; Grabulosa, A.; Lledós, A.; Riera, A.; Verdaguer, X. Direct Asymmetric Hydrogenation of N-Methyl and N-Alkyl Imines with an Ir(III)H Catalyst. *J. Am. Chem. Soc.* **2018**, *140* (49), 16967–16970. (d) Cabré, A.; Khaizourane, H.; Garçon, M.; Verdaguer, X.; Riera, A. Total Synthesis of (*R*)-Sarkomycin Methyl Ester via Regioselective Intermolecular Pauson-Khand Reaction and Iridium-Catalyzed Asymmetric Isomerization. *Org. Lett.* **2018**, *20* (13), 3953–3957. (e) Biosca, M.; Salomó, E.; De La Cruz-Sánchez, P.; Riera, A.; Verdaguer, X.; Pàmies, O.; Diéguez, M. Extending the Substrate Scope in the Hydrogenation of Unfunctionalized Tetrasubstituted Olefins with Ir-P Stereogenic Aminophosphine-Oxazoline Catalysts. *Org. Lett.* **2019**, *21* (3), 807–811.

(13) Smilovic, I. G.; Cluzeau, J.; Richter, F.; Nerdinger, S.; Schreiner, E.; Laus, G.; Schottenberger, H. Synthesis of Enantiopure Antiobesity Drug Lorcaserin. *Bioorg. Med. Chem.* **2018**, *26* (9), 2686–2690.

(14) (a) Boger, D. L.; Boyce, C. W.; Garbaccio, R. M.; Goldberg, J. A. CC-1065 and the Duocarmycins: Synthetic Studies. *Chem. Rev.* **1997**, *97* (3), 787–828. (b) Kuwano, R.; Kaneda, K.; Ito, T.; Sato, K.; Kurokawa, T.; Ito, Y. Highly Enantioselective Synthesis of Chiral 3-Substituted Indolines by Catalytic Asymmetric Hydrogenation of Indoles. *Org. Lett.* **2004**, *6* (13), 2213–2215. (c) Groth, U.; Köttgen, P.; Langenbach, P.; Lindenmaier, A.; Schütz, T.; Wiegand, M. Enantioselective Synthesis of 3,3-Disubstituted Indolines via Asymmetric Intramolecular Carbolithiation in the Presence of (-)-Sparteine 1. *Synlett* **2008**, No. 9, 1301–1304. (d) Sieber, J. D.; Rivalti, D.; Herbage, M. A.; Masters, J. T.; Fandrick, K. R.; Fandrick, D. R.; Haddad, N.; Lee, H.; Yee, N. K.; Gupton, B. F.; Senanayake, C. H. Rh-Catalysed Asymmetric Conjugate Addition of Boronic Acids to Nitroalkenes Employing a: P -Chiral P,π-Hybrid Ligand. *Org. Chem. Front.* **2016**, *3* (9), 1149–1153.

(15) Yamada, K.; Kurokawa, T.; Tokuyama, H.; Fukuyama, T. Total Synthesis of the Duocarmycins. *J. Am. Chem. Soc.* **2003**, *125* (22), 6630–6631.

(16) Glennon, R. A. Central Serotonin Receptors as Targets for Drug Research. *J. Med. Chem.* **1987**, *30* (1), 1–12.

(17) Certal, V.; Carry, J. C.; Halley, F.; Virone-Oddos, A.; Thompson, F.; Filoche-Rommé, B.; El-Ahmad, Y.; Karlsson, A.; Charrier, V.; Delorme, C.; Ray, A.; Abecassis, P.-Y.; Amara, C.; Vincent, L.; Bonneveaux, H.; Nicolas, J.-P.; Mathieu, M.; Bertrand, T.; Marquette, J.-P.; Michot, N.; Benard, T.; Perrin, M.-A.; Lemaitre, O.; Guerif, S.; Perron, S.; Monget, S.; Gruss-Leleu, F.; Doerflinger, G.; Guizani, H.; Brollo, M.; Delbarre, L.; Bertin, L.; Richepin, P.; Loyau, V.; Garcia-Echevarria, C.; Lengauer, C.; Schio, L. Discovery and Optimization of Pyrimidone Indoline Amide PI3Kβ Inhibitors for the Treatment of Phosphatase and Tensin Homologue (PTEN)-Deficient Cancers. *J. Med. Chem.* **2014**, *57* (3), 903–920.

(18) Shafir, A.; Buchwald, S. L. Highly Selective Room-Temperature Copper-Catalyzed C-N Coupling Reactions. *J. Am. Chem. Soc.* **2006**, *128* (27), 8742–8743.

Experimental Part

General procedures and materials

Unless otherwise indicated, materials were obtained from commercial suppliers and used without further purification. All reactions that required anhydrous conditions were performed in dried glassware under a dry nitrogen atmosphere. Dichloromethane and THF were degassed and dried with a solvent purification system (SPS PS-MD-3). Anhydrous dichloroethane and DMF were used from Sigma Aldrich. Solvents were removed under reduced pressure with a rotary evaporator. Silica gel chromatography was performed using an automated chromatography system (PuriFlash® 430, Interchim).

Instrumentation

NMR spectroscopy: ^{1}H and ^{13}C were recorded on the NMR spectrometers of the *Centres Científics i Tecnològics de la Universitat de Barcelona*. The employed spectrometers were a Varian Mercury 400 MHz. Chemical shifts (δ) were referenced to internal solvent resonances and reported relative to TMS (tetramethylsilane). The coupling constants (*J*) are reported in Hertz (Hz). The following abbreviations are used to define multiplicities: s (singlet), d (doublet), t (triplet), q (quartet), dd (doublet of doublets), ddd (doublet of doublet of doublets), ddd (doublet of doublet of triplets), dddd (doublet of doublet of doublet of doublets), dt (doublet of triplets), td (triplet of doublets), ddq (doublet of doublet of quartets), dtd (doublet of triplet of doublets), dq (doublet of quartets), tt (triplet of triplets), qt (quartet of triplets), m (multiplet), br s (broad signal).

High Resolution Mass Spectrometry: High resolution ESI-MS spectra were recorded in an LC/MSD-TOF G1969A (Agilent Technologies) of the *Centres Científics i Tecnològics de la Universitat de Barcelona.*

IR spectroscopy: IR spectra were measured in a Thermo Nicolet 6700 FT-IR spectrometer using an ATR system, of the Department of Organic Chemistry in the Universitat de Barcelona.

Optical rotations were measured at room temperature (25°C) using a Jasco P-2000 iRM- 800 polarimeter. Concentration is expressed in g/100 mL. The cell sized 10 cm long and had 1 mL of capacity, measuring λ was 589 nm, which corresponds to a sodium lamp.

Melting points were determined using a Büchi melting point apparatus and were not corrected.

Experimental procedures.

Synthesis of catalyst MaxPHOX 9-2c

Following the experimental procedure described in the literature[1], catalysts were afforded after 4 synthetic steps.

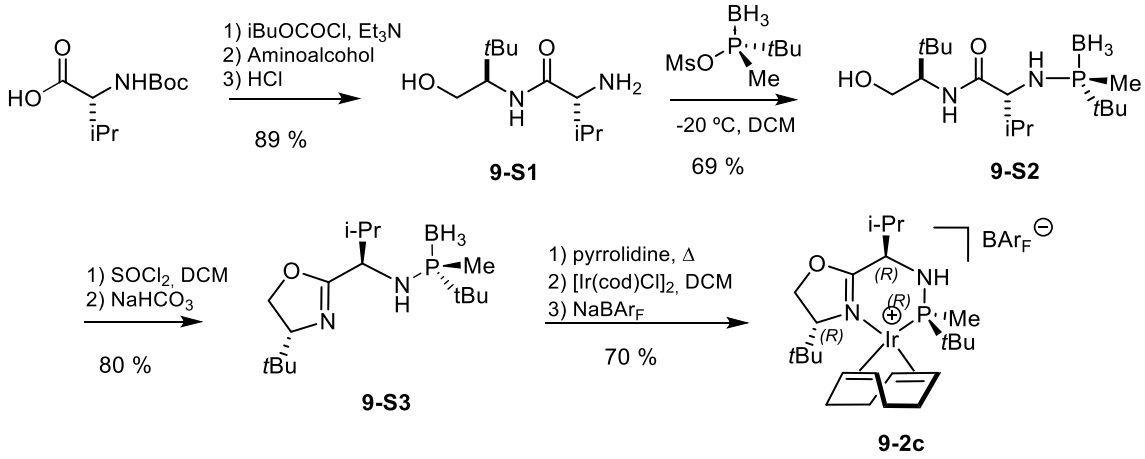

((*R*)-2-amino-N-((*R*)-1-hydroxy-3,3-dimethylbutan-2-yl)-3-methylbutanamide, 9-S1

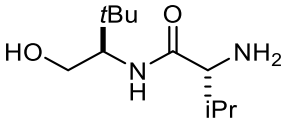

Et_3N (2 eq) and isobutylchloroformate (1.1 equiv) were slowly added to a solution of the N-Boc-protected aminoacid (1 eq, 28 mmol) in THF (0.13 M) at –30 ºC (white solid was observed when adding *i*BuOCOCl). The reaction mixture was stirred for 45 min at –30 ºC, and then the corresponding aminoalcohol (1.1 equiv) was added. The resulting mixture was left stirring at room temperature overnight. Then the THF was removed under reduced pressure and the oily solid was dissolved in H_2O and EtOAc. The phases were separated and the aqueous layer was extracted twice with EtOAc. The organic layers were combined, dried over $MgSO_4$ and the solvent evaporated under reduced pressure. The crude obtained was dissolved in a 1:1 mixture of MeOH and HCl (3 M, aq) (0.1 M) and stirred overnight at room temperature. The MeOH was removed under vacuum and the resulting aqueous phase was extracted with EtOAc twice to remove impurities. Then EtOAc was added over the aqueous phase and it was basified using NaOH (40%, aq) at 0 ºC. The layers were separated and the aqueous phase was extracted thrice with EtOAc. The organic phases were combined, dried over $MgSO_4$ and the solvent was removed under reduced pressure to yield the deprotected aminoalcohol **9-S1** as a white solid (5.52 g, 89% yield). This was used on the next step without further purification.

m.p. 87 - 91 ºC. **$[\alpha]_D^{25}$**: +36 (c 0.7, $CHCl_3$). **^{1}H NMR** ($CDCl_3$, 400 MHz) δ: 7.80 (d, *J* = 8.4 Hz, 1H), 3.90 (ddd, *J* = 11.0, 3.1, 0.6 Hz, 1H), 3.76 (td, *J* = 8.6, 3.1 Hz, 1H), 3.54 (ddd, *J* = 11.0, 8.6, 0.6 Hz, 1H), 3.33 (d, *J* = 3.6 Hz, 1H), 2.42 – 2.31 (m, 1H), 1.99 (s, 2H), 1.02 (d, *J* = 7.0 Hz, 3H), 0.97 (s, 9H), 0.83 (d, *J* = 6.9 Hz, 3H) ppm. **^{13}C NMR** (101 MHz, $CDCl_3$) δ: 176.3, 64.3, 60.3, 33.2, 30.6, 27.1, 19.9, 16.1 ppm. **HRMS** (ESI) calculated for $C_{11}H_{25}N_2O_2$ 217.1911, found 217.1917 $[M+H]^+$. **IR** (ATR-FTIR) ν_{max} = 3324, 3292, 2953, 2869, 1650, 1629, 1537 cm^{-1}.

[1] (a) León, T.; Riera, A.; Verdaguer, X. *J. Am. Chem. Soc.* **2011**, *133*, 5740-5743. (b) Orgué, S.; Flores, A.; Biosca, M.; Pàmies, O.; Diéguez, M.; Riera, A.; Verdaguer, X. *Chem. Commun.* **2015**, *51*, 17548-17551. (c) E. Salomó, S. Orgué, A. Riera, X. Verdaguer, *Angew. Chem. Int. Ed.* **2016**, *55*, 7988-7992.

(*R*)-2-(((*S*)-*tert*-butyl(methyl)phosphanyl)amino)-N-((*R*)-1-hydroxy-3,3-dimethylbutan-2-yl)-3-methylbutanamide borane, 9-S2

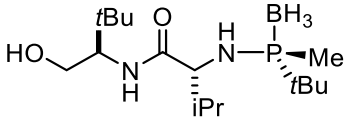

A solution of optically pure *tert*-butyl(methyl)phosphinous acid borane (1 equiv, 9.14 mmol) and methansulfonic anhydride (1.2 equiv) in CH_2Cl_2 (0.2M) was cooled to –20 ºC. To this solution, anhydrous NEt_3 (2.5 eq) was slowly added, and the mixture was stirred 1 h at –20 ºC. The corresponding amine (1.5 equiv) was then added and the solution was stirred overnight at –20 ºC. Water was added and the mixture was allowed to warm to room temperature. The organic layer was separated and the aqueous phase was extracted twice with CH_2Cl_2. The combined extracts were washed with brine and concentrated under reduced pressure. Purification by column chromatography (SiO_2, hexanes:EtOAc) yielded **9-S2** as a white solid (2.06 g, 69% yield). This was used on the next step without further purification.

m.p. 150-152 ºC. **[α]$_D^{25}$**: +27 (c 0.8, $CHCl_3$). **^{1}H NMR** (400 MHz, $CDCl_3$) δ 6.07 (d, *J* = 8.8 Hz, 1H), 3.87 (dd, *J* = 11.2, 3.1 Hz, 1H), 3.79 (ddd, *J* = 8.9, 7.7, 3.1 Hz, 1H), 3.58 (dd, *J* = 11.2, 7.7 Hz, 2H), 2.15 (s, 1H), 2.12 – 2.05 (m, 1H), 1.36 (d, *J* = 8.9 Hz, 3H), 1.14 (d, *J* = 14.1 Hz, 9H), 1.00 (d, *J* = 6.8 Hz, 3H), 0.97 (s, 9H), 0.93 (d, *J* = 6.9 Hz, 3H). **^{13}C NMR** (101 MHz, $CDCl_3$) δ 174.5, 110.2, 63.7, 62.8, 60.4, 33.3, 32.8, 32.7, 31.1, 30.7, 27.2, 24.7, 24.7, 19.7, 17.9, 10.7, 10.3. **^{31}P NMR** (202 MHz, $CDCl_3$) δ 71.0 – 71.0 (m, P-BH_3) ppm. **HRMS** (ESI) calculated for $C_{16}H_{39}BN_2O_2P$ 333.2842, found 333.2849 $[M+H]^+$. **IR** (ATR-FTIR) ν_{max} = 3312, 3244, 2960, 2861, 2367, 2328, 1644, 1556, 1366, 1067, 1052 cm^{-1}.

(*S*)-1-*tert*-butyl-N-((*R*)-1-((*R*)-4-(tert-butyl)-4,5-dihydrooxazol-2-yl)-2-methylpropyl)-1-methylphosphanamine borane, 9-S3

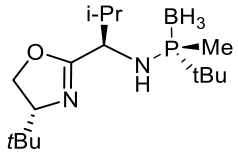

The corresponding aminophosphane (1 eq, 4.0 mmol) was dissolved in CH_2Cl_2 (0.08 M) and $SOCl_2$ (2.4 equiv) was added drop wise at 0 ºC. The solution was stirred 4 h at room temperature. The solution was then cooled down to 0 ºC and $NaHCO_3$ saturated aqueous solution was added slowly until pH 8-9. The mixture was left stirring for 15 min at room temperature. The two phases were separated and the aqueous phase was extracted twice with CH_2Cl_2. The combined organic layers were washed with brine. The organic layer was dried over $MgSO_4$ and concentrated on a rotary evaporator under reduced pressure. Purification by column chromatography (SiO_2, hexanes:EtOAc of increasing polarities 90:10 to 60:40) yielded the desired product **9-S3** as an oil (1.02 g, 81% yield).

[α]$_D^{25}$: +28 (c 0.6, $CHCl_3$). **^{1}H NMR** ($CDCl_3$, 400 MHz) δ 4.22 (dd, *J* = 10.2, 8.7 Hz, 1H), 4.06 (t, *J* = 8.6 Hz, 1H), 3.95 (dt, *J* = 10.0, 5.0 Hz, 1H), 3.84 (ddd, *J* = 10.2, 8.5, 0.7 Hz, 1H), 2.35 (d, *J* = 10.0 Hz, 1H), 2.00 (dtd, *J* = 13.8, 6.9, 4.6 Hz, 1H), 1.33 (d, *J* = 9.0 Hz, 3H), 1.14 (d, *J* = 14.0 Hz, 9H), 0.94 (d, *J* = 6.8 Hz, 3H), 0.90 (s, 9H), 0.89 (d, *J* = 6.9 Hz, 4H). **^{13}C NMR** (101 MHz, $CDCl_3$) δ 75.5, 69.1, 56.7 (d, *J* = 2.6 Hz), 33.6 (d, *J* = 2.9 Hz), 33.5, 31.3 (d, *J* = 37.8 Hz), 25.9, 24.6 (d, *J* = 3.2 Hz), 18.6, 17.7, 10.6 (d, *J* = 42.2 Hz). **^{31}P NMR** (202 MHz, $CDCl_3$) δ 70.5 – 69.5 (m, P-BH_3) ppm. **HRMS** (ESI) calculated for $C_{16}H_{37}BN_2OP$ 315.2731, found 315.2742 $[M+H]^+$. **IR** (ATR-FTIR) ν_{max} = 3332, 2958, 2865, 2390, 2368, 2336, 1668, 1464, 1357, 1137 cm^{-1}.

Catalyst 9-2c

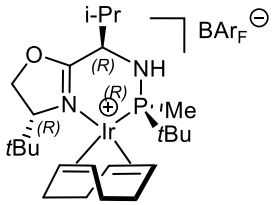

The corresponding borane protected ligand (1 eq, 0.16 mmol) was dissolved in freshly distilled pyrrolidine (0.06 M) and stirred for 16 h, heating at 90 ºC in an oil bath. Afterwards, pyrrolidine was removed *in vacuo*. When no pyrrolidine remained, the crude was further dried under vacuum for 30 min at 50 ºC in an oil bath (the crude was under N_2 during all the procedure). A solution of $[Ir(COD)(Cl)]_2$ (0.5 equiv) in CH_2Cl_2 (0.06 M) was added to the free ligand via cannula. The resulting mixture was stirred for 40 min at room temperature. $NaBAr_F$ (1 eq) was then added and the solution was stirred 1 h more at room temperature. The resulting crude was filtered through a small plug of silica gel, (first washed with Et_2O) under N_2, eluting with hexanes:CH_2Cl_2 (50-100%). The intense orange fraction was collected and concentrated to yield the corresponding Ir complex **9-2c** was obtained as an orange solid (162 mg, 70% yield).

m. p. 228 - 230 ºC (descomposition). **[α]$_D^{25}$**: -76 (c 0.3, $CHCl_3$). **^{1}H NMR** ($CDCl_3$, 400 MHz) δ 7.71 (s, 5H), 7.53 (s, 4H), 4.87 (s, 1H), 4.59 (dd, *J* = 9.7, 3.4 Hz, 2H), 4.44 (p, *J* = 7.3 Hz, 1H), 4.25 (t, *J* = 9.7 Hz, 1H), 3.92 (dd, *J* = 9.1, 3.4 Hz, 2H), 3.28 (ddd, *J* = 25.2, 9.3, 7.0 Hz, 1H), 2.46 (dd, *J* = 15.6, 7.9 Hz, 1H), 2.40 – 2.17 (m, 4H), 2.16 – 2.04 (m, 2H), 1.91 (dt, *J* = 13.9, 9.0 Hz, 1H), 1.57 (d, *J* = 6.3 Hz, 3H), 1.52 – 1.42 (m, 2H), 1.17 – 1.06 (m, 12H), 1.00 (s, 9H), 0.88 (d, *J* = 6.7 Hz, 3H). **^{13}C NMR** (101 MHz, $CDCl_3$) δ 175.3, 162.6, 162.1, 161.6, 161.1, 134.9, 129.5, 129.5, 129.2, 129.2, 128.9, 128.8, 128.6, 128.6, 126.1, 123.4, 117.7, 117.6, 117.6, 117.6, 93.1, 92.9, 88.2, 88.1, 72.4, 71.1, 63.4, 59.2, 56.3, 38.8, 38.8, 37.8, 37.7, 36.1, 35.7, 34.2, 33.3, 33.3, 28.9, 25.9, 25.9, 25.4, 24.4, 24.3, 21.4, 18.34 16.5, 16.2. **^{31}P NMR** (202 MHz, $CDCl_3$) δ 53.8 ppm. **HRMS** (ESI) calculated for $C_{24}H_{45}N_2OPIr$ 601.2893, found 601.2914 $[M+H]^+$. **IR** (ATR-FTIR) ν_{max} = 3430, 2961, 1624, 1612, 1352, 1273, 1157, 1119, 1094 cm^{-1}.

Experimental procedures for the preparation of substrates.

Synthesis of 2-aryl-substituted N-allyl phthalimides, 9-5

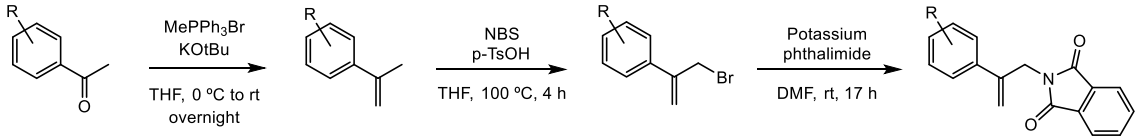

Step 1. In an oven dried flask, methyl triphenylphosphonium bromide (1.2 equiv.) was taken and to this anhydrous THF (1.6 mL/mmol) was added. The suspension was cooled to 0 ºC, KOtBu (1.2 equiv.) was added and the resulting yellow suspension was stirred at 0 ºC for 45 min. To this suspension, a solution of ketone (1.0 equiv.) in THF (0.7 mL/mmol) was added dropwise and the resulting mixture was warmed gradually to r.t. and stirred at r.t. for 16 hours. Afterwards, the reaction mixture was concentrated and redissolved with hexanes. The crude was filtered by a plug of silica and washed (x3) with hexanes, to afford the desired product which was used for the next step without further purification.

Step 2. In an oven dried flask the alkene (1 equiv.) was dissolved in THF (3 mL/mmol). To the resulting solution, NBS (1.05 equiv.) and p-TsOH (0.1 equiv.) were added and the solution was refluxed in an oil bath for 4 hours at 100ºC. Afterwards, the reaction mixture was cooled to room

temperature and taken up with Hexane (15 mL/mmol), washed three times with H_2O (15 mL x 3) and the organic layer dried over $MgSO_4$. The solvent was removed in vacuum and an oil was obtained which was used for the next step without further purification.[2]
Step 3. Potassium phthalimide (1.1 equiv.) was added to a solution of the α-bromo alkene (1 equiv.) in DMF (2.76 mL/mmol) at room temperature. The resulting mixture was stirred for 18 hours. Afterwards, DCM (30 mL) was added and the mixture poured onto water (100 mL). The aqueous phase was separated and extracted with DCM for three times. The combined organic extract was then washed with NaOH aq. (0,2 M) and dried over $MgSO_4$. The solvent was removed in vacuum and the residue purified by column chromatography using hexanes:EtOAc 90:10 to 70:30 as eluent, to afford the protected product as white solid. [3] The purity is 100% for all compounds, unless otherwise indicated.
For the synthesis of the following compounds, 1 g of ketone was used as starting material in all cases.

2-(2-phenylallyl)isoindoline-1,3-dione, 9-5a

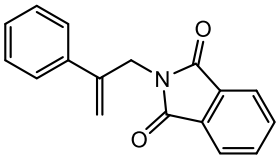

White solid (790 mg, 50% yield), purified by flash chromatography using hexanes:EtOAc 70:30. **^{1}H NMR** (400 MHz, $CDCl_3$) δ 7.85 (dd, *J* = 5.4, 3.1 Hz, 2H), 7.71 (dd, *J* = 5.5, 3.0 Hz, 2H), 7.52 – 7.48 (m, 2H), 7.37 – 7.28 (m, 2H), 5.44 (t, *J* = 0.9 Hz, 1H), 5.16 (t, *J* = 1.6 Hz, 1H), 4.71 (t, *J* = 1.3 Hz, 2H). The analytical data for this compound were in excellent agreement with the reported data.[4]

2-(2-(4-fluorophenyl)allyl)isoindoline-1,3-dione, 9-5b

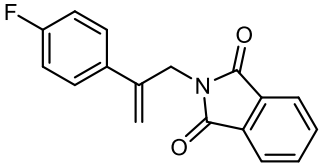

White solid at 96% of purity (696 mg, 34% yield), by flash chromatography using hexanes:EtOAc 70:30. **^{1}H NMR** (400 MHz, $CDCl_3$) δ 7.84 (dd, *J* = 5.5, 3.0 Hz, 2H), 7.74 – 7.69 (m, 2H), 7.49 – 7.43 (m, 2H), 7.05 – 6.98 (m, 2H), 5.39 (s, 1H), 5.19 – 5.16 (m, 1H), 4.67 (t, *J* = 1.3 Hz, 2H). The analytical data for this compound were in excellent agreement with the reported data.[4]

2-(2-(4-chlorophenyl)allyl)isoindoline-1,3-dione, 9-5c

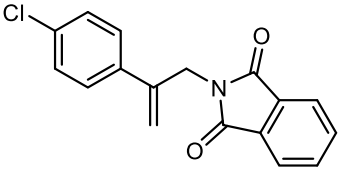

White solid at 98% of purity (845 mg, 44% yield), by flash chromatography using hexanes:EtOAc 70:30. **^{1}H NMR** (400 MHz, $CDCl_3$) δ 7.87 – 7.81 (m, 2H), 7.75 – 7.69 (m, 2H), 7.45 – 7.40 (m, 2H), 7.33 – 7.27 (m, 2H), 5.44 – 5.42 (m, 1H), 5.22 (t, *J* = 1.6 Hz, 1H), 4.67 (dd, *J* = 1.5, 1.0 Hz, 2H). The analytical data for this compound were in excellent agreement with the reported data.[4]

[2] Tripathi, C. B.; Mukherjee, S. *Org. Lett.* **2014**, *16* (12), 3368-3371.
[3] Fort, D. A.; Woltering, T. J.; Bach, T. *Chem. Commun.* **2013**, *49*, 2989-2991.
[4] Wei, Y.; Liang, F.; Zhang, X. *Org. Lett.* **2013**, *15* (20), 5186-5189.

2-(2-(4-bromophenyl)allyl)isoindoline-1,3-dione, 9-5d

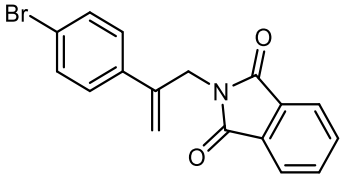

White solid (608 mg, 35% yield) purified by flash chromatography using hexanes:EtOAc 70:30. **^{1}H NMR** (400 MHz, $CDCl_3$) δ 7.84 (dd, *J* = 5.4, 3.1 Hz, 2H), 7.71 (dd, *J* = 5.5, 3.0 Hz, 2H), 7.48 – 7.43 (m, 2H), 7.39 – 7.35 (m, 2H), 5.44 (d, *J* = 1.1 Hz, 1H), 5.23 (t, *J* = 1.5 Hz, 1H), 4.67 (dd, *J* = 1.5, 1.0 Hz, 2H). The analytical data for this compound were in excellent agreement with the reported data.[5]

2-(2-(4-iodophenyl)allyl)isoindoline-1,3-dione, 9-5e

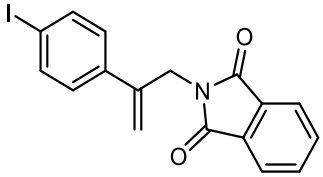

White solid (620 mg, 39% yield) purified by flash chromatography using hexanes:EtOAc 70:30. **m.p.** 178-181°C. **^{1}H NMR** (400 MHz, $CDCl_3$) δ 7.87 – 7.79 (m, 2H), 7.74 – 7.68 (m, 2H), 7.65 (dq, *J* = 8.1, 1.6, 1.2 Hz, 2H), 7.25 – 7.21 (m, 2H), 5.44 (s, 1H), 5.22 (d, *J* = 1.6 Hz, 1H), 4.66 (p, *J* = 0.8 Hz, 2H). **^{13}C NMR** (101 MHz, $CDCl_3$) δ 168.1, 141.8, 138.1, 137.7, 134.2, 132.1, 128.4, 123.6, 115.2, 93.9, 41.4. **HRMS** (ESI) calculated for $C_{17}H_{12}INO_2$ 389.9985, found 389.9988 $[M+H]^+$. **IR** (ATR-FTIR) ν_{max} = 1766, 1703, 1390, 1110 cm^{-1}.

2-(2-(p-tolyl)allyl)isoindoline-1,3-dione, 9-5f

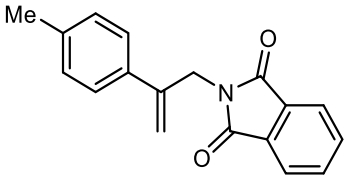

White solid (679 mg, 33% yield) purified by flash chromatography using hexanes:EtOAc 70:30. **^{1}H NMR** (400 MHz, $CDCl_3$) δ 7.86 – 7.82 (m, 2H), 7.71 (dd, *J* = 5.5, 3.1 Hz, 2H), 7.42 – 7.38 (m, 2H), 7.17 – 7.11 (m, 2H), 5.41 (d, *J* = 1.4 Hz, 1H), 5.14 – 5.07 (m, 1H), 4.69 (t, *J* = 1.4 Hz, 2H), 2.33 (s, 3H). The analytical data for this compound were in excellent agreement with the reported data.[4]

2-(2-(3-chlorophenyl)allyl)isoindoline-1,3-dione, 9-5g

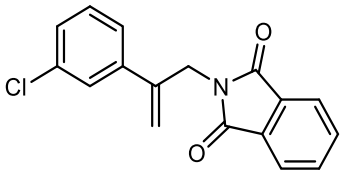

White solid (584 mg, 30% yield) purified by flash chromatography using hexanes:EtOAc 70:30. **m.p.** 122-124 °C. **^{1}H NMR** (400 MHz, $CDCl_3$) δ 7.85 – 7.77 (m, 2H), 7.70 – 7.64 (m, 2H), 7.45 (dt, *J* = 2.5, 1.0 Hz, 1H), 7.35 (ddd, *J* = 6.3, 2.8, 1.7 Hz, 1H), 7.26 – 7.21 (m, 2H), 5.42 (d, *J* = 1.1 Hz, 1H), 5.18 (t, *J* = 1.6 Hz, 1H), 4.64 (t, *J* = 1.4 Hz, 2H). **^{13}C NMR** (101 MHz, $CDCl_3$) δ 167.8, 141.3, 140.3, 134.4, 134.1, 131.9, 129.6, 128.1, 126.7, 124.5, 123.4, 115.2, 41.2. **HRMS** (ESI) calculated for $C_{17}H_{12}ClNO_2$ 298.0629, found 298.0631 $[M+H]^+$. **IR** (ATR-FTIR) ν_{max} = 3029, 2927, 1775, 1709, 1390 cm^{-1}.

[5] Jaganathan, A.; Garzan, A.; Whitehead, D.C.; Staples, R.J.; Borhan, B. *Angew. Chem. Int. Ed.* **2011**, *50* (11), 2593-2596.

2-(2-(3-methoxyphenyl)allyl)isoindoline-1,3-dione, 9-5h

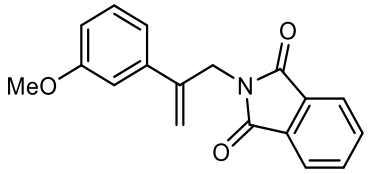

White solid at 96% of purity (834mg, 43% yield), by flash chromatography using hexanes:EtOAc 70:30. **^{1}H NMR** (400 MHz, $CDCl_3$) δ 7.84 (dd, *J* = 5.5, 3.0 Hz, 2H), 7.71 (dd, *J* = 5.4, 3.0 Hz, 2H), 7.25 – 7.22 (m, 1H), 7.09 (ddd, *J* = 7.7, 1.7, 1.0 Hz, 1H), 7.06 – 7.02 (m, 1H), 6.83 (ddd, *J* = 8.2, 2.6, 0.9 Hz, 1H), 5.45 (q, *J* = 1.0 Hz, 1H), 5.17 (t, *J* = 1.6 Hz, 1H), 4.69 (t, *J* = 1.3 Hz, 2H), 3.82 (s, 3H). The analytical data for this compound were in excellent agreement with the reported data.[5]

2-(2-(2-methoxyphenyl)allyl)isoindoline-1,3-dione, 9-5i

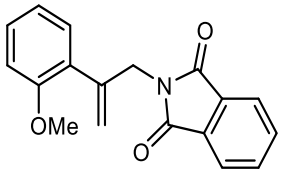

White solid (479 mg, 25% yield) purified by flash chromatography using hexanes:EtOAc 70:30. **^{1}H NMR** (400 MHz, $CDCl_3$) δ 7.81 (ddd, *J* = 5.5, 3.2, 0.4 Hz, 2H), 7.69 (ddd, *J* = 5.7, 2.9, 0.4 Hz, 2H), 7.26 – 7.21 (m, 1H), 7.15 (dd, *J* = 7.6, 1.8 Hz, 1H), 6.89 – 6.83 (m, 2H), 5.26 – 5.21 (m, 1H), 5.19 (dt, *J* = 1.3, 0.7 Hz, 1H), 4.71 (t, *J* = 1.3 Hz, 2H), 3.86 (s, 3H). The analytical data for this compound were in excellent agreement with the reported data.[6]

2-(2-(o-tolyl)allyl)isoindoline-1,3-dione, 9-5j

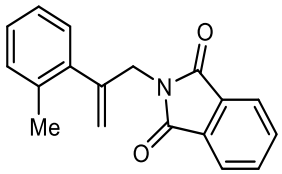

White solid (579 mg, 28% yield) purified by flash chromatography using hexanes:EtOAc 70:30. **m.p.** 102-105 ºC. **^{1}H NMR** (400 MHz, $CDCl_3$) δ 7.85 (dd, *J* = 5.4, 3.0 Hz, 2H), 7.72 (dd, *J* = 5.4, 3.0 Hz, 2H), 7.22 – 7.08 (m, 4H), 5.19 (td, *J* = 1.8, 0.9 Hz, 1H), 5.03 (q, *J* = 1.4 Hz, 1H), 4.49 (t, *J* = 1.6 Hz, 2H), 2.40 (s, 3H). **^{13}C NMR** (101 MHz, $CDCl_3$) δ 167.8 , 143.5, 135.6, 134.0, 132.0, 130.2, 128.7, 127.6, 125.5, 123.3, 114.3, 42.8, 19.6. **HRMS** (ESI) calculated for $C_{18}H_{15}NO_2$ 278.1176, found 278.1175 $[M+H]^+$. **IR** (ATR-FTIR) ν_{max} = 3461, 3018, 2926, 2850, 1770, 1709, 1415, 1388, 1113 cm^{-1}.

2-(2-(2-bromophenyl)allyl)isoindoline-1,3-dione, 9-5k

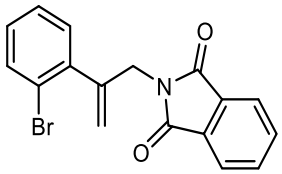

White solid (635 mg, 37% yield) purified by flash chromatography using hexanes:EtOAc 70:30. **m.p.** 120-122 ºC. **^{1}H NMR** (400 MHz, $CDCl_3$) δ 7.86 – 7.80 (m, 2H), 7.74 – 7.68 (m, 2H), 7.58 – 7.54 (m, 1H), 7.25 – 7.18 (m, 2H), 7.13 (ddd, *J* = 7.9, 6.8, 2.3 Hz, 1H), 5.38 (td, *J* = 1.5, 0.7 Hz, 1H), 5.16 (q, *J* = 1.0 Hz, 1H), 4.62 (t, *J* = 1.3 Hz, 2H).. **^{13}C NMR** (101 MHz, $CDCl_3$) δ 167.7, 143.5, 140.8, 133.9, 132.7, 132.0, 130.6, 129.2, 127.2, 123.3, 122.3, 117.3, 42.4. **HRMS** (ESI) calculated for $C_{17}H_{12}BrNO_2$ 342.0124, found 342.0126 $[M+H]^+$. **IR** (ATR-FTIR) ν_{max} = 3069, 2914, 1770, 1705, 1421, 1389, 1108 cm^{-1}.

[6] Olofsson, K.; Sahlin, H.; Larhed, M.; Hallberg, A. *J. Org. Chem.*. **2011**, *66* 544-549.

2-(2-(naphthalen-2-yl)allyl)isoindoline-1,3-dione, 9-5l

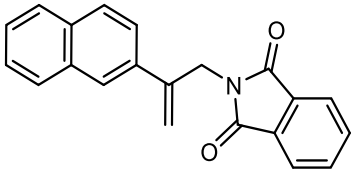

White solid at 97% of purity (713 mg, 39% yield) by flash chromatography using hexanes:EtOAc 70:30. **m.p.** 165-168 ºC. **^{1}H NMR** (400 MHz, $CDCl_3$) δ 7.96 (s, 1H), 7.84 (ddd, *J* = 5.5, 3.1, 0.4 Hz, 2H), 7.82 – 7.78 (m, 2H), 7.72 – 7.68 (m, 2H), 7.64 (dd, *J* = 8.6, 1.9 Hz, 1H), 7.49 – 7.43 (m, 2H), 5.59 (s, 1H), 5.29 (t, *J* = 1.5 Hz, 1H), 4.83 (t, *J* = 1.4 Hz, 2H). **^{13}C NMR** (101 MHz, $CDCl_3$) δ 168.0, 142.3, 135.7, 134.0, 133.2, 133.0, 132.0, 128.3, 128.0, 127.5, 126.2, 126.1, 125.3, 124.6, 123.3, 114.6, 41.5. **HRMS** (ESI) calculated for $C_{21}H_{15}NO_2$ 314.1176, found 314.1171 $[M+H]^+$. **IR** (ATR-FTIR) ν_{max} = 3092, 3056, 3021, 2923, 1770, 1698, 1425, 1397, 1108 cm^{-1}.

2-(2-(4-isobutylphenyl)allyl)isoindoline-1,3-dione, 9-5m

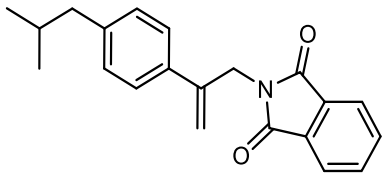

White solid (761 mg, 42% yield) purified by flash chromatography using hexanes:EtOAc 70:30. **m.p.** 87-91 ºC. **^{1}H NMR** (400 MHz, $CDCl_3$) δ 7.87 – 7.82 (m, 2H), 7.73 – 7.68 (m, 2H), 7.43 – 7.39 (m, 2H), 7.14 – 7.09 (m, 2H), 5.42 (q, *J* = 1.0 Hz, 1H), 5.09 (t, *J* = 1.6 Hz, 1H), 4.70 (t, *J* = 1.4 Hz, 2H), 2.45 (d, *J* = 7.2 Hz, 2H), 1.85 (dp, *J* = 13.6, 6.8 Hz, 1H), 0.89 (d, *J* = 6.6 Hz, 6H). **^{13}C** NMR (101 MHz, $CDCl_3$) δ 168.1, 142.2, 141.8, 135.9, 134.1, 132.2, 129.3, 126.1, 123.5, 112.9, 45.2, 41.5, 30.2, 22.5. **HRMS** (ESI) calculated for $C_{21}H_{22}NO_2$ 320.1645, found 320.1643 $[M+H]^+$. **IR** (ATR-FTIR) ν_{max} = 2959, 2919, 2861, 1704, 1425, 1390, 1108 cm^{-1}.

Iridium-Catalyzed Asymmetric Hydrogenation

General procedure GP

Into a low pressure reactor equipped with PTFE-coated stir-bar, the corresponding substrate (0.288 mmol, 1.0 equiv.) was charged and dissolved in anhydrous DCM (1 mL/0.1 mmol substrate). Once sealed, the reactor was purged and charged with 1 bar of H_2. Then, the pressure reactor was placed in a cryocool bath. When it reached -20 ºC, the corresponding catalyst **2c** dissolved in 0.2 mL of anhydrous DCM was then added (4.2 mg, 1 mol%, otherwise indicated) with a pressure-syringe. The reaction was left stirring at -20 ºC overnight. Afterwards, the crude was filtrated with a plug of silica to afford the corresponding isolated product, using hexane:EtOAc 95:5 to 80:20 as eluent. The conversion was measured by ^{1}H NMR spectroscopy from the reaction crude, and the enantiomeric excess using chiral HPLC chromatography.

*Compounds **9-6d**, **9-6e**, **9-6i** and **9-6k** were isolated without the need of column chromatography, as they were already pure by ^{1}H NMR of the reaction crude.

*Compounds **9-6b**, **9-6h** and **9-6l** contained 2-4% of impurity coming from the starting material, which could not be separated after column chromatography but did not interfere in the reaction, as the proportion was maintained.

(*R*)-2-(2-phenylpropyl)isoindoline-1,3-dione, 9-6a

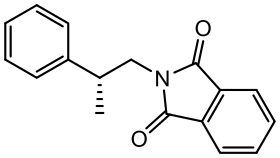

Following GP, the desired product was obtained as an oil (full conversion, 73 mg, 0.277 mmol, 96% yield, 98% ee) purified by flash chromatography using hexanes:EtOAc 4:1. **^{1}H NMR** (400 MHz, $CDCl_3$) δ 7.75 – 7.69 (m, 2H), 7.64 – 7.58 (m, 2H), 7.21 – 7.18 (m, 4H), 7.15 – 7.09 (m, 1H), 3.83 – 3.68 (m, 2H), 3.32 – 3.22 (m, 1H), 1.23 (d, *J* = 7.0 Hz, 3H). **HPLC**: CHIRALPAK IA. Heptane/iPrOH 90:10, 0.5 mL/min, λ = 254 nm. $t_{(R)}$ = 12.5 min, $t_{(S)}$ = 14.3 min. The analytical data for this compound were in excellent agreement with the reported data.[6]

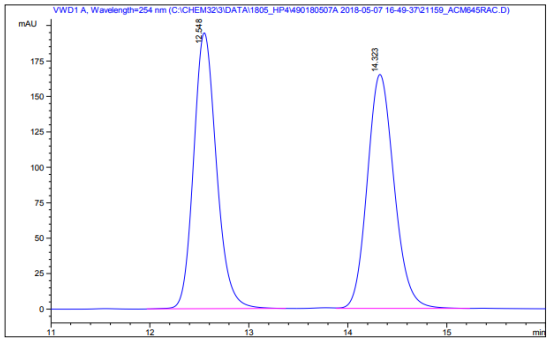

#	Meas. R	Pea	Width	Area	Height	Area %
1	12.548	BB	0.247	3120.488	194.682	50.041
2	14.323	VB	0.292	3115.379	165.081	49.959

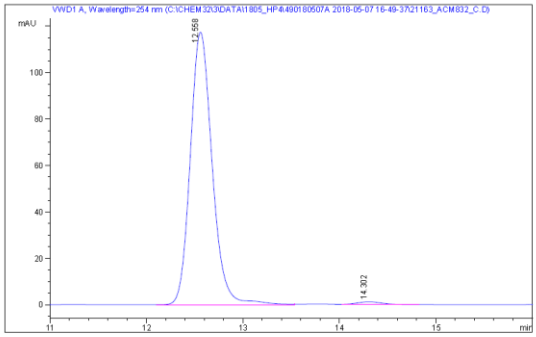

#	Meas. R	Pea	Width	Area	Height	Area %
1	12.558	MF	0.263	1855.440	117.494	98.796
2	14.302	FM	0.305	22.615	1.234	1.204

(*R*)-2-(2-(4-fluorophenyl)propyl)isoindoline-1,3-dione, 9-6b

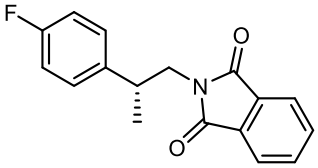

Following GP, the desired product was obtained as a white solid (full conversion, 78 mg, 0.278 mmol, 97% yield, >99% ee) in 96% of purity by flash chromatography using hexanes:EtOAc 4:1**. m.p.** 60-63 °C **[α]$_D$**: +91.5 (c 1.2, $CHCl_3$). **^{1}H NMR** (400 MHz, $CDCl_3$) δ 7.82 – 7.76 (m, 2H), 7.72 – 7.66 (m, 2H), 7.24 – 7.18 (m, 2H), 6.98 – 6.90 (m, 2H), 3.87 – 3.71 (m, 2H), 3.34 (h, *J* = 7.3 Hz, 1H), 1.29 (d, *J* = 7.0 Hz, 3H). **^{13}C NMR** (101 MHz, $CDCl_3$) δ 168.2, 162.9, 160.4, 138.9, 138.9, 133.9, 131.8, 128.7, 128.7, 123.2, 115.3, 115.1, 44.9, 44.8, 37.8, 19.1. **HRMS** (ESI) calculated for $C_{17}H_{14}FNO_2$ 284.1081, found 284.1081 $[M+H]^+$. **IR** (ATR-FTIR) ν_{max} = 2970, 2926, 2853, 2359, 2334, 2249, 1706, 1509, 1395, 1378, 1352, 1223 cm^{-1}. **HPLC**: CHIRALPAK IA. Heptane/EtOH 50:50, 0.5 mL/min, λ = 210 nm. $t_{(R)}$ = 10.9 min, $t_{(S)}$ = 15.4 min.

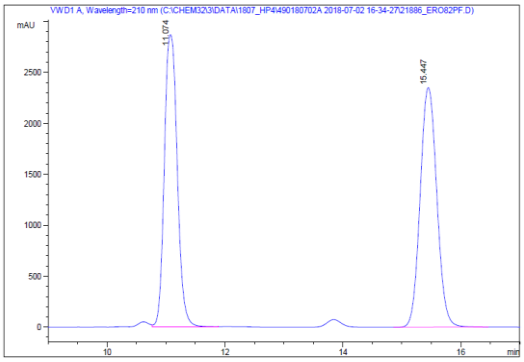

#	Meas. R	Pea	Width	Area	Height	Area %
1	11.074	VV	0.238	43827.660	2.871e3	48.642
2	15.447	MF	0.328	46274.973	2.352e3	51.358

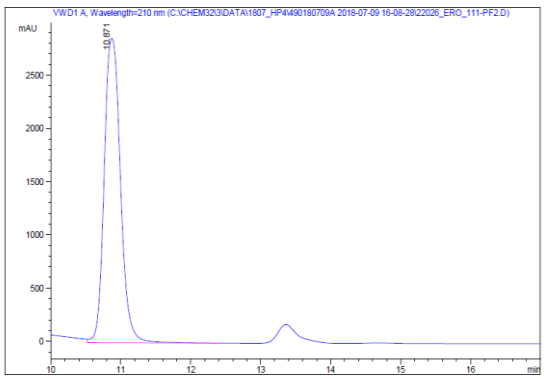

#	Meas. R	Pea	Width	Area	Height	Area %
1	10.871	VV	0.253	46266.938	2.862e3	100.000

(*R*)-2-(2-(4-chlorophenyl)propyl)isoindoline-1,3-dione, 9-6c

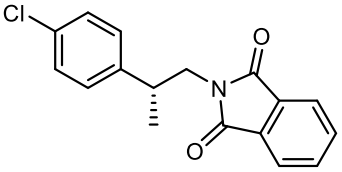

Following GP, the desired product was obtained as a a white solid (full conversion, 80 mg, 0.267 mmol, 93% yield, 97% ee) in 98% of purity by flash chromatography using hexanes:EtOAc 4:1. **m.p.** 69-73 ºC **[α]D**: +98.8 (c 1.1, $CHCl_3$). **^{1}H NMR** (400 MHz, $CDCl_3$) δ 7.75 – 7.69 (m, 2H), 7.64 – 7.58 (m, 2H), 7.19 – 7.07 (m, 4H), 3. 81 – 3.63 (m, 2H), 3.26 (h, *J* = 7.3 Hz, 1H), 1.21 (d, *J* = 7.0 Hz, 3H). **^{13}C NMR** (101 MHz, $CDCl_3$) δ 168.2, 141.7, 133.9, 132.4, 131.8, 128.6, 128.6, 123.2, 77.3, 77.0, 76.7, 44.6, 38.0, 19.1. **HRMS** (ESI) calculated for $C_{17}H_{14}ClNO_2$ 300.0786, found 300.0797 $[M+H]^+$. **IR** (ATR-FTIR) ν_{max} 2970, 2926, 2853, 2363, 2242, 1767, 1708, 1394, 1378, 1351 cm^{-1}. **HPLC**: CHIRALPAK IA. Heptane/EtOH 50:50, 0.5 mL/min, λ = 210 nm. $t_{(R)}$ = 12.0 min, $t_{(S)}$ = 17.1 min.

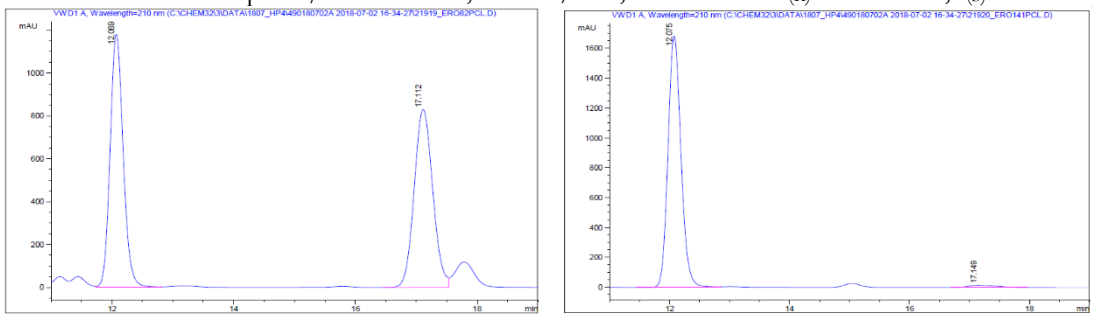

#	Meas. R	Pea	Width	Area	Height	Area %
1	12.069	VV	0.231	17630.529	1.180e3	50.031
2	17.112	BV	0.330	17609.025	830.658	49.969

#	Meas. R	Pea	Width	Area	Height	Area %
1	12.075	VV	0.233	25258.617	1.683e3	98.306
2	17.149	BB	0.432	435.308	14.252	1.694

(*R*)-2-(2-(4-bromophenyl)propyl)isoindoline-1,3-dione, 9-6d

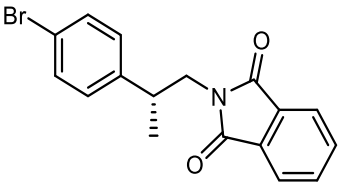

Following GP and using 2 mol% of catalyst, the desired product was obtained as a white solid (full conversion, 96 mg, 0.286 mmol, 99% yield, 97% ee) purified by flash chromatography using hexanes:EtOAc 4:1. **m.p.** 118-121 ºC **[α]D**: +98.4 (c 0.5, $CHCl_3$). **^{1}H NMR** (400 MHz, $CDCl_3$) δ 7.86 – 7.75 (m, 2H), 7.73 – 7.65 (m, 2H), 7.42 – 7.33 (m, 2H), 7.17 – 7.09 (m, 2H), 3.88 – 3.69 (m, 2H), 3.33 (h, *J* = 7.3 Hz, 1H), 1.27 (d, *J* = 7.0 Hz, 3H). **^{13}C NMR** (101 MHz, $CDCl_3$) δ 168.2, 142.2, 133.9, 131.8, 131.5, 129.0, 123.2, 120.5, 44.5, 38.0, 19.0. **HRMS** (ESI) calculated for $C_{17}H_{14}BrNO_2$ 344.0281, found 344.0279 $[M+H]^+$. **IR** (ATR-FTIR) ν_{max} = 2967, 2936, 2843, 2255, 1757, 1708, 1395, 1378, 1352 cm^{-1}. **HPLC**: CHIRALPAK IA. Heptane/EtOH 50:50, 0.5 mL/min, λ = 210 nm. $t_{(R)}$ = 12.9 min, $t_{(S)}$ = 21.8 min.

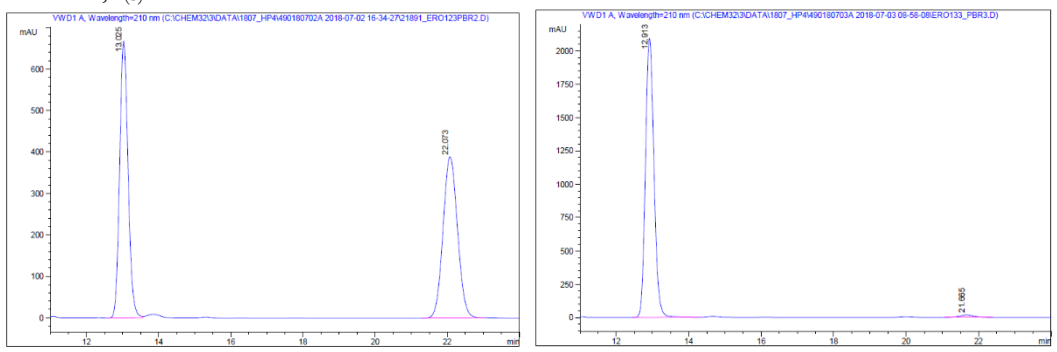

#	Meas. R	Pea	Width	Area	Height	Area %
1	13.025	VV	0.251	10858.039	668.702	49.999
2	22.073	BB	0.436	10858.613	389.493	50.001

#	Meas. R	Pea	Width	Area	Height	Area %
1	12.913	BB	0.255	34319.309	2.094e3	98.471
2	21.665	BB	0.417	532.749	19.881	1.529

(*R*)-2-(2-(4-iodophenyl)propyl)isoindoline-1,3-dione, 9-6e

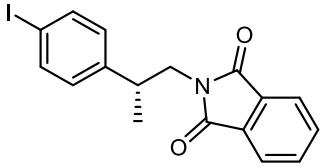

Following GP and using 2 mol% of catalyst, the desired product was obtained as a white solid (full conversion, 111 mg, 99% yield, 98% ee) purified by flash chromatography using hexanes:EtOAc 4:1. **m.p.** 151-155 ºC **[α]$_D$**: +90.2 (c 0.5, $CHCl_3$). **^{1}H NMR** (400 MHz, $CDCl_3$) δ 7.84 – 7.76 (m, 2H), 7.73 – 7.66 (m, 2H), 7.62 – 7.56 (m, 2H), 7.05 – 6.98 (m, 2H), 3.88 – 3.71 (m, 2H), 3.31 (h, *J* = 7.3 Hz, 1H), 1.27 (d, *J* = 7.0 Hz, 3H). **^{13}C NMR** (101 MHz, $CDCl_3$) δ 168.2, 143.0, 137.5, 133.9, 131.8, 129.4, 123.3, 92.0, 44.5, 38.1, 19.0. **HRMS** (ESI) calculated for $C_{17}H_{14}INO_2$ 392.0142, found 392.0142 $[M+H]^+$. **IR** (ATR-FTIR) ν_{max} = 2963, 2927, 2366, 1770, 1697, 1391, 1036, 1004 cm^{-1}. **HPLC**: CHIRALPAK IA. Heptane/IPA 95:5, 0.5 mL/min, λ = 210 nm. $t_{(R)}$ = 11.1 min, $t_{(S)}$ = 13.0 min.

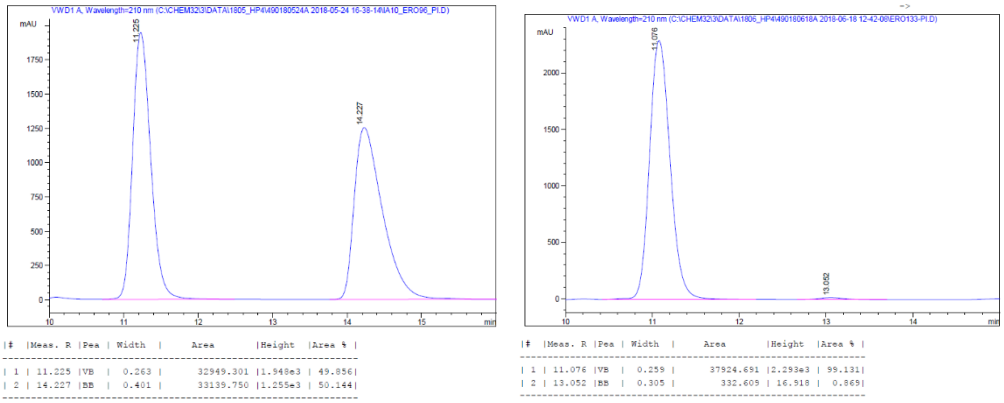

(*R*)-2-(2-(p-tolyl)propyl)isoindoline-1,3-dione, 9-6f

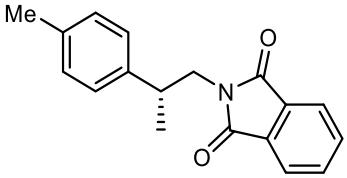

Following GP, the desired product was obtained as a colorless solid (full conversion, 73 mg, 0.263 mmol, 91% yield, 97% ee) purified by flash chromatography using hexanes:EtOAc 4:1. **m.p.** 50-53 ºC **[α]$_D$**: +93.7 (c 1.3, $CHCl_3$). **^{1}H NMR** (400 MHz, $CDCl_3$) δ 7.83 – 7.77 (m, 2H), 7.72 – 7.65 (m, 2H), 7.19 – 7.13 (m, 2H), 7.10 – 7.05 (m, 2H), 3.88 – 3.71 (m, 2H), 3.32 (h, *J* = 7.3 Hz, 1H), 2.29 (s, 3H), 1.28 (d, *J* = 7.0 Hz, 3H). **^{13}C NMR** (101 MHz, $CDCl_3$) δ 168.3, 140.3, 136.2, 133.8, 131.9, 129.1, 127.1, 123.2, 44.9, 38.1, 21.0, 19.0. **HRMS** (ESI) calculated for $C_{18}H_{17}NO_2$, 280.1332 found 280.1333 $[M+H]^+$. **IR** (ATR-FTIR) ν_{max} = 2998, 2927, 2851, 2366, 2242, 1706, 1394, 1376, 1351 cm^{-1}. **HPLC**: CHIRALPAK IA. Heptane/EtOH 50:50, 0.5 mL/min, λ = 210 nm. $t_{(R)}$ = 10.2 min, $t_{(S)}$ = 13.2 min.

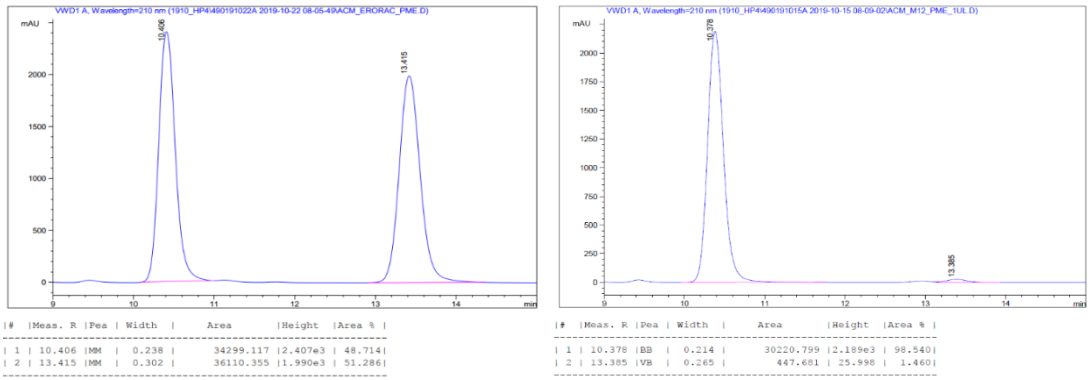

(*R*)-2-(2-(3-chlorophenyl)propyl)isoindoline-1,3-dione, 9-6g

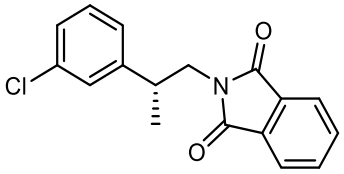

Following GP, the desired product was obtained as an oil (full conversion, 81 mg, 0.270 mmol, 94% yield, 98% ee) purified by flash chromatography using hexanes:EtOAc 4:1.

Gram scale procedure: 1 g of **9-5g** (3.36 mmol) was placed into a low pressure reactor equipped with a PTFE-coated stir-bar. The substrate was dissolved in anhydrous DCM (34 mL, [0.1 M]). Once sealed, the reactor was purged and charged with 1 bar of H_2. Then, the pressure reactor was placed in a cryocool bath. When it reached -20 ºC, the corresponding catalyst **9-2c** (25 mg, 0.5 mol%) dissolved in 1 mL of anhydrous DCM was then added with a pressure-syringe. The reaction was left stirring at -20 ºC for 36 hours. Afterwards, the crude was filtrated with a plug of silica to afford the corresponding isolated product (967 mg, 97% yield), using hexane:EtOAc 90:10 to 80:20 as eluent. The enantiomeric excess (98% ee) was measured by chiral HPLC. **[α]$_D$**: +101.2 (c 1.3, $CHCl_3$). **^{1}H NMR** (400 MHz, $CDCl_3$) δ 7.85 – 7.75 (m, 2H), 7.73 – 7.67 (m, 2H), 7.32 – 7.13 (m, 4H), 3.88 – 3.73 (m, 2H), 3.32 (h, *J* = 7.3 Hz, 1H), 1.29 (d, *J* = 7.0 Hz, 3H). **^{13}C NMR** (101 MHz, $CDCl_3$) δ 168.2, 145.4, 134.2, 133.9, 133.9, 131.8, 129.7, 127.6, 127.0, 125.5, 123.3, 44.6, 38.4, 18.8. **HRMS** (ESI) calculated for $C_{17}H_{14}ClNO_2$ 300.0786, found 300.0788 $[M+H]^+$. **IR** (ATR-FTIR) ν_{max} = 2957, 2971, 2850, 2361, 2337, 2245, 1711, 1396 cm^{-1}. **HPLC**: CHIRALPAK IA. Heptane/EtOH 50:50, 0.5 mL/min, λ = 210 nm. $t_{(R)}$ = 10.3 min, $t_{(S)}$ = 13.8 min.

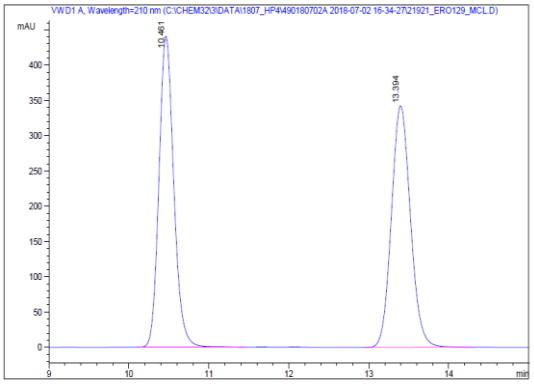

#	Meas. R	Pea	Width	Area	Height	Area %
1	10.461	BB	0.199	5691.042	440.962	50.062
2	13.394	BB	0.257	5676.924	342.438	49.938

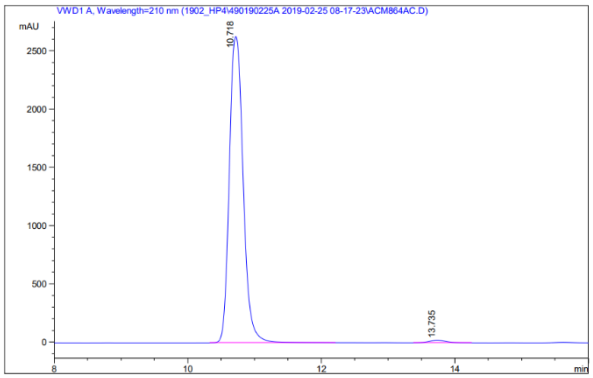

#	Meas. R	Pea	Width	Area	Height	Area %
1	10.718	MM	0.240	37814.063	2.629e3	99.030
2	13.735	MM	0.277	370.449	22.280	0.970

(*R*)-2-(2-(3-methoxyphenyl)propyl)isoindoline-1,3-dione, 9-6h

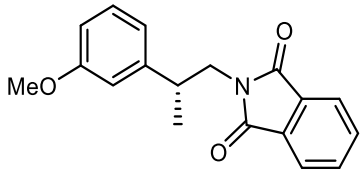

Following GP, the desired product was obtained as an oil (full conversion, 76 mg, 0.259 mmol, 90% yield, 98% ee) in 96% of purity by flash chromatography using hexanes:EtOAc 4:1. **[α]$_D$**: +80.8 (c 1.3, $CHCl_3$). **^{1}H NMR** (400 MHz, $CDCl_3$) δ 7.83 – 7.77 (m, 2H), 7.72 – 7.65 (m, 2H), 7.19 (t, *J* = 7.9 Hz, 1H), 6.88 – 6.71 (m, 3H), 3.90 – 3.77 (m, 2H), 3.76 (s, 3H), 3.33 (h, *J* = 7.3 Hz, 1H), 1.29 (d, *J* = 7.0 Hz, 3H). **^{13}C NMR** (101 MHz, $CDCl_3$) δ 168.3, 159.6, 145.0, 133.8, 131.9, 129.4, 123.2, 119.6, 112.9, 112.2, 55.1, 44.8, 38.5, 19.0. **HRMS** (ESI) calculated for $C_{18}H_{17}NO_3$ 296.1281, found 296.1276 $[M+H]^+$. **IR** (ATR-FTIR) ν_{max} = 3065, 2972, 2936, 2829, 1766, 1708, 1605, 1579, 1394, 1042 cm^{-1}. **HPLC**: CHIRALPAK IA. Heptane/EtOH 50:50, 0.5 mL/min, λ = 210 nm. $t_{(R)}$ = 10.9 min, $t_{(S)}$ = 17.1 min.

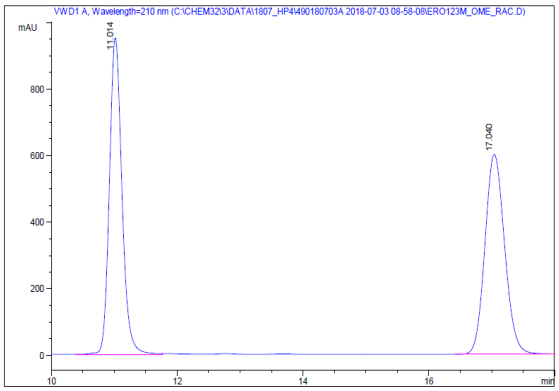

#	Meas. R	Pea	Width	Area	Height	Area %
1	11.014	VV	0.213	13256.500	952.477	50.302
2	17.040	BB	0.340	13097.407	600.842	49.698

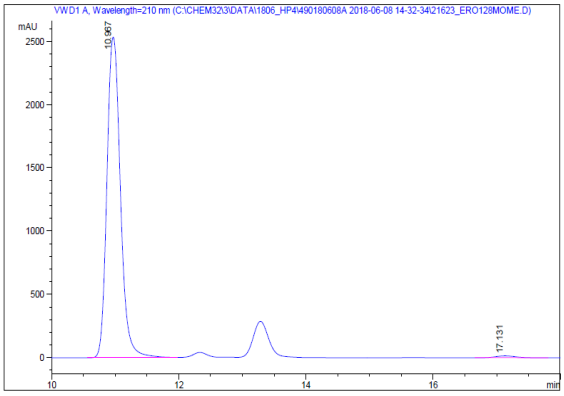

#	Meas. R	Pea	Width	Area	Height	Area %
1	10.967	BV	0.230	37392.113	2.536e3	99.107
2	17.131	VB	0.346	336.769	15.097	0.893

(*R*)-2-(2-(2-methoxyphenyl)propyl)isoindoline-1,3-dione, 9-6i

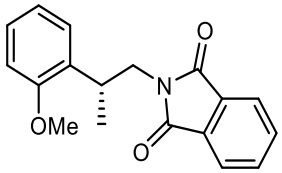

Following GP, the desired product was obtained as an oil (full conversion, 83 mg, 0.281 mmol, 99% yield, 83% ee) purified by flash chromatography using hexanes:EtOAc 4:1. **[α]D**: +64.5 (c 1.3, $CHCl_3$). **^{1}H NMR** (400 MHz, $CDCl_3$) δ 7.78 (ddd, *J* = 5.5, 2.9, 0.4 Hz, 2H), 7.73 – 7.65 (m, 2H), 7.27 – 7.22 (m, 1H), 7.20 – 7.11 (m, 1H), 6.91 (td, *J* = 7.5, 1.2 Hz, 1H), 6.74 (dd, *J* = 8.2, 1.1 Hz, 1H), 3.93 – 3.80 (m, 2H), 3.78 – 3.71 (m, 1H), 3.64 (s, 3H), 1.30 (d, *J* = 6.9 Hz, 3H). **^{13}C NMR** (101 MHz, $CDCl_3$) δ 168.3, 157.3, 133.7, 132.1, 131.5, 127.6, 127.5, 123.0, 120.6, 110.3, 55.1, 43.8, 32.0, 17.6. **HRMS** (ESI) calculated for $C_{18}H_{17}NO_3$ 296.1281, found 296.1281 $[M+H]^+$. **IR** (ATR-FTIR) ν_{max} = 2958, 2932, 2851, 1770, 1708, 1394, 1242 cm^{-1}. **HPLC**: CHIRALPAK IA. Heptane/EtOH 95:5, 0.5 mL/min, λ = 210 nm. $t_{(R)}$ = 16.0 min, $t_{(S)}$ = 17.5 min.

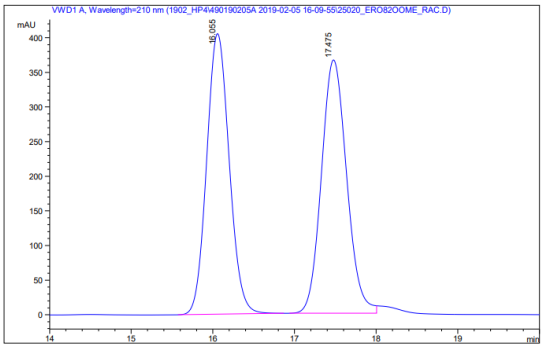

#	Meas. R	Pea	Width	Area	Height	Area %
1	16.055	MM	0.320	7773.294	405.193	49.709
2	17.475	MF	0.358	7864.261	365.842	50.291

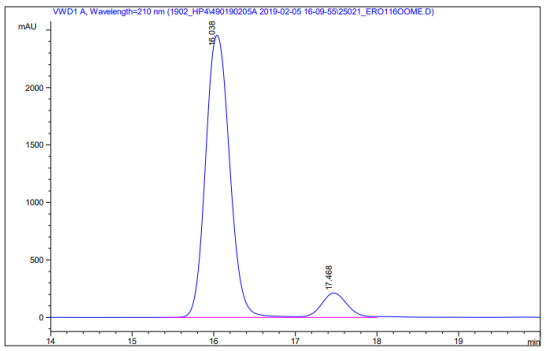

#	Meas. R	Pea	Width	Area	Height	Area %
1	16.038	BV	0.321	50131.250	2.455e3	91.487
2	17.468	VV	0.341	4664.916	212.402	8.513

(*R*)-2-(2-(o-tolyl)propyl)isoindoline-1,3-dione, 9-6j

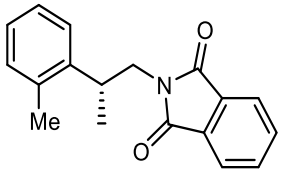

Following GP, using 3 mol% of catalyst and leaving the reaction stirring for 48 hours, the desired product was obtained as an oil (full conversion, 76 mg, 0.274 mmol, 95% yield, 91% ee) purified by

flash chromatography using hexanes:EtOAc 4:1. **[α]$_D$**: +24.5 (c 0.5, $CHCl_3$). **^{1}H NMR** (400 MHz, $CDCl_3$) δ 7.86 – 7.79 (m, 2H), 7.73 – 7.67 (m, 2H), 7.35 (dd, *J* = 7.6, 1.2 Hz, 1H), 7.21 (ddd, *J* = 7.7, 6.7, 2.5 Hz, 1H), 7.16 – 7.08 (m, 2H), 3.87 – 3.73 (m, 2H), 3.69 – 3.56 (m, 1H), 2.40 (s, 3H), 1.26 (d, *J* = 6.9 Hz, 3H). **^{13}C NMR** (101 MHz, $CDCl_3$) δ 168.5, 141.5, 136.0, 133.9, 131.9, 130.4, 126.4, 126.3, 125.7, 123.2, 44.2, 33.6, 19.4, 18.5. **HRMS** (ESI) calculated for $C_{18}H_{17}NO_2$ 280.1332, found 280.1343 $[M+H]^+$. **IR** (ATR-FTIR) ν_{max} = 3461, 3065, 2967, 2923, 2856, 1775, 1706, 1394, 1350, 1276, 1042 cm^{-1}. **HPLC**: CHIRALPAK IA. Heptane/EtOH 98:2, 0.5 mL/min, λ = 210 nm. $t_{(R)}$ = 16.5 min, $t_{(S)}$ = 18.1 min.

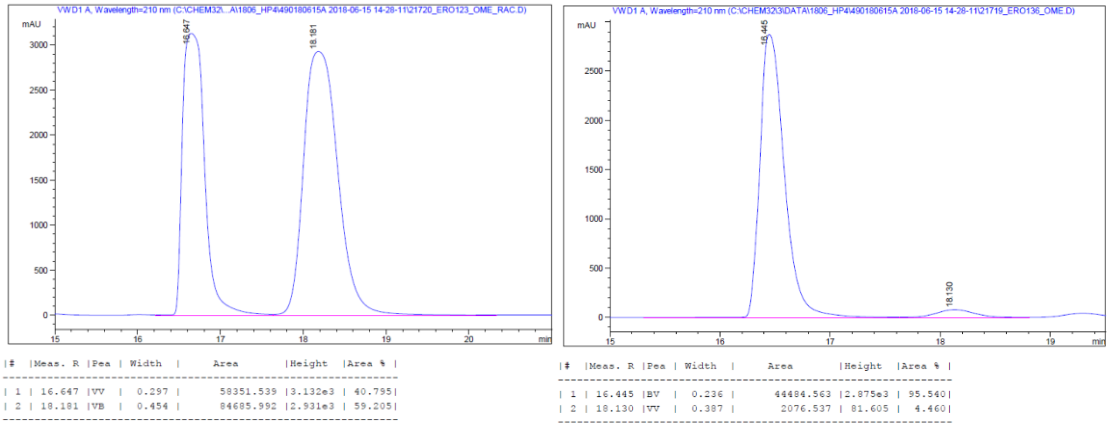

#	Meas. R	Pea	Width	Area	Height	Area %
1	16.647	VV	0.297	58351.539	3.132e3	40.795
2	18.181	VB	0.454	84685.992	2.931e3	59.205

#	Meas. R	Pea	Width	Area	Height	Area %
1	16.445	BV	0.236	44484.563	2.875e3	95.540
2	18.130	VV	0.387	2076.537	81.605	4.460

(*R*)-2-(2-(2-bromophenyl)propyl)isoindoline-1,3-dione, 9-6k

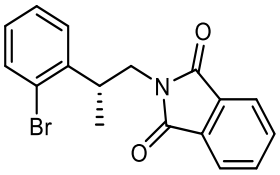

Following GP and using 2 mol% of catalyst, the desired product was obtained as an oil (full conversion, 98 mg, 0.286 mmol, 99% yield, 90% ee) purified by flash chromatography using hexanes:EtOAc 4:1. **[α]$_D$**: +47.2 (c 0.8, $CHCl_3$). **^{1}H NMR** (400 MHz, $CDCl_3$) δ 7.84 – 7.77 (m, 2H), 7.72 – 7.65 (m, 2H), 7.47 (dd, *J* = 8.0, 1.4 Hz, 1H), 7.40 (dd, *J* = 7.8, 1.7 Hz, 1H), 7.31 (td, *J* = 7.6, 1.3 Hz, 1H), 7.05 (ddd, *J* = 8.0, 7.3, 1.7 Hz, 1H), 3.95 – 3.86 (m, 2H), 3.85 – 3.77 (m, 1H), 1.33 – 1.27 (m, 3H). **^{13}C NMR** (101 MHz, $CDCl_3$) δ 168.2, 142.4, 133.9, 132.9, 131.9, 128.2, 127.8, 127.7, 124.8, 123.2, 43.7, 37.2, 18.6. **HRMS** (ESI) calculated for $C_{17}H_{14}BrNO_2$ 344.0281, found 344.0271 $[M+H]^+$. **IR** (ATR-FTIR) ν_{max} = 3466, 3056, 2963, 2923, 2843, 1772, 1706, 1467, 1394, 1378, 1351, 1277, 1043, 1021 cm^{-1}. **HPLC**: CHIRALPAK IA. Heptane/EtOH 98:2, 0.5 mL/min, λ = 210 nm. $t_{(R)}$ = 27.3 min, $t_{(S)}$ = 30.6 min.

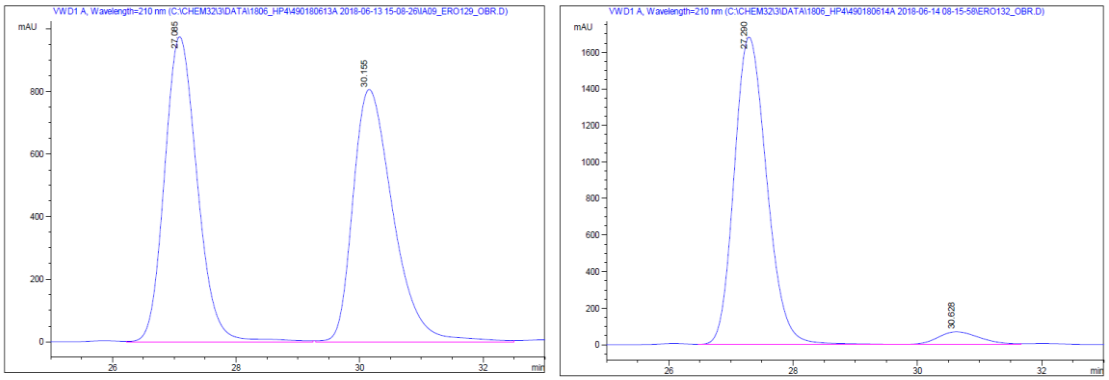

#	Meas. R	Pea	Width	Area	Height	Area %
1	27.085	VB	0.572	36004.203	976.147	49.724
2	30.155	BV	0.695	36404.012	807.428	50.276

#	Meas. R	Pea	Width	Area	Height	Area %
1	27.290	VB	0.570	61353.164	1.682e3	94.842
2	30.628	BV	0.733	3336.870	70.087	5.158

(*R*)-2-(2-(naphthalen-2-yl)propyl)isoindoline-1,3-dione, 9-6l

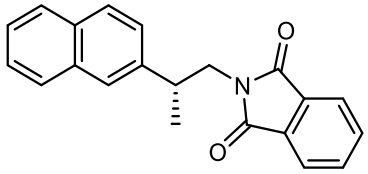

Following GP, the desired product was obtained as a white solid (full conversion, 80 mg, 0.255 mmol, 89% yield, 97% ee) in 97% of purity by flash chromatography using hexanes:EtOAc 4:1. **m.p.** 117-121 °C **[α]$_D$**: +66.1 (c 0.4, $CHCl_3$). **^{1}H NMR** (400 MHz, $CDCl_3$) δ 7.81 – 7.74 (m, 5H), 7.71 – 7.63 (m, 3H), 7.49 – 7.38 (m, 3H), 4.04 – 3.83 (m, 2H), 3.55 (h, *J* = 7.3 Hz, 1H), 1.39 (d, *J* = 7.0 Hz, 3H). **^{13}C NMR** (101 MHz, $CDCl_3$) δ 140.8, 133.8, 133.5, 132.5, 131.9, 128.2, 127.6, 127.6, 125.9, 125.9, 125.9, 125.6, 125.4, 123.2, 44.7, 38.7, 19.2. **HRMS** (ESI) calculated for $C_{21}H_{17}NO_2$ 316.1332, found 316.1329 $[M+H]^+$. **IR** (ATR-FTIR) ν_{max} = 3458, 3050, 2964, 2932, 2872, 1767,1705, 1682, 1397, 1048 cm^{-1}. **HPLC**: CHIRALPAK IA. Heptane/EtOH 70:30, 0.5 mL/min, λ = 210 nm. $t_{(R)}$ = 13.5 min, $t_{(S)}$ = 20.6 min.

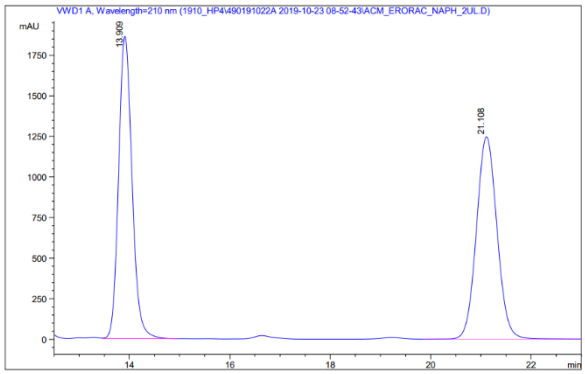

#	Meas. R	Pea	Width	Area	Height	Area %
1	13.909	MM	0.311	34711.523	1.862e3	49.488
2	21.108	VB	0.444	35429.871	1.245e3	50.512

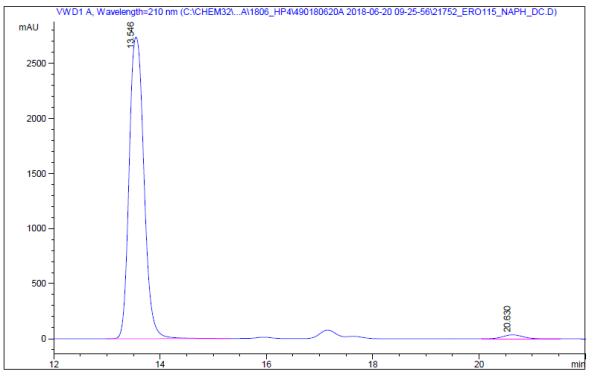

#	Meas. R	Pea	Width	Area	Height	Area %
1	13.546	BV	0.304	52994.035	2.740e3	98.280
2	20.630	BB	0.407	927.394	35.517	1.720

(*R*)-2-(2-(4-isobutylphenyl)propyl)isoindoline-1,3-dione, 9-6m

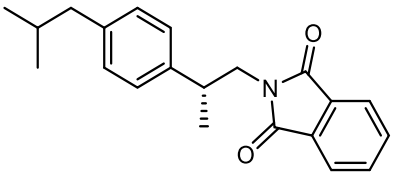

Following GP, the desired product was obtained as an oil (full conversion, 88 mg, 0.276 mmol, 96% yield, 98% ee) purified by flash chromatography using hexanes:EtOAc 4:1. **[α]$_D$**: +70.4 (c 0.3, $CHCl_3$). **^{1}H NMR** (400 MHz, $CDCl_3$) δ 7.74 – 7.67 (m, 2H), 7.63 – 7.57 (m, 2H), 7.10 – 7.05 (m, 2H), 6.99 – 6.93 (m, 2H), 3.78 – 3.65 (m, 2H), 3.23 (h, *J* = 7.2 Hz, 1H), 2.32 (d, *J* = 7.2 Hz, 2H), 1.72 (dp, *J* = 13.6, 6.8 Hz, 1H), 1.21 (d, *J* = 7.0 Hz, 3H), 0.77 (dd, *J* = 6.6, 3.3 Hz, 6H). **^{13}C NMR** (101 MHz, $CDCl_3$) δ 168.4, 140.6, 140.2, 133.9, 132.1, 129.3, 127.1, 123.2, 45.2, 45.1, 38.2, 30.3, 22.4, 18.9. **HRMS** (ESI) calculated for $C_{21}H_{24}NO_2$ 322.1802, found 322.1797 $[M+H]^+$. **IR** (ATR-FTIR) ν_{max} = 2054, 2928, 1708, 1394, 715 cm^{-1}. **HPLC**: CHIRALPAK IA. Heptane/IPA 90:10, 0.5 mL/min, λ = 210 nm. $t_{(R)}$ = 12.5 min, $t_{(S)}$ = 15.2 min.

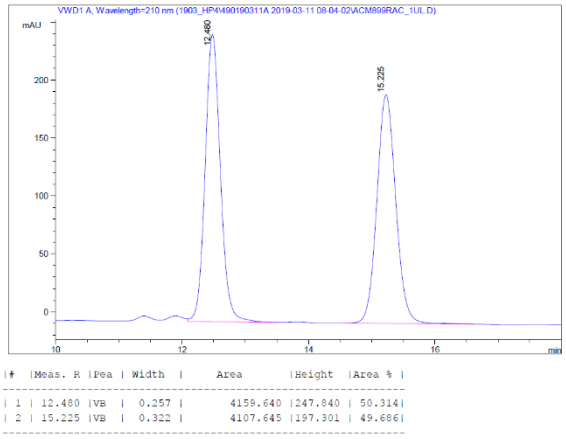

#	Meas. R	Pea	Width	Area	Height	Area %
1	12.480	VB	0.257	4159.640	247.840	50.314
2	15.225	VB	0.322	4107.645	197.301	49.686

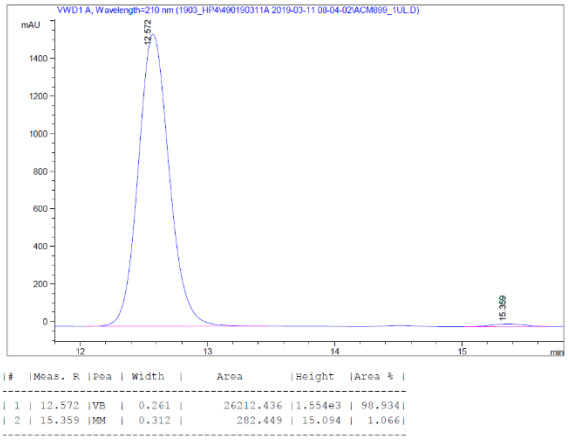

#	Meas. R	Pea	Width	Area	Height	Area %
1	12.572	VB	0.261	26212.436	1.554e3	98.934
2	15.359	MM	0.312	282.449	15.094	1.066

Deprotection of the phthalimido group and derivatization of the amines

(*R*)-2-(3-chlorophenyl)propan-1-amine

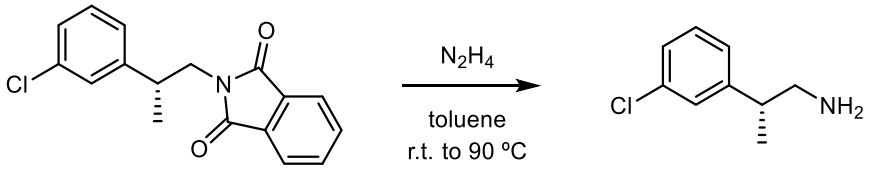

9-6g **9-7**

In a round-bottom flask, chiral amine **9-6g** (440 mg, 1.33 mmol) was placed with a magnetic stirrer. The flask was purged with N_2 and anhydrous toluene (3 mL, [0.45M]) was added. When the solution was homogenous, anhydrous N_2H_4 solution (in THF, [1.0M], 2.0 equiv.) was added dropwise. The reaction was then stirred at room temperature for 3 hours and then heated in an oil bath at 90 °C for 2 hours. Cooled the slurry to room temperature, filtered precipitates through a plug of Celite and the filtrate was concentrated to provide **9-7** as transparent oil which was pure without the need of further purification (210 mg, 93% yield). **^{1}H NMR** (400 MHz, $CDCl_3$) δ 7.25 – 7.17 (m, 3H), 7.09 (dd, J = 7.2, 1.7 Hz, 1H), 2.86 (s, 2H), 2.73 (q, J = 6.8 Hz, 1H), 1.24 (d, J = 7.0 Hz, 3H). The analytical data for this compound were in excellent agreement with the reported data.[7]

tert-butyl (*R*)-(2-(4-bromophenyl)propyl)carbamate

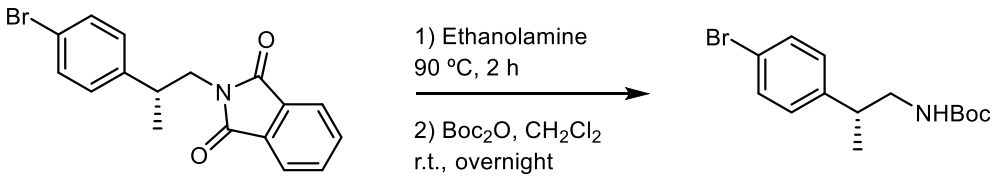

9-6d **9-9**

In a round-bottom flask, chiral amine **9-6d** (60 mg, 0.174 mmol) was placed with a magnetic stirrer. Ethanolamine (0.6 mL, [0.3M]) was then added. The solution was stirred for 10 min and then heated in an oil bath to 90 °C for 2 hours. Afterwards, the mixture was diluted with Et_2O and washed with NaOH 0.1M and brine. The organic phase was dried over $MgSO_4$ and concentrated under vacuum. The resulting oil was dissolved in CH_2Cl_2 and the flask was purged with N_2. Under inert atmosphere, a concentrated solution of Boc_2O in CH_2Cl_2 (1.1 equiv.) was added dropwise. The mixture was left stirring overnight. Then, the solvent was evaporated and the resulting oil was purified by column chromatography (hexanes:EtOAc 90:10) to afford **9** as an oil (42 mg, 76% yield after 2-steps). **^{1}H**

[7] Smilovic, I. G.; Cluzeau, J.; Richter, F.; Nerdinger, S.; Schreiner, E.; Laus, G.; Schottenberger, H. *Bioorganic Med. Chem.* **2018**, *26*, 2686-2690.

NMR (400 MHz, $CDCl_3$) δ 7.44 (dd, *J* = 8.3, 1.7 Hz, 2H), 7.10 – 7.06 (m, 2H), 4.41 (s, 1H), 3.41 – 3.30 (m, 1H), 3.14 (ddd, *J* = 13.6, 8.2, 5.4 Hz, 1H), 2.90 (d, *J* = 8.6 Hz, 1H), 1.41 (s, 9H), 1.23 (d, *J* = 7.0 Hz, 3H). **^{13}C NMR** (101 MHz, $CDCl_3$) δ 146.7, 131.6, 129.0, 120.3, 85.2, 47.2, 39.7, 28.3, 19.0. The analytical data for this compound were in excellent agreement with the reported data.[8]

(R)-3-methylindoline

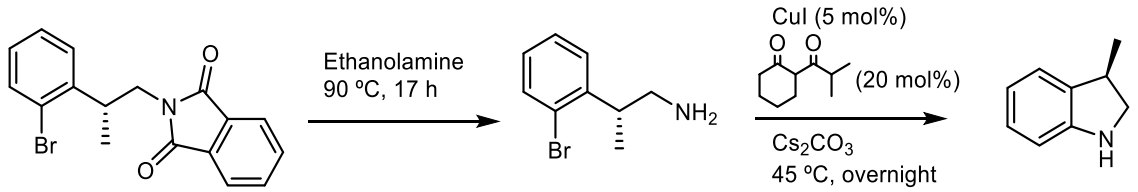

9-6k **9-S4** **9-11**

In a round-bottom flask, chiral amine **9-6k** (142 mg, 0.412 mmol) was placed with a magnetic stirrer. Ethanolamine (1.0 mL, [0.3M]) was then added. The solution was stirred for 10 min at room temperature and then heated in an oil bath to 90 °C for 17 hours. Afterwards, the mixture was diluted with Et_2O and washed with NaOH 0.1M and brine. The organic phase was dried over $MgSO_4$ and concentrated under vacuum to afford **9-S4** as an oil (75 mg, 85% yield), that was used without further purification. **^{1}H NMR** (400 MHz, $CDCl_3$) δ 7.56 (dd, *J* = 8.0, 1.3 Hz, 1H), 7.29 (dddd, *J* = 7.7, 7.2, 1.3, 0.5 Hz, 1H), 7.22 (dd, *J* = 7.8, 1.8 Hz, 1H), 7.06 (ddd, *J* = 7.9, 7.2, 1.8 Hz, 1H), 3.34 (h, *J* = 6.9 Hz, 1H), 2.94 – 2.80 (m, 2H), 1.46 (br s, 2H), 1.24 (d, *J* = 6.9 Hz, 3H). **^{13}C NMR** (101 MHz, $CDCl_3$) δ 143.9, 133.1, 127.9, 127.8, 127.4, 125.5, 48.6, 41.8, 18.5. **HRMS** (ESI) calculated for $C_9H_{13}BrN$ 214.0226, found 214.0220 $[M+H]^+$. **IR** (ATR-FTIR) ν_{max} = 2955, 2923, 2866, 1471, 1438, 1020, 906 cm^{-1}.

The reaction conditions were adapted from the literature procedure.[9] The resulting oil **9-S4** was dissolved in anhydrous DMF [0.3M] and added to a vial containing CuI (5 mol%), 2-isobutyrylcyclohexan-1-one as ligand (20 mol%), Cs_2CO_3 (2.0 equiv.) and a magnetic stirrer. The vial was purged with N_2, sealed and left stirring overnight at 45 °C in an oil bath. Then, the mixture was diluted with water and MTBE. The layers were separated, and the aqueous phase was extracted with MTBE. Combined organic phases were washed with brine, dried with $MgSO_4$ and concentrated under vacuum. Purification of the crude by flash chromatography (hexanes:EtOAc 90:10) afforded **9-11** as an oil (38 mg, 70% yield after 2-steps). **^{1}H NMR** (400 MHz, $CDCl_3$) δ 7.09 (dtd, *J* = 7.3, 1.2, 0.6 Hz, 1H), 7.06 – 7.01 (m, 1H), 6.74 (td, *J* = 7.4, 1.0 Hz, 1H), 6.65 (ddt, *J* = 7.7, 0.9, 0.4 Hz, 1H), 3.71 (t, *J* = 8.6 Hz, 1H), 3.42 – 3.32 (m, 1H), 3.12 (t, *J* = 8.6 Hz, 1H), 1.33 (d, *J* = 6.8 Hz, 3H). **^{13}C NMR** (101 MHz, $CDCl_3$) δ 151.2, 134.3, 127.3, 123.3, 118.7, 109.5, 55.4, 36.6, 18.6. The analytical data for this compound were in excellent agreement with the reported data.[10]

[8] Hebeisen, P.; Weiss, U.; Alker, A.; Staempfli, A. *Tetrahedron Lett.* **2011**, *52*, 5229-5233.
[9] Shafir, A.; Buchwald, S. L. *J. Am. Chem. Soc.* **2006**, *128*, 8742-8743.
[10] Kuwano, R.; Kaneda, K.; Ito, T.; Sato, K.; Kurokawa, T.; Ito, Y. *Org. Lett.* **2004**, *6* (13), 2213-2215.

^{1}H and ^{13}C NMR spectra

(*R*)-2-amino-N-((*R*)-1-hydroxy-3,3-dimethylbutan-2-yl)-3-methylbutanamide

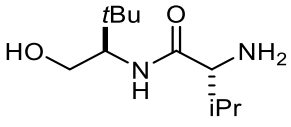

9-S1

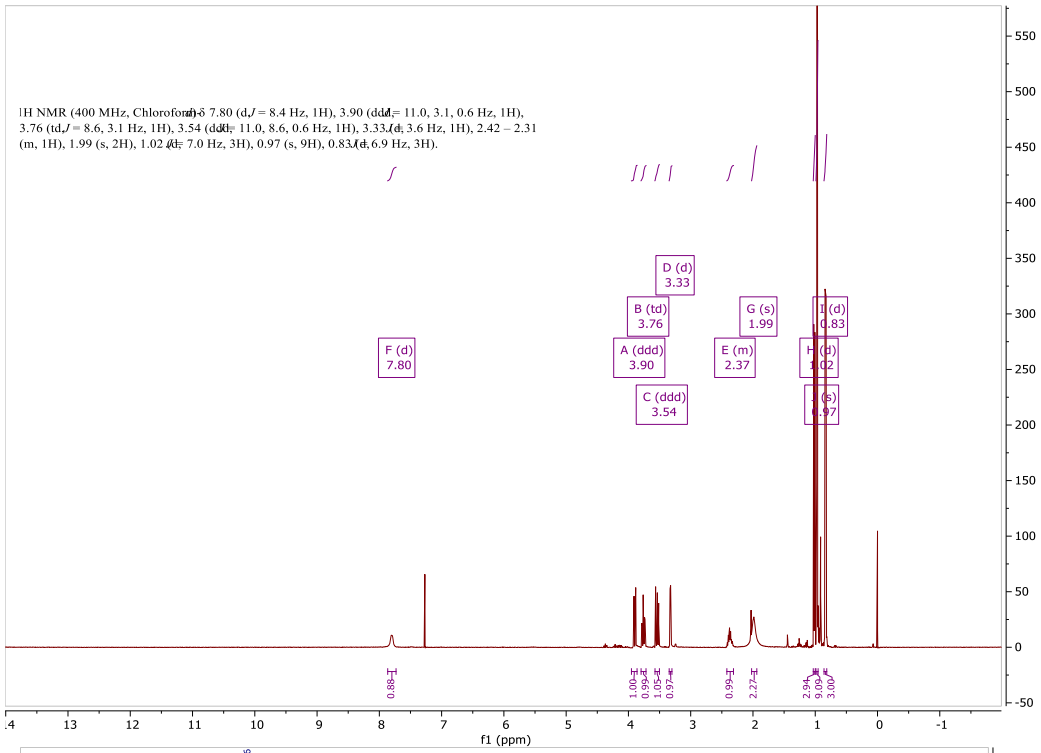

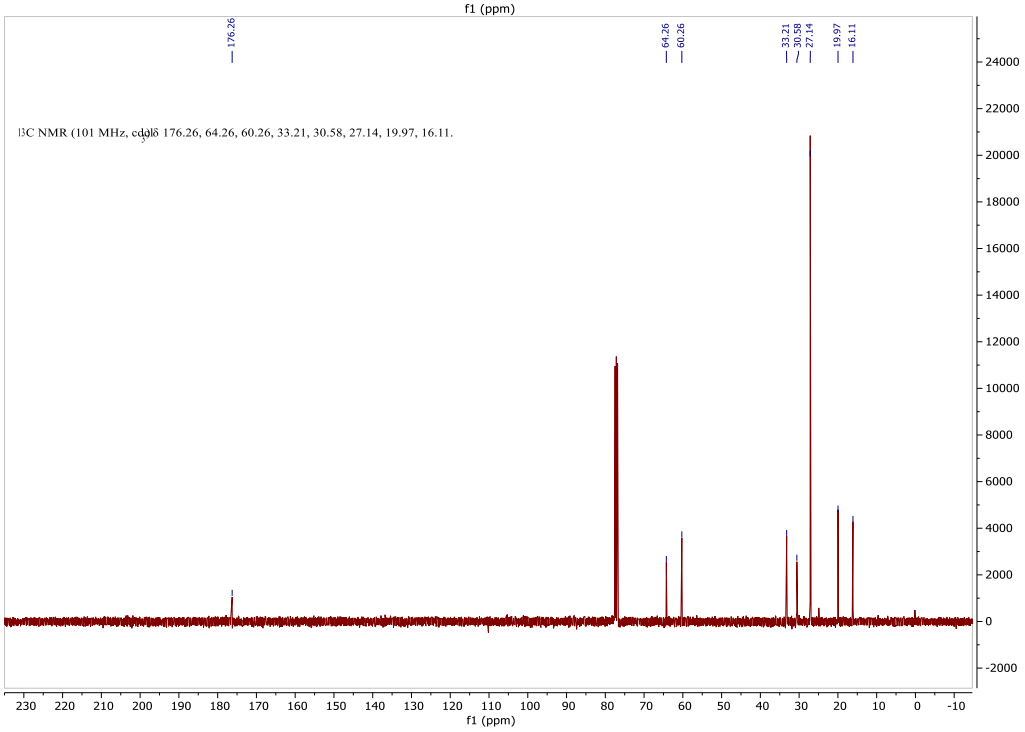

(*R*)-2-(((*S*)-*tert*-butyl(methyl)phosphanyl)amino)-N-((*R*)-1-hydroxy-3,3-dimethylbutan-2-yl)-3-methylbutanamide borane

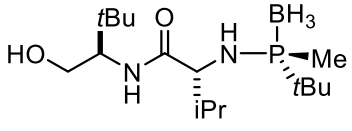

9-S2

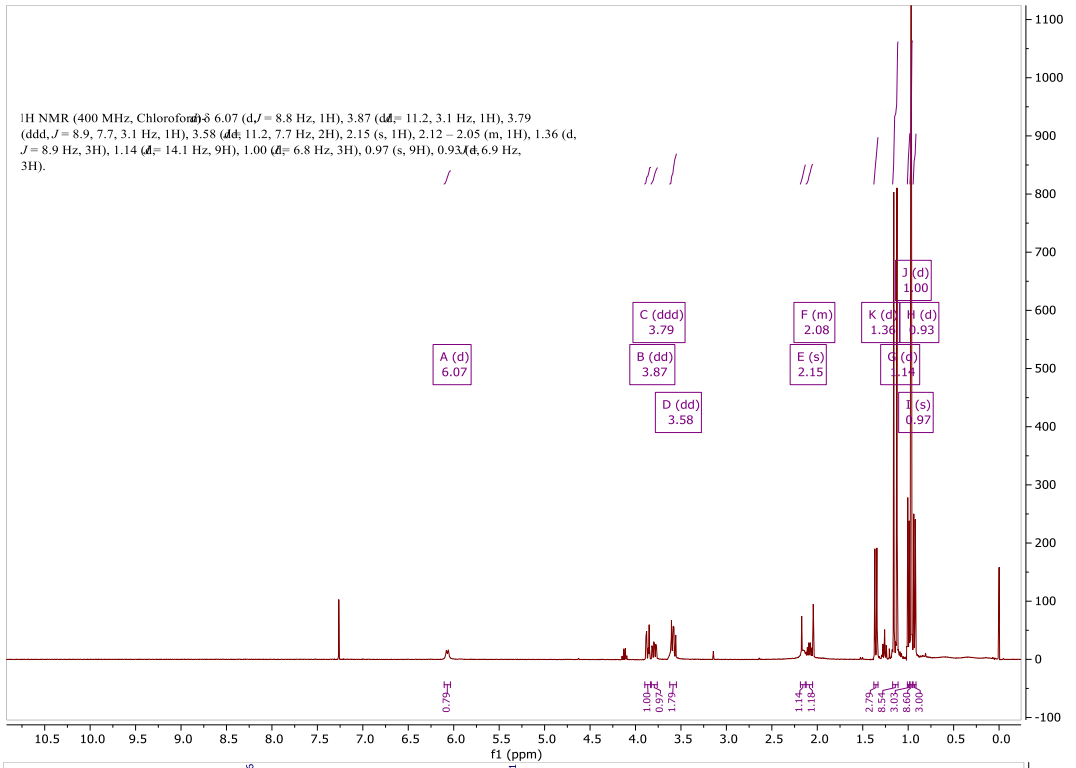

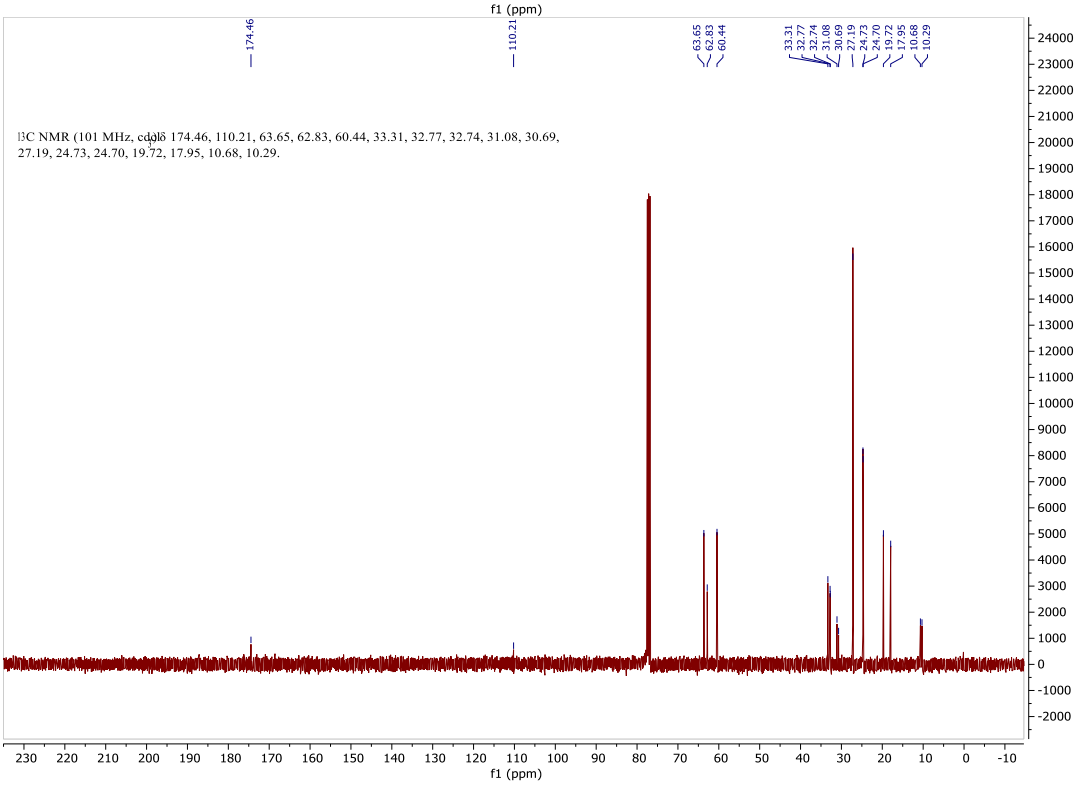

(*S*)-1-*tert*-butyl-N-((*R*)-1-((*R*)-4-(tert-butyl)-4,5-dihydrooxazol-2-yl)-2-methylpropyl)-1-methylphosphanamine borane.

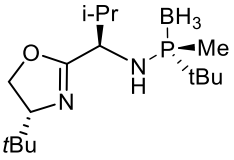

9-S3

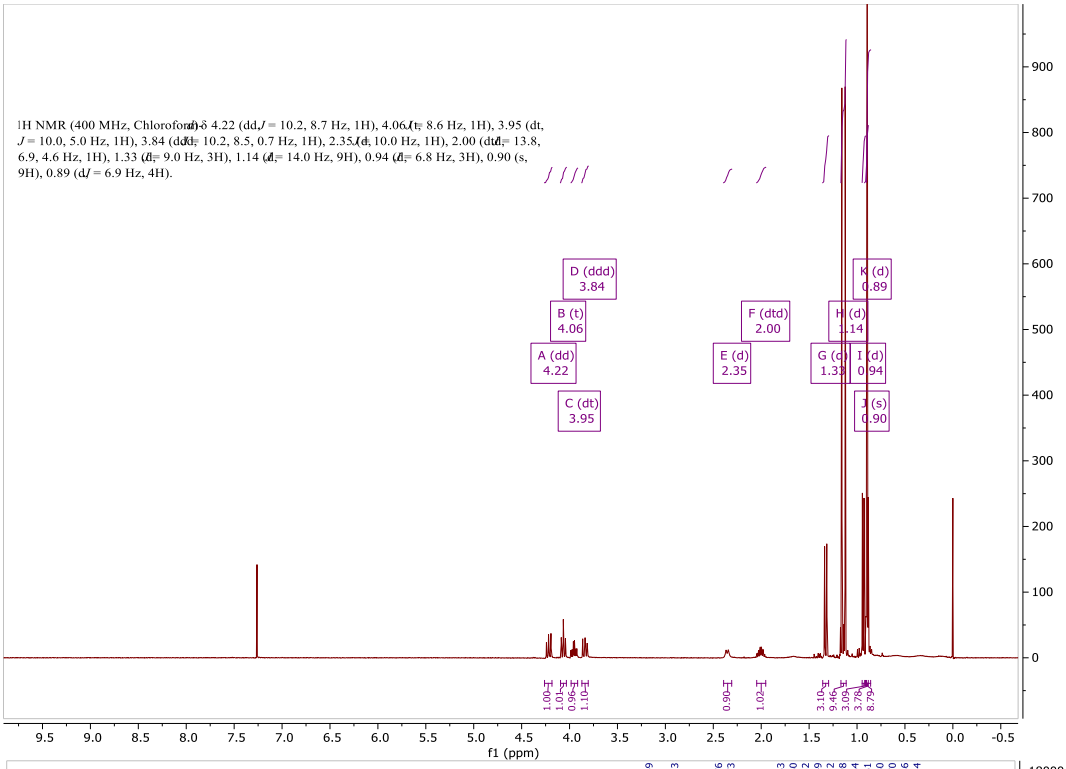

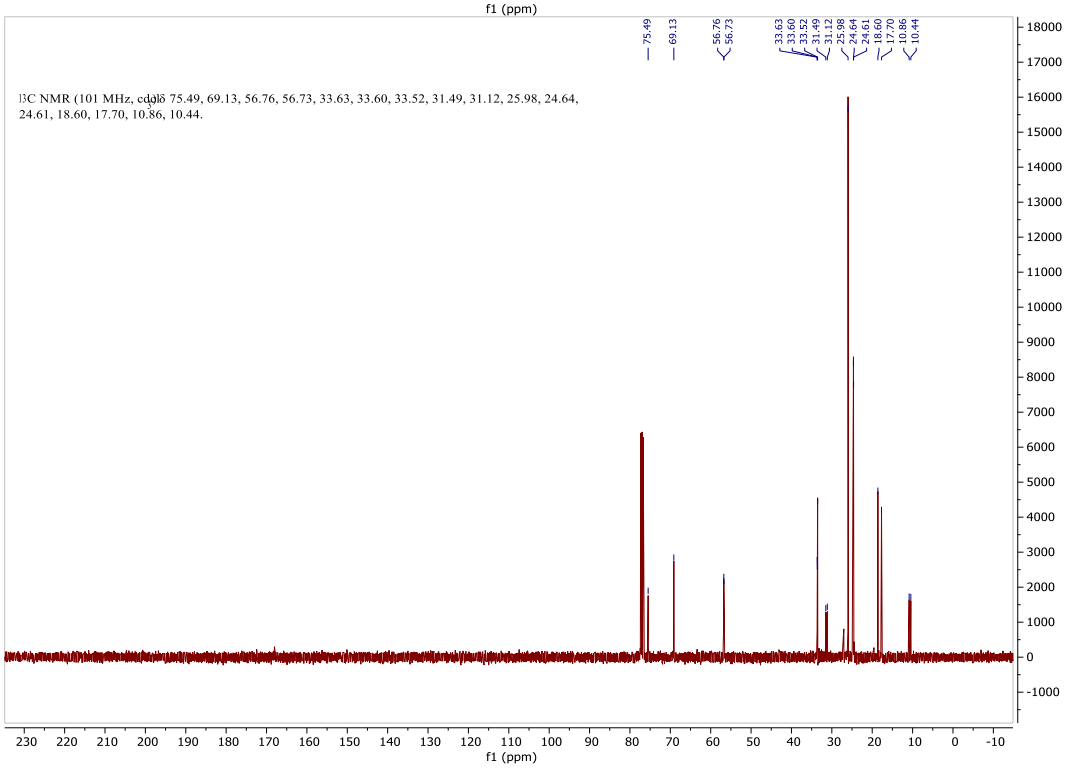

Ir-MaxPHOX tBu (RRR_P)– 2c catalyst

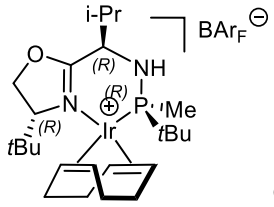

9-2c

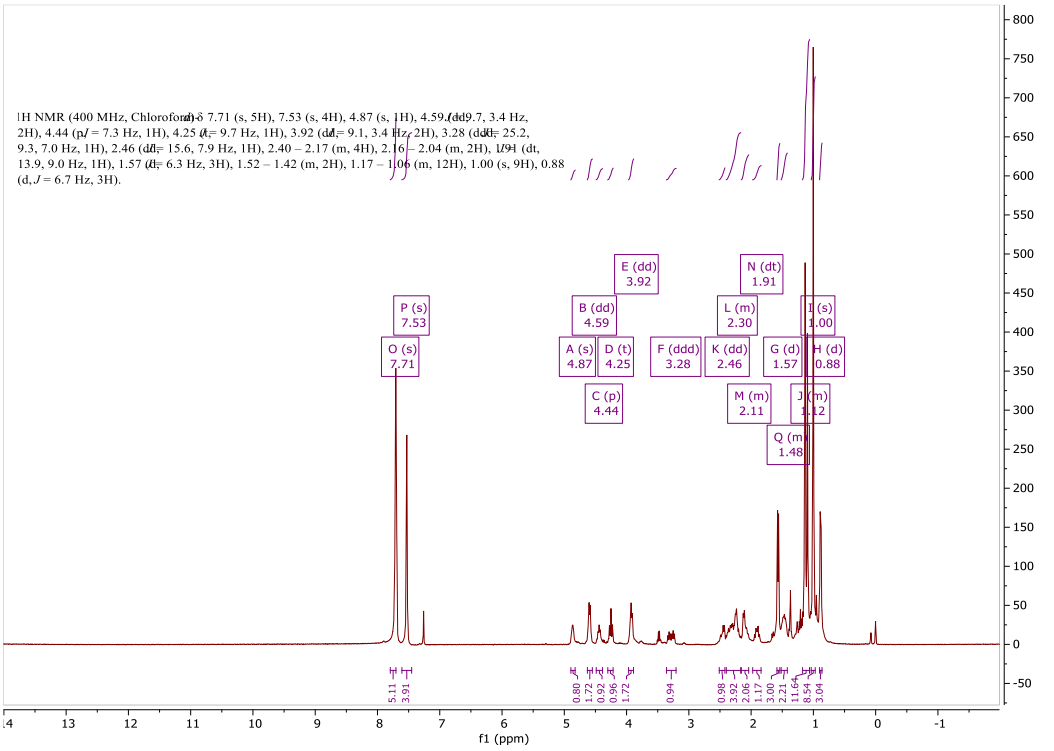

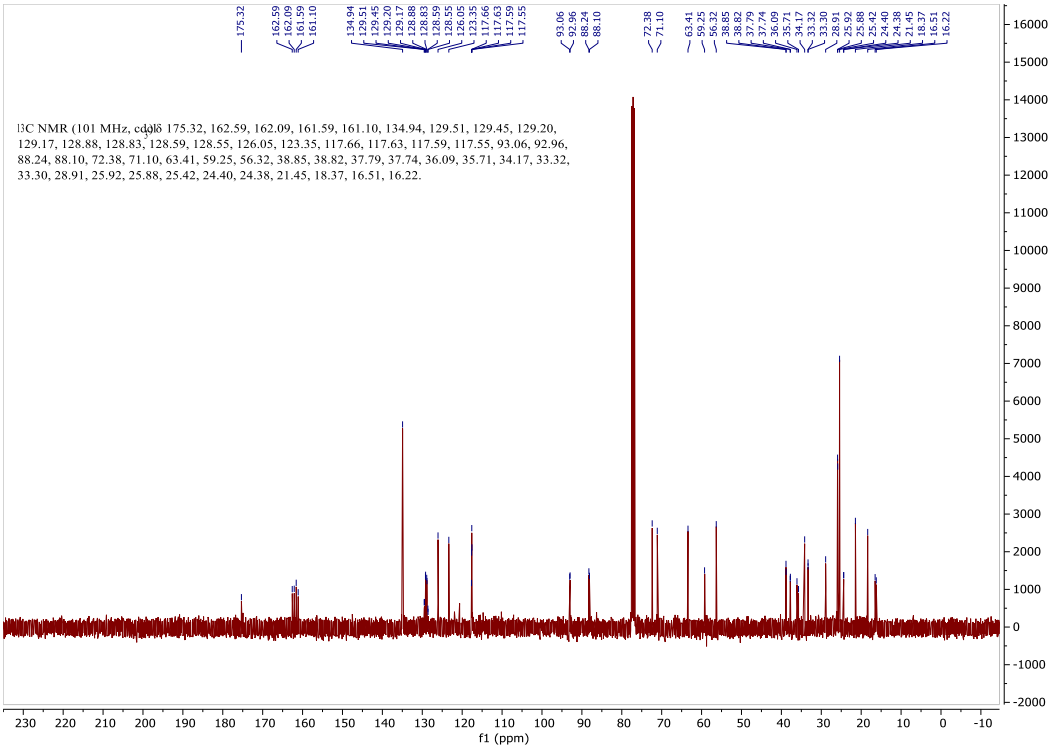

2-(2-(4-iodophenyl)allyl)isoindoline-1,3-dione

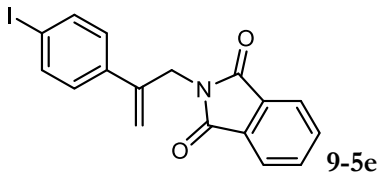

9-5e

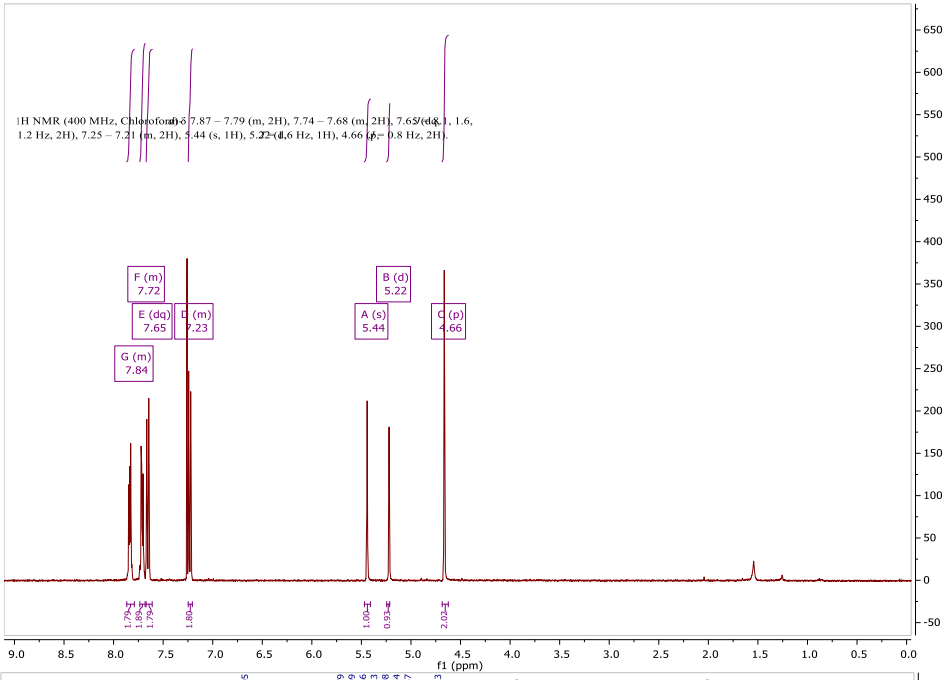

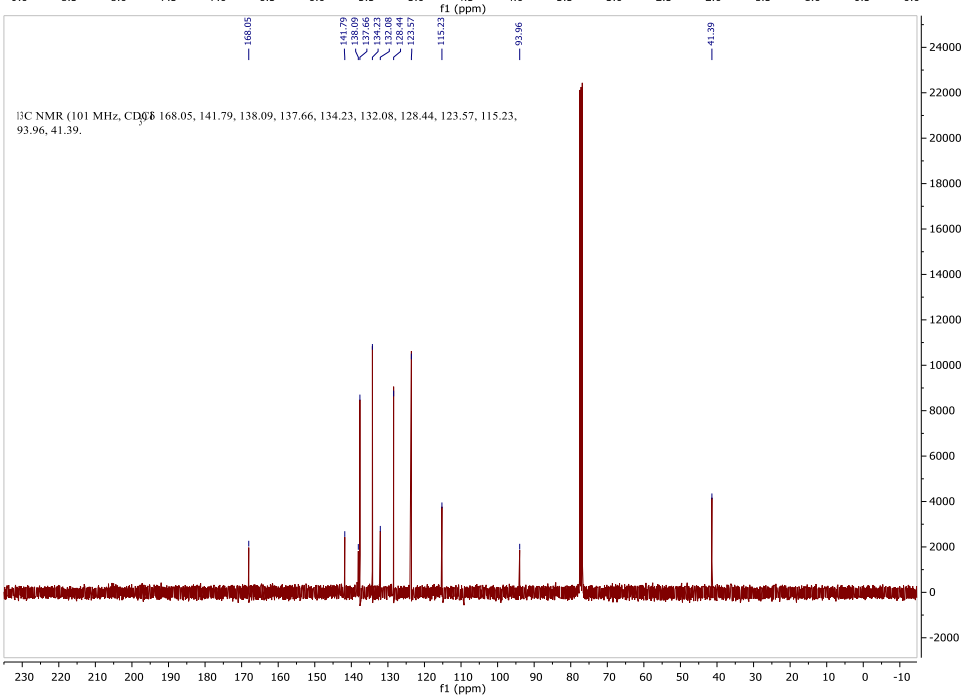

2-(2-(3-chlorophenyl)allyl)isoindoline-1,3-dione

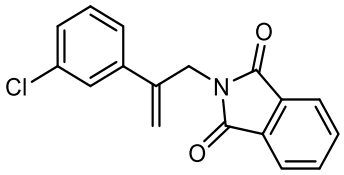

9-5g

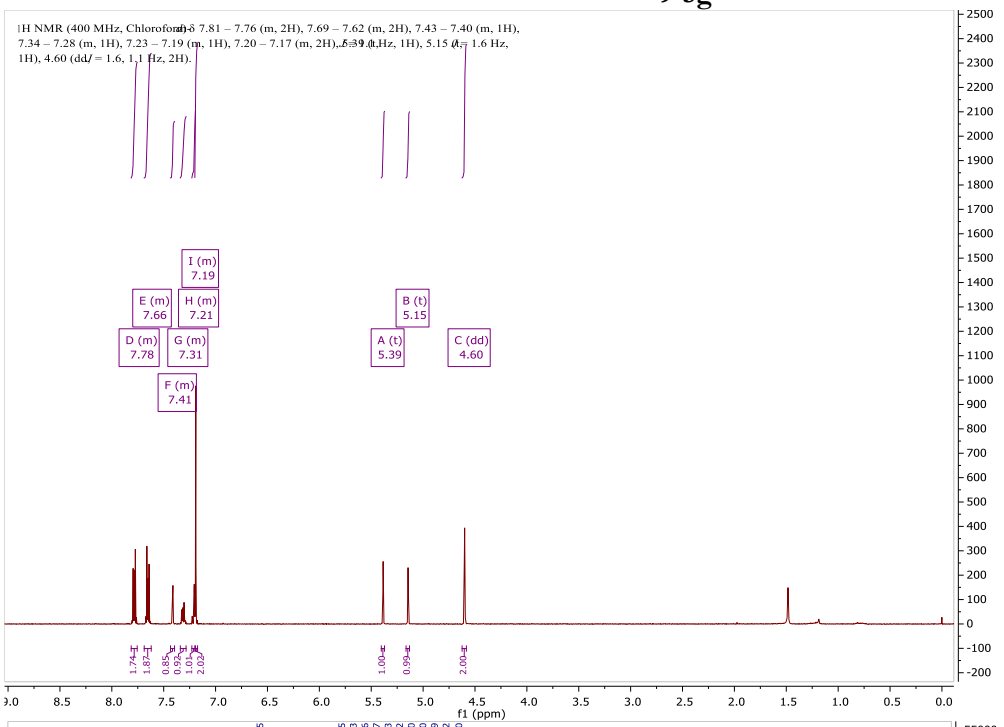

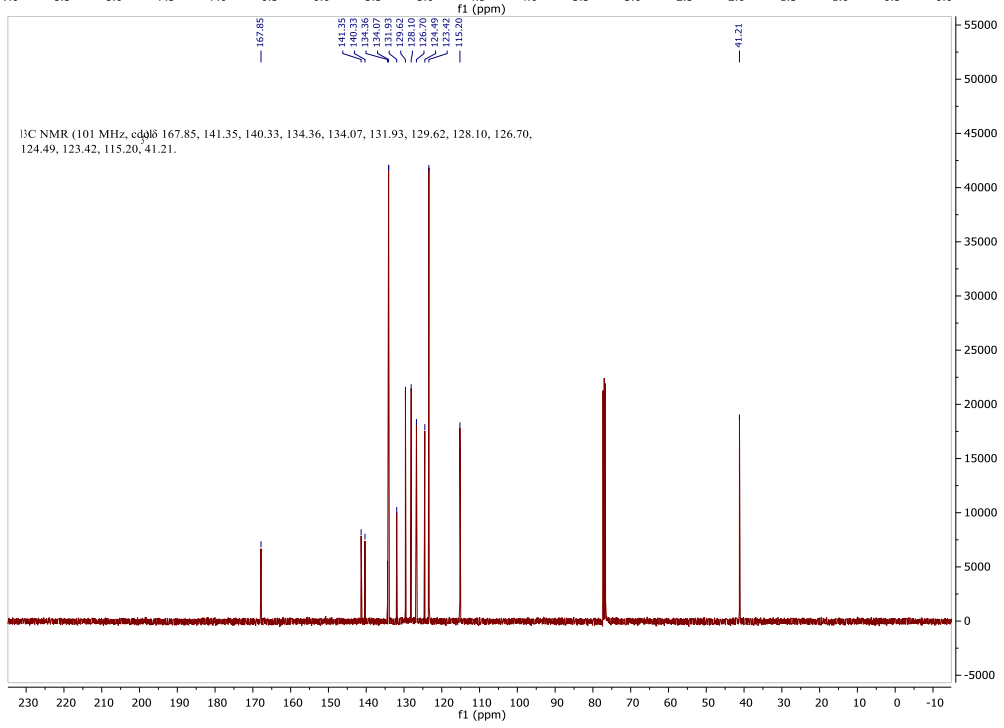

2-(2-(o-tolyl)allyl)isoindoline-1,3-dione

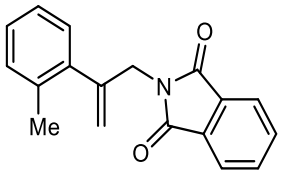

9-5j

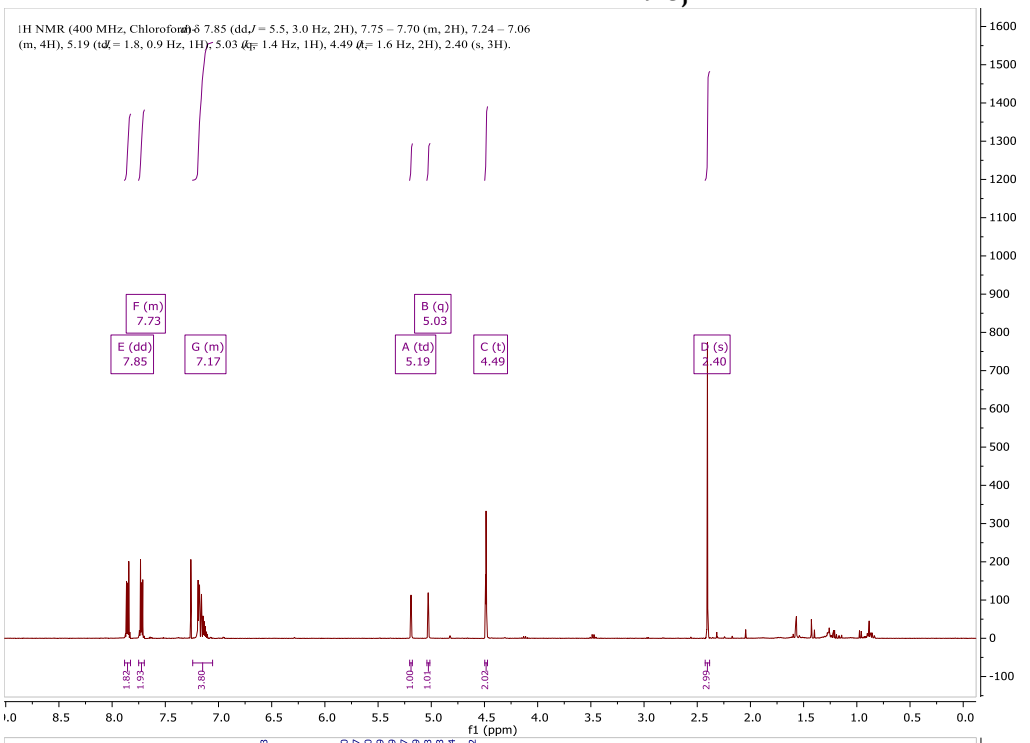

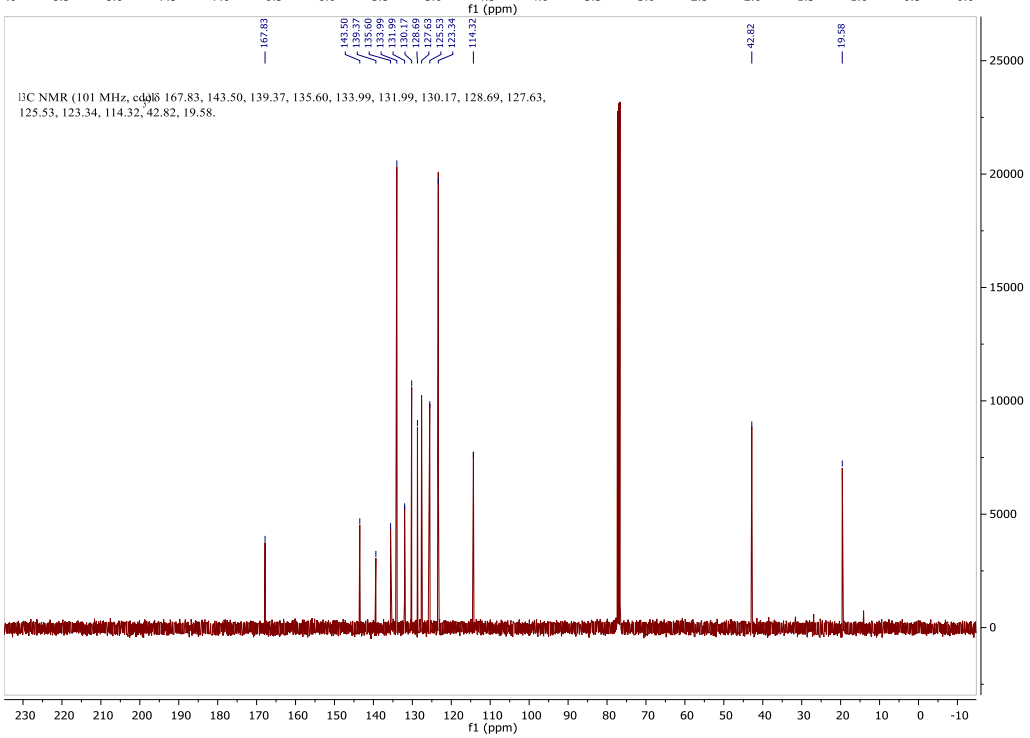

2-(2-(2-bromophenyl)allyl)isoindoline-1,3-dione

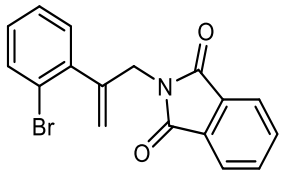

9-5k

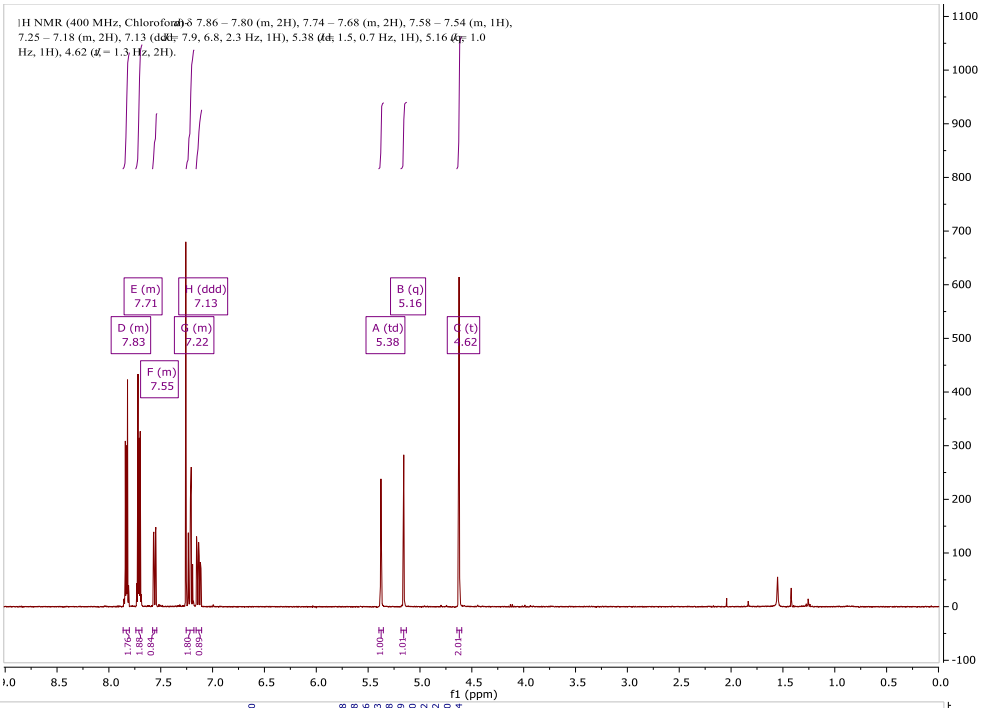

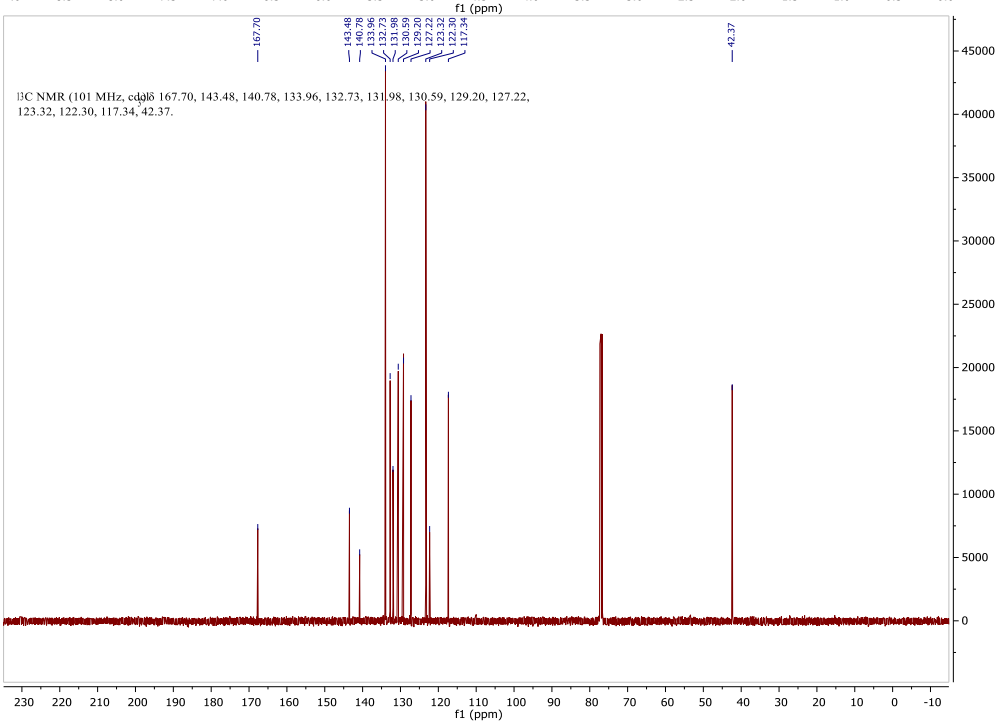

2-(2-(naphthalen-2-yl)allyl)isoindoline-1,3-dione

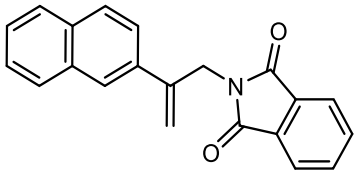

9-51

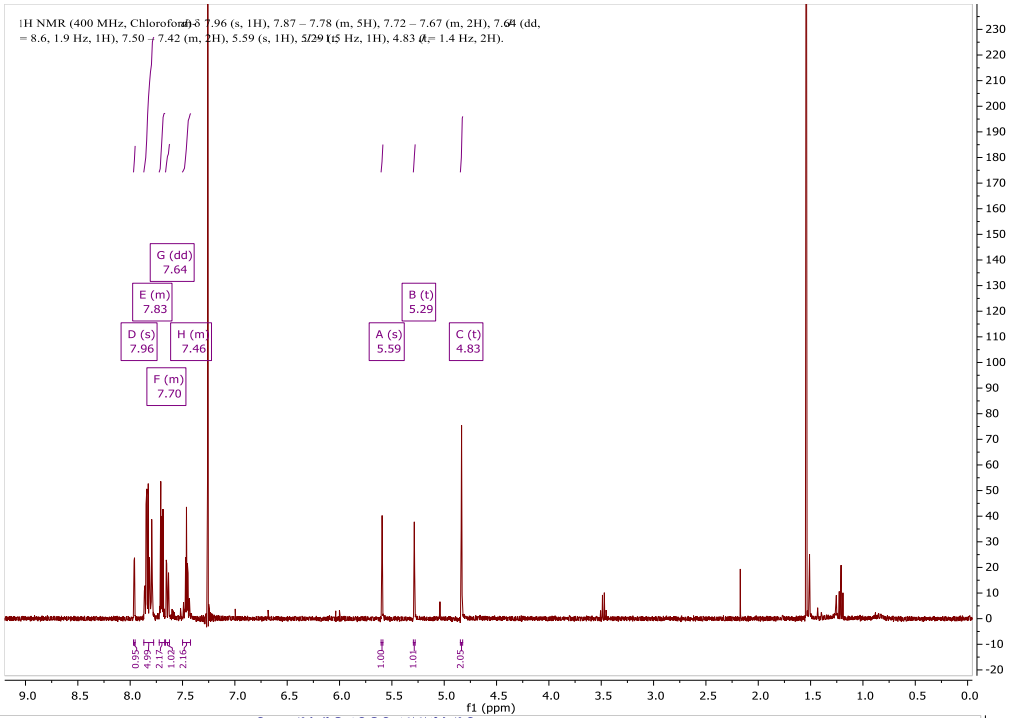

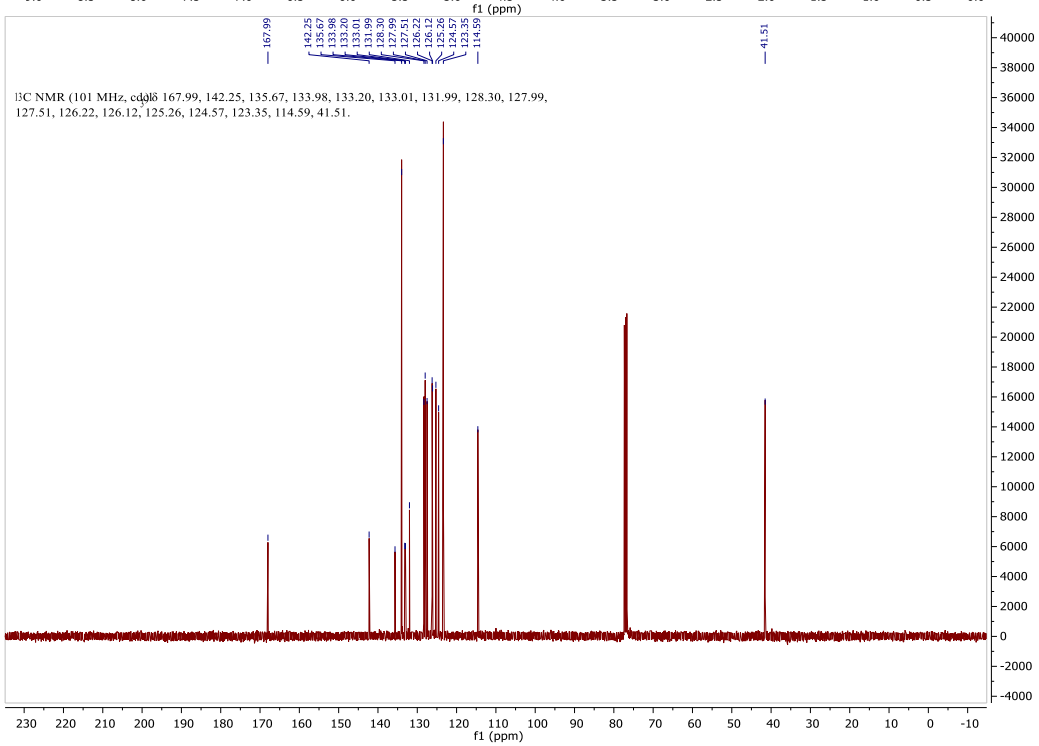

2-(2-(4-isobutylphenyl)allyl)isoindoline-1,3-dione

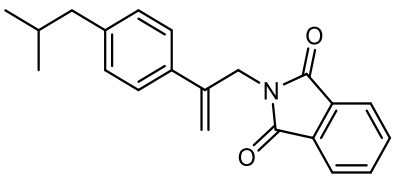

9-5m

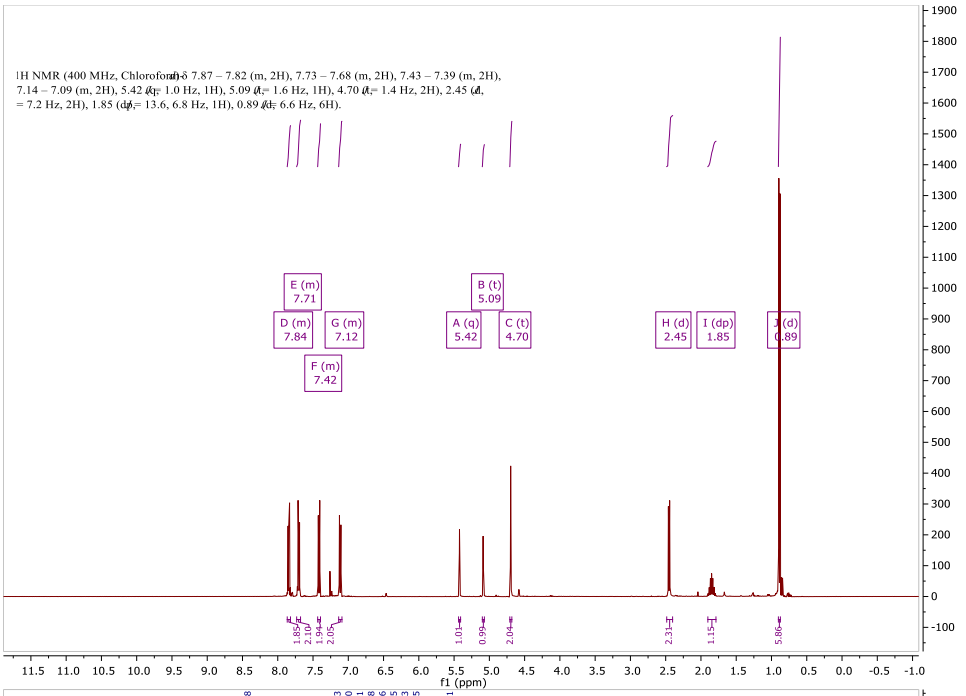

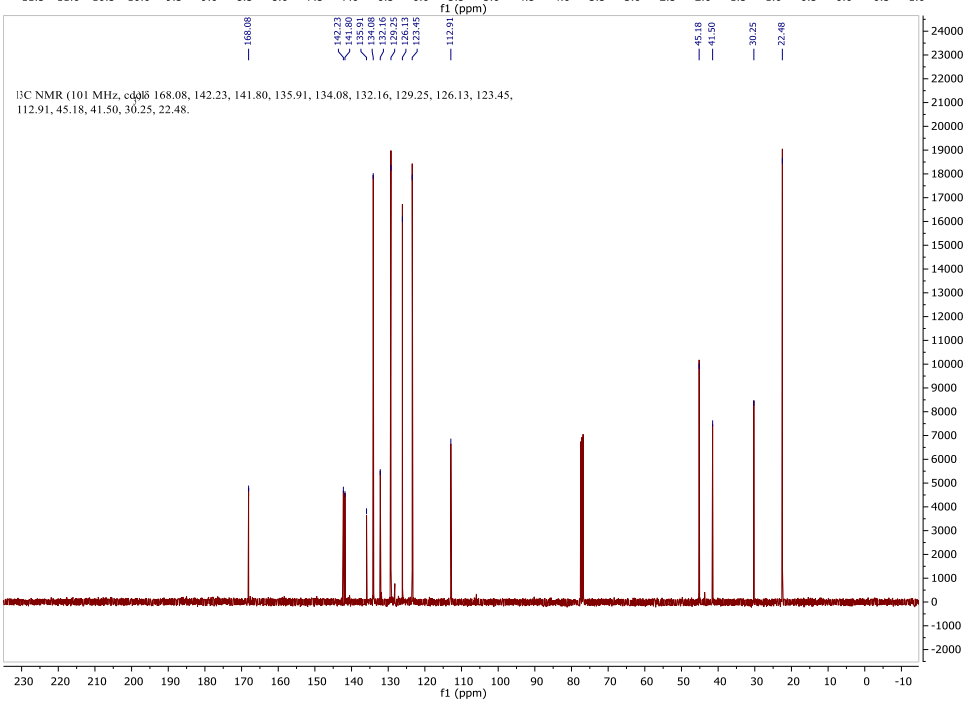

(*R*)-2-(2-(4-fluorophenyl)propyl)isoindoline-1,3-dione

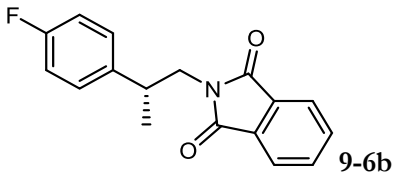

9-6b

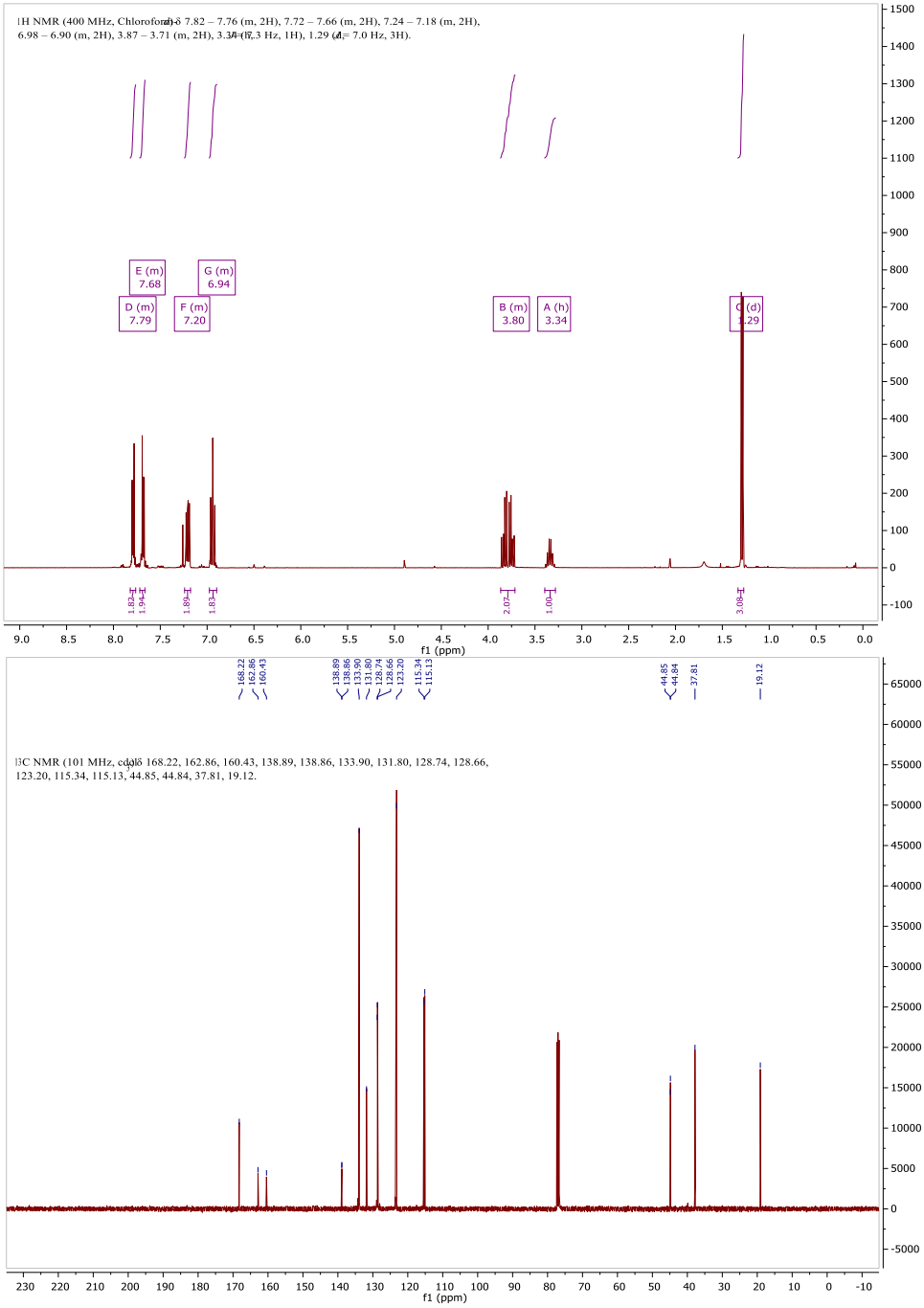

(*R*)-2-(2-(4-chlorophenyl)propyl)isoindoline-1,3-dione

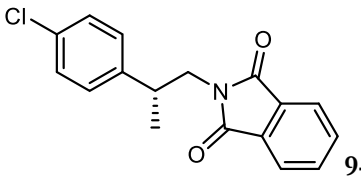

9-6c

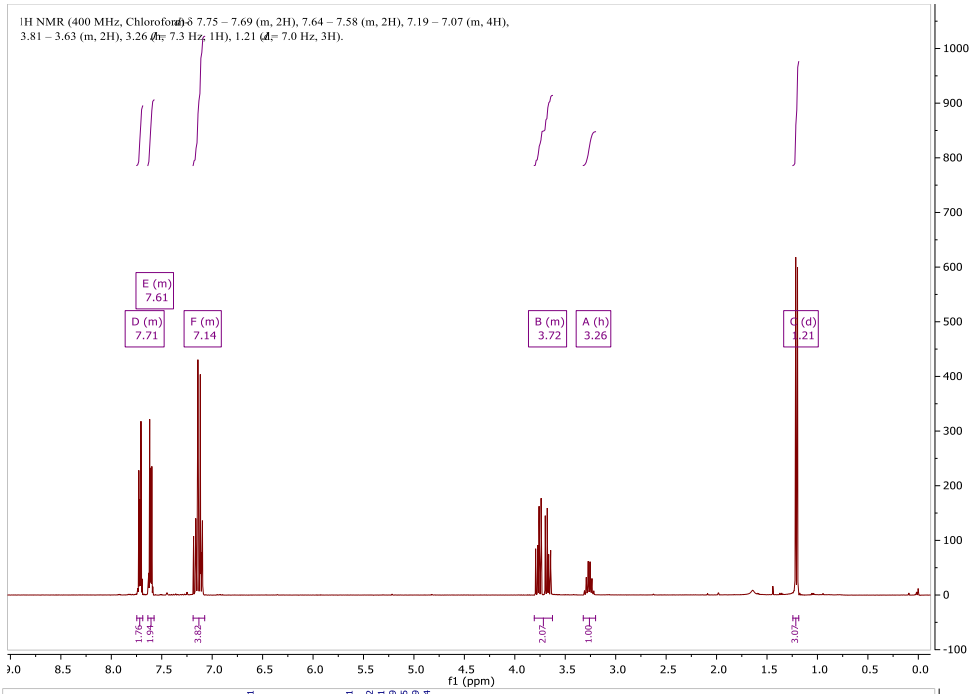

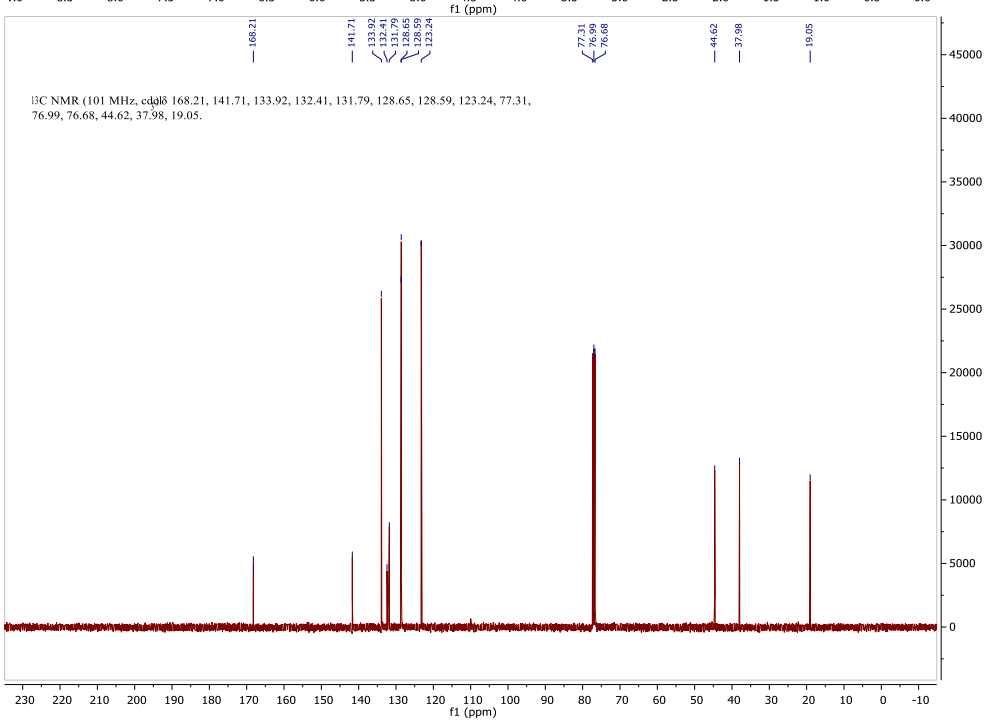

(*R*)-2-(2-(4-bromophenyl)propyl)isoindoline-1,3-dione

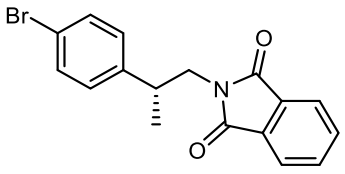

9-6d

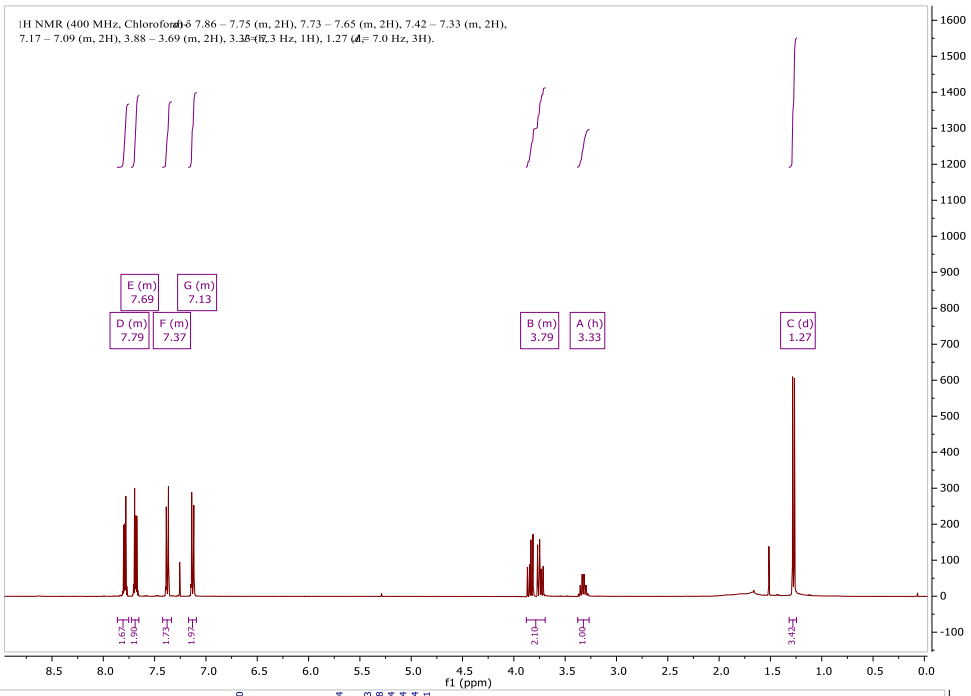

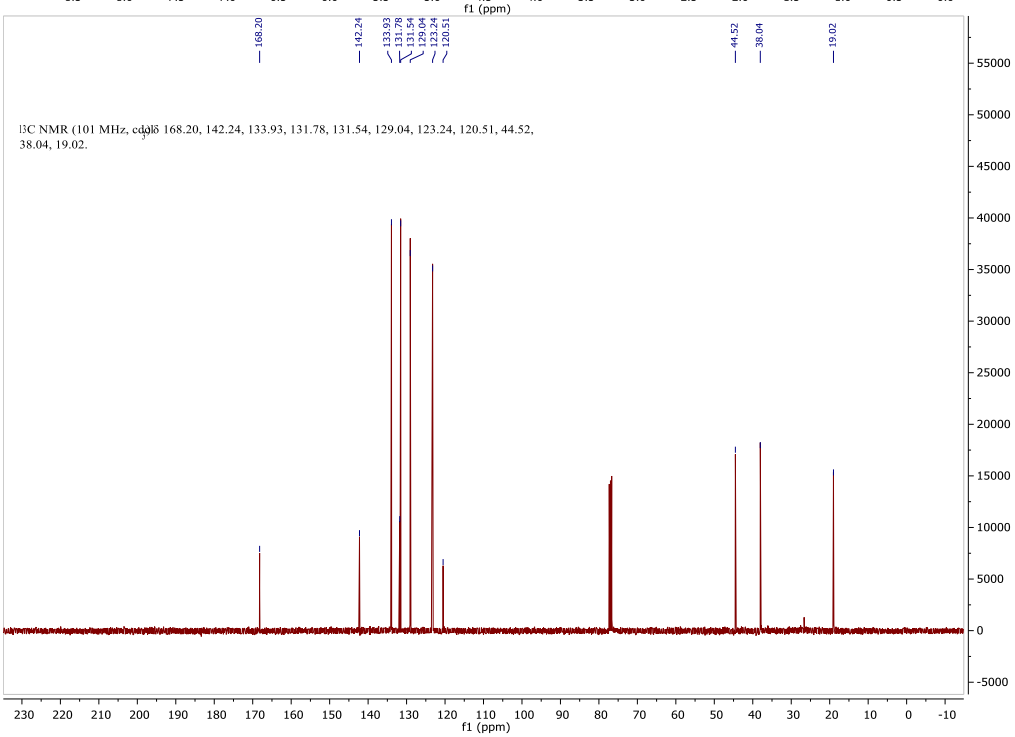

(*R*)-2-(2-(4-iodophenyl)propyl)isoindoline-1,3-dione

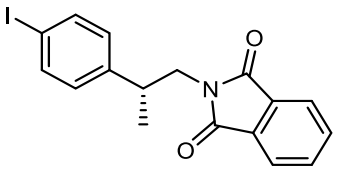

9-6e

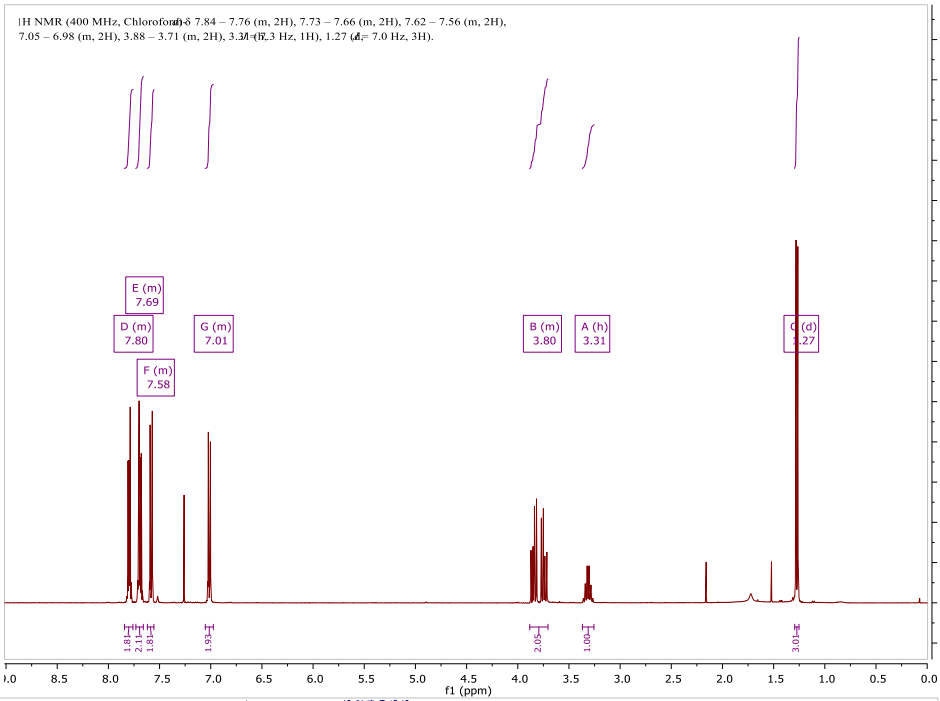

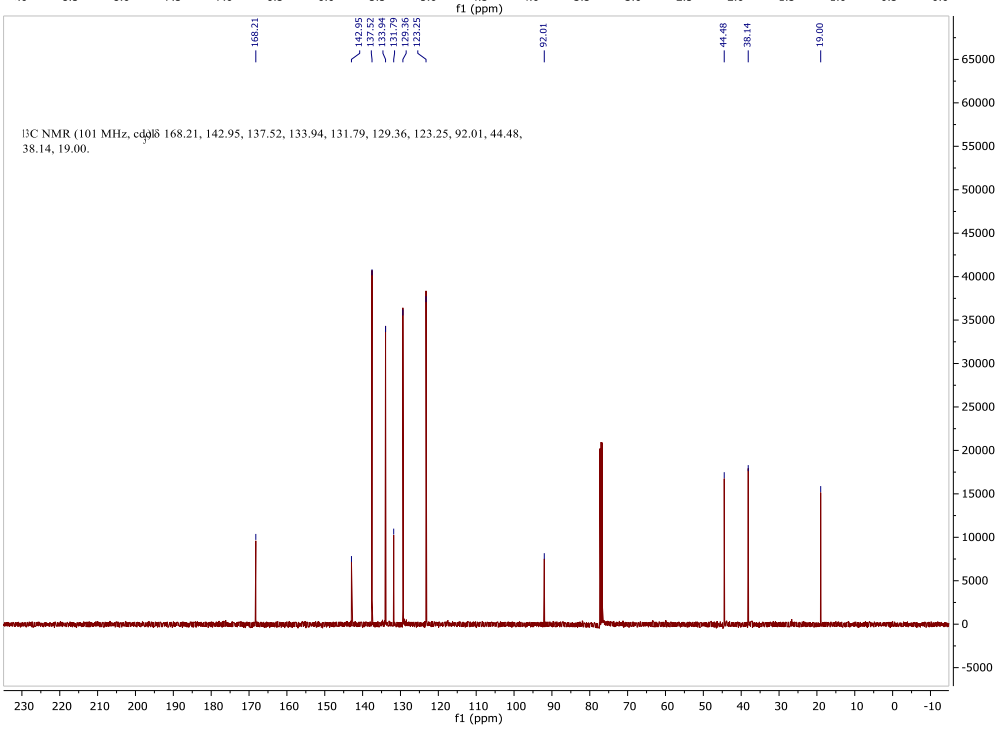

(*R*)-2-(2-(p-tolyl)propyl)isoindoline-1,3-dione

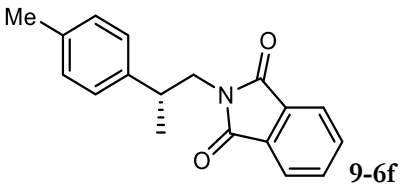

9-6f

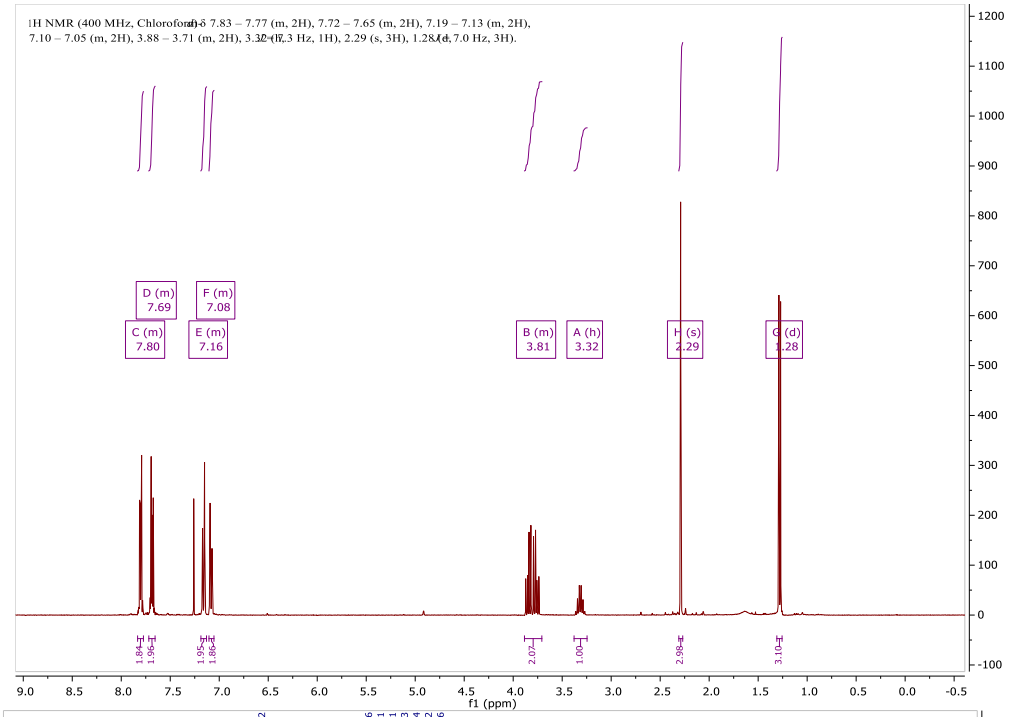

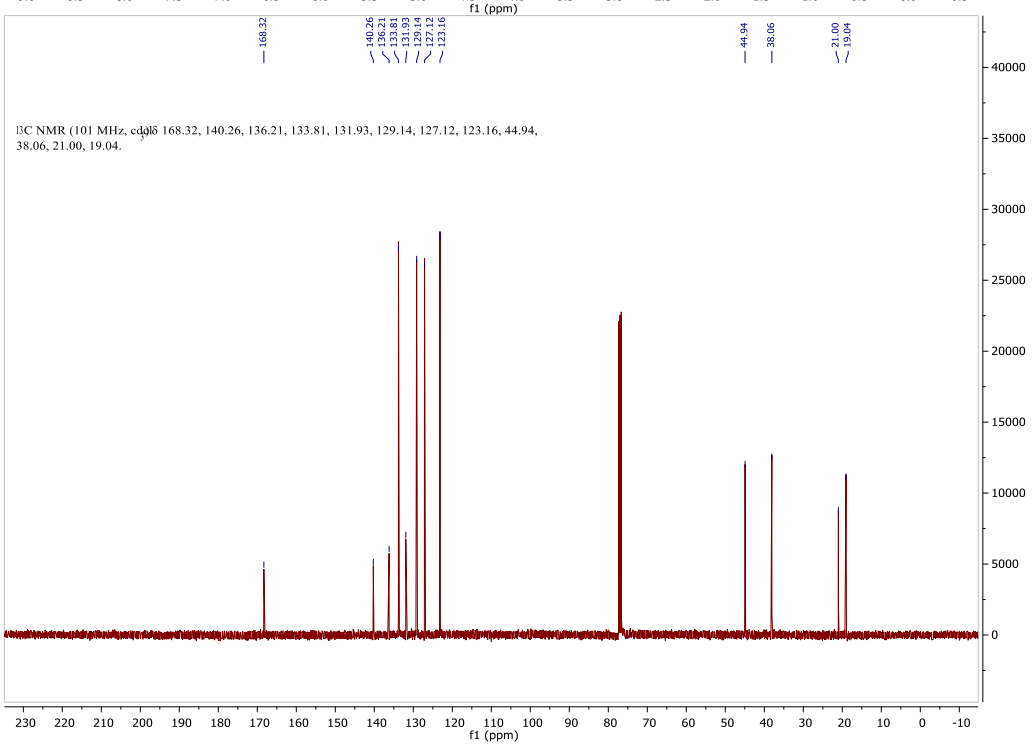

(*R*)-2-(2-(3-chlorophenyl)propyl)isoindoline-1,3-dione

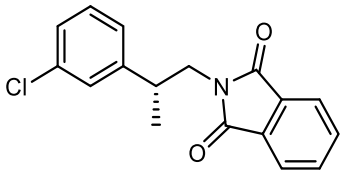

9-6g

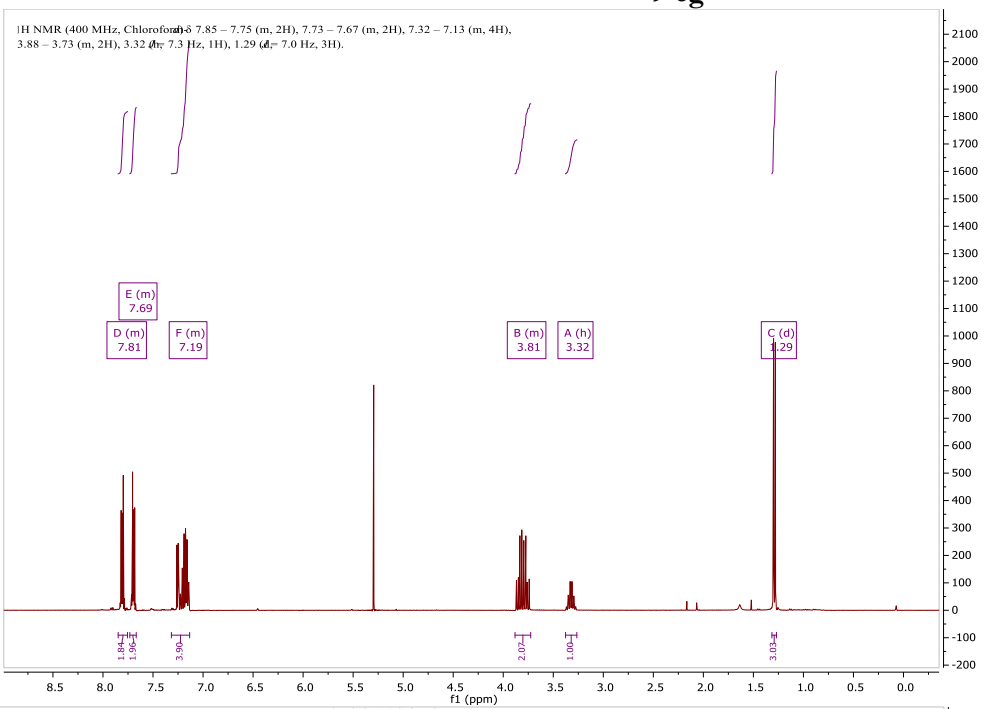

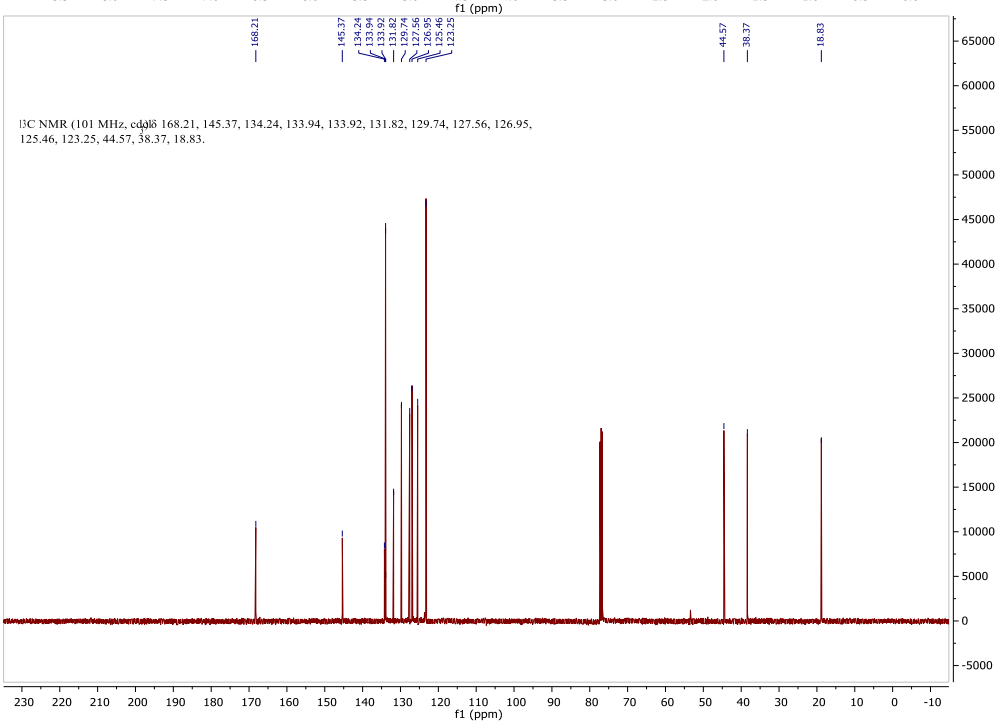

(*R*)-2-(2-(3-methoxyphenyl)propyl)isoindoline-1,3-dione

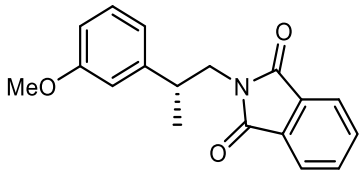

9-6h

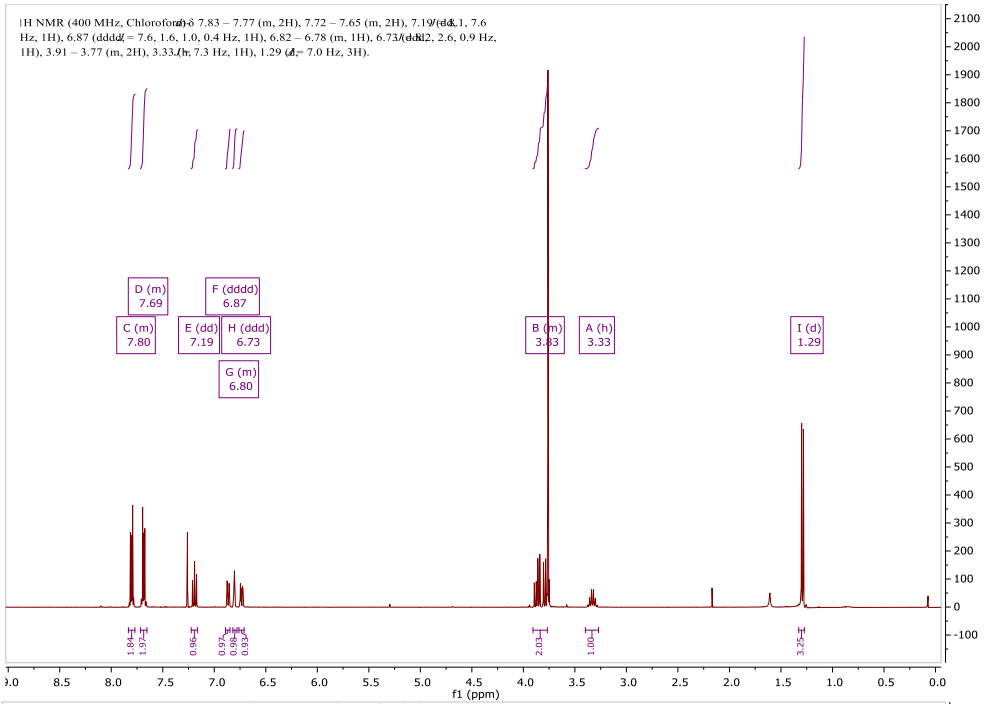

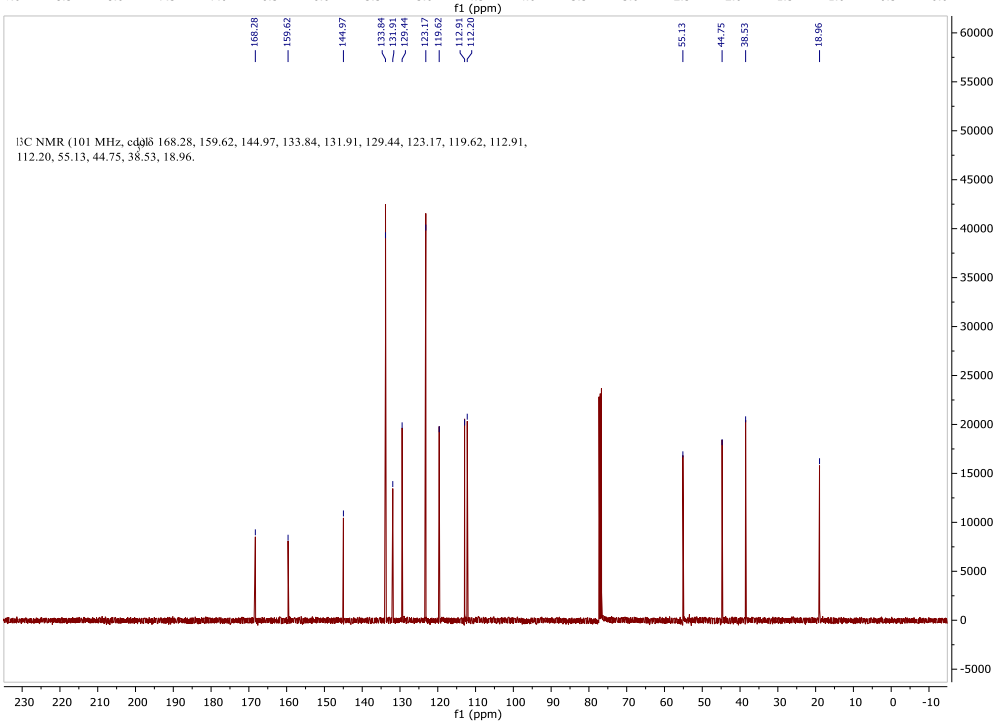

(*R*)-2-(2-(2-methoxyphenyl)propyl)isoindoline-1,3-dione

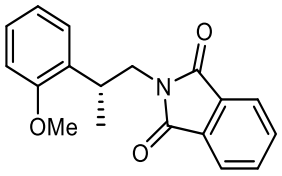

9-6i

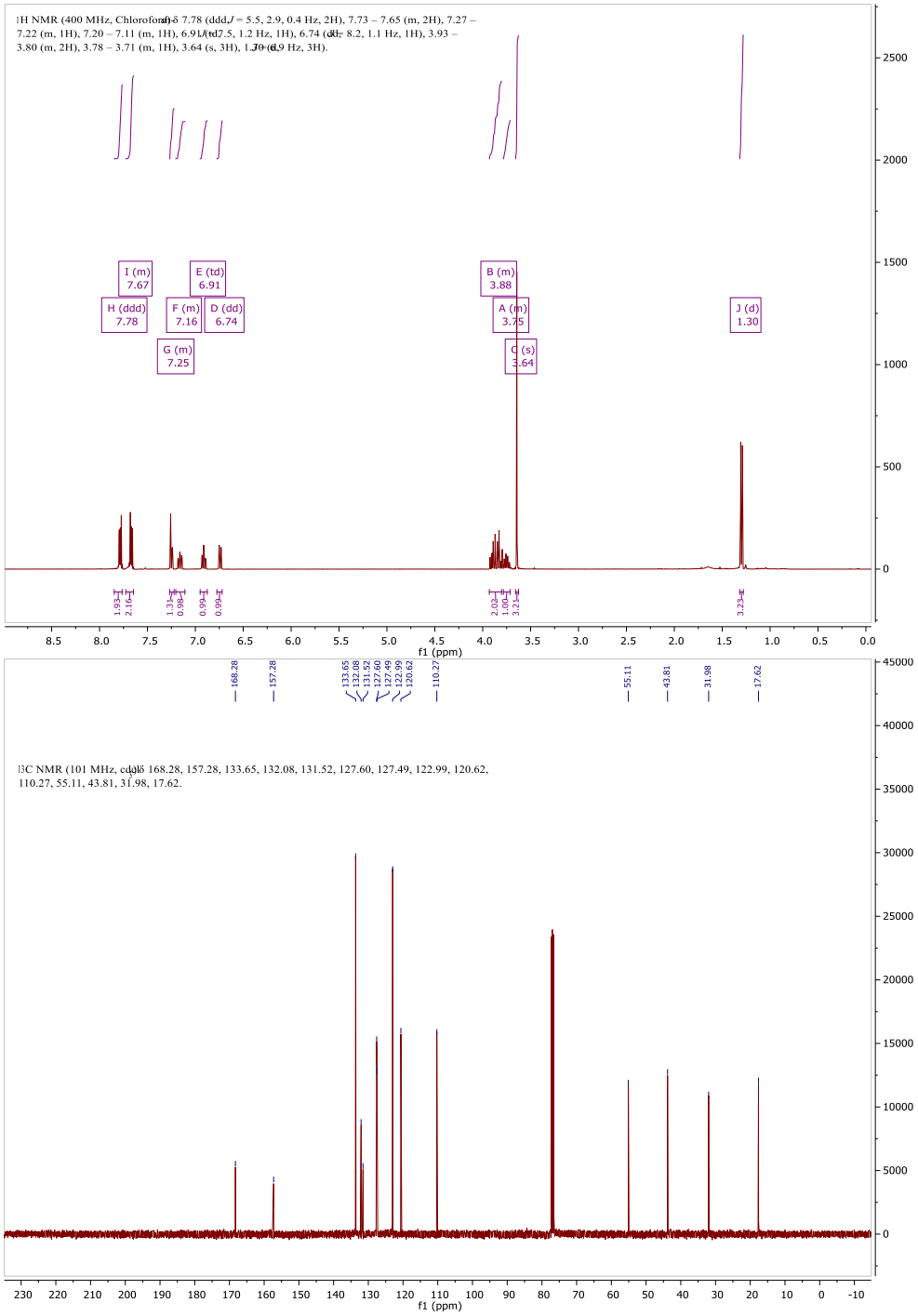

(*R*)-2-(2-(o-tolyl)propyl)isoindoline-1,3-dione

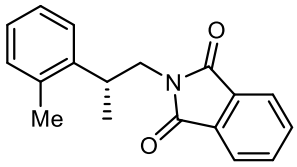

9-6j

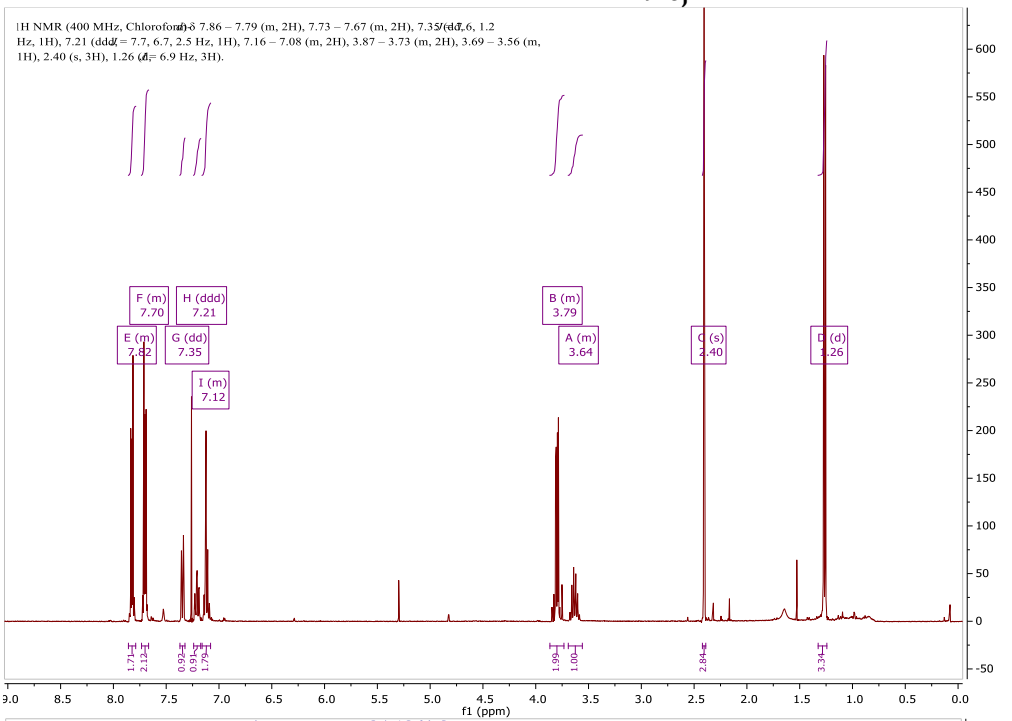

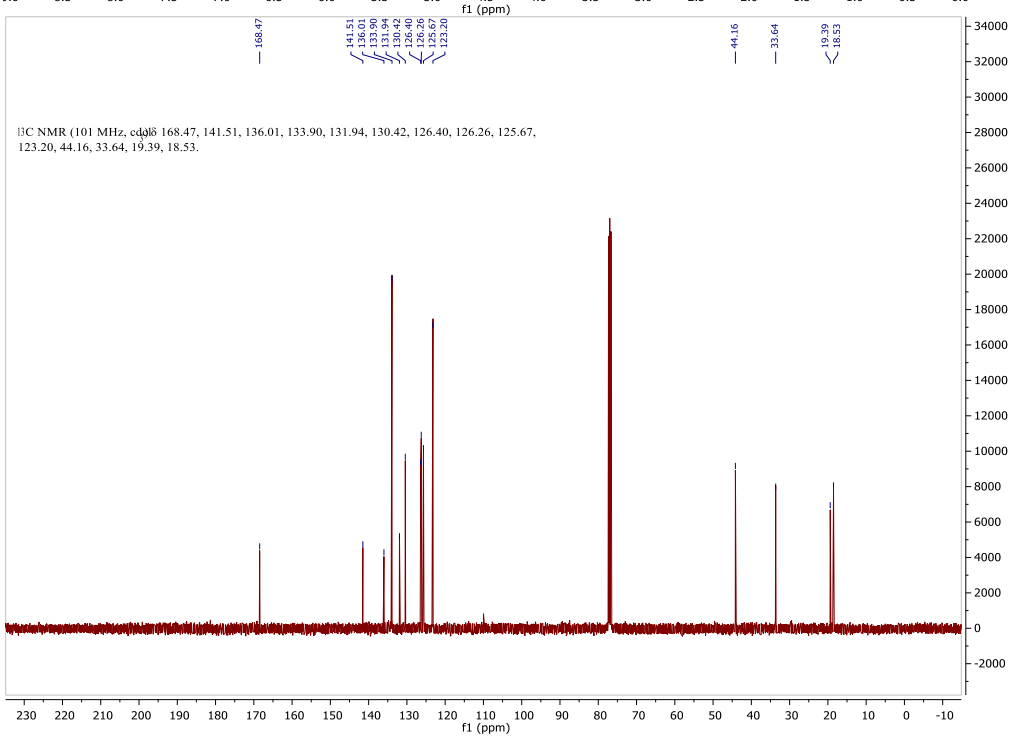

(*R*)-2-(2-(2-bromophenyl)propyl)isoindoline-1,3-dione

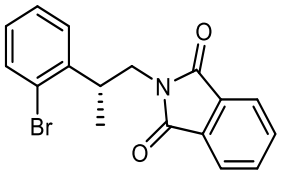

9-6k

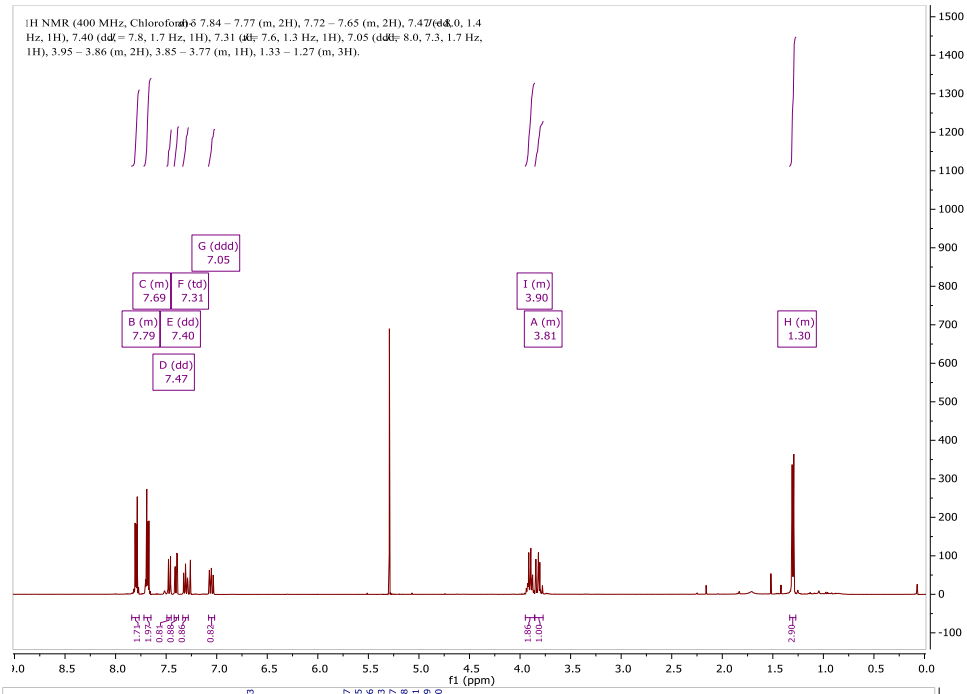

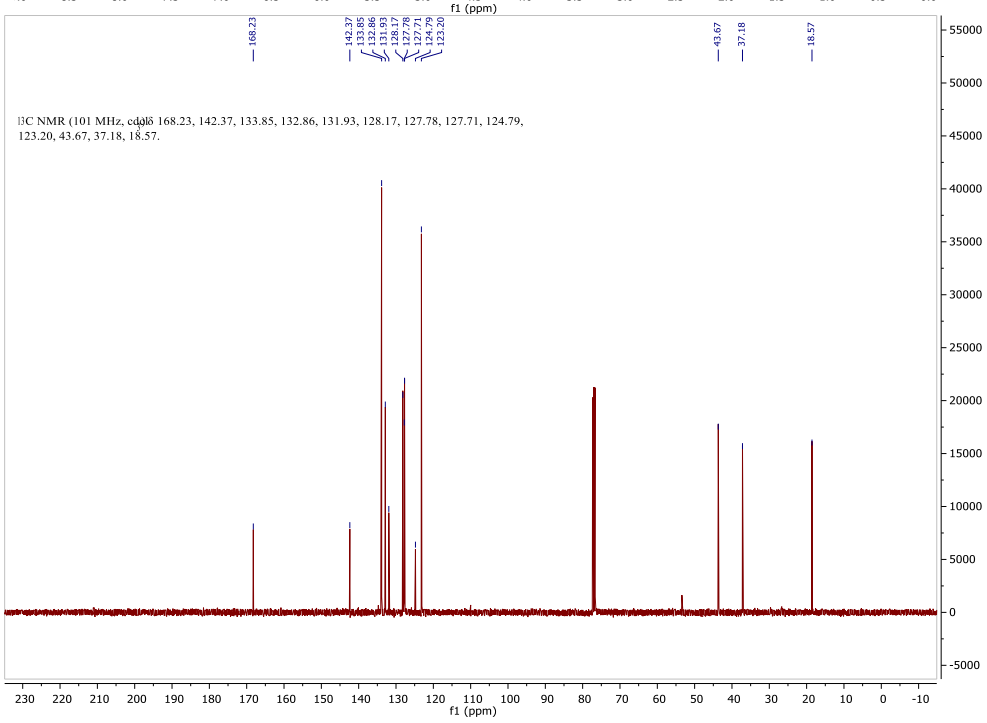

(*R*)-2-(2-(naphthalen-2-yl)propyl)isoindoline-1,3-dione

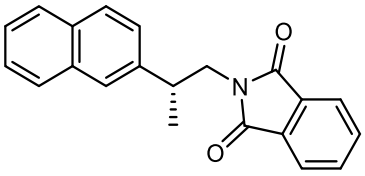

9-61

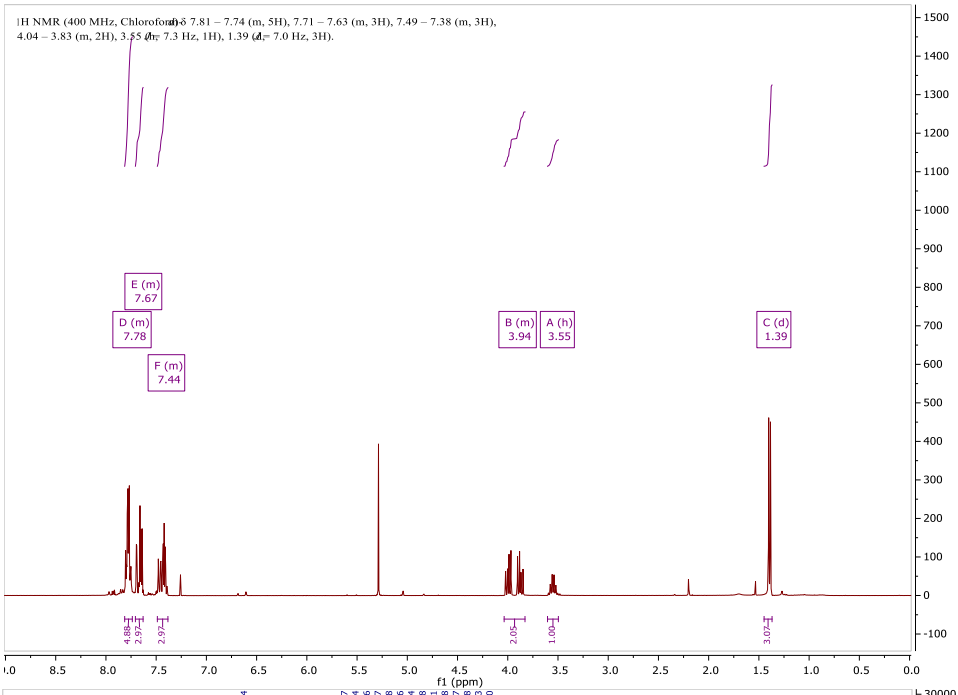

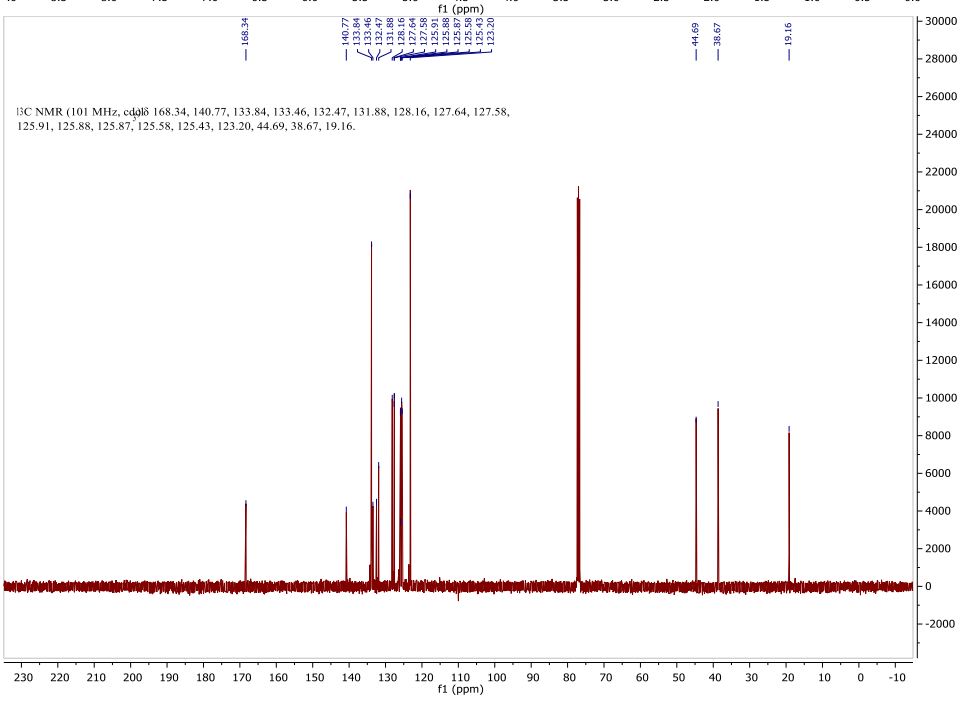

(*R*)-2-(2-(4-isobutylphenyl)propyl)isoindoline-1,3-dione

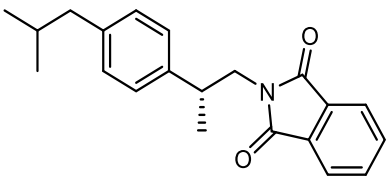

9-6m

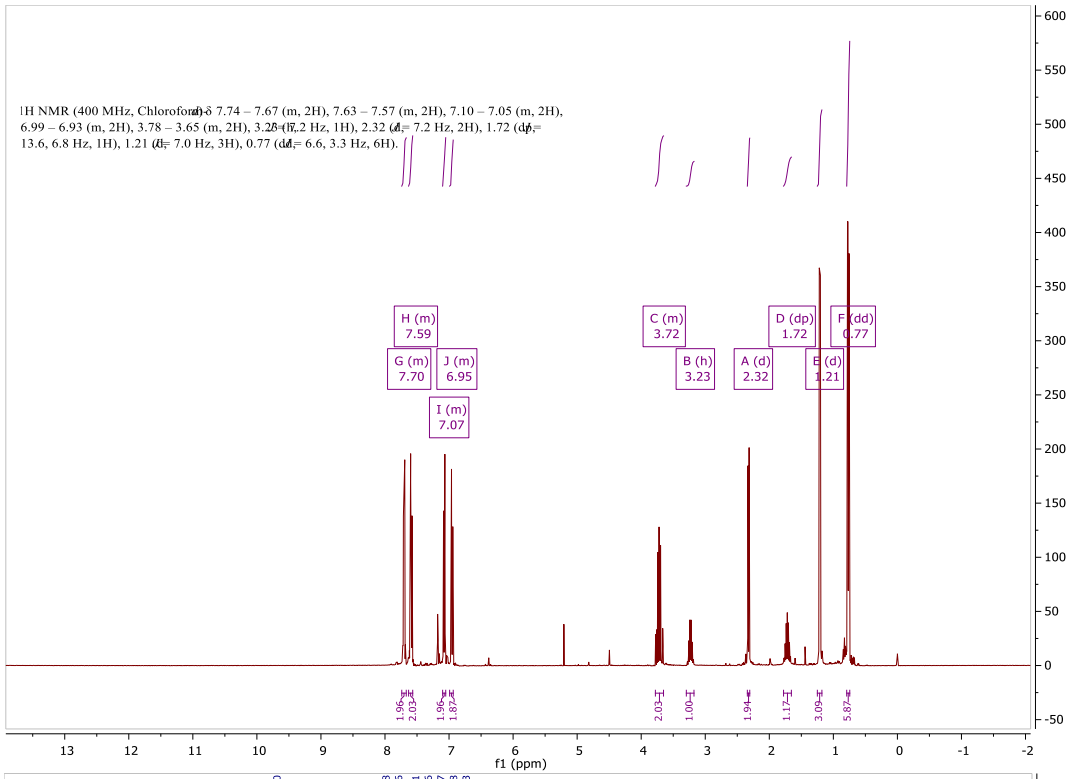

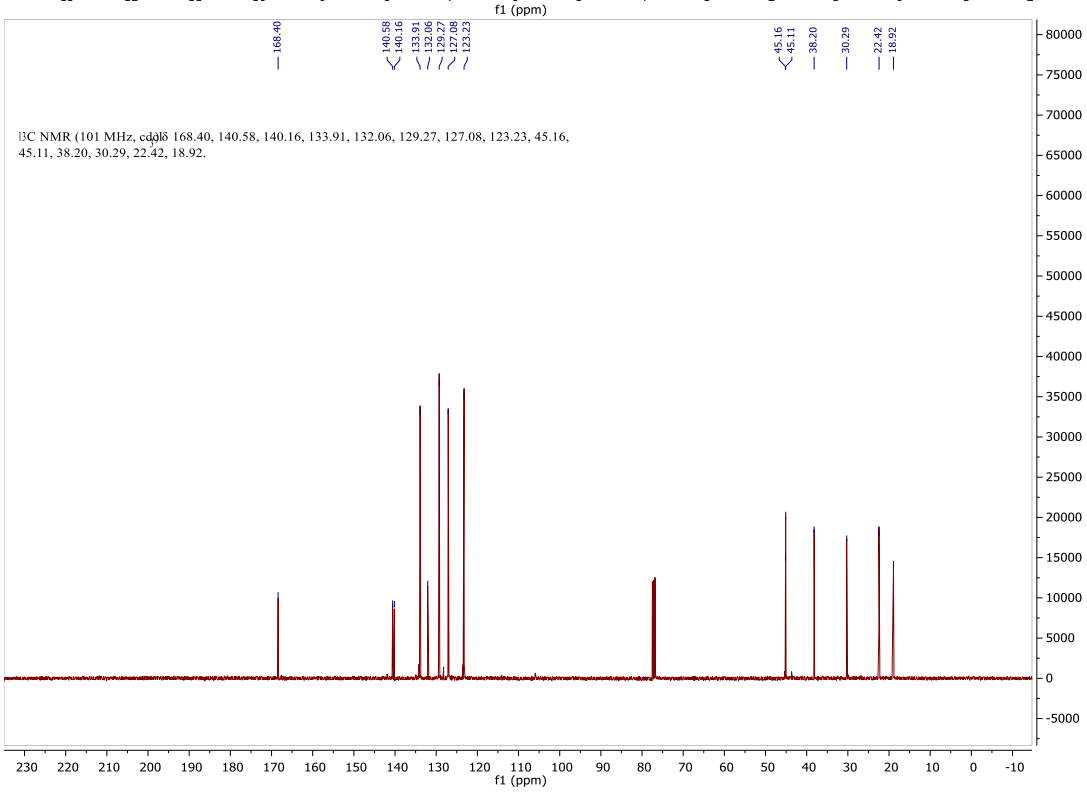

(*R*)-2-(3-chlorophenyl)propan-1-amine

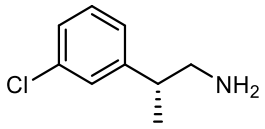

9-7

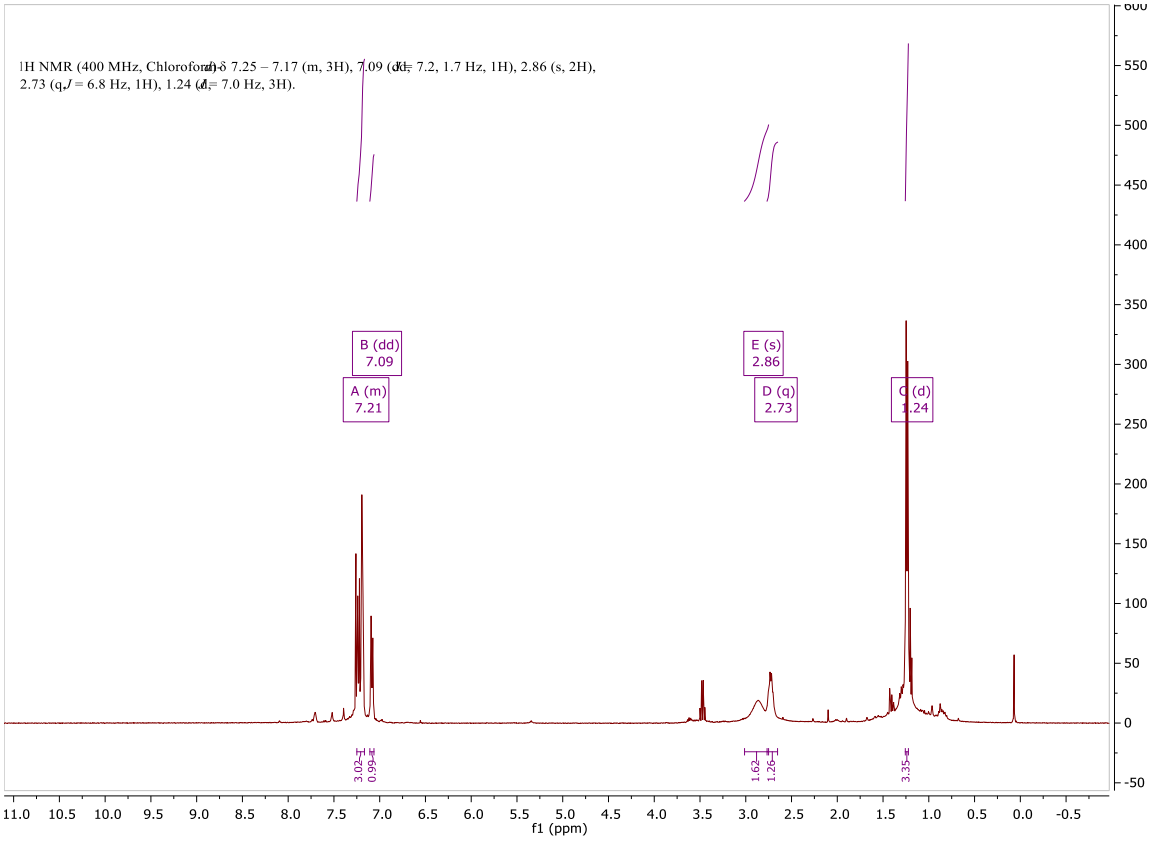

tert-Butyl (R)-(2-(4-bromophenyl)propyl)carbamate

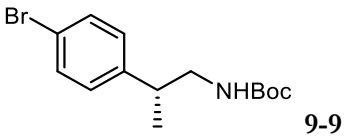

9-9

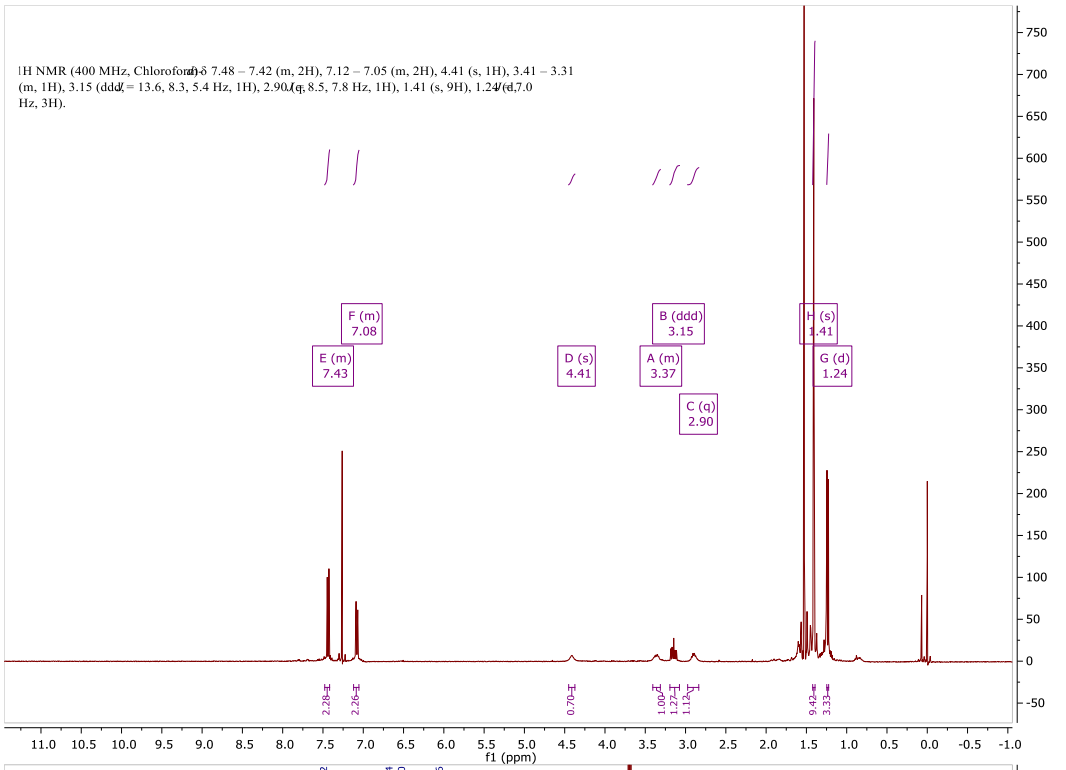

^{1}H NMR (400 MHz, Chloroform-d) δ 7.48 – 7.42 (m, 2H), 7.12 – 7.05 (m, 2H), 4.41 (s, 1H), 3.41 – 3.31 (m, 1H), 3.15 (ddd, J = 13.6, 8.3, 5.4 Hz, 1H), 2.90 (q, 8.5, 7.8 Hz, 1H), 1.41 (s, 9H), 1.24 (d, J = 7.0 Hz, 3H).

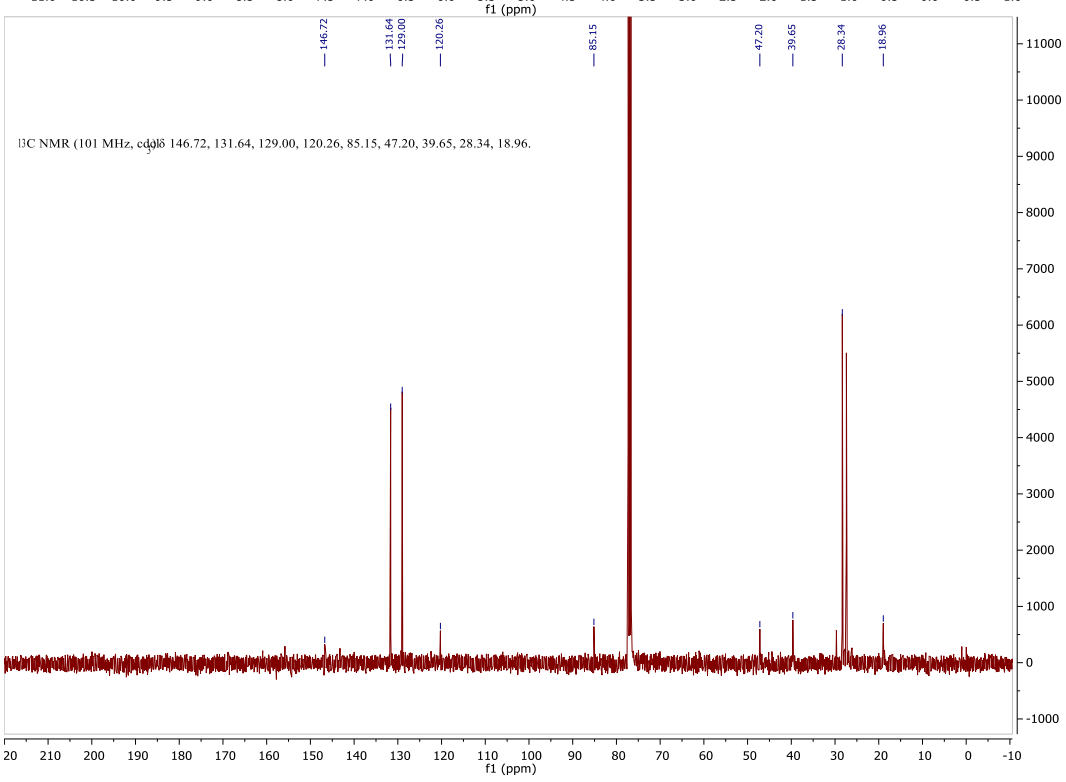

^{13}C NMR (101 MHz, $CDCl_3$) δ 146.72, 131.64, 129.00, 120.26, 85.15, 47.20, 39.65, 28.34, 18.96.

(*R*)-2-(2-bromophenyl)propan-1-amine

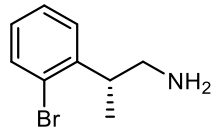

9-S4

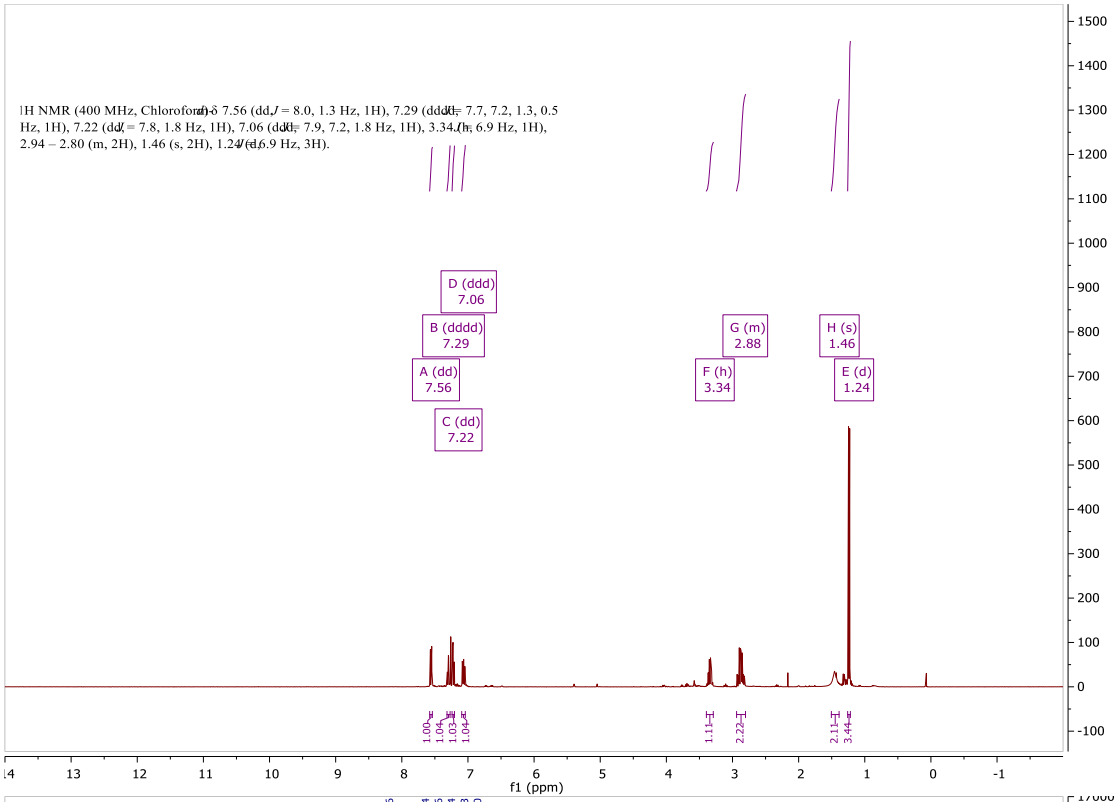

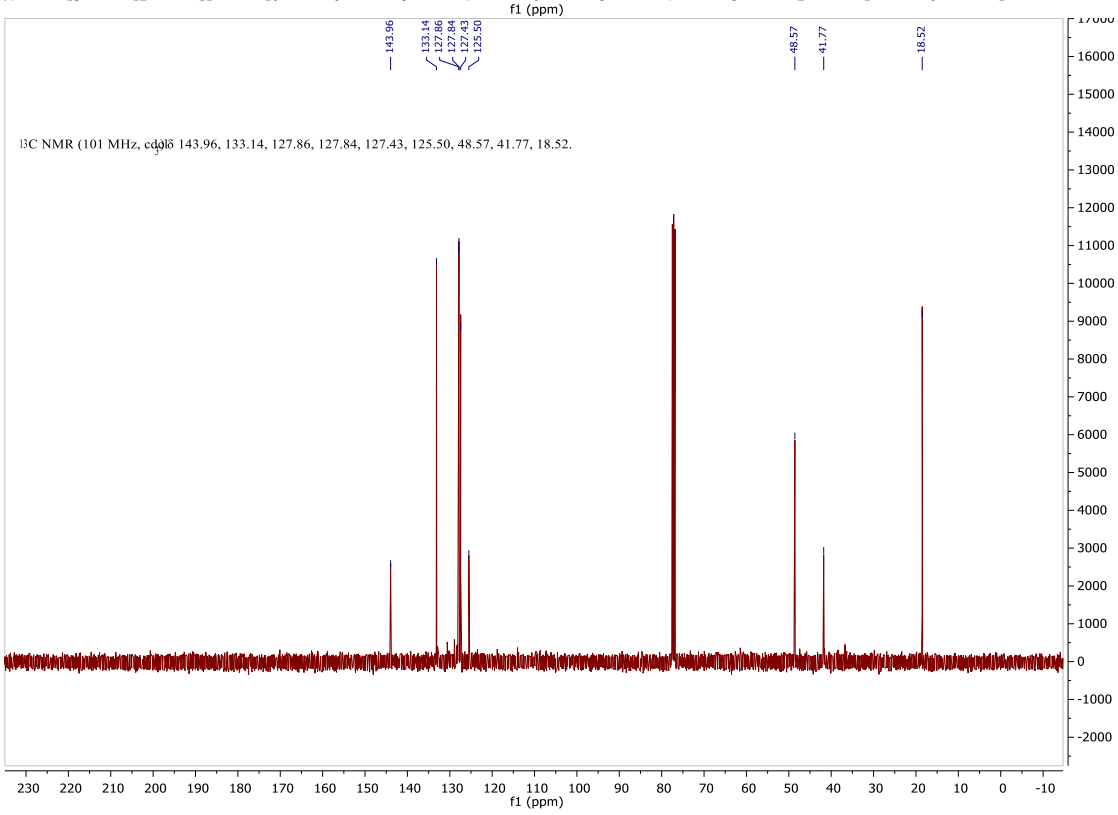

(*R*)-3-methylindoline

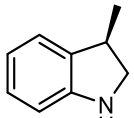

9-11

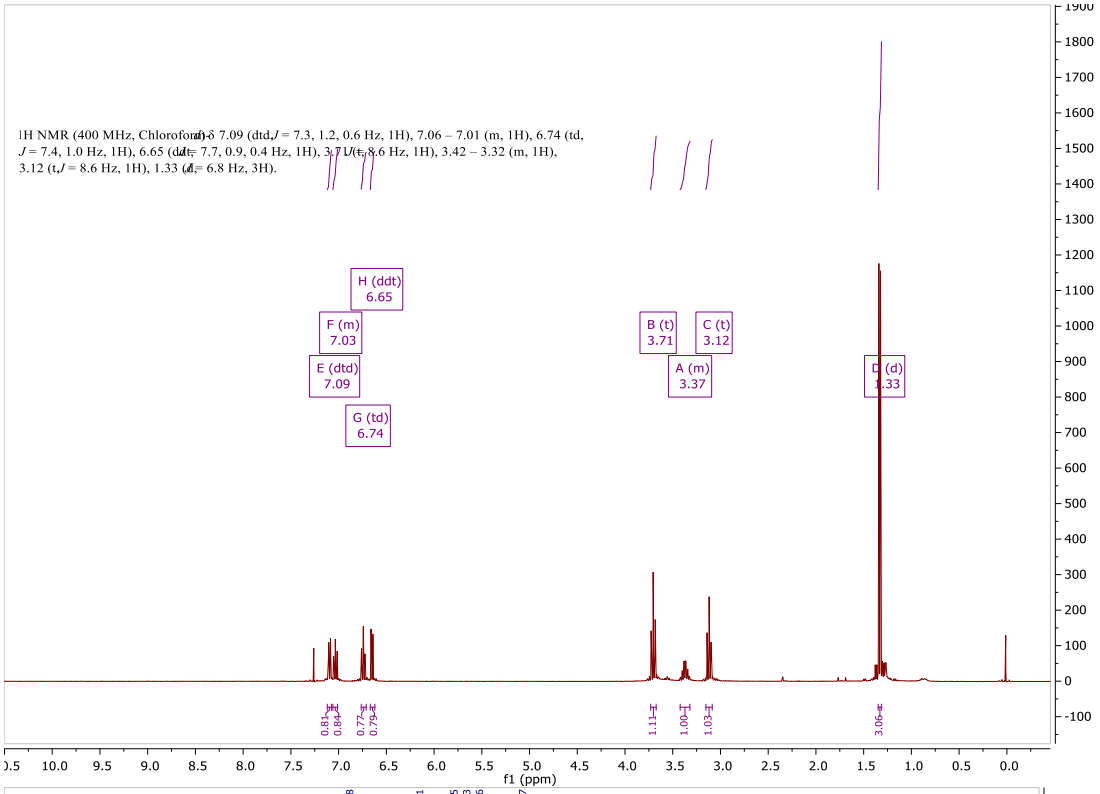

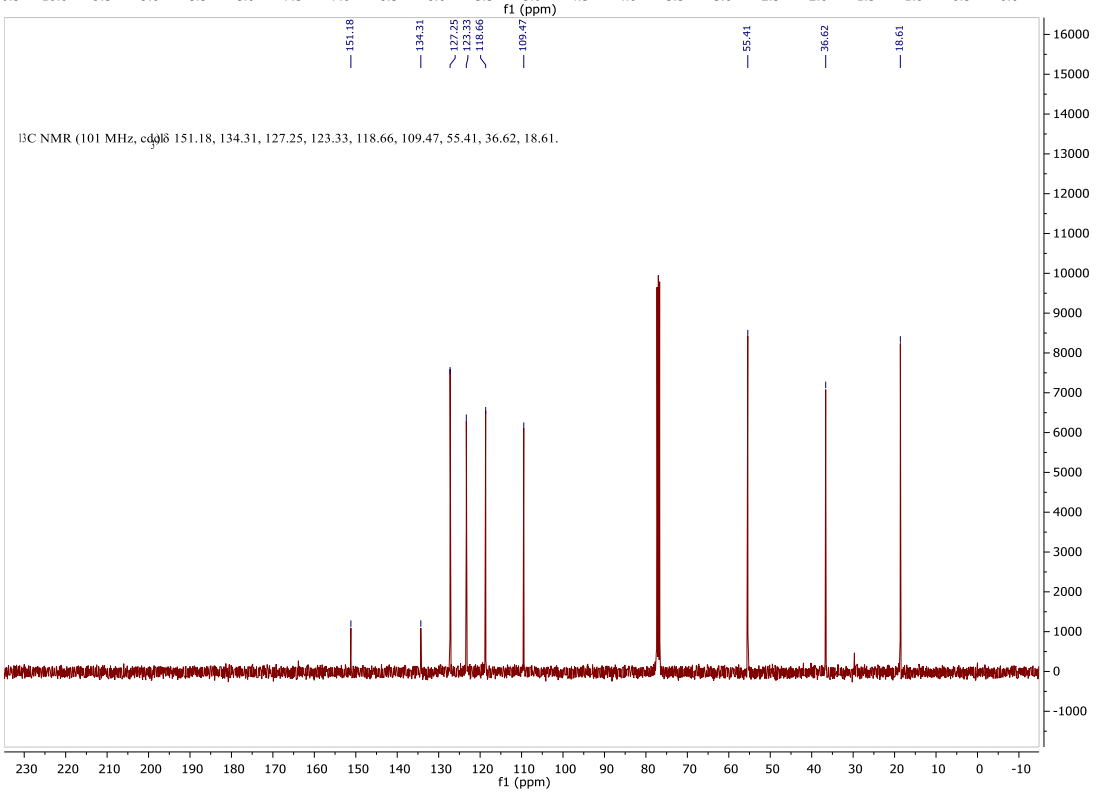

Chapter 10

Conclusions

This Ph.D. dissertion has been divided in three main blocks, regarding to the reaction type: Pauson-Khand cycloaddition, isomerization processes and asymmetric hydrogenation reactions. All three blocks are organized by following a basic idea: the design of novel catalytic methods while understanding the reaction mechanism by experimental and theoretical studies, and applying them to the synthesis of pharmaceuticals and biologically active compounds.

* * *

The Pauson-Khand reaction (PKR) is one of the few direct methods to synthesize five-membered ring carbocycles from acyclic precursors. When executed in an intramolecular fashion, this cobalt-mediated [2+2+1] cyclization has found more limited use due to the narrow scope of the alkene. In fact, only strained olefins or highly unhindered alkenes gave high yields.

- ✓ Related to this, we have reported a novel synthetic protocol to afford Pauson-Khand adducts with enhanced yields by simply **using ethylene glycol as additive** to the reaction mixture. We have postulated that ethylene glycol helps to the stabilization of the cobalt complexes intermediates. Among the benefits, **it has allowed the use of alkenes that did not react with the traditional protocol**, such as cyclopentene, 2,3-dihydrofurane or vinyltrimethylsilane as ethylene surrogate (Scheme 1A) – *see Chapter 2*.
- ✓ Similarly, we have applied the same methodology to the **catalytic Pauson-Khand reaction**. Gratifyingly, we have been able to **enhance the yields and selectivity** of the resulting cyclopentenones and, more importantly, the catalyst could be recycled for the first time through a biphasic toluene-ethylene glycol system (Scheme 1B) – *see Chapter 3*.
- ✓ Our currents efforts in the lab are to expand this methodology towards the synthesis of biologically active compounds that presents a cyclopentanic structure, such as phytoprostanes, prostaglandins, and other new family derivatives.

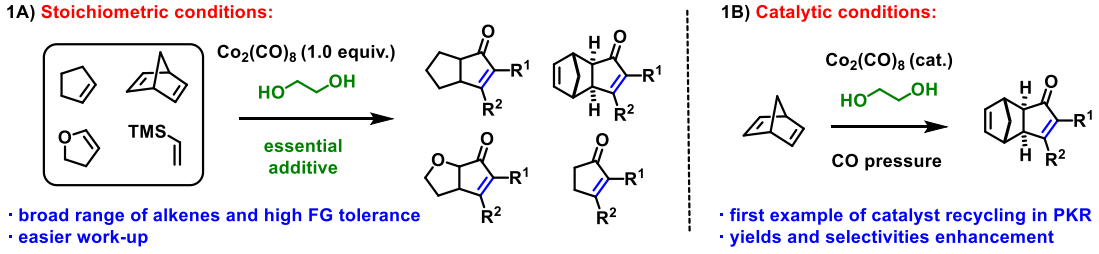

Scheme 1. Ethylene glycol as additive for the intermolecular PKR.

Taking advantage of this new synthetic protocol, we have applied it to the total synthesis of (*R*)-Sarkomycin methyl ester, which is a direct precursor of the (*R*)-Sarkomycin. This is a cyclopentanoid that rapidly emerged as an important drug not only for its antibiotic activity but also for its strong inhibitory effect on several human tumors and carcinoma cell lines. From the chemical point of view, numerous synthesis reported so far suffered from low overall yields or large number of steps were required.

- ✓ To circumvent this, we have reported a new approach to the enantioselective synthesis of (*R*)-Sarkomycin methyl ester using a four-synthetic route. The key steps of this synthesis have been: 1) regioselective intermolecular Pauson-Khand reaction using ethylene glycol as additive, 2) iridium-catalyzed asymmetric isomerization reaction of *N*-Boc allyl amide. After two more steps, (*R*)-Sarkomycin methyl ester has been synthesized in the **shortest enantioselective synthesis** reported so far, with an 28% overall yield (Scheme 2) – *see Chapter 4*.
- ✓ We have been pleased that, using the synthetic protocol developed in Chapter 2, the Pauson-Khand adduct **4-5** is afforded in excellent yield (85%) as **single regioisomer**.
- ✓ An unprecedented, **highly enantioselective isomerization of allyl amides** has been disclosed when using an iridium-P,N complex recently reported in our laboratory (Ir-MaxPHOX catalysts). The corresponding enamide has been afforded in **>99%** of enantiomeric excess. Our current efforts are devoted to expanding the substrate scope for this highly asymmetric isomerization of *N*-protected allyl amides.

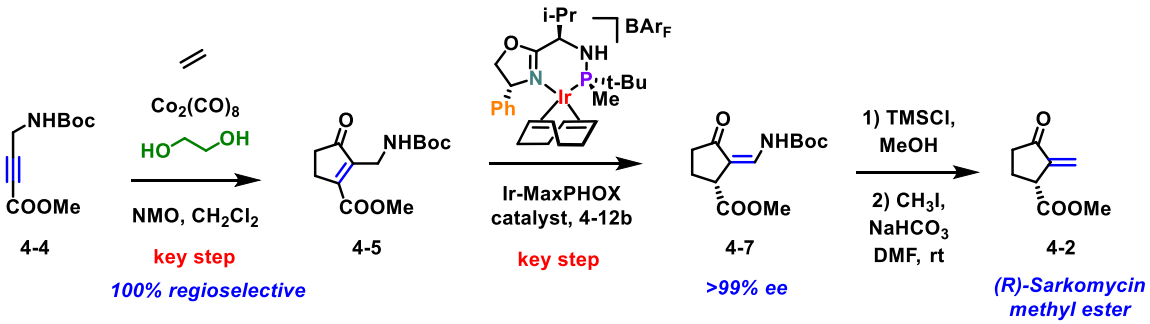

Scheme 2. Total synthesis of (*R*)-Sarkomycin methyl ester.

Inspired by this last result, we have been encouraged to explore the isomerization of other compounds that could be used as versatile, interesting organic intermediates. Isomerization processes provide useful synthetic transformations and constitute an important field in homogeneous catalysis.

However, most of the research in the field is devoted to the isomerization of allylic compounds, while the metal-catalyzed isomerization of heterocyclic compounds remains relatively unexplored. Therefore, we were prompted to better investigate this field using iridium catalysis.

- ✓ We have reported a combined experimental-theoretical study of **the selective isomerization of epoxides into aldehydes using low catalyst loading and very mild conditions**, using the commercially available and well-known **Crabtree's catalyst.** DFT calculations have been performed to disclose the reaction mechanism. The potential of the resulting compounds, which can be used as key intermediates for the synthesis of active molecules, clearly defines this process as a powerful new tool for organic synthesis – *see Chapter 5*.
- ✓ We have performed a **one-pot procedure** to interconvert terminal epoxides into **β-alkyl amines**, in good yields and mild conditions (Scheme 3).

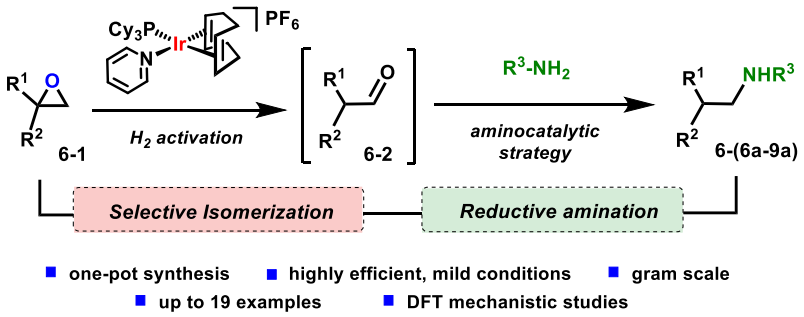

Scheme 3. Mild iridium-catalyzed isomerization of epoxides. One-pot synthesis of β-alkyl amines.

Next, we have been interested in exploring the isomerization reaction of other oxygenated strained rings: 2,2-disubstituted oxetanes. We have applied the catalytic protocol developed for epoxides. However, oxetanes dimerize and/or polymerize due to highly reactive iridium catalytic species. After an exhaustive catalyst screening, we have found that:

- ✓ **$B(C_6F_5)_3$** catalyzes the reaction selectively to the monomeric form, affording the homoallylic alcohol selectively in front of other isomers such as aldehyde or allylic alcohol (Scheme 4). **Exceptionally low catalyst loading** is necessary (0.5 mol%) and, in some cases, full conversion has been reached in only 2 hours. Moreover, DFT calculations have been performed to disclose the reaction mechanism. – *see Chapter 6*.

- ✓ The asymmetric hydrogenation of homoallylic alcohols has been performed as synthetic application, thus obtaining **enantioenriched alcohols with high levels of enantioselectivity**.
- ✓ This **protocol** is very sustainable and **green**, as dimethyl sulfoxide -from the double-Corey-Chaykovsky reaction for the oxetane formation- is the only byproduct.

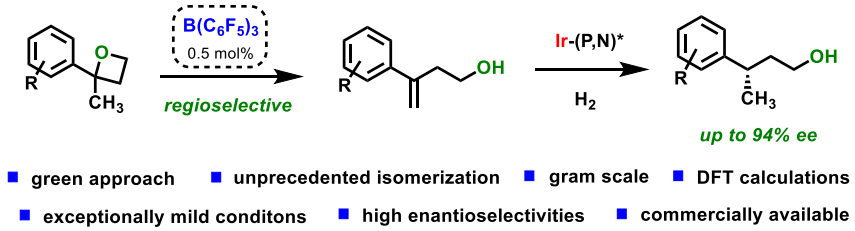

Scheme 4. $B(C_6F_5)_3$-catalyzed isomerization of 2,2-disubstituted oxetanes and applications.

Later, we have wondered if the Crabtree's catalyst could be also used for the regioselective isomerization of nitrogenated heterocyclic compounds. A broad range of *N*-sulfonyl aziridines have been synthesized and the optimal conditions for the isomerization of epoxides were here applied – *see Chapter 7*. Gratifyingly, we have been pleased to observe that:

- ✓ When dealing with *N*-sulfonyl aziridines, **H_2 activation is not necessary**. The Crabtree's catalyst can coordinate to the aziridine, which contain a sulfonyl group, thus displacing the pyridine ligand. Using this much simpler protocol, ***N*-sulfonyl allyl amines have been exclusively formed in front of imines**, allowing the reaction to be performed easily, being air-moisture tolerant, and using low catalyst loadings (Scheme 5).
- ✓ This is the first example in which **Crabtree's catalyst does not need external activation** to catalyze the reaction. The reaction mechanism was supported by **DFT calculations.**

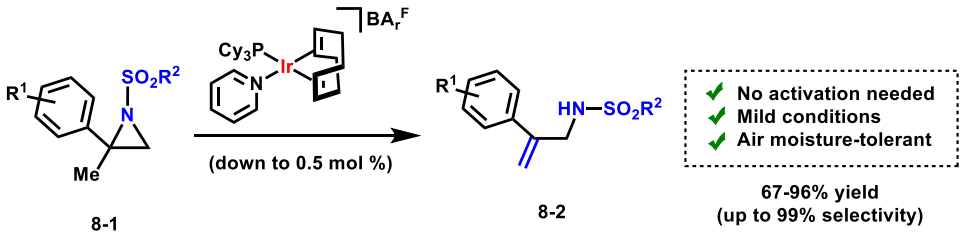

Scheme 5. Iridium-catalyzed isomerization of *N*-sulfonyl aziridines to allyl amines.

Finally, iridium-P,N complexes have been also tested in the asymmetric hydrogenation of minimally functionalized olefins. Particularly, we performed the enantioselective synthesis of β-methyl amines *via* asymmetric hydrogenation of *N*-protected allyl amines (Scheme 6).

- ✓ Commercially available **Ir-Ubaphox** has been chosen as an excellent catalyst for the **asymmetric hydrogenation of *N*-sulfonyl allyl amines** -which were obtained as resulting products of the selective isomerization of *N*-sulfonyl aziridines. Chiral β-methyl amines are afforded with excellent enantioselectivity (up to **94% ee**) – *see Chapter 8*.
- ✓ Alternatively, when dealing with ***N*-allyl phthalimides**, we were pleased to see that **Ir-MaxPHOX** gave impressive results and chiral amines were afforded with an enhanced level of enantioselectivity (up to **99% ee**) – *see Chapter 9*.
- ✓ The applicability of our methodology was further exemplified by the **synthesis of biologically active motifs and other marketed drugs**.

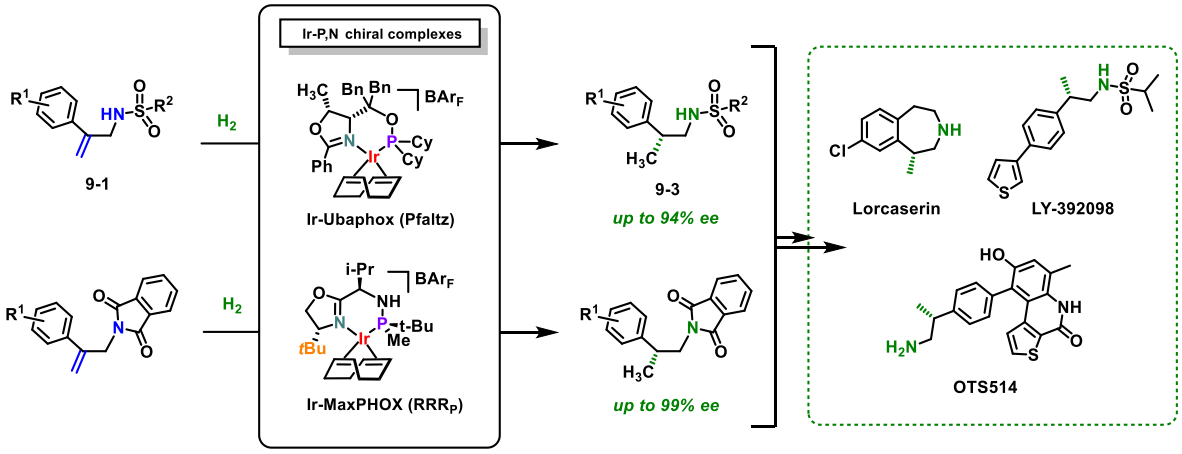

Scheme 6. Asymmetric hydrogenation of *N*-protected allyl amines using iridium-P,N complexes.